

ANALYZING SURFACE ROUGHNESS DEPENDENCE OF LINEAR RF LOSSES *

C. Xu^{1,2#}, M. J. Kelley^{1,2}, C. E. Reece¹

¹Thomas Jefferson National Accelerator Facility, Newport News, VA 23606

²College of William and Mary, Williamsburg, VA 23187

Abstract

Topographic structure on Superconductivity Radio Frequency (SRF) surfaces can contribute additional cavity RF losses describable in terms of surface RF reflectivity and absorption indices of wave scattering theory. At isotropic homogeneous extent, Power Spectrum Density (PSD) of roughness is introduced and quantifies the random surface topographic structure. PSD obtained from different surface treatments of niobium, such as Buffered Chemical Polishing (BCP), Electropolishing (EP), Nano-Mechanical Polishing (NMP) and Barrel Centrifugal Polishing (CBP) are compared. A perturbation model is utilized to calculate the additional rough surface RF losses based on PSD statistical analysis. This model will not consider that superconductor becomes normal conducting at fields higher than transition field. One can calculate the RF power dissipation ratio between rough surface and ideal smooth surface within this field range from linear loss mechanisms.

INTRODUCTION

RF loss induced by roughness is considered in many RF components, such as micro strip transmission line, wave guide and RF resonator. It can be understood as the RF electromagnetic field penetrates the surface and there the induced current will pass and cause RF loss. [1] However, in a RF wave view, the incident wave is reflected, scattered and absorbed by the rough surface. Inside of a resonator, the reflected, scattered wave contributes to standing wave field, while the absorbed RF wave is attributed to the RF surface loss. These two perspectives may both be used to describe the same RF loss.

In a resonator, only several specific RF standing wave modes can exist to meet the boundary condition which is the resonator geometry. The electric and magnetic field at one location is combination a of EM components of those plane waves. Within the resonator, E and M are separated in space and interchange their energy over a distance. Thus the peak E and M field are always not the same location. With special EM setup, TE, TM, TEM are used to describe the EM field direction, if presumed direction is beam axis. In some sense, it is very tedious and difficult to expand the field into plane wave expansion. If so, the incident direction should also be from all directions. Therefore, a RF loss calculation method is required and independent of direction. It also covers all frequencies or wavelengths.

METHODOLOGY

A rough surface will cost more RF loss. [2] One simple reason is that the surface current have more current path. In another word, the RF wave as more radiation absorption surface. This RF loss will contribute into power consumption and aggravate the quality factor.

If we consider a 2D random rough surface $Z = f(x)$ in Fig.1. We can expand the magnetic field into Fourier series as in x and z direction. [3]

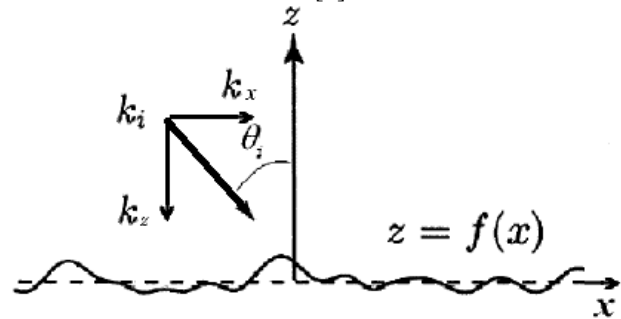


Figure 1: A plane wave incident impinging on a rough surface with incident angle θ_i .

$$\psi(x, z) = \int_{-\infty}^{\infty} dk_x \exp(-jk_x x + jk_{1z} z) \tilde{\psi}(k_x)$$

Where $k_{1z} = \sqrt{k_1^2 - k_x^2}$ and $k_1 = \frac{1-j}{\delta}$. Here δ is the skin depth $\delta = \sqrt{\frac{2}{\omega\mu\sigma}}$ and σ is the superconducting conductivity. The physics behind this equation is that the total magnetic field is combination of field component at each spatial wavelength. In another word, the total magnetic field can be expanded into magnetic contribution from each wavelength in spatial frequency.

If we use a second order small perturbation methods, setting

$$\tilde{\psi}(k_x) = \tilde{\psi}^{(0)}(k_x) + \tilde{\psi}^{(1)}(k_x) + \tilde{\psi}^{(2)}(k_x)$$

In first approximation, a fixed constant magnetic field H_0 is applied on the surface. Thus, the equation above becomes:

$$H_0 = \int_{-\infty}^{\infty} dk_x \exp(-jk_x x + jk_{1z} f(x)) \tilde{\psi}(k_x)$$

Basically, we have done a Fourier transform to redistribute the magnetic field into each surface spatial wavelength in x direction.

By balancing this equation to second order, we obtain:

*Work supported by Jefferson Science Associates. xuchen@jlab.org

FEASIBILITY STUDY OF SHORT PULSE MODE OPERATION FOR MULTI-TURN ERL LIGHT SOURCE*

T. Atkinson[†], A. V. Bondarenko, A. N. Matveenko, Y. Petenev,
Helmholtz-Zentrum Berlin für Materialien und Energie GmbH (HZB), Germany.

Abstract

The optic and simulation group at HZB are designing a light source based on the emerging Energy Recovery Linac superconducting technology, the Femto-Science-Factory (FSF) will provide its users with ultra-bright photons of angstrom wavelength at 6 GeV. The FSF is intended to be a multi-user facility and offer a wide variety of operation modes. A low emittance $\sim 0.1 \mu\text{m rad}$ mode will operate in conjunction with a short-pulse $\sim 10 \text{ fs}$ mode.

INTRODUCTION

This paper continues on from a recent introductory study[1] and highlights the physical limitations when trying to offer interchangeable modes and preserve beam quality. The paper concentrates on the short bunch mode, introducing the multi stage compression schemes in a general manner and presents the first results of the start-to-end beam simulations.

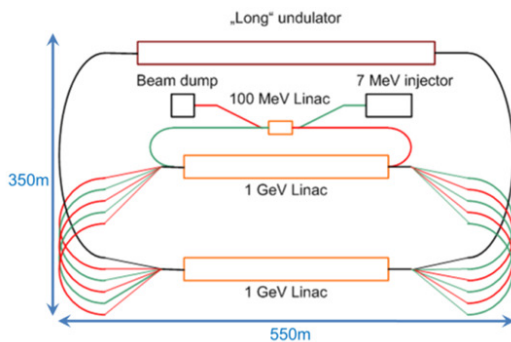


Figure 1: Schematic of the FSF Multi-Turn ERL.

The main design parameters of the FSF are listed in Table 1 and Fig. 1 shows the layout of the light source.

A SRF injector based on the design parameters of the BERLinPro[2] project delivers the 100 MeV electron beam into the main accelerator. Here two 1 GeV linacs are continually traversed until 6 GeV beam energy is reached. Each Arc contains straight sections for undulators and the final energy Arc permits a long straight section for 5000 period undulators.

The beam quality delivered to the long undulators and

* Work supported by German Bundesministerium für Bildung und Forschung, Land Berlin, and grants of Helmholtz Association VH NG 636 and HRJRG-214.

[†] terry.atkinson@helmholtz-berlin.de

Table 1: Main design parameters of FSF

Parameter	High Brilliance Mode	Short Bunch Mode
Energy (GeV)	6	6
Charge (pC)	15	4
Bunch Length (fs)	>200	~ 10
$\langle B \rangle$ (ph/s/mm ² /mrad ² /0.1%)	10^{22}	10^{21}
B_{peak} (ph/s/mm ² /mrad ² /0.1%)	10^{26}	10^{26}

hence the photon brilliance attainable depends on the machine operating mode.

SHORT BUNCH MODE

Single pass machines do not suffer the same fate as storage rings as equilibrium is never reached. A design based on linear uncoupled optic, helps address a proof-of-principle for the short pulse mode, which is later then tested using a realistic input beam distribution from the BERLin-Pro injector project.

Compression in the Injector

Producing a femto-second pulse of low energy spread starts at the Gun, Table 2. Here the longitudinal electron beam properties are restricted by the photo-injector laser pulse and the superconducting RF acceleration. The primary subtle compression in the Merger between the Booster and linac minimizes transverse emittance growth.

Table 2: Injector ASTRA[3] simulations

Component	Bunch Length (mm)	Emittance (keV mm)	Energy (MeV)
Gun	0.7	0.3	1.8
Booster	1.0	2	6.6
Linac	0.45	2.2	50

The injector Arc is then used to prepare the beam for the main accelerator. The combination of a second linac to increase the beam energy to 100 MeV and the R_{56} in the Arc compress the beam to $\sigma_t \sim 660 \text{ fs}$ with a correlated energy spread of $\Delta E/E \sim 1.5 \cdot 10^{-4}$.

LINAC OPTICS DESIGN FOR MULTI-TURN ERL LIGHT SOURCE*

Y. Petenev[#], T. Atkinson, A.V. Bondarenko, A.N. Matveenko, HZB, Berlin, Germany.

Abstract

The optics simulation group at HZB is designing a multi-turn energy recovery linac-based light source. Using the superconducting Linac technology, the Femto-Science-Factory (FSF) will provide its users with ultra-bright photon beams of angstrom wavelength at 6 GeV. The FSF is intended to be a multi-user facility and offer a variety of operation modes. In this paper a design of transverse optic of the beam motion in the Linacs is presented. An important point in the optics design was minimization of the beta-functions in the linac at all beam passes to suppress beam break-up (BBU) instability.

INTRODUCTION

In this document we present a design of a Linac optics for a new 3 pass ERL-based LS with 6 GeV maximum energy of electron beam. This future facility is named Femto-Science Factory (FSF) [1].

The schematic layout of the facility is presented in Fig. 1. A beam is created in 1.3 GHz SRF gun with photo cathode. We consider an SRF injector with similar parameters to the BERLinPro injector under development at HZB [2, 3]. Then it passes a 100 MeV Linac and is accelerated to 6 GeV after passing 3 times through each of two 1 GeV main Linac's. In the arcs between the acceleration stages it is assumed to have undulators with 1000 periods. In the long straight section (see Fig.1) a long undulator with 5000 periods is assumed. The main design parameters of FSF are presented in Table 1.

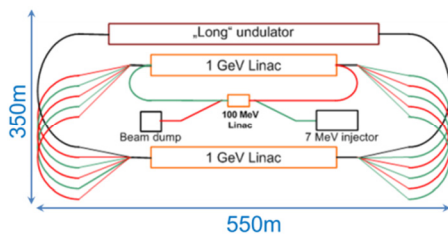


Figure 1: The scheme of FSF.

One potential weakness of the ERLs is transverse beam breakup instability, which may severely limit a beam current. If an electron bunch passes through an accelerating cavity it interacts with dipole modes (e.g. TM_{110}) in the cavity. First, it exchanges energy with the mode; second, it is deflected by the electro-magnetic field of the mode. After recirculation the deflected bunch interacts with the same mode in the cavity again which constitutes the feedback. If net energy transfer from the

beam to the mode is larger than energy loss due to the mode damping the beam becomes unstable.

The actuality of this problem was recognized in early experiments with the recirculating SRF accelerators at Stanford [4] and Illinois [5], where threshold current of this instability was occurring at few microamperes of the average beam current. In the works of Rand and Smith in [6] dipole high order modes were identified as a driver of this instability. In late of the 80's the detailed theoretical model and simulation programs had been developed [7, 8]. Nowadays the interest to this problem was renewed. The requirements for more detailed theory and simulation programs [9-11] are given by the needs of high current (~100 mA) ERLs.

The threshold current for the transverse beam breakup may be estimated for the case of a single cavity and single mode for a multipass ERL in the form as [11]:

$$I_{th} \approx I_0 \frac{\lambda^2}{Q_a L_{eff} \sqrt{\sum_{m=1}^{2N-1} \sum_{n=m+1}^{2N} \frac{\beta_m \beta_n}{\gamma_m \gamma_n}}}, \quad (1)$$

where I_0 - Alfven current, Q_a is the quality factor of HOM, $\lambda = \lambda/2\pi$, λ is the wavelength corresponding to the resonant frequency of the TM_{110} mode, γ_m is the relativistic factor at the m-th pass through the cavity, β_m - is the Twiss parameter, L_{eff} - is the effective length of the cavity, N is the number of passes during acceleration. It should be noted that (1) gives more realistic estimation of the BBU threshold current than a similar expression in [9] with a $1/N(2N-1)$ dependence on the number of passes. This is the result of an assumption in [9] of integer tunes in every turn of the ERL.

Table 1: Main Design Parameters of FSF

Parameter	High brilliance mode	Short bunch mode
E, GeV	6	6
$\langle I \rangle$, mA	20	5
Q, pC	15	4
τ , fs	200-1000	~10
$\langle B \rangle$, ph/s/mm2/mrad2/0.1%	$8 \cdot 10^{22}$	$\sim 4 \cdot 10^{21}$
B_{peak} , ph/s/mm2/mrad2/0.1%	10^{26}	$\sim 10^{26}$

Eq. 1 shows that it is preferable to have low β -functions at low energies. Therefore, the design was optimised to minimize beta functions of the beam in the Linac to increase the threshold current of BBU instability from one

* Work supported by German Bundesministerium für Bildung und Forschung, Land Berlin, and grants of Helmholtz Association VH-NG-636 and HRJRG-214.

[#]yuriy.petenev@helmholtz-berlin.de

STUDY OF BEAM-BASED ALIGNMENT FOR SHANGHAI SOFT X-RAY FEL FACILITY

Duan Gu[#], D.Z.Huang, Meng Zhang, Qiang Gu, M.H.Zhao
Shanghai Institute of Applied Physics, Shanghai 201800, China

Abstract

In linear accelerators, dispersion and transverse wakefield from alignment errors will lead to a significant emittance growth. The performance of the Free Electron Laser (FEL) process imposes stringent demands on the transverse trajectory, dispersion and emittance of the electron beam. So finding an effective Beam-Based Alignment(BBA) procedure is crucial for the success of Shanghai X-Ray FEL facility. This paper presents the preliminary study of different BBA method performances in SXFEL Linac. In addition, a MATLAB based simulation including quadrupole misalignment, dipole field errors and beam position monitor errors have been used to predict the orbit and emittance growth along the beamline and the required corrector current. Comparison with other codes is also presented.

INTRUDUCTION

As a critical development step towards constructing a hard X-ray FEL in China, a soft X-ray FEL facility (SXFEL) was proposed and will be constructed to verify the cascaded HGHG scheme and carry out the research on key technologies for X-Ray FEL. The SXFEL facility will be working at 9 nm soft X-ray band which consists of a 130MeV photo cathode injector, a main linac accelerating the beam to an energy of 840MeV, an undulator section with two stages of HGHG scheme and a diagnostic beamline. The local energy spread is 0.1%-0.15%, the peak current is about 600A and the normalized emittance is 2 mm·mrad[1].

In FEL facilities, misalignments between Quadrupoles and Beam Position Monitors(BPM) cause an increase of the transverse beam size and emittance which turns into an increase of normalized emittance. To keep the normalized emittance due to misalignment below 2 mm·rad, the average Quad-BPM misalignment in the linac must be smaller than 100um.

The traditional optical alignment can no longer meet such strict requirements, but a lot of analytical and numerical studies have been done and proved that Beam-Based Alignment technology can simultaneously eliminate the misalignment and dispersion in linac and undulator section, which obviously will leads to a much smaller emittance growth and transverse beam size. With the method above, a software based on MATLAB has been designed and simulation results have been compared with other software.

[#] gudian@sinap.ac.cn

BBA TECHNOLOGY OVERVIEW

Over past decade, a number of different realizations have been developed to measure the offset of magnetic center of quadrupole magnet[2][4]. Most techniques are based on a common approach, which is to change the quadrupole strength and measure the resulting deflection.

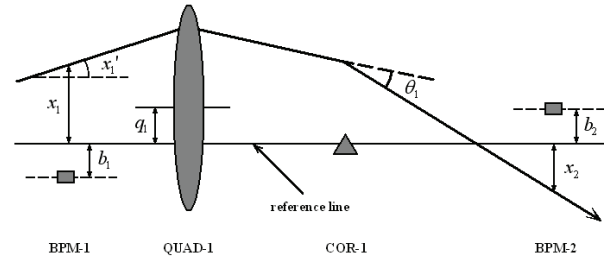


Figure 1: Common approach of BBA.

With respect to the reference line, m_i is the BPM reading at BPM-i. According to Linear optics theory (regardless wakefield effect and Quad-tilt), the transverse misalignment of upstream Quadrupole can be calculated using orbit response matrices, corrector values and inject parameters:

$$m_i = x_i - b_i = (x_i)_i - b_i$$

$$x_i = R^{(B,i)} x_1 + \sum_j^{N_{C_i}} R^{(C_j,i)} c_j + \sum_j^{N_Q} R^{(Q_j,i)} (I - R^{(Q_j)}) q_j \quad (1)$$

Where b_i is BPM reading error due to off-axis between electronic center and geometric center. R is the 2×2 transport matrix from BPM-1 or corrector c_j or Q_j to BPM-i.

x_1 is initial incoming parameters, the unknown c_j the corrector strength and Q_j is Quadrupole misalignments, which are defined as:

$$x_1 = \begin{bmatrix} x_1 \\ x_1' \end{bmatrix}; c_j = \begin{bmatrix} 0 \\ \theta_j \end{bmatrix}; q_j = \begin{bmatrix} q_j \\ 0 \end{bmatrix} \quad (2)$$

Further more, we can simultaneously correct both orbit and dispersion using so called “Dispersion Free Steering” method. The optimal settings are calculated using the orbit and dispersion response matrices, which are defined as the shift of the orbit or dispersion due to corrector strength change:

$$R_{i,j} = \frac{\Delta x_i}{\Delta \theta_j}; D_{i,j} = \frac{\Delta d_i}{\Delta \theta_j} \quad (3)$$

ON-LINE DISPERSION FREE STEERING FOR THE MAIN LINAC OF CLIC

J. Pfingstner*, D. Schulte, CERN, Geneva, Switzerland

Abstract

For future linear colliders as well as for light sources, ground motion effects are a severe problem for the accelerator performance. After a few minutes, orbit feedback systems are not sufficient to mitigate all ground motion effects and additional long term methods will have to be deployed. In this paper, the long term ground motion effects in the main linac of the Compact Linear Collider (CLIC) are analysed via simulation studies. The primary growth of the projected emittance is identified to originate from chromatic dilutions due to dispersive beam orbits. To counter this effect, an on-line identification algorithm is applied to measure the dispersion parasitically. This dispersion estimate is used to correct the beam orbit with an iterative dispersion free steering algorithm. The presented results are not only of interest for the CLIC project, but for all linacs in which the dispersive orbit has to be corrected over time.

INTRODUCTION

Linear colliders and light sources often require very small beam emittances and beam sizes to reach their goals. This fact makes these machines inherently sensitive to ground motion effects. For short time scales orbit feedbacks can be used to mitigate these effects by steering the beam with the help of beam positioning monitors (BPMs) (see [1] for the CLIC case). For longer time scales, this steering is not sufficient to preserve the beam quality as can be seen in Fig. 1. To be able to operate CLIC over longer time periods, it is essential to correct this remaining emittance growth. The development of such an algorithm is the topic of this paper.

The main reason for the remaining emittance growth is that the BPM positions itself will drift from their original position, which results in a dispersive beam orbit. The according chromatic dilutions decrease the beam quality over time. In the literature, a technique named dispersion free steering (DFS) can be found, which has been developed to correct similar chromatic dilutions (see [3] and [4]). In this paper we modify and extent this basic DFS method, such that it can be used to correct long term ground motion effects in an on-line mode. On-line means in this case that the DFS correction is applied during the normal accelerator operation in a parasitic way, without stopping the physics program. The method will be explained and evaluated on the example of CLIC, but can be easily utilised for other accelerators.

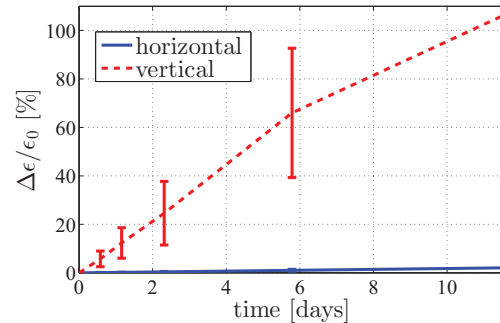


Figure 1: Simulations of the relative emittance growth over long time scales with orbit feedback in the main linac of CLIC. The used ground motion is generated according to the ATL law [2] with a constant A of $0.5 \times 10^{-6} \mu\text{m}^2/\text{m}/\text{s}$, which is the baseline for CLIC. The results have been averaged over 10 random samples of ground motion. For the initial horizontal and vertical emittance 600 nm and 10 nm have been used. The action of the orbit feedback was assumed to be perfect and therefore simulated by applying one-to-one steering without BPM noise, which is an optimistic approximation. It can be seen that already after 1 day the emittance has increased by about 10%.

ON-LINE DFS ALGORITHM

In this section, we will first introduce the basic DFS algorithm. After that the modifications necessary to apply this algorithm in an on-line mode will be discussed.

Basic DFS Algorithm

The DFS algorithm consists of two steps. In the first, the dispersion η at the BPMs is measured by varying the beam energy. This energy change can be created by changing the acceleration gradient, scaling the magnet strength and/or changing the initial beam energy. In the second step, corrector actuations θ are calculated such that at the same time the measured dispersion η as well as the beam orbit b are corrected. Such actuations can be calculated by solving the following system of equations for θ (see [5] for more details)

$$-\begin{bmatrix} b - b_0 \\ \omega(\eta - \eta_0) \\ \mathbf{0} \end{bmatrix} = \begin{bmatrix} R \\ \omega D \\ \beta I \end{bmatrix} \theta, \quad (1)$$

where b_0 and η_0 are the reference beam orbit and target dispersion respectively. The third set of equations in Eq. (1) with the unity matrix I on the right side is used to damp too high corrector actuations. The weights ω and β can be

*juergen.pfingstner@cern.ch

SPECIFICATIONS OF THE DISTRIBUTED TIMING SYSTEM FOR THE CLIC MAIN LINAC

A. Gerbershagen, A. Andersson, D. Schulte, CERN, Geneva, Switzerland
P. N. Burrows, JAI, University of Oxford, Oxford, UK
F. Ömer Ilday, Bilkent University, Ankara, Turkey

Abstract

The longitudinal phase stability of the CLIC main and drive beams is a crucial element of the CLIC design. In order to measure and control the phase a distributed phase monitoring system has been proposed. The system measures the beam phase every 900 m. The relative phase between the measurement points is synchronized with an external reference system via a chain of reference lines. This paper presents the simulations of error propagation in the proposed distributed monitoring system and the impact on the drive and main beam phase errors and the luminosity. Based on the results the error tolerances for the proposed system are detailed.

INTRODUCTION

The Compact Linear Collider (CLIC) is a proposed 3 TeV center-of-mass energy e^+e^- collider. It is designed to extract the RF energy from high-current low-energy drive beams and use this energy for acceleration of the low-current high-energy main beams that are brought into collision.

Since the main beam acceleration is performed by the RF power extracted from the drive beam, the stability of the relative phasing of the drive and main beams is crucial for the preservation of CLIC's luminosity. A relative phase error of 0.2° @ 12 GHz between the drive and the main beam will cause a luminosity loss of 1% if the error is coherent between the 24 decelerator segments. The same luminosity loss can be caused by an incoherent error of 0.8° . [1]

Additionally to these requirements on the relative drive beam - main beam phase, the phase tolerance between the two main beams at the interaction point (IP) has been set to 0.6° @ 12 GHz [2]. Hence, in order to align the main beam phase a global phase reference over 50 km is needed.

The stated tolerance requirements have to be met on the timescale of ≈ 50 ns, since this is the beam loading time of the main beam accelerating structures and errors on the shorter time scale will be (at least partially) filtered out by the structures.

PROPOSED DISTRIBUTED TIMING SYSTEMS

The distributed timing system is required to establish the correct beam phase at each turn-around of the linac. This allows to measure and correct the main and drive beam

phases along the main linac. There are two approaches for the design of such a system.

The first approach (A) is to use the outgoing main beams to transmit the phase information to a number of local oscillators (Fig. 1, top). These can maintain the phase accurately enough until the main beam returns on the way to the interaction point. This system requires accurate phasing between the outgoing main beams at the first booster linac near the interaction point (Fig. 2).

In the other approach (B) the master clock near the interaction point (IP) would define the nominal phase and distribute it as a signal cascade from one 900 m long decelerator segment to another (Fig. 1, bottom). This system would establish the relative phase of the local timing clocks by an optical connection independently of the beams.

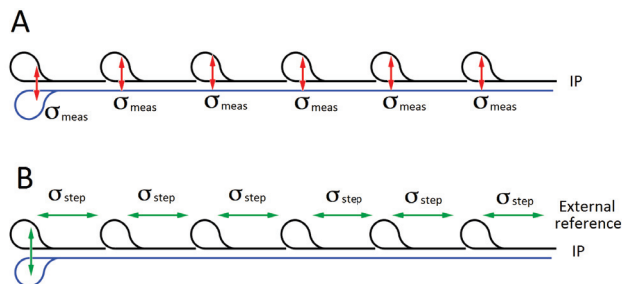


Figure 1: Phase signal propagation for the reference based on the main beam (A) and chained distribution of master clock signal (B).

Approach A has the advantage of having a relatively small error between the main and the drive beams, since the phase measurement at each drive beam decelerator is performed locally and hence no additional error is introduced during the distribution process (see Fig. 3, left). Approach B allows the correction of the main beam at its final turn-around, giving the possibility to reduce the jitter between the e^+ and e^- main beams (Fig. 3, right). However, if the drive beam correction signal is transported from the master clock via the distribution system, the noise introduced by this system would reduce the effectiveness of the phase correction. In the final CLIC design these approaches could be potentially combined.

The proposed timing distribution system is based on state of the art technology for signal distribution via optical fibers tested at XFEL (DESY, Hamburg) [3], [4]. This system is proven to provide <10 fs stability over the distance of several kilometers.

The following analysis determines the specifications of the

LINEAR ACCELERATOR BASED ON PARALLEL COUPLED ACCELERATING STRUCTURE*

Yu. Chernousov, V. Ivannicov, I. Shebolaev, ICKC, Novosibirsk, RUSSIA
 A. Levichev, V. Pavlov, A. Barnyakov, BINP, Novosibirsk, RUSSIA.

Abstract

Linear accelerator based on parallel coupled accelerating structure and RF-controlled electron gun is developed and produced. The structure consists of five accelerating cavities. The RF power feeding of accelerating cavities is provided by common exciting cavity which is performed from rectangular waveguide loaded by reactive pins. Operating frequency is 2450 MHz. RF-controlled Electron gun is made on the basis of RF triode. Linear accelerator was tested with different working regimes. The obtained results are following:

- energy is up to 4 MeV, accelerating current is up to 300 mA with pulse duration of 2.5 ns on the half of the width,
- energy is up to 2.5 MeV, accelerating current is up to 100 mA with pulse duration of 5 μ s,
- energy is up to 2.5 MeV, accelerating current is up to 120 mA with pulse duration of 5 μ s and beam capture of 100%.

The descriptions of the accelerator elements are given in the report. The features of the parallel coupled accelerating structure are discussed. The results of the measuring accelerator's parameters are presented.

INTRODUCTION

Compact linear electron accelerators have wide scientific and industrial applications. The more often linacs are used with energy up to 10 MeV, average beam power up to several kilowatts. In present there are two type of accelerating structures with travelling wave and standing wave. But all of these structures have sequential RF power feeding of the accelerating cells. This is cause of some problems. To supply the accelerating structure total RF power has to go from the first accelerating cell. As the power is attenuated along these structures the initial value of the power must be very high, therefore, there are breakdowns and thermal surface damage in the first accelerating cell. When the breakdown is happened in one of the accelerating cell the operating RF pulse is terminated because of all storage energy of the structure is dissipated in it. Developing of *accelerating structure with given distribution of the power along the cavities is very difficult task. Also there is problem of high order modes, vacuum pumping and etc.

The linear electron accelerator based on new type accelerating structure is developed and produced by Budker Institute of Nuclear Physics of SB RAS, Institute of Chemical Kinetics and Combustion of SB RAS and Insti-

tute of Catalysis of SB RAS [1]. The main elements of accelerator are parallel coupled accelerating structure, injector, waveguide track with vacuum RF window, focusing system and klystron KIU-111. The klystron's frequency is 2450 MHz, average power is 5 kW with pulse power of 5 MW [2]. The main goal of our efforts is to test new ideas and devices which are used in the accelerator. The mass of these elements are used in such accelerator for the first time and have some advantages.

PARALLEL COUPLED ACCELERATING STRUCTURE

The scheme of parallel coupled accelerating structure is shown in the Fig. 1 and Fig. 2. RF power from a klystron feeds the exciting cavity (1) through inductive coupling window (7). The exciting cavity supplies the accelerating cavities (2). The RF connection of the exciting cavity with the accelerating cavities is provided by magnetic field through coupling slots (5). The focusing alternative magnetic field is created along the beam axis by periodic permanent magnets (3) with radial magnetization inserted in the iron yoke (4). This kind of focusing provides large enough magnetic field while keeping the weight of the focusing system considerably small. The copper pins (6) are used to tune the exciting cavity (1) at the resonance frequency.

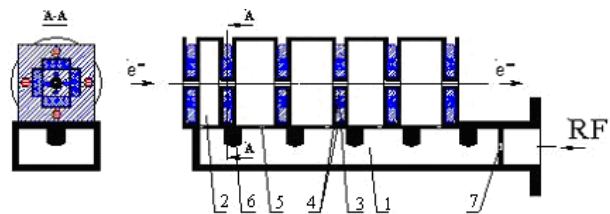


Figure 1: Scheme of the parallel coupled accelerating structure.

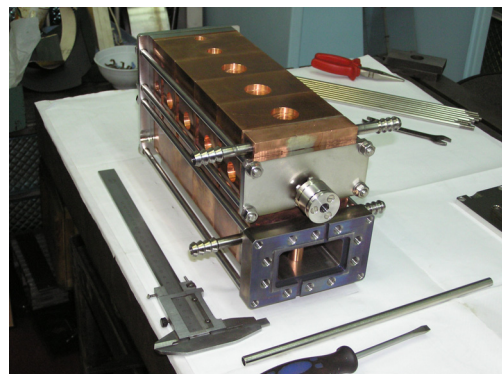


Figure 2: Parallel coupled accelerating structure.

* Work is supported by the Ministry of Education and Science of the Russian Federation, grants N 14.740.11.0836

MEASUREMENTS OF A REDUCED ENERGY SPREAD OF A RECIRCULATING LINAC BY NON-ISOCRONOUS BEAM DYNAMICS*

F. Hug[#], C. Burandt, M. Konrad, N. Pietralla, TU Darmstadt, Darmstadt, Germany
R. Eichhorn, Cornell University, Ithaca, NY, USA

Abstract

The Superconducting Linear Accelerator S-DALINAC at the University of Darmstadt (Germany) is a recirculating linac with two recirculations providing beams for measurements in nuclear physics at small momentum transfers. For these experiments an energy spread of better than 10^{-4} (rms) is needed. Currently acceleration in the linac section is done on crest of the accelerating field. The recirculation path is operated achromatic and isochronous. In this recirculation scheme the energy spread of the resulting beam in the ideal case is determined by the electron bunch length. Taking into account the stability of the RF system the energy spread increases drastically to more than 10^{-3} (rms).

We will present a new non-isochronous recirculation scheme which helps cancelling out these errors coming from the RF-jitters. This scheme uses longitudinal dispersion in the recirculation paths and an acceleration off-crest on a certain phase with respect to the maximum. We will present results of the commissioning of the new system including measurements of the longitudinal dispersion in the recirculation arcs as well as measurements of the resulting energy spread using an electron spectrometer.

INTRODUCTION

Operating since 1987 the Superconducting DArmstadt LINear Accelerator (S-DALINAC) is used as a source for nuclear- and astrophysical experiments at the university of Darmstadt [1]. It can accelerate beams of either unpolarized or polarized electrons [2] to beam energies of 1 up to 130 MeV with beam currents from several pA up to 60 μ A. The layout of the S-DALINAC is shown in Fig. 1.

Acceleration in the injector and main linac is done by superconducting elliptical cavities with a quality factor of $Q_0 \approx 10^9$. These cavities are operating at a frequency of 3 GHz with a maximum accelerating gradient of 5 MV/m.

The main linac consists of 8 standard 20-cell cavities and can provide an energy gain of 40 MeV. By recirculating the beam two times the maximum energy of 130 MeV can be achieved. In the adjacent experimental hall this beam can be used for different experiments such as electron scattering in two electron spectrometers or experiments with tagged photons. For these experiments an energy spread of $\pm 1 \cdot 10^{-4}$ is required.

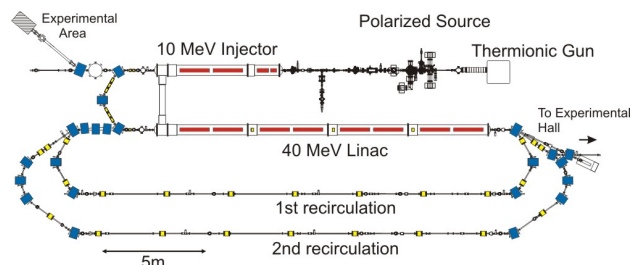


Figure 1: Floor plan of the S-DALINAC.

LONGITUDINAL BEAM DYNAMICS

The S-DALINAC is designed to use an isochronous recirculation scheme originally. On an isochronous working point the electrons are accelerated in the maximum of the accelerating field (on crest) in every turn and the bunch length is kept constantly small ($\pm 1^\circ$) using achromatic and isochronous recirculation paths. Isochronicity is a property of beam optics and can be described as $dL/dE = 0$ meaning that the length of the flight path of all electrons is independent from their energy. Acceleration on crest of the RF-field is the common mode for linear accelerators. Usually amplitude and phase jitters of the cavities are not correlated and the resulting energy spread is mainly determined by the short bunch length. In a recirculating linac the errors can add up coherently throughout the linac passages in a way that every electron sees the same errors in all passes through the linac due to the large time constant of field variations in the superconducting cavities compared to the short time of flight of the ultra relativistic electrons through the linac.

A way to overcome these correlated errors is changing the longitudinal working point to a non-isochronous one. This is the common operation mode for synchrotrons or microtrons. In a non-isochronous recirculation scheme the recirculation paths provide a longitudinal dispersion $dL/dE = D_L \neq 0$ while the accelerating field is operated at a certain synchrotron phase $\Phi_S \neq 0$ (on edge). The electrons then perform synchrotron oscillations in the longitudinal phase space. Compared to synchrotrons a quite large phase advance per turn is needed to cancel out the RF jitters. In fact a half or full integer number of synchrotron oscillations leads to the best energy resolution of the extracted beam in a way that the resulting energy spread at extraction is only determined by the energy spread at injection while the errors caused by the RF jitters of the main linac are cancelled out. [3,4]

The usability of such a non-isochronous recirculation scheme at the S-DALINAC has been verified already by numerical simulations (see Fig. 2). The new longitudinal

* Work supported by DFG through SFB 634

[#] hug@ikp.tu-darmstadt.de

COMPUTATIONAL MODEL ANALYSIS FOR EXPERIMENTAL OBSERVATION OF OPTICAL CURRENT NOISE SUPPRESSION BELOW THE SHOT-NOISE LIMIT

A. Nause, E. Gover, Tel Aviv University, Israel

Abstract

In this paper we present simulation analysis of experimental results which demonstrate noise suppression in the optical regime, for a relativistic e-beam, below the classical shot-noise limit. Shot-noise is a noise resulting from the granular nature of the space-charge in an e-beam. It is linear to the beam current due to its Poissonic distribution in the emission process. Plasma oscillations driven by collective Coulomb interaction during beam drift between the electrons of a cold intense beam are the source of the effect of current noise suppression. The effect was experimentally demonstrated [1] by measuring Optical Transition Radiation (OTR) power per unit e-beam pulse charge. The interpretation of these results is that the beam charge homogenizes due to the collective interaction (sub-Poissonian distribution) and therefore the spontaneous radiation emission from such a beam would also be suppressed (Dicke's sub-radiance [2]). Analysis of the experimental results using GPT simulations will demonstrate the suppression effect. For the simulation results we used a full 3D GPT model of the ATF section in which the experiment took place at.

INTRODUCTION

Shot-noise is a noise resulting from the granular nature of the space-charge in an e-beam. The discreteness of the particles and the randomness of electrons emission from the cathode causes time dependent fluctuations of the charge and current density at any cross section along the beam transport line. This noise was first reported in 1918 by Schottky who made experiments in vacuum tubes.

Noise is best characterized in terms of the Fourier transform of the time-varying fluctuations in electric current, namely, by its spectral density. Gover and Dyunin showed in a 1D model [3] that it is possible to observe and control optical frequency energy and current (shot noise) fluctuations in a dense relativistic charged particles beam. GPT simulations were used to demonstrate this effect for a real-like beam starting from Shot-noise [4]. Moreover, at certain conditions, when the dominant noise in the beam is current shot noise (density fluctuations), it is possible to reduce significantly the beam noise by virtue of a collective interaction process along an interaction length corresponding to a quarter period longitudinal plasma oscillation in the beam. This means that the charge distribution in the beam can be homogenized in this process.

First experimental observation of this phenomenon using OTR from a metallic foil was presented last year [1]. Noise suppression using a dispersive section (dog-leg bend) was demonstrated in SLAC [5]. TR is proportional to the

current-noise amplitude [6], and therefore can be used in order to estimate the suppression in the current noise. In this paper we press analysis of the experimental results and demonstrate this effect using full 3D GPT simulations that were carried out for this purpose.

1D Model of Noise Dynamics in Charged Electron Beams

In electron-beam transport under appreciable space-charge conditions, the microdynamic noise evolution process may be viewed as the stochastic oscillations of Langmuir plasma waves [3]. In the linear regime, the evolution of longitudinal current and velocity modulations of a beam of average current I_b , velocity βc and energy $E = (\gamma - 1)mc^2$, can be described in the laboratory frame by [7]:

$$\frac{d}{d\phi_p} \check{i}(z, \omega) = -\frac{i}{W(z)\check{v}(z, \omega)} \quad (1)$$

$$\frac{d}{d\phi_p} \check{v}(z, \omega) = -iW(z)\check{i}(z, \omega) \quad (2)$$

where $\check{i}(\omega) = \check{I}(\omega)e^{i\omega z/\beta c}$, $\check{v}(\omega) = \check{V}(\omega)e^{i\omega z/\beta c}$. $\check{I}(\omega)$, $\check{V}(\omega)$ are the respective Fourier components of the beam current and kinetic-voltage modulations. The kinetic-voltage modulation is related to energy and longitudinal velocity modulations: $\check{V}(\omega) = -(mc^2/e)\check{\gamma} = -(mc^2/e)\gamma^3\beta\check{\beta}$, $\phi_p(z) = \int_0^z \theta_{pr}(z')dz'$ is the accumulated plasma phase, $W(z) = r_p^2/(\omega A_e \theta_{pr} \epsilon_0)$ is the beam wave-impedance. A_e is the effective beam cross-section area, $\theta_{pr} = r_p \omega_{pl}/\beta c$ is the plasma wavenumber of the Langmuir mode, $r_p < 1$ is the plasma reduction factor, $\omega_{pl} = \omega_{p0}/\gamma^{3/2}$ is the longitudinal plasma frequency in the laboratory frame. The single-frequency Langmuir plasma wave model expressions [3] can be solved straightforwardly in the case of uniform drift transport. After employing an averaging process, this results in a simple expression for the spectral parameters of stochastic current and velocity fluctuations (noise) in the beam assuming that they are initially uncorrelated[]:

$$\check{i}(L, \omega) = \cos \phi_p(L)\check{i}(0, \omega) + (\sin \phi_p(L)/W_d)\check{v}(0, \omega) \quad (3)$$

where $\phi_p = \theta_{pr}z$, $\theta_{pr} = r_p \frac{\omega'_p}{v_0}$, $\omega'_p = (\frac{e^2 n_0}{m \epsilon_0 \gamma^3})$, $W_d = \sqrt{\mu_0/\epsilon_0}/k\theta_{pr}A_e$.

The beam current noise evolution is affected by the initial axial velocity noise through the parameter

$$N^2 = |\check{v}(0, \omega)|^2/W^2|\check{i}(0, \omega)|^2 = (\omega/c\beta k_D)^2 \quad (4)$$

STATUS OF CH CAVITY AND SOLENOID DESIGN OF THE 17 MeV INJECTOR FOR MYRRHA*

D. Mäder[†], H. Klein, H. Podlech, U. Ratzinger,
C. Zhang, IAP, Goethe-Universität, Frankfurt am Main, Germany

Abstract

The multifunctional subcritical reactor MYRRHA (Multi-purpose hybrid research reactor for high-tech applications) will be an accelerator driven system (ADS) located in Mol (Belgium). The first accelerating section up to 17 MeV is operated at 176 MHz and consists of a 4-rod-RFQ followed by two room temperature CH cavities with intertank quadrupole triplet focusing and four superconducting CH structures with intertank solenoids. Each room temperature CH cavity provides about 1 MV effective voltage gain using less than 30 kW of RF power. The superconducting resonators have been optimized for electric peak fields below 30 MV/m and magnetic peak fields below 30 mT. For save operation of the superconducting resonators the magnetic field of the intertank solenoids has to be shielded towards the CH cavity walls. Different coil geometries have been compared to find the ideal solenoid layout.

INTRODUCTION

Transmutation of long-lived radioactive waste and advanced technologies for future power generation will be investigated with the MYRRHA ADS [1]. The IAP of Frankfurt University is responsible for the development of the 17 MeV injector, a 13 meter long front end of the 600 MeV MYRRHA linac. To achieve the extremely high reliability of the beam supply for the reactor, two injectors will be driven at the same time. With this parallel redundancy the beam can be provided even during a failure of one injector. Because of thermal stress in the reactor not more than 11 beam trips of $t > 3s$ per year are allowed. The following accelerating structures up to 60 MeV are using the concept of serial redundancy [2].

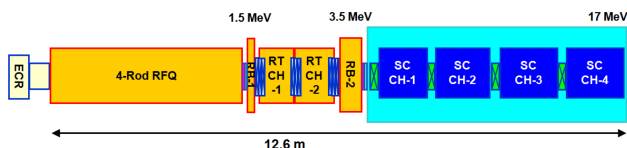


Figure 1: Overview of the MYRRHA injector.

A 4-rod-RFQ will bunch and accelerate the proton beam up to 1.5 MeV [3]. After a five gap CH rebuncher the proton bunches will be accelerated to 3.5 MeV with room temperature CH structures. Quadrupole triplets for focusing and

* Work supported by the EU, FP7 MAX contract number 269565

[†] d.maeder@iap.uni-frankfurt.de

phase probes for diagnostics are placed between the structures. 3 MV/m will be provided by the superconducting accelerators. Four bulk niobium CH cavities are assembled together with four 4.5 Tesla solenoids with coils made of NbTi in one cryomodule [Figure 1].

CH CAVITY DESIGN

Crossbar H-mode (CH) cavities are excellent candidates for acceleration of ions in the low and medium energy range. These resonators driven in the TE₂₁₁-Mode will be used for all accelerating and rebunching cavities after the 4-rod-RFQ from 1.5 to 17 MeV.

Room temperature CH cavities

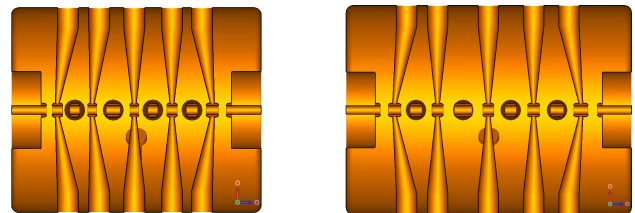


Figure 2: Scheme of the two room temperature CH structures.

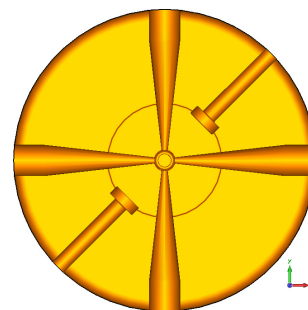


Figure 3: The diagonal tuners act mainly capacitively and provide a total frequency shift of 1 MHz.

CH-1 consists of three and CH-2 of two inclined stems [Figure 2]. Together with the extra volume around the vaults the inclination of the stems increases the induction on the outer stems. This flattens the gap voltage distribution and consequently the thermal load on the stems. The vaults at the resonator ends create additional space outside the cavity and are used for the quadrupole triplet lenses.

Each CH structure is tuned by two mainly capacitively acting tuners that provide a total frequency shift of 1 MHz.

THE BEAM COMMISSIONING PLAN OF INJECTOR II IN C-ADS*

Z.J. Wang, Y. He, H. Jia, S.H. Liu, C. Li, X.B. Xu, B. Zhang,
W. Wu, H.W. Zhao IMP, Lanzhou, 730000, China

Abstract

The design work of the Injector II, which is 10 MeV proton linac, in C-ADS project is being finished and some key hard wares are being fabricated. Now it is necessary to definite the operation mode of beam commissioning, including the selection of the beam current, pulse length and repetition frequency. Also the beam commissions plan should be specified. The beam commissions procedures is simulated with t-mode code GPT [1]. In this paper, the general beam commissioning plan of Injector II in C-ADS and simulation results of commissions procedures are presented.

INTRODUCTION

Nuclear energy as a kind of clean energy will be widely used in Chinese energy program in the future. But one of the serious problems is how to handle radioactive waste produced by nuclear plants. ADS, which is the effective tool for transmuting the long-lived transuranic radionuclides into shorter-lived radionuclides, is being studied in the Chinese Academy of Sciences. The road map of the project is shown in Fig. 1.

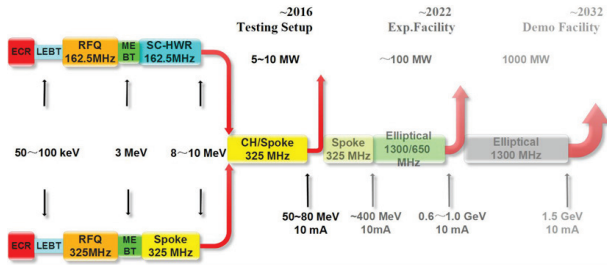


Figure 1: The roadmap of China CAS.

The linac will accelerate the proton with beam current 10mA to about 1.5GeV to produce high flux neutrons for transmutation of nuclear waste.

To ensure technical feasibility in the low energy section, two injectors for the superconduction linac are studied during the first step. One of the injectors, that is Injector II, is been designed and fabricated at Institute of Modern Physics of the Chinese Academy of Sciences. Injector II as part of the ADS is being designed and built at IMP. Injector II is composed of Low Energy Beam transport Line(LEBT), Radio Frequency Quadrupole(RFQ), Medium Energy Beam transport Line(MEBT) and the SC accelerating section. The layout of Injector II is shown in Fig. 2. The LEBT will match the proton beam with 0.035MeV from the ECR source to the RFQ by two solenoids. The RFQ will accelerate and focus the beam

from 0.035 MeV to 2.1 MeV simultaneously. The MEBT has two main functions, which are to match the proton beam from the RFQ to the superconducting accelerating section and to place some on line beam diagnostics devices. The superconducting accelerating section will accelerate proton from 2.1 MeV to 10 MeV with 16 superconducting half wave resonator(HWR) cavities. .

The basic parameters of Injector II are listed in Table. 1.

Table 1: The basic parameters of injector II.

Parameters	Value
Particle type	Proton
Operation frequency(MHz)	162.5
Operation mode	CW
Input beam energy(MeV)	0.035
Output beam energy(MeV)	10
Beam current(mA)	10

In this paper, the general beam commissioning plan of Injector II in C-ADS and simulation results of commissions procedures are presented.

THE BEAM DYNAMICS OF INJECTOR II

The MEBT and superconducting section are simulated by TRACK code. The particles distribution out from the RFQ [2] are transported as the initial distribution of the downstream lianc.

The results of the simulation with three-D field map are shown in Fig. 3. The RMS envelopes in both transverse and longitudinal direction are smooth and periodic in the superconducting section. This depicts that there is good matching between MEBT and the superconducting section.

COMMISSIONS BEAMS OF INJECTOR II

The commissions beams will be chopped for the commissioning of RFQ at first stage, then we plan to use unchopped beam for the bulk of the superconducting section commissioning studies. The beam will be consistent with the beam-handing capabilities of the beam diagnostics system in use at the time.

Beam current

The 0.5mA peak current beam will be chosen to be as the initial commissioning study. The reason is we want to reduce the space charge effect as weak as possible to simply the initial commissioning. At the same time the low limitation of measurement dynamics range of the beam diagnostics device should be considered. Also the low current is

*Supported by the National Natural Science Foundation of China (Grant No.11079001)

RF SETUP OF THE MedAustron RFQ*

B. Koubek, J. Schmidt, A. Schempp, IAP, Goethe University, Frankfurt am Main, Germany
 J. Haeuser, Kress GmbH, Biebergemuend, Germany

Abstract

A Radio Frequency Quadrupole (RFQ) was built for the injector of the cancer treatment facility MedAuston in Austria [1]. For the RF design simulations were performed using CST Microwave Studio® and the structure was manufactured by Firma Kress in Biebergemuend, Germany. The simulations and the RF setup of the delivered RFQ are presented in this paper.

INTRODUCTION

The 216.8 MHz MedAustron RFQ was designed to accelerate protons and carbon ions from 8 keV to 400 keV [2] on an electrode length of 1.25 m. It is a state of the art 4-Rod RFQ with quite slim electrodes and newly developed connections of the stems to the electrodes. Usually clamps were used to fix the electrodes to the stems (see Fig. 2). The accuracy of the machining allows us to remove the clamps. Simulations have shown that these new connections are causing less capacitance and hence less disturbing electric field than the clamps.

Fig. 1 shows the RFQ during its preparation at the Institute of Applied Physics (IAP) in Frankfurt am Main. More details about the RFQ basic design parameter can be found in Table 1.

Table 1: Design Parameters of the MedAustron RFQ

Parameter	Value	
Frequency	216.612	MHz
Input Energy	8	keV
Output Energy	400	keV
Beam Current (max)	4	mA
Aperture (min)	2	mm
Modulation Factor (max)	2	
Electrode Length	1250	mm
Intervane Voltage	70	kV
RF Cells	15	
Beam Height in Tank	19.5	mm
Stem Thickness	20	mm
Stem Distance	68	mm
Tank Length	1233	mm
Wall Thickness	40	mm

SIMULATIONS

Simulations have been performed using CST Microwave Studio® for the RF design. During this process two different shapes of the backside of the electrodes have been in-

* Work supported by BMBF

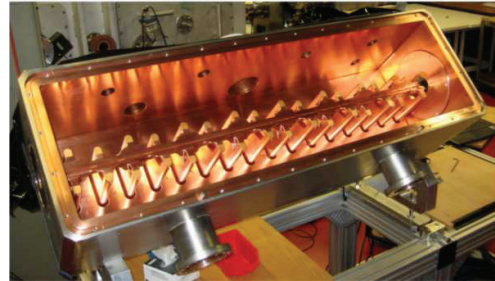


Figure 1: RFQ during preparation at IAP.

vestigated. One is a broad and the other one a more narrow socket of the electrodes backside. A top view of the two different shapes is shown in Fig. 2.

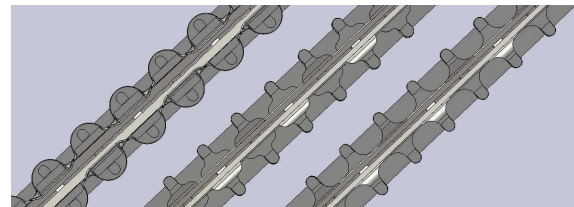


Figure 2: Former clamps (left), new broad (middle) and narrow (right) sockets.

Both shapes are rising the resonance frequency due to less capacitance compared to the old design with clamps. The broad shape increases frequency about one MHz more than the slim one, it shows less inductance and provides a fast and homogenous charge distribution on the electrode tips. Further informations about the RF characteristics of the connections of the electrodes can be found in [3].

MEASUREMENTS AND TUNING

Geometric Measurements

The accuracy of the machining and assembling of the single parts have been checked with a 3-D measurement device. The angle and the distance of the stems, the angle of the electrodes to each other and the position of the beam axis relatively to the reference surfaces have been measured. The measurements have met our expectations. Also no significant longitudinal electrode shift could be measured. Fig. 3 shows the measurement of the angle of the electrodes to each other and the longitudinal shift of the electrodes.

PRODUCTION AND QUALITY CONTROL OF THE FIRST MODULES OF IFMIF-EVEDA RFQ

F. Scantamburlo, A. Pepato, R. Dima, INFN/PD, Padova, Italy,
C. Roncolato INFN/L.N.L., Legnaro, Italy

Abstract

The IFMIF/EVEDA RFQ, designed to accelerate a 125mA D+ beam from 0.1 MeV to 5 MeV at a frequency of 175 MHz, consists of 18 modules with length of ~550 mm each. The production of the modules has been started and 2 prototype modules plus module 16 have undergone all the production steps, including precision milling and brazing. The progress of the construction and especially the fine tuning of the design and engineering phase are reported.

BRAZING PROCEDURE MODIFICATIONS

Once completed the 2 steps brazing of the 1st module prototype, the acquisition of a continuous active scanning measuring machine (Zeiss Accura) allowed a deep and extensive investigation of the internal geometry of the cavity. A wide series of transversal and longitudinal scanning were then performed. The more detailed and reliable measurements showed a lack of symmetry induced by gravitation effect during the 1st step brazing [1]. The final geometry of the cavity resulted still within the acceptable tolerances range for a single module, but not for the complete line, figures 1 and 2. A vertical brazing assembly, which permitted instead a possibility of a single brazing step, has been developed, figure 3. In this respect, the groove geometry, layout and tooling had to be redesigned. We introduced extensive US scanning (destructive test) and inspection (non-destructive) for the qualification of the brazed surfaces (Cu-Cu and Cu-st. steel).

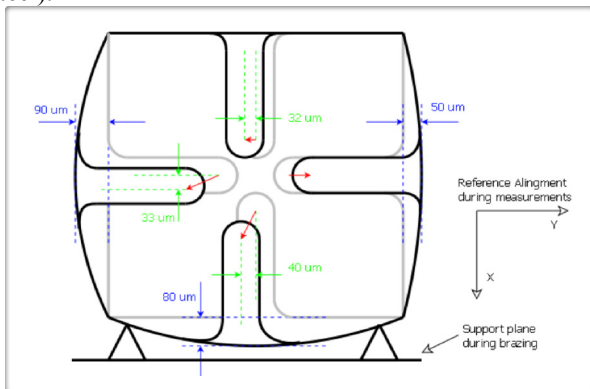
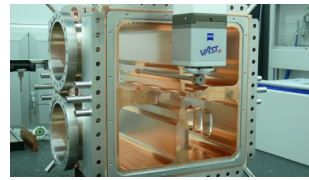


Figure 1: Scheme of the deformation of the cavity of the module 1 prototype after the second brazing



Pole	ΔX [μm]	ΔY [μm]	ΔR_0 [μm]
1	-40	-80	89.44
2	50	0	50.00
3	-32	0	32.00
4	-90	-33	95.86
mean ΔR_0 [μm]			66.83
$\partial f/\partial R_0$ [kHz/ μm]			7.60
Δf [kHz]			507.87

Figure 2: Module 1 prototype during CMM survey (left) and displacements of the tips (right).

R & D FOR SINGLE BRAZING STEP

With a single brazing step, the number of thermal cycles, reducing the mechanical properties of copper (1 annealing step + 1 final brazing step), is minimized.

The overall precision of the final geometry is optimized.

The cost and the timing of the modules production are also optimized.

Some basic tests on specimens having the same groove design, in order to compare vertical to horizontal brazing, have been performed.

Then two almost full scale tests have been performed finalizing an updated tooling set.

A complete inspection by US scan on slices of the brazed surfaces has been done (destructive). The grooves result always completely empty and no significant voids were detected on the brazing planes, figure 4.

Following these results, the production of the final modules started with SuperModule III-HE section. We adopted the vertical brazing approach but still with 2 brazing steps, until all details were well stated.

We completed the production of the module 16 (April '12), the second prototype module (July '12) and the 1st brazing step of module 17 (July '12).

The 1st single brazing step will be adopted on module 15 by October '12.



Figure 3: Full scale single brazing test

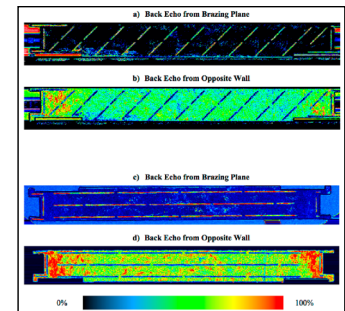


Figure 4: US inspection of two different brazing grooves design

RFQ WITH IMPROVED ENERGY GAIN

A.S. Plastun, NRNU (MEPhI), Moscow, Russia
 A.A. Kolomiets, ITEP, Moscow, Russia

Abstract

RFQ structure is practically only one choice for using in front ends of ion linacs for acceleration up to energy about 3 MeV. This limit is due to its relatively low acceleration efficiency. However it isn't intrinsic feature of RFQ principle. It is defined only by vane geometry of conventional RFQ structure with sinusoidal modulation of vanes. The paper presents results of analysis RFQ with modified vane geometries that allow to reach acceleration efficiency compared with IH DTL structures. RFQ with modified vanes was used for design second section of heavy ion injector of TWAC for acceleration of ions with $Z/A=0.33$ up to 5 MeV/u.

INTRODUCTION

An RFQ output energy doesn't usually exceed several MeV. Using conventional RFQ structure for acceleration of particles for higher energies is impractical because RFQ energy gain decreases rapidly with energy at constant modulation.

Many DTL structures were proposed for beam acceleration following RFQ that use magnetic or radio frequency focusing. The structures are well studied, they can provide good accelerating efficiency and are realized in a number of linacs. In the framework of heavy ion injector development for TWAC facility [1] several designs of second section based on these structures have been studied. In addition it was considered option that uses conventional RFQ with relatively minor modification of RFQ electrodes and resonant structure.

81 MHz RFQ – front end of TWAC injector has been recently successfully commissioned [2]. It is designed to accelerate beam from laser ion source with $Z/A = 0.33$ up to energy 1.57 MeV/u.

This paper presents result of study of TWAC injector second section design based on modified RFQ. The main goal of the modification was to provide maximum energy gain at focusing sufficient for acceleration beam with current 30 mA up to 5 MeV/u.

ENERGY GAIN IN RFQ

Vanes with Sinusoidal Modulation

The energy gain of a particle in RFQ is

$$\Delta W = e \frac{Z}{A} UT \cos \varphi_s, \quad (1)$$

e - electron charge, Z - charge number of the particle, A - mass number of the particle, U - voltage between adjacent vanes, T - accelerating efficiency, φ_s - phase of RF field, when synchronous particle is in a maximum of accelerating field.

Voltage U is usually chosen taking into account many different considerations. However it has to be as high as possible to increase energy gain. Its maximum value in this case is fully defined by acceptable surface electric field $E_{s \text{ lim}}$. Most accurately voltage can be found by numerical simulation for real vane geometry and expressed as

$$U = U_{sim} \frac{E_{s \text{ lim}}}{E_{s \text{ sim}}}, \quad (2)$$

Here U_{sim} is voltage between vanes in computer model and $E_{s \text{ sim}}$ is maximum field at vane surface obtained from simulation result.

Figure 1 shows results of field simulation in RFQ cell with code OPERA 3D. Simulated cell length $L_c = \beta\lambda/2$ corresponds particle energy at TWAC RFQ output. Curve 1 presents maximum field at vane surface calculated for sinusoidal modulation in $1 \leq m \leq 5$ range. Aperture for all modulations was constant $a = 8$ mm, that is average distance from axis to vane was changed as $R_0 = a(m+1)/2$. Simulation results show that for surface field limit $E_{s \text{ lim}} = 250$ kV/cm (about 2 Kilpatrick units for frequency $f = 81$ MHz) maximum voltage can reach according formula (2) $U \cong 500$ kV.

Accelerating efficiency T was calculated from simulated distribution of longitudinal field component E_z on axis. T factor for cell with sinusoidal modulation of vanes is limited by value $T \cong 0.7$. It means that the maximum effective accelerating gain per cell with studied parameters doesn't exceed $UT \cong 350$ kV.

Curve 1 shows that there is no sense to increase modulation factor more than $m = 4 \div 5$ because maximum field $E_{s \text{ sim}}$ reduces very slowly for higher m while focusing efficiency rapidly decreases. Figure 2 shows transverse phase advance calculated with the following expression [3]:

$$\sigma^2 = \frac{2}{\pi^2} K^4 + \frac{\pi e UT}{W_{kin}} \sin \varphi,$$

$$K^2 = \frac{Z}{A} \frac{e \bar{G}}{4 W_0} \lambda^2.$$

Here \bar{G} is mean value of simulated transverse field gradient along RFQ cell, W_0 - rest mass of proton, λ - wavelength of RF field. Estimation shows that transverse motion is very close to stability border at $m \cong 4$. It defines limiting capability of conventional RFQ with sinusoidal modulation for higher energy gain acceleration.

It is possible to improve accelerating efficiency using trapezoidal modulation proposed in [4]. Cell with this modulation type is shown in Figure 3. The trapezoidal

TUNING STUDIES ON 4-ROD RFQs*

J. Schmidt, B. Koubek, A. Schempp, B. Klump, IAP, Univ. Frankfurt, Germany

Abstract

A NI LabVIEW based Tuning Software has been developed to structure the tuning process of 4-rod Radio Frequency Quadrupoles (RFQs). Its results are compared to measurement data of 4-rod RFQs in different frequency ranges. For the optimization of RFQ design parameters, a certain voltage distribution along the electrodes of an RFQ is assumed. Therefore an accurate tuning of the voltage distribution is very important for the beam dynamic properties of an RFQ. A variation can lead to particle losses and reduced beam quality especially at higher frequencies. Our electrode design usually implies a constant longitudinal voltage distribution. For its adjustment tuning plates are used between the stems of the 4-rod-RFQ. These predictions are based, in contrast to other simulations, on measurements to define the characteristics of the RFQ as it was build - not depending on assumptions of the design. This will lead to a totally new structured process of tuning 4-rod-RFQs in a broad range of frequencies by using the predictions of a software. The results of these studies are presented in this paper.

RESONANT CIRCUITS

A simplified model of the 4-rod RFQ resonator is a chain of LC-oscillators where each RF cell has its own resonance frequency. In these RF cells the stems represent the inductance, while the electrodes form the capacitive part of the circuit. A more detailed model is described in [1].

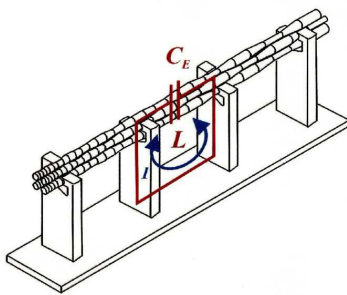


Figure 1: LC Resonator as Equivalent Circuit of a 4-Rod RFQ.

To tune this system, the resonance of each RF cell has to be tuned with tuning plates. They short cut the current path between the stems, to change the inductance of the RF cell. The longitudinal voltage distribution, the so called flatness, is a fundamental parameter in the particle dynamic design of an RFQ. Usually a constant longitudinal voltage along

the electrodes is the basis of our design, but other distributions are possible as well [2].

Following the particle dynamics the longitudinal voltage distribution has to be arranged. It is measured using the capacitive perturbation method. A perturbation capacitor sits on a pair of electrodes of one RF cell to cause a frequency shift due to Thomson's law. The resulting frequency shift of the cell is proportional to its voltage (see Eq. 1).

$$U \propto \Delta f_0 = \frac{1}{\sqrt{LC}} - \frac{1}{\sqrt{L(C + \Delta C)}} \quad (1)$$

THE VOLTAGE TUNING PROCESS

The process of adjusting the flatness is an iterative process of shifting the tuning plates and try to find a set of heights, which results in the desired distribution and total resonance frequency. This process can take some time, especially working on long RFQ structures with a lot of RF cells [3].

Due to several reasons like the changing modulation or differences in the manufacturing, the RFQ has deviations in its characteristics along the electrodes profile [4]. This leads to a different impact of the tuning plates depending on their position in the RFQ.

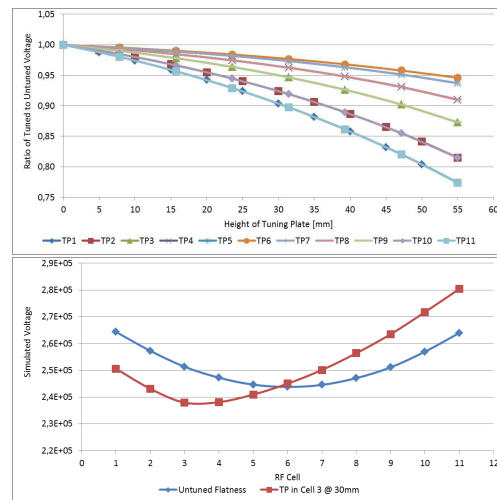


Figure 2: The voltage in $z=k$ from raising tuning plates in all cells (upper graph) and the longitudinal change with a tuning plate in cell $k=3$ (lower graph).

Raising a tuning plate in cell $k \in [1, n]$ decreases the voltage in cell k and its neighboring cells $k \pm i$ with $i < i_0$, while the voltage raises in cells $k \pm i$ with $i \geq i_0$. This behavior is shown in Fig. 2

*Work supported by BMBF

STUDIES OF PARASITIC CAVITY MODES FOR PROPOSED ESS LINAC LATTICES

R. Ainsworth*, Royal Holloway University of London, UK
 S. Molloy, European Spallation Source AB, Lund, Sweden

Abstract

The European Spallation Source (ESS) planned for construction in Lund, Sweden, will be the worlds most intense source of pulsed neutrons. The neutrons will be generated by the collision of a 2.5 GeV proton beam with a heavy-metal target. The superconducting section of the proton linac is split into three different types of cavities, and a question for the lattice designers is at which points in the beamline these splits should occur. This note studies various proposed designs for the ESS lattice from the point of view of the effect on the beam dynamics of the parasitic cavity modes lying close in frequency to the fundamental accelerating mode. Each linac design is characterised by the initial kinetic energy of the beam, as well as by the velocity of the beam at each of the points at which the cavity style changes. The scale of the phase-space disruption of the proton pulse is discussed, and some general conclusions for lattice designers are stated.

INTRODUCTION

The European Spallation Source is a facility, currently in its design phase [1], for the generation of intense pulses of neutrons for studies in applied science. The neutrons are generated through the spallation process when a 5 MW (average) proton pulse is made to impact a heavy metal target.

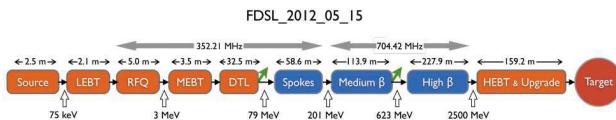


Figure 1: Block diagram of the ESS linac.

	Value	Unit
Final kinetic energy	2.5	GeV
Macropulse current	50	mA
Macropulse repetition rate	14	Hz
Bunch frequency	352.21	MHz

Table 1: Main ESS linac parameters.

A cartoon of the ESS linac is shown in Figure 1, and the main parameters of the proton beam are given in Table 1.

*rob.ainsworth.2009@live.rhul.ac.uk

This note concerns the beam dynamics within the superconducting sections of the machine:

Spokes: Two–spoke cavities operating at 352.21 MHz.

This section accelerates the beam from the exit of the DTL at 79 MeV to 201 MeV.

Medium β : Five–cell elliptical cavities operating at 704.42 MHz. The geometrical beta of this section is still under discussion, but is likely to be set at a value close to, $\beta_g = 0.65$. In this section, the beam is accelerated from 201 MeV to 623 MeV.

High β : Five–cell elliptical cavities operating at 704.42 MHz. As with the previous section, the geometrical beta is still under discussion, but the likely value is close to, $\beta_g = 0.92$. This section accelerates the beam to its final energy of 2.5 GeV

Given the high intensity of the beam, one major concern is that strong resonances will be excited in the superconducting cavities that will then act to disrupt subsequent bunches. In particular parasitic modes that lie close in frequency to that of the accelerating mode. They are of concern due to there small frequency spread and high R/Q relative to the accelerating mode. If they are found to be a problem, the geometric beta of the cavity may need to be altered or the velocity partitioning between the cavity families may need to be shifted.

LINACS

For the studies into Same Order Modes (SOMs), that is, modes that are part of the same passband as the fundamental accelerating mode, four linacs are investigated as shown in Table 2 where cavities per family denotes the number of cavities in the spoke, medium β and high β sections.

Linacs	Cavities per family	Energy In [MeV]
HS_2011_11_23	36-64-12	50
FD_SL_2012_04_13	32-60-120	79
FD_SSCL_2012_04_16	32-52-128	80
FD_SL_2012_05_15	28- 60-120	79

Table 2: Linacs investigated for SOM simulations.

THE MULTIPACTING SIMULATION FOR THE NEW-SHAPED QWR USING TRACK3P*

C. Zhang[#], S. He, Y. He, S. Huang, Y. Huang, T. Jiang, R. Wang, M. Xu, Y. Yang, W. Yue,
S.H. Zhang, S. Zhang, H. Zhao

Institute of Modern Physics, Lanzhou, Gansu 730000, China

Abstract

In order to improve the electro-magnetic performance of the quarter wave resonator, a new-shaped cavity with an elliptical cylinder outer conductor has been proposed [1]. This novel cavity design can provide much lower peak surface magnetic field and much higher R_a/Q_0 and G. The multipacting simulation has been done for this new QWR cavity using ACE3P/TRACK3P code, in this paper the simulation results will be presented and analyzed.

INTRODUCTION

In the Heavy Ion Accelerating Facility (HIAF) of IMP, superconducting quarter wave resonators (QWRs) with frequency of 81.25 MHz and β of 0.041, 0.085 will be applied to accelerate the ion beams from 0.3 MeV/u to 17 MeV/u. Because of the extremely high design voltage for the $\beta = 0.085$ QWR cavity, an elliptical cylinder outer conductor shape has been proposed for it (see Fig. 1).

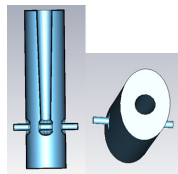


Figure 1: The elliptical cylinder outer conductor QWR model for multipacting simulation.

MULTIPACTING SIMULATION

Parallel codes Omega3P and Track3P which are developed at SLAC have been used, to obtain the field maps and then to analyse the multipacting barriers [2, 3]. When doing the multipacting simulation, one half of the QWR cavity was used taking advantage of the symmetry. Seed particles were initiated on all the RF surfaces. The accelerating gradient was scanned up to 6 MV/m firstly to locate the multipacting band, and then much finer scan interval was used in order to study the multipacting band in detail. 2 eV was used as the initial energy for primary and secondary emissions to study its effect on multipacting and typical niobium secondary electron yield (SEY) was applied to estimate the multipacting strength (see Fig. 2). At each field level, 50 RF cycles were used as total running time to obtain resonant trajectories.

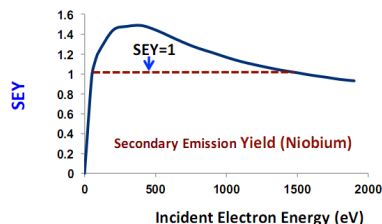


Figure 2: Secondary electron yield (SEY) for Niobium on the dependence of impact energy. The impact energy range relevant to the peak SEY is 150~700 eV. Resonant electrons with impact energies in this range are most dangerous to lead to hard multipacting.

MULTIPACTING SIMULATION RESULTS

Multipacting band at low field level

The distribution of resonant particles identified by Track3P presented the multipacting bands occurred at low field levels, Figure 3, 4 show the expanded plot around this multipacting band and impact positions.

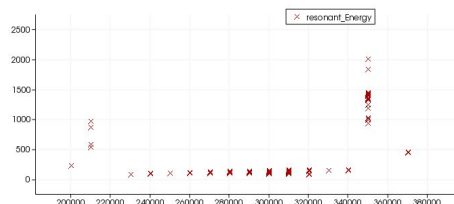


Figure 3: Impact energy vs. accelerating gradient at low field level.

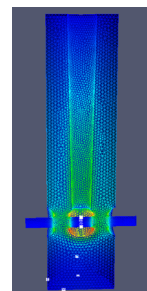


Figure 4: Impact positions at all field levels.

There are two multipacting bands, one at field levels of 0.2 ~0.34 MV/m with impact energies 80~160 eV in the beampipe region (see Fig. 5, 6); the other at around the accelerating gradient of 0.35 MV/m with impact energies 700~2000 eV in the bottom part of the cavity. In consideration of the peak SEY energy for Nb (see Fig. 2), such two bands are expected to be a soft barrier.

* Work supported by 91026001 Nature Science Foundation
claire335@gmail.com

STRUCTURAL ANALYSIS OF THE NEW-SHAPED QWR FOR HIAF IN IMP*

C. Zhang[#], S. He, R. Wang, M. Xu, W. Yue, S. Zhang, S. Huang, Y. Yang, Y. Huang
T. Jiang, S. Zhang, Y. He, H. Zhao

Institute of Modern Physics, Lanzhou, Gansu 730000, China

Abstract

Since the QWR cavity is very successful for the operation with frequency of 48 to 160 MHz and beta value of 0.001 to 0.2, a new-shaped QWR is being designed for the low energy superconducting section of HIAF in the Institute of Modern Physics [1]. The cavity will work at 81.25 MHz and beta of 0.085, with an elliptical cylinder outer conductor to better its electro-magnetic performance and keep limited accelerating space. Structural design is an important aspect of the overall cavity implementation, and in order to minimize the frequency shift of the cavity due to the helium bath pressure fluctuations, the Lorentz force and microphonics excitation, stiffening elements have to be applied. In this paper, structural analyses of the new-shaped QWR are presented and stiffening methods are explored.

INTRODUCTION

A stable resonant frequency for the superconducting cavity is desired, because excessive frequency fluctuations require extra power to control the RF amplitude and phase. The reasons that lead to frequency fluctuations include the fluctuations in the liquid helium pressure, Lorentz force detuning, mechanical vibration modes and the etching effect from the cavity surface treatment. Since the operating temperature for the QWR cavities is 4.5 K, the helium pressure stability will be determined by the extent to which the cryogenic plant can be controlled. The stiffening measures were intended primarily to reduce the pressure sensitivity.

MECHANICAL SIMULATION

When the EM design has been completed, the mechanical performance of the cavity should be evaluated. We tried to figure out the cavity's helium pressure sensitivity, severity of Lorentz Force Detuning plus the vibration frequency of mechanical modes, and further, to minimize the instabilities using different stiffening measures. Simulations and optimizations have been done by the 3D Multiphysics solver ANSYS-APDL [2]. In the simulation, niobium sheet of 3 mm thickness was firstly used, with the mechanical properties of Young

modulus of 105000 N/mm², Poisson ratio of 0.38 (see Fig. 1).

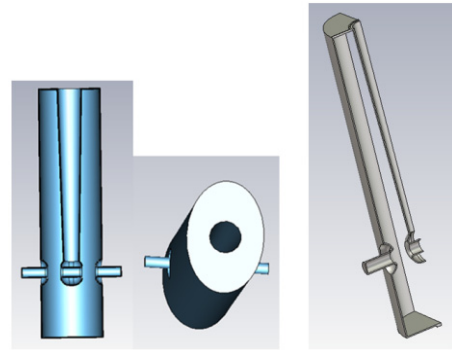


Figure 1: Mechanical model of the elliptical cylinder outer conductor QWR for the structural analysis.

Etching Effects

Surface processing is very important in order to achieve good performance of the superconducting cavity. Either the BCP or the EP is to etch proper thickness of the inner surface, which will change the frequency. According to Slater's perturbation theory, a small deformation in the cavity boundary will lead to a frequency shift.

Using the ANSYS-APDL code, the change in the frequency because of the etching can be calculated. Firstly, you have to get the electro-magnetic field distribution, and then the frequency change caused by the cavity wall's deformation can be obtained. The simulation results show that 1 μm etching thickness will lead to 27Hz increase in the frequency.

Lorentz Force Detuning

The Lorentz force on the cavity surface results from the interaction of the surface electromagnetic fields with the induced surface currents, which will exert pressure to the cavity wall, and the resulting cavity shape deformation ΔV will cause the change in the resonant frequency. The frequency shift caused by Lorentz force is often quantified by K_L which is defined as: $K_L = \Delta f / (E_{acc})^2$.

If the cavity works at the continuous wave mode, then the frequency change will be invariant, it is the static Lorentz force detuning; otherwise, when the cavity works at the pulsed wave mode, the dynamic Lorentz force detuning will be caused. In this paper, only the static situation was considered and 2.5 MV accelerating voltage was to be scaled for the naked cavity whose

*Work supported by 91026001 Nature Science Foundation
#claire335@gmail.com

FIRST MEASUREMENTS ON THE 325 MHz SUPERCONDUCTING CH CAVITY*

M. Busch^{†,1}, F. Dziuba¹, H. Podlech¹, U. Ratzinger¹, W. Barth^{2,3},
S. Mickat^{2,3}, M. Amberg³, M. Pekeler⁴

¹IAP Frankfurt University, 60438 Frankfurt am Main, Germany

²GSI Helmholtzzentrum, 64291 Darmstadt, Germany

³Helmholtz-Institut Mainz (HIM), 55099 Mainz, Germany

⁴RI Research Instruments, Bergisch Gladbach, Germany

Abstract

At the Institute for Applied Physics (IAP), Frankfurt University, a superconducting 325 MHz CH-Cavity has been designed and built. This 7-cell cavity has a geometrical β of 0.16 corresponding to a beam energy of 11.4 AMeV. The design gradient is 5 MV/m. Novel features of this resonator are a compact design, low peak fields, easy surface processing and power coupling. Furthermore a new tuning system based on bellow tuners inside the resonator will control the frequency during operation. After successful rf tests in Frankfurt the cavity will be tested with a 10 mA, 11.4 AMeV beam delivered by the GSI UNILAC. In this paper first measurements and corresponding simulations will be presented.

CAVITY LAYOUT

Worldwide there is a growing interest in applications demanding high beam power and quality (e.g. MYRRHA (Multi Purpose HYbrid Research Reactor for High-Tech Applications) [1]). The superconducting CH-cavity is an appropriate structure for these specifications being characterized by a small number of drift spaces between adjacent cavities compared to conventional low- β ion linacs [2]. Applying KONUS beam dynamics, which decreases the transverse rf defocusing and allows the development of long lens free sections, this results in high real estate gradients with moderate electric and magnetic peak fields. In the past a 19-cell, superconducting 360 MHz CH-prototype has been developed and successfully tested [3]. For future operations a new design proposal for high power applications has been investigated. Presently a new cavity operating at 325.224 MHz, consisting of 7 cells, $\beta = 0.16$ and an effective length of 505 mm (see table 1) is undergoing first measurements. Referring to the previous structure this cavity utilizes some novel features (see fig. 1):

- inclined end stems
- additional flanges at the end caps for cleaning procedures
- two bellow tuners inside the cavity
- two ports for large power couplers through the girders

* Work supported by GSI, BMBF Contr. No. 06FY7102, 06FY9089I

[†] busch@iap.uni-frankfurt.de

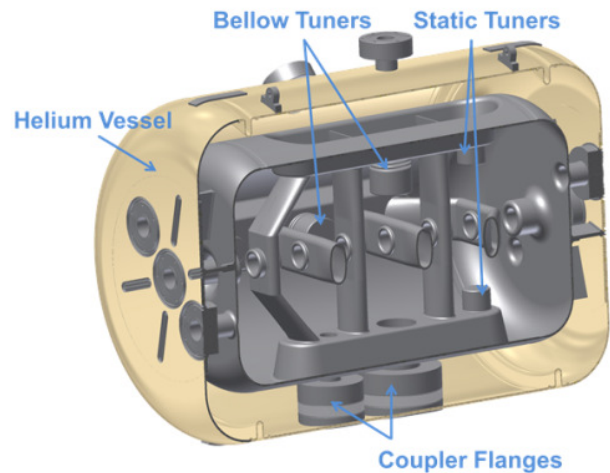


Figure 1: Layout of the superconducting 7-cell CH-Cavity (325.224 MHz, $\beta = 0.16$) [4].

Table 1: Specifications of the 325 MHz CH-Cavity.

β	0.16
frequency [MHz]	325.224
no. of cells	7
length ($\beta\lambda$ -def.) [mm]	505
diameter [mm]	352
E_a [MV/m]	5
E_p/E_a	5
B_p/E_a [mT/(MV/m)]	13
G [Ω]	64
R_a/Q_0	1248
$R_a R_s$ [$k\Omega^2$]	80

SCOPE FOR THE DYNAMIC BELLOW TUNERS

Rf, mechanical properties as well as Multipacting studies of the novel bellow tuner system can be reviewed in [5], [6], [7].

STATUS OF THE SUPERCONDUCTING CW DEMONSTRATOR FOR GSI*

F. Dziuba^{†,1}, M. Amberg^{1,3}, K. Aulenbacher^{3,4}, W. Barth^{2,3}, M. Busch¹,
H. Podlech¹, U. Ratzinger¹, S. Mickat^{2,3}

¹IAP University of Frankfurt, 60438 Frankfurt am Main, Germany

²GSI Helmholtzzentrum, 64291 Darmstadt, Germany

³Helmholtz Institut Mainz (HIM), 55099 Mainz, Germany

⁴KPH Mainz University, 55128 Mainz, Germany

Abstract

Since the existing UNILAC at GSI will be used as an injector for the FAIR facility a new superconducting (sc) continuous wave (cw) LINAC is highly requested by a broad community of future users to fulfill the requirements of nuclear chemistry, especially in the research field of Super Heavy Elements (SHE). This LINAC is under design in collaboration with the Institute for Applied Physics (IAP) of Frankfurt University, GSI and the Helmholtz Institut Mainz (HIM). It will consist of 9 sc Crossbar-H-mode (CH) [1] cavities operated at 217 MHz which provide an energy up to 7.3 AMeV. Currently, a prototype of the cw LINAC is under development. This demonstrator comprises the first sc CH cavity of the LINAC embedded between two sc solenoids mounted in a horizontal cryomodule. One important milestone of the project will be a full performance test of the demonstrator by injecting and accelerating a beam from the GSI High Charge State Injector (HLI) in 2014. The status of the demonstrator is presented.

The demonstrator will be the first section of the new sc cw LINAC at GSI. It will be operated at 217 MHz which is the second harmonic of the existing 1.4 AMeV GSI HLI. A test of the sc 217 MHz CH cavity, which is the key component of the project, under real operational conditions is the main aim of the demonstrator [2, 3]. It is planned to run a full performance test by injecting and accelerating a beam from the HLI in 2014. Figure 1 shows the cw demonstrator setup and the HLI.

STATUS OF THE SC 217 MHz CH CAVITY

The sc 217 MHz CH cavity for the cw LINAC demonstrator (see fig. 2) will consist of 15 accelerating cells at a total length of 690 mm while the maximum gradient is 5.1 MV/m. Furthermore, the cavity is designed with the special EQUUS (EQUidistant mUlti-gap Structure) beam dynamics [4].

THE SUPERCONDUCTING CW LINAC DEMONSTRATOR

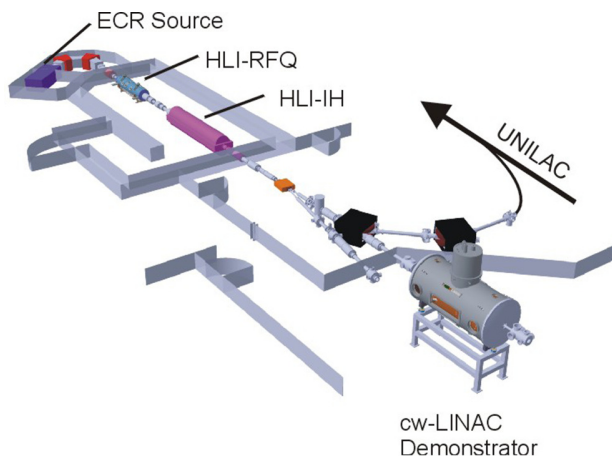


Figure 1: Demonstrator setup with the High Charge Injector at GSI.

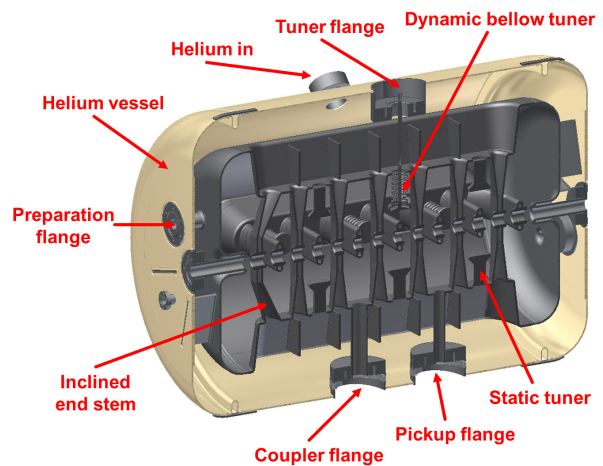


Figure 2: Side view of the sc 217 MHz CH cavity for the cw demonstrator at GSI.

The rf design of the cavity is finished. All main parameters of the cavity are shown in table 1. In June 2012 the production of the cavity has started at Research Instruments (RI) GmbH, Bergisch Gladbach, Germany. It is scheduled to be delivered to the IAP in 2013.

The cavity will be equipped with all necessary auxiliaries like a 10 kW cw power coupler, a titanium helium

* Work supported by HIM, GSI, BMBF Contr. No. 06FY7102
† dziuba@iap.uni-frankfurt.de

DEVELOPMENT OF PERMANENT MAGNET FOCUSING SYSTEM FOR KLYSTRONS

Y. Fuwa, Y. Iwashita, H. Tongu, Institute for Chemical Research, Kyoto University, Kyoto, Japan
S. Fukuda, S. Michizono, High Energy Accelerator Research Organization, Ibaraki, Japan

Abstract

A permanent magnet focusing system for klystrons is under development to improve reliability of RF supply system and reduce power consumption. To save production cost, anisotropic ferrite magnets are used in this system. A test model has been fabricated and the power test of a 750 kW klystron with this focusing magnet is carried out. 60 % of the nominal output power has been achieved at a preliminary power test so far.

INTRODUCTION

Distributed Klystron Scheme (DKS) is proposed as one of the RF supply scheme for International Linear Collider (ILC) to reduce the cost and the down time by raising the reliability [1]. Because thousands of relatively small modulating anode (MA) klystrons were required in DRFS scheme, the failure rate of each component must be reduced. Especially thousands units of electromagnet for klystron beam focusing would cause maintenance problems. Replacing the electromagnets by permanent magnets can eliminate their power supplies and cooling system. Hence the failure rate of the RF supply system can be reduced and cut down the operation cost. A klystron beam focusing system with ferrite magnets is under development is described.

FABRICATION OF FOCUSING MAGNET

Magnetic Materials

There have been precedents for electron beam focusing in klystrons with permanent magnets such as ALNICO, the rare earth (RE) [2,3,4]. Figure 1 shows the B-H curves for these magnet materials and anisotropic ferrite magnets. ALNICO magnets, which have high remanence, shows less coercivity and easily demagnetize. Although RE magnets such as NdFeB has high remanence and coercivity, they are rather expensive and have the resource problem. The anisotropic ferrite magnets have less remanence but higher coercivity than ALNICO. The required magnetic field for beam focusing in klystrons is less than 1 kGauss, therefore the remanence of the anisotropic ferrite magnets is enough high. And the material costs are not expensive, because anisotropic ferrite magnets are composed of iron oxide.

Magnet Field Distributions

Periodic Permanent Magnet (PPM) focusing scheme has relatively well-known magnetic field distribution. In a focusing system with permanent magnet, the alternating magnetic field can be easily generated because an integrated value of magnetic field vector along closed

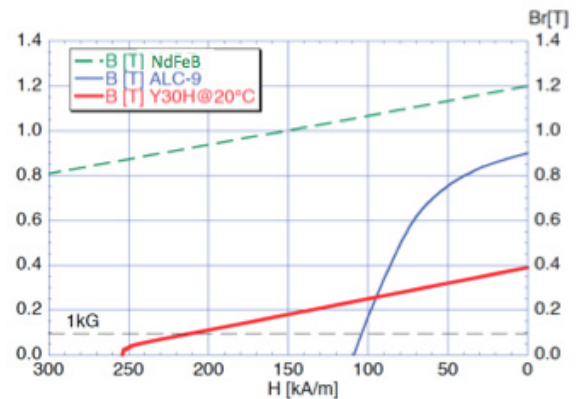


Figure 1: B-H curves of rare earth, ALNICO and ferrite magnets.

curve or infinitely-long axis is zero by the Ampere's law. However, periodicity cause stop bands. For pulse operations, the operating point always crosses such region during pulse rising time and the beam loss causes wall heating and prevents stable operation.

For safe operation, unidirectional magnetic field distribution is applied. Because the required magnet field is not high, anisotropic ferrite magnets can be used. RADIA 4.29[5,6] is used for the magnetic field design. Applied design is shown in Figure 2. Magnets shown in Figure 2 are categorized into two groups. The one group consists of magnets surrounding the klystron body

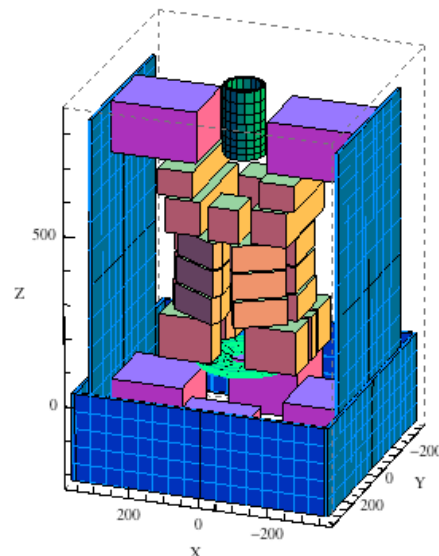


Figure 2: Layout of magnet and iron yoke.

DEVELOPMENT OF SUPERCONDUCTING RADIO-FREQUENCY DEFLECTING MODE CAVITIES AND ASSOCIATED WAVEGUIDE DAMPERS FOR THE APS UPGRADE SHORT PULSE X-RAY PROJECT*

J. Holzbauer[†], A. Nassiri, G. Waldschmidt, G. Wu
 Argonne National Laboratory, Argonne, IL 60439, U.S.A.

Abstract

The Advanced Photon Source Upgrade (APS-U) is a Department of Energy (DoE) funded project to increase the available x-ray beam brightness and add capability to enhance time-resolved experiments on few-ps-scale at APS. A centerpiece of the upgrade is the generation of short pulse x-rays (SPXs) for pump-probe time-resolved capability using SRF deflecting cavities [1]. The SPX project is designed to produce 1-2ps x-ray pulses for some users compared to the standard 100ps pulses currently produced. SPX calls for using superconducting rf (SRF) deflecting cavities to give the electrons a correlation between longitudinal position in the bunch and vertical momentum [2]. The light produced by this bunch can be passed through a slit to produce a pulse of light much shorter than the bunch length at reduced flux. The ongoing work of designing these cavities and associated technologies will be presented. This includes the design and prototyping of higher- (HOM) and lower-order mode (LOM) couplers and dampers as well as the fundamental power coupler (FPC). This work will be given in the context of SPX0, a demonstration cryomodule with two deflecting cavities to be installed in APS in early 2014.

INTRODUCTION

The SPX project calls for the use of an RF deflecting-mode cavity to chirp electron bunches, giving the electrons a correlation between their longitudinal position in the bunch and their vertical momentum. Synchrotron light produced from this bunch can then be passed through a physical slit to create a shorter light pulse at the proportional sacrifice of total flux. This scheme was first proposed by Zholents [1]; the scheme can be seen in Figure 1.

A significant amount of design work has gone into the RF cavities required for this project, details of which can be found in [2, 3, 4, 5, 6, 7]. This cavity application has many specific challenges including the need to heavily damp all non-operational modes to preserve beam quality for other APS users.

CAVITY DESIGN

The current design is a squashed elliptical dipole-mode cavity with a Y-shaped end group and an on-cell damping

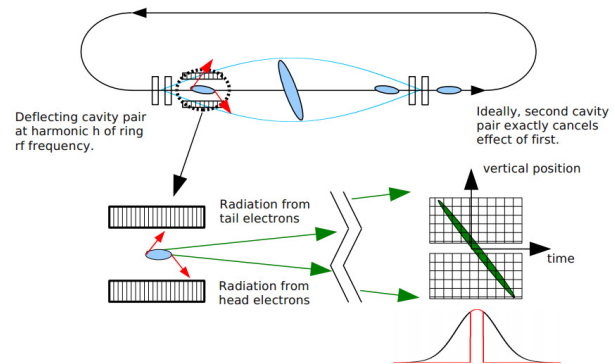


Figure 1: Schematic of Zholtent's short pulse x-ray generation scheme. Image credit to [3].

port which can all be seen in Figure 2. Two of the waveguides from the Y end group will be used for damping of higher-order modes (HOMs) while the third will be primarily used as the forward power coupler. The on-cell damper is used primarily to damp the fundamental mode, called the lower-order mode (LOM). A list of the cavity parameters can be seen in Table 1.

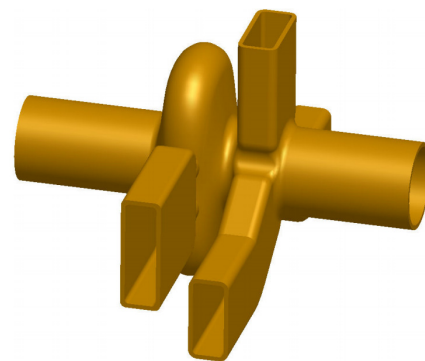


Figure 2: Schematic of a deflecting mode cavity for SPX. The LOM waveguide can be seen on-cell with the Y-end group (HOM dampers and FPC) to the right. Image credit to [3].

At this point, it is expected to use a BCP etching during cavity processing. Given the cavity parameters and this processing technique, 120 mT is the maximum expected reliable peak magnetic field. Given this and the requirement that each deflecting section have a total of 2 MV of

* Work supported by the U.S. Department of Energy, Office of Science, under Contract No. DE-AC02-06CH11357

[†] jholzbauer@aps.anl.gov

MULTIPACTING ANALYSIS OF HIGH-VELOCITY SUPERCONDUCTING SPOKE RESONATORS*

C. S. Hopper[†] and J. R. Delaysen

Center for Accelerator Science, Department of Physics,
Old Dominion University, Norfolk, VA, 23529, USA and
Thomas Jefferson National Accelerator Facility, Newport News, VA 23606, USA

Abstract

Some of the advantages of superconducting spoke cavities are currently being investigated for the high-velocity regime. When determining a final, optimized geometry, one must consider the possible limiting effects multipacting could have on the cavity. We report on the results of analytical calculations and numerical simulations of multipacting electrons in superconducting spoke cavities and methods for reducing their impact.

INTRODUCTION

Superconducting multi-spoke cavities for frequencies of 325, 352, 500, and 700 MHz and velocities of $\beta_0 = 0.82$ and 1 have been designed and optimized [1, 2, 3] for a variety of possible applications. These applications include, but are not limited to, compact machines such as future light sources and high-energy proton or ion linacs. Here we focus on what regions of these resonators are most susceptible to multipacting events.

When the internal surface of a rf cavity is exposed to the high fields maintained in a superconducting cavity, electrons (known as primary electrons) can be emitted from the metal. The kinetic energy and trajectory of these electrons is determined by the electromagnetic fields, and in many cases, they will come in contact with another part of the surface with a certain amount of impact energy. If this energy falls within the secondary emission yield (SEY) range, then additional electrons, known as secondary electrons, will be ejected [4]. Figure 1 shows a generic SEY curve. The parameters E_{oc}^I and E_{oc}^{II} are known as the crossover energies for which $\delta = 1$. E_{om} marks the electron energy for which δ is maximum. These parameters can vary greatly between materials. Even for a given material, these parameters can vary widely based on both the bulk properties and surface condition.

For well prepared niobium cavities, the crossover energies are around 150 eV and 1050 eV, while E_{om} is around 375 eV [5]. We have presented preliminary results for crossover energies of 150 eV and 2000 eV previously [2]. When secondary electrons are in resonant trajectories, and each impact energy is in the range for which $\delta > 1$, then a cascade can occur generating excessive heat, thus leading to thermal breakdown. These regions are commonly called barriers, and they are classified as either "soft" or "hard." Soft barriers are those that can be conditioned

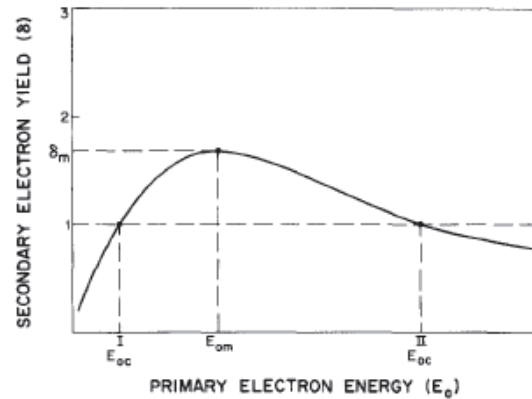


Figure 1: Definition of secondary-electron yield-curve parameters [6]

through and thereby passed. It is believed conditioning occurs because multipacting electrons actually clean the surface to a point where the secondary emission yield is below unity [7]. Hard barriers are those which persist resulting in a limited achievable gradient and quenching.

By improving the quality of the surface, the soft barriers on the gradient can be eliminated. On the other hand, hard barriers can only be overcome by changing the cavity geometry in such a way as to avoid resonant trajectories all together.

Multipacting is also characterized, most commonly, as either one-point or two-point. One-point multipacting occurs when the time of flight of the electron between two impacts is an integer number of rf cycles and that the electron's impact site is approximately the same as its ejection site. This condition can be described in terms of the cyclotron and rf frequencies as [8],

$$\frac{f}{n} = \frac{eB}{2\pi m} \quad (1)$$

In the case of two-point multipacting, the time of flight is an odd number of half rf cycles and the impact site is not the same as the ejection site. The former condition can be described with the same parameters as (1) [9],

$$\frac{2f}{2n-1} = \frac{eB}{2\pi m} \quad (2)$$

* Work supported by U.S. DOE Award No. DE-SC0004094

[†] chop002@odu.edu, chrsthop@jlab.org

MECHANICAL STUDY OF FIRST SUPERCONDUCTING HALF-WAVE RESONATOR FOR INJECTOR II OF CADS PROJECT*

Shoubo He#, Yuan He, Weiming Yue, Shenghu Zhang, Ruoxu Wang, Cong Zhang, Mengxin Xu, Fengfeng Wang, Shichun Huang, Yuzhang Yang, Shengxue Zhang, Hongwei Zhao
 Institute of Modern Physics, Chinese Academy of Sciences, Lanzhou, Gansu 730000, China

Abstract

Within the framework of the China Accelerator Driven Sub-critical System (CADS) project, institute of modern physics (IMP) has proposed a 162.5MHz half-wave resonator (HWR) Superconducting cavity for low energy section ($\beta=0.09$) of high power proton linear accelerators. For the geometrical design of superconducting cavities structure mechanical simulations are essential to predict mechanical eigenmodes and the deformation of the cavity walls due to bath pressure effects and the cavity cool-down. Additionally, tuning analysis has been investigated to control the frequency against microphonics and Lorentz force detuning. Therefore, several RF, static structure, thermal and modal analyses with three-dimensional code Traditional ANSYS have been performed [1]. In this paper, we will present some results about mechanical analysis of the first superconducting HWR cavity in order to further optimization in the near future.

INTRODUCTION

The cavity geometry has been optimized to reach the design frequency 162.5MHz and $\beta=0.09$ and also we want to minimize value of peak electrical and magnetic field on the cavity surface relative to the accelerating electrical field on the cavity axes (B_{pk}/E_{acc} and E_{pk}/E_{acc}) [2]. So the fabrication technology and resonator structural properties including cooling down, vacuum, etching and so on, also should be taken into account at the beginning of design. SC HWR cavities are highly sensitive to mechanical deformations due to the small loaded bandwidth of some SCRF applications. So accordingly for HWR the stability of the cavity structure against any external distortions is the primer design goal. In order to improve df/dP for a low Beta HWR cavity, the typical approach is to add some stiffening ribs on the cavity, but it will not be discussed in this paper. Here, we will investigate this type of structure and then we will improve it in the future. Primarily structural analysis was completed to determine the locations of the model that were beyond yield strength.

Since CADS accelerator will work in CW regime, the main goal of our cavity structural design is a minimization of the resonant frequency dependence on

the external pressure fluctuations. The general basics of the cavity structural design are to avoid using the plane surfaces as illustrated in Figure 1. Besides, four access ports at each cavity (two at the bottom, two at the top) guarantee draining off of the chemical etching and easy access to the inner surfaces during the high pressure water rinsing (HPR).

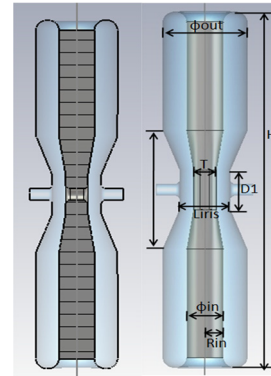


Figure 1: The cross section of HWR cavity with the main geometric parameters: Liris-iris to iris length, T-inner conductor thickness, D1-cavity diameter.

Table 1: Some Properties of HWR Cavity

Para.	Frequency	β	Diameter	Uacc	Epeak	Bpeak
Value	162.5	0.093	40	0.78	25	50
Unit	MHz	---	mm	MV	MV/m	mT

STRUCTURAL ANALYSIS

Injector II of CADS is composed by an ECR ion source, LEPT, RFQ and superconducting accelerating section. And in superconducting accelerating section, there are two cryomodules and each cryomodule is composed of 8 superconducting Half-Wave-resonator cavities and 9 superconducting solenoids. The proton beam will be accelerated from 2.1 MeV to 10MeV. Before structure analysis the geometry of HWR cavity was taken from a sat. model that was generated in software CST Microwave Studio and represented one cavity structure. The ANSYS RF results were compared to CST and to HFSS models of the same cavity for final verification. And the difference among these code result is only about 0.065%.

During mechanical analysis of HWR cavity, the variation of RF Eigen frequency was calculated, including pressure sensitivity, Lorentz force detuning, tuning sensitivity and resonant vibration and etc.. The

*This work is Supported by the National Natural Science Foundation of China (Grant Agreement 91026001)
 #heshoubo@gmail.com

THE SUPERCONDUCTING CH CAVITY DEVELOPING IN IMP*

M.X.XU[#], Y.He, S.H.Zhang, Z.J.Wang, R.X.Wang, SH.B.He, W.M.Yue, C.Zhang, SH.CH.Huang, Y.ZH.Yang, SH.X.Zhang, T.C.Jiang, Y.L.Huang, H.W.Zhao, J.W.Xia, IMP, Lanzhou, Gansu 730000,China

Abstract

The Cross-Bar H-type (CH) cavity is a multi-gap drift tube structure operated in the H21 mode [1]. The Institute of Modern Physics (IMP) has been doing research and development on this type of superconducting CH cavity which can work at the C-ADS (accelerator driver sub-critical system of China). A new geometry CH cavity has been proposed which have smaller radius. It's suitable in fabrication, and it's can reduce cost too .Detailed numerical simulations with CST MicroWave Studio have been performed. An overall surface reduction of 30% against the old structure seems feasible. A copper model CH cavity is being fabrication for validating the simulations and the procedure of fabricating niobium cavity.

INTRODUCTION

C-ADS project with ambitious requirement regarding beam power and quality need new superconducting linac development. Superconducting Crossbar-H-Mode (CH)-cavities have two important features meet with the requirements of C-ADS. Superconducting CH cavity have high real estate gradients compared to conventional low-beta ion linacs, this feature will reduce the amount of cavity prominent. For the cross bar structure, CH cavities are more rigidly. This feature satisfy the harsh requirements of C-ADS about reliable. As this reasons, superconducting CH cavities have been choose as a backup cavity type for the C-ADS(see Fig.1). With respect to C-ADS actual application, one prototype of superconducting CH cavity (f=162.5MHz, beta=0.067, 6 cells) is presently being development in IMP.

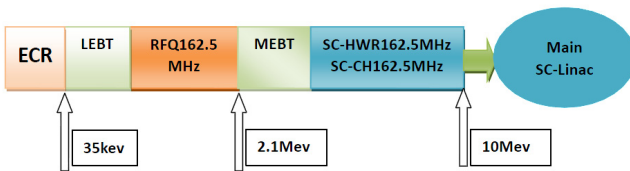


Figure 1: Layout of Injector-II for C-ADS.

*Work supported by 91026001 Nature Science Foundation of China
[#]xumx@impcas.ac.cn

NEW SHAPE SUPERCONDUCTING CH CAVITY

The superconducting CH cavity has electric and magnetic field structure similar with combine the 4-vane RFQ and DTL's. We can use a semi-analytical approach to estimate basic parameters like frequency. The parameter Rt and r1 are represent the radius of CH cavity and the tube radius of CH cavity respectively. Using this equivalent, we can get the resonance frequency with the radius Rt as following [1]:

$$\omega \approx c \left(\frac{0.73}{Rt^2 \left(\frac{25}{144} + \frac{25}{72} \ln\left(\frac{Rt}{r1}\right) - 0.2 \right)} \right)^{1/2} \quad (1)$$

In case of the superconducting CH cavity of IMP, the frequency is 162.5MHz, r1 was 0.03m. Using the formula (1) can give radius Rt of the CH cavity is 0.29 meter. We have using the software CST to simulation. The radius of CH cavity is 0.32 meter [2].

The superconducting CH cavity is a complex cavity. With the radius of 0.32 meter, there are big surface. This means a large amount of high pure niobium needs and a more chance to come across defects. As in superconducting cavity, perfect surface is important for the cavity quality [3]. This size of CH cavity is not easy to protect from defects and contaminates or not suitable in the vacuum chamber of electric beam welding machine.

We try to cut a part of the girder called undercut [4] (see Fig.2).This undercut will increase inductance in the end of cavity, as this will increase the length of current flow. Increased inductance will lower the resonance frequency that we can get a smaller cavity structure in the same frequency (see Fig.3).

When we change the size of undercut in the girder of CH cavity, the radius will reduce with the width of girder liner. At most, we can reduce the radius of cavity by 20% (see Fig.4). As the radius reducing, the surfaces of the cavity reduce by 30% (see Fig.5).

IMPACT OF TRAPPED FLUX AND SYSTEMATIC FLUX EXPULSION IN SUPERCONDUCTING NIOBIUM

J. Vogt, O. Kugeler, J. Knobloch, Helmholtz-Zentrum für Materialien und Energie (HZB)

Abstract

The intrinsic quality factor Q_0 of superconducting cavities is known to depend on various factors like niobium material properties, treatment history and magnetic shielding. To study trapped flux in Niobium we constructed a test stand at Horizontal Bi-Cavity Test Facility (HoBiCaT) at HZB using niobium rods equipped with thermal, electrical and magnetic diagnostics. The focus in this study was on the behaviour of the trapped flux when the sample is slowly warmed up towards the critical temperature T_c . Besides the (incomplete) Meissner effect we observed additional flux expulsion starting at $\approx 0.1K$ below T_c . The reduced level of trapped flux is maintained when the sample is cooled down again and can even be improved by repeating the procedure. Possible explanations for the effect are discussed.

INTRODUCTION

We already reported on the impact of temperature gradients during the cool-down on the obtained Q_0 [1]. In the quest for minimization of RF losses in SRF cavities the impact of trapped vortices is one main topic. The vortices have a normal conducting core with a surface resistance about 6 orders above that of superconducting Niobium. This surface fraction is proportional to the trapped magnetic flux. The surface resistance was determined to be $2.2n\Omega$ per μT for a 1.5GHz cavity [2]. A crucial step in avoiding trapped flux is an improved understanding of flux trapping behaviour of Niobium.

The energetically most favourable state of bulk Niobium at 1.8K (4.2K) is the Meissner phase, in which all magnetic field present in the normal conducting state is expelled. However, expulsion of flux can be incomplete, yielding a remaining magnetization of the material even after removing the external field source. The dynamics of this trapped flux is still not well understood. One approach was the investigation of flux that is permitted to penetrate a marginal type II superconductor in the mixed state. Here, the flux tubes form a lattice and several studies [3, 4] indicate a phase transition from localized (solid, fixed regular lattice) flux tubes towards moveable (liquid) flux tubes when the superconductor exceeds certain temperature / magnetic field combinations as indicated by the black dotted "melting line" in Figure 1.

The behavior of flux that is trapped in the Meissner state is uncertain. A continuation of the melting line in this phase is conceivable, so that flux lines in the check region (Figure 1) may be able to exit the Niobium below T_c . In our study, we examine the properties of the trapped

magnetic flux in the Meissner phase when the rod is slowly warmed up.

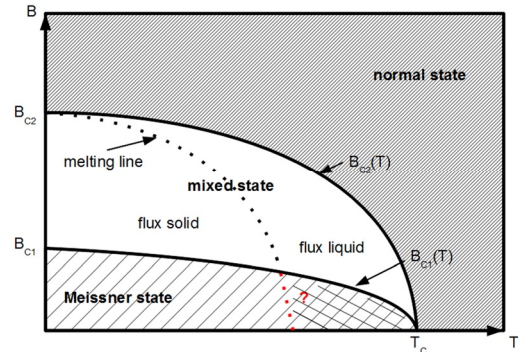


Figure 1: Magnetic phase diagram of marginal Type II superconductor [5]. The added red dotted line indicates a possible extension of the liquid/solid flux interface into the Meissner state. The size of the check region is exaggerated.

EXPERIMENTAL SETUP

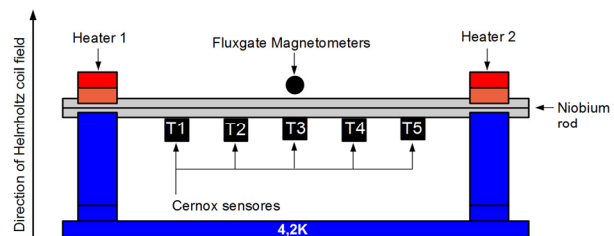


Figure 2: Experimental setup

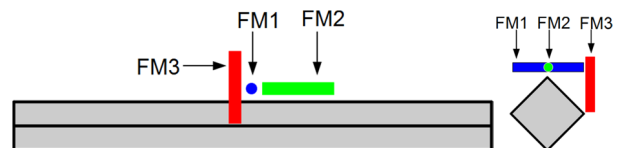


Figure 3: Positions of fluxgate magnetometers (FM): Longitudinal view (left) and cross section (right) of FM1 (black), FM2 (green) and FM3 (red)

For the experiments, a RRR=300 niobium rod (8.4x8.4x300mm) was positioned inside HoBiCaT [6]. It was conduction cooled through the posts to 4.2K. In order to reduce heat transfer into the Helium, heat conductivity was reduced by introducing a kapton foil between rod and support stands. Both ends of the rod were equipped with a resistive heater. They could be individually regulated to control the temperature of the rod with 10mK accuracy. Five Cernox temperature sensors with mK resolution and three fluxgate magnetometers with 1nT resolution (Bartington Mag-01H), one for each spatial direction,

THE NONRESONANT PERTURBATION THEORY BASED FIELD MEASUREMENT AND TUNING OF A LINAC ACCELERATING STRUCTURE *

W. C. Fang[#], Q. Gu, Z. T. Zhao, SINAP, Shanghai, China
D. C. Tong, THU, Beijing, China

Abstract

Assisted by the bead pull technique, nonresonant perturbation theory is applied for measuring and tuning the field of the linac accelerating structure. The method is capable of making non-touching amplitude and phase measurements, real time mismatch feedback and field tuning. Some key considerations of the measurement system and of a C-band traveling-wave structure are discussed, and the bead pull measurement and the tuning of the C-band traveling-wave linac accelerating structure are presented at last.

INTRUCTION

The Shanghai soft X-ray Free Electron Laser test facility(SXFEL)is presently being planned and designed at the Shanghai Institute of Applied Physics, CAS [1]. This facility will be located close to the Shanghai Synchrotron Radiation Facility, which is the first 3rd generation light source in mainland China [2]and it requires a compact linac with a high gradient accelerating structure and high beam quality. As a key R&D item, a room temperature C-band (5712 MHz) accelerating structure has been developed [3, 4]. For fabricating the C-band structure with high performance, the bead pull measurement system based on nonresonant perturbation theory has been developed.

There are several methods for RF structure measurement or tuning, such as the resonant perturbation method [5] and the phase shift method, however several limitations appear when they are applied to a traveling-wave accelerating structure. The resonant perturbation method picks up the amplitude of the electromagnetic field, therefore it is limited in the measurement of the standing-wave accelerating structure and the phase shift method only shows the phase information in the RF structure. For the accurate and fast tuning of a traveling-wave linac RF structure, nonresonant perturbation theory is the preferable method, which can measure the electromagnetic field distribution with both amplitude and phase, and this method is capable of making non-touch measurement, which can maintain the clean inner surface of the accelerating structure and reduce its RF breakdown rate. Furthermore, this method is also very effective in performing an accurate and fast real-time tuning of the accelerating structure, which is economical for mass fabrication of accelerating structures.

In this paper we present a cold test application of nonresonant perturbation theory on a linac RF structure [6]. This method based on the bead pull technique can pick up the amplitude and phase distribution of a linac

structure, particularly for a traveling-wave structure, and is a preferable and efficient method for accelerating structure cold testing and tuning. In the following we describe firstly the theory of nonresonant perturbation and the tuning procedure and then discuss the key considerations of our measurement system with the bead pull technique. At the end we give several experimental results of our newly developed C-band traveling-wave accelerating structure tuning, which verify the feasibility of this method.

NONRESONANT PERTURBATION THEORY AND TUNING PRINCIPLE

According to nonresonant perturbation theory, the variation of the reflection coefficient in the input port is measured with and without a perturbation bead, which is placed at different points along a line to pick up the amplitude and phase distribution of the electromagnetic field strength, a schematic drawing is shown in Figure 1. Based on the results and post-processing, RF tuning is processed with accurate and fast real-time feedback.

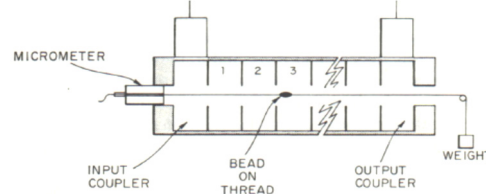


Figure 1: The field measurement based on nonresonant perturbation theory.

Nonresonant Perturbation Theory and Field Measurement

In nonresonant perturbation theory, the desired field strength is calculated as the following [6]:

$$2P_i(\Gamma_p - \Gamma_a) = -j\omega[k_e E_a^2 - k_m H_a^2] \quad (1)$$

For an accelerating structure, the TM mode is used for beam acceleration and the crucial longitudinal electrical field E_z is the unique field component on axis, thus the first equation of equation (1) is used for field measurement, and is renamed as equation(2) with reflected coefficient S_{11} of the Network Analyzer:

$$\Delta S_{11} = \Gamma_p - \Gamma_a = S_{11p} - S_{11a} = -\frac{j\omega k_e E_a^2}{P_i} \quad (2)$$

where S_{11p} and S_{11a} are acquired from the Network Analyzer, respectively corresponding to Γ_p and Γ_a in equation (1) above. In equation (2), E_a is complex data, its amplitude is the square root of the amplitude of ΔS_{11} , and its phase is half of the phase of ΔS_{11} . As the

*Work supported by SINAP project
#fangwencheng@sinap.ac.cn

THE C-BAND RF PULSE COMPRESSION FOR SOFT XFEL AT SINAP

W.C. Wang, Z.T. Zhao, Q. Gu, SINAP, Shanghai, China

Abstract

A compact soft X-ray free electron laser facility is presently being constructed at Shanghai Institute of Applied Physics Chinese Academy of Science (SINAP) in 2012 and will be accomplished in 2014. This facility will be located to the shanghai synchrotron radiation facility (SSRF) which is a third generation light source in china. It requires a compact linac with a high-gradient accelerating structure for a limited overall length less than 230m. The c-band technology which is already used in KEK/Spring-8 linear accelerator is a good compromise for this compact facility and a c-band traveling-wave accelerating structure was already fabricated and tested at SINAP[1], and a c-band pulse compression will be required. There are some reasons, why RF pulse compression devices are quite useful to be applied in RF power supply of the soft XFEL. For it can enhance the peak RF power by expense of RF pulse length, so it will not increase the average power and at the same time reduce the total number of the klystron, it also increases the gradient of the accelerating structure, so we need the c-band pulse compressor. AND a SLED type RF pulse compression scheme is proposed for the C-band RF system of the soft XFEL and this scheme uses TE0.1.15 mode energy storage cavity for high Q-energy storage.

The C-band pulse compression under development at SINAP has a high power gain about 3.1 and it is designed to compress the pulse width from 2.5μs to 0.5μs and multiply the input RF power of 50MW to generate 160MW peak RF power, and the coupling coefficient will be 8.5. It has three components: 3-dB coupler, mode convertors and the resonant cavities. In this paper C-band pulse compression and some components for the c-band pulse compression will be described.

INTRODUCTION

The future c-band accelerator structure of SXFEL is supposed to operate at high acceleration gradient about 40MeV per meter, this requires very high peak RF power about 160MW at frequencies 5712MHz. So as to reduce the total number of the klystron and enhance the peak RF power, the RF pulse compression is needed.

RF pulse compression is one of the methods to compress the RF pulse length and at the same time increase the peak RF power that klystron deliver. RF pulse compression is based on the principle that the RF pulse is stored in a resonance cavity or a delay line and emitted within a short time to create the short RF pulse with high peak power and then deliver it into accelerating section. At present, several RF pulse compressions systems have been already utilized successfully in the s-band or c-band linear accelerator, such RF pulse compression, the SLAC

Energy Double (SLED) was the first, it was successfully applied in SLC operation, and now SLED-I, SLED-II, SLED-III (coupled cavities), BPC, DLDS and VPM (BOC) were already developed.

BPC, SLED-II and DLDS use the delay line as the energy storage cavity, have the flat output, high power gain and high efficiency, but the delay line is long and not economical. SLED-III (coupled cavities) use coupled cavities as the energy storage cavity, reduce the length of the delay line, but the output power irregular. It is applied a complex amplitude modulation on the input RF power, it is hard to control the accuracy and the stable. SLED-I has the simple structure and work stable, but it has the low power gain and less efficiency and a decaying exponential output pulse shape, so the technology AM-PM is applied for the flat output pulse shape.

In the soft XFEL, the design goal of the pulse compression is to compress the pulse width from 2.5μs to 0.5μs and to multiply the input RF power of 50MW to generate 160MW peak RF power. To satisfy this requirement for the soft XFEL, we adopted a SLED type pulse compression as the c-band pulse compressor. This scheme use TE0.1.15 mode for the storage cavity to compress an RF pulse into a short square high peak-power pulse for the course of R&D study of the soft XFEL. Figure 1 shows the schematic diagram. This scheme consists of one 3-dB coupler, two mode convertors, and a pair of high-Q resonant cavities.

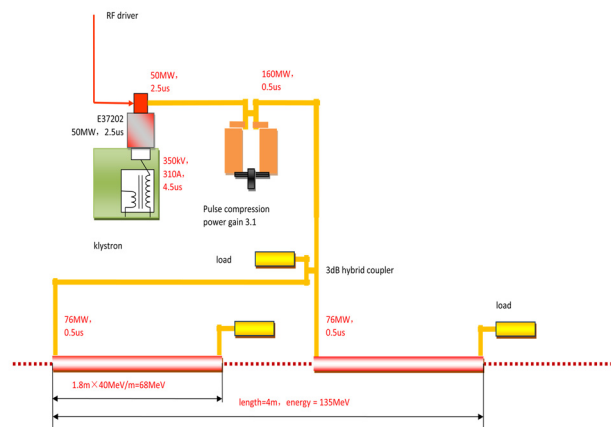


Figure1: C-band 50WM RF Scheme.

C-BAND PULSE COMPRESSOR

C-band Pulse Compressor

For the SLED type RF pulse compression, the expression of the power for the resonant cavity is[2]

$$T_c \frac{dE_e}{dt} + E_e = -\alpha E_K \quad (1)$$

RF PHOTOINJECTOR AND RADIATING STRUCTURE FOR HIGH-POWER THz RADIATION SOURCE

S.M. Polozov, T.V. Bondarenko,

National Research Nuclear University (MEPhI), Moscow, Russia.

Yu.A. Bashmakov, Lebedev Physical Institute of RAS (LPI), Moscow, Russia

Abstract

Sources of high-power electromagnetic radiation in THz band are becoming promising as a new method of a low activation introscopy. Research and development of accelerating RF photoinjector and radiating system for THz radiation source are reported. The photoinjector is based on disk loaded waveguide (DLW). Two different designs of accelerating structure were modelled: widespread 1.6 cell of DLW structure and travelling wave resonator structure (TWR). The resonant models of these structures and the structures with power ports were designed. Electrodynamics characteristics and electric field distribution for all models were acquired. Results of picoseconds photoelectron beam dynamics in simulated structures are reported. Designs of decelerating structures exciting Cherenkov radiation are based on corrugated metal channel or metal channel coated with dielectric. Analysis of radiation intensity and frequency band are presented.

INTRODUCTION

THz radiation is nowadays becoming promising in solving such vital problems as national security, biomedicine and in manufacturing processes control. In national security issue THz radiation can be used in introscopy systems. The definition of the weapons, explosives, drugs and fissionable materials is the main aim of introscopy. The introscopy of cargo transport is much more complicated objective than passenger introscopy issue. The gamma, electron or neutron facilities are used in introscopy system including cargo introscopy at present. The compact electron or ion gun or accelerator is the basic element of such facilities. The main difficulty is the fact that it is necessary to use an electron linear accelerator (LINAC) which can derive the beam with 3-5 times energy variation. LINACs of this type are utterly complex facilities. All of gamma, electron or neutron facilities have a number of disadvantages as needs of environmental shielding and cargo activation.

High-power THz radiation source based on photoinjector and decelerating capillary channel is now one of the most discussable compact facilities providing monochromatic THz radiation of power high enough to be used for cargo introscopy [1].

Facility is based on two main parts: accelerating structure and decelerating radiating channel. Capillary is placed right after the accelerating structures and is made of copper with either dielectric coated inner surface or corrugated surface.

ACCELERATING STRUCTURES

1.6 cell DLW structure

Accelerating structure consists of two accelerators connected sequentially: 1.6 cell DLW and 9 cell TWR structure. First part of facility accelerating system is 1.6 cell standing wave accelerating structure (figure 1). This accelerating structure by itself comes artlessly as a photoinjector part of the accelerating system.

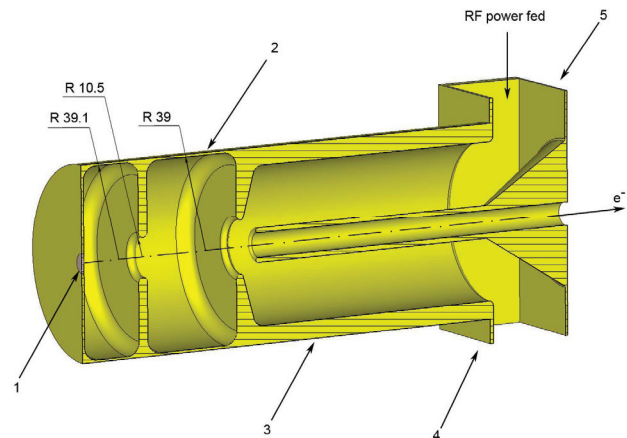


Figure 1. 1.6 accelerating structure: 1 – photocathode, 2 – resonator, 3 – coaxial wave type transformer, 4 – vacuum port, 5 – power input.

This accelerating structure operates on π mode and S-band frequency 2856 MHz ($\lambda=105$ mm). Resonant frequency of the structure was tuned to the desired value by means of cell radius variation. Iris profile was made with rounding to eliminate the possibility of breakdown. First cell length is 0.6 of full-sized cell to obtain maximum field amplitude in the center of the photocathode arranged in the cell's sidewall. Performance of the structures was also increased by rounding of shells edges. The rounding radius value was chosen to provide the highest possible shunt impedance and Q-factor.

Structure RF power input is organized by S-band standard rectangular waveguide with the coaxial coupler. RF power is fed into the structure through only one of the connected waveguides; another is used for structure field symmetry and will be applied for vacuum and other accompanying connections. This scheme provides high level of field symmetry in the system that leads to better quality of the accelerated beam.

This type of wave transformer differs from recently used RF power inputs in photoinjectors like ones in BNL Guns [2]. That type was exploiting the scheme of power

04 Extreme Beams, Sources and Other Technologies

4E Sources: Guns, Photo-Injectors, Charge Breeders

THE DEVELOPMENT OF TIMING CONTROL SYSTEM FOR RFQ

J. Bai, L. Zeng, S. Xiao, T. Xu

Institute of High Energy Physics, CAS, Beijing, 100049, P.R China

Abstract

In order to meet the need of RFQ accelerator, Timing extension hardware based on VME configuration has been developed. In the future, it will be used in the diagnostics system of CSNS. This paper introduces the function of Timing extension hardware, EPICS driver for Timing extension hardware and MEDM operator interface.

BACKGROUND

The core research of intense-proton beam accelerator is mainly concentrated in the field of beam loss control. Based on the intense-beam RFQ accelerator [1] which accelerates proton beam of 46mA pulse current to 35MeV at more than 7% duty factor, a beam line has been built. In order to do beam loss control experiment, many devices have been developed, one of which is Timing extension hardware. Timing extension hardware, as an important device in the running of RFQ accelerator, provides high accuracy and high stability timing trigger signals for the whole system. In the future, it will be used in the CSNS (Chinese Spallation Neutron Source).CSNS adopts EPICS [2] (Experimental Physics and Industrial Control System) as its software environment. So it is necessary to develop EPICS driver [3] for timing extension hardware.

INTRODUCTION OF TIMING EXTENSION HARDWARE

Timing extension hardware uses VME bus of A24 nonprivileged data access address modifier [6]. It is listed below as fig. 1. Since A24 space is of predicable size 16MB, default window encompassing the full space is always provided. The A24 window is for VME bus address from 0x000000 to 0xfffff, which is usually mapped by VxWorks subroutine sysBusToLocalAdrs to local memory from 0xfa000000 to 0xfaffffff [6].

```
#define VME_AM_STD_USR_DATA 0x39 /* A24, nonprivileged data access*/
```

Figure 1: Address Modifiers of A24 nonprivileged data access

Timing extension hardware based on VME configuration is not only consistent with RFQ requirement, it but also avoids the disadvantage of original timing control system, achieving parameters remedy on line. When operators need to remedy parameters of original timing control system, they have to stop the accelerator and calculate the parameters according to the request of experiments, and then use dip switch to change the parameters. The whole process will

last almost two hours and affect the efficiency, stability and continuity. Besides, Timing extension hardware based on VME architecture achieves utility of the same hardware to perform different functions by using reconfiguration of the FPGA, which enhances the flexibility of timing extension hardware.

Timing extension hardware has two types of functions [4]. One is providing primary timing signals for RFQ and secondary timing signals which divide frequency of primary timing signals for beam commissioning and RF system. The other is providing delaying or broadening timing signals according to the needs of various devices. In fact, the principle of these two functions is calculating clock signals. For example, primary timing outputs a timing pulse when it calculates the clock signal to the certain amount. Broadening hardware is triggered by timing signal and starts counting program. It will output a TTL pulse with the width of 3us when counting program reaches to the setting value.

Fig. 2 shows timing signals of RFQ, and the timing extension hardware is shown in Fig. 3.

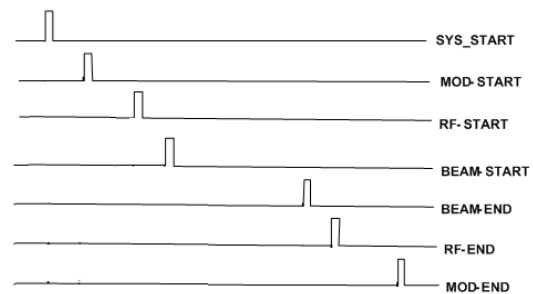


Figure 2: Timing signals of RFQ



Figure 3: The timing extension hardware

MULTIPOLE FIELD EFFECTS FOR THE SUPERCONDUCTING PARALLEL-BAR/RF-DIPOLE DEFLECTING/CRABBING CAVITIES*

S. U. De Silva^{1,2#}, J. R. Delayen^{1,2},

¹Center for Accelerator Science, Old Dominion University, Norfolk, VA 23529, USA.

²Thomas Jefferson National Accelerator Facility, Newport News, VA 23606, USA.

Abstract

The superconducting parallel-bar deflecting/crabbng cavity is currently being considered as one of the design options in rf separation for the Jefferson Lab 12 GeV upgrade and for the crabbng cavity for the proposed LHC luminosity upgrade. The knowledge of multipole field effects is important for accurate beam dynamics study of rf structures. The multipole components can be accurately determined numerically using the electromagnetic surface field data in the rf structure. This paper discusses the detailed analysis of those components for the fundamental deflecting/crabbng mode and higher order modes in the parallel-bar deflecting/crabbng cavity.

INTRODUCTION

The parallel-bar/RF-dipole deflecting/crabbng cavity has been optimized from a rectangular-shaped design with cylindrical-shaped parallel bars into a design with a cylindrical-shaped outer conductor with trapezoidal-shaped parallel bars [1,2], named the rf-dipole cavity. The improved rf-dipole deflecting/crabbng cavity design operating in TE₁₁-like mode has attractive properties with low and balanced surface fields, high shunt impedance and well separated higher order modes (HOMs). The deflecting/crabbng mode is the lowest mode in the rf-dipole design.

Currently the rf-dipole design is being considered as one of the rf separator options for the Jefferson Lab 12 GeV upgrade and as one of the crabbng cavity options for proposed LHC luminosity upgrade operating at 499 MHz and 400 MHz respectively. A 750 MHz design is also being considered as a crabbng cavity for the proposed medium energy electron-ion collider (MEIC) at Jefferson Lab [3]. The first prototypes of the cylindrical-shaped 499 MHz and 400 MHz rf-dipole cavities (Fig. 1 (A) and (B)) are being fabricated and are in preparation for rf testing [4].

The 400 MHz crabbng cavity design was further modified into a square-shaped outer conductor (Fig. 1(C)) with fixed transverse dimensions of <295 mm, to meet the dimensional constraints of the LHC crabbng system. The design was further improved by curving the bar geometry at the beam aperture (Fig. 1(D)) to reduce the transverse field variation across the beam aperture.

*Authored by Jefferson Science Associates, LLC under U.S. DOE Contract No. DE-AC05-06OR23177. The U.S. Government retains a non-exclusive, paid-up, irrevocable, world-wide license to publish or reproduce this manuscript for U.S. Government purposes.

Part of this work was done in collaboration with and supported by Niowave Inc. under the DOE STTR program.

#sdesilva@jlab.org

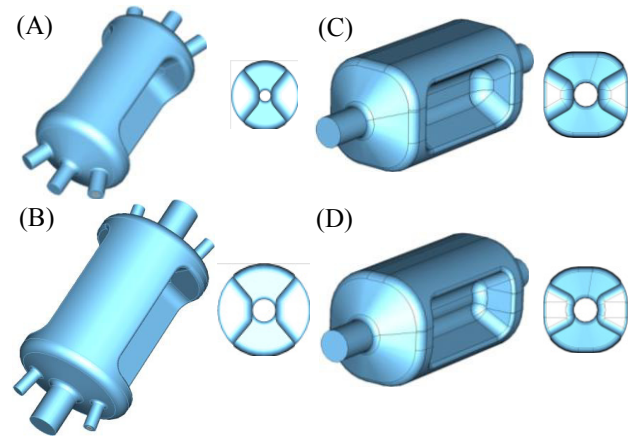


Figure 1: RF-dipole geometries and cross sections of (A) 499 MHz design, (B) cylindrical-shaped 400 MHz design, (C) square-shaped 400 MHz design and (D) square-shaped 400 MHz design with curved inner bar surfaces.

MULTIPOLE FIELD ANALYSIS

In the rf-dipole design, the field varies across the beam aperture off the beam axis generating a non-uniform transverse deflection. The field variation in x and y directions are shown in Fig. 2, for all the rf-dipole designs mentioned in Fig. 1.

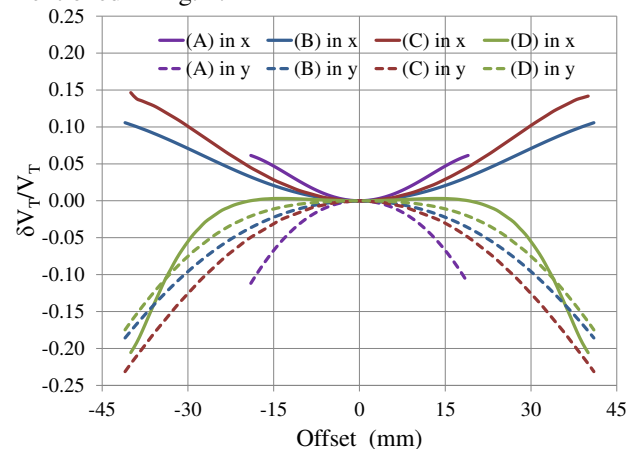


Figure 2: Normalized transverse voltage in x and y directions for designs (A), (B), (C) and (D) in Fig. 1.

The non-uniform transverse fields can generate higher orders of transverse momentum apart from the first order transverse momentum that corresponds to the deflecting or crabbng voltage. These higher order transverse multipole components may lead to perturbations in the beam. This paper presents the higher order multipole components present in the rf-dipole cavity and suppressing of those components by modifying the geometry.

04 Extreme Beams, Sources and Other Technologies

4D Beam Dynamics, Computer Simulation, Beam Transport

COMPACT SUPERCONDUCTING CRABBING AND DEFLECTING CAVITIES*

S. U. De Silva^{1,2#}

¹Center for Accelerator Science, Old Dominion University, Norfolk, VA 23529, USA.

²Thomas Jefferson National Accelerator Facility, Newport News, VA 23606, USA.

Abstract

Recently, new geometries for superconducting crabbing and deflecting cavities have been developed that have significantly improved properties over those of the standard TM_{110} cavities. They are smaller, have low surface fields, high shunt impedance and, more importantly for some of them, no lower-order-mode with a well-separated fundamental mode. This talk will present the status of the development of these cavities.

INTRODUCTION

Primarily the crabbing and deflecting structures are used to restore luminosity in particle colliders or in separating a single beam into multiple beams. The crabbing concept was initially proposed by R.B. Palmer for collider rings [1] and was later proven for linear colliders [2] as well. The applications of crabbing and deflecting cavities are not limited to the above-mentioned applications but also can be used in many applications for beam diagnostics, emittance exchange, in generating compressed x-ray beams etc. Some of the potential applications at present are the deflecting cavity needed for the Jefferson Lab 12 GeV upgrade [3] to separate the maximum energy beam into the three experimental halls and the deflecting cavity system required for the multi experimental project under Project-X [4]. One of the crabbing applications is the LHC luminosity upgrade that requires a crabbing system for vertical and horizontal crossing at the integrations regions of IP_1 and IP_5 [5].

The stringent dimensional constraints set by these current applications especially operating at low frequencies demands the design and development of compact crabbing and deflecting cavities. Compared to the crabbing and deflecting cavities operating in TM_{110} these compact designs that has been developed have improved properties with low surface fields, high shunt impedance. Most of the designs have no lower order modes (LOMs) with a widely separated higher order mode (HOM) spectrum.

The First Superconducting Deflecting Cavity

The early research in superconducting crabbing and deflecting structures was done in 1970s where the first superconducting rf deflecting cavity as shown in Fig. 1

* Authored by Jefferson Science Associates, LLC under U.S. DOE Contract No. DE-AC05-06OR23177. The U.S. Government retains a non-exclusive, paid-up, irrevocable, world-wide license to publish or reproduce this manuscript for U.S. Government purposes.

Part of this work was done in collaboration with and supported by Niowave Inc. under the DOE STTR program.

#sdesilva@jlab.org

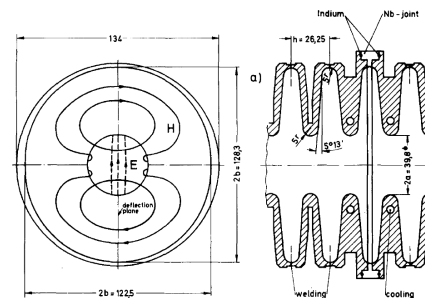
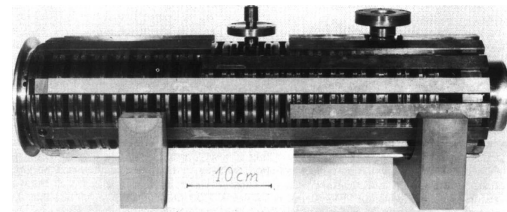


Figure 1: 19-cell end section of the 2.865 GHz rf separator cavity (top) and bi-periodic TM_{110} operating mode (bottom).

was designed and developed in KfK, Karlsruhe in collaboration with CERN [6]. The 2.865 GHz, 104-cell cylindrical-shaped standing wave rf particle separator shown in Fig. 1 installed at CERN in 1977 was capable of delivering a deflection in the vertical plane. The rf separator driven at 1.8 K, in a bi-periodic TM_{110} -type mode (Fig. 1) was in operation until 1981.

The First Superconducting Crabbing Cavity

The first crabbing cavity system was developed and installed in 2007 at KEK [7] for the KEKB electron-positron collider. The crabbing cavity shown in Fig. 2, operating in TM_{110} mode at 508.9 MHz was the only crabbing cavity system that has been in operation in a particle collider until 2010 after the installation in 2007.

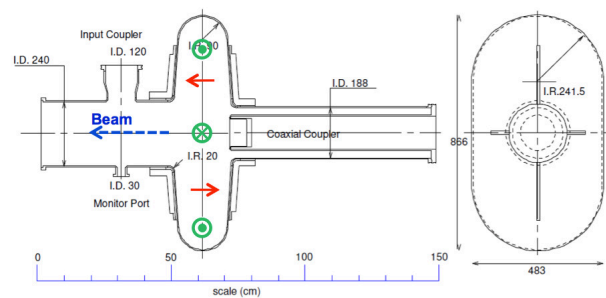


Figure 2: Superconducting 508.9 MHz KEK crabbing cavity.

OPERATIONAL EXPERIENCE AND FUTURE GOALS OF THE SARAF PROTON / DEUTERON LINAC

D. Berkovits[#], L. Weissman, A. Arenshtam, Y. Ben Aliz, Y. Buzaglo, O. Dudovich, Y. Eisen, I. Eliyahu, G. Feinberg, I. Fishman, I. Gavish, I. Gertz, A. Grin, S. Halfon, D. Har-Even, Y. Haruvy, T. Hirsh, D. Hirschmann, Z. Horvitz, B. Kaizer, D. Kijel, A. Kreisel, G. Lempert, Y. Luner, I. Mardor, A. Perry, E. Reinfeld, J. Rodnizki, G. Shimel, A. Shor, I. Silverman, E. Zemach
Soreq NRC Yavne 81800, Israel

Abstract

The Soreq Applied Research Accelerator Facility (SARAF) is built as a user facility. An intense fast neutrons source, a thermal neutrons source and apparatuses for production of isotopes for basic and applied research will be available at the end of construction, foreseen in several years. SARAF is based on a high intensity CW proton / deuteron RF superconducting linear accelerator. Several novel technologies are used in order to build this demanding linac. To reduce technological risks, the construction was divided in two Phases. Phase-I was constructed in order to test and characterize the novel technologies and is in routine operation since 2010. SARAF phase-I, with its single 6 half-wave resonators separated vacuum cryomodule, is the first high current, superconducting low-beta linac in operation and it is presently delivering CW mA proton beams for target developments. Phase-II of this linac will allow acceleration up to 40 MeV and 5 mA CW proton and deuteron beams. Phase-II is now under conceptual redesign. The project status, the operational experience and the future goals of SARAF are described and discussed in this paper.

INTRUDUCTION

System Requirements

The goals of the Soreq Applied Research Accelerator Facility (SARAF) are: 1) to enlarge the experimental nuclear science infrastructure and promote research in Israel, 2) to develop and produce radioisotopes for biomedical applications and 3) to modernize the source of neutrons at Soreq and extend neutron based research and applications [1,2]. SARAF, when it fulfils its goals, is intended to replace the aging research reactor in Soreq. These goals define the requirements from the accelerator. The requirements were optimized to fulfil all of the above goals, within domestic cost constraints. Production of isotopes for radiopharmaceuticals is mainly done by tens of MeV protons, so this is a basic requirement. Variable energy protons allow optimizing the production yield, while minimizing parasitic isotopes production. Deuterons have two main advantages in isotopes production; the production yield in the (d,2n) reaction is significantly higher than the (p,n) reaction for several targets with mass higher than 100 a.m.u [3]. In addition, at tens of MeV, the neutron yield of deuterons is

significantly higher than of protons bombarding the same target [4].

Although linac based neutrons sources are usually based on high energy proton based spallation reactions [5], for tens of MeVs projectiles the neutron yield of deuterons on light element targets is higher by more than a factor of 3 with respect to spallation.

For example, while using a beryllium target, deuterons of 2 mA at 40 MeV, or 5 mA at 25 MeV, are enough to generate a thermal neutron flux that is equivalent to the flux available at the image plane of the neutron radiography apparatus at the Soreq IRR1 5 MW reactor [6].

Tens of MeV deuterons on light element targets generate fast neutrons with a forward flux and neutron energy peaked around the beam energy divided by 2.5 [4]. Such a spectrum is ideal to produce isotopes using (n,2n), (n,p), (n, α) and (n,f) reactions and therefore open new and interesting opportunities for basic and applied research. These reactions are the basis for niche intense radioactive beams at SARAF Phase-II [7,8]. For these reactions, the total amount of fast neutrons is two orders of magnitudes lower than in the spallation reaction. However, the neutron flux in the relevant range for these reactions (5-25 MeV) is higher by an order of magnitude (Fig. 1). The sources of this advantage are the low energy deuteron range in the target, which is shorter than spallation protons by an order of magnitude and the forward peaked structure of the stripping reaction.

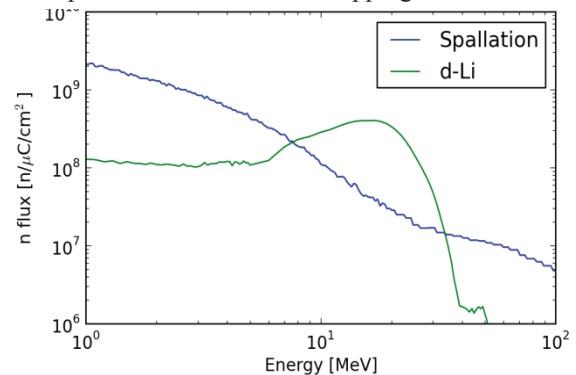


Figure 1: Forward neutron spectra comparison between 40 MeV deuterons on lithium (SARAF/IFMIF [9] like) and spallation 1400 MeV protons on tungsten (ISOLDE [10]). The spectra were measured and simulated 8 cm downstream the targets at zero degrees.

[#] berkova@soreq.gov.il

STATUS OF THE EUROPEAN XFEL – CONSTRUCTING THE 17.5 GeV SUPERCONDUCTING LINEAR ACCELERATOR

W. Decking, DESY, Hamburg, Germany
for the European XFEL Accelerator Construction Consortium*

Abstract

The European XFEL is presently under construction in Hamburg, Germany. It consists of a 1.2 km long superconducting linac serving an about 3 km long electron beam transport system [1]. Three undulator systems of up to 200 m length each produce hard and soft x-rays via the self-amplified spontaneous emission (SASE) process. We will present the status of the civil construction and the accelerator components. The production of the 100 superconducting accelerator modules is distributed between industries and a collaboration of accelerator laboratories. We describe the carefully orchestrated production sequence, quality assurance measures and risk mitigation mechanisms. The last module is scheduled to be installed in the accelerator in spring 2015 and commissioning with beam will start in summer of that year.

OVERVIEW

The European XFEL is being constructed as an European Research Infrastructure under the participation of 12 European countries. The construction of the electron accelerator is entrusted to a consortium of 16 laboratories led by DESY, Hamburg. The laboratories contribute to the accelerator 'in-kind', i.e. by delivering sub-systems and parts under their own responsibility.

The facility will provide hard and soft X-rays for a wide range of scientific applications. In its initial stage it will host three independent photon beam lines serving two experiments each. Final extension will show three experiments for each of the five independent photon beam lines.

The European XFEL employs superconducting accelerator technology, leading to unique features compared to other X-ray FELs being constructed or in operation worldwide. It is capable of accelerating up to 27000 bunches per second, distributed into 10 pulses of 600 μ s length. Bunches can be injected into two separate electron beam lines hosting two resp. up to three undulators in a row. Flexible bunch patterns and plans to provide individual bunch properties will make the European XFEL a true multi-user facility.

Progress in the electron gun development for the European XFEL and the success of LCLS led to a redefinition of the expected accelerator performance. The final energy of 17.5 GeV, together with the long undulators and the anticipated low emittance beams out of

a photo-cathode gun will allow reaching photon wavelength as short as 0.5 nm [2].

The installed linac and its infrastructure bear the possibility to be converted into a CW (or quasi-CW) accelerator in the future with the potential to reach up to 6 GeV final energy (for an update on the R&D towards this option see [3]).

Table 1 gives an overview of the main parameters of the facility.

Table 1: European XFEL Parameters

Quantity	Value
maximum electron energy	17.5 GeV
macro pulse repetition rate	10 Hz
RF pulse length (flat top)	600 μ s
bunch repetition frequency within pulse	4.5 MHz
bunch charge	0.02 – 1 nC
electron bunch length after compression (FWHM)	2 – 180 fs
beam power	500 kW
# of modules containing eight 9-cell superconducting 1.3 GHz cavities	101
accelerating gradient for 17.5 GeV	23.6 MV/m
# of 10 MW multi-beam klystrons	27
average klystron power for 0.03 mA beam current at 17.5 GeV	5.2 MW
photon wavelength	0.05 – 4 nm

A normal-conducting photo-cathode RF gun produces high brightness electron beams. The injector building allows the later installation of a second, completely independent injector. The main linear accelerator is sectioned into three units with 4, 12 and 84 modules each, intercepted by normal conducting bunch compressor and diagnostic sections. A collimation and beam distribution section follows the linac, where the beam can be fed into the two separate undulator beam-lines and/or a commissioning and pulse-picker dump. Each beam-line is terminated by a solid state beam dump capable of accepting up to 300 kW of continuous beam power. The SASE photon beam is delivered through up to 800 m long photon beam lines to the experimental hall. See Fig. 1 for a bird's eye view of the facility.

* BINP Novosibirsk, CEA Saclay, CIEMAT Madrid, CNRS Orsay, DESY Hamburg&Zeuthen, IFJ-PAN Krakow, IHEP Protvino, INFN Milano, INR Troitsk, NCBJ Swierk, NIIIEFA St. Petersburg, PSI Villigen, SU Stockholm, UPM Madrid, UU Uppsala, WUT Wroclaw

SRF LINAC TECHNOLOGY DEVELOPMENT AT FERMILAB*

Vyacheslav Yakovlev[#] and Camille Ginsburg, Fermilab, Batavia, IL 60510, USA

Abstract

Superconducting linear accelerators are being developed for different applications: for fundamental research at the high-energy and high-intensity frontiers, in nuclear physics, for spallation neutron sources, for synchrotron radiation sources, etc. The linac applications dictate the requirements for the superconducting acceleration system, and, thus, for SRF technology. Fermilab is currently involved in two projects: ILC and Project X, both based on SRF technology. For high-intensity frontier investigations, Project X – a multi-experiment facility – is being developed based by a wide collaboration of US National and Indian Laboratories. In the CW H⁻ linac several families of SC cavities are used: half-wave resonators (162.5 MHz); single-spoke cavities, SSR1 and SSR2 (325 MHz); elliptical 5-cell beta=0.61 and beta=0.9 cavities (650 MHz). The pulsed 3-8 GeV linac is based on 9-cell 1.3 GHz cavities. In this paper the basic requirements for the CW superconducting Project X linac are considered as well as its specific technology challenges.

INTRODUCTION

The application of SRF technology to electron and hadron linacs has a long – almost 50 years long – and successful history. Superconducting RF cavities are now widely used and are planned to be used in linear accelerators for different applications, for example: (i) high-energy physics (SPL [1], ILC [2]) and the high-intensity frontier (Project X [3]); (ii) new X-ray free electron lasers (XFEL [4], NGLS [5], Cornell ERL [6]), (iii) spallation neutron sources (SNS [7], ESS [8]), (iv) nuclear physics and rare isotope production (ATLAS [9], ISAC-II [10], CEBAF [11], SARAF [12], SPIRAL –II [13]), (v) ADS accelerators (MYRRHA [14], Indian ADS [15], China ADS [16]). The recent progress in development of superconducting acceleration cavities was achieved substantially in connection with the ILC project, see Fig 1, where a sketch of the ILC is presented. For such a long machine, high acceleration gradient is essential: 35 MeV/m with a duty factor of 0.5%. The 9-cell ILC cavity (see Fig. 2) operates at 1.3 GHz. The ILC collaboration [2], which includes Fermilab, achieved impressive results in the development of cavity processing (which includes electro-polishing and 120°C baking, see Fig. 3) and clean assembly techniques. These developments allowed the achievement of cavity gradients at quite high and gradually increasing production yields, see Fig. 4 [17]. At Fermilab, the work on building ILC-type cavities and cryo-modules is continuing.

*Operated by Fermi Research Alliance, LLC, under Contract DE-AC02-07CH11359 with the U.S. DOE
#yakovlev@fnal.gov

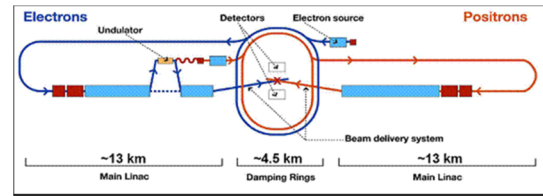


Figure 1: The ILC project sketch (2007 Reference Design).

The new large accelerator facility which is under development at Fermilab, Project X [18], is based on a CW H⁻ superconducting linac, which has requirements very different from what is suitable for ILC, creating new problems and new challenges.



Figure 2: Photo of the ILC 1.3 GHz 9-cell SC cavity [Fermilab Visual Media Services].

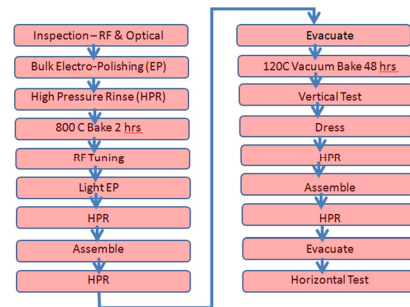


Figure 3: ILC Cavity Processing Basic Recipe.

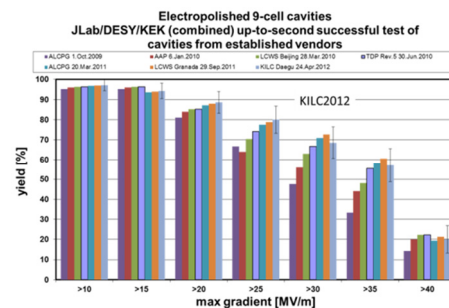


Figure 4: ILC gradient yield. ILC cavities reach 35 MV/m in vertical test more than half the time after one or two processing cycles.

DISCUSSION

Project-X, a multi-MW proton source, is under development at Fermilab. The Project X configuration is shown in Fig. 5. It enables a world-leading program in neutrino physics, and a broad suite of rare decay experiments. The facility is based on 3-GeV 1-mA CW

INCREASED UNDERSTANDING OF BEAM LOSSES FROM THE SNS LINAC PROTON EXPERIMENT *

J. Galambos[#], A. Aleksandrov, M. Plum, A. Shishlo, ORNL, Oak Ridge, TN 37831, USA,
E. Laface, ESS, Lund Sweden, V. Lebedev, FNAL, Batavia, IL 60510, USA

Abstract

Beam loss is a major concern for high power hadron accelerators such as the Spallation Neutron Source (SNS). An unexpected beam loss in the SNS superconducting linac (SCL) was observed during the power ramp up and early operation. Intra-beam-stripping (IBSt) loss, in which interactions between H⁺ particles within the accelerated bunch strip the outermost electron, was recently identified as a possible cause of the beam loss. Results from a set of experiments using proton beam acceleration in the SNS linac support IBSt as the primary beam loss mechanism in the SNS SCL.

SNS BEAM LOSS EXPECTATIONS

The SNS accelerator consists of an RFQ (output energy of 2.5 MeV), a Drift Tube Linac (output energy of 85 MeV), a Coupled Cavity structure (output energy of 186 MeV) and an elliptical cell superconducting cavity structure with design output energy of 1 GeV. The SNS linac accelerates a 1 msec pulse H⁺ beam, which is subsequently captured in a storage ring to produce a sub μ s intense pulsed neutron source.

A major advantage of superconducting RF linacs for H⁺ and proton acceleration is the inherently large beam aperture, which greatly alleviates the issue of beam loss relative to copper accelerating structures. During the design stage of SNS the multi-particle beam simulations indicated no beam loss in the superconducting linac (SCL) region [1,2]. Nonetheless, there was a reluctance to assume no superconducting linac beam loss and a minimal loss in this area was allocated in the beam loss budget [3], attributed to gas stripping in the warm sections between cryomodules.

OBSERVED SCL BEAM LOSS

Loss History

Early in the power ramp-up phase of the SNS operation, unexpected residual activation was measured along the SNS superconducting linac, in the warm sections between the cryomodules. The warm sections are the limiting aperture restrictions in the SCL, so it is not surprising that the observed beam loss is located in these regions. The build-up of measured residual activation over the period of the SNS power ramp-up and initial operation is shown in Fig. 1, where the the average warm section residual activation levels are superimposed on the operational beam power level. Initially, the loss detectors

did not register the beam loss causing this activation, but they were moved closer to the beam pipe in the warm sections, and subsequently did detect the beam loss. Beam loss is rather uniformly distributed along the SCL.

Beam Loss Magnitude

Based on the measured residual activation levels, the beam loss can be expected to be $< \sim 1$ W/warm-section, which corresponds to $< 10^{-4}$ fractional beam loss throughout the SCL at 1 MW. Quantifying beam loss fractions at this level is difficult. One method of producing very small fractional controllable beam spills in the SNS SCL is with a laser profile device [4]. The short pulse laser strips the outermost H⁺ electron from about 10^{-6} of a nominal beam pulse, creating H⁰ that is subsequently lost downstream. By comparing the additional beam loss signal produced by the known amount of beam lost from the laser pulse to the measured beam loss during production, we estimate the fractional beam loss during neutron production in the SNS SCL to be a few $\times 10^{-5}$.

Possible Loss Causes

Initially, causes of the unexpected beam loss were suggested to be poor matching (transverse or longitudinal); beam halo from the ion source, or produced during acceleration; and residual gas stripping. Longitudinal tails were considered a likely loss contributor because of the sensitivity of SCL beam loss to the longitudinal setup of the upstream warm linac. Different longitudinal tunes were applied in the SCL, trading final energy for increased acceptance, but minimal impact was observed on the baseline SCL beam-loss level. The transverse match is a natural suspect, however adjustments of matching quadrupoles at the linac lattice transitions generally affect beam loss at local loss points, as opposed to the observed uniform beam loss through the SCL. Additionally, for the design transverse optics, beam mis-steering does not affect beam loss, indicating the presence of additional aperture available for the transverse tune. Finally, residual gas stripping in the upstream warm linac was addressed by measuring the change in beam loss with deteriorated warm linac vacuum to determine the impact from gas stripping and extrapolating back to ideal vacuum conditions. This indicated that gas stripping was not a major contributor to the SCL beam loss. The measured vacuum level in the warm sections between superconducting RF cryomodules is much lower than the design assumptions, and is too low to contribute to significant gas stripping beam loss.

[#] jdg@ornl.gov

DEVELOPMENT OF H-MODE LINACS FOR THE FAIR PROJECT*

G. Clemente[†], W. Barth, L. Groening, S. Mickat, B. Schlitt, W. Vinzenz, GSI, Darmstadt, Germany
 U.Ratzinger, H.Podlech, R.Brodhage, M.Busch, F.Dziuba,
 Goethe University, Frankfurt am Main, Germany

Abstract

H-mode cavities offer outstanding shunt impedances at low beam energies and enable the acceleration of intense protons and ion beams. Crossed-bar H-cavities extend these properties to energies even beyond 100 MeV. Thus, the designs of the new injector linacs for FAIR, i.e. a 70 MeV, 70 mA proton driver for pbar-production and a cw intermediate mass, superconducting ion linac are based on these novel cavities. Several prototypes (normal and superconducting) have been built and successfully tested. Moreover, designs for a replacement of the 90 MV Alvarez section of the GSI - Unilac will be discussed to improve the capabilities as the future FAIR heavy ion injector.

INTRODUCTION

The scientific program of FAIR requires the construction of a new 70 MeV, 325 MHz proton injector [1] for the SIS18. This machine will provide at least 35 mA of protons at a repetition rate of 4 Hz.

Beside the new proton linac, FAIR also requires a massive upgrade of the GSI UNILAC linear accelerator [2].

The UNILAC started operation in 1975 and it is one of the eldest DTL still active. Almost 40 years of high duty factor operation (up to 25 %) led to the increasing number of failures occurred in the last years. That represents a strong reliability issue for the new FAIR facility.

Additionally, the Alvarez-DTL is equipped with DC quadrupoles, which is a disadvantage for short pulse operation and limits the machine flexibility in case of the multibeam operation (different ion beam with specific magnetic rigidities and beam currents). That constraint, together with the challenging requirements of 15 mA of U^{28+} , favours the replacement of the existing DTL section by a new high energy linac with short beam pulses at low repetition rate (HE-Linac).

The linac upgrade program will be completed by a new superconducting cw heavy-ion linac [3] with an adjustable energy from 3.5 to 7.3 AMeV for the super heavy elements program (SHE-Linac).

The choice of the RF cavity type represents the most critical key for such a massive upgrade. The experience with high current operation at the HSI and HLI led to the natural decision to base the UNILAC replacement on IH-DTL cavities. On the other hand, the successful R&D performed at the Frankfurt University on room temperature [4] and superconducting CH-DTL [5] justifies the use of that kind of structures for the new proton linac and for the cw SHE linac.

* Work supported by HicforFAIR and BMBF

[†] g.clemente@gsi.de

H-MODE CAVITIES

H-Mode cavities are characterized by a slim tube geometry resulting in a high shunt impedance and a uniform power loss distribution (see Fig.1). Beam dynamics is designed according to an asynchronous injection energy lattice like the KONUS [6] or the EQUUS [3]. Alternatively an APF [7] lattice can be used.

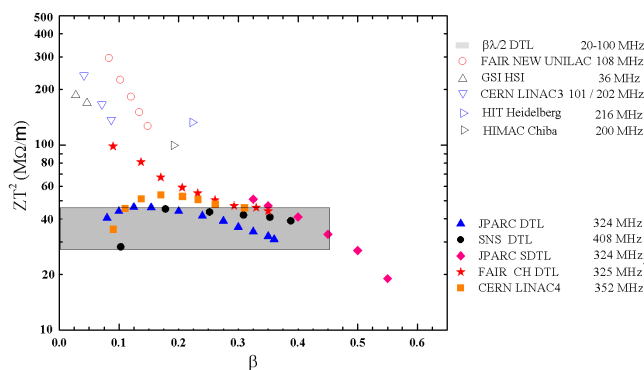


Figure 1: Effective shunt impedance of several ion and proton accelerators as function of the velocity profile.

The IH-DTL, excited in the $TE_{11(0)}$ mode is by far the most efficient RF structure in the β range from 0.01 to 0.2. For $\beta \leq 0.1$ it is competitive with superconducting structures, concerning the plug power demand, even at cw operation. Several IH-DTL are routinely in operation and this structure has established as standard solution for heavy ion in the frequency range between 30 and 200 MHz.

The CH-structure, excited in the $H_{21(0)}$ mode has a larger diameter for a given frequency compared with the IH-structure. Cavities with frequencies from 150 MHz to 3 GHz can be realized, making the CH-structure feasible for proton and ion acceleration up to 100 AMeV. Additionally, the crossbar geometry is so robust to ensure the mechanical stability required for superconducting operation. At present, the s.c CH-DTL is the only multi gap superconducting structure available at low energy.

THE CH-DTL FOR FAIR

The FAIR requirement of a dedicated proton injector pushed an intensive R&D activity in order to explore the capabilities of the room temperature CH-DTL. In 2006 a first test model was successfully built at the University of Frankfurt and later copper plated at the galvanic workshop of GSI. This 340 MHz cavity comprises eight equidistant cells of length $\beta\lambda/2=45$ mm, and was used to test all fabrication steps including welding, copper plating and designing of an efficient cooling system. Moreover, a tuning strat-

COMMISSIONING OF A NEW INJECTOR FOR THE RIKEN RI-BEAM FACTORY

N. Sakamoto^{a*}, M. Fujimaki^a, Y. Higurashi^a, H. Hasebe^a, O. Kamigaito^a,
R. Koyama^b, H. Okuno^a, K. Suda^a, T. Watanabe^a, and K. Yamada^a

a) RIKEN Nishina Center, Wako, Saitama, Japan

b) Sumitomo Accelerator Service Ltd., Shinagawa, Tokyo, Japan

Abstract

A new injector for the RIKEN RI-Beam Factory (RIBF) was fully commissioned in October 2011. The injector accelerates ions of $m/q = 6.8$ up to 670 keV/u. To save cost and space, a direct coupling scheme was adopted for RF coupling between the DTL cavity and amplifier, based on an elaborate design with the Microwave Studio software package. The new injector has been successfully commissioned and worked very stably for beam service time, increasing the uranium beam intensity by an order of magnitude. Moreover, it is now possible to independently operate the RIBF and GARIS facilities for super-heavy element synthesis.

INTRODUCTION

Role of new injector

Since 2008, the accelerator complex at the RIKEN RI-Beam Factory (RIBF) has provided various heavy ion beams according to the programs of the RIBF experiments. The developed beams so far are polarized- and unpolarized-deuteron, ⁴He, ¹⁴N, ¹⁸O, ⁴⁸Ca, ⁷⁰Zn, ¹²⁴Xe and ²³⁸U. Among them the experiments of the new RI production require intense beams. Initial experiment using the uranium beams was carried out in November 2008, at 0.4 pA. This intensity is insufficient for radio isotope production experiments at the RIBF. Our final goal is to realize a 1 pμA beam current for each ion.

The new injector project started because the main injector, the RIKEN Heavy Ion Linear Accelerator (RILAC) [1], was tasked with super-heavy elements (SHE) search [2]. This was a problem because the RIBF experiments could not be performed when SHE search experiments were performed. Also, the beam currents for uranium and xenon beams were unsatisfactory. Therefore we designed and built a new injector, the RIKEN Heavy Ion Linear Ac-

celerator (RILAC2), dedicated for the acceleration of intense uranium and xenon beams to energies of 670 keV/u, which is the injection energy of the RIKEN Ring Cyclotron (RRC) [3].

Xe and U acceleration by cyclotron cascades

In RIBF, Xe and U beams are accelerated by cyclotron cascades of RRC, the fixed frequency ring cyclotron (fRC) [4], the intermediate-stage ring cyclotron (IRC) [5], and the world first separate-sector superconducting ring cyclotron (SRC) [6]. In this scheme shown in Fig. 1, the intense ²³⁸U³⁵⁺ beams from the ion source can be accelerated by the RRC without charge stripping, before injection to the RRC. Using the stripper after the RRC, the charge state is converted to 71+ at an energy of 10.75 MeV/u for injection into the fRC. Then ²³⁸U⁷¹⁺ beams are accelerated using the fRC with velocity gain of about 2 to suit the injection energy of the IRC. Before injection to the IRC, the charge state is converted to 86+.

For uranium, the first stripper (CS1) utilizes a 0.3 mg/cm² carbon foil and the stripping efficiency is about 18%. The second stripper (CS2) utilizes 17~19 mg/cm² carbon foil, and the stripping efficiency is about 33%. Owing to the heat load by the intense beams, these efficiency values go down with increased beam dose.

To maximize the average current, the stripper foils are changed frequently, typically 2 or 3 times/day. To increase the beam current, the stripper foil lifetime must be extended.

Injection to RRC

The beams from the RILAC2 are injected into the RRC. Layout of the key devices of the RRC is shown in Fig. 2. The function of the isochronous cyclotron is to increase the velocity of ions by the ratio of the extraction radius to the injection radius. The velocity gain of the RRC is four and the energy of the extracted beams is 10.75 MeV/u. In the case of ²³⁸U³⁵⁺ acceleration, the magnetic rigidity is 3.2 T·m, which is 91% of the maximum value of the RRC. The operating dee-voltage of the resonator is about 60 kV. The resonators of double-gap type with a dee angle of 23.5° provide 230 kV/turn acceleration voltage with a harmonic number of 9, resulting the total number of revolutions of 325. The gap between turns at the extraction radius is only 5.5 mm, excluding the effect of betatron motion. Therefore beam loss during cyclotron acceleration is prone to occur in the electrostatic deflection channel (EDC). Acceleration

Copyright © 2012 by the respective authors — cc Creative Commons Attribution 3.0 (CC BY 3.0)

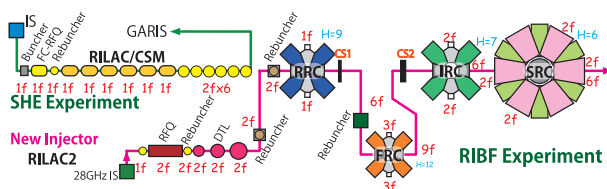


Figure 1: RIBF accelerator complex.

* nsakamot@ribf.riken.jp

FRANZ – ACCELERATOR TEST BENCH AND NEUTRON SOURCE

O. Meusel, L.P. Chau, M. Heilmann, H. Podlech, U. Ratzinger, K. Volk, C. Wiesner
IAP, University Frankfurt/Main, Germany

Abstract

Accelerator based neutron sources are used for different kinds of research programs in nuclear astrophysics, material science and for the development of next generation nuclear power plants. The challenge of existing and planned neutron sources is to provide highly brilliant ion beams with high reliability.

The Frankfurt neutron source FRANZ is not only a neutron source but also a test bench for novel accelerator and diagnostic concepts for intense ion beams. The experiment consists of a compact linear accelerator for the acceleration of an intense proton beam to 2MeV producing neutrons via the ${}^7\text{Li}(p,n)$ reaction. The final beam intensity will be 200mA. Therefore the space charge and space charge compensation effects can be studied with high statistical significance along the accelerator.

The hot filament-driven gas discharge ion source already delivers 240mA beam current with a proton fraction of 92%. The low energy beam transport LEBT section is equipped with four solenoids matching the beam into a chopper system and into a RFQ-IH combination already under construction. Coupling of the RFQ accelerator stage and the IH drift tube cavity offers the possibility to use only one power amplifier as a driver for both of these resonators and reduces investment costs. The compact design of the low- β accelerator stage is optimized for high beam intensities to overcome the expected strong space charge forces in this accelerator test bench.

The presentation will give a brief overview of the FRANZ accelerator and discusses the beam dynamics, comparing numerical and experimental results.

INTRODUCTION

To advance the development of accelerator technology a dedicated test bench was needed. Different work groups are now able to test their devices under realistic conditions with respect to the interplay of each of the accelerator components. The main focus of the planned experiments is to reach the intensity and power limits for conventional RF accelerator technics. The question of these limits is highly relevant for several future accelerator projects and the basis of next generation accelerator concepts.

It is planned to use a proton beam with beam energies of 2MeV with energy variation of about $\pm 0.2\text{MeV}$. These parameters enable various experiments by the use of thermal neutrons produced by the ${}^7\text{Li}(p,n)$ reaction at the end of the accelerator test bench. Therefore an astrophysical research program was launched for the measurement of neutron capture cross sections relevant for nucleosynthesis [1].

Figure 1 shows the scheme of the experimental setup of the FRANZ facility. It consists of a high voltage terminal facilitating ion source operation, a low energy beam transport section including a chopper system, the main accelerator, a bunch compressor and target stations. Two operation modes for the experiments will be available. The compressor mode will deliver a 1ns beam pulse with a repetition rate of 250 kHz and an estimated peak beam current of 9.6A. The activation mode uses a cw beam to produce a continuous neutron flux. Because of the average power density the proton beam in activation mode is limited to a current of about 8 mA for the use of solid targets and up to 30 mA for liquid metal targets.

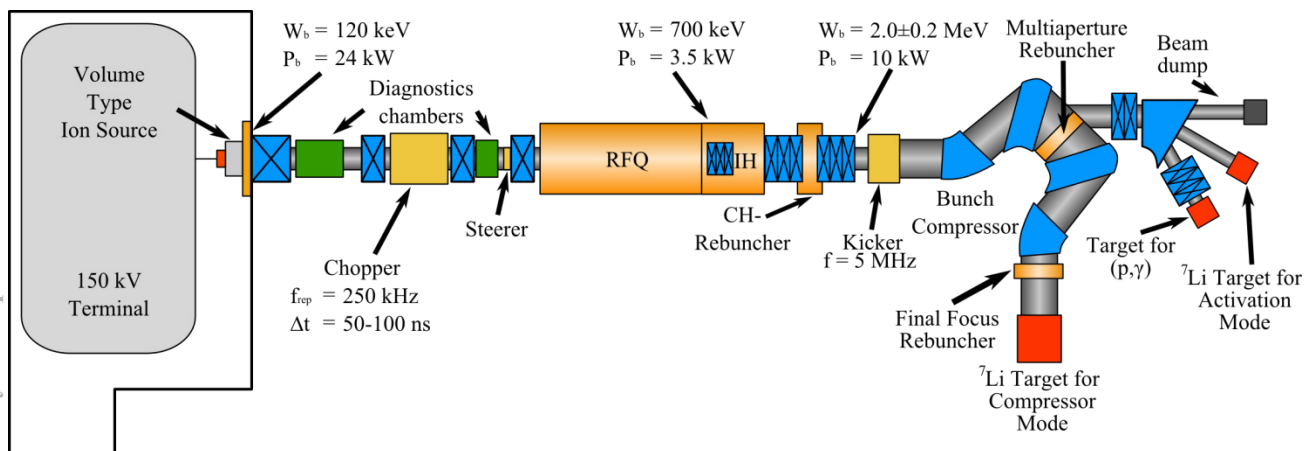


Figure 1: Experimental setup of the FRANZ facility. The accelerator test bench and neutron source consist of a 2MeV proton accelerator equipped with bunch compressor and several target stations.

ACCELERATOR/DECELERATOR OF SLOW NEUTRONS

M. Kitaguchi, KURRI, Osaka, Japan

Y. Arimoto, KEK, Ibaraki, Japan

P. Geltenbort, ILL, Grenoble, France

S. Imajo, Y. Iwashita, Kyoto University, Kyoto, Japan

Y. Seki, RIKEN, Saitama, Japan

H. M. Shimizu, Nagoya University, Aichi, Japan

T. Yoshioka, Kyushu University, Fukuoka, Japan

Abstract

An accelerator/decelerator for slow neutron beams has been demonstrated. The energy of a neutron can be increased or decreased by flipping the neutron spin (directly coupled to magnetic dipole moment) in magnetic field. This device is a combination of a gradient magnetic field and an RF magnetic field. Test experiments were performed by using very slow neutrons at High-Flux Reactor at Institut Laue-Langevin. Acceleration and deceleration for focusing of neutrons at the detector position was observed. Focusing neutrons enables us to transport the neutrons while maintaining density from source to experimental position. This will be a powerful technique for measurement of the permanent electric dipole moment of neutrons, which require a high density of neutrons.

INTRODUCTION

Particle accelerators have continually evolved since their invention, and nowadays are applied not only in physics experiments but also in various fields such as medical science. The properties of the beam should be optimized for each use by accelerating, decelerating, focusing and/or defocusing. Recently the neutron beam becomes important as a probe for new science including particle physics with extremely high precision. Although the ray of neutrons has been handled by some optical devices, for example, mirrors and lenses, it is impossible to control the velocity by the electric field used in an ordinary accelerator because the neutron is an electrically neutral particle. A neutron accelerator which manipulates the velocity has the advantage that experiments can be performed with high precision.

One of the most useful applications of the neutron accelerator is space-time focusing. In the case of pulsed neutrons, during transport of the neutrons to the experimental area, the neutron pulses spatially spread as some neutrons travel faster whereas some travel slower. The density decreases according to the velocity spread of the neutron pulse. When fast neutrons are magnetically decelerated and/or slow neutrons are accelerated properly in the middle of the transport, these neutrons can reach the experimental area at the same time (Fig. 1) [1, 2, 3, 4]. The density can be kept from the source to the arrival position

by focusing. This enables us to utilize instantaneous-intense pulsed neutrons in order to suppress the systematic errors for some experiments which require dense neutrons, for example, search for neutron electric dipole moment (nEDM) to reveal the origin of matter in the universe. Although experimental searches have been pursued in the world [5, 6, 7, 8, 9], the nEDM has not yet been observed. The present upper limit is $|d_n| < 2.9 \times 10^{-26} ecm$ (90% C.L.) [9], which is very close to the predictions of some physics beyond the standard model of particle physics, for example, supersymmetry. Using the space-time focusing and high power pulsed neutron source, we can improve experimental sensitivity by one or two orders of magnitude to search for nEDM.

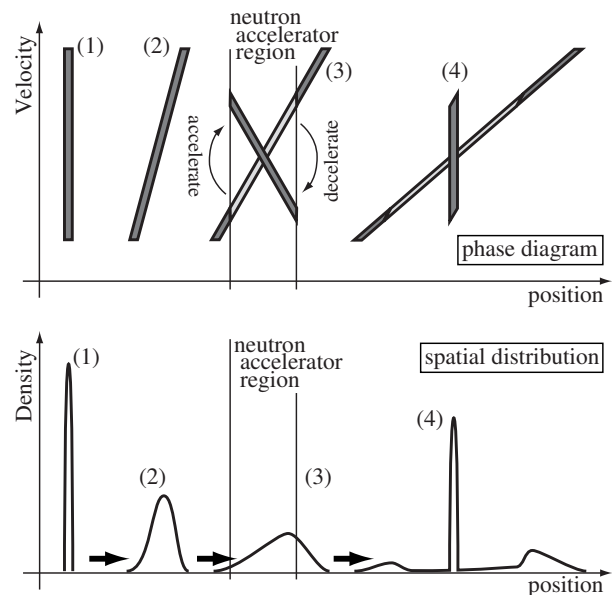


Figure 1: Concept of space-time focusing by using neutron accelerator. (1) Neutrons are generated as a pulse. (2) Neutrons spread spatially during transport. (3) Neutrons are accelerated/decelerated properly. (4) Some neutrons are focused at the experimental position. This figure illustrates the behavior of polarized neutrons.

EMITTANCE CONTROL FOR DIFFERENT FACET BEAM SETUPS IN THE SLAC LINAC*

F.-J. Decker, W. Colocho, N. Lipkowitz, Y. Nosochkov, J. Sheppard, H. Smith, Y. Sun, M.-H. Wang,
G.R. White, U. Wienands, M. Woodley, G. Yocky, SLAC, Menlo Park, CA 94025, USA

Abstract

The linac beam at SLAC requires different setups for different users at the FACET (Facility for Advanced Accelerator Experimental Tests) area, like highly compressed, intense bunches, or lower charge, long bunches. These require typically a lengthy tuning effort since with an energy-time correlation (or "chirp") the bunch transverse wakefield kicks can be compensated with dispersive trajectory oscillations and vice versa. Lowering the charge or changing the bunch length will destroy this delicate balance. Besides the typical steering to minimize BPMs (Beam Position Monitors) with correctors, we applied different techniques to try to localize beam disturbances like dispersion with phase changes, RF-kicks and RF quadrupole fields turning a klystron off and on, or varying the phase, and finally wakefield kicks with different beam intensities. It is also important to quantify BPM to quadrupole offsets with "bowtie" plots and that the correctors give the expected kicks with orbit response matrix measurements.

INTRODUCTION

Good transverse beam emittances at different places along the SLAC Linac get typically achieved in the following way. The beam gets steered relatively flat (< 0.5 mm) using BPMs (Beam Position Monitors) and then with a lengthy tuning scheme, linac oscillations or bumps are introduced which minimize the emittance measured with wire scanners. Over the years this process typically achieved small emittance growth numbers of 50 to 100% over the initial values of 30 and 2.5 mm-mrad for x and y , so 50 by 5 mm-mrad was expected for the FACET beam in Sector 20.

Typically twice that amount and often more was only achieved. There are a few explanations (excuses) which could cause this. The typical beam rate was 10 Hz, so tuning was three times slower than at 30 Hz. The FACET chicane needed special attention, so linac tuning was cut short. And the final spot sizes after the chicane and final focus were about the same, like 30 μm , even if the emittance just in front of the chicane changed by a factor of three (300 \rightarrow 100 mm-mrad in x), discouraging further linac tuning.

Additionally, frequent user requested beam changes in current and bunch length made it necessary to tune the beam emittances up again, which would make it even trickier for smaller emittances. It is assumed that the main root cause for this is that after just steering flat the initial emittance is as high as 1200 mm-mrad, and the

subsequent tuning cancels this with equally large corrections. When these cancelations are not local, or are charge / bunch length dependant, small say 10% variations will create 10% of 1200 mm-mrad = 120 mm-mrad.

So the goal is to localize and reduce emittance increasing effects. For that we try to find and categorize all possible mechanisms, like dispersion, wakefield, RF-kicks, and develop procedures like special steering methods and component alignment.

Goal: Get Linac closer to good emittances with BPMs etc. so the tuning part is less.

1. BPMs
2. Correctors
3. Quads (old BBA: straight orbit)
4. BPM-to-Quad: bowtie plot or Quad change
5. Corrector strength (LOCO, R12 meas.)
6. Lattice (Quad) strength: Oscillation data
7. RF-kicks: a) sin-cos, b) dipole-quadrupole-lens
8. Measure dispersion
9. Measure with different charge (wakefield)
10. Measure with different bunch lengths
11. Others

The different methods (numbers in () below) and their relevance are discussed in the following sections.

STEERING TECHNIQUES

Steering the beam to the center of a BPM (1) gets the beam down the linac relatively fast, but usually ends up with big beam emittances. Additionally we can look at the corrector (2) values along z and check for certain patterns, e.g. stronger values with $+ - +$ might indicate a BPM with a big unreal offset. With our "SVD Steering" we can adjust a gain parameter to prefer BPMs (gain high) or correctors (gain low), but this method just supports what is believed more correct.

The next step is also using the quadrupole (3) strengths in a way to get a straight trajectory. When a BPM reading is say $\Delta x = 1$ mm and the corrector strength is $cor = 0.03$ kG-m, the two can be compared by dividing cor by the quadrupole strength $Q = 20$ kG: $cor/Q = 1.5$ mm. So the beam gets more bend up by the corrector than the $Q\Delta x$ bends it down (focussing magnet). Figure 1 shows an example where the orbit was steered flat (below 0.3 mm) but its corresponding cor/Q -values are up to 1.3 mm. This led to a global alignment of the Linac of up to 7 mm [1]. Equalizing the two locally will give a straight non-bend beam orbit and therefore no dispersion is generated. But an offset in a BPM might indicate also an offset in the RF nearby structure, causing wakefield kicks.

*Work supported by U.S. Department of Energy, Contract DE-AC02-76SF00515.

POSITRON INJECTOR LINAC UPGRADE FOR SUPERKEKB

T. Kamitani*, M. Akemoto, Y. Arakida, D. Arakawa, A. Enomoto, S. Fukuda, K. Furukawa, Y. Higashi, T. Higo, H. Honma, N. Iida, M. Ikeda, E. Kadokura, K. Kakihara, H. Katagiri, M. Kurashina, H. Matsushita, S. Matsumoto, T. Matsumoto, S. Michizono, K. Mikawa, T. Miura, F. Miyahara, T. Mori, H. Nakajima, K. Nakao, T. Natsui, S. Ohsawa, Y. Ogawa, M. Satoh, T. Shidara, A. Shirakawa, T. Suwada, H. Sugimoto, T. Takatomi, T. Takenaka, Y. Yano, K. Yokoyama, M. Yoshida, L. Zang, X. Zhou, KEK, Tsukuba, Japan
D. Satoh, Graduate School of Science and Engineering, Tokyo Inst. of Technology, Tokyo, Japan

Abstract

This paper reports on a present status of a positron injector linac upgrade for SuperKEKB. A development status of a flux concentrator for positron focusing is shown. An influence of offset layout of the flux concentrator and the target on a positron yield is described. Positron capture by L-band and large aperture S-band accelerating structures are compared in a viewpoint of satellite bunch elimination. Beam optical design compatible to electrons and positrons of different beam energies is discussed.

INTRODUCTION

The KEKB-factory is now under an upgrade to SuperKEKB for a forty times higher luminosity [1]. The injector linac is required to supply beams of higher charge and smaller emittance as shown in Table 1.

Table 1: Linac Beam Specifications

	KEKB (e^-/e^+)	SuperKEKB (e^-/e^+)
Injection Energy (GeV)	8.0 / 3.5	7.0 / 4.0
Bunch Intensity (nC)	1.0 / 1.0	5.0 / 4.0
Number of Bunch /pulse	2 / 2	2 / 2
Emittance (μm)	300 / 2100	20 / 92 _{[H]:7[V]}

To generate low emittance electron beams of 5 nC bunch intensity for injection, a photo-cathode RF gun is introduced [2] to replace the existing thermionic gun and the RF bunching section. The electron beams are accelerated up to 7.0 GeV over the entire linac and injected into the HER. Electron beams of 10 nC for positron production will also be generated with the RF gun. In a case high intensity operation of the RF gun is not stable, the thermionic gun is also used and the beams from these two guns are switched. To generate low emittance positron beams, a damping ring (DR) of 136 m circumference is introduced at a side of the linac and connected at the beam switch-yard No.2 (SY2). Beams generated in a positron capture section (PCS) are accelerated up to 1.1 GeV and injected into the DR. Positrons are extracted after 40 ms from the DR, injected back to the linac and accelerated up to 4.0 GeV for

injection to the LER. Energy gain of the positrons from existing six accelerator modules (typically 160 MeV per each module) from the PCS to the SY2 is not sufficient for this 1.1 GeV injection to the DR. The PCS is relocated 40 m upstream to have a sufficient energy margin for the DR. To increase positron beam intensity four times as much, capture efficiency is enhanced in two aspects. At first, an existing 2-T pulsed coil of short field length (45 mm) right behind a positron production target, is replaced with a flux concentrator (FC) type of 5-T pulsed solenoid of long field length (200 mm). An adiabatic matching characteristics of a solenoidal field distribution with a FC, gives wider energy acceptance for positrons. As a second aspect, existing S-band accelerating structures with conventional aperture (21 mm in diameter) used in a solenoidal field of the PCS are replaced with large aperture S-band (LAS) structures (30 mm) or L-band structures (35 mm) to enlarge transverse phase space acceptance. Total length of the PCS is extended from 8 m to 16 m to boost positron beam energy from the PCS from 80 to 120 MeV. This increase of the beam energy at a transition from solenoidal to quadrupole focusing region is effective in reducing beam loss around an optical matching section.

In December of 2013, we will start a preliminary positron beam commissioning of the injector linac within limited operation parameters. A beam commissioning with the DR will be started in February of 2015. Development, fabrication and installation of the components are ongoing to be in time for the schedule.

In the following sections, as topics of significance in the positron injector linac upgrade, flux concentrator development, target protection and offset positron production, large aperture accelerating structures development, satellite bunch elimination and electron/positron compatible optics design are described.

FLUX CONCENTRATOR DEVELOPMENT

Flux concentrator is a pulsed solenoid composed of a primary coil and a copper cylinder with a conical hole inside. Induced eddy current flows through a thin slit to a inner surface and generates a strong field of several Tesla. Achievable field strength is mainly determined by a hole diameter and a primary pulsed current. They are constrained from a required aperture size, a power supply capacity and break-

*E-mail: < takuya.kamitani@kek.jp >

ADVANCES IN BEAM TESTS OF DIELECTRIC BASED ACCELERATING STRUCTURES*

S. P. Antipov^{1,2}, C. Jing^{1,2}, A. Kanareykin^{1,#}, J.E. Butler¹, V.Yakimenko³, W. Gai²

¹Euclid Techlabs LLC, Solon, OH, USA,

²Argonne National Laboratory, Argonne, IL, USA

³Brookhaven National Laboratory, Upton, NY, USA

Abstract

Diamond is being evaluated as a dielectric material for dielectric loaded accelerating structures. It has a very low microwave loss tangent, high thermal conductivity, and supports high RF breakdown fields. We report on progress in our recent beam tests of the diamond based accelerating structures of the Ka-band and THz frequency ranges. Wakefield breakdown test of a diamond-loaded accelerating structure has been carried out at the ANL/AWA accelerator. The high charge beam from the AWA linac (~ 70 nC, $\sigma_z \sim 2$ mm) was passed through a rectangular diamond loaded resonator and induce an intense wakefield. A groove is cut on the diamond to enhance the field. Electric fields up to 300 MV/m has been generated on the diamond surface to attempt to initiate breakdown. Wakefield effects in a 250 GHz planar diamond accelerating structure has been observed at BNL/ATF accelerator as well. We have directly measured the mm-wave wake fields induced by subpicosecond, intense relativistic electron bunches in a diamond loaded accelerating structure via the dielectric wake-field acceleration mechanism. A surface analysis of the diamond has been performed before and after the beam test.

INTRODUCTION

Diamond has been proposed as a dielectric material for dielectric loaded accelerating (DLA) structures [1-3]. Dielectric Loaded Accelerator structures using ceramics or other materials and excited by a high current electron beam or an external high frequency high power RF source have been under extensive study for many years [4-7]. Low loss microwave ceramics, fused silica, and CVD polycrystalline and single crystal diamonds [11] have been considered as materials for dielectric based accelerating structures to study of the physical limitations encountered in developing field strengths > 100 MV/m at microwave [4-6] and $> \text{GV/m}$ at THz frequencies in a dielectric based wakefield accelerator [6,7,11,12]. THz radiation has been generated recently by a short ~ 10 GV/m pulse within a 100 μm diameter quartz fiber [7]. A planar diamond-based DLA structure was proposed recently by Omega-P, Inc., where the dielectric loading of this structure was to be made of diamond slabs fabricated

using CVD (chemical vapor deposition) technology [2].

Our choice of CVD (Chemical Vapor Deposition) diamond as a loading material will allow demonstration of high accelerating gradients; up to 0.5-1.0 GV/m as long as the diamond surface can sustain a 0.5-1.0 GV/m short pulse (~ 10 ns) rf field without breaking down. Diamond has the lowest coefficient of thermal expansion, highest thermal conductivity ($2 \times 10^3 \text{ Wm}^{-1} \text{ K}^{-1}$) and extremely low loss tangent ($< 10^{-4}$) at Ka-W frequency bands. Secondary emission from the CVD diamond surface can be dramatically suppressed by diamond surface dehydrogenation or oxygen termination [3,6,8-12]. The CVD process technology is rapidly developing, making the CVD diamond fabrication process fast and inexpensive. Given these remarkable properties, diamond should find numerous applications in advanced accelerator technology [3]. Planar diamonds are available commercially in various grades including single crystal diamonds. The goal of this research is to perform a wakefield acceleration experiment using a diamond loaded structure and to test diamond for breakdown.

Euclid Techlabs had performed two wakefield experiments with diamond loaded accelerating structures: a 25 GHz structure at the Argonne Wakefield Accelerator of ANL and a 250 GHz structure at the Accelerator Test facility of BNL [9].

BEAM EXPERIMENTS WITH THE DIAMOND BASED DLA STRUCTURES

Significant progress has been made in the development and testing of high gradient dielectric accelerating structures (DLA) [1]. As various engineering challenges (breakdown, dielectric losses, efficient RF coupling) have been overcome, the technology of high gradient RF or wakefield driven dielectric loaded structures appears increasingly attractive as a viable option for high energy accelerators. Typical DLA considered in experiments is a cylindrical, dielectric tube with an axial vacuum channel inserted into a conductive sleeve or a rectangular waveguide loaded with planar dielectric pieces. In this paper we will focus on the latter structure. The dielectric constant, thickness of dielectric and the size of a vacuum gap are chosen to adjust the phase velocity of the fundamental mode at certain frequency to the beam velocity $\sim c$. In the application to particle acceleration, the dominant TM_{01} mode is of main interest.

*Work supported by the Department of Energy SBIR program.

#alexkan@euclidtechlabs.com

A 10 MeV L-BAND LINAC FOR THE IRRADIATION APPLICATIONS IN CHINA

G.[#] Pei, Y. Chi, R. Shi, Z. Zhou, Q. Yuan, F. Zhao, D. He, X. Yang, C. Yu, M. Dai, J. Liu, Y. Feng, X. Li, X. He, X. Wang, Z. Zhu, E. Tang, H. Huang, J. Zhao, C. Ma,
 Institute of High Energy Physics, IHEP, Beijing, P. O. Box 918, 100049, China
 Z. Li, X. Zhang, Wuxi EL PONT Radiation Technology, Ltd, No 8 Weiye Road,
 Qianqiaoqian District, Wuxi, 214151, Jiangsu, China

Abstract

The electron linear accelerator has wide applications, and the demands for the irradiation applications are keeping growing in China. A high beam power 10 MeV L-band Linac has been developed recently as a joint venture of Institute of High Energy Physics (IHEP) and Wuxi EL-PONT Company in China. The Thales TH2104U klystron, 2 A thermionic electron gun and 3 m long L-band disk-loaded constant impedance RF structure were adopted. A stable electron beam of 10 MeV / 40 kW has been obtained in the last April. In this paper the detailed design issues and beam commissioning results are reported.

INTRODUCTION

IHEP in China has very rich experience in the electron linac design and development. When requested to transfer the technology to industry, many S-band electron linacs have been developed for medical and irradiation applications. For the S-band irradiation linac, the beam power is limited to be ~20 kW because of the RF structure heating/cooling issues. Due to the scaling law of $P \sim f^1$ between the RF power consumption of the accelerating structure and the frequency, L-band structure [1][2] is usually adopted for the nature extending to much higher beam power up to ~100 kW level. For any high beam power machines the power efficiency is a concern. According to Eq. (1), the maximum conversion efficiency η_{max} of the RF power to the beam power depends only on the attenuation factor τ [3], and smaller τ is preferred.

$$\eta_{max} = \frac{1}{2} \left[\frac{(1 - e^{-2\tau})^2}{(1 - e^{-2\tau}) - 2\tau e^{-2\tau}} \right] \quad (1)$$

However, there is a compromise among power efficiency, power dissipation as well as heating, peak beam current and beam energy. It is known that τ is independent of frequency, and for SLAC type 3m long disk-loaded TW structure τ is ~0.57. Suppose a 3 m long L-band structure of 34 cavities is used, τ can be roughly estimated to be $0.57 \cdot 34 / 86 = 0.225$. With SUPERFISH simulation and cold test, τ is shown [4] to be 0.22, which is in good agreement with the simple scaling. By putting 0.22 into Eq. (1) one can get an efficiency η_{max} of 90%, which is very excellent. In this condition, the beam

current is ~900 mA according to Eq. (2).

$$i_{\eta_{max}} = \left(\frac{P_r}{rl} \right)^{1/2} \left[\frac{(1 - e^{-2\tau})^{3/2}}{(1 - e^{-2\tau}) - 2\tau e^{-2\tau}} \right] \quad (2)$$

Table 1 shows the design parameters for the 10 MeV / 40 kW L-band linac. The linac is a machine with very heavy beam loading; the beam energy range of 8 to 12 MeV can be easily controlled by simply adjusting the gun bias voltage (i.e. the gun emitting beam current), but above 10 MeV is not recommended for prevention of the neutron production.

Table 1: Design parameters for the 10MeV L-band linac

Beam energy (MeV)	10
Beam power (kW)	40
RF frequency (GHz)	1.3
Peak beam current (mA)	530
Duty cycle (%)	0.75
Klystron peak power (MW)	10

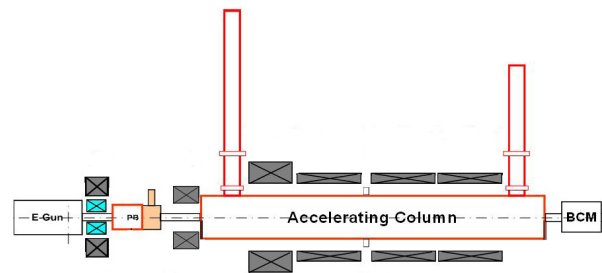


Figure 1: The schematic of the L-band linac.

DETAILED DESIGN AND SIMULATION

Figure 1 shows the schematic of the high power 10 MeV L-band linac, which mainly consists of an electron gun, an RF power source and an accelerating column. The electron gun is the 80 kV BEPC type [5] gun with 2 A Y646B cathode grid assembly. The gun system is separated from the other subsystems, which makes it easy for maintenance. The gun emitting current and the beam energy are adjustable. The RF power source is a 10 MW Thales TH2104U klystron with 130 kW average power, and the modulator was designed to make it work at 100 kW. Fig. 2 shows the Thales TH2104U klystron and its parameters.

*Work supported by the joint venture foundation of IHEP and the Wuxi EL-PONT Company in China.
 #peigx@ihep.ac.cn

APPLICATIONS OF COMPACT DIELECTRIC BASED ACCELERATORS*

C. Jing#, S. Antipov, P. Schoessow, and A. Kanareykin, Euclid Techlabs LLC, Solon, OH, USA
J.G. Power, M. Conde, and W. Gai, ANL, IL, USA

Abstract

Important progress on the development of dielectric based accelerators has been made both experimentally and theoretically in the past few years. One advantage of dielectric accelerators over their metallic counterparts is their compact size, which make them attractive for industrial or medical applications. In this article, we discuss the design of dielectric based accelerators focusing on those technologies relevant toward these needs.

DIELECTRIC LOADED ACCELERATOR

The first studies of using RF driven dielectric-loaded circular waveguide for particle acceleration can be traced back to the early 1950's [1]. In recent years, because of its geometrical simplicity and availability of low loss dielectrics, theoretical and experimental investigations on dielectric based accelerators have been intensively revived. Among them, externally powered Dielectric-Loaded Accelerators (DLA), dielectric wakefield accelerators, and dielectric laser accelerators have attracted the most attention. In this paper, we concentrate on externally powered DLA technologies and possible application.

DLA structures can be made as simple as a dielectric tube surrounded by a conducting cylinder. Most of them use uniform, linear ceramic tubes so that they work as constant impedance accelerating structures. The TM_{01} mode (traveling wave accelerator) or TM_{01n} mode (standing wave) are the fundamental accelerating modes. Unlike conventional metallic accelerating structures, DLA structures do not require any structure periodicity to slow the phase velocity of the guided wave below the speed of light. For a given radius, the phase velocity of each guided wave mode in a DLA structure is governed by the dielectric constant of the material and its wall thickness. In general, for the same a/λ , where a is the radius of the beam opening and λ is the wavelength, the DLA structure can be made much smaller than a disk-loaded accelerating structure due to the high dielectric constant of the material used. This small size may be favored for applications with tight space requirements. It also facilitates the use of quadrupole lenses or a permanent solenoid around the structure to prevent the beam from breaking up in the case of high current beam acceleration. For example, for an X-band structure, given $a/\lambda=0.156$, the diameter of a cell of a 120-degree traveling wave disk-loaded accelerating structure is larger than 2 cm, but the outer diameter of the dielectric tube in a DLA structure is only 1 cm if the

dielectric constant of the tube is 20.

However, the choice of dielectric constant should be considered as far more complicated than the requirement of a reduced transverse dimension. It is strongly linked with other accelerating parameters as well. A very good estimate of the group velocity of a traveling wave DLA structure is given by $V_g/c \approx 1/\varepsilon_r$ (where c is the speed of light and ε_r is the relative dielectric constant of the loaded material) when a/λ is less than 15%. The quality factor of a DLA structure can be roughly estimated as $Q \approx 5.22 \times 10^4 / \{ \sqrt{[f < \text{GHz} > \times (\varepsilon_r - 1)] + 5.22 \times 10^4 \times \tan \delta} \}$, where f is the frequency of the TM_{01} mode in units of GHz and $\tan \delta$ is the loss tangent of the loaded material.

PARAMETER CHOICE

DLA structures are generally preferred for use in a short structure powered by short, high frequency RF pulses, which reduces the probability of RF breakdown but needs a short filling time to achieve a high RF-to-beam efficiency [2]. Consider the rough design of an X-band travelling wave DLA structure. From the group velocity estimate, we choose $\varepsilon_r = 10$ for a structure with $V_g = 10\% c$. Then Q can be estimated to be 3400. Since the size of the beam opening ($2a$) is independent of Q but tightly related to the R/Q (figure of merit of an accelerating structure) and shunt impedance R (they both increase as the beam opening decreases), we can choose a as small as the beam emittance allows to obtain both a large R/Q and R . Meanwhile the filling time (defined as L/V_g , where L is the length of the structure) remains short since the group velocity is unrelated to the beam opening. It should be pointed out that a/λ of DLA structures cannot be chosen too small since it will increase the wakefield and thus the risk of beam break-up.

Transverse wakefield damping in DLA structures has been well studied [3]. Its implementation is rather simple: an axially slotted copper jacket filled with RF absorber or metallized strips on the outer surface of the dielectric tube surrounded with RF absorber. The low Q of the DLA structures also helps the damping of long range wakefields.

Figure 1 shows a few parameters of X-band (11.7GHz) travelling wave DLA structures. Three different dielectric constants are used in the plots, representing three commonly used low loss materials: Alumina ($\varepsilon_r=10$, $\tan \delta=1 \times 10^{-4}$), MgCaTiO ($\varepsilon_r=20$, $\tan \delta=1 \times 10^{-4}$) and Quartz ($\varepsilon_r=3.8$, $\tan \delta=6 \times 10^{-5}$). Figure 1(a) clearly shows that the group velocity is bounded by the reciprocal of the dielectric constant as the beam opening decreases. The quality factor of a DLA structure is the combined contribution of metal wall losses and dielectric losses, but

*Work supported by the Department of Energy SBIR program.

#jingchg@hep.anl.gov

FERMILAB 1.3 GHz SUPERCONDUCTING RF CAVITY AND CRYOMODULE PROGRAM FOR FUTURE LINACS*

C.M. Ginsburg[#], Fermilab, Batavia, IL 60510, USA

Abstract

The proposed Project X accelerator and the International Linear Collider are based on superconducting RF technology. As a critical part of this effort, Fermilab has developed an extensive program in 1.3 GHz SRF cavity and cryomodule development. This program includes cavity inspection, surface processing, clean assembly, low-power bare cavity tests and pulsed high-power dressed cavity tests. Well performing cavities have been assembled into cryomodules for pulsed high-power tests and will be tested with beam. In addition, peripheral hardware such as tuners and couplers are under development. The current status and accomplishments of the Fermilab 1.3 GHz activity will be described, as well as the R&D program to extend the existing SRF pulsed operational experience into the CW regime.

INTRODUCTION

Work by the International Linear Collider (ILC) [1,2] community, which includes Fermilab, has motivated substantial world-wide infrastructure development and cavity performance progress. At Fermilab, this has translated to a very large commitment of resources for infrastructure and personnel development. The developed capability has led to the possibility to use the 1.3 GHz infrastructure for development of Project X [3,4], although the performance requirements are somewhat different [5]. The Project X 3 GeV CW linac requires high Q_0 at gradients (E_{acc}) in the range $15 < E_{acc} < 20$ MV/m; 1.3 GHz cavities can be used to investigate high Q_0 . In addition, the Project X 3-8 GeV pulsed section operates at 1.3 GHz and requires ILC-like cavities with $E_{acc} \sim 25$ MV/m. The status of Fermilab 1.3 GHz infrastructure, accomplishments and plans are described.

INFRASTRUCTURE

The cavities are fundamentally of the Tesla design [6], made of high RRR niobium with an elliptical cell shape, for superconducting operation at 2K. Cavity qualification has been described in detail elsewhere [7] and includes cavity inspection, surface processing, clean assembly, and one or more cryogenic qualification tests which typically include performance diagnostics. Cavities which reach the performance requirement in vertical (bare) qualification test, typically $E_{acc} > 35$ MV/m, are dressed and horizontally tested. Cavities which reach the performance specification in horizontal (dressed) qualification test, also typically $E_{acc} > 35$ MV/m, are

assembled into cryomodules.

The joint ANL/FNAL facility is the primary infrastructure [7] for surface processing of 1.3 GHz cavities, and includes electropolishing (EP). New infrastructure at Fermilab includes two high temperature furnaces for hydrogen degassing, see Fig.1. In addition, a centrifugal barrel polishing (CBP) machine for 1-cell and 9-cell 1.3 GHz cavities has been introduced for R&D and may be used for production cavity preparation in the future, see Fig.2. CBP may be used in place of the standard bulk electropolishing step, to reduce acid use. CBP has been demonstrated to be a useful repair technique [8], and may have other benefits as well, such as reducing cavity performance sensitivity to minor manufacturing or material defects; these studies are not yet complete. A new R&D surface processing facility [9] is now fully operational for the full suite of standard EP processing for 1-cell 1.3 GHz cavities. The R&D EP tool is shown in Fig.3.



Figure 1: One of the two new vacuum furnaces.



Figure 2: Centrifugal barrel polishing machine.

*Operated by Fermi Research Alliance, LLC, under Contract DE-AC02-07CH11359 with the U.S. DOE
#ginsburg@fnal.gov

NON-DESTRUCTIVE INSPECTIONS FOR SC CAVITIES

Y. Iwashita, Y. Fuwa, M. Hashida, K. Otani, S. Sakabe, S. Tokita, H. Tongu,
Kyoto University, Uji, Kyoto, JAPAN
H. Hayano, K. Watanabe, Y. Yamamoto, KEK, Ibaraki, JAPAN

Abstract

Starting from the high-resolution camera for inspection of the cavity inner surface – so-called Kyoto Camera, high resolution T-map, X-map and eddy current scanner have been developed. R&D for radiography techniques is also going on to detect small voids inside the Nb EBW seam, where the target resolution is 0.1 mm. Some radiography tests with X-rays induced from an ultra short pulse intense laser were carried out. The local treatment technique on the found defects is also realized by the Micro-Grinder.

INTRODUCTION

Non-destructive Inspections play important roles in improving yield on production of high performance SC Cavities. Starting from the high-resolution camera for inspection of the cavity inner surface [1], high-resolution T-map, X-map and eddy current scanner [2,3,4,5,6] have been developed. We are also investigating radiography to detect small voids inside the Nb EBW seam, where the target resolution is 0.1 mm. We are carrying out radiography tests with X-rays induced by irradiations of an ultra short pulse intense laser on a target metal sheet. Defects found by the inspection technique can be locally treated by the Micro-Grinder.

CAVITY CAMERA UPDATE

In order to inspect the SPL cavity at CERN, whose frequency is about a half of ILC cavity and the diameter is about twice larger, the illumination system has been enhanced to illuminate the wider surface area (see Fig. 1). Although the iris diameter is about twice larger than that of ILC's, the bore diameter at the flange position is limited (just below $\varnothing 80\text{mm}$). This limits the camera cylinder diameter is $\varnothing 70\text{mm}$. Fig. 2 shows the modification on the illumination system to illuminate the wider area with enough strength. While the former system used two LED's for each strip, the new system uses 14 LED chips on a line and two lines consist one strip. Thus 28 LED chips are used for a strip. Furthermore, the LED chip has three LED's in a package. This illumination system should provide enough light for the wider cavity surface area. Because of the larger cavity size, the working distance is longer than former model and a bigger lens system is adopted. Fig. 3 shows the overview of this system. The illumination plate on the cylinder is shown in Fig. 4. The camera cylinder can be rotated to see the annular area in a cavity without movement of the cavity, while the cavity table can rotate the cavity if it does not wear its He jacket around. The table has a function to move the cavity in its axial direction.

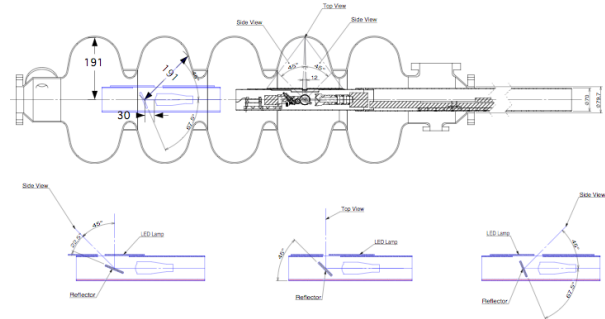


Figure 1: CavCam3 in SPL cavity.

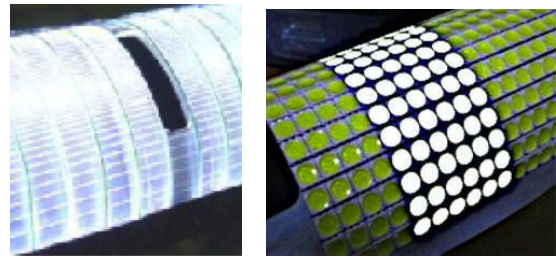


Figure 2: Enhanced illumination for wider surface area (Armadillo Illumination). 28 LED chips (right) instead of 2 LED's per strip (left) are installed.



Figure 3: Latest CavCam-3 for SPL cavity at CERN.



Figure 4: All the LED's are lighten. A diffusing panel will be install on the LED's to form the light strip. 14 chips/line x 2 lines/strip x 10 strips/side x 2 sides = 560 chips are used.

NORMAL CONDUCTING DEFLECTING CAVITY DEVELOPMENT AT THE COCKCROFT INSTITUTE

G. Burt, P. K. Ambattu, A. C. Dexter, B. Woolley, C. Lingwood, Cockcroft Institute, Lancaster, UK
 S. Buckley, P. Goudket, C. Hill, P. A. McIntosh, J. Mackenzie, A. Wheelhouse,
 STFC, Daresbury, UK
 V. Dolgashev SLAC, USA
 A. Grudiev, CERN, Geneva, Switzerland
 R. M. Jones, UMAN, Manchester, UK

Two normal conducting deflecting structures are currently being developed at the Cockcroft Institute, one as a crab cavity for CERN linear collider CLIC and one for bunch slice diagnostics on low energy electron beams for Electron Beam Test Facility EBTF at Daresbury. Each has its own challenges that need overcome. For CLIC the phase and amplitude tolerances are very stringent and hence beamloading effects and wakefields must be minimised. Significant work has been undertaken to understand the effect of the couplers on beamloading and the effect of the couplers on the wakefields. For EBTF the difficulty is avoiding the large beam offset caused by the cavities internal deflecting voltage at the low beam energy. Prototypes for both cavities have been manufactured and results will be presented.

INTRODUCTION

Transverse deflecting cavities are required for many applications on accelerators, including crab cavities, bunch separators, emittance exchange and for bunch length diagnostics. These cavities usually operate in a TM_{110} -like mode. The Cockcroft Institute in the UK is participating in the design of several deflectors for a range of applications including crab cavities for ILC [1], CLIC [2] and LHC [3] and a bunch length diagnostic for EBTF [4]. In this paper we concentrate on the normal conducting rf deflectors for CLIC and EBTF.

CLIC CRAB CAVITY

CLIC requires a crab cavity to rotate the bunches prior to the interaction point (IP) to achieve an effective head-on collision. As the bunch size at the IP is very small (~ 5 nm) the luminosity is very sensitive to the crab cavities RF phase and amplitude. This means that the beamloading must be minimised and correction applied. The beamloading is dependent on the longitudinal electric field experienced by the bunch. In crab cavities the longitudinal electric field is zero on axis but has a linear variation as the bunch goes off axis. This means the beamloading could be positive or negative depending on the beam offset. As the bunch train for CLIC is short (~ 200 ns), the beamloading cannot be compensated for in a single bunch train, the feedback would occur over several trains. Unless the jitter on the beam offset is much less than the bunch size the compensation will not be successful, hence the beamloading must be minimised

instead [5]. In order to reduce the effect of beamloading the cavity is designed with a large power flow so that any power induced by beamloading is smaller in comparison. This is achieved by using a high group velocity travelling wave structure.

Another issue affecting beamloading is the perturbation of the input and output couplers. Couplers break the symmetry of the cavity and can give rise to monopole components to the deflecting field. A dual feed coupler keeps the symmetry of the structure and avoids monopole components but is more complex coupling arrangement requiring splitters. A single feed is the simpler coupling arrangement however this gives the end cells a large monopole component of the rf field. We have investigated methods of single feed coupling without inducing monopole component.

Single-feed Couplers

In order to minimise the monopole component of rf field in the end cells while using a single-feed coupler a number of options were investigated. Initially cancelling the monopole kick from the two end cells was studied. Consider particle moving at the speed of light. If the cell is rotated the monopole component has the sign of the real part of the voltage flipped. Hence if the input and output couplers are mounted on opposite side the real parts should cancel. If the lengths of the cells are adjusted so that the voltage is entirely real then the entire monopole component is cancelled. This however is not sufficient in travelling wave deflecting structures as the power put into the output cell will be extracted through the output coupler while the power in the input cell will travel down the structure. Hence it is necessary to cancel the beamloading in each cell individually.

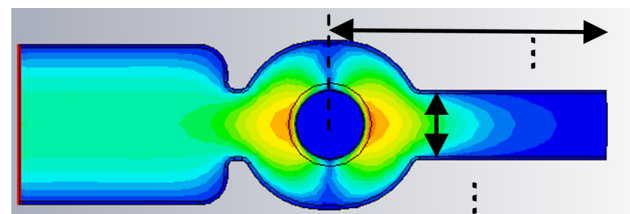


Figure 1: Dummy waveguide and input coupler on the CLIC crab cavity

In order to restore the symmetry of the cell a dummy waveguide opposite the coupler was studied. Using a

STATUS OF THE C-BAND RF SYSTEM FOR THE SPARC-LAB HIGH BRIGHTNESS PHOTOINJECTOR

R. Boni, D. Alesini, M. Bellaveglia, G. Di Pirro, M. Ferrario, A. Gallo, B. Spataro, INFN-LNF, Frascati, Italy
A. Mostacci, L. Palumbo, ULRS, Rome, Italy

Abstract

The high brightness photo-injector in operation at the SPARC-LAB facility of the INFN-LNF, Italy, consists of a 150 MeV S-band electron accelerator aiming to explore the physics of low emittance high peak current electron beams and the related technology. Velocity bunching techniques, SASE and Seeded FEL experiments have been carried out successfully. To increase the beam energy so improving the performances of the experiments, it was decided to replace one S-band travelling wave accelerating cavity, with two C-band cavities that allow to reach higher energy gain per meter. The new C-band system is in advanced development phase and will be in operation early in 2013. The main technical issues of the C-band system and the R&D activities carried out till now are illustrated in detail in this paper.

THE SPARC-LAB AT FRASCATI LNF

The SPARC-LAB is a research facility of the INFN Frascati Laboratory (LNF) whose purpose is to conduct advanced research in the field of high brightness, low emittance electron beams [1]. The facility, able to operate also in the velocity bunching configuration, feeds six 2m. long undulators and integrates the 150 MeV S-band photo-injector with a 220 Terawatt, Ti:Sa ultrashort laser system. FEL radiation in the SASE, Seeded and HHG modes have been performed from 500 nm down to 40 nm wavelength. The photo-injector SPARC, a single bunch electron accelerator, consists of a laser driven RF Gun followed by three traveling wave (TW), constant gradient, $2\pi/3$ accelerating cavities, with the first two immersed in a solenoidal field to keep down the beam emittance growth. A second beam line has been also installed and is now hosting a narrow band THz radiation source.

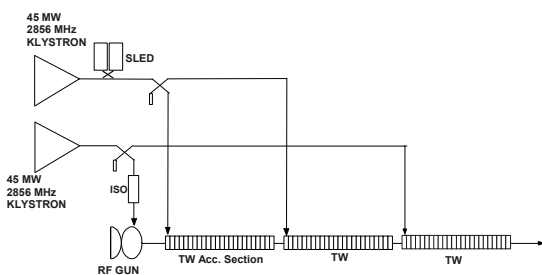


Figure 1: the SPARC photoinjector present layout

To improve the performances of the experiments and recuperate the energy that is lost in the velocity bunching configuration, it was decided to increase the beam energy by replacing the third S-band section with two, 1.4 m.

long, C-band TW accelerating structures that allow to operate at higher gradient. The choice of a higher frequency, e.g. the X-band, was also considered but then discarded because more expensive and technically more challenging.

THE C-BAND RF SYSTEM

The C-band technology is relatively new in linear accelerators compared to the standard and widely used S-band systems. Nevertheless it can be considered sufficiently mature since it is already employed in other accelerator laboratories like the Spring8 (JP) and the PSI FEL (CH) facilities.

R&D of the accelerating structure

The third S-band accelerating section, that is a 3 m. long SLAC-type unit, shown in Fig.1 will be replaced with two, 1.4 m., C-band sections supplied with a 50 MW, 5712 MHz Toshiba klystron through a SKIP-type pulse-compressor [2]. In order to ease design and construction, the C-band sections are constant impedance (CI) structures with large (14 mm) iris diameter to minimize the surface electric field on the iris edges and improve the pumping speed. Also, the group velocity increases and this reduces the filling time. It must be remarked that the typical exponential decay of the input compressed pulse is partially compensated by the RF losses of the CI structure, resulting in a quasi-constant field amplitude along the section. Input and output waveguides are coupled to the beam-pipe instead of to the end-cells. A 50 cm long prototype was designed at LNF and built by a local firm. Brazing and vacuum test have been made at LNF [3].

The prototype, shown in figure 2, has been power tested at KEK, in the frame of a collaboration established ad hoc with the INFN.

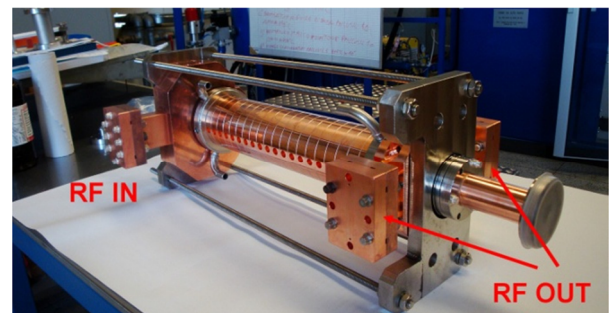


Figure 2: The C-band prototype tested at KEK.

The KEK RF station consists of a 50 MW - 2.5 μ sec Toshiba E37202 klystron, followed by a pulse

FRIB TECHNOLOGY DEMONSTRATION CRYOMODULE TEST*

J. T. Popielarski^{*}, E. C. Bernard, S. Bricker, C. Compton, S. Chouhan, A. Facco[#], A. Fila, L. Harle, M. Hodek, L. Hodges, S. Jones, M. Klaus[†], M. Leitner, D. Miller, S. Miller, D. Morris, J. P. Ozelis, R. Oweiss, L. Popielarski, K. Saito, N. Usher, J. Weisend, Yan Zhang, Z. Zheng, S. Zhao
FRIB, East Lansing, Michigan, USA

[#]INFN/LNL, Legnaro (PD), Italy, [†] Technische Universität Dresden, Dresden, Germany

Abstract

A Technology Demonstration Cryomodule (TDCM) has been developed for a systems test of technology being developed for FRIB. The TDCM consists of two half wave resonators (HWRs) which have been designed for an optimum velocity of $\beta=v/c=0.53$ and a resonant frequency of 322 MHz. The resonators operate at 2 K. A superconducting 9T solenoid is placed in close proximity to one of the installed HWRs. The 9T solenoid operates at 4 K. A complete systems test of the cavities, magnets, and all ancillary components is presented in this paper.

INTRODUCTION

The SRF Department at Michigan State University had developed and tested four cryomodules prior to the first demonstration cryomodule for FRIB. Two of the cryomodules are working reliably in the ReA3 linac at MSU [1]. The TDCM, shown in figure 1, is the first cryomodule that demonstrates FRIB specific technology and encourages a transition to large scale engineering and quality assurance methods [2].

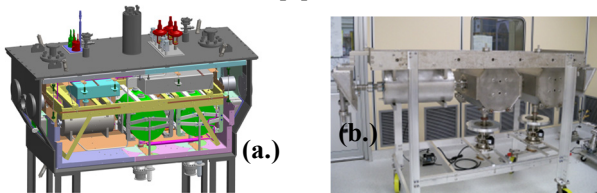


Figure 1: (a.) Rendering of TDCM in cryostat (b.) Cold mass assembly in cleanroom.

In developing the FRIB TDCM, a baseline cryomodule production method evolved for FRIB. The technical and schedule related setbacks encountered during the TDCM campaign eventually yielded reliable fabrication, processing, and certification techniques. SRF-related infrastructure and utility usage required for the TDCM assisted in finalizing planning for a new SRF high bay which will support FRIB cavity processing, vertical testing, cold mass assembly, and cryomodule bunker tests.

TDCM RELEVANCE TO FRIB

The TDCM is a developmental snapshot, and much of the technology improved as more detailed engineering

*This material is based upon work supported by the U.S. Department of Energy Office of Science under Cooperative Agreement DE-SC0000661.

[#]popielar@frib.msu.edu

analysis and sub component testing programs provided opportunities for design optimization [3- 5]. Some of the key differences are: a “bottom-up” style from the “top-down” TDCM style [4]; the rail system, support system, heat and magnetic shields assemblies were simplified; Improvements to alignment methods; an internal heat exchanger replaces the external heat exchanger; the 4K thermal intercepts will be parallel circuits as opposed the series connection in the TDCM.

With much of the cryogenic circuitry and alignment systems optimized in the baseline design before TDCM testing took place, alignment and continuous 2K operation aspects were not tested. The plumbing of the RF coupler 4K intercepts [6] required steady flow in the static state required continuous overfilling of the 4K header to ensure the couplers stayed cooled during RF conditioning.

TDCM DEVELOPMENT

Individual tests or more detailed engineering analyses conducted on the cavities, couplers, tuners, and cryogenic circuits used in the TDCM led to design optimizations and improved processing [7- 9].

Initial dunk tests showed low field emission onset values and thermal breakdown below the operating gradient; FRIB processing optimization for the HWR began during the TDCM campaign. The TDCM cavities were field emission-free [10] prior to the installation of the helium vessels.

Initial tests still showed signs of multipacting in the cavity. Repeated measurements on several cavities show a recurring barrier at 2 MV/m E_{acc} . This barrier self-conditioned as the RF power was raised, and in most tests only observed during initial 4K measurements.

During the initial dunk tests, it was discovered Q_0 was lower after a thermal cycle with no change otherwise. A closer investigation for Q -disease showed a strong reduction in the Q_0 after a 15 hour soak at 100K. The cavities were sent to JLAB for a furnace treatment to remove hydrogen from the bulk. Subsequent ‘ Q -soaks’ and thermal cycles showed no signs of degradation. A 600°C furnace treatment was added to the baseline processing plan and a furnace has been installed at MSU [9].

After being jacketed with a helium vessel, the 1st cavity was certified using the vertical cryostat configuration [5], and no field emission was observed. This helium vessel design utilized a titanium bellows at the beamport to reduce the tuning force required for the scissor-jack tuner.

THE UPGRADED ARGONNE WAKEFIELD ACCELERATOR FACILITY (AWA): A TEST-BED FOR THE DEVELOPMENT OF HIGH GRADIENT ACCELERATING STRUCTURES AND WAKEFIELD MEASUREMENTS*

M.E. Conde[#], D.S. Doran, W. Gai, R. Konecny, W. Liu, J.G. Power, Z. Yusof,
ANL, Argonne, IL 60439, U.S.A.
S. Antipov, C. Jing, Euclid Techlabs LLC, Solon OH 44139, U.S.A.
E. Wisniewski, IIT, Chicago IL 60616, U.S.A.

Abstract

Electron beam driven wakefield acceleration is a bona fide path to reach high gradient acceleration of electrons and positrons. With the goal of demonstrating the feasibility of this concept with realistic parameters, well beyond a proof-of-principle scenario, the AWA Facility is currently undergoing a major upgrade that will enable it to achieve accelerating gradients of hundreds of MV/m and energy gains on the order of 100 MeV per structure. A key aspect of the studies and experiments carried out at the AWA facility is the use of relatively short RF pulses (15 – 25 ns), which is believed to mitigate the risk of breakdown and structure damage. The upgraded facility will utilize long trains of high charge electron bunches to drive wakefields in the microwave range of frequencies (8 to 26 GHz), generating RF pulses with GW power levels.

AWA FACILITY

The mission of the Argonne Wakefield Accelerator Facility (AWA) is to develop technology for future accelerator facilities. The AWA facility has been used to study and develop new types of accelerating structures based on electron beam driven wakefields. In order to carry out these studies, the facility employs a photocathode RF gun capable of generating electron beams with high bunch charges and short bunch lengths. This high intensity beam is used to excite wakefields in the structures under investigation.

The facility is also used to investigate the generation and propagation of high brightness electron beams, and to develop novel electron beam diagnostics.

The AWA high intensity electron beam is generated by a photocathode RF gun, operating at 1.3 GHz. This one-and-a-half cell gun typically runs with 12 MW of input power, which generates an 80 MV/m electric field on its Magnesium photocathode surface. A 1.3 GHz linac structure increases the electron beam energy, from the 8 MeV produced by the RF gun, to 15 MeV. The linac is an iris loaded standing-wave structure operating in the $\pi/2$ mode with an average accelerating gradient of 7 MV/m; it has large diameter irises to minimize the undesirable wakefields generated by the passage of high charge electron bunches.

The charge of the electron bunches can be easily varied

from 1 to 100 nC, with bunch lengths of 2 – 2.5 mm rms, and normalized emittances of 3 to 100 π mm mrad.

The AWA laser system consists of a Spectra Physics Tsunami oscillator followed by a Spitfire regenerative amplifier and two Ti:Sapphire amplifiers (TSA 50). It produces 1.5 mJ pulses at 248 nm, with a pulse length of 2 to 8 ps FWHM and a repetition rate of up to 10 pps. A final KrF Excimer amplifier is optionally used to increase the energy per pulse to 15 mJ.

The generation of electron bunch trains (presently up to 16 bunches) requires each laser pulse to be divided by means of beam splitters into a laser pulse train. The charge in each electron bunch is determined by the energy in each laser pulse and the quantum efficiency of the photocathode material. Typically, single bunches of 100 nC can be produced (with a maximum of 150 nC occasionally reached).

WAKEFIELD ACCELERATION

The use of electron beam driven wakefields to achieve high gradient acceleration has received considerable attention. It offers the advantage of using a relativistic beam to transport the energy to the accelerating structures, decreasing the difficulties of generating and distributing RF power by conventional means; wakefields naturally constitute RF pulses that are of short duration and high peak intensity [1].

Research at the AWA facility has been exploring various types of wakefield structures, including photonic band gap structures, metallic iris loaded structures, and also more exotic schemes using metamaterials. The main focus of the facility, however, has clearly been the development of dielectric loaded structures. They offer the advantage of simple geometry and easy fabrication with accelerating properties that compare favourably with conventional iris loaded metallic structures: the axial electric field is uniform across the transverse cross section of cylindrical structures, and the uniform cross section of the structures presents no geometric features to cause field enhancement. The damping of the undesirable deflecting dipole modes seems to be more easily accomplished in dielectric loaded structures as well; planned experiments will explore the use of longitudinal slots on the metallic outer shell of dielectric structures, as a possible scheme to damp dipole modes. Dielectric structures also hold the promise of withstanding higher electric fields without material breakdown. A significant advantage offered by wakefield structures, in comparison

*Work supported by the U.S. Department of Energy under contract No. DE-AC02-06CH11357.

[#]conde@anl.gov

X-RAY LOCAL ENERGY SPECTRUM MEASUREMENT AT TSINGHUA THOMSON SCATTERING X-RAY SOURCE (TTX)*

Y.-C. Du[#], Z. Zhang, L.-X. Yan, J.-F. Hua, H. Zha, W.-H. Huang, C.-X. Tang

Accelerator laboratory, department of engineering physics, Tsinghua University, Beijing, China
Key laboratory of Particle & Radiation Imaging (Tsinghua University), Ministry of Education, Beijing, 100084, China

Key laboratory of High Energy Radiation Imaging Fundamental Science for National Defense, Beijing, 100084, China

Abstract

Thomson scattering X-ray source, in which the TW laser pulse is scattered by the relativistic electron beam, can provide ultra short, monochromatic, high flux, tunable polarized hard X-ray pulse which is can widely used in physical, chemical and biological process research, ultra-fast phase contrast imaging, and so on. Since the pulse duration of X-ray is as short as picosecond and the flux in one pulse is high, it is difficult to measure the x-ray spectrum with traditional spectra measurement methods. In this paper, we introduce an iterative statistical algorithm (Expectation-Maximization) to reconstruct the spectra from the attenuation data, and the results of the X-ray spectrum measurement experiment on Tsinghua Thomson scattering is also presented.

INTRODUCTION

Thomson Scattering sources (also called Inverse Compton Scattering), which can be bright X-ray sources typically produce photons, have attracted a lot of interest as the technologies for producing low-emittance high-brightness relativistic electron sources and ultra-short high-power lasers have progressed. The X-rays that are generated by the interactions between laser and electron, exhibit high directivity, and have a polarized tunable quasi-monochromatic spectrum. The knowledge of the spectrum of an X-ray source is a key point for the development of any kind of application, for example in imaging both contrast and absorbed dose strongly depend on energy. However, direct methods performing a standard spectrometric measurement based on single photon energy measurement to detect the X-ray spectrum of Thomson Scattering sources have always been considered troublesome to implement because the beam is too intense to cause pulse pile up problems. Thomson Scattering source can produce up to 10^8 photons, bunched in 10ps long pulse^[1]. An alternative way to measure the spectrum might request the measurement to be integral-type, which will not be affected by the high rate of incidence of photons. The analysis of attenuation data (transmission curves), which can provide some information about the spectral distribution of an X-ray

source, as not affected by the rate of incidence of photons, is a good candidate to measure the X-ray spectrum of the Thomson Scattering X-ray source. Although there are several problems with this method, such as low accuracy, non-unique solution to ill-condition system and instability with different measurement error^[2], this method can still give good estimation and reconstruction of spectra with some improvements based on the property of the measured spectra.

In this article, we introduce an iterative statistical algorithm (Expectation-Maximization)^[3] to reconstruct the spectra from the attenuation data on simulated measurement. Results show that this method can give good approximations for the mean energy of the spectra, while it is not sensitive to the specific spectral distribution and the energy broadening. In order to reconstruct the shape of the spectra, especially the energy broadening, we present a new method based on the Expectation-Maximization algorithm. An preliminary experiment is also carried out on Tsinghua Thomson scattering X-ray source, the measured maximum X-ray energy is about 53keV, which is agreed well with the simulations.

OVERVIEW OF TTX

The scheme of TTX is shown in figure 1. This machine includes a 50MeV electron linac based on the photocathode RF gun and a Ti: Sapphire TW laser system. The laser system generates both the 266nm UV pulse for photocathode and the 800nm IR pulse for scattering interaction. The two pulses are derived from one 79.3MHz Ti:Sapphire oscillator in order to reduce the time jitter between the electron beam and the IR pulse. The linac system consists of a BNL/KEK/SHI type 1.6 cell S-band photocathode RF gun, a 3m S-band SLAC type travelling wave accelerating section, generates 40~50MeV ultra-short high brightness electron pulse for scattering interaction. The laser system is synchronized with the RF system through a timing circuit, with a timing jitter no greater than 0.5ps. The parameters of electron and laser were listed in the table 1.

In previous experiment, we succeed to generate and detect the X-ray signal with head-on colliding mode. The results from the MCP and X-ray CCD are shown in figure 2.

*Work supported by work is supported by NSFC under Grant Nos. 10735050, 10805031, 10975088 and 10875070 and by the 973 Program under Grant No. 2007CB815102.

[#] dych@mail.tsinghua.edu.cn

EMITTANCE CONTROL FOR DIFFERENT FACET BEAM SETUPS IN THE SLAC LINAC*

F.-J. Decker, W. Colocho, N. Lipkowitz, Y. Nosochkov, J. Sheppard, H. Smith, Y. Sun, M.-H. Wang,
G.R. White, U. Wienands, M. Woodley, G. Yocky, SLAC, Menlo Park, CA 94025, USA

Abstract

The linac beam at SLAC requires different setups for different users at the FACET (Facility for Advanced Accelerator Experimental Tests) area, like highly compressed, intense bunches, or lower charge, long bunches. These require typically a lengthy tuning effort since with an energy-time correlation (or "chirp") the bunch transverse wakefield kicks can be compensated with dispersive trajectory oscillations and vice versa. Lowering the charge or changing the bunch length will destroy this delicate balance. Besides the typical steering to minimize BPMs (Beam Position Monitors) with correctors, we applied different techniques to try to localize beam disturbances like dispersion with phase changes, RF-kicks and RF quadrupole fields turning a klystron off and on, or varying the phase, and finally wakefield kicks with different beam intensities. It is also important to quantify BPM to quadrupole offsets with "bowtie" plots and that the correctors give the expected kicks with orbit response matrix measurements.

INTRODUCTION

Good transverse beam emittances at different places along the SLAC Linac get typically achieved in the following way. The beam gets steered relatively flat (< 0.5 mm) using BPMs (Beam Position Monitors) and then with a lengthy tuning scheme, linac oscillations or bumps are introduced which minimize the emittance measured with wire scanners. Over the years this process typically achieved small emittance growth numbers of 50 to 100% over the initial values of 30 and 2.5 mm-mrad for x and y , so 50 by 5 mm-mrad was expected for the FACET beam in Sector 20.

Typically twice that amount and often more was only achieved. There are a few explanations (excuses) which could cause this. The typical beam rate was 10 Hz, so tuning was three times slower than at 30 Hz. The FACET chicane needed special attention, so linac tuning was cut short. And the final spot sizes after the chicane and final focus were about the same, like 30 μm , even if the emittance just in front of the chicane changed by a factor of three (300 \rightarrow 100 mm-mrad in x), discouraging further linac tuning.

Additionally, frequent user requested beam changes in current and bunch length made it necessary to tune the beam emittances up again, which would make it even trickier for smaller emittances. It is assumed that the main root cause for this is that after just steering flat the initial emittance is as high as 1200 mm-mrad, and the

subsequent tuning cancels this with equally large corrections. When these cancelations are not local, or are charge / bunch length dependant, small say 10% variations will create 10% of 1200 mm-mrad = 120 mm-mrad.

So the goal is to localize and reduce emittance increasing effects. For that we try to find and categorize all possible mechanisms, like dispersion, wakefield, RF-kicks, and develop procedures like special steering methods and component alignment.

Goal: Get Linac closer to good emittances with BPMs etc. so the tuning part is less.

1. BPMs
2. Correctors
3. Quads (old BBA: straight orbit)
4. BPM-to-Quad: bowtie plot or Quad change
5. Corrector strength (LOCO, R12 meas.)
6. Lattice (Quad) strength: Oscillation data
7. RF-kicks: a) sin-cos, b) dipole-quadrupole-lens
8. Measure dispersion
9. Measure with different charge (wakefield)
10. Measure with different bunch lengths
11. Others

The different methods (numbers in () below) and their relevance are discussed in the following sections.

STEERING TECHNIQUES

Steering the beam to the center of a BPM (1) gets the beam down the linac relatively fast, but usually ends up with big beam emittances. Additionally we can look at the corrector (2) values along z and check for certain patterns, e.g. stronger values with $+ - +$ might indicate a BPM with a big unreal offset. With our "SVD Steering" we can adjust a gain parameter to prefer BPMs (gain high) or correctors (gain low), but this method just supports what is believed more correct.

The next step is also using the quadrupole (3) strengths in a way to get a straight trajectory. When a BPM reading is say $\Delta x = 1$ mm and the corrector strength is $cor = 0.03$ kG-m, the two can be compared by dividing cor by the quadrupole strength $Q = 20$ kG: $cor/Q = 1.5$ mm. So the beam gets more bend up by the corrector than the $Q\Delta x$ bends it down (focussing magnet). Figure 1 shows an example where the orbit was steered flat (below 0.3 mm) but its corresponding cor/Q -values are up to 1.3 mm. This led to a global alignment of the Linac of up to 7 mm [1]. Equalizing the two locally will give a straight non-bend beam orbit and therefore no dispersion is generated. But an offset in a BPM might indicate also an offset in the RF nearby structure, causing wakefield kicks.

*Work supported by U.S. Department of Energy, Contract DE-AC02-76SF00515.

POSITRON INJECTOR LINAC UPGRADE FOR SUPERKEKB

T. Kamitani*, M. Akemoto, Y. Arakida, D. Arakawa, A. Enomoto, S. Fukuda, K. Furukawa, Y. Higashi, T. Higo, H. Honma, N. Iida, M. Ikeda, E. Kadokura, K. Kakihara, H. Katagiri, M. Kurashina, H. Matsushita, S. Matsumoto, T. Matsumoto, S. Michizono, K. Mikawa, T. Miura, F. Miyahara, T. Mori, H. Nakajima, K. Nakao, T. Natsui, S. Ohsawa, Y. Ogawa, M. Satoh, T. Shidara, A. Shirakawa, T. Suwada, H. Sugimoto, T. Takatomi, T. Takenaka, Y. Yano, K. Yokoyama, M. Yoshida, L. Zang, X. Zhou, KEK, Tsukuba, Japan
D. Satoh, Graduate School of Science and Engineering, Tokyo Inst. of Technology, Tokyo, Japan

Abstract

This paper reports on a present status of a positron injector linac upgrade for SuperKEKB. A development status of a flux concentrator for positron focusing is shown. An influence of offset layout of the flux concentrator and the target on a positron yield is described. Positron capture by L-band and large aperture S-band accelerating structures are compared in a viewpoint of satellite bunch elimination. Beam optical design compatible to electrons and positrons of different beam energies is discussed.

INTRODUCTION

The KEKB-factory is now under an upgrade to SuperKEKB for a forty times higher luminosity [1]. The injector linac is required to supply beams of higher charge and smaller emittance as shown in Table 1.

Table 1: Linac Beam Specifications

	KEKB (e^-/e^+)	SuperKEKB (e^-/e^+)
Injection Energy (GeV)	8.0 / 3.5	7.0 / 4.0
Bunch Intensity (nC)	1.0 / 1.0	5.0 / 4.0
Number of Bunch /pulse	2 / 2	2 / 2
Emittance (μm)	300 / 2100	20 / 92 _[H] :7 _[V]

To generate low emittance electron beams of 5 nC bunch intensity for injection, a photo-cathode RF gun is introduced [2] to replace the existing thermionic gun and the RF bunching section. The electron beams are accelerated up to 7.0 GeV over the entire linac and injected into the HER. Electron beams of 10 nC for positron production will also be generated with the RF gun. In a case high intensity operation of the RF gun is not stable, the thermionic gun is also used and the beams from these two guns are switched. To generate low emittance positron beams, a damping ring (DR) of 136 m circumference is introduced at a side of the linac and connected at the beam switch-yard No.2 (SY2). Beams generated in a positron capture section (PCS) are accelerated up to 1.1 GeV and injected into the DR. Positrons are extracted after 40 ms from the DR, injected back to the linac and accelerated up to 4.0 GeV for

injection to the LER. Energy gain of the positrons from existing six accelerator modules (typically 160 MeV per each module) from the PCS to the SY2 is not sufficient for this 1.1 GeV injection to the DR. The PCS is relocated 40 m upstream to have a sufficient energy margin for the DR. To increase positron beam intensity four times as much, capture efficiency is enhanced in two aspects. At first, an existing 2-T pulsed coil of short field length (45 mm) right behind a positron production target, is replaced with a flux concentrator (FC) type of 5-T pulsed solenoid of long field length (200 mm). An adiabatic matching characteristics of a solenoidal field distribution with a FC, gives wider energy acceptance for positrons. As a second aspect, existing S-band accelerating structures with conventional aperture (21 mm in diameter) used in a solenoidal field of the PCS are replaced with large aperture S-band (LAS) structures (30 mm) or L-band structures (35 mm) to enlarge transverse phase space acceptance. Total length of the PCS is extended from 8 m to 16 m to boost positron beam energy from the PCS from 80 to 120 MeV. This increase of the beam energy at a transition from solenoidal to quadrupole focusing region is effective in reducing beam loss around an optical matching section.

In December of 2013, we will start a preliminary positron beam commissioning of the injector linac within limited operation parameters. A beam commissioning with the DR will be started in February of 2015. Development, fabrication and installation of the components are ongoing to be in time for the schedule.

In the following sections, as topics of significance in the positron injector linac upgrade, flux concentrator development, target protection and offset positron production, large aperture accelerating structures development, satellite bunch elimination and electron/positron compatible optics design are described.

FLUX CONCENTRATOR DEVELOPMENT

Flux concentrator is a pulsed solenoid composed of a primary coil and a copper cylinder with a conical hole inside. Induced eddy current flows through a thin slit to a inner surface and generates a strong field of several Tesla. Achievable field strength is mainly determined by a hole diameter and a primary pulsed current. They are constrained from a required aperture size, a power supply capacity and break-

*E-mail: <takuya.kamitani@kek.jp>

RECENT IMPROVEMENTS TO THE CONTROL OF THE CTF3 HIGH-CURRENT DRIVE BEAM

B. Constance, R. Corsini, D. Gamba, P. K. Skowroński, CERN, Geneva, Switzerland

Abstract

In order to demonstrate the feasibility of the CLIC multi-TeV linear collider option, the drive beam complex at the CLIC Test Facility (CTF3) at CERN is providing high-current electron pulses for a number of related experiments. By means of a system of electron pulse compression and bunch frequency multiplication, a fully loaded, 120 MeV linac is used to generate 140 ns electron pulses of around 28 Amperes. Subsequent deceleration of this high-current drive beam demonstrates principles behind the CLIC acceleration scheme, and produces 12 GHz RF power for experimental purposes. As the facility has progressed toward routine operation, a number of studies aimed at improving the drive beam performance have been carried out. Additional feedbacks, automated steering programs, and improved control of optics and dispersion have contributed to a more stable, reproducible drive beam with consequent benefits for the experiments.

INTRODUCTION

The Compact Linear Collider [1] (CLIC) is a leading contender for the next generation of high energy lepton colliders. As an essential precursor to proceeding with such a facility, the CLIC Test Facility (CTF3) at CERN has been built to demonstrate many of the technologies required for stable drive beam generation and RF power production. The complex consists of a 120 MeV e^- linac, a chicane for bunch length control, a 42 m Delay Loop (DL), an 84 m Combiner Ring (CR) and finally the CLIC Experimental Area (CLEX). A thermionic gun produces 4 Amp pulses of 1.4 μ s, typically at a repetition rate of 0.83 or 1.67 Hz. A sub-harmonic buncher operating at 1.5 GHz, followed by a 3 GHz buncher, generates a beam bunched at half the acceleration frequency. Since energy efficiency is key to the CLIC design, the 3 GHz CTF3 linac operates in a fully loaded configuration. In order to maximise the RF power available, 5.5 μ s pulses from the klystrons are compressed to around 1.4 μ s using resonant cavities, increasing peak power by a factor of two to over 30 MW.

As laid out in the CLIC design, at CTF3 a system of bunch frequency multiplication and pulse compression is used to generate a high-current drive beam. Injection into the DL and CR is achieved using transverse deflecting RF cavities. By coding the beam phase with a series of 180° phase shifts, 140 ns sections of the pulse may be alternately injected or allowed to bypass the DL. On exiting the DL, the delayed sections interleave with those sections bypassing. This results in a train of four 140 ns sub-pulses, sep-

arated by 140 ns, with a current of some 8 Amps and a 3 GHz bunch frequency. These four sub-pulses are then stacked in the CR before extraction to CLEX, where the final 12 GHz pulse is 140 ns long. The combined current is typically around 28 Amps before transport, since some fraction of the charge is lost to satellite bunches in the unused RF buckets.

In CLEX, the combined pulse may be directed to one of two experimental beamlines. The Test Beam Line (TBL) contains at present 12 Power Extraction and Transfer Structures (PETS), with 16 expected by end of the 2012, and is used primarily for studies into the phase and amplitude stability of the produced 12 GHz RF power and the transport of the decelerated drive beam [2]. The second beamline serves the Two-Beam Test Stand (TBTS), an experiment which is also provided a probe e^- beam by the CALIFES accelerator. The probe beam fills the role of the CLIC main beam, allowing for two-beam acceleration studies [3].

OPTICAL MODEL VERIFICATION

Control of the transverse linear optics at CTF3 is achieved using a MAD-X model of the machine. Optical transition radiation screens at key points in the lattice allow measurements of the beam emittance and Twiss parameters using standard quadrupole scan techniques. Based on these measurements, quadrupole currents are rematched using the model predictions to ensure the correct beam parameters at critical locations. Of course, the success of this method depends on the validity of the model.

Discrepancies between the predicted and measured optical functions at some screens inspired a campaign to verify the MAD-X model using beam-based optics measurements. The horizontal and vertical planes were assumed to be uncoupled and treated independently. Using a pair of calibrated dipole corrector magnets separated by a drift length, a series of beam orbits may be injected into the lattice with arbitrary positions and angles. The series of orbits can be chosen in such a way that they map out, or paint, the matched phase space ellipse expected at the location of the second corrector. In effect, each orbit behaves as a macroparticle on the matched ellipse. The orbits evolve as they propagate through the lattice in a way governed by the linear transport matrix, and thus so too does the ellipse they describe. By spacing the orbits at regular intervals covering the full phase space, and observing how the ellipse has changed at some downstream position, information is obtained about all four elements of the two-dimensional transfer matrix.

DESIGN AND OPERATION OF A COMPACT 1 MeV X-BAND LINAC

G. Burt, P.K. Ambattu, C. Lingwood, T. Abram, Cockcroft Institute, Lancaster University, UK
 I. Burrows, P. Corlett, A. Goulden, T. Hartnett, P. Hindley, P.A. McIntosh, K. Middleman,
 Y. Saveliev, R. Smith, C. White, STFC, Daresbury Laboratories, UK

Abstract

A compact 1 MeV linac has been produced at the Cockcroft Institute using X-band RF technology. The linac is powered by a high power X-band magnetron and has a 17 keV 200 mA thermionic gun with a focus electrode for pulsing. A bi-periodic structure with on-axis coupling is used to minimise the radial size of the linac and to reduce the surface electric fields.

INTRODUCTION

Small, low-energy linacs are required by industry for the production of X-rays to be utilised in security applications and for non-destructive testing. Mobile cargo scanning systems used in the security industry typically use S-band (3 GHz) RF linacs to accelerate electrons produced from a pulsed electron gun to the required energy (typically 1-5 MeV depending on the type and thickness of the material to be scanned) [1]. Typically all the power supplies, control electronics and water cooling are placed on the back of a truck along with a robotic arm which will have the linac cavity, electron gun and target attached, along with a substantial amount of lead shielding. For mobile security applications the weight of the linac is critical to the mobility of the linac. Using higher frequency linacs reduces the cavity radius and hence the weight of the lead shielding required. For this reason an ultra-compact 9.3 GHz, 1 MeV linac has been designed at the Cockcroft Institute.

LINAC DESIGN

The linac is to be driven from a 1 MW e2v magnetron. As magnetrons are not very frequency stable the structure must be tolerant to changes in frequency. This is made more difficult by the requirement to have a small iris to have the maximum possible R/Q. In order to increase stability the structure was chosen to work in a $\pi/2$ mode. As every 2nd cell is empty there are two options to keep the R/Q high, to use a side coupled structure or an on-axis coupled bi-periodic structure. As we also want to keep the structure diameter small it was decided to use the latter. The structure is electrically coupled through the iris, this doesn't have as much coupling as magnetic coupling through slots in the wall, but is simpler to manufacture and operate. A 5 mm iris diameter was chosen to give sufficient coupling between the cells.

Although the electron gun is pulsed it has a pulse width that is several thousand RF periods hence it is necessary to bunch the electron beam within the linac cavity before acceleration. The electron beam is injected into the cavity from the gun at a relatively low energy (17 keV) and the electron velocity will not become close to the speed of

light until after several cells of the cavity. This requires the length of each cell to be carefully optimised using beam dynamics codes to track each electron through the cavity such that the synchronous phase varies along the structure. As the electron velocity is dependent on the accelerating gradient, the electric field amplitude must be chosen before optimising the cavity. A peak accelerating gradient of 30 MV/m was chosen as a compromise between structure length and peak surface electric field, and this resulted in a structure with 8 accelerating cells.

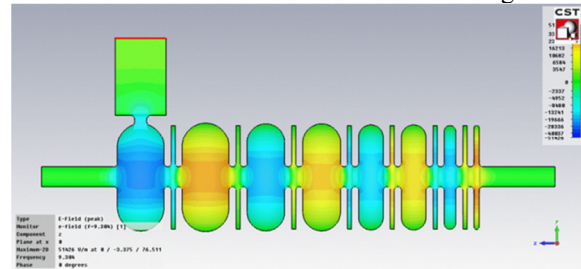


Figure 1: Compact Linac Cavity modelled in CST [4].

Particle tracking including space charge has been performed in ASTRA[2] as well as full PIC simulations in VORPAL [3], shown in Figure 2 and 3. It is observed that space charge forces are quite large in the front end of the linac where the cavity field is very low, resulting in particles spreading and hitting the cavity walls. This however is not expected to cause much heating or radiation as the impact energy is low. As the particles travel further downstream, they get bunched and transversely focused and at the exit of the linac reach 1 MeV and 50 to 70 mA on average which is sufficient to produce the desired range of X-ray dose for many applications.

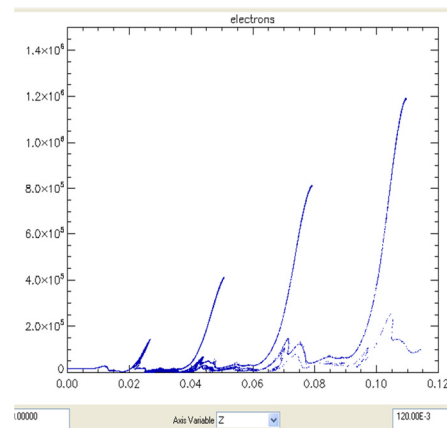


Figure 2: Electron energy, in eV, as a function of longitudinal position in the linac, in metres.

HIGH GRADIENT OPERATION OF 8-GeV C-BAND ACCELERATOR IN SACLA

T. Inagaki[#], T. Sakurai, C. Kondo, Y. Otake, RIKEN SPring-8 Center, Hyogo, 679-5148, Japan.

Abstract

In X-ray free electron laser facility, SACLA, C-band high gradient accelerator was employed in order to shorten the 8-GeV accelerator length. In total, 64 klystrons, 64 RF pulse compressors, and 128 accelerating structures are used in SACLA. Since the C-band accelerator generates high acceleration gradient (nominal 35 MV/m), associated with a high RF breakdown rate, reliability of the high power RF components and the reduction of the trip rate less than several trips per an hour are the key issues for the stable operation. At beginning of beam commissioning in 2011, the trip rate of the C-band accelerator was still high. Major causes of the trips were an RF breakdown in an accelerator cavity and an abnormal discharge in a thyatron tube. After the RF conditioning time of 700 hours, the RF breakdown rate was reduced to be 1/10 comparing with the beginning stage of the RF conditioning. Concerning the thyatron discharge, we confirmed most of the discharges do not influenced to the next pulse generated by a klystron modulator and it can be excluded from the trip items of an interlock system. We currently operate the accelerator with the beam energy as much as 8.5 GeV, and the acceleration gradient of 38 MV/m in average, with an acceptable trip rate of once per 20-30 minutes, which provides stable laser for XFEL user experiments. Availability of the C-band high gradient accelerator for compact accelerator is confirmed.

INTRODUCTION

SACLA (SPring-8 Angstrom Compact Free Electron Laser) [1] is a unique X-ray free electron laser (XFEL) facility, aiming to generate an X-ray laser with a compact electron accelerator and an in-vacuum undulator. The compactness is important to be able to construct within an available space in the SPring-8 campus, and for lower construction costs. In order to shorten the 8 GeV accelerator length, a C-band (5712 MHz) accelerator is employed. A higher frequency is chosen to produce a higher acceleration gradient. The nominal acceleration gradient is about 35 MV/m, which is twice higher than that of conventional S-band accelerators.

Figure 1 shows the configuration of the SACLA accelerator. For the energy from 400 MeV to 1.4 GeV, 12 C-band acceleration units accelerate an electron beam at -48 degree off crest phase, which provides an energy chirp for the following bunch compression chicane BC3. After BC3, the 52 C-band acceleration units accelerate the beam up to the target energy around 5 GeV to 8 GeV, dependent on a laser wavelength.

Since SACLA is the single-pass FEL facility, if only one unit out of 64 makes a trip (interlocked failure), it

surely changes the beam energy and makes a serious influence to the laser properties. For example, when each unit makes one trip per 3 days on average, the beam trip is almost hourly occurred in total. Therefore reduction of the trip rate is the crucial point for stable laser provision.

The beam commissioning was started in March 2011 and the first lasing at a 0.12 nm wavelength was achieved in June [1]. At that time the trip rate was high due to the insufficient conditioning time for RF components [2]. Major causes of these trips were RF breakdown (arcing) in cavities and abnormal discharge (pre-trigger) of thyratrons. Then we lowered the beam energy to 7 GeV, and a pulse repetition rate up to 10 pps, because the beam energy and the repetition rate were not so important for immediate beam commissioning. Instead, a high beam energy of over 8 GeV and low trip rate were required for user runs. Hence we spent much effort to reduce the trip rate. Careful RF conditioning effectively reduced the number of the RF breakdowns. Since March 2012, the SACLA accelerator is stably operated for the user experiments with the energy up to 8.5 GeV and the acceleration gradient of 38 MV/m in 10 pps.

C-BAND ACCELERATOR SYSTEM

Figure 2 shows the configuration of the C-band accelerator system. Two 1.8 m long accelerating structures are connected to a 50 MW pulse klystron with

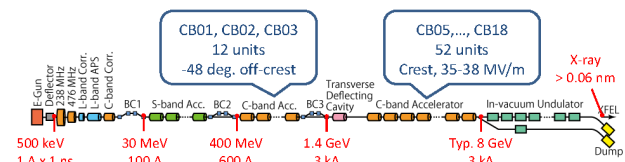


Figure 1: Configuration of the SACLA accelerator.

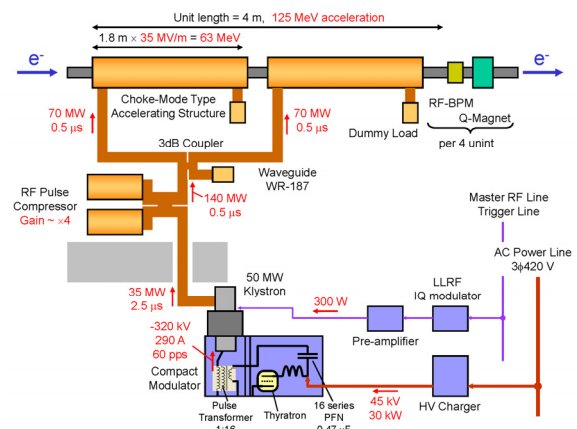


Figure 2: Configuration of the C-band accelerator system. Typical parameters for nominal operation are noted in red.

STUDY OF MICROBUNCHING INSTABILITY IN THE LINAC OF THE SHANGHAI SOFT X-RAY FEL FACILITY*

Dazhang Huang[#], Qiang Gu[†], Meng Zhang, SINAP, Shanghai, China

Abstract

The microbunching instability (μ BI) in the LINAC of a FEL facility has always been an issue which may degrade the electron beam quality. As the result, the whole facility may not be working properly. Therefore, learning how to control and reduce the instability is the key to the success of a FEL project. Shanghai soft X-ray FEL project (SXFEL) has been proposed and the feasibility study is finished. Once it is built, it will be the first X-ray FEL facility in China. In this article, detailed study will be given based on the design parameters of the facility to gain better understanding and control over the possible microbunching instability in SXFEL, which is critical to the success of the FEL project.

INTRODUCTION

The proposed Shanghai soft X-ray FEL facility is planned to be built in a few years. It will be a cascading HGHG FEL facility which will be working at 9 nm soft X-ray band. The electron beam energy of it at the exit of the LINAC will be around 840 MeV, the peak current will be around 600 A. The normalized emittance of the electron beam at the LINAC exit will be 2.0 – 2.5 mm.mrad.

Both the analytical and numerical studies show that μ BI- induced growth of the global/slice energy spread in the LINAC is not ignorable; it also reduces the smoothness of the longitudinal beam current profile. Therefore, without proper control, the instability will be a serious problem and may impair the FEL process thereafter.

One way to control the instability is to increase the uncorrelated energy spread of the beam, which can be done by a laser heater [2][8], and it will also be implemented in SXFEL.

COMPUTATION AND ANALYSIS OF THE INSTABILITY

The basic principle of the microbunching instability in the LINAC of a FEL device has already been well-studied [1][2][3]. It is similar to the amplification mechanism in a klystron amplifier. The initial density modulation or white noise can be transferred into energy modulation by the impedances when the beam is being accelerated including the longitudinal space charge (LSC), coherent synchrotron radiation (CSR) and the structural impedance. When the beam is passing through the dispersive section such as the bunch compressor

(chicane), the energy modulation will be turned back into the much stronger density modulation, in such a way that the microbunching instability is developed. Moreover, the CSR effect in the dispersive section will also form a positive feedback to enhance the instability. More dispersive sections in the LINAC will have more serious μ BI problem. Figure 1 is the schematic description of the instability process.

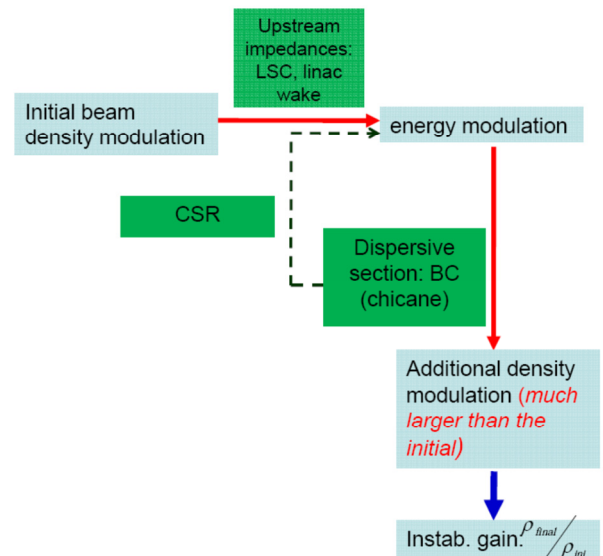


Figure 1: The microbunching instability process.

As discussed above, in the LINAC, the microbunching instability is mainly driven by the LSC, CSR and structural impedances. Since the structural impedance is more complicated and its effect on the instability is not as significant as the other two, in this article, we will be focusing on the microbunching instability introduced by the LSC and the CSR impedance.

The basic layout of the SXFEL LINAC is the following:



Figure 2: The layout of the SXFEL LINAC.

The SXFEL LINAC includes both S-band and C-band accelerating structures, one X-band structure to suppress the non-linear higher order mode (HOM), and two chicane-type bunch compressors (BC1 & BC2). Since there are two bunch compressors, the microbunching instability in the SXFEL LINAC is not negligible. The computation and simulation in the following is based on the design parameters of the LINAC, and the beam parameters out of the injector tracked by PARMELA [4]. Those parameters are listed in table 1.

*Work supported by National Science Foundation of China (NSFC).

Project No. 11275253

[#] huangdazhang@sinap.ac.cn

[†] guqiang@sinap.ac.cn

PHOTOINJECTOR OF THE EBTF/CLARA FACILITY AT DARESBURY

B.L. Militsyn*, D. Angal-Kalinin, N. Bliss, C. Hill, S.P. Jamison, J.K. Jones, J.W. McKenzie, K.J. Middleman, M.D. Roper, B.J.A. Shepherd, R.J. Smith, R. Valizadeh, A.E. Wheelhouse, STFC ASTeC, Daresbury Laboratory, Warrington, WA4 4AD, UK

Abstract

A photoinjector designed for Electron Beam Test Facility (EBTF) and Compact Linear Accelerator for Research and Applications (CLARA), a proposed FEL test facility is described. The photoinjector is based on a 2.5 cell S-band photocathode RF gun operating with a copper photocathode which is driven by a third harmonic of Ti: Sapphire laser (266 nm) installed in dedicated thermally stabilized room. The injector will be operated with laser pulses with energy of up to 2 mJ, a pulse duration of 80 fs RMS and initially a repetition rate of 10 Hz, with the aim of increasing this eventually to 400 Hz. At a field gradient of 100 MV/m provided by a 10 MW klystron, the gun is expected to deliver beam pulses with energy of up to 6 MeV. Bunch length and emittance of electron bunches essentially depend on the bunch charge and vary from 0.1 ps at 20 pC to 5 ps at 200 pC and from 0.2 to 2 mm-mrad respectively. Additional compression of the electron bunches required for CLARA will be provided with a velocity bunching scheme and a dedicated chicane.

INTRODUCTION

The Electron Beam Test Facility (EBTF) is a 6 MeV electron accelerator designed to provide low emittance, short pulse beams to two user stations [1-2]. It will also act as the front end for the proposed CLARA accelerator [3-4]. Initially, the beam for EBTF will be delivered by a 2.5-cell, S-band, normal-conducting, RF gun originally designed for the ALPHA-X project [5]. The front end of EBTF (Fig. 1) has been designed as a photoinjector diagnostics suite to fully characterise 6D phase space of bunches. A variety of YAG screens and

slits will be used to characterise the beam transversely. Longitudinal characterisation of the beam will be provided with energy spectrometer comprising a dipole magnet and a YAG screen. Bunch length will be measured using a Transverse Deflecting Cavity (TDC) [7] to streak the longitudinal position of the particles onto the transverse plane, thus making it viewable on the YAG screen. Furthermore, if the streak is performed in the vertical plane as planned, then passing the beam around the horizontal spectrometer will make the longitudinal phase-space directly viewable on the screen. Combining the TDC with the transverse beam diagnostics will allow time-sliced emittance measurements to be made. For better thermal stability the injector is mounted on an artificial granite support.

PHOTOINJECTOR BEAM DYNAMICS

The EBTF photoinjector has been modelled both in ASTRA and GPT. The simulations presented are at the maximum bunch charge of 250 pC to show the effects of space charge. For the simulations, an intrinsic emittance of 0.9 mm-mrad per mm RMS beam size is used [6]. The simulations presented here are based on the factory measured laser pulse length of 80 fs RMS. An optimisation of the photoinjector beam line was performed looking at the beam parameters at 1, 3, and 10 m from the photocathode to observe their evolution, as shown in Fig. 2. It was found that energy spread is highly sensitive to solenoid strength due to space charge. The energy spread could be controlled by operating further off-crest in the gun, at a phase of -35° from that of maximum energy gain.

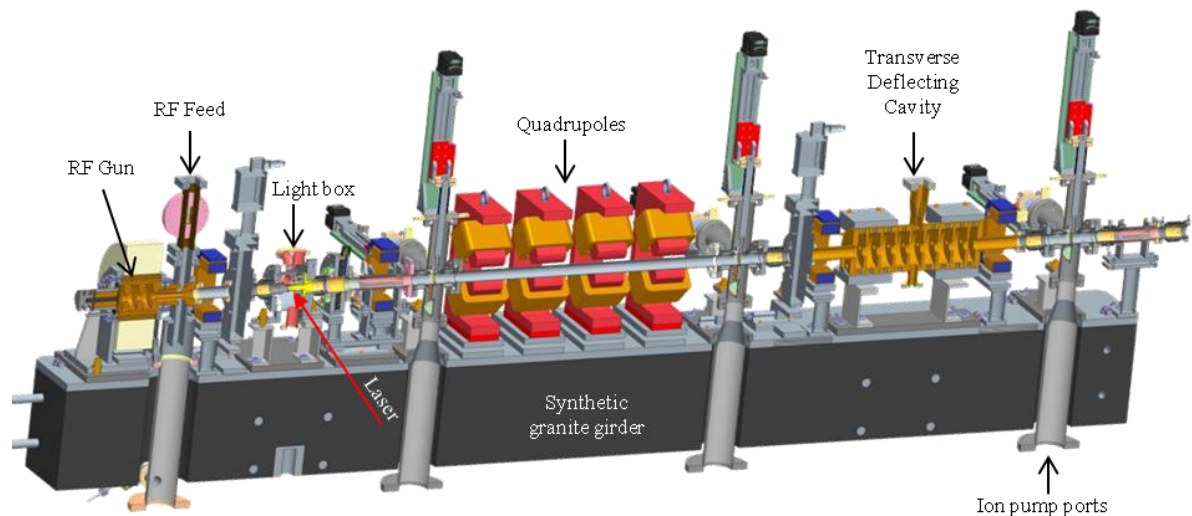


Figure 1: CAD drawing of the EBTF photoinjector

*boris.militsyn@stfc.ac.uk

FIRST RF MEASUREMENT RESULTS FOR THE EUROPEAN XFEL SC CAVITY PRODUCTION

A. Sulimov, P. Borowiec, V. Gubarev, J. Iversen, D. Kostin, G. Kreps, K. Krzysik, A. Matheisen, W.-D. Moeller, D. Reschke, W. Singer, DESY, Notkestrasse 85, 22603 Hamburg, Germany

Abstract

The first reference cavities (RCV) for the European XFEL Project are being tested within the collaboration of Research Instruments (RI), E. ZANON, IFJ-PAN and DESY:

- production and warm RF measurements of cavities and their components at RI and ZANON;
- surface preparation at DESY;
- cold RF tests at DESY by IFJ-PAN.

Purpose of the RCV is to establish a stable cavity fabrication and qualification of the surface preparation infrastructure at industry.

All necessary RF measurements were done, starting with mechanical fabrication in 2011, till the tuning and cold cavity RF tests in 2012.

We present the first results of RF measurements within RCV production for the European XFEL.

INTRODUCTION

For the first time the superconducting (SC) cavities for the XFEL are not only fabricated by industry, but also the full preparation “ready for cold RF test”.

Before starting the (pre-)serial production each supplier of XFEL SC cavities (RI and ZANON) has produced 4 dummy (DCV) and 4 reference (RCV) cavities to qualify the new equipment and check the sequence of the fabrication process.

The main aspects of the RF measurements procedure for the European XFEL were described in [1].

These measurements allow checking the RF quality of the cavity (tuning, cold RF tests) and help to predict the mechanical parameters (length after tuning or deformation during transportation).

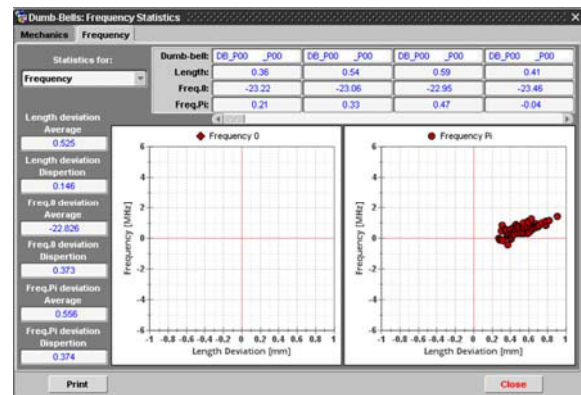
PRODUCTION OF PARTS

The main ideas of cavity parts (dumb-bells (DB) and end-groups (EG)) control are quick tests of their shapes before final cutting and checking the correspondence of the pi-mode frequency to part’s length after trimming.

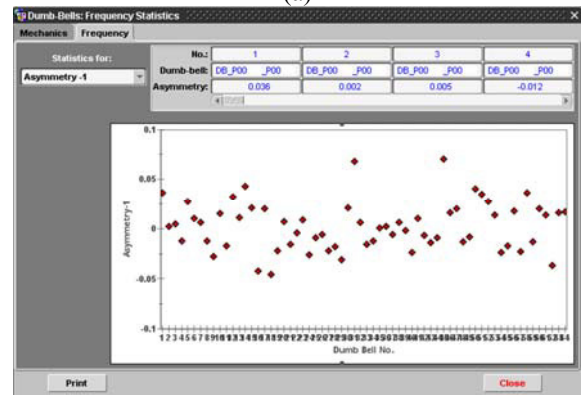
Only extensive 3D shape measurements can give the final results of the cell shape status, but RF measurements can give a prognosis for a series of 32 DB in one hour. The necessary field distribution for the fundamental mode can be obtained relatively easy by cavity tuning even for a wrong shape, but the behaviour of the higher order modes (HOM) spectrum is not predictable in this case. So a wrong shape is more critical and dangerous for HOM and beam dynamics.

The results of final RF measurements, when the parts are ready to be welded together in a cavity, are collected in the XFEL database [2].

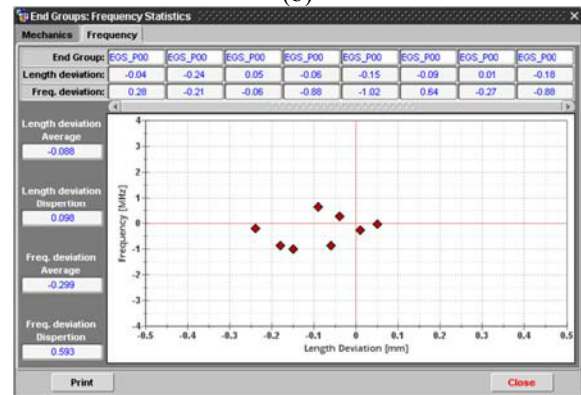
Some examples of statistical values are shown in figure 1: the correspondence of pi-mode frequency to the length for DB (a) and EG (c). As a DB consists of two half-cells the symmetry of their volumes is additionally checked (b). These values are limited by ± 0.1 . In case a DB is out of tolerance, it has to be checked mechanically and additionally compensated or reshaped.



(a)



(b)



(c)

Figure 1: Statistical data for dumb-bells (a, b) and end-groups (c) are in tolerance.

EXPERIMENTAL RESULTS ON THE PHIL PHOTO-INJECTOR TEST STAND AT LAL

R. Roux, F. Blot, J. Brossard, C. Bruni, S. Cavalier, J.-N. Cayla, V. Chaumat, A. Gonnin, M. El Khaldi, P. Lepercq, E. Ngo Mandag, B. Mercier, H. Monard, C. Prevost, V. Soskov, A. Variola, LAL, Université Paris-Sud, CNRS/IN2P3 Orsay, France

Abstract

The PHIL accelerator is in operation since November 2009. Its main goals are the R&D on photo-injectors and to provide electron beam to users. We report on the experimental characterization of the electron beam produced by a 3 GHz 2,5 cells RadioFrequency (RF) gun and operation with a Magnesium photo-cathode.

INTRODUCTION

The PHIL beamline [1,2] is rather simple : the photo-injector at 3 GHz called AlphaX [3] equipped with a couple of solenoids, a pair of steerers, a third solenoid to transport and focus the electron beam and a dipole to analyse the beam energy. The main diagnostics are Integrated Current Transformers (ICT) from the Bergoz Company to measure the charge and YAG screens coupled with a CCD camera to measure the transverse profile of the beam. Main parameters of the electron beam are summarized in table 1.

Table 1: PHIL Electron Beam Parameters, with Cu Photo-Cathode Except Few Runs with Mg*.

Energy (MeV)	< 5
Charge (nC), single pulse	0.01-0.4; 1*
Energy spread (%)	< 1
Emittance (π mmrad)	< 5
Repetition rate (Hz)	5

COMMISSIONING

The RF gun has been commissioned several times rather easily. Generally it took a day to reach 5.5 MW with a RF pulse duration of 2.5 μ s which is equivalent to an accelerating field of 70 MV/m. The RF commissioning has been repeated several times due to some changes of photo-cathode; we tried raw copper, copper polished with diamond paper and magnesium photo-cathodes. The commissioning took place smoothly thanks to the elliptical shape of the irises between the cells. It leads to a ratio of the surface electrical to the accelerating field close to one, thus reducing breakdown hazards.

Dark Current

The dark current or charge has been measured as a function of the accelerating field for raw copper and hand

polished photo-cathodes. It was not possible to compare with the optically polished photo-cathode because of a breakdown in the RF circulator which did not allow us to increase the electrical field above 40 MV/m.

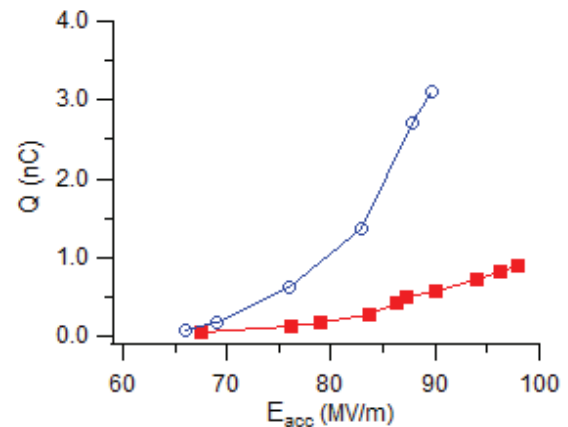


Figure 1: dark charge produced by field emission in the gun for raw copper (round points) and hand polished copper (square points) photo-cathodes.

The reduction of dark current due to the use of a polished photo-cathode is spectacular. At 90 MV/m, the dark charge with polished photo-cathode is 5.5 times lower than in the raw copper case. However, the analysis of these results according to the Fowler-Nordheim formula [4] showed that the field amplification factor, β , has the same order of magnitude, around 100. The lower charge with the polished copper comes actually from a reduction of the emission area.

BEAM PERFORMANCES

To compare performances of different photo-injectors and also for user experiment, it is important to characterize the electron beam as a function of parameters as the relative phase between the RF and the laser, the accelerating gradient, the energy and spot size of the laser.

Dephasing Curve

The best performances of the electron beam are obtained when the electron beam is accelerated near the crest of the RF wave. However there is a range around the optimum phase on which the gun can be operated. Measurements of the beam charge as a function of the relative phase between the laser and the RF is shown in figure 2.

ELECTRON MODEL OF A DOGBONE RLA WITH MULTI-PASS ARCS *

S.A. Bogacz[#], G.A. Krafft, V.S. Morozov, Y.R. Roblin, Jefferson Lab, Newport News, VA, USA
 K.B. Beard, Muons, Inc., Batavia, IL, USA

Abstract

The design of a dogbone Recirculated Linear Accelerator, RLA, with linear-field multi-pass arcs was earlier developed [1] for accelerating muons in a Neutrino Factory and a Muon Collider. It allows for efficient use of expensive RF while the multi-pass arc design based on linear combined-function magnets exhibits a number of advantages over separate-arc or pulsed-arc designs. Such an RLA may have applications going beyond muon acceleration. This paper describes a possible straightforward test of this concept by scaling a GeV scale muon design for electrons. Scaling muon momenta by the muon-to-electron mass ratio leads to a scheme, in which a 4.5 MeV electron beam is injected at the middle of a 3 MeV/pass linac with two double-pass return arcs and is accelerated to 18 MeV in 4.5 passes. All spatial dimensions including the orbit distortion are scaled by a factor of 7.5, which arises from scaling the 200 MHz muon RF to the frequency readily available at CEBAF: 1.5 GHz. The footprint of a complete RLA fits in an area of 25 by 7 m. The scheme utilizes only fixed magnetic

fields including injection and extraction. The hardware requirements are not very demanding, making it straightforward to implement.

MUON RLA WITH TWO-PASS ARCS

A schematic layout of a dog-bone-shaped muon RLA, proposed for future Neutrino Factory [2] is illustrated in the top portion of Fig. 1. Reusing the same linac for multiple (4.5) beam passes provides for a more compact accelerator design and leads to significant cost savings. In the conventional scheme with separate return arcs [4], different energy beams coming out of the linac are separated and directed into appropriate arcs for recirculation. Therefore, each pass through the linac would require a separate fixed-energy arc, increasing the complexity of the RLA. We propose a novel return-arc optics design based on linear combined-function magnets with variable dipole and quadrupole field components, which allows two consecutive passes with very different energies to be transported through the same string of magnets [6].

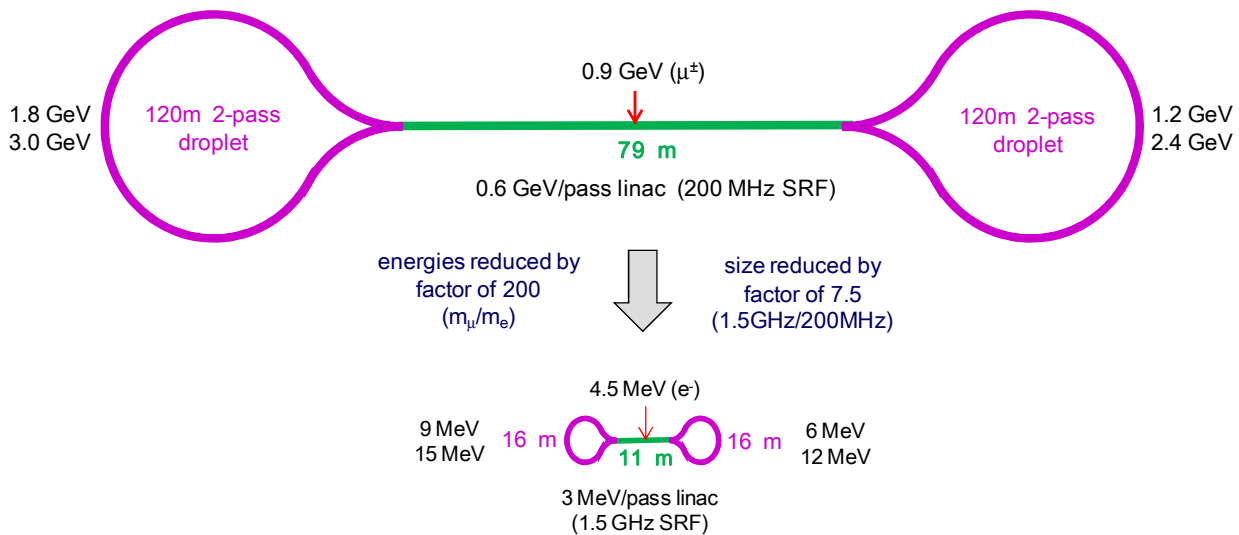


Figure 1: Schematic layout of a GeV-scale muon RLA with two-pass return arcs. A path to an ‘electron model’ is outlined: scaling 3.6 GeV muon RLA to 18 MeV model and replacing 200 MHz RF with a 1.5 GHz CEBAF cavity

* Supported in part by US DOE STTR Grant DE-FG02-08ER86351.
 Notice: Authored by Jefferson Science Associates, LLC under U.S. DOE Contract No. DE-AC05-06OR23177. The U.S. Government retains a non-exclusive, paid-up, irrevocable, world-wide license to publish or reproduce this manuscript for U.S. Government purposes.

[#] bogacz@jlab.org

IN-SITU MEASUREMENT OF BEAM-INDUCED FIELDS IN THE S-BAND ACCELERATING STRUCTURES OF THE DIAMOND LIGHT SOURCE LINAC

C. Christou

Diamond Light Source, Oxfordshire, UK

Abstract

Higher order modes induced by beam in the accelerating structures of the Diamond Light Source pre-injector linac have been directly measured using directional couplers in the high-power waveguide network. These modes are compared with an electromagnetic simulation of the structures and the use of the higher order modes for alignment of the beam to the structure is investigated.

DETECTION OF INDUCED FIELDS

Much work has been done on the analysis of wake fields using dedicated test accelerators, particularly at the ASSET facility in SLAC [1, 2] and the SBTF at DESY [3]. Extension of the method to a low-energy device in a user facility with minimal disturbance to the installed hardware offers scope for cost-effective physics studies and diagnostic development. In the work presented here, wake fields and structure higher order modes are studied in the Diamond Light Source pre-injector linac. This device uses two 5.2 m DESY linac II-type accelerating structures to generate a 100 MeV electron beam suitable for injection into the booster synchrotron [4]: the layout of the linac is shown in Figure 1. The structures are normal-conducting constant gradient designs, operating in the $2\pi/3$ mode at 3 GHz. Each structure is independently powered by a TH2100 klystron amplifier which provides a 5 μ s pulse of around 20 MW five times per second in normal operation.

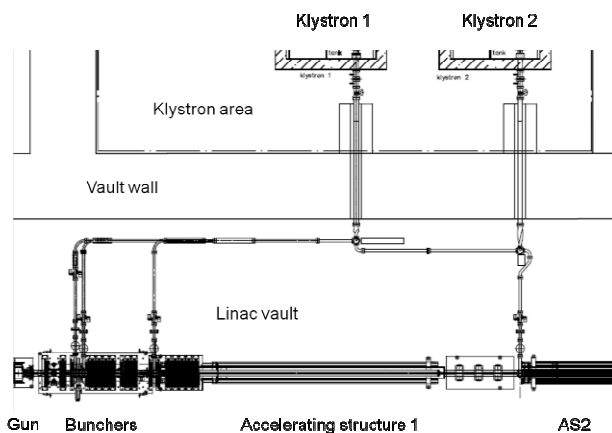


Figure 1: The Diamond linac

Directional couplers, manufactured by Spinner, are mounted in the waveguide network at the exits of the klystrons and at the windows of the accelerating

structures. These couplers measure forward and reverse power and monitor operation and protect the klystrons. If either one of the klystrons is left unpowered, the beam can drift through the accelerating structure and the directional coupler can be used as a monitor of the beam-induced wake fields in the structure.

Signals were discernible on an Agilent DS091304A 13 GHz-bandwidth oscilloscope for beam drifting through bunchers and through both accelerating structures in single-bunch mode and in multibunch mode. The most intense signals were obtained for high charge (1 nC) single bunches drifting through the second accelerating structure at 47 MeV (corresponding to the standard operating gradient of the first accelerating structure) with good temporal bunching; Figure 2 shows an oscilloscope trace recorded for these parameters.

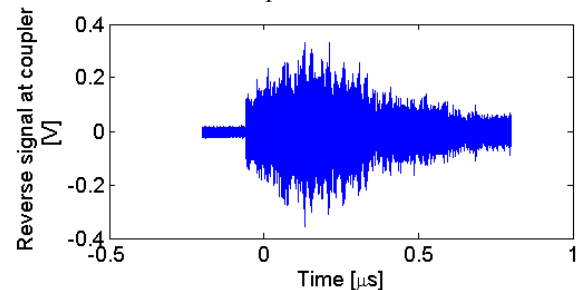


Figure 2: Passage of single bunch detected at the directional coupler in the non-powered RF line

There is rich spectral content to this induced signal, as can be seen in Figure 3. Two measurements are shown in this figure, recorded with and without beam in the structure, establishing that the most intense peaks in the spectrum are the third and fourth harmonics of the 3 GHz RF power fed to the first accelerating structure. The fundamental 3 GHz signal is not transmitted from structure to structure.

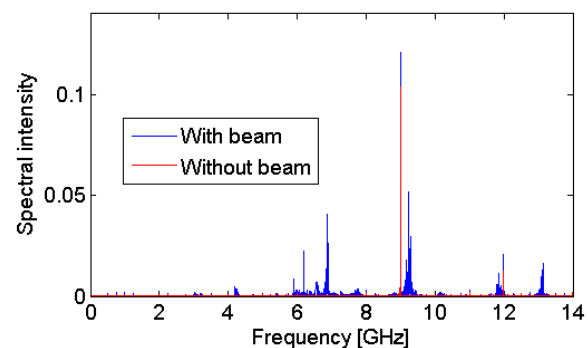


Figure 3: Frequency content of induced pulse

INTEGRATION OF THE EUROPEAN XFEL ACCELERATING MODULES

E. Vogel, S. Barbanotti, J. Branlard, H. Brueck, S. Choroba, L. Hagge, K. Jensch, D. Kaefer, V. Katalev, D. Kostin, L. Lilje, A. Matheisen, W.-D. Moeller, D. Noelle, B. Petersen, J. Prenting, D. Reschke, H. Schlarb, M. Schmoekel, J. Sekutowicz, W. Singer, H. Weise, DESY, Hamburg, Germany, S. Berry, C. Madec, O. Napoly, B. Visentin, CEA, Saclay, France, P. Borowiec, J. Swierblewski, HNINP, Kraków, Poland, A. Bosotti, P. Michelato, INFN, Milan, Italy, W. Kaabi, LAL, Orsay, France, E. Plawski, NCBJ, Świerk, Poland, F. Toral, CIEMAT, Madrid, Spain

Abstract

The production of the 103 superconducting accelerating modules for the European XFEL is an international effort. Institutes and companies from seven different countries (China, France, Germany, Italy, Poland, Russia and Spain), organized in 12 different work packages contribute with parts, capacity for work and facilities to the production of the modules. Currently the series production of the individual parts started or is approaching. Personnel is trained for the assembly and testing of parts and as well for the complete modules. Here we present an overview and the status of all these activities.

INTRODUCTION

In the early 1990s the Tera Electronvolt Superconducting Linear Accelerator (TESLA) collaboration started working on the development of a pioneering superconducting accelerator technology [1]. The concept has proved so successful that it was also chosen for the European XFEL [2].

Each superconducting accelerating module for the European XFEL consists of several parts provided by different work packages (WPs). The core parts are the superconducting 1.3 GHz nine-cell cavities provided by WP04. They are used for beam acceleration. For beam focusing and steering each module contains a superconducting quadrupole magnet from WP-11. A beam position monitor produced by WP-17 is attached to the magnet. The rf power is fed into the cavities via power couplers delivered by WP-05. The frequency tuners from WP-07 are used for keeping the cavities on resonance. Bellows connecting the individual cavities are part of the WP-08, the ‘cold vacuum’, likewise the coupler vacuum system. WP-06 organizes the Higher Order Mode (HOM) and pick up (PU) antennas. All these parts are installed inside the cryostat. The cryostat is also called ‘cold mass’ and part of the WP-03.

The final assembly is done in the responsibility of WP-09 (string assembly) and WP-03 (module assembly) at CEA, Saclay and the final module operation test is performed by WP-10 at the Accelerator Module Test Facility (AMTF) at DESY, Hamburg. Proper rf control in the later accelerator will base on properties measured during the modules tests. This item is the task of WP-02. Before transportation into the XFEL tunnel for installation, each module receives a waveguide system tailored by WP-01 to

the cavity performances.

Providing infrastructure and support needed for parts tracking, quality control and nonconformity handling for all these activities is the task of the WP-40.

SUPERCONDUCTING CAVITIES

More than 800 superconducting TESLA type cavities [3] will be used for the European XFEL. They are mechanically manufactured and surface treated [4] by the two companies Ettore Zanon (EZ) and Research Instruments (RI) and delivered to DESY ready for vertical testing in the AMTF by a Polish team from IFJ-PAN, Krakow. Always eight cavities with similar performance will be put together and shipped to CEA for the string and module assembly.

Both companies manufactured reference cavities which have been surface treated at DESY and vertically tested. These cavities showed promising maximum gradients above 28 MV/m. They are used for the qualification of the companies’ infrastructure created for the cavity treatment (clean room, degreasing and ultrasonic cleaning, HPR, (electro) chemical surface treatment, annealing furnaces, slow venting slow pumping systems etc.). The commissioning of the infrastructure is ongoing. The series delivery to DESY will start in November (RI) and in December (EZ).

COLD MAGNETS

The accelerating modules of the XFEL linac will be equipped with one combined superconducting magnet [5] per module, which consists of a main superferric quadrupole for focusing and two nested corrector dipoles for beam steering. The magnet series production is being done under the supervision of CIEMAT in Spain: ANTEC produces the magnets while Trinos Vacuum Projects takes care of the helium vessel, assembly and tests (electrical, pressure and vacuum). The magnetic measurements are done at DESY as a common German and Polish in-kind contribution. The conduction cooled current leads are produced at CECOM in Italy under DESY supervision while the copper coating of the beam pipe is being done by Galvano-T in Germany.

The three pre-series units have been successfully produced and tested. Green light has been given to series production in June, 2012.

ANALYZING SURFACE ROUGHNESS DEPENDENCE OF LINEAR RF LOSSES *

C. Xu^{1,2#}, M. J. Kelley^{1,2}, C. E. Reece¹

¹Thomas Jefferson National Accelerator Facility, Newport News, VA 23606

²College of William and Mary, Williamsburg, VA 23187

Abstract

Topographic structure on Superconductivity Radio Frequency (SRF) surfaces can contribute additional cavity RF losses describable in terms of surface RF reflectivity and absorption indices of wave scattering theory. At isotropic homogeneous extent, Power Spectrum Density (PSD) of roughness is introduced and quantifies the random surface topographic structure. PSD obtained from different surface treatments of niobium, such as Buffered Chemical Polishing (BCP), Electropolishing (EP), Nano-Mechanical Polishing (NMP) and Barrel Centrifugal Polishing (CBP) are compared. A perturbation model is utilized to calculate the additional rough surface RF losses based on PSD statistical analysis. This model will not consider that superconductor becomes normal conducting at fields higher than transition field. One can calculate the RF power dissipation ratio between rough surface and ideal smooth surface within this field range from linear loss mechanisms.

INTRODUCTION

RF loss induced by roughness is considered in many RF components, such as micro strip transmission line, wave guide and RF resonator. It can be understood as the RF electromagnetic field penetrates the surface and there the induced current will pass and cause RF loss. [1] However, in a RF wave view, the incident wave is reflected, scattered and absorbed by the rough surface. Inside of a resonator, the reflected, scattered wave contributes to standing wave field, while the absorbed RF wave is attributed to the RF surface loss. These two perspectives may both be used to describe the same RF loss.

In a resonator, only several specific RF standing wave modes can exist to meet the boundary condition which is the resonator geometry. The electric and magnetic field at one location is combination a of EM components of those plane waves. Within the resonator, E and M are separated in space and interchange their energy over a distance. Thus the peak E and M field are always not the same location. With special EM setup, TE, TM, TEM are used to describe the EM field direction, if presumed direction is beam axis. In some sense, it is very tedious and difficult to expand the field into plane wave expansion. If so, the incident direction should also be from all directions. Therefore, a RF loss calculation method is required and independent of direction. It also covers all frequencies or wavelengths.

METHODOLOGY

A rough surface will cost more RF loss. [2] One simple reason is that the surface current have more current path. In another word, the RF wave as more radiation absorption surface. This RF loss will contribute into power consumption and aggravate the quality factor.

If we consider a 2D random rough surface $Z = f(x)$ in Fig.1. We can expand the magnetic field into Fourier series as in x and z direction. [3]

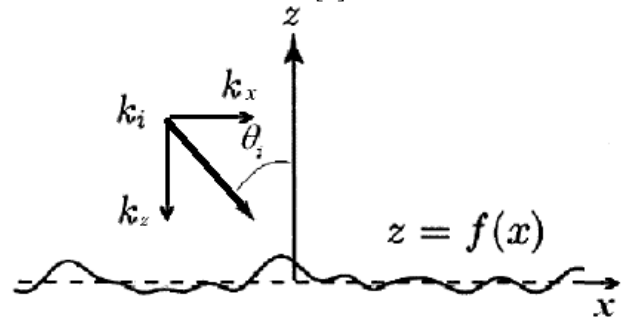


Figure 1: A plane wave incident impinging on a rough surface with incident angle θ_i .

$$\psi(x, z) = \int_{-\infty}^{\infty} dk_x \exp(-jk_x x + jk_{1z} z) \tilde{\psi}(k_x)$$

Where $k_{1z} = \sqrt{k_1^2 - k_x^2}$ and $k_1 = \frac{1-j}{\delta}$. Here δ is the skin depth $\delta = \sqrt{\frac{2}{\omega\mu\sigma}}$ and σ is the superconducting conductivity. The physics behind this equation is that the total magnetic field is combination of field component at each spatial wavelength. In another word, the total magnetic field can be expanded into magnetic contribution from each wavelength in spatial frequency.

If we use a second order small perturbation methods, setting

$$\tilde{\psi}(k_x) = \tilde{\psi}^{(0)}(k_x) + \tilde{\psi}^{(1)}(k_x) + \tilde{\psi}^{(2)}(k_x)$$

In first approximation, a fixed constant magnetic field H_0 is applied on the surface. Thus, the equation above becomes:

$$H_0 = \int_{-\infty}^{\infty} dk_x \exp(-jk_x x + jk_{1z} f(x)) \tilde{\psi}(k_x)$$

Basically, we have done a Fourier transform to redistribute the magnetic field into each surface spatial wavelength in x direction.

By balancing this equation to second order, we obtain:

*Work supported by Jefferson Science Associates. xuchen@jlab.org

LLRF SYSTEM IMPROVEMENT FOR HLS LINAC UPGRADE*

G. Huang, H. Lin, Y. Liu, W. Zhou, K. Jin, D. Jia,
NSRL USTC Anhui Hefei 230029 P. R. China

Abstract

The linac beam energy will be upgraded from 200MeV to 800MeV, in order to realize the full-energy injection of storage ring at Hefei Light Source. This paper introduces the improvement of linac LLRF system, which is composed of phase reference and driver signal transmission and distribution, phase stability system, phase reversal device for SLED. The LLRF prototype has been constructed, and the test results are described in the paper.

800MEV LINAC INTRODUCTION

The layout of 800MeV linac is shown in Figure 1, and the parameters in Table 1.

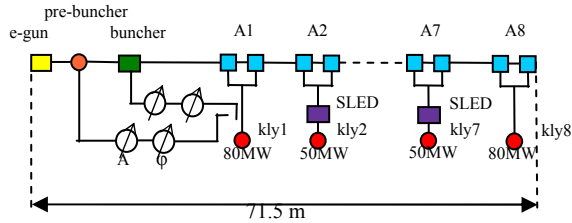


Figure 1: 800MeV Linac layout

Table 1: Linac parameters

	200 MeV	800 MeV
Beam current	50mA	1 A
Beam pulse	0.1-1 μ s	1 ns
Repetition /Hz	0.5	1
Energy spread	0.8%	0.5%
RF freq. / MHz	2856	2856
Acc. section	4	8
klystron	5 (20MW)	6 (50MW)
SLED	0	+2 (80MW)

The 800MeV Linac is composed of injector (prebuncher, buncher) and eight accelerating sections. The prebuncher is a single resonant cavity, and the buncher is a 1-meter travelling wave accelerating construct. Each accelerating section contains two 3-meter constant gradient travelling wave accelerators. The design energy of linac is 1GeV, one accelerating section may stand by when linac beam energy is 800MeV.

PHASE REVERSAL DEVICE FOR SLED

Six SLEDs will be installed in RF stations from the 2nd

*Work supported by NFSC-CAS(11079034)
grhuang@ustc.edu.cn

to 7th. The SLED parameters are listed in table 2, and the test result of the SLED prototype is shown in Figure 2.

Table 2: Parameters of SLED

Freq. /MHz	2856
Q_0	~ 100000
β	5
Insert Loss /dB	0.2
Tuning range /kHz	± 500
Pulse time / μ s	4
Power Gain /dB	7
VSWR	1.05

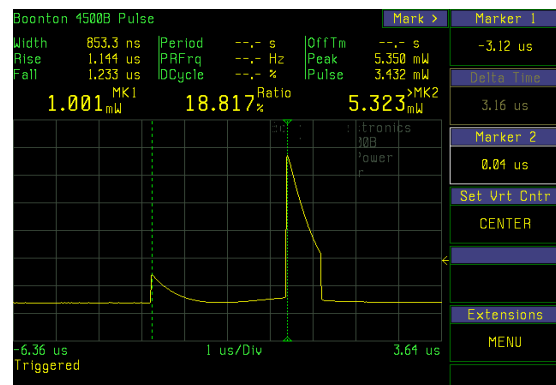


Figure 2: SLED RF output profile

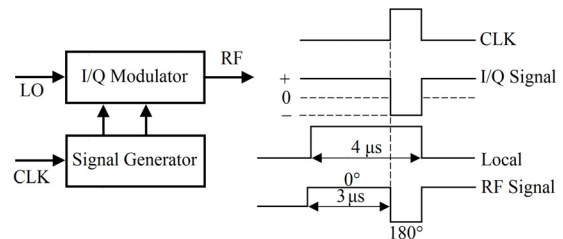


Figure 3: Schematics of the 180° phase reversal system

Table 3: Parameters of IDOH-01-45

Carrier (LO) Freq. /MHz	2000-4000
RF Freq. /MHz	LO ± 100
I & Q Freq. /MHz	DC-100
Conv. Loss /dB	10
Amplitude Balance /dB	1.0
Max. Phase Balance /°	8.0
Isolation /dB	30
VSWR min.	1.5:1

The phase reversal device for SLED showed in figure 3 is consist of fast pulse signal generator and I/Q modulator. The I/Q Modulator is the IDOH-01-45 manufactured by Pulsar Microwave company, and the parameters are

BUNCH-BY-BUNCH PHASE MODULATION FOR LINAC BEAM LOADING COMPENSATION*

G. Huang, Y. Liu, H. Lin, W. Zhou, K. Jin, D. Jia,
NSRL USTC Anhui Hefei 230029 P. R. China

Abstract

If the linac is loaded by a high intensity, long pulse multi-bunch beam, the energy of the beam drops with time during the pulse within the accelerating structure filling time [1, 2]. The bunch phase modulation method is introduced to compensate the beam loading effect. In this method the bunch phase in the RF accelerating field is changed bunch-by-bunch, the bunch energy gain in the RF field gradually grows up, which cancels out the drop due to beam loading. The relationship between the beam phase distribution and the linac parameters is calculated in this paper.

BEAM LOADING EFFECT

When a bunch train passes through a travelling wave accelerating structure, the loaded accelerating fields U_{acc} is defined by [3].

$$U_{acc}(t) = U_{rf}(t) \cdot \cos \varphi - U_b(t) \quad (1)$$

Where U_{rf} is the accelerating voltage conducted by input RF power (unloaded accelerating voltage), φ is the bunch phase in RF field, U_b is the beam loading voltage,

There are two kinds of travelling-wave accelerating structure—constant impedance and constant gradient, normally used in linac. In case of constant impedance structure, the U_{rf} and U_b is expressed by

$$U_b(t) = \begin{cases} I \cdot R_M \left[(L - z - \frac{1}{\alpha})(1 - e^{-\alpha z}) + z \right] & t < T_F \\ I \cdot R_M \cdot L \left(1 - \frac{1 - e^{-\tau}}{\tau} \right) & t \geq T_F \end{cases} \quad (2)$$

$$U_{rf}(t) = \begin{cases} \sqrt{2\alpha P_0 R_M} \cdot L \left(\frac{1 - e^{-\alpha v_g \tau}}{\tau} \right) & t < T_F \\ \sqrt{2\alpha P_0 R_M} \cdot L \left(\frac{1 - e^{-\tau}}{\tau} \right) & t \geq T_F \end{cases} \quad (3)$$

$$z = v_g \cdot t \quad \tau = \alpha L$$

Where I is beam current, T_F is the filling time, R_M is shunt impedance per length, L is the length of accelerating structure, α is attenuation coefficient, P_0 is RF input power, v_g is group velocity.

U_b is the sum of each bunch induced voltage U_i . The attenuation and superposition of bunch induced voltage is shown in Figure 2.

$$U_b = \sum_{i=1}^n U_i \quad (4)$$

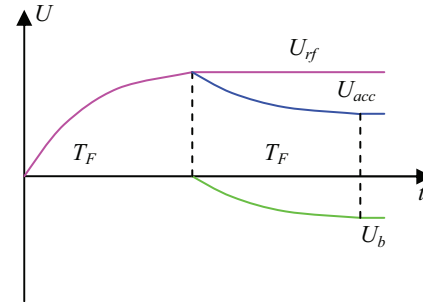


Figure 1: Transient beam loading effect.

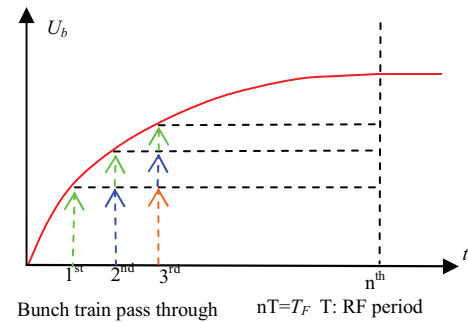


Figure 2: Attenuation and superposition of bunch induced voltage.

Some methods are used to compensate the transient beam loading. For a short pulse beam, the beam is injected before RF power is filled up (early injection method) [4]. In case of long pulse beam, the amplitude or phase of RF power is ramped to keep the U_{acc} constant during the filling time of beam injection [5, 6].

PRINCIPLE OF PHASE MODULATION METHOD

We propose the bunch phase modulation method to compensate the transient beam loading. The idea is that the bunch phase (φ) in the RF accelerating field is changed bunch-by-bunch, therefore the bunch energy gain in the RF field gradually changes. If the trends of the gain change is exactly contrast of the rise up of beam loading, all bunches will obtain the same energy.

Since the bunch phase shifts continuously, the beam loading is the vector superposition of all bunch's induced voltage, which is shown in Figure 4.

*Work supported by NFSC-CAS(11079034)
grhuang@ustc.edu.cn

RF CHARACTERISTIC STUDIES ON THE WHOLE ACCELERATING STRUCTURE FOR THE BEPCII LINEAR ACCELERATOR

S. Pei[#], J. Zhang, M. Hou, X. Li, IHEP, Beijing 100049, P. R. China
 B. Wang, SINAP, Shanghai 201800, P. R. China

Abstract

An accelerating structure is one device to boost the particle energy. 2856 MHz 3 m long travelling wave disk-loaded accelerating structure is applied in BEPCII linac, its RF characteristics are mainly determined by the 84 regular cells located between the input and output couplers. Input and output couplers need to be included when the whole structure RF characteristics are simulated before fabrication; otherwise it would be difficult to obtain the travelling wave fields excited in the whole structure. If the real 3D couplers are modelled during the design process, a large amount of computer resources and time need to be used. However, if the redesigned azimuth symmetric coupler is used to replace the real 3D one during the simulation process, much less computer resources and time are required. With this method proposed here, the simulation results agree well with the theoretically calculated and experimentally measured ones.

INTRODUCTION

The travelling wave (TW) disk-loaded accelerating structure is one of the key components in normal conducting (NC) linear accelerators, such as the BEPC and BEPCII linacs [1, 2], and has been studied for many years. Usually after the dimensions of each cell and the two couplers are finalized, the structure is fabricated and tuned, and then the whole structure RF characteristics are measured by using a vector network analyzer. Before the fabrication, the whole structure RF characteristics are less simulated. This is because of the structural scale (couples of meters long and centimeters in diameter at S-band) and also the personal computer capability limitations.

Because the RF characteristics of the TW structures with several tens of cells are mainly decided by the regular cells, one method to use redesigned power couplers with azimuth symmetry to replace the original 3D waveguide ones in finite element analysis (FEA) can be used. Then the whole structure RF characteristics, such as the electric field amplitude distribution along the structure's axis and the VSWR curve, can be analyzed by using the multi-physics software package ANSYS [3] with much less computer resources required.

In BEPC and BEPCII linear accelerators, 56 units of 3 m long constant gradient disk-loaded accelerating structure are employed. Table 1 shows the main specifications. Fig. 1 shows the schematic of the input/output coupler. To balance the electromagnetic field asymmetry existed in this kind of single feed input/output coupler, appropriate eccentricity offset is applied. If this

[#]peisl@mail.ihep.ac.cn

real coupler shape shown in Fig. 1 is used to simulate the whole structure RF characteristics, at least 1/2 model (180° azimuth angle) needs to be created, which is impossible to do with only one PC.

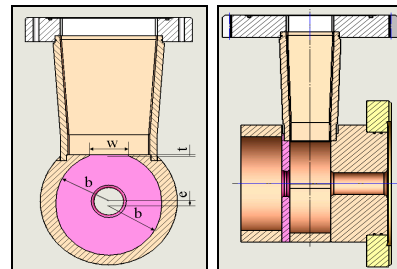


Figure 1: Schematic of the input/output coupler for the accelerating structure of the BEPCII linac. b —radius; e —eccentricity offset; w —coupling aperture width; t —coupling aperture thickness.

Table 1: Main Specifications of the TW Structure for BEPCII Linac

Parameters	Units	Values
Operating frequency	MHz	2856
Operating temperature	°C	45.0±0.1
Number of cells		84 regular cells 2 coupler cells
Section length	mm	3009 (86 cells)
Phase advance per cell		$2\pi/3$
Cell length	mm	34.99
Disk thickness	mm	5.84
Iris diameter ($2a$)	mm	26.231–19.243
Cell diameter ($2b$)	mm	83.460–81.781
Shunt impedance (r_0)	MΩ/m	54.6–63.9
Q factor		13990–13836
Group velocity	v_g/c	0.0208–0.0070
Filling time	ns	830
Attenuation coefficient	Np	0.57

ANSYS SIMULATION METHODOLOGY

The high frequency modal and harmonic solver modules in ANSYS can be used to perform the numerical finite element analysis on the whole structure RF characteristics. By using one program for all of the simulations any problems of meshing inconsistency between different types of software were eliminated.

PROGRESS ON THE DESIGN AND CONSTRUCTION OF THE 100 MeV / 100 kW ELECTRON LINAC FOR THE NSC KIPT NEUTRON SOURCE

S. Pei[#], Y. Chi, G. Pei, S. Wang, J. Cao, M. Hou, W. Liu, Z. Zhou, F. Zhao, R. Liu, X. Kong, J. Zhao, C. Deng, H. Song, J. Liu, J. Yue, Q. Yang, D. He, K. Lv, X. He, Q. Le, X. Li, L. Wang, X. Wang, H. Ma, H. Guo, B. Deng, J. Zhang, J. Zhao, C. Ma, IHEP, Beijing, China

A. Zelinsky, M. Ayzatskiy, V. Kushnir, V. Mytrochenko, I. Karnaukhov, KIPT, Kharkov, Ukraine
Y. Gohar, ANL, Illinois, USA

Abstract

IHEP in China is designing and constructing a 100 MeV / 100 kW electron linac for NSC KIPT, which will be used as the driver of a neutron source based on a subcritical assembly. Recently, the physical design has been finalized. The chicane scheme instead of the RF chopper one has been selected. The mechanical design is on-going and will be finished in the very near future. The injector part of the machine has been installed in the experimental hall #2 of IHEP and is being commissioned and tested. The progress on the machine design and construction are reported, initial testing and commissioning results of the injector are also presented.

INTRODUCTION

One 100 MeV / 100 kW electron linac in NSC KIPT is being constructed, which will be used to drive a neutron source based on a subcritical assembly. This neutron source is a joint project between ANL (USA) and NSC KIPT (Ukraine), and IHEP in China is responsible for the linac (including the transport line to the target) design and construction. Due to the high average beam power of 100 kW and the low beam loss of ~3 kW (including intended and unintended) along the entire linac, the whole machine is being designed and constructed elaborately. Table 1 shows the main parameters of the NSC KIPT linac.

Table 1: Main Parameters of the NSC KIPT Linac

Parameters	Values	Units
RF frequency	2856	MHz
Beam energy / power	100 / 100	MeV / kW
Beam current (max.)	0.6	A
Energy spread (p-to-p)	±4	%
Emittance	5×10^{-7}	m-rad
Beam pulse length	2.7	μs
RF pulse length	3	μs
Pulse repetition rate	625	Hz
Klystron	6×30MW / 50kW	Units
Accelerating structures	10×1.336m	Units
Gun high voltage	~120	kV
Nominal gun beam current	~1–1.2	A

[#]peisl@mail.ihep.ac.cn

ISBN 978-3-95450-122-9

222

The beam energy spread at the linac exit has been changed to ±4% for peak-to-peak rather than 1% for 1σ [1] [2]. This is determined by the energy spread acceptance of the beam transport line with 90° bending angle located at the linac end. With ±4% peak-to-peak energy spread, the beam power losses along the transport line can be reduced to less than 1 kW with ±0.2 mm alignment error, ±2° phasing jitter, ±0.15% modulator voltage jitter, ±0.5% gun high voltage jitter and ±1% RF pulse flatness.

Figure 1 shows the mechanical layout of the linac including the beam transport line. The klystron gallery is located at the downstairs of the accelerator tunnel.

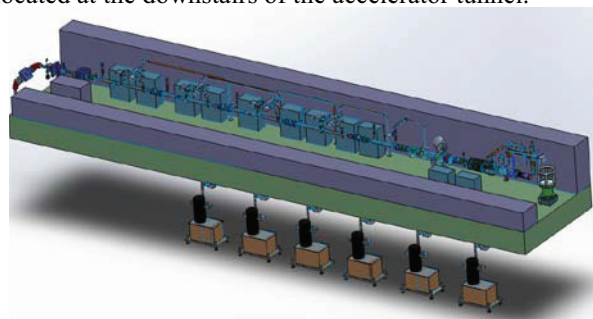


Figure 1: Mechanical layout of the linac including the beam transport line.

INJECTOR DESIGN AND TEST

To get a clean bunch without any satellite electrons in each RF period downstream the chicane system, the phases of all the RF structures (the prebuncher, the buncher and the 1st accelerating structure A0) and the solenoid field distribution in the injector are re-optimized. Finally one can obtain the phase and energy spectrums as shown in Fig. 2, which are appropriate for the beam collimation process with the chicane system to eliminate all particles with very large energy and phase spreads relative the reference particle located at the 0° phase. By this way, the beam power losses along the transport line can be minimized to the largest extent.

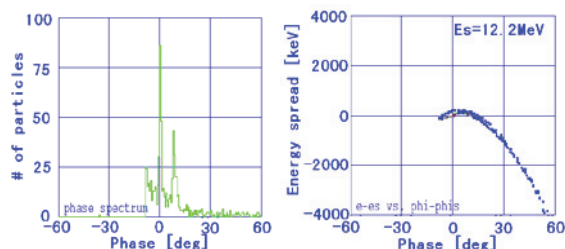


Figure 2: Phase and energy spectrums at the injector exit.

01 Electron Accelerators and Applications

1A Electron Linac Projects

BEAM DYNAMICS SIMULATION AND OPTIMIZATION FOR 10 MeV SUPERCONDUCTING E-LINAC INJECTOR FOR VECC-RIB FACILITY

S.Dechoudhury[#], Vaishali Naik, Alok Chakrabarti, DAE/VECC, Kolkata, India

Gabriel Goh, SFU, Burnaby, British Columbia, Canada

Friedhelm Ames, Richard Baartman, Yu-Chiu Chao, Robert Edward Laxdal,

Marco Marchetto, Lia Merminga, Fang Yan, TRIUMF, British Columbia, Canada

Abstract

In the first phase of ongoing collaboration between VECC (India) and TRIUMF (Canada) a 10 MeV superconducting (SC) electron linac injector will be installed at VECC. This will constitute a 100 keV DC thermionic gun with grid delivering pulsed electron beam at 650 MHz. Owing to low beam energy from the gun, a capture cryomodule (CCM) consisting of two $\beta=1$, 1.3 GHz single cell elliptical cavities will be installed for pre-acceleration of electron beam to around before it enters an Injector Cryomodule (ICM). The ICM consists of one 9-cell $\beta=1$ elliptical cavity that will provide acceleration to 10 MeV. The present paper depicts the beam dynamics simulation and optimization of different parameters for the injector with a realistic simulated beam emittance from the electron gun.

INTRODUCTION

The proposed electron linac would eventually accelerate 10mA CW electron beam (16 pC/bunch) to 50 MeV with 1.3 GHz superconducting RF cavities. The e-Linac consist of a thermionic gun with 650MHz RF modulated grid followed by a buncher and the two cryomodules. The injector cryomodule (ICM) consisting of a single 9-cell 1.3 GHz niobium cavity followed by an accelerator cryomodule (ACM) having two 9-cell cavities [1]. Systematic optimization of the beam line with wide range of objectives and constraints has been carried out for this e-Linac. The TRIUMF machine would also be used in ERL or RLA mode [3]. Keeping this in mind, option of accelerating high brightness beam of 100pC/bunch charge with better longitudinal beam quality has been kept in the base-line design considering a 300 keV thermionic gun [2].

However, for the VECC facility a 100 keV electron gun would be developed for initial tests of the injector [1] because the present site has several limitations. The ICM would be identical to the TRIUMF machine and would be built and tested at TRIUMF and will be shipped to VECC. Since the 100 keV beam with a $\beta \approx 0.55$ is ill suited to be directly injected into the ICM, some pre-acceleration of the beam to an energy ≥ 300 keV will be needed. To achieve this, a capture cryo-module having two independently phased $\beta = 1$ single cell cavities will be added before the Injector Cryo Module (ICM). The beam dynamics optimization of the 10 MeV injector for the VECC e-Linac facility will be presented.

[#] sdc@vecc.gov.in

ELECTRON GUN SIMULATION

The electron gun consists of a cathode with a grid placed 150 micron away from the electron emitting surface, on which the modulating voltage would be applied. First the electrostatic field between electron emitting surface and grid and finally up-to anode was simulated using SIMION [4]. The electric field distribution thus generated was then used in GPT [5] for estimating the longitudinal and transverse emittance of 100keV electron beam. GPT simulation was done for different geometries essentially varying the cathode angle and cathode-anode distance. An optimum gap of 9.5 cm was chosen between the anode and cathode for good beam quality and a robust solution [6]. The conduction angle of the gun was varied in order to estimate the beam structure both longitudinally and transversely for $\pm 16^\circ$ and $\pm 20^\circ$ beam.

For both the cases the bunch charge was 16pC which yields 10mA average current for conduction angle of $\pm 20^\circ$. Two factors are expected to influence transverse emittance growth - temperature of electron emitting surface (1400 K \sim 0.13eV) and influence of grid due to the lens action of the micro holes in the mesh. It can be seen analytically that grid induced emittance dominates over the thermal effect. The "Reiser model" [7] for grid induced emittance cannot be used since the angle is not $\ll 1$. The analytically calculated grid effect was therefore included in the simulation.

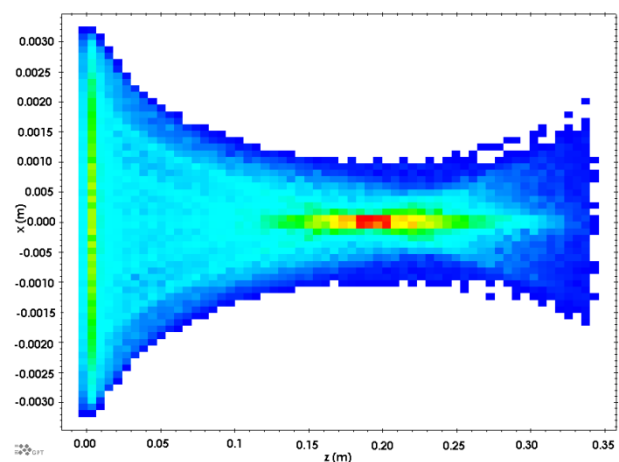


Figure 1: GPT simulated density distribution of 100 keV electron beam with 16pC, conduction angle of $\pm 20^\circ$

1 ms MULTI-BUNCH ELECTRON BEAM ACCELERATION BY A NORMAL CONDUCTING RF GUN AND SUPERCONDUCTING ACCELERATOR*

M. Kuriki[†], H. Iijima, S. Hosoda, HU/AdSM, Higashi-Hiroshima, Japan
 K. Kawase, G. Isoyama, R. Kato, ISIR, Osaka, Japan
 K. Watanabe, H. Hayano, J. Urakawa, KEK, Tsukuba, Japan
 A. Kuramoto, Sokendai, Hayama, Japan
 S. Kashiwagi, Tohoku U., Sendai, Japan
 K. Sakaue, RISE, Tokyo, Japan

Abstract

KEK-STF (Superconducting Test Facility) has been constructed to establish super-conducting accelerator technology for ILC (International Linear Collider). This facility is also used to demonstrate a high-brightness quasi-monochromatic X-ray generation by inverse laser Compton scattering. For the both purposes, high intensity electron beam in multi-bunch and long macro-pulse formats is important. The beam commissioning has been started since February 2012. 1 ms macro pulse train is successfully generated and 40 MeV acceleration was confirmed. We report the progress of the beam commissioning including the basic beam properties.

INTRODUCTION

Aim of KEK-STF(Superconducting Test Facility) is establish the super-conducting accelerator technology for ILC(International Linear Collider) which is a future project of high-energy physics. In STF, a beam acceleration test will be performed with parameters almost equivalent to those in the real ILC, 8.7 mA average current in 0.9 ms length macro-pulse. In super-conducting accelerator, the input RF power and phase should be well controlled by monitoring RF field of the cavity for stable beam acceleration which can be examined only with a real beam. In ILC beam format, the 3.2 nC bunch is repeated with 369 ns spacing up to 0.9 ms. Total number of bunch is 2625 in a macro pulse. We call this operation mode as ILC mode.

Another purpose of STF is MEXT Quantum Beam project, generating high brightness and quasi-monochromatic X-ray by inverse Compton Scattering[1]. In this case, 62 pC bunch is repeated each 6.15 ns up to 1 ms macro pulse. We call this mode as Q-beam mode.

These high-average and long macro pulse beam formats are generated by a normal conducting 1.3 GHz photo-cathode RF gun. It was originally developed by DESY for FLASH/XFEL[2]. The Gun cavity fabricated by FNAL was installed at KEK-STF. The design peak field of the gun is 50 MV/m at 4.5 MW RF power. Cs₂Te photo-cathode is employed for beam generation. It is prepared as thin-film by evaporation on Mo cathode block in a vacuum chamber (preparation chamber)[3].

*Work supported by Quantum Beam Project of MEXT, Japan.

[†] mkuriki@hiroshima-u.ac.jp

By switching laser systems, the macro pulse in ILC mode and Q-beam mode are produced with this RF gun system. A laser system for ILC mode was developed as a collaborative work between KEK, Hiroshima Univ., IAP, and JINR in Russia in 2010[4][5]. This system is based on 3 MHz Yb fiber oscillator. The pulse train is amplified by Nd:YLF laser pumped by flash lump. 266 nm UV pulse train up to 0.9 ms was obtained as 4th harmonics of the fundamental mode. Another laser system based on 162.5 MHz mode-lock oscillator with MOPA system was developed for Q-beam mode[6]. UV laser pulse train was obtained as FHG by LBO and BBO. Typical UV laser energy per bunch is 500nJ or less.

The STF beam line setup for Q-Beam mode is schematically shown in Fig. 1. The beam properties are observed by various beam monitors set in the beam line, FC(Faraday Cup), ICT(Integrated Current Transformer), BPM(Beam Position Monitor), etc. SC accelerator boost up the beam energy up to 40 MeV. The beam size at IP (Interaction Point) for laser-Compton scattering after acceleration is designed to be 10 μ m[7].

In this article, we report successful generation and acceleration of 1 ms macro pulse by this photo-cathode RF gun and super-conducting accelerator.

STF INJECTOR

The injector is based on 1.3 GHz L-band normal conducting RF gun originally developed by DESY for FLASH/XFEL[2]. The design peak field is 47 MV/m with 4.0 MW input RF power. To generate 1 ms long macro pulse with RF gun, suppressing dark-current, i.e. field-emission from the cavity wall, is an important issue. The dark-current should be well below the average beam current in the macro pulse for a stable operation and clear X-ray signal detection from the laser-Compton scattering. The gun cavity conditioning was performed with nominal high power RF processing and ethanol rinse. The detail of the conditioning was explained elsewhere[8][9][3].

The cavity processing was performed in three stages. Between the first and second stages, ethanol rinse for the cavity was performed. The summary of the cavity conditioning was given in Fig.2; The dark current is shown as a function of accelerating field. The dark current was decreased roughly more than an order of magnitude by the

TRIUMF/VECC E-LINAC INJECTOR BEAM TEST

R.E. Laxdal, F. Ames, Y.C. Chao, K. Fong, C. Gong, A. Laxdal, M. Marchetto, W.R. Rawnsley, S. Saminathan, V. Verzilov, Q. Zheng, V. Zvyagintsev, TRIUMF, Vancouver, Canada
 J. Abernathy, D. Karlen, D. Storey, U. of Victoria, Victoria, Canada
 V. Naik, A. Chakrabarti, VECC, Kolkata, India

Abstract

TRIUMF is collaborating with VECC on the design of a 10 MeV injector cryomodule to be used as a front end for a high intensity electron linac. A electron gun and low energy beam transport (LEBT) have been installed in a test area to act as the injector for the cryomodule test. The LEBT includes a wide variety of diagnostics to fully characterize the beam from the gun. A series of beam tests are being conducted during the stage installation. The test configuration details and results of beam tests will be presented.

INTRODUCTION

TRIUMF is now preparing a new high intensity (10mA) 50MeV superconducting electron linear accelerator [1], e-Linac, as a key element of the ARIEL project. In brief the e-Linac consists of five 1.3GHz nine-cell niobium cavities each providing 10MV acceleration with two 50kW power couplers supplying the required beam loaded rf power. The five cavities are housed in three cryomodules, with a single cavity in an injector cryomodule, EINJ, and two identical accelerating cryomodules EACA and EACB with two cavities in each module.

TRIUMF began developing EINJ in 2010 in collaboration with the VECC laboratory in Kolkata. As part of the collaboration two EINJs will be fabricated and beam tested at TRIUMF. One EINJ will be shipped and installed at VECC and the second will be installed in the e-Linac. The initial EINJ is presently in fabrication [2].

A beam test area is being installed in the ISAC-II building to eventually test the two injector cryomodules with beam. The site utilizes the existing ISAC-II cryogenics infrastructure and enables testing of the cryomodules well before the expected availability of the e-Linac cryogenics in 2014. The schedule calls for accelerated beam tests in early 2013. Moreover, the injector test facility provides an ideal proving ground for e-linac design and operation strategies. It duplicates the front-end of the e-linac up to the exit of the injector cryomodule with enhanced diagnostics capability for benchmarking both the performance of the gun but also of the various diagnostics themselves. In addition the test installation allows early demonstration and troubleshooting of various e-Linac sub-systems including MPS, controls, beam modes, safety, LLRF, HPRF, cryogenics and important feedback on beam quality, halo formation and high intensity operation. Commissioning this facility began Nov 2011.

INJECTOR LAYOUT

The test layout, shown in Fig. 1 includes an electron gun, a low energy beam transport (LEBT) complete with a beam diagnostics leg, the EINJ cryomodule, a medium energy beam transport and diagnostic end station (MEBT) and beam dump. Two guns are envisaged. In the first phase (present) a 100kV thermionic gun with rf modulated gridded cathode bias is utilized. The cathode rf drive is at 650MHz providing rf bunches for one of every two accelerating buckets. This will soon be replaced by a 300kV gun also with rf modulated gridded cathode bias at 650MHz. The higher energy is needed to achieve efficient capture in the EINJ while the 100kV gun is perfectly sufficient to characterize the rf modulation and commission the LEBT and diagnostics. In both cases the specified peak current is 10mA, with a bunch length of $\leq \pm 20^\circ$ of 650 MHz (170 ps), a bunch charge of 15.3 pC, an energy spread of $\leq \pm 1$ keV and a transverse emittance of $\leq 30 \mu\text{m}$ normalized to a $2\sigma \times 2\sigma$ cylindrical beam. The rf modulation can also be pulsed to provide a macro duty cycle varying from 0.1% to 99.9% duty cycle at various macro periods.

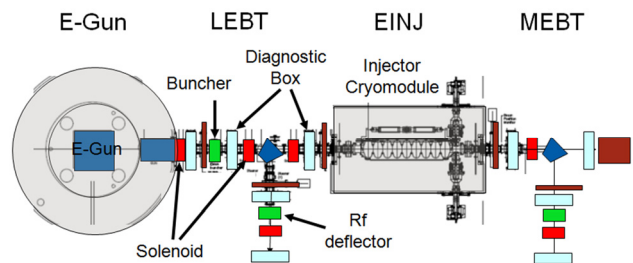


Figure. 1: TRIUMF/VECC beam test configuration.

The LEBT straight section is designed to prepare the beam for acceleration. Three solenoids are used to provide transverse matching and transportation. An initial solenoid provides a waist at the buncher while the two downstream solenoids match the beam to the cryomodule. A 1.3GHz room temperature buncher provides longitudinal matching to the EINJ. An analyzing diagnostic line includes a 90° bending spectrometer, diagnostic boxes and a 1.3GHz rf deflector for bunch length measurements.

DIAGNOSTICS

The diagnostics used in the LEBT are shown in Fig. 2. The diagnostics fit in multi-port custom chambers machined out of solid stainless steel bulk material. The

COMMISSIONING OF THE X-BAND TEST AREA AT SLAC[#]

C.G. Limborg-Deprey*, C. Adolphsen, M. Dunning, S. Gilevich, C. Hast, K. Jobe, D. McCormick, A. Miahnahri, T. Raubenheimer, A.E. Vliks, S. Weathersby, and D. Walz, SLAC, Menlo Park, California, R. Marsh, LLNL, Livermore, California, USA

Abstract

The X-Band Test Area (XTA) was installed in the NLCTA tunnel at SLAC over the spring and summer of 2012. The first gun to be tested is an upgraded version of a 5.5 cell, 200 MV/m peak field X-band gun designed at SLAC in 2003 for a Compton scattering experiment run in ASTA [1]. The first photo-electron beam was generated at the end of July. We report on the results of the first eleven days of commissioning.

X-BAND TEST AREA

The X-Band Test Area (XTA) is a gun test facility located in the SLAC NLCTA tunnel that uses exclusively X-Band technology. In its initial configuration, a 5.5 cell photo-rf gun is followed by a 1-m long accelerator structure (denoted T105) that had been built for NLC rf breakdown studies. Both are driven by a single klystron whose power is compressed (x4 in magnitude) with a SLED-II system. A combination of high power phase shifters and 3 dB hybrids allows the phase and amplitude of the gun and accelerator to be controlled independently.

Simulations [2] have shown that such a photoinjector has great potential to be a compact driver for X-ray FELs [3], for a compact Compton-generated photon source [4] and for Ultra-Fast Electron Diffraction. The main challenges of this technology were expected to be alignment and high dark current levels. Early operation of the facility indicates that these issues are manageable. Detailed tuning and full beam characterization will continue this year.

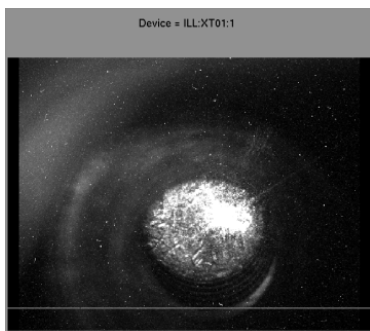


Figure 1: Green alignment laser striking the cathode.

LASER SYSTEM

Photo-Injector Laser

A Spectra Physics Tsunami oscillator locked at 79.3 MHz to the rf master clock provides a 305 mW, 65 nm

[#] Work supported by the U.S. Department of Energy under contract DE-AC02-76SF00515.

*corresponding author: limborg@slac.stanford.edu

bandwidth seed to a Coherent Elite regenerative Ti:Sapphire amplifier. The regenerative amplifier produces 600Hz, 3.5 mJ pulses of IR. This amplifier is shared with another experiment so pulses are sent to the XTA line at 300 Hz. The stretched IR pulses are transported through 26 m of vacuum pipe via relay imaging, yielding 2.6 mJ of IR at the XTA laser table. The IR is then compressed to 70 fs pulses of 1.7 mJ each. A non-linear tripling of the frequency with two 0.3 mm thick BBO crystals yields 120 uJ UV pulses. Finer tuning should provide a higher conversion efficiency, up to 10%, which this is not required initially.

Alignment Laser

A green laser was used to align the optics to the cathode – the image of this laser on the cathode is shown in Fig. 1. This procedure had to be implemented for two reasons: the rf gun does not have a removable cathode and the laser injection chamber was installed after the gun had already been positioned. The UV pulse follows the path defined by the green laser. A leakage of 10% before entering the injection chamber is sent to a virtual cathode camera as shown in Fig. 2.

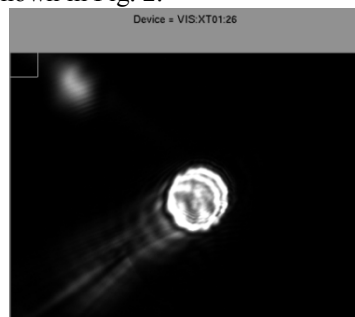


Figure 2: Virtual cathode image (4x6 mm): the main spot is the non-attenuated UV and the upper left spot is the green laser attenuated with filters.

Injection Chamber

The gun irises are 4 mm in radius which translates into a laser half-opening angular aperture of 45 mrad from the last adjustable mirror. Optimum emittance compensation requires having the first accelerator positioned as close as possible to the gun exit. However the injection mirror, which is located in between, has to be far enough away from the cathode to allow a reasonable beam stay-clear. As a compromise, the ~ 45 degree injection mirror was located 53 cm from the cathode plane. It is a 12.7 mm diameter Al substrate mirror with a UV protected Al coating. An extraction mirror for viewing the cathode is located symmetrically opposite of the injection mirror with a 7 mm gap between them. The injection chamber also accommodates a YAG screen combined with a

PERFORMANCE OF THE FIRST C100 CRYOMODULES FOR THE CEBAF 12 GeV UPGRADE PROJECT*

M. Drury, A. Burrill, G. K. Davis, J. Hogan, L. King, F. Marhauser, H. Park, J. Preble, C. E. Reece, R. Rimmer, A. Reilly, H. Wang, and M. Wiseman,
Thomas Jefferson National Accelerator Facility, Newport News, VA 23606 USA

Abstract

The Thomas Jefferson National Accelerator Facility is currently engaged in the 12 GeV Upgrade Project. The goal of the 12 GeV Upgrade is a doubling of the available beam energy of CEBAF from 6 GeV to 12 GeV. This increase in beam energy will be due primarily to the construction and installation of ten “C100” cryomodules in the CEBAF linacs. The C100 cryomodules are designed to deliver an average 108 MV each from strings of eight seven-cell, electropolished, superconducting RF cavities operating at an average accelerating gradient of 19.2 MV/m. The new cryomodules fit in the same available linac space as the original CEBAF 20 MV cryomodules. Cryomodule production started in September 2010. Initial Acceptance Testing started in June 2011. Four C100 cryomodules were installed and tested from August 2011 through July 2012. The first two of these cryomodules were successfully operated during the last period of the CEBAF 6 GeV era, which ended in May 2012. This paper will present the results of Acceptance Testing and Commissioning of the C100 style cryomodules to date.

INTRODUCTION

Since July 2011, six C100 cryomodules have been delivered to the Cryomodule Test Facility (CMTF) for Acceptance Testing. Four of these cryomodules have been installed in the South Linac of CEBAF and commissioned. Two of these, C100-1 and C100-2, have been operated with beam during the final 6 GeV operations period for CEBAF which started in November 2011 and ended in May 2012.

Each cryomodule goes through two testing cycles, acceptance testing prior to installation in the linac and a final commissioning after installation.

Acceptance testing is generally a more comprehensive set of tests than the final commissioning and is meant to uncover any major problems before delivery to the linac. An example of such a problem would be the failure of an instrumentation feedthru during cooldown that leads to the loss of insulating vacuum. Such problems are more easily addressed while the cryomodule is in the CMTF.

During acceptance testing, each cavity is tested to insure proper operation of the mechanical and piezo tuners. Low power measurements using a network analyser are made to characterize the seven passbands of each cavity once the cavities have been tuned to 1497.000 MHz. The higher order modes of each cavity are also

characterized at low power. Each cavity is then characterized in terms of maximum gradient, field emission, and unloaded Q (Q_0). Measurements of microphonics, pressure sensitivity, static Lorentz coefficients and static heat loads are also conducted.

Once the cryomodule has been installed in a linac, it is commissioned. Commissioning consists of a subset of the acceptance tests. The focus for commissioning is determining stable operating gradients, measuring field emitted x-ray production, Q_0 and microphonics.

MICROPHONICS

The measurement of cavity detuning due to external vibration sources is conducted in both the CMTF and in the tunnel. The results of these measurements, however, are location and time dependent. We now know that the CMTF has a large number of vibration sources that are not present in the tunnel environment. This paper will focus on measurements made on installed cryomodules.

A maximum peak detuning of 25 Hz was budgeted for the C100 cavities. Microphonics testing of the first unit (C100-1) met design goals, but results were higher than expected based on prototype testing. C100-1 as measured during operation in the CEBAF tunnel ranged as high as 21 Hz peak detuning during a 500 second sample time period [1]. While within the specification, the results were higher than predicted. These results led to a modification of the mechanical tuner system in order to gain margin. The tuner modification was first installed on the cavities in C100-4. Thicker plates at either end of the tuning structure led to an average reduction in peak detuning of 42% [1].

TUNING SENSITIVITY

Two other properties related to cavity detuning are measured during Acceptance testing. These are pressure sensitivity and the static Lorentz coefficient. As Tables 1 and 2 illustrate, these properties were also affected by the tuner modifications.

Table 1: Pressure Sensitivity (Hz / torr)

	C100-1	C100-2	C100-3	C100-4	C100-5
1	435	404	420	250	254
2	322	323	352	226	234
3	300	357	323	215	203
4	252	321	355	200	188
5	273	356	323	205	183
6	314	338	325	230	203
7		379	355	213	214
8		399	426	243	243

* Authored by Jefferson Science Associates, LLC under U.S. DOE Contract No. DE-AC05-06OR23177.

VIBRATION RESPONSE TESTING OF THE CEBAF 12 GeV UPGRADE CRYOMODULES*

K. Davis, J. Matalевич, T. Powers, and M. Wiseman

Thomas Jefferson National Accelerator Facility, Newport News, VA 23606, USA

Abstract

The CEBAF 12 GeV upgrade project includes 80 new 7-cell cavities to form 10 cryomodules. These cryomodules were tested during production to characterize their microphonic response *in situ*. For several early cryomodules, detailed (vibration) modal studies of the cryomodule string were performed during the assembly process to identify the structural contributors to the measured cryomodule microphonic response. Structural modifications were then modelled, implemented, and verified by subsequent modal testing and *in-situ* microphonic response testing. Interim and latest results from this multi-stage process will be reviewed.

VIBRATION TEST PROGRAM

A vibration test program was conducted during construction of the first C100 cryomodules, with the goal of improving the operational vibration response of the cryomodules. Beginning with C100-4, a simple modification was introduced that reduces the peak microphonic detuning to less than one-half of the original project design requirements.

The 12 GeV project “budgeted” for 25 Hz peak total detuning (4 Hz static plus 21 Hz dynamic) based on the available klystron power (13 kW), the design Q_{ext} (3.2×10^7) for the fundamental power couplers, and maximum beam load (465 μA) [1]. Tuner performance allowed the static detuning budget to be reduced, allowing the full 25 Hz for the peak dynamic detuning. Operational experience in CEBAF has established a 6 \times rule-of-thumb between standard deviation to peak detuning, giving us approximately 4.2 Hz rms detuning (one σ , assuming a Gaussian distribution).

Commissioning of the cryomodules in CEBAF includes measurement of the ambient microphonic response of each cavity in the cryomodule using established procedures and test equipment [2]. Microphonics testing of the first unit (C100-1) met design goals marginally, but results were higher than expected based on prototype testing. C100-1, as measured during operation in the CEBAF tunnel ranged as high as 21 Hz peak detuning over a 500 second time period. Early measurements taken in the cryomodule test facility were even higher, but were eventually attributed to anomalous local driving sources in that facility. The last full upgrade-style pre-

production cryomodule (“Renaissance”) measured less than 15 Hz peak detuning for all cavities in the cryomodule test facility (historically, half this amplitude would be expected in the CEBAF tunnel due to the different vibration environment found there). The most relevant design changes between the two modules comprised removal of the stiffening rings from the cavity design and a completely different tuner design.

A typical spectrum from one of the noisier cavities in the first production cryomodule (C100-1) is shown in Figure 1. The spectrum is dominated by the peak at approximately 10.5 Hz. This peak shows up in the spectrum of all eight cavities, and is typically highest in amplitude in the middle of the string (cavities 4 and 5), becoming lower in amplitude as you move out to the ends of the string (cavities 1 and 8).

Vibration testing of the CEBAF 12 GeV upgrade cryomodules comprised FEA modelling, modal testing of cryomodule components, and operational RF testing of the completed, cold cryomodules. The end goal was to improve our understanding of the vibrational response of the cryomodule to the extent that it affects RF performance, and to improve that performance with minimal risk to the 12 GeV project.

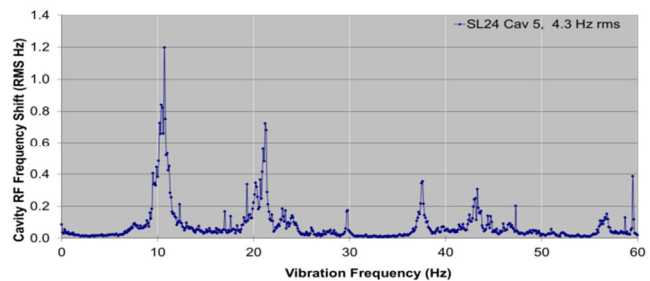


Figure 1: Spectra of Baseline (C100-1) Design

FEA Modelling

ANSYS™ finite element analysis software was used to create a 1-D simplified model of the string assembly. Once the model was validated against the modal test data, the model was used to vet various proposed design modifications including stiffening inside the cavity helium vessels, adding damping to the cavity string assembly, and changes to the cavity tuner. The conclusion of this analysis was that the tuner pivot plates were the least stiff component in the tuner assembly. Stiffening the pivot plate was judged to present low schedule, budget, and technical risk.

* Authored by Jefferson Science Associates, LLC under U.S. DOE Contract No. DE-AC05-06OR23177. The U.S. Government retains a non-exclusive, paid-up, irrevocable, world-wide license to publish or reproduce this manuscript for U.S. Government purposes.

STABILIZATION OF THE BEAM INTENSITY IN THE LINAC AT THE CTF3 CLIC TEST FACILITY

A. Dubrovskiy, JINR, Dubna, Russia
 F. Tecker, CERN, Geneva, Switzerland
 B.N. Bathe, S. Srivastava, BARC, Mumbai, India

Abstract

A new electron beam stabilization system has been introduced in CTF3 in order to open new possibilities for CLIC beam studies in ultra-stable conditions and to provide a sustainable tool to keep the beam intensity and energy at its reference values for long term operations. The stabilization system is based on a pulse-to-pulse feedback control of the electron gun to compensate intensity deviations measured at the end of the injector and at the beginning of the linac. Thereby it introduces negligible beam distortions at the end of the linac and it significantly reduces energy deviations. A self-calibration mechanism has been developed to automatically configure the feedback controller for the optimum performance. The residual intensity jitter of 0.045% of the stabilized beam was measured whereas the CLIC requirement is 0.075%.

INTRODUCTION

CTF3 is a test facility, which is extensively used to uncover new frontiers of the Compact Linear Collider (CLIC) and to develop new technologies of normal conducting linear accelerators [1, 2]. In spite that the feasibility of most of the critical CLIC components has been demonstrated the demands on the beam with parameters closer to the CLIC ones are only rising [3]. The quality, the performance and the relevance to CLIC of each beam shot reduces with the beam deviation from the nominal parameters. In CLIC the beam stability and reproducibility are essential properties and they are required in order to keep the maximum luminosity up to $5.9 \times 10^{34} \text{ cm}^{-2} \text{ s}^{-1}$ at energies from 500 GeV to 3TeV during 20 years of high energy experiments [4]. The beam stability in CTF3 needs to be improved in order to meet CLIC requirements.

DRIVE BEAM GENERATION

In CTF3 an electron beam with the intensity of 4.5 A and the pulse length of 1.5 μs is created by a thermionic

gun, bunched at 1.5 GHz or 3 GHz in the bunching system and then pre-accelerated up to 20 MeV (see Fig. 1). After the injector the beam passes through the cleaning chicane, where low energy particles are eliminated and the bunch length is reduced. The beam of 4.0 A with a low energy spread is injected into the linac. It is accelerated in the fully loaded mode at the average gradient of 7 MV/m up to 125 MeV. Then the beam goes through the stretching chicane, where the bunch length is increased. After that the beam goes around the delay loop and combiner ring, where the intensity is increased by the factor four or eight. The generated high-intensity, high-energy beam is delivered to the tests lines, where the beam is most required to be stable.

BEAM STABILITY OUTLINES

Beam current variations and drifts at the level of 10^{-4} in CTF3 cannot be associated with any one particular device as dominant source of influence. Apparently, it is a combination of imperfections of all components together: the electron gun, RF sources and the current control of magnets. On top of this each of components changes its properties due to fatigue processes, temperature variations and unknown sources. This study is limited to the consideration of the treatment of integrated deviations only in the linac.

The intensity and energy stabilities are the main properties of the beam, which are responsible for the stable pulse-to-pulse beam combination and delivery to the tests areas. In the fully loaded operation the beam energy deviation at the end of the linac can be approximated as follows:

$$\Delta E \propto -\frac{1}{2} I_L \Delta \phi_L^2 - \Delta I_L + \frac{I_L}{E_L} \Delta E_I, \quad (1)$$

where I_L and ϕ_L – the intensity and phase at the beginning of the linac and E_I is the energy at the end of the injector. The beam phase and intensity deviations propagate from the injector to the linac and they are coupled through the energy deviation in the cleaning chicane:

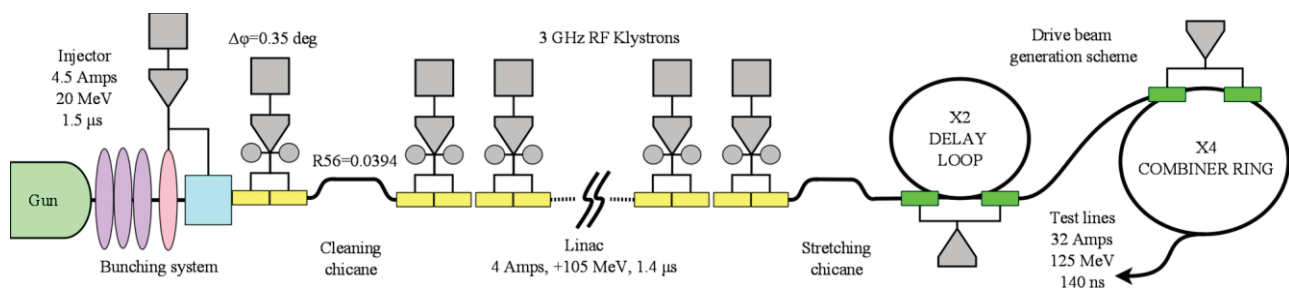


Figure 1: CTF3 layout.

HIGH POWER COUPLER TEST FOR TRIUMF E-linac SC CAVITIES

A.K. Mitra, Z. Ang, S. Calic, P. Harmer, S. Koscielniak, R.E Laxdal, W.R. Rawnsley, R. Shanks
TRIUMF, 4004 Wesbrook Mall, Vancouver, BC, Canada, V6T 2A3

Abstract

TRIUMF has been funded to build an electron linac with a final energy of 50 MeV and 500 kW beam power using TESLA type 9-cell superconducting cavities operating at 1.3 GHz at 2 K [1]. The e-linac consists of an electron gun, buncher cavity, injector cryomodule (ICM), and two accelerator cryomodules (ACMs). The ICM has one 9-cell cavity whereas each of the ACMs contains two 9-cell cavities. One ICM and one ACM are scheduled to be installed by 2014. Six power couplers, each rated for 60 kW CW, have been procured for three cavities. The ICM will be fed by a 30 kW CW Inductive Output Tube (IOT) and each ACM will be powered by a 290 kW CW klystron. Before installing the power couplers with the cavities, they are to be assembled and conditioned with a high power RF source. A power coupler test station has been built and tests of two power couplers have begun. A 30 kW IOT has been commissioned to full output power and it will be used for the power coupler tests. In this paper, test results of the RF conditioning of the power couplers in pulse and CW mode will be described.

is on the order of 10^{-9} mbar and the warm window is a safeguard in the event of a failure of the cold window. Since the waveguide box and the couplers are at room temperature, the CW power applied to the couplers is kept to a level < 10 kW so as to limit the temperature of the inner conductor to 80 °C maximum. The couplers have Mega Industries WR650 coaxial to waveguide transitions which are at atmospheric pressure.

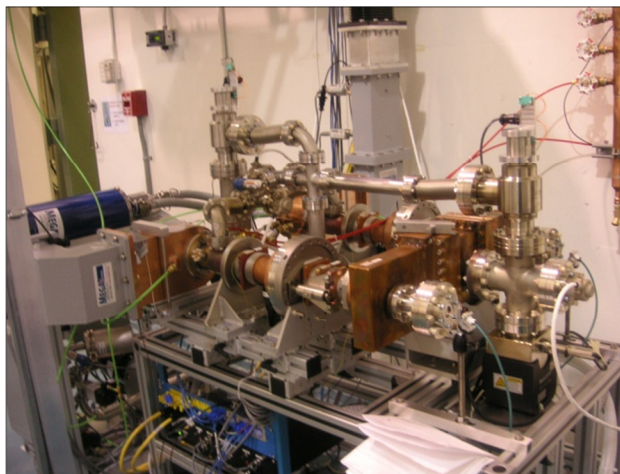


Figure 2: The power coupler test set up.

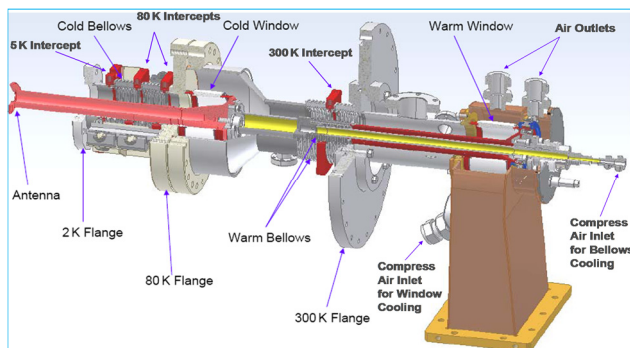


Figure 1: The CPI coupler is based on the Cornell 60 kW TTF-III coupler design.

INTRODUCTION

The power couplers that are being tested are manufactured by CPI, USA and have been adapted from the Cornell coupler shown in figure 1. The couplers, prior to installation with the accelerating cavities, are to be fully RF conditioned. A 30 kW IOT amplifier has been tested to full power and it will be used for RF conditioning of the couplers in both CW and pulse mode. Two couplers are mounted on to a waveguide box which has been designed such that RF power can be transmitted from the input coupler through the waveguide box and out through a second coupler to a 50 Ω waveguide load with minimum standing wave [2]. The coupler station is shown in figure 2. Each coupler has two ceramic windows, one cold and one warm. The cold window is the barrier for the ultra high vacuum pressure inside the SRF cavities which

HIGH POWER TEST OF COUPLERS

The waveguide box was baked and found to be leak tight. The cold windows and the waveguide box were assembled in a clean room environment and leak checked. The warm window and waveguide to coaxial transition were assembled on the coupler test stand and all monitoring and instrumentation were attached.

Signal Level Measurement

The strength of the coupling to the waveguide box can be varied by moving the inner conductors of the couplers. Both couplers are adjusted for best matching (minimum VSWR). Measured values of S11 and S21 are 1.065:1 and 0.166 dB respectively. From the S21 measurement, the power loss in the two couplers and the waveguide box in total will be 39 W for an input power of 1 kW. Hence no cooling is required. However for 10 kW input power, the power loss increases to 390 W which requires cooling if run for a long time.

Interlocks and Monitoring

The vacuum system for the coupler test stand uses two systems; one vacuum common to the cold windows of the couplers and the waveguide box and the second system common to both of the warm windows of the couplers.

NOVEL TECHNIQUE OF SUPPRESSING TBBU IN HIGH-ENERGY ERLS*

Vladimir N. Litvinenko [#], Brookhaven National Laboratory, Upton, NY, USA
 Department of Physics and Astronomy, Stony Brook University, Stony Brook, NY, USA

Abstract

Energy recovery linacs (ERLs) is an emerging generation of accelerators that promise to revolutionize the fields of high-energy physics and photon sciences. These accelerators combine the advantages of linear accelerators with that of storage rings, and augur the delivery of electron beams of unprecedented power and quality. However, one potential weakness of these devices is transverse beam break-up instability that could severely limit the available beam current. In this paper, I propose a novel method of suppressing these dangerous effects using the chromaticity of the transverse motion.

In this short paper I am able only to touch the surface of the method and a complete description of the method with all relevant derivations can be found in [1].

INTRODUCTION

Energy-recovery linacs (ERLs, see Fig.1) belong to a family of recirculating linacs (RLs) that accelerate a beam of charged particles multiple times in the same linear accelerator, accumulating the beam's energy on each pass.

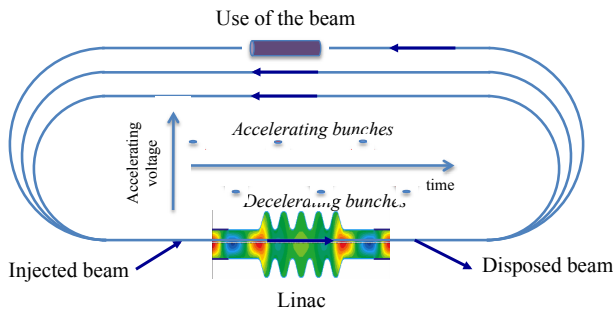


Figure 1: A sketch of a three-pass ERL.

One main challenge for these accelerators is the transverse beam break-up instability (TBBU) that especially is severe for SRF recirculating linacs. Early experiments with recirculating SRF accelerators at Stanford [2] and Illinois [3], where this instability occurred at a few microamperes of the average beam current, highlighted this problem. Dipole high-order modes (HOMs) of the SRF cavities were identified as the culprits driving this instability [4-5], and several remedies were developed for raising this threshold [6].

Detailed theoretical approaches and TBBU simulation programs were developed in the late 80s [7-9]. The renewed interest also stimulated refinements of the TBBU

theory, simulation programs [10-12] and their experimental verification [13] all are driven by the need for high current ERLs, and also by the rewards of resolving this complex problem. Nevertheless, strong damping of HOMs in SRF linacs while maintaining high accelerating gradients remains one of the major unsolved issues. In the general ERL case, we can write a complete matrix of dispersion relations [7-12], but an analytical solution of the TBBU's instability threshold can be derived only for a single HOM mode, and a single-pass ERL, and as detailed in [5]:

$$I_{th} = \frac{2c^2}{e R_g \cdot Q \cdot \omega} \cdot \frac{1}{T_{12} \sin(\omega t_r)} \quad (1)$$

where c is the speed of the light, e is the elementary charge, $R_g \cdot Q$ is the HOM's impedance (measured in Ω), ω is its frequency, and t_r is the beam's travel time through the returning loop. Since there are many HOM modes in the cavities encompassing a large range of the spectrum, there can be modes with $|\sin(\omega t_r)| \sim 1$; then, the only meaningful way of increasing the threshold is by reducing the values of Q and the $|T_{12}|$. As shown in [10], eq. (66), in an ERL with N passes through its linac, we can estimate the TBBU threshold by

$$I_{th} = \frac{2c^2}{e R_g \cdot Q \cdot \omega} \cdot \frac{1}{\sum_{J=1}^{2N} \sum_{I=J+1}^{2N} T^{IJ} \sin \omega(t_I - t_J)}, \quad (2)$$

where $T^{IJ} \equiv T_{12}(s_J | s_I)$ is the element of transport matrix between the J^{th} and I^{th} pass through the linac. Analyzing eq. (3) the authors of ref. [10] offered their natural conjecture that the TBBU threshold scales as follows:

$$I_{th} \propto \left(R_g \cdot Q \cdot N^2 \langle |T^{IJ}| \rangle \right)^{-1}. \quad (3)$$

The unfavorable scaling discussed above may have major implications on the cost of a high-energy ERL. Since an SRF linac usually more expensive than magnetic elements, cost-effective solutions [14-16] lead to three- to six-pass ERLs. If the current in such ERL designs suffer from severe beam current limitation, then the extent of their use and their energy reach will be restricted.

One way of resolving these confines lies in reducing the Q of all dangerous HOMs by developing complex HOM-damping schemes, and in addition, circumscribing the number of cells per linac module so to avoid trapping high- Q HOMs.

The other way of increasing the threshold current is by lowering $\langle |T^{IJ}| \rangle$. The latter is the topic of this paper.

*Work supported by Brookhaven Science Associates under Contract No. DE-AC02-98CH10886 with the U.S. DOE
[#]vl@bnl.gov

THE LINEAR ACCELERATING STRUCTURE DEVELOPMENT FOR HLS UPGRADE *

K. Jin, S. C. Zhang, Y. L. Hong, G. R. Huang, D. C. Jia
National Synchrotron Radiation Laboratory, NSRL USTC,
P.O. Box 6022, Hefei Anhui 230029, China

Abstract

Hefei Light Source (HLS) is mainly composed of an 800 MeV electron storage ring and a 200 MeV constant-impedance Linac functioning as its injector. A new Linac is developed in view of the Full Energy Injection and the Top-up Injection scheme will be adopted in the HLS upgrade. In this paper, an 800MeV linear accelerating system construction, the constant-gradient structure design and the symmetry couplers consideration will be described in detail. The manufacture technology, the RF measurement, the high power test results and the accelerating system operation are presented.

INTRODUCTION

In order to ensure the low-emittance focusing parameters steady operation in the HLS Storage Ring, it's necessary to increase the injector energy to 800MeV. After realize Full Energy Injection, each system of Storage Ring can keep single operation state, the light source stability will be improved eminently. A new Linac is developed in view of the Full Energy Injection and the Top-up Injection scheme will be adopted in the HLS upgrade. An 800MeV Linac layout is shown in Fig.1.

The project is proceeding as planned at present. In this paper, an 800MeV linear accelerating system construction, the constant-gradient structure design and the symmetry couplers consideration will be described in detail. One section of accelerator structure has been fabricated successfully. The manufacture technology, the RF measurement, the high power test results and the project schedule are presented.

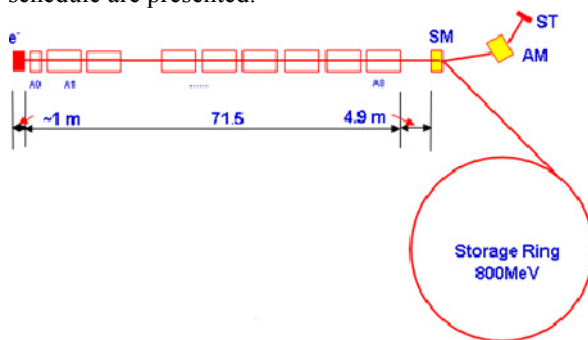


Figure 1: HLS 800MeV Linac layout

800MEV LINEAR ACCELERATING SYSTEM DESIGN

HLS accelerating system consists of a pre-buncher, a buncher and eight units of constant-gradient accelerating structures (6m accelerator unit). Total length is about 73meter. The electron beam energy can be achieved to

ISBN 978-3-95450-122-9

800MeV~1GeV. In general, seven such as units is in operation condition and another one is in standby state so that to assure storage-ring stability running (Fig.2).

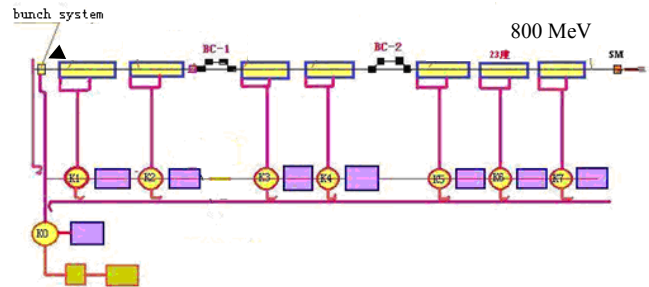


Figure 2: 800MeV electron Linac energy, phase and microwave System

Pre-buncher

Pre-buncher or velocity modulation cavity is a cylindrical reentrant resonator. Its resonance frequency is 2856 MHz, working at TM_{010} mode. Cavity dimensions and physical parameters are calculated with SUPERFISH. To reduce the errors of resonance frequency caused by temperature, beam loading etc., stainless steel is selected to make this cavity to reduce Q (~ 500), the cavity shunt impedance is $R_s/Q = 220$. So when 2kW power is feeding in, it will produce about 15kV microwave voltage in the cavity. According to beam dynamics calculation, bunching parameter is selected $r = 1.92$. The beam waist of electron beam from gun is focused at the center of pre-buncher. Through the preliminary bunching cavity and drift 35 cm, its phase width will be focused from 260° to 90° . The work was finished in a HLS phase I project. It is in good condition still. So it will continue to use after upgrading.

The fundamental mode buncher

The bunching system work frequency is 2856 MHz, including pre-buncher and fundamental mode buncher. The beam from the gun is focused initially in the pre-buncher, then electron beam get into buncher to further complete beam phase bunching process, and further increase the beam energy. The fundamental mode buncher is constant gradient disk load accelerating structure. Solenoids are used to focus in the transverse direction. The length of fundamental mode buncher is 1.63 m, the accelerating gradient is about 8.2 MV/m, and beam energy is about 13.1 MeV after bunching section.

In order to optimize bunching effect, pre-buncher voltage is optimized to 15kV and the distance between buncher and pre-buncher is optimized to 35 cm. The

FEASIBILITY STUDY OF SHORT PULSE MODE OPERATION FOR MULTI-TURN ERL LIGHT SOURCE*

T. Atkinson[†], A. V. Bondarenko, A. N. Matveenko, Y. Petenev,
Helmholtz-Zentrum Berlin für Materialien und Energie GmbH (HZB), Germany.

Abstract

The optic and simulation group at HZB are designing a light source based on the emerging Energy Recovery Linac superconducting technology, the Femto-Science-Factory (FSF) will provide its users with ultra-bright photons of angstrom wavelength at 6 GeV. The FSF is intended to be a multi-user facility and offer a wide variety of operation modes. A low emittance $\sim 0.1 \mu\text{m rad}$ mode will operate in conjunction with a short-pulse $\sim 10 \text{ fs}$ mode.

INTRODUCTION

This paper continues on from a recent introductory study[1] and highlights the physical limitations when trying to offer interchangeable modes and preserve beam quality. The paper concentrates on the short bunch mode, introducing the multi stage compression schemes in a general manner and presents the first results of the start-to-end beam simulations.

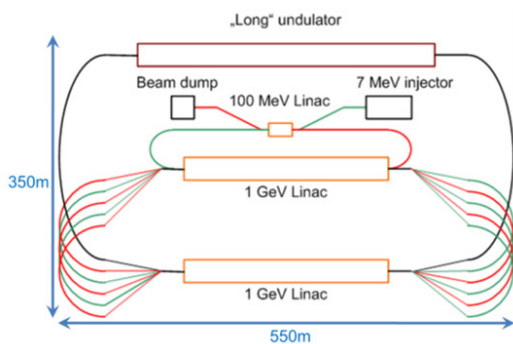


Figure 1: Schematic of the FSF Multi-Turn ERL.

The main design parameters of the FSF are listed in Table 1 and Fig. 1 shows the layout of the light source.

A SRF injector based on the design parameters of the BERLinPro[2] project delivers the 100 MeV electron beam into the main accelerator. Here two 1 GeV linacs are continually traversed until 6 GeV beam energy is reached. Each Arc contains straight sections for undulators and the final energy Arc permits a long straight section for 5000 period undulators.

The beam quality delivered to the long undulators and

* Work supported by German Bundesministerium für Bildung und Forschung, Land Berlin, and grants of Helmholtz Association VH NG 636 and HRJRG-214.

[†] terry.atkinson@helmholtz-berlin.de

Table 1: Main design parameters of FSF

Parameter	High Brilliance Mode	Short Bunch Mode
Energy (GeV)	6	6
Charge (pC)	15	4
Bunch Length (fs)	>200	~ 10
$\langle B \rangle$ (ph/s/mm ² /mrad ² /0.1%)	10^{22}	10^{21}
B_{peak} (ph/s/mm ² /mrad ² /0.1%)	10^{26}	10^{26}

hence the photon brilliance attainable depends on the machine operating mode.

SHORT BUNCH MODE

Single pass machines do not suffer the same fate as storage rings as equilibrium is never reached. A design based on linear uncoupled optic, helps address a proof-of-principle for the short pulse mode, which is later then tested using a realistic input beam distribution from the BERLinPro injector project.

Compression in the Injector

Producing a femto-second pulse of low energy spread starts at the Gun, Table 2. Here the longitudinal electron beam properties are restricted by the photo-injector laser pulse and the superconducting RF acceleration. The primary subtle compression in the Merger between the Booster and linac minimizes transverse emittance growth.

Table 2: Injector ASTRA[3] simulations

Component	Bunch Length (mm)	Emittance (keV mm)	Energy (MeV)
Gun	0.7	0.3	1.8
Booster	1.0	2	6.6
Linac	0.45	2.2	50

The injector Arc is then used to prepare the beam for the main accelerator. The combination of a second linac to increase the beam energy to 100 MeV and the R_{56} in the Arc compress the beam to $\sigma_t \sim 660 \text{ fs}$ with a correlated energy spread of $\Delta E/E \sim 1.5 \cdot 10^{-4}$.

LINAC OPTICS DESIGN FOR MULTI-TURN ERL LIGHT SOURCE*

Y. Petenev[#], T. Atkinson, A.V. Bondarenko, A.N. Matveenko, HZB, Berlin, Germany.

Abstract

The optics simulation group at HZB is designing a multi-turn energy recovery linac-based light source. Using the superconducting Linac technology, the Femto-Science-Factory (FSF) will provide its users with ultra-bright photon beams of angstrom wavelength at 6 GeV. The FSF is intended to be a multi-user facility and offer a variety of operation modes. In this paper a design of transverse optic of the beam motion in the Linacs is presented. An important point in the optics design was minimization of the beta-functions in the linac at all beam passes to suppress beam break-up (BBU) instability.

INTRODUCTION

In this document we present a design of a Linac optics for a new 3 pass ERL-based LS with 6 GeV maximum energy of electron beam. This future facility is named Femto-Science Factory (FSF) [1].

The schematic layout of the facility is presented in Fig. 1. A beam is created in 1.3 GHz SRF gun with photo cathode. We consider an SRF injector with similar parameters to the BERLinPro injector under development at HZB [2, 3]. Then it passes a 100 MeV Linac and is accelerated to 6 GeV after passing 3 times through each of two 1 GeV main Linac's. In the arcs between the acceleration stages it is assumed to have undulators with 1000 periods. In the long straight section (see Fig.1) a long undulator with 5000 periods is assumed. The main design parameters of FSF are presented in Table 1.

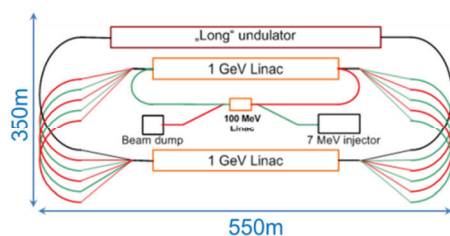


Figure 1: The scheme of FSF.

One potential weakness of the ERLs is transverse beam breakup instability, which may severely limit a beam current. If an electron bunch passes through an accelerating cavity it interacts with dipole modes (e.g. TM_{110}) in the cavity. First, it exchanges energy with the mode; second, it is deflected by the electro-magnetic field of the mode. After recirculation the deflected bunch interacts with the same mode in the cavity again which constitutes the feedback. If net energy transfer from the

beam to the mode is larger than energy loss due to the mode damping the beam becomes unstable.

The actuality of this problem was recognized in early experiments with the recirculating SRF accelerators at Stanford [4] and Illinois [5], where threshold current of this instability was occurring at few microamperes of the average beam current. In the works of Rand and Smith in [6] dipole high order modes were identified as a driver of this instability. In late of the 80's the detailed theoretical model and simulation programs had been developed [7, 8]. Nowadays the interest to this problem was renewed. The requirements for more detailed theory and simulation programs [9-11] are given by the needs of high current (~100 mA) ERLs.

The threshold current for the transverse beam breakup may be estimated for the case of a single cavity and single mode for a multipass ERL in the form as [11]:

$$I_{th} \approx I_0 \frac{\tilde{\lambda}^2}{Q_a L_{eff} \sqrt{\sum_{m=1}^{2N-1} \sum_{n=m+1}^{2N} \frac{\beta_m \beta_n}{\gamma_m \gamma_n}}}, \quad (1)$$

where I_0 - Alfven current, Q_a is the quality factor of HOM, $\tilde{\lambda} = \lambda/2\pi$, λ is the wavelength corresponding to the resonant frequency of the TM_{110} mode, γ_m is the relativistic factor at the m-th pass through the cavity, β_m - is the Twiss parameter, L_{eff} - is the effective length of the cavity, N is the number of passes during acceleration. It should be noted that (1) gives more realistic estimation of the BBU threshold current than a similar expression in [9] with a $1/N(2N-1)$ dependence on the number of passes. This is the result of an assumption in [9] of integer tunes in every turn of the ERL.

Table 1: Main Design Parameters of FSF

Parameter	High brilliance mode	Short bunch mode
E, GeV	6	6
$\langle I \rangle$, mA	20	5
Q, pC	15	4
τ , fs	200-1000	~10
$\langle B \rangle$, ph/s/mm2/mrad2/0.1%	$8 \cdot 10^{22}$	$\sim 4 \cdot 10^{21}$
B_{peak} , ph/s/mm2/mrad2/0.1%	10^{26}	$\sim 10^{26}$

Eq. 1 shows that it is preferable to have low β -functions at low energies. Therefore, the design was optimised to minimize beta functions of the beam in the Linac to increase the threshold current of BBU instability from one

* Work supported by German Bundesministerium für Bildung und Forschung, Land Berlin, and grants of Helmholtz Association VH-NG-636 and HRJRG-214.

[#]yuriy.petenev@helmholtz-berlin.de

SINGLE SHOT BUNCH-BY-BUNCH BEAM EMITTANCE MEASUREMENT OF THE SPRING-8 LINAC

Yoshihiko Shoji[#] and Kouji Takeda, NewSUBARU/SPring-8, University of Hyogo, Japan

Abstract

The bunch-by-bunch emittance of a single shot beam from the SPring-8 electron linac was measured utilizing phase rotation in an electron storage ring. The linac beam was injected into the ring and the beam profiles of several revolutions were recorded using a dual sweep streak camera. The fast sweep separated the linac bunches in 1 ns macro pulse and the slow sweep separated the profiles at different turns. The bunch emittances were reconstructed from the profiles. The stability of the linac beam was evaluated from the recorded shot-to-shot fluctuation. We also identified differences in the orbit and the emittance of different bunches in a pulse.

INTRODUCTION

The SPring-8 linac has been operated as an injector to the electron storage ring, NewSUBARU. However, fine parameter tuning is required for stable top-up injection because of the small ring acceptance. In that process, single shot linac beam monitors were necessary to understand the shot-to-shot fluctuation of the injection. A single shot bunch-by-bunch emittance monitor would be a powerful tool to understand the shot-to-shot fluctuation of the injection efficiency.

We used the visible light profile monitor of the electron storage ring as a diagnostic for the linac beam. The dual sweep streak camera recorded multiple profiles of the injected beam in a single camera frame. The fast sweep separated linac bunches in a macro pulse and the slow sweep separated profiles of different turns. The betatron oscillation in the ring produced phase rotation allowing the reconstruction of the beam emittance. It was possible to fully optimize the ring parameters for our measurements since beam storage was not required.

A stability of the linac beam was evaluated from the shot-to-shot variation. We could also see differences in the bunch at the front of a macro pulse compared to the bunch at the rear.

PARAMETERS OF DAILY OPERATION

Averaged Beam Parameters

Figure 1 shows the layout of the SPring-8 linac, the booster synchrotron, and NewSUBARU storage ring. Table 1 shows the main parameters for the linac. The macro pulse width of the linac beam is normally 1 ns, which contains 3 linac bunches. The rf synchronization system between the linac and the ring [1] enables an injection to a single rf bucket of the ring with rf frequency of 500 MHz.

[#] shoji@lasti.u-hyogo.ac.jp

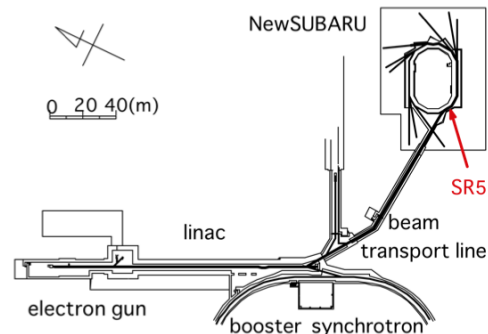


Figure 1: Layout of the 1 GeV SPring-8 linac, the booster synchrotron, and the NewSUBARU storage ring.

Table 1: Main Parameters of the Linac

Electron energy	1 GeV
Rf frequency	2856 MHz
Common pulse rate	1 Hz
Common pulse width	1 ns
FWHM bunch length; front/middle	10 ps / 14ps
Full energy spread; front / middle	0.4% / 0.6%
Transverse emittance (FWHM ²)	100 π nmrad.

The listed transverse emittance was calculated from the average over many shots, measured by Q-scanning at the beam transport line. The longitudinal parameters were obtained from the measurements of the synchrotron oscillation in the ring just after injection [2]. The listed bunch length and the energy spread were calculated from the average of 10 shots.

Bunch Structure and Injection Efficiency

The bunch structure was fluctuated by a jittering of the gate pulse of the electron gun. Figure 2 shows six typical dual sweep images of the streak camera with six typical bunch structures. The vertical axis in the images is the ring rf phase and the horizontal axis the revolution. The time structure at 1/4 of the synchrotron oscillation period (41 μ s) gives the energy profile.

Figure 3 shows the injection efficiency with the ring parameters characteristic of daily operation. Shots with images A and B had comparatively worse efficiency. A separated data shows that the ring has a large enough longitudinal acceptance for the injected beam, suggesting that dependence on transverse parameters caused fluctuations in the injection efficiency.

ADVANCES IN BEAM TESTS OF DIELECTRIC BASED ACCELERATING STRUCTURES*

S. P. Antipov^{1,2}, C. Jing^{1,2}, A. Kanareykin^{1,#}, J.E. Butler¹, V.Yakimenko³, W. Gai²

¹Euclid Techlabs LLC, Solon, OH, USA,

²Argonne National Laboratory, Argonne, IL, USA

³Brookhaven National Laboratory, Upton, NY, USA

Abstract

Diamond is being evaluated as a dielectric material for dielectric loaded accelerating structures. It has a very low microwave loss tangent, high thermal conductivity, and supports high RF breakdown fields. We report on progress in our recent beam tests of the diamond based accelerating structures of the Ka-band and THz frequency ranges. Wakefield breakdown test of a diamond-loaded accelerating structure has been carried out at the ANL/AWA accelerator. The high charge beam from the AWA linac (~ 70 nC, $\sigma_z \sim 2$ mm) was passed through a rectangular diamond loaded resonator and induce an intense wakefield. A groove is cut on the diamond to enhance the field. Electric fields up to 300 MV/m has been generated on the diamond surface to attempt to initiate breakdown. Wakefield effects in a 250 GHz planar diamond accelerating structure has been observed at BNL/ATF accelerator as well. We have directly measured the mm-wave wake fields induced by subpicosecond, intense relativistic electron bunches in a diamond loaded accelerating structure via the dielectric wake-field acceleration mechanism. A surface analysis of the diamond has been performed before and after the beam test.

INTRODUCTION

Diamond has been proposed as a dielectric material for dielectric loaded accelerating (DLA) structures [1-3]. Dielectric Loaded Accelerator structures using ceramics or other materials and excited by a high current electron beam or an external high frequency high power RF source have been under extensive study for many years [4-7]. Low loss microwave ceramics, fused silica, and CVD polycrystalline and single crystal diamonds [11] have been considered as materials for dielectric based accelerating structures to study of the physical limitations encountered in developing field strengths > 100 MV/m at microwave [4-6] and $> \text{GV/m}$ at THz frequencies in a dielectric based wakefield accelerator [6,7,11,12]. THz radiation has been generated recently by a short ~ 10 GV/m pulse within a 100 μm diameter quartz fiber [7]. A planar diamond-based DLA structure was proposed recently by Omega-P, Inc., where the dielectric loading of this structure was to be made of diamond slabs fabricated

using CVD (chemical vapor deposition) technology [2].

Our choice of CVD (Chemical Vapor Deposition) diamond as a loading material will allow demonstration of high accelerating gradients; up to 0.5-1.0 GV/m as long as the diamond surface can sustain a 0.5-1.0 GV/m short pulse (~ 10 ns) rf field without breaking down. Diamond has the lowest coefficient of thermal expansion, highest thermal conductivity ($2 \times 10^3 \text{ Wm}^{-1} \text{ K}^{-1}$) and extremely low loss tangent ($< 10^{-4}$) at Ka-W frequency bands. Secondary emission from the CVD diamond surface can be dramatically suppressed by diamond surface dehydrogenation or oxygen termination [3,6,8-12]. The CVD process technology is rapidly developing, making the CVD diamond fabrication process fast and inexpensive. Given these remarkable properties, diamond should find numerous applications in advanced accelerator technology [3]. Planar diamonds are available commercially in various grades including single crystal diamonds. The goal of this research is to perform a wakefield acceleration experiment using a diamond loaded structure and to test diamond for breakdown.

Euclid Techlabs had performed two wakefield experiments with diamond loaded accelerating structures: a 25 GHz structure at the Argonne Wakefield Accelerator of ANL and a 250 GHz structure at the Accelerator Test facility of BNL [9].

BEAM EXPERIMENTS WITH THE DIAMOND BASED DLA STRUCTURES

Significant progress has been made in the development and testing of high gradient dielectric accelerating structures (DLA) [1]. As various engineering challenges (breakdown, dielectric losses, efficient RF coupling) have been overcome, the technology of high gradient RF or wakefield driven dielectric loaded structures appears increasingly attractive as a viable option for high energy accelerators. Typical DLA considered in experiments is a cylindrical, dielectric tube with an axial vacuum channel inserted into a conductive sleeve or a rectangular waveguide loaded with planar dielectric pieces. In this paper we will focus on the latter structure. The dielectric constant, thickness of dielectric and the size of a vacuum gap are chosen to adjust the phase velocity of the fundamental mode at certain frequency to the beam velocity $\sim c$. In the application to particle acceleration, the dominant TM_{01} mode is of main interest.

*Work supported by the Department of Energy SBIR program.

#alexkan@euclidtechlabs.com

ON-LINE DISPERSION FREE STEERING FOR THE MAIN LINAC OF CLIC

J. Pfingstner*, D. Schulte, CERN, Geneva, Switzerland

Abstract

For future linear colliders as well as for light sources, ground motion effects are a severe problem for the accelerator performance. After a few minutes, orbit feedback systems are not sufficient to mitigate all ground motion effects and additional long term methods will have to be deployed. In this paper, the long term ground motion effects in the main linac of the Compact Linear Collider (CLIC) are analysed via simulation studies. The primary growth of the projected emittance is identified to originate from chromatic dilutions due to dispersive beam orbits. To counter this effect, an on-line identification algorithm is applied to measure the dispersion parasitically. This dispersion estimate is used to correct the beam orbit with an iterative dispersion free steering algorithm. The presented results are not only of interest for the CLIC project, but for all linacs in which the dispersive orbit has to be corrected over time.

INTRODUCTION

Linear colliders and light sources often require very small beam emittances and beam sizes to reach their goals. This fact makes these machines inherently sensitive to ground motion effects. For short time scales orbit feedbacks can be used to mitigate these effects by steering the beam with the help of beam positioning monitors (BPMs) (see [1] for the CLIC case). For longer time scales, this steering is not sufficient to preserve the beam quality as can be seen in Fig. 1. To be able to operate CLIC over longer time periods, it is essential to correct this remaining emittance growth. The development of such an algorithm is the topic of this paper.

The main reason for the remaining emittance growth is that the BPM positions itself will drift from their original position, which results in a dispersive beam orbit. The according chromatic dilutions decrease the beam quality over time. In the literature, a technique named dispersion free steering (DFS) can be found, which has been developed to correct similar chromatic dilutions (see [3] and [4]). In this paper we modify and extend this basic DFS method, such that it can be used to correct long term ground motion effects in an on-line mode. On-line means in this case that the DFS correction is applied during the normal accelerator operation in a parasitic way, without stopping the physics program. The method will be explained and evaluated on the example of CLIC, but can be easily utilised for other accelerators.

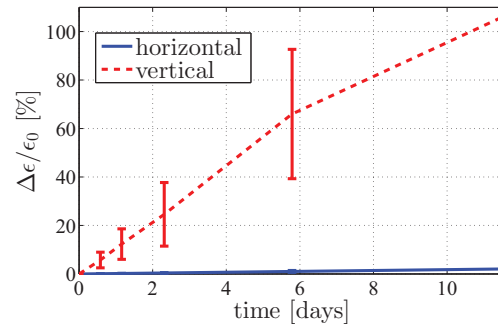


Figure 1: Simulations of the relative emittance growth over long time scales with orbit feedback in the main linac of CLIC. The used ground motion is generated according to the ATL law [2] with a constant A of $0.5 \times 10^{-6} \mu\text{m}^2/\text{m}/\text{s}$, which is the baseline for CLIC. The results have been averaged over 10 random samples of ground motion. For the initial horizontal and vertical emittance 600 nm and 10 nm have been used. The action of the orbit feedback was assumed to be perfect and therefore simulated by applying one-to-one steering without BPM noise, which is an optimistic approximation. It can be seen that already after 1 day the emittance has increased by about 10%.

ON-LINE DFS ALGORITHM

In this section, we will first introduce the basic DFS algorithm. After that the modifications necessary to apply this algorithm in an on-line mode will be discussed.

Basic DFS Algorithm

The DFS algorithm consists of two steps. In the first, the dispersion η at the BPMs is measured by varying the beam energy. This energy change can be created by changing the acceleration gradient, scaling the magnet strength and/or changing the initial beam energy. In the second step, corrector actuations θ are calculated such that at the same time the measured dispersion η as well as the beam orbit b are corrected. Such actuations can be calculated by solving the following system of equations for θ (see [5] for more details)

$$-\begin{bmatrix} b - b_0 \\ \omega(\eta - \eta_0) \\ 0 \end{bmatrix} = \begin{bmatrix} R \\ \omega D \\ \beta I \end{bmatrix} \theta, \quad (1)$$

where b_0 and η_0 are the reference beam orbit and target dispersion respectively. The third set of equations in Eq. (1) with the unity matrix I on the right side is used to damp too high corrector actuations. The weights ω and β can be

* juergen.pfingstner@cern.ch

DETAILED ANALYSIS OF THE LONG-RANGE WAKEFIELD IN THE BASELINE DESIGN OF CLIC MAIN LINAC

V.F. Khan and A. Grudiev
CERN, Geneva, Switzerland.

Abstract

The baseline design of the accelerating structure of the CLIC main linac relies on strong damping of transverse higher order modes (HOMs). Each accelerating cell is equipped with four damping waveguides that causes HOM energy to propagate to damping loads. Most of the HOMs decay exponentially with a Q -factor of about 10, however there are modes with higher Q -factors. Though the amplitude of the high Q modes is nearly two orders of magnitude smaller than the dominating lowest dipole mode, their cumulative effect over the entire bunch train may be significant and dilute the beam emittance to unacceptable level. In this paper we report on an accurate calculation of the long-range wakefield and its overall effect on beam dynamics. We also discuss possible measures to minimise its effect in a tapered structure.

INTRODUCTION

The CLIC baseline design of the main linac operates at 12 GHz [1]. Preserving the beam quality in linacs operating at high frequencies is primarily limited by the beam induced fields known as wakefields [2]. Inadequate suppression of wakefields may result in emittance dilution; hence it is essential to employ a damping mechanism. In the first section of this paper we present detailed calculation of the wakefields in the CDR [1] baseline design of the CLIC accelerating structure (CLIC AS) [3], which is based on strong waveguide damping of HOMs. We also investigate the presence of so called persistent wakefield [4] in this structure. In the CLIC scheme, the bunch train consists of 312 bunches [1]; in such multi-bunch acceleration, wakefield generated by a bunch often leads to kicking the following bunches. An analytical estimate of the effect of multi-bunch long range wakefields on the beam profile is presented in [5]. However, in [5], by considering the strong damping of the HOMs, it is assumed that only the first trailing bunch experiences a kick due to an off-axis driving bunch. Herein we calculate the very long range wakefields in CLIC AS which allows HOM kicks to be considered on all trailing bunches by applying the analytical model to estimate the long range multi-bunch wakefield effect. These results are discussed in the second section.

WAKEFIELDS IN CLIC AS

The CLIC AS is designed with tapered irises so as to keep the accelerating gradient (nearly) constant. The wakefield is strongly damped by means of four waveguides attached to each accelerating cell [1, 3]. The time domain code GdfidL [6] was utilised to calculate the long-range wakefields excited in the structure. The

wakefield can also be reconstructed using the frequencies, kicks and Q factors of the dominating modes. The lowest dipole mode has the strongest impact on the off-axis beam as it contains the largest kick factor. The damping waveguides are carefully designed, in particular to damp this mode with a $Q \sim 10$ [3]. The envelopes of transverse wakefields of the sample cells, namely the first, middle and last are illustrated in the Fig. 1, and a disc of the CLIC AS is also shown inset. Beyond 1 m wake-length it is clear that only one mode dominates, which has low amplitude but high Q -factor. However, modes with high group velocity (v_g) and poor damping via these waveguides travel along the structure and are damped by means of evacuation from the structure volume through the input and output power couplers. Whereas the wakefield in the last cell does not seem to be affected by

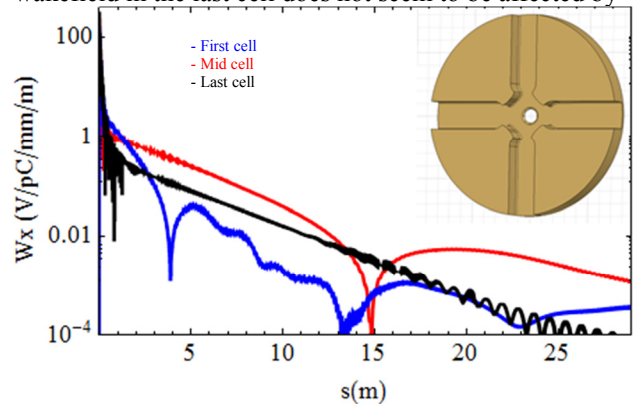


Figure 1: Envelope of transverse wakefield in single cells of CLIC AS.

the group velocity of the mode, the wakefields in the first and the middle cells are, resulting in reduction of the wakefield envelope at about 4 m and at about 15 m respectively. In this case, the wakefield is calculated including the group velocity term (β) as [1, 2]

$$W_{\perp}(s) = 2 \sum_p K_p \text{Exp} \left[i \frac{\omega_p s}{c} \left(1 + \frac{i}{2(1-\beta_p)Q_p} \right) \right] \left(1 - \frac{\beta_p s}{L(1-\beta_p)} \right) \quad (1)$$

where K_p and ω_p are the frequency and kick factor of the mode p respectively, L is the structure length and $\beta = v_g/c$. The modes with non-negligible β_p travel rapidly through the structure which expedites wake suppression, hence it is necessary to include this term in the calculation. In order to understand the modal contribution in the wake beyond 1 m, we study the transverse impedance (Fourier transform of the wake) in these cells. The impedance of these cells is shown in Fig. 2. As can be seen, the first mode around 17 GHz has the largest impedance (i.e. kick factor) and better damping (width of the peak) compared to the other modes. The modes at 21 GHz, 26 GHz, 40

SPECIFICATIONS OF THE DISTRIBUTED TIMING SYSTEM FOR THE CLIC MAIN LINAC

A. Gerbershagen, A. Andersson, D. Schulte, CERN, Geneva, Switzerland
P. N. Burrows, JAI, University of Oxford, Oxford, UK
F. Ömer Ilday, Bilkent University, Ankara, Turkey

Abstract

The longitudinal phase stability of the CLIC main and drive beams is a crucial element of the CLIC design. In order to measure and control the phase a distributed phase monitoring system has been proposed. The system measures the beam phase every 900 m. The relative phase between the measurement points is synchronized with an external reference system via a chain of reference lines. This paper presents the simulations of error propagation in the proposed distributed monitoring system and the impact on the drive and main beam phase errors and the luminosity. Based on the results the error tolerances for the proposed system are detailed.

INTRODUCTION

The Compact Linear Collider (CLIC) is a proposed 3 TeV center-of-mass energy e^+e^- collider. It is designed to extract the RF energy from high-current low-energy drive beams and use this energy for acceleration of the low-current high-energy main beams that are brought into collision.

Since the main beam acceleration is performed by the RF power extracted from the drive beam, the stability of the relative phasing of the drive and main beams is crucial for the preservation of CLIC's luminosity. A relative phase error of 0.2° @ 12 GHz between the drive and the main beam will cause a luminosity loss of 1% if the error is coherent between the 24 decelerator segments. The same luminosity loss can be caused by an incoherent error of 0.8° . [1]

Additionally to these requirements on the relative drive beam - main beam phase, the phase tolerance between the two main beams at the interaction point (IP) has been set to 0.6° @ 12 GHz [2]. Hence, in order to align the main beam phase a global phase reference over 50 km is needed.

The stated tolerance requirements have to be met on the timescale of ≈ 50 ns, since this is the beam loading time of the main beam accelerating structures and errors on the shorter time scale will be (at least partially) filtered out by the structures.

PROPOSED DISTRIBUTED TIMING SYSTEMS

The distributed timing system is required to establish the correct beam phase at each turn-around of the linac. This allows to measure and correct the main and drive beam

phases along the main linac. There are two approaches for the design of such a system.

The first approach (A) is to use the outgoing main beams to transmit the phase information to a number of local oscillators (Fig. 1, top). These can maintain the phase accurately enough until the main beam returns on the way to the interaction point. This system requires accurate phasing between the outgoing main beams at the first booster linac near the interaction point (Fig. 2).

In the other approach (B) the master clock near the interaction point (IP) would define the nominal phase and distribute it as a signal cascade from one 900 m long decelerator segment to another (Fig. 1, bottom). This system would establish the relative phase of the local timing clocks by an optical connection independently of the beams.

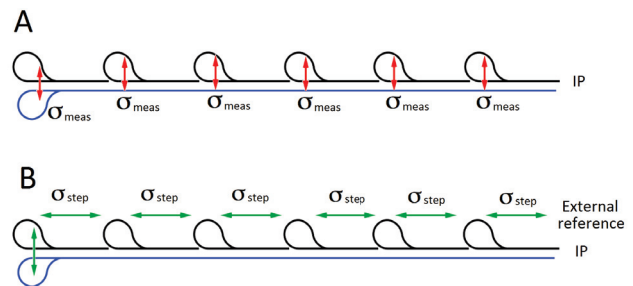


Figure 1: Phase signal propagation for the reference based on the main beam (A) and chained distribution of master clock signal (B).

Approach A has the advantage of having a relatively small error between the main and the drive beams, since the phase measurement at each drive beam decelerator is performed locally and hence no additional error is introduced during the distribution process (see Fig. 3, left). Approach B allows the correction of the main beam at its final turn-around, giving the possibility to reduce the jitter between the e^+ and e^- main beams (Fig. 3, right). However, if the drive beam correction signal is transported from the master clock via the distribution system, the noise introduced by this system would reduce the effectiveness of the phase correction. In the final CLIC design these approaches could be potentially combined.

The proposed timing distribution system is based on state of the art technology for signal distribution via optical fibers tested at XFEL (DESY, Hamburg) [3], [4]. This system is proven to provide <10 fs stability over the distance of several kilometers.

The following analysis determines the specifications of the

A 10 MeV L-BAND LINAC FOR THE IRRADIATION APPLICATIONS IN CHINA

G.[#] Pei, Y. Chi, R. Shi, Z. Zhou, Q. Yuan, F. Zhao, D. He, X. Yang, C. Yu, M. Dai, J. Liu, Y. Feng, X. Li, X. He, X. Wang, Z. Zhu, E. Tang, H. Huang, J. Zhao, C. Ma,
Institute of High Energy Physics, IHEP, Beijing, P. O. Box 918, 100049, China
Z. Li, X. Zhang, Wuxi EL PONT Radiation Technology, Ltd, No 8 Weiye Road,
Qianqiaoqian District, Wuxi, 214151, Jiangsu, China

Abstract

The electron linear accelerator has wide applications, and the demands for the irradiation applications are keeping growing in China. A high beam power 10 MeV L-band Linac has been developed recently as a joint venture of Institute of High Energy Physics (IHEP) and Wuxi EL-PONT Company in China. The Thales TH2104U klystron, 2 A thermionic electron gun and 3 m long L-band disk-loaded constant impedance RF structure were adopted. A stable electron beam of 10 MeV / 40 kW has been obtained in the last April. In this paper the detailed design issues and beam commissioning results are reported.

INTRODUCTION

IHEP in China has very rich experience in the electron linac design and development. When requested to transfer the technology to industry, many S-band electron linacs have been developed for medical and irradiation applications. For the S-band irradiation linac, the beam power is limited to be ~20 kW because of the RF structure heating/cooling issues. Due to the scaling law of $P \sim f^1$ between the RF power consumption of the accelerating structure and the frequency, L-band structure [1][2] is usually adopted for the nature extending to much higher beam power up to ~100 kW level. For any high beam power machines the power efficiency is a concern. According to Eq. (1), the maximum conversion efficiency η_{max} of the RF power to the beam power depends only on the attenuation factor τ [3], and smaller τ is preferred.

$$\eta_{max} = \frac{1}{2} \left[\frac{(1 - e^{-2\tau})^2}{(1 - e^{-2\tau}) - 2\tau e^{-2\tau}} \right] \quad (1)$$

However, there is a compromise among power efficiency, power dissipation as well as heating, peak beam current and beam energy. It is known that τ is independent of frequency, and for SLAC type 3m long disk-loaded TW structure τ is ~0.57. Suppose a 3 m long L-band structure of 34 cavities is used, τ can be roughly estimated to be $0.57 * 34 / 86 = 0.225$. With SUPERFISH simulation and cold test, τ is shown [4] to be 0.22, which is in good agreement with the simple scaling. By putting 0.22 into Eq. (1) one can get an efficiency η_{max} of 90%, which is very excellent. In this condition, the beam

current is ~900 mA according to Eq. (2).

$$i_{\eta_{max}} = \left(\frac{P_r}{rl} \right)^{1/2} \left[\frac{(1 - e^{-2\tau})^{3/2}}{(1 - e^{-2\tau}) - 2\tau e^{-2\tau}} \right] \quad (2)$$

Table 1 shows the design parameters for the 10 MeV / 40 kW L-band linac. The linac is a machine with very heavy beam loading; the beam energy range of 8 to 12 MeV can be easily controlled by simply adjusting the gun bias voltage (i.e. the gun emitting beam current), but above 10 MeV is not recommended for prevention of the neutron production.

Table 1: Design parameters for the 10MeV L-band linac

Beam energy (MeV)	10
Beam power (kW)	40
RF frequency (GHz)	1.3
Peak beam current (mA)	530
Duty cycle (%)	0.75
Klystron peak power (MW)	10

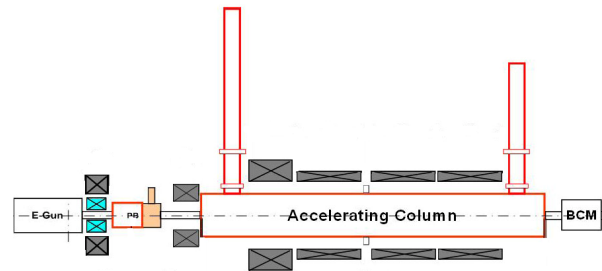


Figure 1: The schematic of the L-band linac.

DETAILED DESIGN AND SIMULATION

Figure 1 shows the schematic of the high power 10 MeV L-band linac, which mainly consists of an electron gun, an RF power source and an accelerating column. The electron gun is the 80 kV BEPC type [5] gun with 2 A Y646B cathode grid assembly. The gun system is separated from the other subsystems, which makes it easy for maintenance. The gun emitting current and the beam energy are adjustable. The RF power source is a 10 MW Thales TH2104U klystron with 130 kW average power, and the modulator was designed to make it work at 100 kW. Fig. 2 shows the Thales TH2104U klystron and its parameters.

*Work supported by the joint venture foundation of IHEP and the Wuxi EL-PONT Company in China.
#peigx@ihep.ac.cn

APPLICATIONS OF COMPACT DIELECTRIC BASED ACCELERATORS*

C. Jing#, S. Antipov, P. Schoessow, and A. Kanareykin, Euclid Techlabs LLC, Solon, OH, USA
J.G. Power, M. Conde, and W. Gai, ANL, IL, USA

Abstract

Important progress on the development of dielectric based accelerators has been made both experimentally and theoretically in the past few years. One advantage of dielectric accelerators over their metallic counterparts is their compact size, which make them attractive for industrial or medical applications. In this article, we discuss the design of dielectric based accelerators focusing on those technologies relevant toward these needs.

DIELECTRIC LOADED ACCELERATOR

The first studies of using RF driven dielectric-loaded circular waveguide for particle acceleration can be traced back to the early 1950's [1]. In recent years, because of its geometrical simplicity and availability of low loss dielectrics, theoretical and experimental investigations on dielectric based accelerators have been intensively revived. Among them, externally powered Dielectric-Loaded Accelerators (DLA), dielectric wakefield accelerators, and dielectric laser accelerators have attracted the most attention. In this paper, we concentrate on externally powered DLA technologies and possible application.

DLA structures can be made as simple as a dielectric tube surrounded by a conducting cylinder. Most of them use uniform, linear ceramic tubes so that they work as constant impedance accelerating structures. The TM_{01} mode (traveling wave accelerator) or TM_{01n} mode (standing wave) are the fundamental accelerating modes. Unlike conventional metallic accelerating structures, DLA structures do not require any structure periodicity to slow the phase velocity of the guided wave below the speed of light. For a given radius, the phase velocity of each guided wave mode in a DLA structure is governed by the dielectric constant of the material and its wall thickness. In general, for the same a/λ , where a is the radius of the beam opening and λ is the wavelength, the DLA structure can be made much smaller than a disk-loaded accelerating structure due to the high dielectric constant of the material used. This small size may be favored for applications with tight space requirements. It also facilitates the use of quadrupole lenses or a permanent solenoid around the structure to prevent the beam from breaking up in the case of high current beam acceleration. For example, for an X-band structure, given $a/\lambda=0.156$, the diameter of a cell of a 120-degree traveling wave disk-loaded accelerating structure is larger than 2 cm, but the outer diameter of the dielectric tube in a DLA structure is only 1 cm if the

dielectric constant of the tube is 20.

However, the choice of dielectric constant should be considered as far more complicated than the requirement of a reduced transverse dimension. It is strongly linked with other accelerating parameters as well. A very good estimate of the group velocity of a traveling wave DLA structure is given by $V_g/c \approx 1/\varepsilon_r$ (where c is the speed of light and ε_r is the relative dielectric constant of the loaded material) when a/λ is less than 15%. The quality factor of a DLA structure can be roughly estimated as $Q \approx 5.22 \times 10^4 / \{ \sqrt{[f(\text{GHz}) \times (\varepsilon_r - 1)] + 5.22 \times 10^4 \times \tan \delta} \}$, where f is the frequency of the TM_{01} mode in units of GHz and $\tan \delta$ is the loss tangent of the loaded material.

PARAMETER CHOICE

DLA structures are generally preferred for use in a short structure powered by short, high frequency RF pulses, which reduces the probability of RF breakdown but needs a short filling time to achieve a high RF-to-beam efficiency [2]. Consider the rough design of an X-band travelling wave DLA structure. From the group velocity estimate, we choose $\varepsilon_r = 10$ for a structure with $V_g = 10\% c$. Then Q can be estimated to be 3400. Since the size of the beam opening ($2a$) is independent of Q but tightly related to the R/Q (figure of merit of an accelerating structure) and shunt impedance R (they both increase as the beam opening decreases), we can choose a as small as the beam emittance allows to obtain both a large R/Q and R . Meanwhile the filling time (defined as L/V_g , where L is the length of the structure) remains short since the group velocity is unrelated to the beam opening. It should be pointed out that a/λ of DLA structures cannot be chosen too small since it will increase the wakefield and thus the risk of beam break-up.

Transverse wakefield damping in DLA structures has been well studied [3]. Its implementation is rather simple: an axially slotted copper jacket filled with RF absorber or metallized strips on the outer surface of the dielectric tube surrounded with RF absorber. The low Q of the DLA structures also helps the damping of long range wakefields.

Figure 1 shows a few parameters of X-band (11.7GHz) travelling wave DLA structures. Three different dielectric constants are used in the plots, representing three commonly used low loss materials: Alumina ($\varepsilon_r=10$, $\tan \delta = 1 \times 10^{-4}$), MgCaTiO ($\varepsilon_r=20$, $\tan \delta = 1 \times 10^{-4}$) and Quartz ($\varepsilon_r=3.8$, $\tan \delta = 6 \times 10^{-5}$). Figure 1(a) clearly shows that the group velocity is bounded by the reciprocal of the dielectric constant as the beam opening decreases. The quality factor of a DLA structure is the combined contribution of metal wall losses and dielectric losses, but

*Work supported by the Department of Energy SBIR program.
#jingchg@hep.anl.gov

LINEAR ACCELERATOR BASED ON PARALLEL COUPLED ACCELERATING STRUCTURE*

Yu. Chernousov, V. Ivannicov, I. Shebolaev, ICKC, Novosibirsk, RUSSIA
A. Levichev, V. Pavlov, A. Barnyakov, BINP, Novosibirsk, RUSSIA.

Abstract

Linear accelerator based on parallel coupled accelerating structure and RF-controlled electron gun is developed and produced. The structure consists of five accelerating cavities. The RF power feeding of accelerating cavities is provided by common exciting cavity which is performed from rectangular waveguide loaded by reactive pins. Operating frequency is 2450 MHz. RF-controlled Electron gun is made on the basis of RF triode. Linear accelerator was tested with different working regimes. The obtained results are following:

- energy is up to 4 MeV, accelerating current is up to 300 mA with pulse duration of 2.5 ns on the half of the width,
- energy is up to 2.5 MeV, accelerating current is up to 100 mA with pulse duration of 5 μ s,
- energy is up to 2.5 MeV, accelerating current is up to 120 mA with pulse duration of 5 μ s and beam capture of 100%.

The descriptions of the accelerator elements are given in the report. The features of the parallel coupled accelerating structure are discussed. The results of the measuring accelerator's parameters are presented.

INTRODUCTION

Compact linear electron accelerators have wide scientific and industrial applications. The more often linacs are used with energy up to 10 MeV, average beam power up to several kilowatts. In present there are two type of accelerating structures with travelling wave and standing wave. But all of these structures have sequential RF power feeding of the accelerating cells. This is cause of some problems. To supply the accelerating structure total RF power has to go from the first accelerating cell. As the power is attenuated along these structures the initial value of the power must be very high, therefore, there are breakdowns and thermal surface damage in the first accelerating cell. When the breakdown is happened in one of the accelerating cell the operating RF pulse is terminated because of all storage energy of the structure is dissipated in it. Developing of *accelerating structure with given distribution of the power along the cavities is very difficult task. Also there is problem of high order modes, vacuum pumping and etc.

The linear electron accelerator based on new type accelerating structure is developed and produced by Budker Institute of Nuclear Physics of SB RAS, Institute of Chemical Kinetics and Combustion of SB RAS and Insti-

tute of Catalysis of SB RAS [1]. The main elements of accelerator are parallel coupled accelerating structure, injector, waveguide track with vacuum RF window, focusing system and klystron KIU-111. The klystron's frequency is 2450 MHz, average power is 5 kW with pulse power of 5 MW [2]. The main goal of our efforts is to test new ideas and devices which are used in the accelerator. The mass of these elements are used in such accelerator for the first time and have some advantages.

PARALLEL COUPLED ACCELERATING STRUCTURE

The scheme of parallel coupled accelerating structure is shown in the Fig. 1 and Fig. 2. RF power from a klystron feeds the exciting cavity (1) through inductive coupling window (7). The exciting cavity supplies the accelerating cavities (2). The RF connection of the exciting cavity with the accelerating cavities is provided by magnetic field through coupling slots (5). The focusing alternative magnetic field is created along the beam axis by periodic permanent magnets (3) with radial magnetization inserted in the iron yoke (4). This kind of focusing provides large enough magnetic field while keeping the weight of the focusing system considerably small. The copper pins (6) are used to tune the exciting cavity (1) at the resonance frequency.

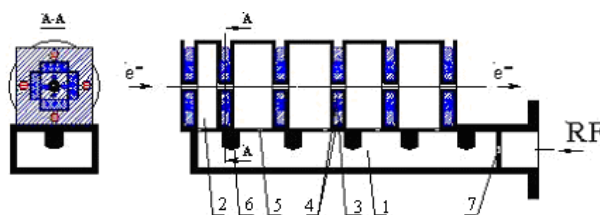


Figure 1: Scheme of the parallel coupled accelerating structure.

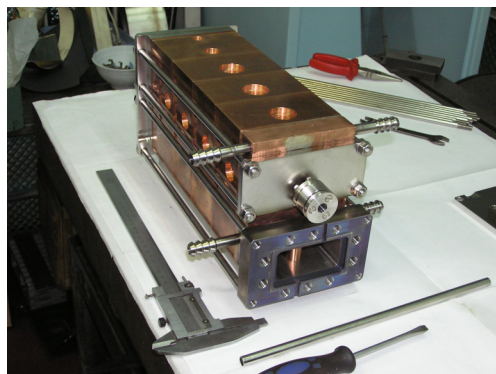


Figure 2: Parallel coupled accelerating structure.

* Work is supported by the Ministry of Education and Science of the Russian Federation, grants N 14.740.11.0836

DESIGN OF COMPACT C-BAND STANDING-WAVE ACCELERATOR FOR MEDICAL RADIOTHERAPY*

H. R. Yang[#], M. H. Cho, and W. Namkung

Pohang University of Science and Technology, Pohang 790-784, Korea

S. H. Kim, Argonne National Laboratory, Argonne, Illinois 60439, USA

J. S. Oh, National Fusion Research Institute, Daejeon 305-333, Korea

Abstract

We design a C-band standing-wave accelerator for an X-ray and electron source of medical radiotherapy. The accelerator system is operated two modes, using the X-ray and electron beams. Since two modes require different energy, the accelerator is capable of producing 6-MeV, 100-mA pulsed electron beams with peak 2-MW RF power, and 7.5-MeV, 50 mA electron beams with peak 2.5-MW RF power. The beam is focused by less than 1 mm without external magnets. The accelerating structure is a bi-periodic and on-axis-coupled structure with a built-in bunching section, which consists of 3 bunching cells, 14 normal cells and a coupling cell. It is operated with the $\pi/2$ -mode standing-wave. The bunching cells are designed to enhance the RF phase focusing. Each cavity is designed by the MWS code within 3.5% inter-cell coupling. In this paper, we present design details of RF cavities and the beam dynamics.

INTRODUCTION

The electron accelerator is widely used for industrial and medical applications: a contraband detection, material processing, a medical diagnosis and therapy, sterilizing food, and environmental processing [1, 2]. For the medical applications, the electron beam with 3 ~ 15 MeV, pulsed tens mA is required. These applications require the small beam spot size at the X-ray conversion target for reducing the penumbra [3]. In order to achieve such a small beam spot size, the RF focusing effect is maximized instead of the magnetic focusing with external magnets for a compact accelerator system.

We are developing a C-band standing-wave electron accelerator for an X-ray and electrons source of medical radiotherapy. This accelerator system is operated two modes, using the X-ray and electron beams. The X-ray beam is used to irradiate the viscera, and the electron beam is used to irradiate the inner and outer layers of skin. There is energy loss by two scattering foils which are between the accelerating column and the affected area in the electron mode, as shown in Fig. 1 [4]. The beam energy at the end of column has to be higher than irradiated energy in the affected area, 6 MeV which are widely used in the medical radiotherapy [5]. For such reasons, the accelerator is designed to produce 6-MeV, pulsed 100-mA electron beam with peak 2-MW power in the X-ray mode, and 7.5-MeV, pulsed 50-mA electron beam with peak 2.5-MW power in the electron mode. It is

operated with a pulse length of 4 μ s and with a pulse repetition rate of 250 Hz. The bunching cells are designed with beam dynamics simulation for enhancing the RF phase focusing. We design the RF cavities in the bi-periodic and on-axis-coupled accelerating structure with the MWS code. The beam dynamics simulations are conducted with PARMELA codes.

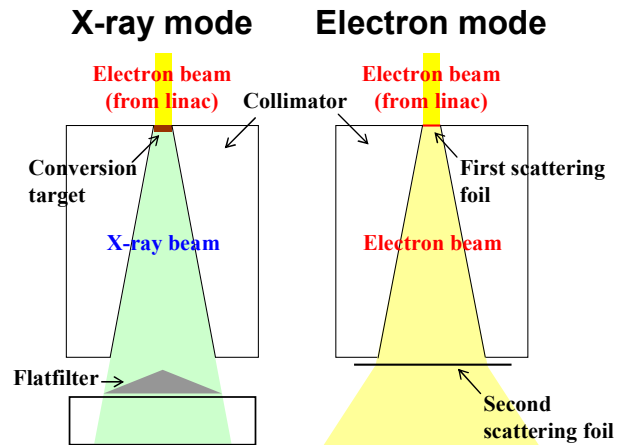


Figure 1: Schematic diagram of the X-ray and electron modes.

Table 1: The design parameters of the accelerator

Parameters	X-ray Mode	Electron mode
Operating Frequency	5712 GHz	
Input Pulsed RF Power	2.0 MW	2.5 MW
Pulse Length	4 μ s	
Repetition Rate	250 Hz	
E-gun Voltage	19.0 kV	20 kV
Input Pulsed Beam Current	80 mA	180 mA
Output Beam Energy	6 MeV	7.5 MeV
Output Pulsed Beam Current	50 mA	100 mA
Type of Structure	Bi-periodic, On-axis coupled	
Operating Mode	SW $\pi/2$ mode	
Beam Aperture Diameter*	6 mm	
Average Accelerating Gradient	134 MV/m	16.7 MV/m
Number of Cells	18	
Inter-cell Coupling	3.5%	
Quality Factor*	9000	
Shunt Impedance*	113 M Ω /m	
Transit-time Factor*	0.84	

*Values for normal cells.

*Work supported by POSTECH Physics BK21 Program.

[#]highlong@postech.ac.kr

CHANGING ATTITUDE TO RADIATION HAZARDS AND CONSEQUENT OPPORTUNITIES FOR LINAC APPLICATIONS

Y. Socol, Falcon Analytics, POB 82 Netanya 42100, Israel

Abstract

High-energy LINACs unavoidably yield ionizing radiation. This fact makes them subject to strict regulations and considerably limits their possible applications. During the last two decades the attitude to ionizing radiation hazards seems to become more balanced, as opposed to "radiophobia" of the Cold-War era. Scientifically, the Linear No-Threshold (LNT) model of radiation damage is more frequently questioned. Moreover, the hypothesis of radiation hormesis – beneficial effect of low-dose radiation – is studied. While this scientific debate has not yet given fruit in terms of changes in radiation regulation policy, we may expect this to happen in the near to middle term. Namely, the ALARA (as low as reasonably achievable) demand is anticipated to be substituted by some tolerance level, which in turn is anticipated to be very high according to the present standards. The presentation will review the present status of the radiation-hazard debate, and outline anticipated opportunities for LINAC applications, like compact designs and wider industrial outreach.

TOLERANCE LEVEL VS. LINEAR NO-THRESHOLD

High-energy LINACs unavoidably yield ionizing radiation. Adverse effects of high doses of ionizing radiation were discovered nearly immediately after the discovery of X-rays and radioactivity back in the XIX century. However, it took about two decades before early medical practitioners began to control their exposures to ionizing radiation. For example, the British X-ray and Radium Protection Committee was formed in 1921. In 1924, at a meeting of the American Roentgen Ray Society, Arthur Mutscheller recommended "tolerance" (permissible) dose rate for radiation workers, a dose rate that could be tolerated indefinitely. This rate was 0.2 roentgen per day (R/day), based on applying a factor of 1/100 to the commonly accepted average erythema dose of 600 R (not accidentally – lethal dose in case of acute whole-body irradiation), spread over 30 days [1]. The International Commission on Radiological Protection (ICRP), established in 1928, accepted in 1931 this tolerance dose rate as a universal recommendation that was in effect for more than quarter of a century. This level corresponds to 70 R/year or about 700 mSv/year – 35 times higher than the present-day occupational (professional) exposure limit, and 700 times higher than the present-day public one. It was assumed that no harm will be caused by radiation below this tolerance level. To illustrate the extent of public confidence in the usefulness and safety of ionizing radiation we will remind that until

after the Second World War X-ray machines were typical equipment of shoe shops (this fact was mentioned in passing in Rudolf Peierls' book from 1956 [2]).

It should be stressed that until now nobody succeeded to disprove the assumption of tolerance level (while it is clear that high dose is harmful: acute dose of 100 R leads to radiation sickness and 200 R may be already lethal). For example, a study of British radiological society members [3] reveals that while the pre-1921 radiologists (who had not controlled their exposure and therefore received high doses of ionizing radiation) had a 75% (4σ of the expected value) higher cancer mortality than other medical practitioners, the post-1920 radiologists had an insignificant 5% (0.4σ) excess. Furthermore, the studies of radium dial-painters, exposed to huge cumulative doses (mostly at low rates), revealed that no cancer excess was observed below the life-time dose of about 1000 rad [4]. For α -particles, emitted by radium, the radiation weighting factor $w_R=20$, i.e. 1000 rad = 10 Gray correspond to 200,000 mSv!

However, geneticists strongly believed the theory that the number of genetic mutations is linearly proportional to radiation dose just like the number of ionized atoms, that mutagenic damage was cumulative and therefore no tolerant (safe) dose for radiation could be set. According to this view, there is no absolute radiation safety, so that the safety level should only be weighed against the cost to achieve it [1].

After the bombing of Hiroshima and the start of the nuclear arms race, geneticists greatly amplified their concerns that exposure to radiation of atomic bomb fall-out would likely have devastating consequences on the gene pool of the human population. Hermann Muller was awarded the Nobel Prize in 1946 for his discovery of radiation-induced mutations. In his Nobel Prize Lecture, he argued that the dose-response for radiation-induced germ cell mutations was linear and that there was "no escape from the conclusion that there is no threshold" [5].

There was great controversy and extensive arguments during the following decade. Probably, both super-powers became interested in exaggerating the nuclear fall-out hazard. Ultimately all kinds of ionizing radiation became connected in public perception with nuclear apocalypse. As a result of (or at least in the wake of) this change in public perception, the ICRP and the national regulators changed their radiation protection policies in the mid-1950s. They rejected the tolerance dose concept and adopted the ALARA (as low as reasonably achievable) policy, i.e., to keep the radiation exposure ALARA. The accepted model for low-dose radiation-induced health damage became the so-called Linear No-Threshold (LNT) model. In LNT, the acute exposure, high-dose cancer

FERMILAB 1.3 GHz SUPERCONDUCTING RF CAVITY AND CRYOMODULE PROGRAM FOR FUTURE LINACS*

C.M. Ginsburg[#], Fermilab, Batavia, IL 60510, USA

Abstract

The proposed Project X accelerator and the International Linear Collider are based on superconducting RF technology. As a critical part of this effort, Fermilab has developed an extensive program in 1.3 GHz SRF cavity and cryomodule development. This program includes cavity inspection, surface processing, clean assembly, low-power bare cavity tests and pulsed high-power dressed cavity tests. Well performing cavities have been assembled into cryomodules for pulsed high-power tests and will be tested with beam. In addition, peripheral hardware such as tuners and couplers are under development. The current status and accomplishments of the Fermilab 1.3 GHz activity will be described, as well as the R&D program to extend the existing SRF pulsed operational experience into the CW regime.

INTRODUCTION

Work by the International Linear Collider (ILC) [1,2] community, which includes Fermilab, has motivated substantial world-wide infrastructure development and cavity performance progress. At Fermilab, this has translated to a very large commitment of resources for infrastructure and personnel development. The developed capability has led to the possibility to use the 1.3 GHz infrastructure for development of Project X [3,4], although the performance requirements are somewhat different [5]. The Project X 3 GeV CW linac requires high Q_0 at gradients (E_{acc}) in the range $15 < E_{acc} < 20$ MV/m; 1.3 GHz cavities can be used to investigate high Q_0 . In addition, the Project X 3-8 GeV pulsed section operates at 1.3 GHz and requires ILC-like cavities with $E_{acc} \sim 25$ MV/m. The status of Fermilab 1.3 GHz infrastructure, accomplishments and plans are described.

INFRASTRUCTURE

The cavities are fundamentally of the Tesla design [6], made of high RRR niobium with an elliptical cell shape, for superconducting operation at 2K. Cavity qualification has been described in detail elsewhere [7] and includes cavity inspection, surface processing, clean assembly, and one or more cryogenic qualification tests which typically include performance diagnostics. Cavities which reach the performance requirement in vertical (bare) qualification test, typically $E_{acc} > 35$ MV/m, are dressed and horizontally tested. Cavities which reach the performance specification in horizontal (dressed) qualification test, also typically $E_{acc} > 35$ MV/m, are

assembled into cryomodules.

The joint ANL/FNAL facility is the primary infrastructure [7] for surface processing of 1.3 GHz cavities, and includes electropolishing (EP). New infrastructure at Fermilab includes two high temperature furnaces for hydrogen degassing, see Fig.1. In addition, a centrifugal barrel polishing (CBP) machine for 1-cell and 9-cell 1.3 GHz cavities has been introduced for R&D and may be used for production cavity preparation in the future, see Fig.2. CBP may be used in place of the standard bulk electropolishing step, to reduce acid use. CBP has been demonstrated to be a useful repair technique [8], and may have other benefits as well, such as reducing cavity performance sensitivity to minor manufacturing or material defects; these studies are not yet complete. A new R&D surface processing facility [9] is now fully operational for the full suite of standard EP processing for 1-cell 1.3 GHz cavities. The R&D EP tool is shown in Fig.3.

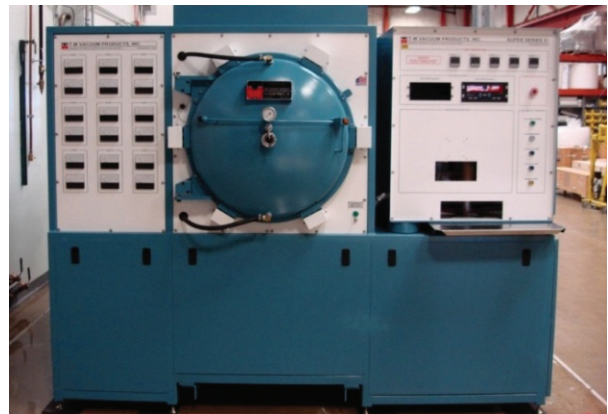


Figure 1: One of the two new vacuum furnaces.



Figure 2: Centrifugal barrel polishing machine.

*Operated by Fermi Research Alliance, LLC, under Contract DE-AC02-07CH11359 with the U.S. DOE
#ginsburg@fnal.gov

NON-DESTRUCTIVE INSPECTIONS FOR SC CAVITIES

Y. Iwashita, Y. Fuwa, M. Hashida, K. Otani, S. Sakabe, S. Tokita, H. Tongu,
Kyoto University, Uji, Kyoto, JAPAN
H. Hayano, K. Watanabe, Y. Yamamoto, KEK, Ibaraki, JAPAN

Abstract

Starting from the high-resolution camera for inspection of the cavity inner surface – so-called Kyoto Camera, high resolution T-map, X-map and eddy current scanner have been developed. R&D for radiography techniques is also going on to detect small voids inside the Nb EBW seam, where the target resolution is 0.1 mm. Some radiography tests with X-rays induced from an ultra short pulse intense laser were carried out. The local treatment technique on the found defects is also realized by the Micro-Grinder.

INTRODUCTION

Non-destructive Inspections play important roles in improving yield on production of high performance SC Cavities. Starting from the high-resolution camera for inspection of the cavity inner surface [1], high-resolution T-map, X-map and eddy current scanner [2,3,4,5,6] have been developed. We are also investigating radiography to detect small voids inside the Nb EBW seam, where the target resolution is 0.1 mm. We are carrying out radiography tests with X-rays induced by irradiations of an ultra short pulse intense laser on a target metal sheet. Defects found by the inspection technique can be locally treated by the Micro-Grinder.

CAVITY CAMERA UPDATE

In order to inspect the SPL cavity at CERN, whose frequency is about a half of ILC cavity and the diameter is about twice larger, the illumination system has been enhanced to illuminate the wider surface area (see Fig. 1). Although the iris diameter is about twice larger than that of ILC's, the bore diameter at the flange position is limited (just below $\varnothing 80\text{mm}$). This limits the camera cylinder diameter is $\varnothing 70\text{mm}$. Fig. 2 shows the modification on the illumination system to illuminate the wider area with enough strength. While the former system used two LED's for each strip, the new system uses 14 LED chips on a line and two lines consist one strip. Thus 28 LED chips are used for a strip. Furthermore, the LED chip has three LED's in a package. This illumination system should provide enough light for the wider cavity surface area. Because of the larger cavity size, the working distance is longer than former model and a bigger lens system is adopted. Fig. 3 shows the overview of this system. The illumination plate on the cylinder is shown in Fig. 4. The camera cylinder can be rotated to see the annular area in a cavity without movement of the cavity, while the cavity table can rotate the cavity if it does not wear its He jacket around. The table has a function to move the cavity in its axial direction.

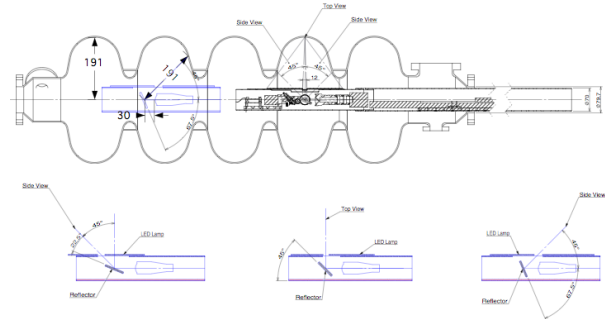


Figure 1: CavCam3 in SPL cavity.

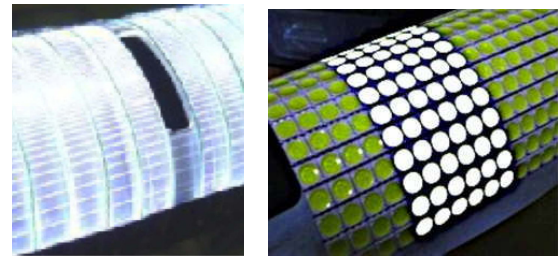


Figure 2: Enhanced illumination for wider surface area (Armadillo Illumination). 28 LED chips (right) instead of 2 LED's per strip (left) are installed.



Figure 3: Latest CavCam-3 for SPL cavity at CERN.



Figure 4: All the LED's are lighten. A diffusing panel will be install on the LED's to form the light strip. 14 chips/line x 2 lines/strip x 10 strips/side x 2 sides = 560 chips are used.

TEST RESULTS OF TESLA-STYLE CRYOMODULES AT FERMILAB *

E. Harms[#], K. Carlson, B. Chase, D. Crawford, E. Cullerton, D. Edstrom, A. Hocker, M. Kucera, J. Leibfritz, O. Nezhevenko, D. Nicklaus, Y. Pischalnikov, P. Prieto, J. Reid, W. Schappert, P. Varghese, Fermilab, Batavia, IL 60510 USA

Abstract

Commissioning and operation of the first Tesla-style Cryomodule (CM-1) at Fermilab was concluded in recent months. A second Tesla Type III+ module, RFCA002, will be replacing it. CM-1 is the first 8-cavity ILC style cryomodule to be built at Fermilab and also the first accelerating cryomodule of the Advanced Superconducting Test Accelerator (ASTA). We report on the operating results of both of these cryomodules.

- 5 Hz repetition rate
- 700 μs fill time
- 500 μs flattop
- 2 Kelvin / 23.4 Torr temperature
- 3.9 MW peak Klystron power.

INTRODUCTION

An electron Linac based on Superconducting RF technology has been proposed and is under construction at Fermilab. This Advanced Superconducting Test Accelerator (ASTA) has as its main components a Cs-Te 1-1/2 cell Photoinjector gun, two Capture cavities, and Tesla-style SRF cryomodules as well as low (40 MeV) and high energy user beam lines. This facility has been described previously [1]. It currently serves as the only test bed for multi-cavity cryomodules at Fermilab until a dedicated facility, the Cryomodule Test Facility (CMTF), now under construction is completed.

The setup for testing cryomodules at ASTA contains all of the necessary infrastructure including:

- 5MW 1.3 GHz klystron capable of pulsed operation at 10 Hz
- Cryogenics plant capable of providing 120 Watts of refrigeration at 2 Kelvin
- Interlock/protection systems
- Low Level RF (Feedforward & Feedback) system
- Vacuum system
- Controls integrated to Fermilab's Accelerator Controls system, ACNET.

CRYOMODULE 1

CM-1 was the first Tesla Type III Cryomodule to be placed into operation in the United States and the first multi-cavity cryomodule of any type to become operational at Fermilab. It was provided to Fermilab as a 'kit' from DESY in exchange for a 4-cavity 3.9 GHz module, ACC39, which was designed and assembled at Fermilab and is now in operation at DESY's FLASH facility. Table 1 highlights the major steps in bringing CM-1 into operation and completing the test program.

The test plan for CM-1 has been described previously as has been the performance characteristics of individual cavities [2]. Typical operating conditions were:

Table 1: CM-1 Commissioning Milestones

Milestone	Date
Cryomodule moved into final position and aligned	22 January 2010
5 MW RF/Klystron commissioning	June - July 2010
Warm coupler conditioning - one cavity at a time (4 - 14 days/cavity)	August – October 2010
Cool down from room temperature to 4 then 2 Kelvin	17 – 22 November 2010
Individual Cavity cold conditioning and evaluation	December 2010 – June 2011
Installation of Waveguide Distribution system and Water System upgrade	13 June - 5 July 2011
First powering of the entire module	6 July 2011
Long Pulse (9ms) tests	December 2011
Thermal cycling and IN ₂ leak repair	January - February 2012
Cease operation/Removal	March 2012

Figure 2 provides a comparison of peak cavity gradients during qualification tests at DESY as well as during CM-1 full module operation while Table 2 summarizes individual cavity performance in CM-1. On average, the cavities' peak gradients in CM-1 are 85% of that measured previously.

Module Evaluation

The previous report [2] on CM-1 indicated some outstanding measurements to be performed including

- Demonstration of Lorentz Force Detuning Compensation on the entire module,
- Additional processing to attempt to improve the performance of deficient cavities,

*Operated by Fermi Research Alliance, LLC under Contract No. DE-AC02-07CH11359 with the United States Department of Energy.

[#]Harms@fnal.gov

DEVELOPMENT OF SUPERCONDUCTING RADIO-FREQUENCY DEFLECTING MODE CAVITIES AND ASSOCIATED WAVEGUIDE DAMPERS FOR THE APS UPGRADE SHORT PULSE X-RAY PROJECT*

J. Holzbauer[†], A. Nassiri, G. Waldschmidt, G. Wu
Argonne National Laboratory, Argonne, IL 60439, U.S.A.

Abstract

The Advanced Photon Source Upgrade (APS-U) is a Department of Energy (DoE) funded project to increase the available x-ray beam brightness and add capability to enhance time-resolved experiments on few-ps-scale at APS. A centerpiece of the upgrade is the generation of short pulse x-rays (SPXs) for pump-probe time-resolved capability using SRF deflecting cavities [1]. The SPX project is designed to produce 1-2ps x-ray pulses for some users compared to the standard 100ps pulses currently produced. SPX calls for using superconducting rf (SRF) deflecting cavities to give the electrons a correlation between longitudinal position in the bunch and vertical momentum [2]. The light produced by this bunch can be passed through a slit to produce a pulse of light much shorter than the bunch length at reduced flux. The ongoing work of designing these cavities and associated technologies will be presented. This includes the design and prototyping of higher- (HOM) and lower-order mode (LOM) couplers and dampers as well as the fundamental power coupler (FPC). This work will be given in the context of SPX0, a demonstration cryomodule with two deflecting cavities to be installed in APS in early 2014.

INTRODUCTION

The SPX project calls for the use of an RF deflecting-mode cavity to chirp electron bunches, giving the electrons a correlation between their longitudinal position in the bunch and their vertical momentum. Synchrotron light produced from this bunch can then be passed through a physical slit to create a shorter light pulse at the proportional sacrifice of total flux. This scheme was first proposed by Zholents [1]; the scheme can be seen in Figure 1.

A significant amount of design work has gone into the RF cavities required for this project, details of which can be found in [2, 3, 4, 5, 6, 7]. This cavity application has many specific challenges including the need to heavily damp all non-operational modes to preserve beam quality for other APS users.

CAVITY DESIGN

The current design is a squashed elliptical dipole-mode cavity with a Y-shaped end group and an on-cell damping

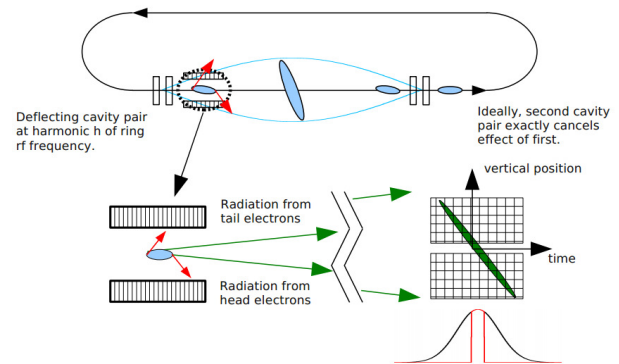


Figure 1: Schematic of Zholent's short pulse x-ray generation scheme. Image credit to [3].

port which can all be seen in Figure 2. Two of the waveguides from the Y end group will be used for damping of higher-order modes (HOMs) while the third will be primarily used as the forward power coupler. The on-cell damper is used primarily to damp the fundamental mode, called the lower-order mode (LOM). A list of the cavity parameters can be seen in Table 1.

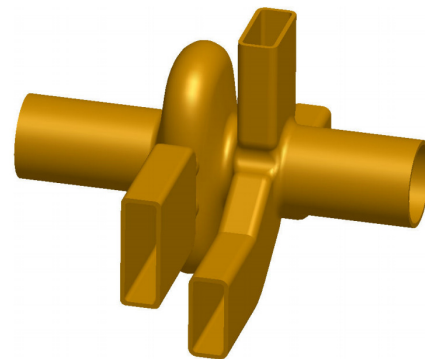


Figure 2: Schematic of a deflecting mode cavity for SPX. The LOM waveguide can be seen on-cell with the Y-end group (HOM dampers and FPC) to the right. Image credit to [3].

At this point, it is expected to use a BCP etching during cavity processing. Given the cavity parameters and this processing technique, 120 mT is the maximum expected reliable peak magnetic field. Given this and the requirement that each deflecting section have a total of 2 MV of

* Work supported by the U.S. Department of Energy, Office of Science, under Contract No. DE-AC02-06CH11357

[†] jholzbauer@aps.anl.gov

MULTIPACTING ANALYSIS OF HIGH-VELOCITY SUPERCONDUCTING SPOKE RESONATORS*

C. S. Hopper[†] and J. R. Delayan

Center for Accelerator Science, Department of Physics,
Old Dominion University, Norfolk, VA, 23529, USA and
Thomas Jefferson National Accelerator Facility, Newport News, VA 23606, USA

Abstract

Some of the advantages of superconducting spoke cavities are currently being investigated for the high-velocity regime. When determining a final, optimized geometry, one must consider the possible limiting effects multipacting could have on the cavity. We report on the results of analytical calculations and numerical simulations of multipacting electrons in superconducting spoke cavities and methods for reducing their impact.

INTRODUCTION

Superconducting multi-spoke cavities for frequencies of 325, 352, 500, and 700 MHz and velocities of $\beta_0 = 0.82$ and 1 have been designed and optimized [1, 2, 3] for a variety of possible applications. These applications include, but are not limited to, compact machines such as future light sources and high-energy proton or ion linacs. Here we focus on what regions of these resonators are most susceptible to multipacting events.

When the internal surface of a rf cavity is exposed to the high fields maintained in a superconducting cavity, electrons (known as primary electrons) can be emitted from the metal. The kinetic energy and trajectory of these electrons is determined by the electromagnetic fields, and in many cases, they will come in contact with another part of the surface with a certain amount of impact energy. If this energy falls within the secondary emission yield (SEY) range, then additional electrons, known as secondary electrons, will be ejected [4]. Figure 1 shows a generic SEY curve. The parameters E_{oc}^I , and E_{oc}^{II} are known as the crossover energies for which $\delta = 1$. E_{om} marks the electron energy for which δ is maximum. These parameters can vary greatly between materials. Even for a given material, these parameters can vary widely based on both the bulk properties and surface condition.

For well prepared niobium cavities, the crossover energies are around 150 eV and 1050 eV, while E_{om} is around 375 eV [5]. We have presented preliminary results for crossover energies of 150 eV and 2000 eV previously [2]. When secondary electrons are in resonant trajectories, and each impact energy is in the range for which $\delta > 1$, then a cascade can occur generating excessive heat, thus leading to thermal breakdown. These regions are commonly called barriers, and they are classified as either "soft" or "hard." Soft barriers are those that can be conditioned

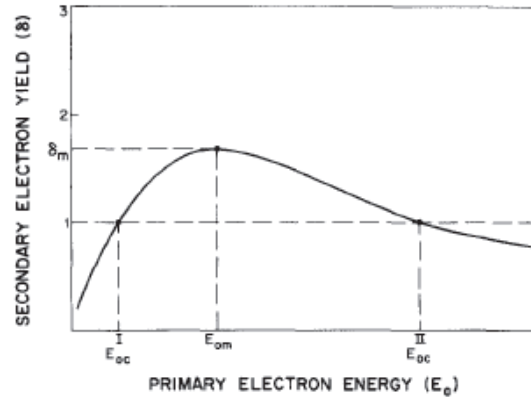


Figure 1: Definition of secondary-electron yield-curve parameters [6]

through and thereby passed. It is believed conditioning occurs because multipacting electrons actually clean the surface to a point where the secondary emission yield is below unity [7]. Hard barriers are those which persist resulting in a limited achievable gradient and quenching.

By improving the quality of the surface, the soft barriers on the gradient can be eliminated. On the other hand, hard barriers can only be overcome by changing the cavity geometry in such a way as to avoid resonant trajectories all together.

Multipacting is also characterized, most commonly, as either one-point or two-point. One-point multipacting occurs when the time of flight of the electron between two impacts is an integer number of rf cycles and that the electron's impact site is approximately the same as its ejection site. This condition can be described in terms of the cyclotron and rf frequencies as [8],

$$\frac{f}{n} = \frac{eB}{2\pi m} \quad (1)$$

In the case of two-point multipacting, the time of flight is an odd number of half rf cycles and the impact site is not the same as the ejection site. The former condition can be described with the same parameters as (1) [9],

$$\frac{2f}{2n - 1} = \frac{eB}{2\pi m} \quad (2)$$

* Work supported by U.S. DOE Award No. DE-SC0004094

[†] chop002@odu.edu, chrsthop@jlab.org

MECHANICAL STUDY OF FIRST SUPERCONDUCTING HALF-WAVE RESONATOR FOR INJECTOR II OF CADS PROJECT*

Shoubo He[#], Yuan He, Weiming Yue, Shenghu Zhang, Ruoxu Wang, Cong Zhang, Mengxin Xu, Fengfeng Wang, Shichun Huang, Yuzhang Yang, Shengxue Zhang, Hongwei Zhao
Institute of Modern Physics, Chinese Academy of Sciences, Lanzhou, Gansu 730000, China

Abstract

Within the framework of the China Accelerator Driven Sub-critical System (CADS) project, institute of modern physics (IMP) has proposed a 162.5MHz half-wave resonator (HWR) Superconducting cavity for low energy section ($\beta=0.09$) of high power proton linear accelerators. For the geometrical design of superconducting cavities structure mechanical simulations are essential to predict mechanical eigenmodes and the deformation of the cavity walls due to bath pressure effects and the cavity cool-down. Additionally, tuning analysis has been investigated to control the frequency against microphonics and Lorentz force detuning. Therefore, several RF, static structure, thermal and modal analyses with three-dimensional code Traditional ANSYS have been performed [1]. In this paper, we will present some results about mechanical analysis of the first superconducting HWR cavity in order to further optimization in the near future.

INTRODUCTION

The cavity geometry has been optimized to reach the design frequency 162.5MHz and $\beta=0.09$ and also we want to minimize value of peak electrical and magnetic field on the cavity surface relative to the accelerating electrical field on the cavity axes (Bpk/Eacc and Epk/Eacc) [2]. So the fabrication technology and resonator structural properties including cooling down, vacuum, etching and so on, also should be taken into account at the beginning of design. SC HWR cavities are highly sensitive to mechanical deformations due to the small loaded bandwidth of some SCRF applications. So accordingly for HWR the stability of the cavity structure against any external distortions is the primer design goal. In order to improve df/dP for a low Beta HWR cavity, the typical approach is to add some stiffening ribs on the cavity, but it will not be discussed in this paper. Here, we will investigate this type of structure and then we will improve it in the future. Primarily structural analysis was completed to determine the locations of the model that were beyond yield strength.

Since CADS accelerator will work in CW regime, the main goal of our cavity structural design is a minimization of the resonant frequency dependence on

the external pressure fluctuations. The general basics of the cavity structural design are to avoid using the plane surfaces as illustrated in Figure 1. Besides, four access ports at each cavity (two at the bottom, two at the top) guarantee draining off of the chemical etching and easy access to the inner surfaces during the high pressure water rinsing (HPR).

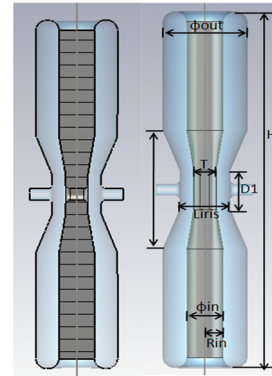


Figure 1: The cross section of HWR cavity with the main geometric parameters: Liris-iris to iris length, T-inner conductor thickness, D1-cavity diameter.

Table 1: Some Properties of HWR Cavity

Para.	Frequency	β	Diameter	Uacc	Epeak	Bpeak
Value	162.5	0.093	40	0.78	25	50
Unit	MHz	---	mm	MV	MV/m	mT

STRUCTURAL ANALYSIS

Injector II of CADS is composed by an ECR ion source, LEPT, RFQ and superconducting accelerating section. And in superconducting accelerating section, there are two cryomodels and each cryomodel is composed of 8 superconducting Half-Wave-resonator cavities and 9 superconducting solenoids. The proton beam will be accelerated from 2.1 MeV to 10MeV. Before structure analysis the geometry of HWR cavity was taken from a sat. model that was generated in software CST Microwave Studio and represented one cavity structure. The ANSYS RF results were compared to CST and to HFSS models of the same cavity for final verification. And the difference among these code result is only about 0.065%.

During mechanical analysis of HWR cavity, the variation of RF Eigen frequency was calculated, including pressure sensitivity, Lorentz force detuning, tuning sensitivity and resonant vibration and etc.. The

*This work is Supported by the National Natural Science Foundation of China (Grant Agreement 91026001)

[#]heshoubo@gmail.com

THE SUPERCONDUCTING CH CAVITY DEVELOPING IN IMP*

M.X.XU[#], Y.He, S.H.Zhang, Z.J.Wang, R.X.Wang, SH.B.He, W.M.Yue, C.Zhang, SH.CH.Huang, Y.ZH.Yang, SH.X.Zhang, T.C.Jiang, Y.L.Huang, H.W.Zhao, J.W.Xia, IMP, Lanzhou, Gansu 730000,China

Abstract

The Cross-Bar H-type (CH) cavity is a multi-gap drift tube structure operated in the H21 mode [1]. The Institute of Modern Physics (IMP) has been doing research and development on this type of superconducting CH cavity which can work at the C-ADS (accelerator driver sub-critical system of China). A new geometry CH cavity has been proposed which have smaller radius. It's suitable in fabrication, and it's can reduce cost too .Detailed numerical simulations with CST MicroWave Studio have been performed. An overall surface reduction of 30% against the old structure seems feasible. A copper model CH cavity is being fabrication for validating the simulations and the procedure of fabricating niobium cavity.

INTRODUCTION

C-ADS project with ambitious requirement regarding beam power and quality need new superconducting linac development. Superconducting Crossbar-H-Mode (CH)-cavities have two important features meet with the requirements of C-ADS. Superconducting CH cavity have high real estate gradients compared to conventional low-beta ion linacs, this feature will reduce the amount of cavity prominent. For the cross bar structure, CH cavities are more rigidly. This feature satisfy the harsh requirements of C-ADS about reliable. As this reasons, superconducting CH cavities have been choose as a backup cavity type for the C-ADS(see Fig.1). With respect to C-ADS actual application, one prototype of superconducting CH cavity (f=162.5MHz, beta=0.067, 6 cells) is presently being development in IMP.

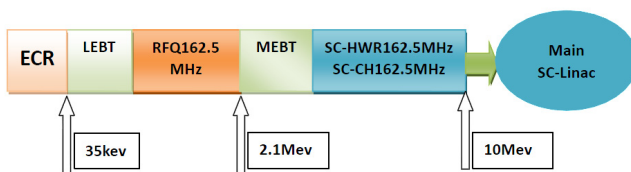


Figure 1: Layout of Injector-II for C-ADS.

*Work supported by 91026001 Nature Science Foundation of China
[#]xumx@impcas.ac.cn

NEW SHAPE SUPERCONDUCTING CH CAVITY

The superconducting CH cavity has electric and magnetic field structure similar with combine the 4-vane RFQ and DTL's. We can use a semi-analytical approach to estimate basic parameters like frequency. The parameter Rt and r1 are represent the radius of CH cavity and the tube radius of CH cavity respectively. Using this equivalent, we can get the resonance frequency with the radius Rt as following [1]:

$$\omega \approx c \left(\frac{0.73}{Rt^2 \left(\frac{25}{144} + \frac{25}{72} \ln\left(\frac{Rt}{r1}\right) - 0.2 \right)} \right)^{1/2} \quad (1)$$

In case of the superconducting CH cavity of IMP, the frequency is 162.5MHz, r1 was 0.03m. Using the formula (1) can give radius Rt of the CH cavity is 0.29 meter. We have using the software CST to simulation. The radius of CH cavity is 0.32 meter [2].

The superconducting CH cavity is a complex cavity. With the radius of 0.32 meter, there are big surface. This means a large amount of high pure niobium needs and a more chance to come across defects. As in superconducting cavity, perfect surface is important for the cavity quality [3]. This size of CH cavity is not easy to protect from defects and contaminates or not suitable in the vacuum chamber of electric beam welding machine.

We try to cut a part of the girder called undercut [4] (see Fig.2).This undercut will increase inductance in the end of cavity, as this will increase the length of current flow. Increased inductance will lower the resonance frequency that we can get a smaller cavity structure in the same frequency (see Fig.3).

When we change the size of undercut in the girder of CH cavity, the radius will reduce with the width of girder liner. At most, we can reduce the radius of cavity by 20% (see Fig.4). As the radius reducing, the surfaces of the cavity reduce by 30% (see Fig.5).

RF SURFACE IMPEDANCE CHARACTERIZATION OF POTENTIAL NEW MATERIALS FOR SRF-BASED ACCELERATORS*

B. P. Xiao^{1,2#}, G. V. Eremeev¹, M. J. Kelley^{1,2}, H. L. Phillips¹, C. E. Reece¹

¹Thomas Jefferson National Accelerator Facility, Newport News, VA 23606, USA

²College of William and Mary, Williamsburg, VA 23187, USA

Abstract

In the development of new superconducting materials for possible use in SRF-based accelerators, it is useful to work with small candidate samples rather than complete resonant cavities. The recently commissioned Jefferson Lab RF Surface Impedance Characterization (SIC) system [1] can presently characterize the central region of 50 mm diameter disk samples of various materials from 2 to 40 K exposed to RF magnetic fields up to 14 mT at 7.4 GHz. We report the recent measurement results of bulk Nb, thin film Nb on Cu and sapphire substrates, Nb₃Sn sample, and thin film MgB₂ on sapphire substrate provided by colleagues at JLab and Temple University.

INTRODUCTION

SRF accelerating cavities for particle accelerators made from bulk niobium materials are the state-of-art for particle accelerators. Other materials, like thin film Nb on Cu, Nb₃Sn, and MgB₂ are of interest because of their potential cost and performance benefits in SRF applications. In this paper, we report the measurement results from bulk Nb, thin film Nb on Cu substrates and thin film MgB₂ on sapphire provided by colleagues at JLab and Temple University.

DESCRIPTION OF APPARATUS

The sample has been put at the open end of a TE₀₁₁ cylindrical Nb cavity with a sapphire rod inside, described in [1]. The system provides a resonant field at 7.4 GHz. The cavity body, from which the sample is thermally isolated, is surrounded by liquid helium during the test, which differs from the previous measurements [2-4] by making the RF effect on sample the only contribution to the induced heat and resonance frequency change. Heat can be conducted from the sample only via the calorimeter. The effective surface impedance of the sample is derived by directly substituting heater heat for RF heat under controlled RF field and temperature conditions. This system can detect as little as 1 μW dissipated on the sample, enabling the resolution of surface resistance as low as 1.2 nΩ at 5 mT peak magnetic field. A cross-section of the SIC system is shown in Figure 1.

The effective surface impedance can be calculated from:

$$Z_s = \frac{E_z}{H_y} = \frac{P_{rf}}{\frac{1}{2} \int H^2(S) dS} + i\omega\mu_0\lambda = \frac{P_{rf}}{kB_{pk}^2} + i\omega\mu_0(\lambda_{ref} + \frac{f-f_{ref}}{M})$$

$$\text{with: } k = \frac{1}{2} \int B^2(S) dS / (\mu_0 B_{pk})^2$$

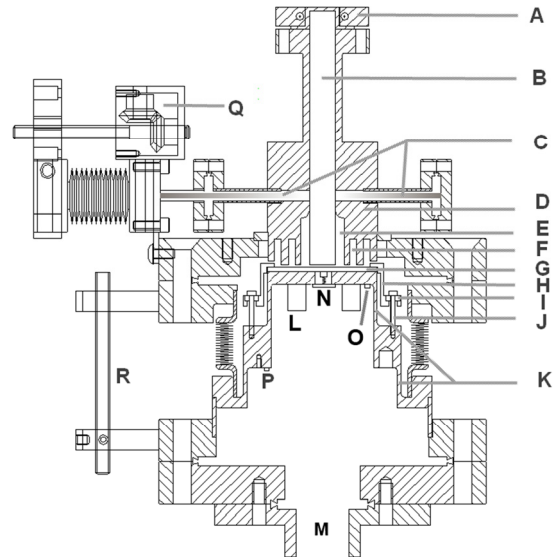


Figure 1: SIC system cross-section. A. Cap for sapphire rod, B. Sapphire rod, C. RF coupler, D. Nb cavity body, E. TE₀₁₁ cavity, F. Double choke joints, G. Sample on top of copper sample holder, H. Stainless steel sample clamp, I. G-10 washer, J. Aluminium bolt, K. Upper and lower thermal insulators, L. Ring heater, M. Port for vacuum and wires. (Vacuum port of the cavity is not shown), N. Thermal sensor mounted on spring, O&P. Thermal sensor, Q. Coupler tuning mechanism, R. Gap tuning mechanism (1 of 3).

The real part is the effective surface resistance and imaginary part is the effective surface reactance. P_{rf} is the RF induced heat, $B(S)$ is the magnetic field distribution on the sample, M is the tuning sensitivity that represents the ratio between frequency change and penetration depth change. k and M are geometry dependent coefficients and ω is the resonant circular frequency. The RF induced heat is calculated from the difference between the power from the heater required to keep a constant sample temperature without RF fields in the cavity and the power from the heater required to keep the sample's equilibrium temperature unchanged when RF fields are present, so called power compensation technique. The change of effective surface reactance is proportional to the change of penetration depth. It may be discerned from the

* Authored by Jefferson Science Associates, LLC under U.S. DOE Contract No. DE-AC05-06OR23177. The U.S. Government retains a non-exclusive, paid-up, irrevocable, world-wide license to publish or reproduce this manuscript for U.S. Government purposes.

THE NEW 2ND-GENERATION SRF R&D FACILITY AT JEFFERSON LAB: TEDF*

C. E. Reece and A. Reilly

Thomas Jefferson National Accelerator Facility, Newport News, VA 23606, USA

Abstract

The US Department of Energy has funded a near-complete renovation of the SRF-based accelerator research and development facilities at Jefferson Lab. The project to accomplish this, the Technology and Engineering Development Facility (TEDF) Project has completed the first of two phases. An entirely new 3,100 m² purpose-built SRF technical work facility has been constructed and was occupied in summer of 2012. All SRF work processes with the exception of cryogenic testing have been relocated into the new building. All cavity fabrication, processing, thermal treatment, chemistry, cleaning, and assembly work is collected conveniently into a new LEED-certified building. An innovatively designed 800 m² cleanroom/chemroom suite provides long-term flexibility for support of multiple R&D and construction projects as well as continued process evolution. The detailed characteristics of this first 2nd-generation SRF facility are described.

JLAB SRF FACILITY HISTORY

In 1987 the construction of CEBAF began on a green-field site in Newport News, Virginia. Since CEBAF was to be the first major research institution fully dependent on superconducting RF (SRF) technology in the US, a self-contained set of facilities using then-current technology were setup to support construction of CEBAF. To assure project success and on-going support capability, investments were made in chemical, cleanroom, assembly, and testing facilities that have served multiple needs for the subsequent +20 years.

These facilities enabled the construction of the 42 cryomodules for CEBAF, two cryomodules for the JLab FEL, 24 cryomodules for SNS, rework with upgraded techniques of the ten weakest cryomodules from CEBAF as part of the “C50 program” to establish a 6 GeV program, several prototype cryomodules, and most recently ten “C100” cryomodules for the CEBAF 12 GeV Upgrade project. These projects plus additional R&D programs accumulated over 4200 cavity preparation and vertical cryogenic testing cycles.

Participation in the SNS construction project and the ILC R&D program provided opportunities to make some improvement to the cavity cleaning and testing capabilities. The evolution and aging of the infrastructure resulted in adequate, but constrained capabilities and significant on-going maintenance challenges.

* Authored by Jefferson Science Associates, LLC under U.S. DOE Contract No. DE-AC05-06OR23177. The U.S. Government retains a non-exclusive, paid-up, irrevocable, world-wide license to publish or reproduce this manuscript for U.S. Government purposes.

DOE SLI PROGRAM

The US Department of Energy has a program designed to upgrade existing substandard facility infrastructure within the Office of Science laboratory system. Jefferson Lab won a competitive award from this system, the Science Laboratory Infrastructure (SLI) program, to build the Technology and Engineering Development Facility Project (TEDF). The project allows elimination of substandard structures and provides improved:

- Energy efficiency
- Life-safety code compliance
- Work-flow efficiency
- Facility sustainability
- Human work environment
- Technical quality of facilities for future work

The completed TEDF project will provide new homes for members of several Jefferson Lab organizational units, including the SRF staff, most of the Engineering Division, and Physics Division instrumentation groups. The new building set will meet the “green building” standards of LEED Gold™.

TEDF CONCEPTUAL DESIGN

The architectural engineering firm EwingCole was retained to integrate user requirements into a coherent package. The firm took a blank-page approach to facility design, seeking to incorporate improved safety, energy efficiency, and work flow for SRF cavity development, fabrication, processing, assembly, testing, and provide increased build-out space for cryomodule assembly. Replacement of the cryomodule test facility and cavity vertical dewar test facility was briefly considered, but even simple duplication would have been much too expensive.

Lessons learned over the past +30 years of SRF cavity preparation were folded into facility requirements, as was equipment and support systems expertise from the semiconductor industry. This new facility was composed so as to strengthen our support of four parallel missions:

- Reliable on-going support for the CEBAF nuclear physics research program
- Research on performance-limiting aspects of SRF technology to push the net system costs down
- Development of new accelerating structures, improved SRF cavity processing methods, and prototype cryomodules for new applications
- Construction and delivery of SRF-based accelerator modules for Jefferson Lab and partner laboratories.

Anticipating the continued evolution of the designs, materials, and processes used in SRF cryomodules, the

A NEW INTERNAL OPTICAL PROFILOMETRY SYSTEM FOR CHARACTERIZATION OF RF CAVITY SURFACES – CYCLOPS*

C. E. Reece¹, A. D. Palczewski¹, H. Tian¹, J. Bearden², and L. Jacobs²

¹Thomas Jefferson National Accelerator Facility, Newport News, VA 23606, USA

²MicroDynamics Inc., Woodstock, GA 30189, USA

Abstract

Jefferson Lab has received and is commissioning a new interferometric optical profilometer specifically designed to provide internal surface mapping of elliptical rf cavities. The CavitY CaLibrated Optical Profilometry System – CYCLOPS – provides better than 2 μm lateral resolution and 0.1 μm surface height resolution of programmatically selected locations on the interior surface of multi-cell cavities. The system is being used to provide detailed characterization of surface topographic evolution as a function of applied surface treatments and to investigate particular localized defects. We also intend to use the system for 3D mapping of actual interior rf surface geometry for feedback to structure design model and fabrication tooling. First uses will be illustrated. CYCLOPS was developed and fabricated by MicroDynamics Inc., Woodstock, GA, USA.

INTRODUCTION

The performance of superconducting resonant rf structures used for particle acceleration is quite often limited by localized surface defects. Developing an understanding of the nature of such defects and their origin is critical to confidently avoiding their occurrence. The surface of interest is the interior of a complex three-dimensional object, which presents a major impediment to the development of such an understanding.

External thermometry during cryogenic rf testing provides confident localization of anomalous heating to within ~ 1 cm. Use of such thermometric mapping has been followed up with visual inspection by careful non-contacting insertion of a camera and illumination system such as that developed at Kyoto University [1], and by use of long-range microscopes with mirror and lighting inserted into the cavity [2]. Such visual inspection provides valuable information about the morphology of the defect region, but is very difficult to interpret quantitatively. In addition to characterization of defects, quantitative topographical information is needed to refine the understanding of cavity surface topography evolution as a function of applied processing steps, whether mechanical or chemical, to optimize those processes for both effectiveness and economy.

One route to obtain quantitative topographic information from a location of interest is by forming a replica mold of the region which may then be examined

with external profilometry tools. This has been successfully accomplished for a few defect spots in multi-cell cavities [3, 4], and even accomplished without affecting the performance of the cavity. Such technique, however, can hardly be envisioned for extensive use.

A more attractive solution would be provided by optical interferometric profilometry accomplished on the interior of the finished cavity. Though perhaps conceptually straightforward, the realization of such a system presents significant motion control challenges.

MicroDynamics Inc. [5] has developed such a system, called CavitY CaLibrated Optical Profilometry System (CYCLOPS) and delivered it to Jefferson Lab. Commissioning of the CYCLOPS is underway.

SYSTEM DESCRIPTION

This unique system provides optical inspection and quantitative profilometry of the interior surface of cylindrically symmetric structures that have axial clearance of at least 48 mm diameter. The system can accommodate structures up to 1.5 m in length and diameter up to 34 cm. See Figure 1.



Figure 1: CYCLOPS setup at Jefferson Lab.

The system is oriented vertically with the non-contacting optical probe traveling down the cylindrical axis. The probe consists of two concentric hollow cylinders, an outer probe which positions a lower mirror,

* Authored by Jefferson Science Associates, LLC under U.S. DOE Contract No. DE-AC05-06OR23177. The U.S. Government retains a non-exclusive, paid-up, irrevocable, world-wide license to publish or reproduce this manuscript for U.S. Government purposes.

SUPERCONDUCTING RF LINAC FOR eRHIC*

S. Belomestnykh^{1,2#}, I. Ben-Zvi^{1,2}, J. C. Brutus¹, H. Hahn¹, D. Kayran¹, V. Litvinenko^{1,2}, G. Mahler¹, G. McIntyre¹, V. Ptitsyn¹, R. Than¹, J. Tuozzolo¹, Wencan Xu¹, A. Zaltsman¹

¹⁾ Brookhaven National Laboratory, Upton, NY 11973-5000, U.S.A.

²⁾ Stony Brook University, Stony Brook, NY 11794, U.S.A.

Abstract

eRHIC will collide high-intensity hadron beams from RHIC with a 50-mA electron beam from a six-pass 30-GeV Energy Recovery Linac (ERL), which will utilize 704 MHz superconducting RF accelerating structures. This paper describes the eRHIC SRF linac requirements, layout and parameters, five-cell SRF cavity with a new HOM damping scheme, project status, and plans.

INTRODUCTION

The proposed electron-ion collider eRHIC will collide ions from one of the rings of the existing heavy-ion collider RHIC with electrons from a new accelerator to be installed in the RHIC tunnel [1, 2]. eRHIC will utilize several superconducting RF accelerators. Layout of the SRF systems in the RHIC tunnel, their description, and main parameters were presented elsewhere [3]. The main electron accelerator, the subject of this paper, is a six-pass ERL with two 2.45-GeV SRF linac sections. After six re-circulations, the electron beam energy will be as high as 30 GeV.

SRF LINAC

Each SRF linac section will be 200-meters long. Due to rapid increase of the synchrotron radiation power at high energies, the beam current will be lowered at energies above 20 GeV to keep the total power loss below 10 MW. Thus, the highest luminosity will be achieved at 20 GeV. Parameters of the SRF linac are listed in Table 1.

Installing a shorter linac first and then gradually adding more SRF cryounits will stage the energy of the machine. The initial energy of the main ERL will be 10 GeV with three or four re-circulations. Only one linac section will be installed at this stage of the project.

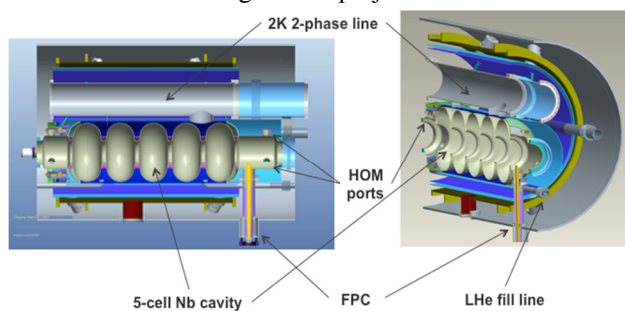


Figure 1: Preliminary layout of a cryounit for eRHIC.

*Work is supported by Brookhaven Science Associates, LLC under contract No. DE-AC02-98CH10886 with the US DOE.

#sbelomestnykh@bnl.gov

Table 1: Parameters of the Main ERL Linacs

Energy gain per linac section at 30 GeV	2.45 GeV
Beam current per pass ($E \leq 20$ GeV)	50 mA
Bunch frequency	14.1 MHz
Bunch length	2 mm rms
RF frequency	703.8 MHz
Linac length	2×200 m
No. of cavities per linac	2×120
Filling factor	0.64
Cavity type	Elliptical, 5-cell
E_{acc} at 30 (20) GeV	19.2 (12.7) MV/m
Peak detuning due to microphonics	6 Hz
Q_{ext} FPC	5.9×10^7
RF power per cavity	10 kW
Total heat load at 1.9 K	5,700 W
Total heat load at 50 K	12,000 W

The SRF linac utilizes five-cell, 704-MHz cavities, described in the next section. Each cavity will be housed in an individual cryounit (Figure 1). A series of such cryounits will form one long cryomodule per section of the linac, with one-meter long transitions to room temperature at each end. The linac's accelerating gradient will reach 19.2 MV/m when operating at the highest energy. At 6 Hz peak detuning due to microphonic noise, the RF power is under 10 kW per cavity. The cavities will be powered from individual solid-state RF amplifiers.

FIVE-CELL CAVITY AND OTHER COMPONENTS

Cavity and HOM Damping

A superconducting cavity for high-current applications [4-6] is shown in Figure 2. The cavity, named BNL3, has an optimized geometry that supports strong damping of higher order modes (HOMs) while maintaining good properties of the fundamental mode. The damping is accomplished via six antenna-type couplers attached to the large diameter beam pipes [7]. The simulations show that this HOM damping scheme provides sufficient suppression of the parasitic impedance to satisfy eRHIC requirements. The cavity parameters are listed in Table 2.

DEVELOPING OF SUPERCONDUCTING RF GUNS AT BNL*

S. Belomestnykh^{1,2#}, Z. Altinbas¹, I. Ben-Zvi^{1,2}, C.H. Boulware³, J. C. Brutus¹, A. Burrill⁴, R. Calaga⁵, M. Cole⁶, J. Dai², A. Favale⁶, D. Gassner¹, T.L. Grimm³, H. Hahn¹, L. Hammons^{1,2}, D. Holmes⁶, J. Jamilkowski¹, D. Kayran¹, J. Kewisch¹, X. Liang², V. Litvinenko^{1,2}, G. Mahler¹, G. McIntyre¹, D. Pate¹, D. Phillips¹, T. Rao¹, J. Rathke⁶, M. Ruiz-Osés², T. Schultheiss⁶, S. Seberg¹, T. Seda¹, B. Sheehy¹, J. Skaritka¹, K. Smith¹, R. Than¹, A. Todd⁶, J. Tuozzolo¹, E. Wang¹, Q. Wu¹, T. Xin², Wencan Xu¹, A. Zaltsman¹

¹⁾ Brookhaven National Laboratory, Upton, NY 11973-5000, U.S.A.

²⁾ Stony Brook University, Stony Brook, NY 11794, U.S.A.

³⁾ Niowave, Inc., Lansing, MI 48906, U.S.A.

⁴⁾ JLab, Newport News, VA 23606, U.S.A.

⁵⁾ CERN, Geneva, Switzerland

⁶⁾ Advanced Energy System, Inc., Medford, NY 11763, U.S.A.

Abstract

BNL is developing several superconducting RF guns for different applications. The first gun is based on a half-cell 1.3-GHz elliptical cavity. This gun is used to study generation of polarized electrons from GaAs photocathodes. The second gun, also of a half-cell elliptical cavity design, operates at 704 MHz and is designed to produce a high average current electron beam for the R&D ERL from multi-alkali photocathodes. The third gun is of a quarter-wave resonator type, operating at 112 MHz. This gun will be used for photocathode studies, including a diamond-amplified cathode, and to generate a high charge, low repetition rate beam for the coherent electron cooling experiment. In this paper we describe the gun designs, present recent test results, and discuss future plans.

INTRODUCTION

Developing superconducting RF (SRF) photoinjectors is a part of the SRF program that is important for several projects in progress or under consideration at the Collider-Accelerator Department of BNL. The SRF photocathode guns promise to generate high-bunch-charge, high-average-current, low-emittance electron beams. The three SRF guns described in this paper address different issues, from generating polarized electrons, to experimenting with different photocathodes, to producing high-intensity beams for energy recovery linacs and electron coolers.

1.3 GHz SRF PLUG GUN FOR GaAs PHOTOCATHODES

SRF guns, which combine excellent vacuum conditions of DC guns and high accelerating gradients of RF guns, potentially can generate very low emittance polarized electron beams from GaAs photocathodes with long

lifetime. Our simulations show that a SRF gun can exceed the ILC's requirement for vertical beam emittance by a factor of two, if an ellipsoid charge distribution is used. There will be no need for a damping ring.

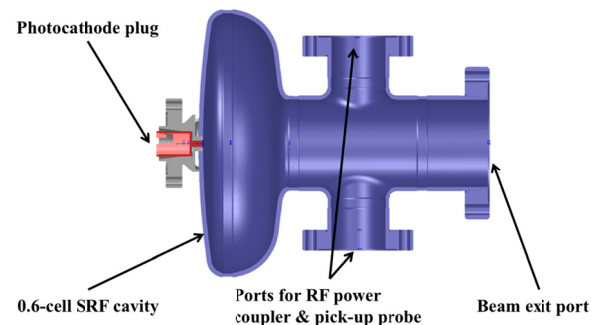


Figure 1: BNL 1.3-GHz plug SRF gun cavity.

Table 1: Parameters of the 1.3 GHz SRF gun

RF frequency	1300 MHz
Cavity active length	0.6 cell
Energy gain	0.6 MeV
Maximum field at the cathode	15 MV/m
e^- emission RF phase at 2.5 MV	20°
Cavity Q_0 at 2 K	7×10^9
Cavity operating temperature	2 K
Bunch repetition frequency	81.25 MHz
Bunch charge	0.12 pC
Bunch length	10 ps
Cathode spot size	2 mm dia.

We are using a 0.6-cell 1.3-GHz SRF plug gun to test the quantum efficiency (QE) and lifetime of a GaAs photocathode. It has got its name from a removable niobium plug holding a cathode and located at the back of the gun. The gun and cathode transfer system were

*Work is supported by Brookhaven Science Associates, LLC under contract No. DE-AC02-98CH10886 with the US DOE. The work at Niowave is supported by the US DOE under SBIR contract No. DE-FG02-07ER84861.

#sbelomestnykh@bnl.gov

IMPACT OF TRAPPED FLUX AND SYSTEMATIC FLUX EXPULSION IN SUPERCONDUCTING NIOBIUM

J. Vogt, O. Kugeler, J. Knobloch, Helmholtz-Zentrum für Materialien und Energie (HZB)

Abstract

The intrinsic quality factor Q_0 of superconducting cavities is known to depend on various factors like niobium material properties, treatment history and magnetic shielding. To study trapped flux in Niobium we constructed a test stand at Horizontal Bi-Cavity Test Facility (HoBiCaT) at HZB using niobium rods equipped with thermal, electrical and magnetic diagnostics. The focus in this study was on the behaviour of the trapped flux when the sample is slowly warmed up towards the critical temperature T_c . Besides the (incomplete) Meissner effect we observed additional flux expulsion starting at $\approx 0.1K$ below T_c . The reduced level of trapped flux is maintained when the sample is cooled down again and can even be improved by repeating the procedure. Possible explanations for the effect are discussed.

INTRODUCTION

We already reported on the impact of temperature gradients during the cool-down on the obtained Q_0 [1]. In the quest for minimization of RF losses in SRF cavities the impact of trapped vortices is one main topic. The vortices have a normal conducting core with a surface resistance about 6 orders above that of superconducting Niobium. This surface fraction is proportional to the trapped magnetic flux. The surface resistance was determined to be $2.2n\Omega$ per μT for a 1.5GHz cavity [2]. A crucial step in avoiding trapped flux is an improved understanding of flux trapping behaviour of Niobium.

The energetically most favourable state of bulk Niobium at 1.8K (4.2K) is the Meissner phase, in which all magnetic field present in the normal conducting state is expelled. However, expulsion of flux can be incomplete, yielding a remaining magnetization of the material even after removing the external field source. The dynamics of this trapped flux is still not well understood. One approach was the investigation of flux that is permitted to penetrate a marginal type II superconductor in the mixed state. Here, the flux tubes form a lattice and several studies [3, 4] indicate a phase transition from localized (solid, fixed regular lattice) flux tubes towards moveable (liquid) flux tubes when the superconductor exceeds certain temperature / magnetic field combinations as indicated by the black dotted "melting line" in Figure 1.

The behavior of flux that is trapped in the Meissner state is uncertain. A continuation of the melting line in this phase is conceivable, so that flux lines in the check region (Figure 1) may be able to exit the Niobium below T_c . In our study, we examine the properties of the trapped

magnetic flux in the Meissner phase when the rod is slowly warmed up.

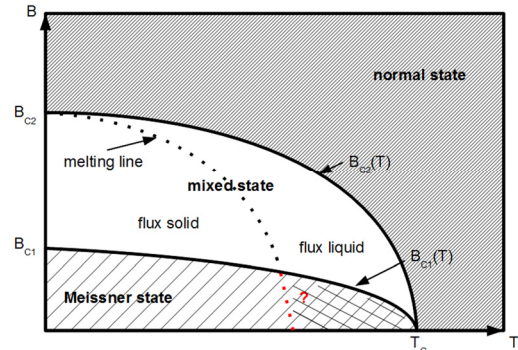


Figure 1: Magnetic phase diagram of marginal Type II superconductor [5]. The added red dotted line indicates a possible extension of the liquid/solid flux interface into the Meissner state. The size of the check region is exaggerated.

EXPERIMENTAL SETUP

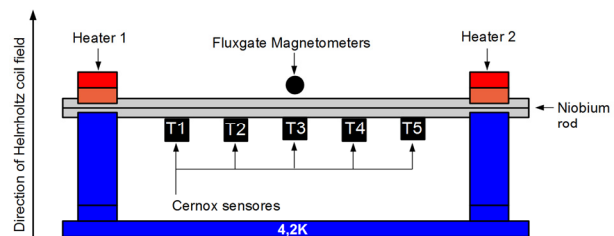


Figure 2: Experimental setup

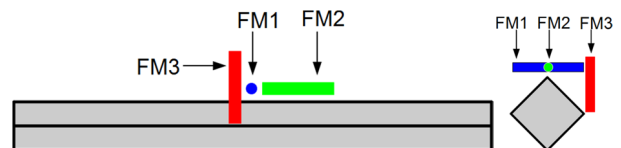


Figure 3: Positions of fluxgate magnetometers (FM): Longitudinal view (left) and cross section (right) of FM1 (black), FM2 (green) and FM3 (red)

For the experiments, a RRR=300 niobium rod (8.4x8.4x300mm) was positioned inside HoBiCaT [6]. It was conduction cooled through the posts to 4.2K. In order to reduce heat transfer into the Helium, heat conductivity was reduced by introducing a kapton foil between rod and support stands. Both ends of the rod were equipped with a resistive heater. They could be individually regulated to control the temperature of the rod with 10mK accuracy. Five Cernox temperature sensors with mK resolution and three fluxgate magnetometers with 1nT resolution (Bartington Mag-01H), one for each spatial direction,

ALTERNATIVE APPROACHES FOR HOM-DAMPED CAVITIES*

Bernard Riemann[†], TU Dortmund University, Dortmund, Germany
 Axel Neumann, Helmholtz-Zentrum Berlin, Berlin, Germany
 Thomas Weis, TU Dortmund University, Dortmund, Germany

Abstract

In this paper, we present two different ideas that may be useful for design and simulation of (superconducting) radio frequency cavities.

To obtain longitudinal and transverse voltages resp. shunt impedances in cavities without rotational symmetry, one or two integration paths are often used to get an approximate difference relation for the transverse voltage of higher order modes (HOMs). The presented approach uses a multipole decomposition that is valid in vicinity of the central axis to compute voltage multipole decomposition directly for paths of arbitrary number and position.

Elliptical cavities have been a standard in SRF linac technology for 30 years. We present another approach to base cell geometry based on Bezier splines that is much more flexible in terms of optimization, while reaching equal performance levels.

POLAR PATH INTEGRAL ANALYSIS

In the following section, the longitudinal and transverse voltages are expressed using a multipole decomposition. By pseudo-inversion of the resulting equation system (similar to polynomial interpolation), one can calculate the corresponding coefficients directly from an arbitrary number and position of integration paths.

This method also allows to check a) if the position and number of paths is appropriate to extract the desired coefficients, b) if there is any “noise” in the voltage paths that stem from computational errors or from a too large distance of the path from the central axis.

Signed Effective Voltages

The effective longitudinal and transverse acceleration voltages can be written as complex Fourier integrals

$$\tilde{V}_{\parallel} = \int E_s(s) \exp(ik_{\beta}s) ds \in \mathbb{C}, \quad (1)$$

$$\tilde{\vec{V}}_{\perp} = \frac{1}{q} \int \vec{F}_{\perp}(s) \exp(ik_{\beta}s) ds \in \mathbb{C}^2, \quad (2)$$

where \vec{F}_{\perp} is the total transverse Lorentz force, and E_s is the longitudinal electric field at the path position s . The complex angle $\Psi_0 = \arg(\tilde{V}_{\parallel})$ corresponds to an optimal acceleration phase, and its magnitude to the acceleration

voltage for this phase (see [6] for a special derivation of this relation with a fixed $\Psi_0 = 0$).

For each mode, the phases of \tilde{V}_{\parallel} on all paths are equal up to an additional shift by π , corresponding to a sign change (deceleration). Using a fixed phase Ψ_0 that is one of the two possible optimal phases, we may define a real acceleration voltage for the optimal phase by

$$V_{\parallel} := \tilde{V}_{\parallel} \cdot e^{-i\Psi_0} \in \mathbb{R}. \quad (3)$$

and, using the Panofsky-Wenzel theorem, a corresponding real transverse voltage may be defined by

$$\frac{\partial}{\partial t} \tilde{\vec{V}}_{\perp} = i\omega \tilde{\vec{V}}_{\perp} = -\vec{\nabla}_{\perp} \tilde{V}_{\parallel} \quad (4)$$

$$\vec{V}_{\perp} = \begin{pmatrix} V_x \\ V_y \end{pmatrix} = -i \tilde{\vec{V}}_{\perp} \cdot e^{-i\Psi_0} \in \mathbb{R}^2. \quad (5)$$

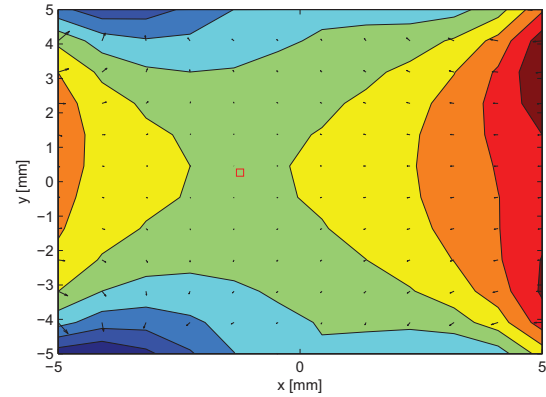


Figure 1: Reconstruction of the transverse (arrows) and longitudinal (isolines) voltages in the beam area with contributions from different multipole components. The corresponding coefficients were computed from voltages on circularly arranged integration paths at 5mm offset from beam axis for an eigenmode of the BERLinPro main linac cavity. The red square marks the transverse forceless point z_0 which deviates from the axis by more than 1 mm.

Holomorphic Multipole Expansion

By using a complex analytic multipole decomposition

$$F(z) \approx \sum_p c_p z^p, \quad (6)$$

where $z = x+iy = re^{i\phi}$ is the transverse position of the integration path, and $c_p = a_p + ib_p$ are complex numbers that

* this work is supported by BMBF contract 05K10PEA

[†] bernard.riemann@tu-dortmund.de

RESULTS AND PERFORMANCE SIMULATIONS OF THE MAIN LINAC DESIGN FOR *BERLinPro**

A. Neumann[†], W. Anders, J. Knobloch, Helmholtz-Zentrum Berlin, Berlin, Germany

B. Riemann, T. Weis, TU Dortmund University, Dortmund, Germany

K. Brackebusch, T. Flisgen, T. Galek, K. Papke, U. van Rienen, Rostock University, Rostock, Germany

Abstract

The Berlin Energy Recovery Linac Project (*BERLinPro*) is designed to develop and demonstrate CW LINAC technology for 100-mA-class ERLs. High-current operation requires an effective damping of higher order modes (HOMs) of the 1.3 GHz main linac cavities.

We have studied elliptical seven cell cavities damped by five waveguides at the adjacent beam tubes. Eigenmode calculations for geometrical figures of merit show that the present design should allow successful cw linac operation at the maximum beam current of 100 mA / 77pC bunch charge.

In this paper the progress in HOM calculations to avoid beam-breakup instabilities for the favored cavity structure is presented.

INTRODUCTION

BERLinPro will be a CW driven ERL machine with a maximum current of 100 mA beam and a maximum energy of 50 MeV, while preserving a normalized emittance of better than 1 mm mrad at a pulse length of 2 ps [1]. The main linac cavity has strong HOM damping requirements since it is passed by two 100 mA beams that both resonantly interact with transverse deflecting (e.g. TM_{110}) cavity modes, leading to beam break up (BBU) [2].

An ERL cavity design must minimize the HOM's R/Q_{\perp} and external quality factors Q_{ext} [8]. The mid-cell design influences the HOM spectrum, dispersion relation and operational mode acceleration performance (see [8] for op. mode parameters of the tuned structure). By proper end-cell tuning that preserves field flatness for the fundamental $TM_{010-\pi}$ mode, mode localization (trapping) can be avoided and the Q_{ext} can be receded to a sufficient extent.

In this paper updated HOM calculations of the main linac cavity using new methods are presented [8], and an outlook on ongoing activities to decompose the cavity structure into smaller parts is given [5] [9].

STRUCTURE EIGENMODE CALCULATIONS

The design under consideration is a seven cell structure using the Cornell ERL mid-cell design [6] and combining it

*Work supported by Federal Ministry for Research and Education BMBF under contract 05K10HRC and 05K10PEA

[†] Axel.Neumann@helmholtz-berlin.de

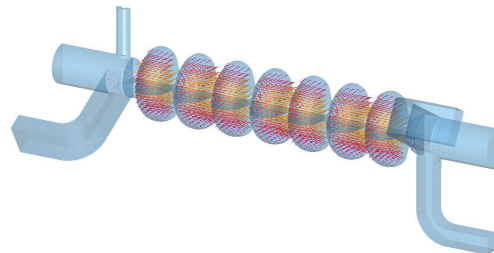


Figure 1: Rendering of the cavity design under consideration for *BERLinPro* with a cut through the symmetry (FPC) plane and electric field magnitude of the operational mode.

	ERL shape Cornell U.	Spline shape TU Do, v_4 / v_5
$E_{\text{surf}}/E_{\text{acc}}$ (π mode)	2.07	2.08 / 2.07
R_{\parallel}/Q (π mode)	111 Ω	113 Ω / 112 Ω
intercell coupling κ	2.1 %	1.7 % / 1.9 %
Geometry factor G	272.7 Ω	- / 269.5 Ω

Table 1: Cavity mid-cell figures of merit comparison.

with JLab 3-fold symmetric waveguide HOM couplers [7] (see Figure 1). Flexible input power coupling is enabled by replacing one waveguide with a TTF-III type coaxial fundamental power coupler (thus breaking the 3-fold symmetry). The design aims at combining the peak field properties of the Cornell design with the advantage of waveguide couplers having a natural cutoff above the fundamental, and further limiting the possibility of dust intruding from ferrite beam tube absorbers into the cavity.

Base cells

In parallel to periodic boundary mid-cell calculations, such calculations were also performed using Spline-based cells [4]. Table 1 shows a preliminary comparison between 36 mm radius mid-cells for both designs. At the moment, development concentrates on the Cornell ERL mid-cell. Further development and degree elevation of the spline design may lead to a mid-cell shape with higher performance.

Transverse shunt impedance

The final goal will be to minimize the product $R/Q_{\perp} \cdot Q_{\text{ext}}$ for all HOMs. $|\vec{V}_{\perp}|^2 \propto R_{\perp}/Q$ can be computed di-

STUDY OF HPR CREATED OXIDE LAYER AT Nb SURFACES

P. V. Tyagi[#], GUAS, Tsukuba, Japan

T. Saeki, M. Sawabe, H. Hayano, S. Kato, KEK, Tsukuba, Japan

Abstract

The performance of superconducting radio frequency (SRF) niobium (Nb) cavities mainly depends on final surface condition therefore the surface preparation of these SRF cavities becomes very important. The preparation of surface includes two steps; surface chemistry (in order to get a smooth surface) and cleaning/rinsing (in order to remove contaminants left after the surface chemistry). As high pressure rinsing (HPR) with ultra pure water (UPW) is most commonly used surface cleaning method after the surface chemistry, it's very interesting to characterize the Nb surfaces after HPR. The surface characterizations show the presence of a thicker oxide layer at Nb surface as an outcome of HPR. In this article, we report the production of oxide layer (FWHM thickness) based on different conditions such as high pressure and doses. The surface characterization was done by XPS (x-ray photoelectron spectroscopy) with depth profiling.

INTRODUCTION

Final surface preparations [1] of niobium (Nb) superconducting radio frequency (SRF) cavities play a critical role in order to achieve high performances. Final surface preparation includes mainly two steps 1) surface chemistry in order to make surface smoother and 2) post cleaning processes in order to remove chemical residues left after the surface chemistry. As a step two, the High Pressure Rinsing (HPR) with ultra pure water/deionized water (UPW/DI), is most commonly used surface cleaning procedure worldwide [2,3]. The HPR seems to be a most effective cleaning procedure and HPR treated cavities have shown high field gradient with a high Q value. For the last two decades, HPR has been successfully used on SRF cavity surfaces and became an integral part of the final surface preparation of Nb SRF cavities. In order to make HPR more effectively for removal of the contaminants from cavity surface, the HPR operating parameters such as high pressures and doses should be carefully determined.

In this paper, we report our efforts towards finding of the optimized pressure and doses for HPR. In this regard, three samples were initially buffer chemical polished (BCPed) and subjected to HPR with three different pressures and two doses. For the HPR experiments, a commercial high pressure washer machine was used which can reach to a maximum pressure of 15 MPa. After the experiments, sample surfaces were analyzed by XPS (x-ray photo-electron spectroscopy).

Email: puneet.tyagi@helmholtz-berlin.de

[#]Presently at Helmholtz Zentrum Berlin

Work was conducted in KEK, Tsukuba Japan.

ISBN 978-3-95450-122-9

EXPERIMENTAL DETAILS

Surface Analysis

After the experiments, all the samples surfaces were analysed by XPS and a depth profile can be obtained. Our surface analysis system contains one main chamber along with three loadlock mechanism. The main chamber is equipped with an electron energy analyzer, an ion mass spectrometer, a x-ray source, an electron gun, an ion gun for depth profiling, an extractor gauge, and a residual gas analyzer. The analysis system is capable of executing Auger electron spectroscopy (AES), secondary ion mass spectrometry (SIMS) with argon ion etching, and XPS with probing area of 2 mm. Fig. 1 is the overview of our surface analysis system. The main chamber is maintained at extremely high vacuum [4].

The three loadlock mechanism provides the facility to transfer the samples from vacuum environment to main chamber without exposing them in to air. A vacuum suitcase (maintained at UHV) can be attached to one of the loadlock chambers with it and sample can be transferred from the suitcase to the analysis chamber keeping in vacuum. A sample storage chamber, which maintains the base pressure of 10^{-8} Pa, is also connected to one of the loadlock chambers to keep remaining samples in the carousel in UHV. Also, samples can be mounted to one of the loadlock chambers directly from the atmosphere and can be transferred to main chamber after achieving UHV.

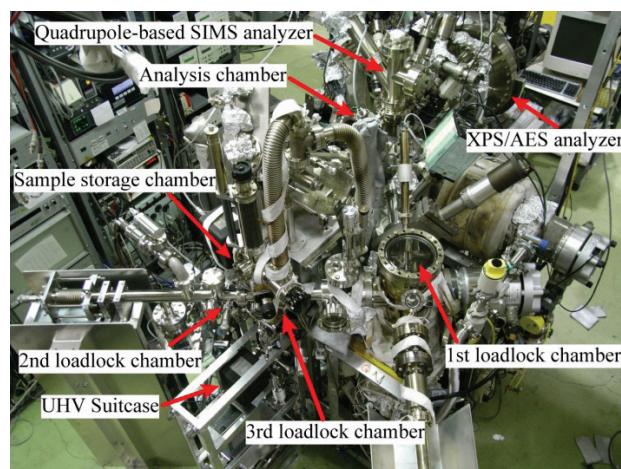


Figure 1: Overview of the surface analysis chamber.

HPR Experiments

We have conducted a series of HPR experiments on three Nb samples with three different pressures and two doses. The dose can be defined as the total injected

QUALITY CONTROL OF CLEANROOM PROCESSING PROCEDURES OF SRF CAVITIES FOR MASS PRODUCTION*

R. Oweiss[#], K. Elliott, A. Facco⁺, M. Hodek, I. Malloch, J. Popielarski, L. Popielarski, K. Saito
 Facility for Rare Isotope Beams (FRIB), Michigan State University, East Lansing, MI 48824, USA
⁺INFN - Laboratori Nazionali di Legnaro, Padova, Italy

Abstract

Quality control is a key factor in the SRF cavity mass production. This paper summarizes ongoing research at the facility of Rare Isotope Beams (FRIB) to validate the quality assurance of SRF cavities while optimizing processing procedures for mass production. Experiments are conducted to correlate surface cleanliness for niobium surfaces with high pressure rinse time using $\beta=0.085$ quarter-wave resonators (QWR) cavities. Diagnostic devices, a liquid particle counter, a surface particle detector and a total organic carbon (TOC) analyzer are used to monitor key parameters for quality control. Rinse water samples are collected during high pressure rinsing to measure liquid particle counts. The SLS 1200 Sampler is used to detect the presence of liquid particles of $0.2\mu\text{m}$ and up to $1\mu\text{m}$ to set standards for acceptable cleaning thresholds and optimize high pressure rinse time. The QIII+ surface particle detector is used to scan the high electric field region of the $\beta=0.085$ QWR to ensure high pressure rinsing efficiency. The $\beta=0.085$ QWR RF testing data are analyzed and results are presented to investigate the correlation between attained acceleration gradients and surface cleanliness.

INTRODUCTION

A quality control (QC) system is in place for cleanroom processing of SRF cavities at FRIB. The FRIB QC system embeds diagnostic tools and stringent cavity processing procedures to control particle contamination, increase field emission onset level and attain high acceleration gradients. The e-traveler system is launched to document procedures and to provide a reporting tool for data mining and decision-making. This paper presents the findings of the commissioning and use of the liquid particle counter during the high pressure rinsing process. The paper also focuses on the QC steps for the clean assembly of $\beta=0.085$ QWR, and investigates the potential of predicting the cavity attained gradient (E_{acc}) at field emission onset based on its QC data collected during processing.

QUALITY CONTROL FOR CLEANROOM PROCEDURES

High Pressure Rinsing (HPR)

HPR is a key step that precedes the final SRF cavity assembly for RF vertical testing. HPR is proven the most

effective tool as a final surface treatment to remove particles and to reduce field emission [1]. The FRIB HPR tool for production is still under development. The current HPR tool resides in an ISO5 cleanroom. Cavities are high pressure rinsed by rotating the cavity on a rotary aluminum cylinder flange as illustrated in Figure 1. A stainless steel spray nozzle wand with 8 jets moves in and out from below the rotating cavity. The HPR system utilizes a 3HP CAT pump and a final $0.1\mu\text{m}$ filter; both of which are located outside the cleanroom. The CAT pump pressurizes the ultra-pure water to ~ 8300 kPa.



Figure 1: $\beta=0.085$ QWR on high pressure rinse in ISO5 cleanroom

Ultra-pure Water (UPW) Quality Control

A reliable ultra-pure water system is essential to the successful operation and process quality of the HPR system. The current ultrapure water system is fed by a 7.6 l/m reverse osmosis system (RO). The resistivity of the ultrapure water system ranges between $17.2\text{--}17.6$ $\text{M}\Omega\text{-cm}$. The resistivity is monitored by an inline resistivity meter. The TOC is measured routinely for all points of use on the UPW distribution line using a TOC analyzer. The UPW TOC levels are consistently below 50 ppb. The microbiological quality of the system is analyzed every year to detect any bacterial buildup and assess the need for the system sterilization. Ultimately, a well-defined maintenance schedule is followed to replace critical system components. [2]

Another integral component for monitoring the UPW and the HPR process is the liquid particle counter. The Liquid particle counter (SLS-1200) is a device that pressurizes the water sample using a built in pump and a syringe. The device is capable of detecting $0.2\mu\text{m}$ size particles and up to $1\mu\text{m}$. A $\frac{1}{4}$ " stainless steel national pipe tapered thread (NPT) fitting was installed on HPR system tray to collect drain water samples during cavity HPR.

* Work supported by the U.S. Department of Energy Office of Science under Cooperative Agreement DE-SC0000661.

[#]oweiss@frib.msu.edu

PROCESS DEVELOPMENTS FOR SUPERCONDUCTING RF LOW BETA RESONATORS FOR THE ReA3 LINAC AND FACILITY FOR RARE ISOTOPE BEAMS*

L. Popielarski[#], C. Compton, L. Dubbs, K. Elliott, A. Facco(*), L. Harle, I. Malloch, R. Oweiss, J. Ozelis, J. Popielarski, K. Saito

Facility for Rare Isotope Beams (FRIB), Michigan State University (MSU), East Lansing, MI 48824, USA (*), INFN-Laboratori Nazionali di Legnaro, I-35020 Legnaro, Padova, Italy

Abstract

The Facility for Rare Isotope Beams (FRIB) will utilize over 330 superconducting radio frequency (SRF) low beta cavities for its heavy ion driver linac. The SRF department will process and test all cavities prior to string assembly in the cleanroom. The baseline processing procedures have been established. The methods are being optimized for production rate benchmarking. Additional processes are being developed to increase flexibility and reduce technical risks. This paper will describe developments and experimental results. Topics include high temperature heat treatment for hydrogen degassing, selective chemical etching for cavity frequency tuning, low-temperature bake out and process quality control.

INTRODUCTION

The ReAccelerator (ReA) and FRIB projects at MSU both utilize a 80.5 MHz $\beta=0.085$ quarter wave resonator (QWR) design [1]. For the ReA3 project eleven cavities have been fabricated and eight need to be certified, while for the FRIB project, 126 cavities need to be fabricated with 94 qualified for use in a cryomodule. The ReA project allows for the chance to gain valuable production experience. To meet the ReA3 cavity frequency specifications a differential etching technique with Buffered Chemical Polish (BCP) was developed for post fabrication tuning. The technical risks regarding cavity performance for ReA linac operation were reduced by establishing a low temperature bakeout method and a high temperature heat treatment - both of which improved cavity Q_0 values. The process steps for the ReA3 cavities are shown in Table 1. The process procedures will be optimized from lessons learned during the ReA cavity production.

Table 1: Summary of process steps for ReA3 cavities.

Step	Cavity Process Steps
1	Degrease, bulk BCP, dry, frequency measurements
2	Differential BCP, dry, frequency measurement
3	Degrease & hydrogen degas
4	Degrease, light BCP, High Pressure Rinse (HPR)
5	Clean assembly, evacuation, 120°C low temperature bake
6	Test preparations and RF Dewar testing
7	Clean removal from test stand and install to coldmass

*Work supported by the U.S. Department of Energy Office of Science under Cooperative Agreement DE-SC0000661.

[#]lpopiela@frib.msu.edu

In preparation for FRIB production, a comprehensive program is in place to improve process quality control and documentation. Innovative diagnostic tools allow for the quantification of process and assembly parameters for quality control [2]. The cavity fabrication, processing and vertical test parameters are recorded in a computer database (electronic traveler system), for cavity characterization and analysis. The database is accessible through a web-based interface, and will ease the analysis of 50 cavities before FRIB production.

HYDROGEN DEGASSING

The risk of Q-disease has been mitigated by implementing a hydrogen degassing step to the cavities after the bulk chemistry. The cavities are fired in a high temperature vacuum furnace for 10 hours at 600°C, while maintaining vacuum less than 5×10^{-6} Torr. The heat treatment removes much of the hydrogen from the bulk niobium material. Multiple QWRs and half wave resonators (HWRs) have been heat treated, using furnaces at Jefferson Lab and Fermilab, in an effort to quantify the benefits of the treatment both at 4.2 K and 2 K. The furnace design and heat treatment cycle have been optimized for production, considering both mechanical impacts to the cavity structure and overall schedule constraints. The current FRIB cavity furnace cycle is about 40 hours and includes pump down, temperature ramp up, steady state bake at 600 °C and cool down.



Figure 1: T-M Vacuum[®] high temperature vacuum furnace commissioned and being used to heat treat cavities at MSU.

MULTIPOLE EXPANSION OF THE FIELDS IN SUPERCONDUCTING HIGH-VELOCITY SPOKE CAVITIES *

R. G. Olave, J. R. Delayen, C. S. Hopper, Center for Accelerator Science, Old Dominion University and Thomas Jefferson National Accelerator Facility, VA, USA †

Abstract

Multi-spokes superconducting cavities in the high-beta regime are being considered for a number of applications. In order to accurately model the dynamics of the particles in such cavities, knowledge of the fields off-axis are needed. We present a study of the multipoles expansion of the fields from an EM simulation field data for two-spokes cavities operating at 325 MHz, $\beta = 0.82$, and 500 MHz, $\beta = 1$.

INTRODUCTION

In recent years there has been considerable progress in the optimization and characterization of accelerating multi-spoke cavities in the high-velocity regime ($\beta_0 = v_0/c > 0.6$). Multi-spokes cavities have several advantages over the more traditional multi-cell elliptical cavities [1, 2], such as increased longitudinal acceptance, lower superconducting surface resistance and therefore lower heat load allowing for operation at 4K, and a cavity diameter on the order of half the rf wavelength, which allows for lower operating frequencies for a given size.

The lack of cylindrical symmetry of the multi-spokes cavities might result in the presence of non-negligible higher order multipole components of the operating mode. In order to study the impact of the cavity fields on the beam dynamics, it is necessary to characterize off-axis fields. To this end, we present a study of the multipoles expansion of the fields for the operating (fundamental) cavity mode for spokes operating at 325 MHz, $\beta = 0.82$, and 500 MHz, $\beta = 1$.

MULTIPOLAR RF KICKS AND FIELD EXPANSION

It has recently been demonstrated that surface fitting of field data around a virtual cylinder in the proximity of the beamline can be used to compute high-order transfer maps, interior fields, and non-linear beam dynamics including high-order multipole effects [3, 4].

From the interpolation of the electromagnetic fields on the surface of a virtual cylinder of radius R through the length of the cavity in a region with no charge, a general complete solution to the fields can be found. The acceler-

ating electric field can then be expressed as:

$$E_{acc}(r, \phi, z) = E_z e^{i\omega t} = E_{acc-c}^{(0)} + \left(\sum_{n=1}^{\infty} r^n (E_{acc-c}^{(n)} \cos(n\phi) + E_{acc-s}^{(n)} \sin(n\phi)) \right) e^{i\omega t} \quad (1)$$

Where E_{acc} is the accelerating electric field along the beamline direction z and ω is the rf frequency. If the field $E_{acc}(R, \phi, z)$ is known, then the coefficients $E_{acc-c}^{(0)}$, $E_{acc-c}^{(n)}$ and $E_{acc-s}^{(n)}$ can be found via inverse Fourier integration of the surface fitted field.

Inserting this series into the Panofsky-Wenzel theorem we may then calculate the transverse change in momentum (kick) of the particles as a series of multipolar RF kicks:

$$\Delta p_{\perp} = \left(\frac{e}{\omega} \right) \int_{-\infty}^{+\infty} (-i) \nabla_{\perp} E_{acc}|_{t=z/v_z} dz \quad (2)$$

To get an idea of the impact of the nonlinear effects of the higher order field multipoles, it is useful to compare the strength of the multipolar RF-kicks with that of magnetic multipoles [7]. It is usual to express the magnetic potential and static magnetic kick to incoming particles as a Taylor series expansion [5, 6]. In magnets, the a_n and b_n terms are determined by the orientation of the magnet, such that a_1 corresponds to a vertical bend of the particle trajectory, b_1 to a horizontal bend, and in general a_n correspond to skew oriented magnets and b_n to normal oriented magnets. For simplicity we will continue to use this nomenclature. Obviously, the b_0 or monopole term is not dependent on the orientation of the cavity and corresponds to the accelerating voltage across the cavity. Following this idea, we find:

$$\begin{aligned} b_0 &= \int_{-\infty}^{+\infty} E_{acc-c}^{(0)}(z) dz, \propto V_{acc} \\ b_n &= \int_{-\infty}^{+\infty} \frac{ni}{\omega} E_{acc-c}^{(n)}(z) dz, (n = 1, 2, \dots) \\ a_n &= \int_{-\infty}^{+\infty} \frac{ni}{\omega} E_{acc-s}^{(n)}(z) dz, (n = 1, 2, \dots) \end{aligned} \quad (3)$$

Additionally, the rf multipole strength depends of the rf phase of particles traversing the cavity; so we can express them as complex numbers, where the real part corresponds to particles on crest, and the imaginary part corresponds to particles off-crest.

* Part of this work supported by U.S. DOE Award No. DE-SC0004094 Part of this work was done in collaboration with and supported by Niowave Inc. under the DOE STTR program.

† rolave@odu.edu

COLD TESTING OF SUPERCONDUCTING 72 MHz QUARTER-WAVE CAVITIES FOR ATLAS

M. P. Kelly, Z. A. Conway, S. M. Gerbick, M. Kedzie, T. C. Reid, R. C. Murphy,
P. N. Ostroumov, Argonne National Laboratory, Argonne, IL 60439, U.S.A.

Abstract

A set of seven 72 MHz $\beta=0.077$ superconducting quarter-wave cavities for a beam intensity upgrade of the ATLAS heavy-ion accelerator has been completed. Cavities have been fabricated using lessons learned from the worldwide effort to push the performance limits for niobium cavities close to the fundamental limits. Key developments include the use of electropolishing on the completed cavity. Polishing parameters, including temperature, are better controlled compared to the standard horizontal electropolishing systems for elliptical cavities. Wire EDM, used instead of traditional niobium machining, looks well suited for preparing weld joints that are, with respect to quench, defect free. Hydrogen degassing at 625 C has been performed after electropolishing, removing the need for fast cool down in with 2 K or 4 K operation. Tested cavities have useful accelerating voltages of >3 MV/cavity at 4 K, as for ATLAS, and 5 MV or more per cavity at 2 K with $B_{PEAK}>130$ mT in 3 of 4 cases.

INTRODUCTION

The essential components of the ATLAS Efficiency and Intensity Upgrade [1] are a new CW radio frequency quadrupole injector and one new cryomodule of 7 SC cavities for $\beta=0.077$, scheduled to replace three existing cryomodules of split-ring resonators in the middle portion of the ATLAS SC ion linac. This upgrade follows upon the 2009 $\beta=0.15$ ATLAS Energy Upgrade cryomodule, presently the world leading cryomodule for low velocity ions, providing 14.5 MV accelerating voltage over 4.5 meters.

The new cryomodule will nominally provide 17.5 MV of accelerating potential at a lower beta of 0.077 in a 5



Figure 1: Initial mock up of the 72 MHz cavity clean room assembly.

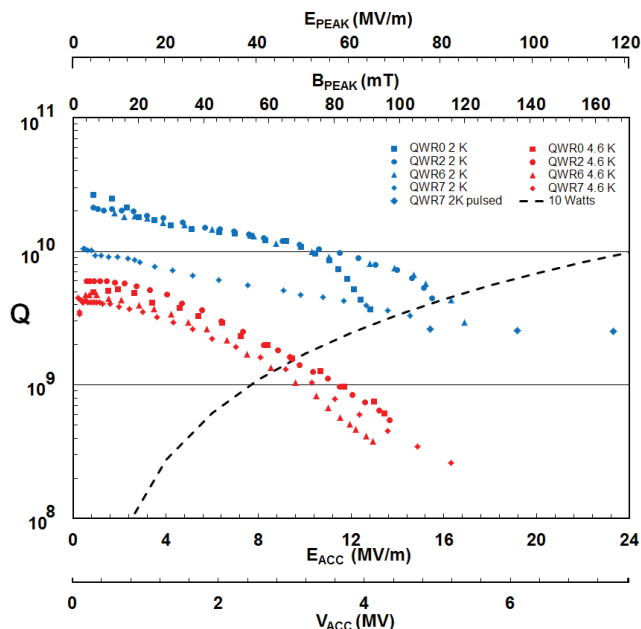


Figure 2: Quality factor versus accelerating gradient, voltage and surface fields at 2 and 4 K ($l_{eff}=\beta\lambda=0.32$ m)

meter cavity string (see Figure 1). ATLAS beam transport efficiency for both stable and radioactive ion beams will be improved dramatically by increasing overall acceptance and reducing emittance growth inherent in the split-ring designs.

The planned cavity operating voltage of $V_{ACC}=2.5$ MV/cavity is roughly two times higher than for the present state-of-the-art at this beta, however, cavities and subsystems, including power couplers and cryogenics are all designed for operation with at least $V_{ACC}\sim 3$ MV/cavity. Several improvements have been made since 2009 to achieve this performance, however, the two critical pieces are the improved rf design [2] and the unique capability to electropolish complete quarter-wave cavity/helium jacket assemblies [3].

CAVITY PERFORMANCE

Cold tests at 2 K and 4 K for four out of eight new 72 MHz cavities are complete and test results are shown in Figure 2. Seven of these cavities will be installed into ATLAS as part of the intensity upgrade and the eighth is for R&D and intended to advance the performance for this class of cavity [4]. Of the seven ATLAS cavities, four will be tested individually in the ANL test cryostat while the remaining three will be tested in the full cryomodule before installation into the ATLAS beamline. If a cavity requires a second round of cleaning, it can be removed

THERMO-MECHANICAL SIMULATIONS OF THE FREQUENCY TUNING PLUNGER FOR THE IFMIF HALF-WAVE RESONATOR

N. Bazin, P. Bosland, S. Chel, G. Devanz, N. Grouas, P. Hardy, J. Migne, F. Orsini, F. Peauger, CEA, F-91191, Gif-sur-Yvette, France

Abstract

In the framework of the International Fusion Materials Irradiation Facility (IFMIF), which consists of two high power CW accelerator drivers, each delivering a 125 mA deuteron beam at 40 MeV [1], a Linear IFMIF Prototype Accelerator (LIPAc) is presently under design for the first phase of the project. A superconducting option has been chosen for the 5 MeV RF Linac, based on a cryomodule composed of 8 low-beta Half Wave Resonators (HWR), 8 Solenoid Packages and 8 RF couplers. The initial solution for the frequency tuning system of the HWR was an innovated system based on a capacitive plunger located in the electric field region, allowing a large tuning range of ± 50 kHz, while keeping the cavity rigid enough to fulfill the Japanese regulations on pressurized vessel. Following the cold test results obtained on HWR equipped with the first design of plunger in 2011 [2], the project decided to change the tuning system by a more conservative solution based on the HWR wall deformation.

Nevertheless RF and thermal simulations were realized to understand the previous test results and the conceptual design of a new plunger in niobium was proposed to resolve the issue. The mechanical constraint is to sufficiently deform the plunger to tune the cavity while staying in the elastic range of the niobium material. For the thermal simulations, all the non-linear properties of the materials and the effects of the RF fields are taken into account: thermal conductivity and surface resistance are depending on the temperature, RF fields computed with dedicated software are leading to thermal dissipations in the materials and the vacuum seal.

FIRST DESIGN OF THE HWR PROTOTYPE TUNING SYSTEM

The low- β HWR prototype, whose RF and mechanical design has already been presented in [3] is made of niobium with a titanium helium vessel and niobium-titanium alloy flanges.

The tuning system is based on a capacitive plunger located in the electric field region of the HWR, perpendicular to the beam axis. This plunger, filled with liquid helium, is connected to a thin membrane – 1.7 mm thick – via a 5 mm stem where the tuning force is applied. In order to clean the cavity, the whole tuning system is dismountable from the cavity body and a Garlock Helicoflex joint is used for the vacuum tightness.

For mechanical reasons, the membrane was made of niobium-titanium alloy, whereas the stem and the plunger are made of pure niobium. The membrane can be deformed in the range of ± 1 mm which is sufficient to achieve the required tuning sensitivity of ± 50 kHz.

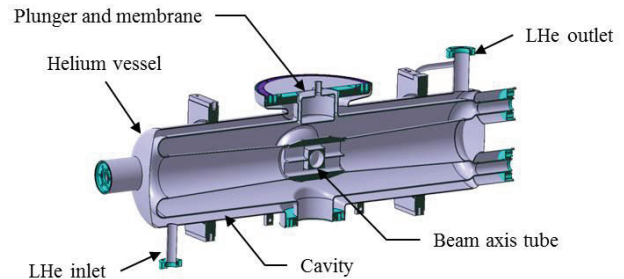


Figure 1: the IFMIF HWR prototype.

Vertical Test Results

After a proper preparation at IPN Orsay (BCP treatment, high pressure rinsing and assembly in an ISO 4 clean room), the prototype equipped with the tuning system was tested in a vertical cryostat at 4.2K.

Several multipactor barriers were observed starting at very low accelerating field (first barrier at 12 kV/m) and up to 500 kV/m. To pass these barriers, the input power was increased on the incident antenna but the consequence was a quench of the NbTi membrane at the $E_{acc} \geq 1$ MV/m.

According to RF simulations, the magnetic field distribution over the membrane shows a maximum value of $\sim 20\%$ of peak field located on the centre of the membrane, which represents ~ 2.5 mT (Figure 2). This value may be sufficient to heat the membrane until its critical temperature.

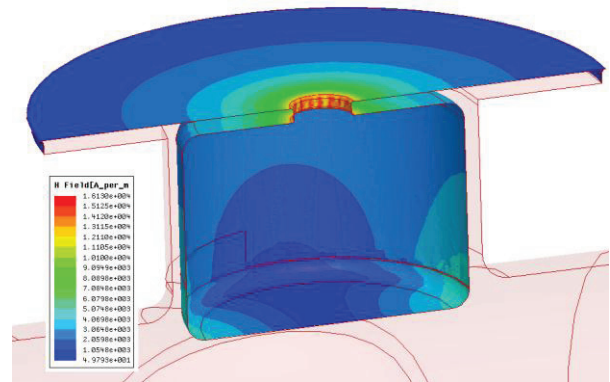


Figure 2: H-field in the plunger region.

Thermal Model of the Tuning System

In order to understand the behaviour of the tuning system, a thermal model has been developed taking into account all the non-linear properties of the materials and the effect of the RF field.

LORENTZ FORCE DETUNING COMPENSATION STUDIES FOR LONG PULSES IN ILC TYPE SRF CAVITIES

N.Solyak, G.Cancelo, B.Chase, D. Crawford, D. Edstrom, E. Harms, Y.Pischalnikov, W.Schappert, Fermilab, Batavia, IL 60510, USA

Abstract

Project-X 3-8 GeV pulsed linac is based on ILC type 1.3 GHz elliptical cavities. The cavity will operate at 25 MV/m accelerating gradient, but in contrast with XFEL and ILC projects the required loaded Q is much higher ($Q \sim 10^7$) and RF pulse is much longer (~ 8 ms or even 26ms). For these parameters Lorentz force detuning (LFD) and microphonics should be controlled at the level < 30 Hz to minimize power overhead from the klystron. A new algorithm of LFD compensation, developed at Fermilab for ILC cavities was applied for Lorentz force compensation studies for 8ms pulses. In these studies two cavities inside TESLA-type cryomodule at Fermilab NML facility have been powered by one klystron. Studies done for different cavity gradients and different values of loaded Q demonstrated that required level of LFD frequency compensation is achievable. Detuning measurements and compensation results are presented.

INTRODUCTION

For the proposed second stage of Project X at Fermilab a 1mA H⁻ beam will be accelerated from 3 to 8 GeV in pulsed linac, based on XFEL/ILC technology. Each of 28 cryomodules with 8 cavities and one quadrupole will be powered by one RF power source. Efficient operation of the linac requires cavities operating at 25 MV/m with a higher loaded Q_L driven by longer pulses, (4ms fill and 4.3ms flattop) than has typically been used with Tesla style cavities until now. The period of the dominant mechanical modes of the cavities is typically several milliseconds and if left uncompensated, the Lorentz force at the planned gradient of 25MV/m can drive the cavities several bandwidths off resonance during the pulse. The RF power required to drive a detuned cavity for different values of Q_L is shown in Figure 1. Since detuned cavity requires extra power, it is critical to have LFD compensated to 30 Hz or better to keep RF power below 50 kW, enough to cover cavity detuning, RF distribution losses and provide overhead for LLRF control. The chosen value $Q_L=10^7$ is a compromise between cavity bandwidth and required power.

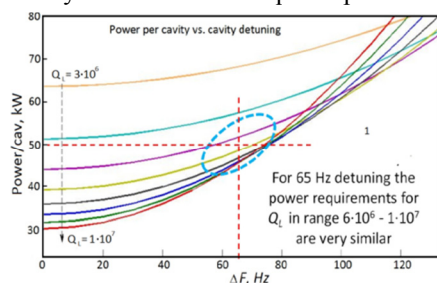


Figure 1: Required power per cavity vs. cavity detuning

The feasibility of actively compensating Lorentz force during long pulses to the levels required for efficient operation of the linac under consideration for Project X was assessed during recent studies using two cavities from CM1 at the Fermilab SRF Test Facility.

EXPERIMENTAL SETUP

CM1 is a DESY Type II cryomodule containing eight 9-cell elliptical superconducting Tesla style cavities operating at a frequency of 1.3 GHz [1], see Fig.2.



Figure 2: Cryomodule in NML at Fermilab

Following the successful commissioning of the cryomodule, the RF distribution system and modulator were reconfigured to drive only the two highest gradient cavities, C5 and C6, with 9 ms pulses from a 120 kW klystron at repetition rates of up to 1 Hz. These two cavities can operate at accelerating gradients, E_{acc} , of 25MV/m and 27MV/m respectively. The vector sum of the two cavities was controlled using an Esecon digital controller and the LFD compensation system developed for CM1 was adapted to handle the modified cavity configuration. The loaded Q_L of both cavities can be varied between 10^6 ($f_{1/2}=650$ Hz) and to 10^7 ($f_{1/2}=65$ Hz) by adjusting the ratios of the power couplers. Cavity baseband waveforms were recorded for the following matrix of operating conditions:

- Q_L : $3 \cdot 10^6$; $6 \cdot 10^6$; $1 \cdot 10^7$;
- E_{acc} : 15MV/m; 20 MV/m; 25 MV/m;
- RF power per cavity: 40 kW; 50 kW; 60 kW.

Current plans for the candidate Project X linac call for the cavities to operate with $Q_L=10^7$ at a gradient of 25 MV/m while driven by 50 kW of RF power required for RF distribution losses, control overhead and compensation of residual frequency detuning from LFD and microphonics.

NORMAL CONDUCTING DEFLECTING CAVITY DEVELOPMENT AT THE COCKCROFT INSTITUTE

G. Burt, P. K. Ambattu, A. C. Dexter, B. Woolley, C. Lingwood, Cockcroft Institute, Lancaster, UK
 S. Buckley, P. Goudket, C. Hill, P. A. McIntosh, J. Mackenzie, A. Wheelhouse,
 STFC, Daresbury, UK
 V. Dolgashev SLAC, USA
 A. Grudiev, CERN, Geneva, Switzerland
 R. M. Jones, UMAN, Manchester, UK

Two normal conducting deflecting structures are currently being developed at the Cockcroft Institute, one as a crab cavity for CERN linear collider CLIC and one for bunch slice diagnostics on low energy electron beams for Electron Beam Test Facility EBTF at Daresbury. Each has its own challenges that need overcome. For CLIC the phase and amplitude tolerances are very stringent and hence beamloading effects and wakefields must be minimised. Significant work has been undertaken to understand the effect of the couplers on beamloading and the effect of the couplers on the wakefields. For EBTF the difficulty is avoiding the large beam offset caused by the cavities internal deflecting voltage at the low beam energy. Prototypes for both cavities have been manufactured and results will be presented.

INTRODUCTION

Transverse deflecting cavities are required for many applications on accelerators, including crab cavities, bunch separators, emittance exchange and for bunch length diagnostics. These cavities usually operate in a TM_{110} -like mode. The Cockcroft Institute in the UK is participating in the design of several deflectors for a range of applications including crab cavities for ILC [1], CLIC [2] and LHC [3] and a bunch length diagnostic for EBTF [4]. In this paper we concentrate on the normal conducting rf deflectors for CLIC and EBTF.

CLIC CRAB CAVITY

CLIC requires a crab cavity to rotate the bunches prior to the interaction point (IP) to achieve an effective head-on collision. As the bunch size at the IP is very small (~5 nm) the luminosity is very sensitive to the crab cavities RF phase and amplitude. This means that the beamloading must be minimised and correction applied. The beamloading is dependent on the longitudinal electric field experienced by the bunch. In crab cavities the longitudinal electric field is zero on axis but has a linear variation as the bunch goes off axis. This means the beamloading could be positive or negative depending on the beam offset. As the bunch train for CLIC is short (~200 ns), the beamloading cannot be compensated for in a single bunch train, the feedback would occur over several trains. Unless the jitter on the beam offset is much less than the bunch size the compensation will not be successful, hence the beamloading must be minimised

instead [5]. In order to reduce the effect of beamloading the cavity is designed with a large power flow so that any power induced by beamloading is smaller in comparison. This is achieved by using a high group velocity travelling wave structure.

Another issue affecting beamloading is the perturbation of the input and output couplers. Couplers break the symmetry of the cavity and can give rise to monopole components to the deflecting field. A dual feed coupler keeps the symmetry of the structure and avoids monopole components but is more complex coupling arrangement requiring splitters. A single feed is the simpler coupling arrangement however this gives the end cells a large monopole component of the rf field. We have investigated methods of single feed coupling without inducing monopole component.

Single-feed Couplers

In order to minimise the monopole component of rf field in the end cells while using a single-feed coupler a number of options were investigated. Initially cancelling the monopole kick from the two end cells was studied. Consider particle moving at the speed of light. If the cell is rotated the monopole component has the sign of the real part of the voltage flipped. Hence if the input and output couplers are mounted on opposite side the real parts should cancel. If the lengths of the cells are adjusted so that the voltage is entirely real then the entire monopole component is cancelled. This however is not sufficient in travelling wave deflecting structures as the power put into the output cell will be extracted through the output coupler while the power in the input cell will travel down the structure. Hence it is necessary to cancel the beamloading in each cell individually.

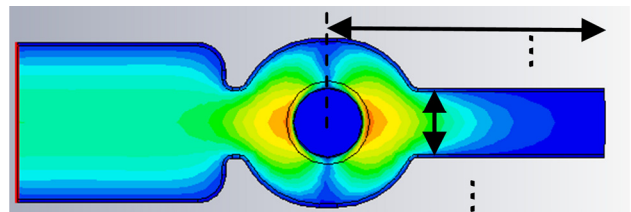


Figure 1: Dummy waveguide and input coupler on the CLIC crab cavity

In order to restore the symmetry of the cell a dummy waveguide opposite the coupler was studied. Using a

STATUS OF THE C-BAND RF SYSTEM FOR THE SPARC-LAB HIGH BRIGHTNESS PHOTOINJECTOR*

R. Boni, D. Alesini, M. Bellaveglia, G. Di Pirro, M. Ferrario, A. Gallo, B. Spataro,
INFN-LNF, Frascati, Italy
A. Mostacci, L. Palumbo, ULRS, Rome, Italy

Abstract

The high brightness photo-injector in operation at the SPARC-LAB facility of the INFN-LNF, Italy, consists of a 150 MeV S-band electron accelerator aiming to explore the physics of low emittance high peak current electron beams and the related technology. Velocity bunching techniques, SASE and Seeded FEL experiments have been carried out successfully. To increase the beam energy so improving the performances of the experiments, it was decided to replace one S-band travelling wave accelerating cavity, with two C-band cavities that allow to reach higher energy gain per meter. The new C-band system is in advanced development phase and will be in operation early in 2013. The main technical issues of the C-band system and the R&D activities carried out till now are illustrated in detail in this paper.

THE SPARC-LAB AT FRASCATI LNF

The SPARC-LAB is a research facility of the INFN Frascati Laboratory (LNF) whose purpose is to conduct advanced research in the field of high brightness, low emittance electron beams [1]. The facility, able to operate also in the velocity bunching configuration, feeds six 2m. long undulators and integrates the 150 MeV S-band photo-injector with a 220 Terawatt, Ti:Sa ultrashort laser system. FEL radiation in the SASE, Seeded and HHG modes have been performed from 500 nm down to 40 nm wavelength. The photo-injector SPARC, a single bunch electron accelerator, consists of a laser driven RF Gun followed by three traveling wave (TW), constant gradient, $2\pi/3$ accelerating cavities, with the first two immersed in a solenoidal field to keep down the beam emittance growth. A second beam line has been also installed and is now hosting a narrow band THz radiation source.

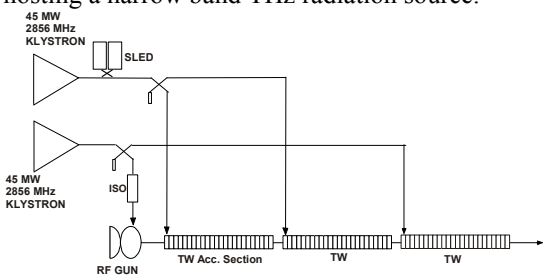


Figure 1: the SPARC photoinjector present layout.

To improve the performances of the experiments and

recuperate the energy that is lost in the velocity bunching configuration, it was decided to increase the beam energy by replacing the third S-band section with two, 1.4 m. long, C-band TW accelerating structures that allow to operate at higher gradient. The choice of a higher frequency, e.g. the X-band, was also considered but then discarded because more expensive and technically more challenging.

THE C-BAND RF SYSTEM

The C-band technology is relatively new in linear accelerators compared to the standard and widely used S-band systems. Nevertheless it can be considered sufficiently mature since it is already employed in other accelerator laboratories like the Spring8 (JP) and the PSI FEL (CH) facilities.

R&D of the Accelerating Structure

The third S-band accelerating section, that is a 3 m. long SLAC-type unit, shown in Fig.1 will be replaced with two, 1.4 m., C-band sections supplied with a 50 MW, 5712 MHz Toshiba klystron through a SKIP-type pulse-compressor [2]. In order to ease design and construction, the C-band sections are constant impedance (CI) structures with large (14 mm) iris diameter to minimize the surface electric field on the iris edges and improve the pumping speed. Also, the group velocity increases and this reduces the filling time. It must be remarked that the typical exponential decay of the input compressed pulse is partially compensated by the RF losses of the CI structure, resulting in a quasi-constant field amplitude along the section. Input and output waveguides are coupled to the beam-pipe instead of to the end-cells. A 50 cm long prototype was designed at LNF and built by a local firm. Brazing and vacuum test have been made at LNF [3].

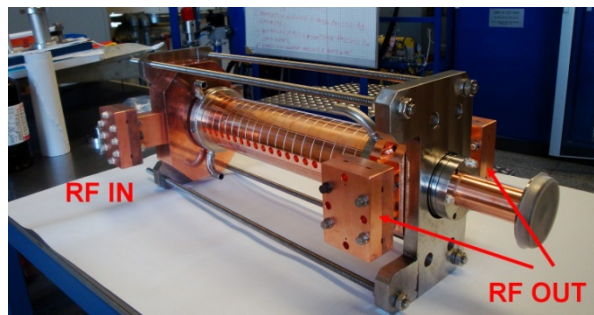


Figure 2: The C-band prototype tested at KEK.

* This research has received funding from the European Commission under the FP7-INFRASTRUCTURES-2010-1/INFRA-2010-2.2.11 project TIARA (CNI-PP). Grant agreement no 261905

TRAVELING WAVE ACCELERATING STRUCTURES WITH A LARGE PHASE ADVANCE

V. Paramonov *, INR of the RAS, Moscow, 117312, Russia

Abstract

The Traveling Wave (TW) accelerating structures, operating with phase advance for the whole field more than 180° per period (up to 1300°) are considered in this report. To realize such phase advance, the structures should operate in higher branches of the Brillouine diagram for TM_{01} wave and have similar to TM_{01n} mode field distribution in the cell. RF parameters of the Disk Loaded Waveguide (DLW) cells are considered for such phase advance and some additions to improve RF efficiency are presented.

INTROSUCTION

There are a lot of papers, describing traveling wave structures with phase advance $\Theta \geq 180^\circ$ and particularities of particle acceleration. For example, see [1] and related references, higher current electron beams can be accelerated. If such structures operate in the first Brillouine zone for TM_{01} wave and field distribution in the cell corresponds to TM_{010} mode, it means acceleration with higher spatial harmonics. The subject of this paper is consideration of DLW structures, in which the main, dominating spatial harmonic has a phase advance $\Theta \geq 180^\circ$.

FIELD DISTRIBUTION

In Fig. 1 is shown well known formation of the DLW dispersion diagram from TM_{01} wave parabola in smooth waveguide, [2], and numbers of Brillouine zones are marked. For traveling wave the field distribution in the

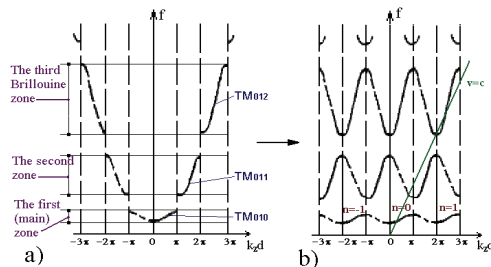


Figure 1: DLW dispersion diagram formation for TM_{01} wave.

aperture all time can be represented in complex form as:

$$E_j(r, z) = \Re E_j(r, z) - i \Im E_j(r, z) = e^{-\frac{i\Theta_0 z}{d}} \sum_{n \rightarrow -\infty}^{n \rightarrow +\infty} a_{jn}(r) e^{-\frac{i2n\pi z}{d}}, \quad (1)$$

* paramono@inr.ru

where d is the DLW period and $0 \leq \Theta_0 \leq 180^\circ$ is the phase advance. In the main zone, Fig. 1, the TM_{010} mode is implemented in DLW cell and expansion (1) starts with $n = 0$. For the second zone the field distribution is TM_{011} -like. For symmetrical DLW cell there is no $n = 0$ harmonic in the expansion (1), which starts now with $n = -1$, and field phase advance is in range $180^\circ \leq \Theta \leq 360^\circ$, including 180° leap due to TM_{011} mode field structure. So on, in higher zones with TM_{01N} -like field in the cell, we can provide field phase advance $N \cdot 180^\circ \leq \Theta \leq N \cdot 180^\circ + 180^\circ$.

DLW CELLS PARAMETERS

RF parameters of DLW cells in higher TM_{01} passbands investigated assuming operating frequency $3.0GHz$ in wide range of aperture radius a and Θ_0 similar to [3] with powerful 2D software. In each passband the cell length is defined from synchronism condition:

$$d_2 = \frac{\lambda(2\pi - \Theta_0)}{2\pi}, \quad d_3 = \frac{\lambda(2\pi + \Theta_0)}{2\pi}, \quad (2)$$

where d_2 and d_3 are the DLW cell length for the second and the third passband, respectively.

In Fig. 2 the surfaces of the group velocity β_g and effective shunt impedance Z_e are shown with parameters $\frac{a}{\lambda}$ and Θ_0 for the second and the third TM_{01} passbands.

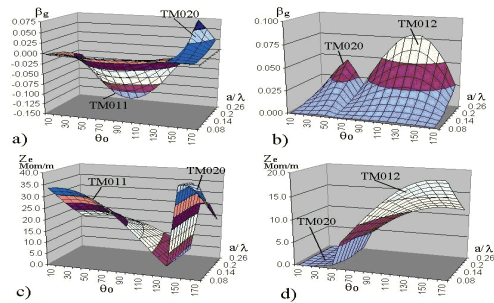


Figure 2: The surfaces $\beta_g(\frac{a}{\lambda}, \Theta_0)$, (a,b) and $Z_e(\frac{a}{\lambda}, \Theta_0)$, (c,d) for the second (a,c) and the third (b,d) passbands.

The regions of TM_{01} wave existence in each higher passbands are limited by interaction with TM_{02} wave, see Fig. 2. For the first and the second passbands possible Θ_0 values are in limits $0 < \Theta_0 < 140^\circ$ and $70^\circ < \Theta_0 < 180^\circ$, respectively. Outside these limits the cell radius R_c becomes large enough and TM_{02} wave comes in appropriate passband.

Without 2D investigations, these Θ_0 limitations were accepted and for appropriate higher passbands (the fourth and so on).

RF PARAMETERS OF A TE - TYPE DEFLECTING STRUCTURE FOR THE S-BAND FREQUENCY RANGE *

V. Paramonov †, L. Kravchuk, INR RAS, Moscow, Russia
K. Floettmann, DESY, Hamburg, Germany

Abstract

In [1] an effective compact deflecting structure has been proposed preferably for the L-band frequency range. RF parameters of this structure are now considered for S-band frequencies both for traveling and standing wave operation. Some methodical topics of the structure are discussed too.

INTRODUCTION

In [1] a deflecting structure was proposed with the original design idea to separate the functions of RF efficiency and RF coupling, which are coupled in the well known Disk Loaded Waveguide (DLW) by a single parameter - the aperture radius r_a . Two protrusions are introduced at the disk in order to concentrate the transverse electric field at the axis, Fig. 1b. The magnetic field around the protrusions, Fig. 1d, provides the required flux for the transverse RF voltage. The structure has a small transverse diameter $2r_c \sim (0.6 \div 0.8)\lambda_0$, where λ_0 is the operating wavelength and looks promising at lower frequencies, including the L-band range. The structure dispersion is positive with a passband width $\Delta f \sim (0.10 \div 0.15)f_0$. It reaches a significant group velocity β_g for a Traveling Wave (TW) with a phase advance $0 < \theta < \pi$, which results in a significant power flow and thus suggest a Standing Wave (SW) operation, [2].

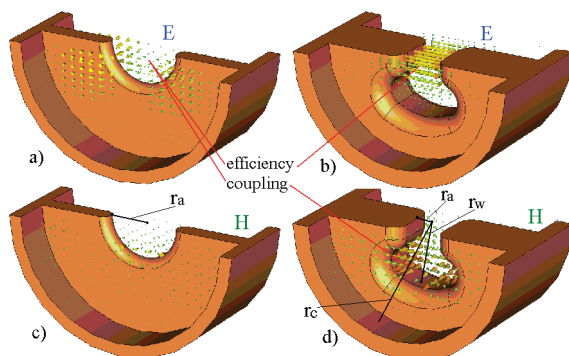


Figure 1: Electric (a, b) and magnetic (c, d) field distributions for the classical DLW structure (a, c) and the TE-deflector, (b, d).

The attractive features of the structure stimulate an additional study, including possible applications in the S - band frequency range.

* Work supported in part by RBFN N12-02-00654-a

† paramono@inr.ru

FIELD DISTRIBUTION

The classification of a structure with a complicated field distribution is always rather conditional. In the field distributions, Fig. 1b,d, one can see a strong transverse electric field, providing an argument for a structure classification in the RF sense as TE - type. But for the description of a deflecting field at $\beta = 1$ the generating hybrid waves HM_n and HE_n are used, see [3] for explanations, both with simultaneously non vanishing E_z and H_z components. For the deflecting force - the transverse component of the Lorentz force - in cylindrical or Cartesian coordinates we have:

$$\vec{F}_{r,x}^L = e(\vec{E} + [\vec{v}, \vec{B}]) = e(E_r - \beta Z_0 H_\varphi) = e(E_x - \beta Z_0 H_y), \quad Z_0 = \sqrt{\mu_0 \epsilon_0}. \quad (1)$$

In contrast to a DLW, the structure under consideration has the same phasing for both transverse components E_r, H_φ or E_x, H_y and the deflecting effect of the electric field is partially compensated by an opposite deflection of the magnetic field. The phasing of transverse E, H components defines also the sign of the group velocity, which is positive in our case. For a deflection of particles this structure can be described as HE_1 -dominating structure.

The effective transverse shunt impedance Z_e in the structure,

$$Z_e = \frac{\frac{1}{k} \int_0^L \frac{\partial E_z}{\partial z} e^{ikz} dz|^2}{P_s L}, \quad \beta = 1, \quad (2)$$

where L is the structure length and P_s is the dissipated RF power, depends mainly on the distance between the ends of the protrusions, i.e. the effective aperture diameter $2r_a$, Fig. 1d, Fig. 2.

The structure has no rotational symmetry, which removes

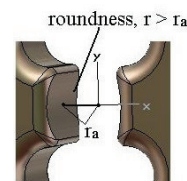


Figure 2: The structure shape near the axis for the reduction of multipole additions.

the problem of overlapping modes with perpendicular field orientation. But in the field distribution exist, together with the desirable dipole components $\sim \cos(\varphi), \sin(\varphi)$, multipole components $\sim \cos(n\varphi), \sin(n\varphi), n = 3, 5, 7, \dots$,

OPERATIONAL EXPERIENCE WITH THE FERMI@ELETTRA S-BAND RF SYSTEM*

A. Fabris[#], P. Delgiusto, F. Gelmetti, M. Milloch, A. Milocco, F. Pribaz, C. Serpico, N. Sodomaco,
R. Umer, L. Veljak, Sincrotrone Trieste, S.S. 14 – km. 163,5, in Area Science Park, 34149
Basovizza, Trieste, Italy

Abstract

FERMI@Elettra is a single-pass linac-based FEL user-facility covering the wavelength range from 100 nm (12 eV) to 4 nm (310 eV) and is located next to the third generation synchrotron radiation facility Elettra in Trieste, Italy. The machine is presently under commissioning and the first FEL line (FEL-1) will be opened to the users by the end of 2012. The 1.5 GeV linac is based on S-band technology. The S-band system is composed of fifteen 3 GHz 45 MW peak RF power plants powering the gun, eighteen accelerating structures and the RF deflectors. The S-band system has been set into operation in different phases starting from the second half of 2009. This paper provides an overview of the performance of the system, discussing the achieved results, the strategies adopted to assure them and possible upgrade paths to increase the operability of the system.

INTRODUCTION

The FERMI@Elettra FEL facility is based on a warm linac followed by a single pass seeded FEL [1]. Two FEL lines are foreseen: FEL-1 which produces fundamental output wavelength from 100 to 20 nm and FEL-2 which will extend the operation down to 4 nm applying High Gain Harmonic Generation schemes. The main parameters of the machine are reported in Table 1.

Table 1: Machine Parameters

Parameter	FEL-1	FEL-2	Unit
Wavelength	100-20	20-4	nm
Electron beam energy	1.2	1.5	GeV
Bunch charge	0.8	1	nC
Peak current	850	500	A
Bunch length (FWHM)	400	600	fs
Norm. emittance (slice)	0.8-1.2	1.0-2.0	mm mrad
Energy spread (slice)	150-250	100-200	keV
Repetition rate	10-50	50	Hz

The accelerator consists of an RF photocathode gun, an S-band linac, an X-band structure, a laser heater to control the uncorrelated energy spread and the beam

transport system to the undulators. The machine is presently working at a repetition frequency of 10 Hz, which will be increased to 50 Hz in May 2013.

The commissioning of the facility is rapidly advancing and FEL-1 will be opened to external users at the end of the present year. Commissioning of FEL-2 will progress in the remaining time with the target of the first test experiment during 2013.

PRESENT STATUS OF THE S-BAND SYSTEM

Sixteen S-band accelerating structures are installed in the FERMI linac (Fig.1). The first nine structures are TW ones, while the last seven are BTW type and are equipped with SLED. Two more TW structures will be added in the future. They will replace the first two structures that will be finally relocated along the machine.

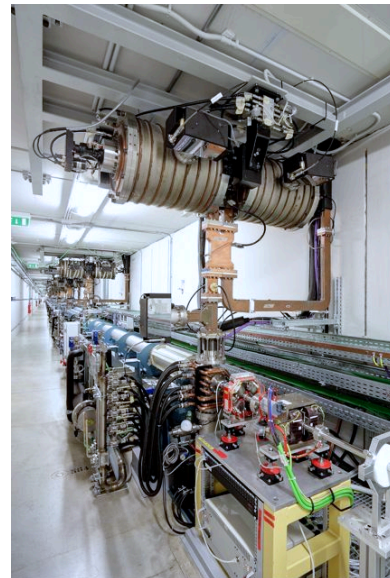


Figure 1: View of the linac from the high-energy end.

Fifteen 45 MW peak klystron (TH2132A) are installed, each one powered by pfn based modulators (Fig.2). Fourteen klystrons provide RF power to the accelerating structures, to the gun and to the low and high-energy RF deflectors. Two main power distribution schemes are used: one klystron feeding two TW structures or one klystron feeding one high gradient BTW structures. A spare power plant provides a backup solution to the first two, powering either the RF gun or the structures before the laser heater. The change of the operating mode is

*Work supported by the Italian Ministry of University and Research under grants FIRB-RBAP045JF2 and FIRB-RBAP06AWK3
[#]alessandro.fabris@elettra.trieste.it

DESIGN OF A C-BAND DISK-LOADED TYPE ACCELERATING STRUCTURE FOR A HIGHER PULSE REPETITION RATE IN THE SACLA ACCELERATOR

Tatsuyuki Sakurai[#], Takahiro Inagaki and Yuji Otake, RIKEN SPring-8 center, Hyogo, Japan
Hiroyasu Ego, JASRI/SPring-8, Hyogo, Japan

Abstract

It is expected that the high pulse-repetition rate of the SACLA accelerator provide a higher rate of X-ray laser pulses to expand ability of user experiments, such as simultaneously providing the laser to several beamlines and reducing a measuring time in the experiment. Therefore, we studied on a C-band accelerating structure for the higher pulse rate above 120 pps than the present rate of 60 pps. Since the higher repetition rate operation is inclined to increase vacuum electrical discharges, it is required to reduce the surface electric fields in the structure without decrease in accelerating voltage. We designed a cross sectional shape of ellipsoidal curvature, which reduces the maximum surface electric or rf field by 20%. The designed structure adopts a TM₀₁-2 π /3 mode disk-loaded type with a quasi-constant gradient. Since the high repetition rate also increases the heat load to the structure, in simulation, we optimized cooling channels. As a result of the design, an accelerating gradient of more than 40 MV/m will be expected, when an input RF power of 80 MW is fed into the structure.

INTRODUCTION

The SACLA (SPring-8 Angstrom Compact free electron LAser) facility succeeded to generate of the X-ray free electron laser (XFEL) with a wavelength of 0.12 nm in June, 2011[1]. Since March 2012, the X-ray laser is provided to the user experiments by mainly using one beamline.

To expend user experiment ability, SACLA has a space of five beamlines for the future expansion. The electron beam must be distributed to the beamlines by using a fast switching magnet in order to supply X-ray laser to many experiments users. However, the repetition rate of each beamline decreases inevitably. Therefore, we plan to operate SACLA with a repetition rate up to 120 pps for the upgrade of the beamlines.

Our present C-band (5712 MHz) accelerating structure to adopt multi-bunch operation has a choke-mode cavities [2] and an SiC absorbers outside of each cavity. The present structure generates an accelerator gradient of 37 MV/m to obtain a 8GeV electron beam and has a phase advance per cell of 3 π /4 mode in order to machine the choke-mode cavity. Due to the heat dissipation, this complicated structure has distortions of the cavity, which leads large shifts of a resonant frequency and an RF phase. This distortion is a serious problem for 120 pps operation. Therefore, the newly designed accelerating structure does not have complicated choke structures and

SiC absorbers. Furthermore, the simple structure gives reduction of the production costs and enable us high precise adjustment of the resonant frequency with the dimpling method after the brazed of the structure.

NEW STRUCTURE DESIGN

The designed disk-loaded structure has a phase advance per cell of 2 π /3 for the accelerating TM₀₁-mode and quasi-constant gradient. The highest shunt impedance for a travelling-wave structure occurs in the neighborhood of the phase advance. Therefore, an accelerating gradient of the new structure should be higher than the existing structure. Due to the compatibility of future replacement with the present choke-mode structure for future replacement, a structure length, a filling time and an attenuation parameter of new structure are designed to be the same as those of the choke-mode one.

We used the 3D electromagnetic field simulation codes, ANSYS-HFSS [3], in order to design the structure. By the simulation, the iris diameter (2a) of each cell is linearly changed over 100 cells and a quasi-constant gradient is obtained. The cell diameter (2b) was adjusted so that the resonance frequency for every cell is equal to the operation frequency of 5712 MHz. Table 1 shows the parameters of a new C-band disk-load type accelerating structure. Figure 1 shows variations of the 2a and the accelerating gradient at an input power of 80 MW. The averaged accelerating gradient is expected to be 43 MV/m, when an input RF power of 80 MW is fed into the structure.

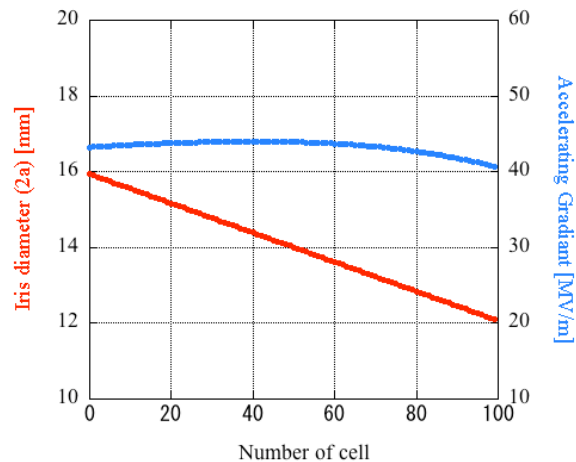


Figure 1: Variation of the iris diameters (red line/left axis) and an accelerating gradient at an input power of 80 MW (blue line/right axis).

[#]t-sakura@spring8.or.jp

THE NONRESONANT PERTURBATION THEORY BASED FIELD MEASUREMENT AND TUNING OF A LINAC ACCELERATING STRUCTURE *

W. C. Fang[#], Q. Gu, Z. T. Zhao, SINAP, Shanghai, China
D. C. Tong, THU, Beijing, China

Abstract

Assisted by the bead pull technique, nonresonant perturbation theory is applied for measuring and tuning the field of the linac accelerating structure. The method is capable of making non-touching amplitude and phase measurements, real time mismatch feedback and field tuning. Some key considerations of the measurement system and of a C-band traveling-wave structure are discussed, and the bead pull measurement and the tuning of the C-band traveling-wave linac accelerating structure are presented at last.

INTRUCTION

The Shanghai soft X-ray Free Electron Laser test facility(SXFEL)is presently being planned and designed at the Shanghai Institute of Applied Physics, CAS [1]. This facility will be located close to the Shanghai Synchrotron Radiation Facility, which is the first 3rd generation light source in mainland China [2]and it requires a compact linac with a high gradient accelerating structure and high beam quality. As a key R&D item, a room temperature C-band (5712 MHz) accelerating structure has been developed [3, 4]. For fabricating the C-band structure with high performance, the bead pull measurement system based on nonresonant perturbation theory has been developed.

There are several methods for RF structure measurement or tuning, such as the resonant perturbation method [5] and the phase shift method, however several limitations appear when they are applied to a traveling-wave accelerating structure. The resonant perturbation method picks up the amplitude of the electromagnetic field, therefore it is limited in the measurement of the standing-wave accelerating structure and the phase shift method only shows the phase information in the RF structure. For the accurate and fast tuning of a traveling-wave linac RF structure, nonresonant perturbation theory is the preferable method, which can measure the electromagnetic field distribution with both amplitude and phase, and this method is capable of making non-touch measurement, which can maintain the clean inner surface of the accelerating structure and reduce its RF breakdown rate. Furthermore, this method is also very effective in performing an accurate and fast real-time tuning of the accelerating structure, which is economical for mass fabrication of accelerating structures.

In this paper we present a cold test application of nonresonant perturbation theory on a linac RF structure [6]. This method based on the bead pull technique can pick up the amplitude and phase distribution of a linac

structure, particularly for a traveling-wave structure, and is a preferable and efficient method for accelerating structure cold testing and tuning. In the following we describe firstly the theory of nonresonant perturbation and the tuning procedure and then discuss the key considerations of our measurement system with the bead pull technique. At the end we give several experimental results of our newly developed C-band traveling-wave accelerating structure tuning, which verify the feasibility of this method.

NONRESONANT PERTURBATION THEORY AND TUNING PRINCIPLE

According to nonresonant perturbation theory, the variation of the reflection coefficient in the input port is measured with and without a perturbation bead, which is placed at different points along a line to pick up the amplitude and phase distribution of the electromagnetic field strength, a schematic drawing is shown in Figure 1. Based on the results and post-processing, RF tuning is processed with accurate and fast real-time feedback.

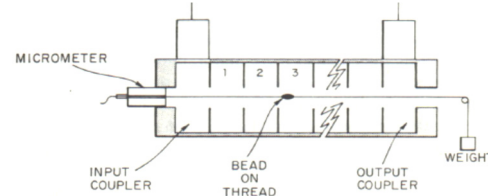


Figure 1: The field measurement based on nonresonant perturbation theory.

Nonresonant Perturbation Theory and Field Measurement

In nonresonant perturbation theory, the desired field strength is calculated as the following [6]:

$$2P_i(\Gamma_p - \Gamma_a) = -j\omega[k_e E_a^2 - k_m H_a^2] \quad (1)$$

For an accelerating structure, the TM mode is used for beam acceleration and the crucial longitudinal electrical field E_z is the unique field component on axis, thus the first equation of equation (1) is used for field measurement, and is renamed as equation(2) with reflected coefficient S_{11} of the Network Analyzer:

$$\Delta S_{11} = \Gamma_p - \Gamma_a = S_{11p} - S_{11a} = -\frac{j\omega k_e E_a^2}{P_i} \quad (2)$$

where S_{11p} and S_{11a} are acquired from the Network Analyzer, respectively corresponding to Γ_p and Γ_a in equation (1) above. In equation (2), E_a is complex data, its amplitude is the square root of the amplitude of ΔS_{11} , and its phase is half of the phase of ΔS_{11} . As the

*Work supported by SINAP project
#fangwencheng@sinap.ac.cn

S-BAND LOADS FOR SLAC LINAC*

A. Krasnykh, F.-J. Decker, SLAC National Accelerator Lab, Menlo Park, CA 94025, USA
 R. LeClair, INTA Technologies, Santa Clara, CA 95051, USA

Abstract

The S-Band loads on the current SLAC linac RF system were designed, in some cases, 40+ years ago to terminate 2-3 MW peak power into a thin layer of coated Kanthal material as the high power absorber [1]. The technology of the load design was based on a flame-sprayed Kanthal wire method onto a base material. During SLAC linac upgrades, the 24 MW peak klystrons were replaced by 5045 klystrons with 65+ MW peak output power. Additionally, SLED cavities were introduced and as a result, the peak power in the current RF setup has increased up to 240 MW peak. The problem of reliable RF peak power termination and RF load lifetime required a careful study and adequate solution. Results of our studies and three designs of S-Band RF load for the present SLAC RF linac system is discussed. These designs are based on the use of low conductivity materials.

INTRODUCTION

The original RF system setup of the SLAC linac (see Fig. 1) was based on an array of 24 MW peak klystrons [1].

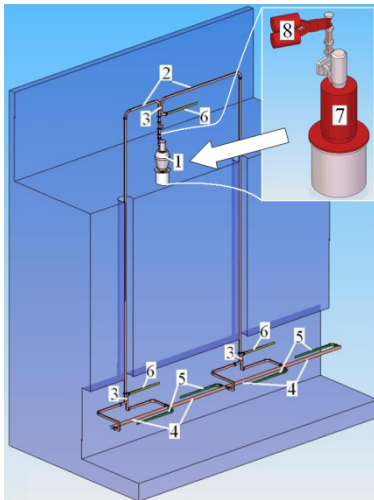


Figure 1: Original RF setup of the SLAC linac; 1 is XK-5 Klystron, 2 is WR284 Waveguide Branches, 3 is Power Dividers, 4 is Accelerating Sections, 5 is High Power RF Loads, 6 – Low Power RF Loads

Each RF station is equipped with a XK-5 klystron (1), feeding two branches of WR284 waveguide (2) and three 3dB power splitters (3) to supply four 10ft travelling accelerating sections (4). The residual klystron power after passing through the accelerator structure is absorbed by four high power loads (5).

* Work supported by the U.S. Department of Energy under contract number DE-AC02-76SF00515 and SBIR grant number DE-SC0007661

Three low power RF loads (6) absorb any mismatched (reflected) RF power. 240 such stations were in service of the original SLAC linac.

A high energy physics program (to reach 50 GeV output beam energy) was initiated and completed at the end of 1980 [2]. The original XK-5 klystrons were replaced by 5045 series klystrons with a 50 MW peak (subsequent production improvements the output power reached 65+ MW peak). SLED cavities were also introduced into the RF system thereby increasing the beam energy by a factor 1.7. The present typical RF setup is depicted in Fig. 1 where the new RF components (5045 klystron (7) and the SLED assembly (8)) are shown in right corner. A white arrow shows the location of the upgrade.

The residual power termination performance of the RF loads was not a concern during many years of service. For example, there were not any problems when the linac is used as the PEP-II injector. The RF absorption performance only became an item of concern after analyses of the LCLS RF phase stability issues [3].

It was found that the RF amplitude and phase of the reflected signals are unstable. It was shown also that these RF instabilities are associated with the processes inside of the load vacuum envelope. A detail of the RF structure layout that helps illustrate the high power load problem is shown in Fig.2.

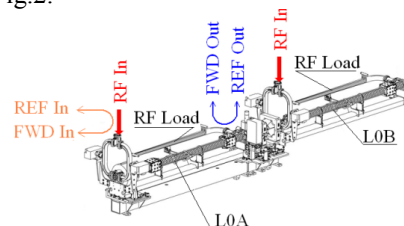


Figure 2: LCLS Injector layout

These two stations are working with detuned SLED cavities. The input and output couplers are employed for the monitoring of forward (FWD In and FWD Out) and reflection (REF In and REF Out) signals. The waveforms of these signals are shown in Fig. 3.

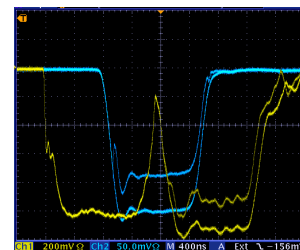


Figure 3: Waveforms of reflection signals

Ch1 (yellow trace) shows the reflection power from the input of the accelerating structure. Ch2 (blue trace) shows the reflection signal from the output of the accelerating

FABRICATION TESTS FOR IMP 162.5 MHz RFQ*

Bin Zhang, Yuan He, Xiaofeng Jin, Jing Wang, Junhui Zhang, Aiming Shi, Xiaonan Du, Zhouli Zhang, IMP, CAS, China
 Derun Li, Matthew, D. Hoff, Steve Vireostek, Andrew Lambert, LBNL, USA

Abstract

The RFQ for one of front ends of C-ADS is designed. The frequency of the RFQ is 162.5 MHz and the energy is 2.1 MeV. The beam intensity is 15 mA and it works at CW mode. Because of low frequency, the four-wing structure is big size. It makes fabrication will take more risks. Therefore, four fabrication tests were planned and done to minimize the technic risks. The description about fabrication and testing results are presented .

STRUCTURE DESIGN

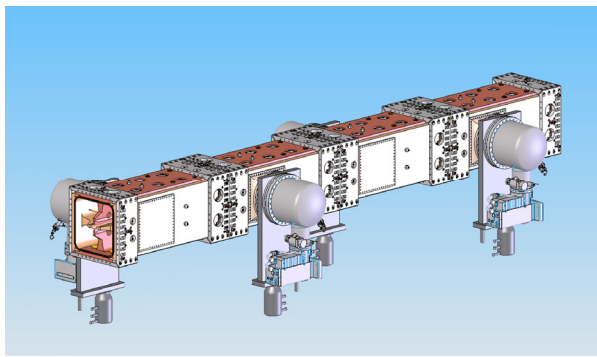


Figure 1: Structure of the ADS-Linac RFQ

Four 1.05 m long cavity modules were bolted together with a total length of 4.20 m, approximately 1000 kg for each complete module. All OFHC copper body were machined from solid billets, 4-vane cavity structure be choose with fly cut modulated vane tips. In this structure it includes 32 Pi-mode rods for mode stabilization, 20 fixed slug tuners/module 12 field sensing loops were designed per module. RF power feed through two loop couplers. 20 cooling channels per module will take the heat of RF power.

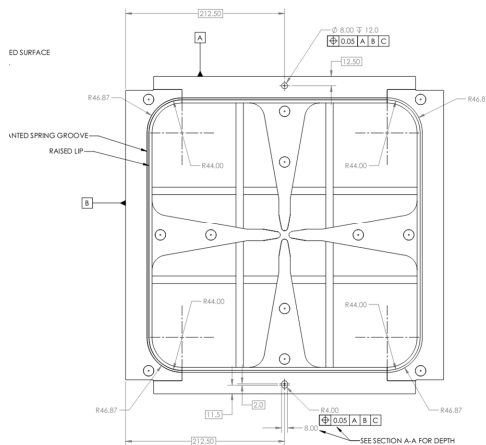


Figure 2: Section of RFQ

FABRICATION TESTS

Since the RFQ work in a low frequency, the four-wing structure is big size (425mm×425mm at section), four fabrication tests were planned and done to ensure fabricated process and minimize technic risks. It include fly cutting test, full length vane test, braze and clamp test and half-length test module. Two of them had finished the last one were rough machining now, as for hydrogen braze test, more tests were necessary before the last braze to take.

Flying cutting test

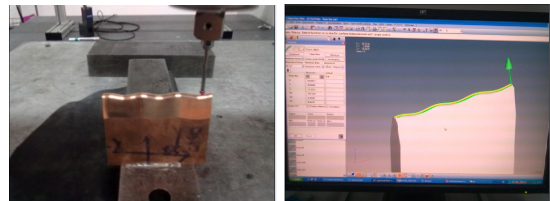


Figure 2: measurement vane

Flying cutting method were choice for RFQ modulation machined instead of ball drill. Two short pieces were cut and measurement with CMM. the result of measurement shows some point were out of tolerance ,some improvement with cutting tool will be take and the pieces will be measurement again in new CMM device.

Table 1: result of modulation measurement

	Max (mm)	Min(mm)
Profile tolerance	+0.0067	-0.0070
Section 1	+0.0056	-0.0097
Section 5	+0.0103	-0.0185
Section9	+0.0431	-0.0856
Radius of tip	8.5685	8.5315
Angle	19.9332	19.5164

Full length vane fabricated test

Full length of a single vane is about 1050mm, include all mechanic structure of RFQ, such as braze groove, cooling water deep hole, modulation of vane, vacuum seal groove etc. Main task were focused on the Gun-drill for deep hole, EBW for water plunger and the tolerance for vane pale. So far, it had been finished and all ports, holes and outside surface geometry tolerance will be checked by CMM this month.

X-RAY LOCAL ENERGY SPECTRUM MEASUREMENT AT TSINGHUA THOMSON SCATTERING X-RAY SOURCE (TTX)*

Y.-C. Du[#], Z. Zhang, L.-X. Yan, J.-F. Hua, H. Zha, W.-H. Huang, C.-X. Tang

Accelerator laboratory, department of engineering physics, Tsinghua University, Beijing, China
Key laboratory of Particle & Radiation Imaging (Tsinghua University), Ministry of Education, Beijing, 100084, China

Key laboratory of High Energy Radiation Imaging Fundamental Science for National Defense, Beijing, 100084, China

Abstract

Thomson scattering X-ray source, in which the TW laser pulse is scattered by the relativistic electron beam, can provide ultra short, monochromatic, high flux, tunable polarized hard X-ray pulse which is can widely used in physical, chemical and biological process research, ultra-fast phase contrast imaging, and so on. Since the pulse duration of X-ray is as short as picosecond and the flux in one pulse is high, it is difficult to measure the x-ray spectrum with traditional spectra measurement methods. In this paper, we introduce an iterative statistical algorithm (Expectation-Maximization) to reconstruct the spectra from the attenuation data, and the results of the X-ray spectrum measurement experiment on Tsinghua Thomson scattering is also presented.

INTRODUCTION

Thomson Scattering sources (also called Inverse Compton Scattering), which can be bright X-ray sources typically produce photons, have attracted a lot of interest as the technologies for producing low-emittance high-brightness relativistic electron sources and ultra-short high-power lasers have progressed. The X-rays that are generated by the interactions between laser and electron, exhibit high directivity, and have a polarized tunable quasi-monochromatic spectrum. The knowledge of the spectrum of an X-ray source is a key point for the development of any kind of application, for example in imaging both contrast and absorbed dose strongly depend on energy. However, direct methods performing a standard spectrometric measurement based on single photon energy measurement to detect the X-ray spectrum of Thomson Scattering sources have always been considered troublesome to implement because the beam is too intense to cause pulse pile up problems. Thomson Scattering source can produce up to 10^8 photons, bunched in 10ps long pulse^[1]. An alternative way to measure the spectrum might request the measurement to be integral-type, which will not be affected by the high rate of incidence of photons. The analysis of attenuation data (transmission curves), which can provide some information about the spectral distribution of an X-ray

source, as not affected by the rate of incidence of photons, is a good candidate to measure the X-ray spectrum of the Thomson Scattering X-ray source. Although there are several problems with this method, such as low accuracy, non-unique solution to ill-condition system and instability with different measurement error^[2], this method can still give good estimation and reconstruction of spectra with some improvements based on the property of the measured spectra.

In this article, we introduce an iterative statistical algorithm (Expectation-Maximization)^[3] to reconstruct the spectra from the attenuation data on simulated measurement. Results show that this method can give good approximations for the mean energy of the spectra, while it is not sensitive to the specific spectral distribution and the energy broadening. In order to reconstruct the shape of the spectra, especially the energy broadening, we present a new method based on the Expectation-Maximization algorithm. An preliminary experiment is also carried out on Tsinghua Thomson scattering X-ray source, the measured maximum X-ray energy is about 53keV, which is agreed well with the simulations.

OVERVIEW OF TTX

The scheme of TTX is shown in figure 1. This machine includes a 50MeV electron linac based on the photocathode RF gun and a Ti: Sapphire TW laser system. The laser system generates both the 266nm UV pulse for photocathode and the 800nm IR pulse for scattering interaction. The two pulses are derived from one 79.3MHz Ti:Sapphire oscillator in order to reduce the time jitter between the electron beam and the IR pulse. The linac system consists of a BNL/KEK/SHI type 1.6 cell S-band photocathode RF gun, a 3m S-band SLAC type travelling wave accelerating section, generates 40~50MeV ultra-short high brightness electron pulse for scattering interaction. The laser system is synchronized with the RF system through a timing circuit, with a timing jitter no greater than 0.5ps. The parameters of electron and laser were listed in the table 1.

In previous experiment, we succeed to generate and detect the X-ray signal with head-on colliding mode. The results from the MCP and X-ray CCD are shown in figure 2.

*Work supported by work is supported by NSFC under Grant Nos. 10735050, 10805031, 10975088 and 10875070 and by the 973 Program under Grant No. 2007CB815102.

[#] dych@mail.tsinghua.edu.cn

FRIB TECHNOLOGY DEMONSTRATION CRYOMODULE TEST*

J. T. Popielarski^{*}, E. C. Bernard, S. Bricker, C. Compton, S. Chouhan, A. Facco[#], A. Fila, L. Harle, M. Hodek, L. Hodges, S. Jones, M. Klaus[†], M. Leitner, D. Miller, S. Miller, D. Morris, J. P. Ozelis, R. Oweiss, L. Popielarski, K. Saito, N. Usher, J. Weisend, Yan Zhang, Z. Zheng, S. Zhao
FRIB, East Lansing, Michigan, USA

[#]INFN/LNL, Legnaro (PD), Italy, [†] Technische Universität Dresden, Dresden, Germany

Abstract

A Technology Demonstration Cryomodule (TDCM) has been developed for a systems test of technology being developed for FRIB. The TDCM consists of two half wave resonators (HWRs) which have been designed for an optimum velocity of $\beta=v/c=0.53$ and a resonant frequency of 322 MHz. The resonators operate at 2 K. A superconducting 9T solenoid is placed in close proximity to one of the installed HWRs. The 9T solenoid operates at 4 K. A complete systems test of the cavities, magnets, and all ancillary components is presented in this paper.

INTRODUCTION

The SRF Department at Michigan State University had developed and tested four cryomodules prior to the first demonstration cryomodule for FRIB. Two of the cryomodules are working reliably in the ReA3 linac at MSU [1]. The TDCM, shown in figure 1, is the first cryomodule that demonstrates FRIB specific technology and encourages a transition to large scale engineering and quality assurance methods [2].

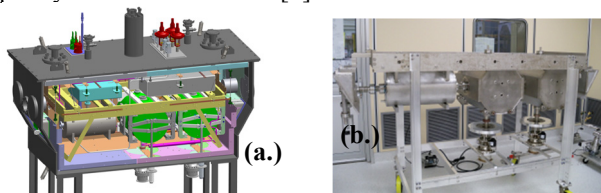


Figure 1: (a.) Rendering of TDCM in cryostat (b.) Cold mass assembly in cleanroom.

In developing the FRIB TDCM, a baseline cryomodule production method evolved for FRIB. The technical and schedule related setbacks encountered during the TDCM campaign eventually yielded reliable fabrication, processing, and certification techniques. SRF-related infrastructure and utility usage required for the TDCM assisted in finalizing planning for a new SRF high bay which will support FRIB cavity processing, vertical testing, cold mass assembly, and cryomodule bunker tests.

TDCM RELEVANCE TO FRIB

The TDCM is a developmental snapshot, and much of the technology improved as more detailed engineering

*This material is based upon work supported by the U.S. Department of Energy Office of Science under Cooperative Agreement DE-SC0000661.
[#]popielar@frib.msu.edu

analysis and sub component testing programs provided opportunities for design optimization [3- 5]. Some of the key differences are: a “bottom-up” style from the “top-down” TDCM style [4]; the rail system, support system, heat and magnetic shields assemblies were simplified; Improvements to alignment methods; an internal heat exchanger replaces the external heat exchanger; the 4K thermal intercepts will be parallel circuits as opposed the series connection in the TDCM.

With much of the cryogenic circuitry and alignment systems optimized in the baseline design before TDCM testing took place, alignment and continuous 2K operation aspects were not tested. The plumbing of the RF coupler 4K intercepts [6] required steady flow in the static state required continuous overfilling of the 4K header to ensure the couplers stayed cooled during RF conditioning.

TDCM DEVELOPMENT

Individual tests or more detailed engineering analyses conducted on the cavities, couplers, tuners, and cryogenic circuits used in the TDCM led to design optimizations and improved processing [7- 9].

Initial dunk tests showed low field emission onset values and thermal breakdown below the operating gradient; FRIB processing optimization for the HWR began during the TDCM campaign. The TDCM cavities were field emission-free [10] prior to the installation of the helium vessels.

Initial tests still showed signs of multipacting in the cavity. Repeated measurements on several cavities show a recurring barrier at 2 MV/m E_{acc} . This barrier self-conditioned as the RF power was raised, and in most tests only observed during initial 4K measurements.

During the initial dunk tests, it was discovered Q_0 was lower after a thermal cycle with no change otherwise. A closer investigation for Q -disease showed a strong reduction in the Q_0 after a 15 hour soak at 100K. The cavities were sent to JLAB for a furnace treatment to remove hydrogen from the bulk. Subsequent ‘ Q -soaks’ and thermal cycles showed no signs of degradation. A 600°C furnace treatment was added to the baseline processing plan and a furnace has been installed at MSU [9].

After being jacketed with a helium vessel, the 1st cavity was certified using the vertical cryostat configuration [5], and no field emission was observed. This helium vessel design utilized a titanium bellows at the beamport to reduce the tuning force required for the scissor-jack tuner.

THE INJECTOR CRYOMODULE FOR THE ARIEL E-LINAC AT TRIUMF

R.E. Laxdal, N. Muller, A. Koveshnikov, W.R. Rawnsley, G. Stanford, V. Zvyagintsev
 TRIUMF, Vancouver, Canada
 M. Ahammed, M. Mondrel, VECC, Kolkata, India

Abstract

The ARIEL project at TRIUMF includes a 50 MeV-10 mA electron linear accelerator (e-Linac) using 1.3 GHz superconducting technology. The accelerator is divided into three cryomodules including a single cavity injector cryomodule (ICM) and two accelerating cryomodules with two cavities each. The ICM is being built first. The ICM utilizes a unique top-loading box vacuum vessel. The shape readily allows the addition of a 4K/2K cryogenic unit that accepts near atmospheric LHe and converts to 2K liquid inside the cryomodule. The cryomodule design is complete and in fabrication. The 4K/2K cryogenic unit has been assembled with tests scheduled next month. The paper describes the design and status of the cryomodule.

INTRODUCTION

TRIUMF is now preparing a new high intensity superconducting electron linear accelerator[1], e-Linac, as a key element of the ARIEL project. The e-Linac is specified to produce 10mA of 50MeV electrons as a powerful 0.5MW photo-fission driver to add a complimentary second source of radioactive ion beams for the existing ISAC experimental infrastructure. The e-Linac consists of five 1.3GHz nine-cell niobium cavities each supplying 10MV acceleration with two 50kW power couplers supplying the required beam loaded rf power. The five cavities are housed in three cryomodules, with a single cavity in an injector cryomodule, EINJ, and two identical accelerating cryomodules EAC1 and EAC2 with two cavities in each module. The fully funded first phase of the e-Linac includes the first two cryomodules for a final energy and intensity of 30MeV and 5mA for 150kW driver capability by 2014. The EINJ is presently being fabricated and will serve as the working prototype for EAC1.

TRIUMF began developing EINJ in 2010 in collaboration with the VECC laboratory in Kolkata. VECC requires a photo-fission driver for the proposed ANURIB[2] facility. TRIUMF and VECC have an agreement to jointly design the EINJ cryomodule. Two EINJs are being fabricated and beam tested at TRIUMF with one EINJ being shipped to VECC and the second installed in the e-Linac. The initial EINJ is presently in fabrication. A beam test area is being installed in the ISAC-II building to utilize the existing cryogenics infrastructure with beam tests scheduled for early 2013.

CONCEPTUAL DESIGN

Cryomodules for 1.3GHz elliptical cavities utilize typically round vacuum chambers with end loaded cold mass assemblies. In applications such as X-FEL involving long linac structures the gas return pipe in the cryomodule acts as both the support strongback for the cold mass and the helium cold return distribution line for the overall cryogenic system. Operation is at 2K with the 2K produced either in a central 2K cold box or in a JT expansion valve close to the cryomodule that transforms a typical 3 bar stream from a 4K cold box to He-II. Heavy ion linacs such as the ISAC-II 40MV linac[3] operate at 4K due to typically lower rf frequencies and hence lower BCS resistance and are typically designed as box cryomodules with the cold mass loaded from above due to the large transverse size of the low frequency low beta cavities.

Although non-standard a top-loading box design (Fig. 1) has some advantages for the e-Linac over an end-loading round variant. Firstly the modular and staged testing/installation sequence of the e-Linac suggests that each cryomodule be self-reliant to convert 4K atmospheric LHe available from dewars or ISAC-II cryogenic system into 2K He-II. To this end the box

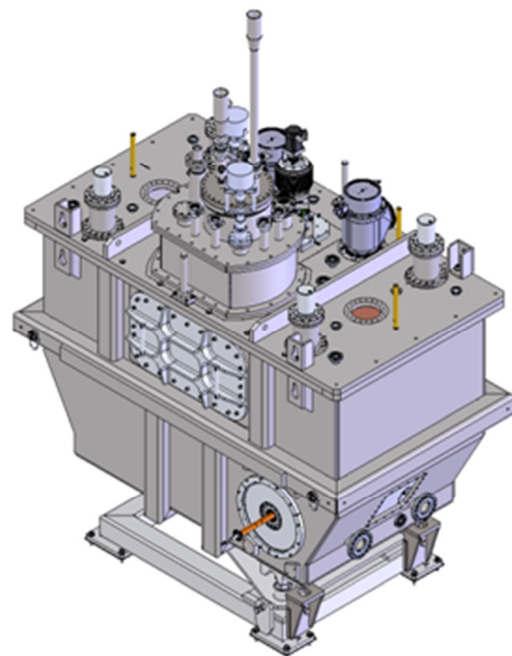


Figure 1: Model of the e-Linac Injector cryomodule.

THE UPGRADED ARGONNE WAKEFIELD ACCELERATOR FACILITY (AWA): A TEST-BED FOR THE DEVELOPMENT OF HIGH GRADIENT ACCELERATING STRUCTURES AND WAKEFIELD MEASUREMENTS*

M.E. Conde[#], D.S. Doran, W. Gai, R. Konecny, W. Liu, J.G. Power, Z. Yusof,
ANL, Argonne, IL 60439, U.S.A.
S. Antipov, C. Jing, Euclid Techlabs LLC, Solon OH 44139, U.S.A.
E. Wisniewski, IIT, Chicago IL 60616, U.S.A.

Abstract

Electron beam driven wakefield acceleration is a bona fide path to reach high gradient acceleration of electrons and positrons. With the goal of demonstrating the feasibility of this concept with realistic parameters, well beyond a proof-of-principle scenario, the AWA Facility is currently undergoing a major upgrade that will enable it to achieve accelerating gradients of hundreds of MV/m and energy gains on the order of 100 MeV per structure. A key aspect of the studies and experiments carried out at the AWA facility is the use of relatively short RF pulses (15 – 25 ns), which is believed to mitigate the risk of breakdown and structure damage. The upgraded facility will utilize long trains of high charge electron bunches to drive wakefields in the microwave range of frequencies (8 to 26 GHz), generating RF pulses with GW power levels.

AWA FACILITY

The mission of the Argonne Wakefield Accelerator Facility (AWA) is to develop technology for future accelerator facilities. The AWA facility has been used to study and develop new types of accelerating structures based on electron beam driven wakefields. In order to carry out these studies, the facility employs a photocathode RF gun capable of generating electron beams with high bunch charges and short bunch lengths. This high intensity beam is used to excite wakefields in the structures under investigation.

The facility is also used to investigate the generation and propagation of high brightness electron beams, and to develop novel electron beam diagnostics.

The AWA high intensity electron beam is generated by a photocathode RF gun, operating at 1.3 GHz. This one-and-a-half cell gun typically runs with 12 MW of input power, which generates an 80 MV/m electric field on its Magnesium photocathode surface. A 1.3 GHz linac structure increases the electron beam energy, from the 8 MeV produced by the RF gun, to 15 MeV. The linac is an iris loaded standing-wave structure operating in the $\pi/2$ mode with an average accelerating gradient of 7 MV/m; it has large diameter irises to minimize the undesirable wakefields generated by the passage of high charge electron bunches.

The charge of the electron bunches can be easily varied

from 1 to 100 nC, with bunch lengths of 2 – 2.5 mm rms, and normalized emittances of 3 to 100 π mm mrad.

The AWA laser system consists of a Spectra Physics Tsunami oscillator followed by a Spitfire regenerative amplifier and two Ti:Sapphire amplifiers (TSA 50). It produces 1.5 mJ pulses at 248 nm, with a pulse length of 2 to 8 ps FWHM and a repetition rate of up to 10 pps. A final KrF Excimer amplifier is optionally used to increase the energy per pulse to 15 mJ.

The generation of electron bunch trains (presently up to 16 bunches) requires each laser pulse to be divided by means of beam splitters into a laser pulse train. The charge in each electron bunch is determined by the energy in each laser pulse and the quantum efficiency of the photocathode material. Typically, single bunches of 100 nC can be produced (with a maximum of 150 nC occasionally reached).

WAKEFIELD ACCELERATION

The use of electron beam driven wakefields to achieve high gradient acceleration has received considerable attention. It offers the advantage of using a relativistic beam to transport the energy to the accelerating structures, decreasing the difficulties of generating and distributing RF power by conventional means; wakefields naturally constitute RF pulses that are of short duration and high peak intensity [1].

Research at the AWA facility has been exploring various types of wakefield structures, including photonic band gap structures, metallic iris loaded structures, and also more exotic schemes using metamaterials. The main focus of the facility, however, has clearly been the development of dielectric loaded structures. They offer the advantage of simple geometry and easy fabrication with accelerating properties that compare favourably with conventional iris loaded metallic structures: the axial electric field is uniform across the transverse cross section of cylindrical structures, and the uniform cross section of the structures presents no geometric features to cause field enhancement. The damping of the undesirable deflecting dipole modes seems to be more easily accomplished in dielectric loaded structures as well; planned experiments will explore the use of longitudinal slots on the metallic outer shell of dielectric structures, as a possible scheme to damp dipole modes. Dielectric structures also hold the promise of withstanding higher electric fields without material breakdown. A significant advantage offered by wakefield structures, in comparison

*Work supported by the U.S. Department of Energy under contract No. DE-AC02-06CH11357.

[#]conde@anl.gov

SIMULATION STUDY ON THE LONGITUDINAL BUNCH SHAPE MEASUREMENT BY RF CHOPPER AT J-PARC LINAC

T. Maruta*, J-PARC center, Japan Atomic Energy Agency, Tokai, Ibaraki, Japan
M. Ikegami, High Energy Accelerator Research Organization, Tsukuba, Ibaraki, Japan

Abstract

We propose to measure the longitudinal rms beam size by existing apparatuses in MEBT1 at J-PARC linac. The RF chopper cavity horizontally deflects beam particles at the frequency of 324 MHz, which is the same frequency as other accelerator cavities. By setting an adequate driving phase of the chopper, a horizontal deflection is proportional to relative phase difference from the centroid of a beam bunch. Then, the deflected beam distribution is measured by a wire scanner monitor. It is also possible to measure the longitudinal rms emittance by varying the amplitude of a buncher upstream. In this paper, we confirm the feasibility of the measurement scheme with particle simulation.

INTRODUCTION

The J-PARC linac is comprised from a 50 keV negative hydrogen (H^-) ion source (IS), a 3 MeV Radio Frequency Quadrupole (RFQ), a 50 MeV Drift Tube Linac (DTL), and a 181 MeV Separate-type DTL (SDTL). There is a medium energy beam transport section (MEBT1) between the RFQ and DTL. We place an RF chopper system in the middle of MEBT1 to shape a macro pulse configuration in accordance with RF frequency of following 3 GeV rapid cycling synchrotron (RCS).

In the J-PARC linac, a beam intensity upgrade project is currently underway. The project will replace the front end part (IS to RFQ) for the extension of the peak current to 50 mA in the next summer. A simulation study indicates that the longitudinal beam emittance in the 50 mA operation is 20 % larger than present one. The beam rejection power of the RF chopper system is inversely correlated to a beam width in phase direction, it motivated us to consider a reinforcement of the chopper. It is important to understand the current beam width for an inquest of the reinforcement. However, we have no monitors for the beam width measurement, and moreover, there is no space to install an additional monitors in MEBT1.

We devise a beam width measurement method only with an existing apparatus in MEBT1 to overcome the situation. Then we evaluate the feasibility with a three dimensional particle-in-cell code IMPACT [1].

MEBT1

MEBT1 is a 3 m long transport line between RFQ and DTL as shown in Fig. 1. There are two major issues. One is a matching of the beam to the DTL acceptance in both longitudinal and transverse phase space by eight

quadrupole magnets and two buncher cavities while transferring the beam to DTL. To measure the beam qualitatively, we place beam current monitors (CT), beam position monitors (BPM) and wire scanner monitors (WSM) [2] throughout MEBT1. The other issue is a shaping of a macro pulse in accordance with the RF frequency of following RCS. The RF chopper system is involved in the shaping. It is comprised from an RF chopper cavity and a scraper which is located at 0.72 m downstream from the cavity. Unnecessary beam bunches are horizontally (x) deflected by the cavity and then they hit to the scraper.

RF Chopper Cavity

We employ an RF deflector (RFD) for beam chopping [3]. The RFD is operated in a TE_{11} -like mode with the frequency of 324 MHz, which is same as RFQ and DTL. The deflection angle of a RF gap is 6 mrad at the electric field of 1.6 MV/m of which an RF power is 22 kW. There are two RF gaps in the cavity at intervals of $3\beta\lambda$, where β is the velocity of beam normalized by the speed of light and λ is RF wave length. The two RF gaps are currently connected in series via a coaxial tube with length of 2λ to supply an RF from a single semiconductor amplifier. In this summer, we modify the configuration to individually supply an RF to each RF gap by introduction of an additional amplifier. It enable us to tune an asynchronous phase and an amplitude of each RF gap individually. The current amplifier stably supply an RF power up to 35 kW which corresponds a gap field of 2.0 MV/m. Moreover, we have a plan to upgrade the amplifier to 60 kW in the next summer.

MEASUREMENT METHOD

In the measurement, we use the RF chopper cavity, the upstream buncher and a WSM downstream of the chopper cavity. The measurement is comprised of two steps. In the first step, we measure the beam width in phase direction by the chopper cavity and the WSM. Then, the second step measures a longitudinal emittance and a Courant-Snyder parameter by adding the buncher to the beam width measurement. This measurement is similar to a transverse emittance measurement so-called "Q-scan" [4] in principle.

Beam Width in Phase Direction

In the nominal operation of J-PARC linac, the chopper is tuned to give a maximum deflection to a beam bunch. It is equivalent that we adjust the RF to be maximum when a beam bunch arrives at the middle of an RF gap as shown in Fig. 2(a). The integrated RF of a beam particle gradually attenuates in accordance with a phase difference from the

* tmaruta@post.j-parc.jp

DESIGN OF MEBT FOR THE PROJECT X INJECTOR EXPERIMENT AT FERMILAB

A. Shemyakin[#], C. Baffes, A. Chen, Y. Eidelman, B. Hanna, V. Lebedev, S. Nagaitsev, J.-F. Ostiguy, R. Pasquinelli, D. Peterson, L. Prost, G. Saewert, V. Scarpine, B. Shteynas, N. Solyak, D. Sun, M. Wendt, V. Yakovlev, Fermilab*, Batavia, IL 60510, USA
 T. Tang, SLAC, Menlo Park, CA 94025

Abstract

The Project X Injector Experiment (PXIE) [1], a test bed for the Project X front end, will be completed at Fermilab at FY12-16. One of the challenging goals of PXIE is demonstration of the capability to form a 1 mA H- beam with an arbitrary selected bunch pattern from the initially 5 mA 162.5 MHz CW train. The bunch selection will be made in the Medium Energy Beam Transport (MEBT) at 2.1 MeV by diverting undesired bunches to an absorber. This paper presents the MEBT scheme and describes development of its elements, including the kickers and absorber.

REQUIREMENTS

The PXIE MEBT will be a ~10 m beam line between RFQ and the first Half-Wave Resonator cryomodule (HWR). It should form the required bunch pattern, match the optical functions between RFQ and SRF, include tools to measure properties of the beam coming out of RFQ and coming to SRF, and clean transverse halo particles while transporting the bunches selected for the following acceleration with a low emittance dilution and a low beam loss. The main MEBT requirements are listed in Table 1.

Table 1. The main MEBT functional requirements

Parameter	Value	Unit
Beam kinetic energy	2.1 +/-1%	MeV
Input frequency of bunches	162.5	MHz
Nominal input beam current	5	mA
Beam current operating range	1-10	mA
Nominal output beam current	1	mA
Relative residual charge of removed bunches	< 10 ⁻⁴	
Beam loss of pass through bunches	< 5%	
Nominal transverse emittance	< 0.27	μm
Nominal longitudinal emittance	0.8	eV-μs
Relative emittances increase	<10%	

FOCUSING SCHEME

Transverse focusing in the MEBT is provided mainly by equidistantly placed quadrupole triplets (Fig.1); the only exception is two doublets at the MEBT upstream

end. Below the regions between neighboring triplets or doublets are referred to as MEBT sections. These sections are represented in Fig. 2 by rectangles color-coded according to their main function. The regular period is 1140 mm, which leaves 650 mm (flange-to-flange) space for equipment (350 mm in the section #0).

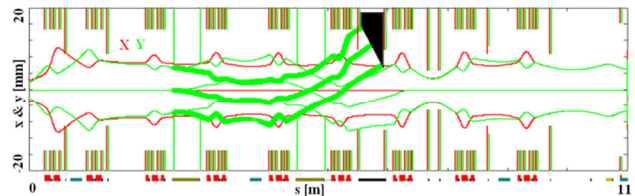


Figure 1: Scheme of MEBT optics [2] and the beam envelope. The thin lines are the central trajectory and 3σ envelope (ε_{rms,n}=0.25 mm mrad) of the passing beam, and the thick lines are the Y envelope of the chopped-out beam. Red- quadrupoles, blue- bunching cavities.

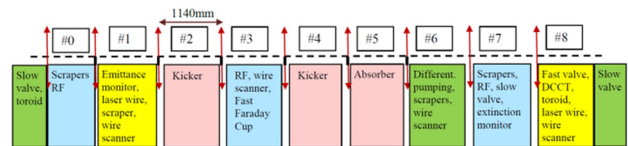


Figure 2: MEBT structure. Red - chopping system, blue-RF, yellow – diagnostics, green – vacuum.

Longitudinally the beam is focused (Fig.3) by three bunching cavities (Fig.4).

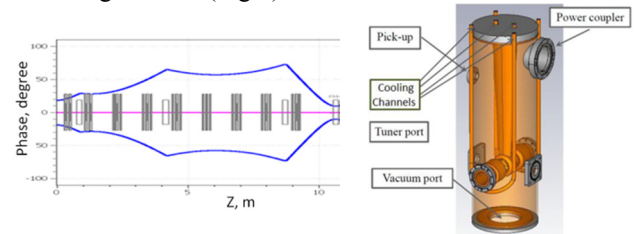


Figure 3: 3-σ bunch length through MEBT. Figure 4: Conceptual design of the MEBT bunching cavity.

CHOPPING SYSTEM

The undesired beam bunches will be removed in the MEBT by a chopping system consisting of two identical kickers separated by 180° transverse phase advance and an absorber at 90° from the last kicker. In the broadband, travelling-wave kickers [3], the transverse electric field propagates through their structures with the phase velocity equal to the speed of H- ions, 20 mm/ns. Depending on polarity, bunches are either kicked toward the absorber surface or on a pass through path. In either

[#] shemyakin@fnal.gov

* Operated by Fermi Research Alliance, LLC, under Contract No. DE-AC02-07CH11359 with the United States Department of Energy

BEAM LOSS MITIGATION IN J-PARC LINAC AFTER THE TOHOKU EARTHQUAKE

M. Ikegami, K. Futatsukawa, Z. Fang, T. Miyao, Y. Liu, KEK/J-PARC, Tokai, Japan
T. Maruta, A. Miura, H. Sako, J. Tamura, G. Wei, JAEA/J-PARC, Tokai, Japan

Abstract

In the course of the beam commissioning of J-PARC linac after nine-month shutdown due to an earthquake, we have experienced beam losses which were not seen before the earthquake. One of the main cause for the beam loss was the irregular RF setting for accelerating cavities to avoid multipactor at one of them, which started to pose difficulty in the nominal operation after the earthquake. In this paper, we discuss the beam loss mitigation effort putting the emphasis on the optimization of the RF setting for SDDL.

INTRODUCTION

We had a magnitude-9.0 earthquake in Tohoku region in Eastern Japan in March 2011. It caused severe damage to J-PARC facilities which forced us to shutdown for nearly nine months [1]. After significant restoration efforts, we started beam operation of J-PARC linac in December 2011 and user operation in January 2012. The linac beam power when we resumed the user operation was 7.2 kW. Then, it is increased to 13.3 kW in March 2012, which is the same as just before the earthquake. While the linac beam operation was restored in terms of the beam power, we have experienced higher beam losses than before the earthquake. Thus, we have been trying to mitigate the beam loss while supporting the user operation. The initial beam start-up in December 2011 and January 2012 was reported in another literature [2]. Therefore, we focus on the beam loss mitigation effort after restoring the user operation in this paper. It should be noted here that the history of residual radiation during the beam commissioning was summarized in the reference [3].

J-PARC linac consists of a 50-keV negative hydrogen ion source, 3-MeV RFQ (Radio Frequency Quadrupole linac), 50-MeV DTL (Drift Tube Linac), and 181-MeV SDDL (Separate-type DTL) [4]. For later reference, we should note here that the SDDL section consists of 30 SDDL tanks with $2\beta\lambda$ inter-tank spacing with β and λ being the particle velocity scaled by the speed of light and the RF wavelength, respectively. Then, each SDDL tank consists of five β -graded cells, and two neighboring SDDL tanks are driven by a klystron.

As reported in reference [2, 3], we experienced significant beam loss at the straight section after SDDL immediately after we resumed the beam operation. A main cause of the beam loss was identified to be insufficient alignment of some of the beam ducts. After conducting urgent realignment of the beam ducts [5], the beam loss was sub-

stantially reduced and become significantly less sensitive to the beam steering. However, multipactor of one of SDDL cavity has been gradually worsened and the irregular RF setting we adopted to avoid the multipactor started to cause beam losses.

In this paper, we mainly discuss the method we adopted to circumvent the SDDL multipactor while suppressing the beam losses.

MULTIPACTOR AT AN SDDL CAVITY

As mentioned above, a pair of SDDL tanks are driven by a klystron. The relative RF amplitude and phase of the tank pair are supposed to be kept balanced with the low-level RF control system. However, we noticed just before the resumption of beam operation in December 2011 that the fifth tank pair, or SDDL5, shows some unstable behavior. For this tank pair, one of the tanks tends to have arcing, or presumably multipactor, which makes the balance of RF amplitude and phase easily lost. This unstable behavior arises in a certain range of RF amplitude which contains its design amplitude. Although similar behavior has been noticed for SDDL1 to SDDL6 since before the earthquake, it caused no difficulty in operating with the design tank level [6]. Therefore, we suspect that the multipactor in SDDL5 become severer at the earthquake for some reason to cause practical difficulty in the nominal operation.

As we can avoid the multipactor by adopting higher or lower RF amplitude for SDDL5, we adopt 109 % of the design amplitude in starting the user operation in January 2012. The unstable band in the RF amplitude was widened during the beam operation and forced us to increase the operating amplitude to 116 % later. As of June 2012, we are operate SDDL5 with the same amplitude. However, the unstable region for SDDL5 is still widening gradually and reducing the operational margin.

We don't delve into the details on the multipactor itself in this paper. Instead, we discuss the irregular RF setting for SDDL we adopt to avoid the multipactor, its effect on the beam losses, and the countermeasure for the beam loss we adopted in the beam commissioning. Further detail of the multipactor will be found in the reference [7].

BEAM LOSS MITIGATION WITH IRREGULAR SDDL SETTING

Operation with 109 % Amplitude for SDDL5

In setting the RF amplitude and phase for SDDL tanks after the earthquake, it was required for us to perform the

PLANNING FOR EXPERIMENTAL DEMONSTRATION OF TRANSVERSE EMITTANCE TRANSFER AT THE GSI UNILAC THROUGH EIGEN-EMITTANCE SHAPING

C. Xiao, O.K. Kester, Institute of Applied Physics, Goethe-University of Frankfurt a.M, Germany
L. Groening, GSI Helmholtzzentrum für Schwerionenforschung, Darmstadt, Germany

Abstract

The minimum transverse emittances achieved in a beam line are determined by the two transverse eigen-emittances of the beam. Without coupling, they are equal to the transverse rms-emittances. Eigen-emittances are constants of motion for all symplectic beam line elements. To allow for rms-emittance transfer, the eigen-emittances are changed by a non-symplectic action to the beam, preferably preserving the four-dimensional rms-emittance.

Unlike emittance swapping, the presented concept will allow the transformation of a beam of equal rms-emittances into a beam of different rms-emittances while preserving the four-dimensional rms-emittance. This contribution will introduce the concept for eigen-emittance shaping and rms-emittance transfer at an ion beam line. The actual work status towards the experimental demonstration of the concept at the GSI UNILAC is presented.

INTRODUCTION

For injection of beams into circular machines with different horizontal and vertical emittance acceptances, the injection efficiency can be increased if these beams are flat. However, beams provided from the linear accelerator are generally round, and the horizontal and vertical emittances are quite equal.

Round-to-flat transformation requires a change of the beam eigen-emittances by a non-symplectic transformation [1]. Such a transformation can be performed by placing a charge state stripper foil inside a longitudinal field region as proposed in [2]. Inside such a solenoidal stripper, the transverse inter-plane correlations are created non-symplectically. Afterwards they are removed symplectically with a coupling correction section. The new set-up providing round-to-flat transformation is shown in Fig. 1. Such an emittance transfer section is proposed to be integrated into the existing beam line between the UNILAC [3] and the SIS synchrotron.

EMITTANCE

The four-dimensional symmetric beam matrix C contains ten unique elements, four of which describe the coupling. The rms-emittances, ε_x and ε_y , are defined as the square roots of the determinants of the on-diagonal submatrices. If one or more of the elements of the off-diagonal

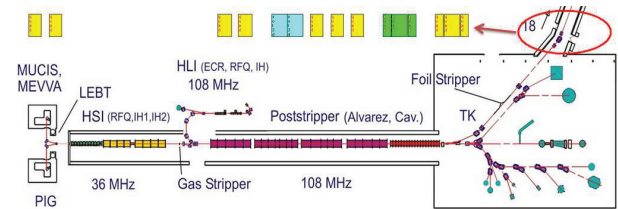


Figure 1: Conceptual layout of the transverse emittance transfer section in the GSI UNILAC.

submatrix is non-zero, the beam is x - y coupled. Diagonalization of the beam matrix yields the beam eigen-emittances, ε_1 and ε_2 , and the values are calculated as:

$$\varepsilon_1 = \frac{1}{2} \sqrt{-\text{tr}(CJ)^2 - \sqrt{\text{tr}^2(CJ)^2 - 16|C|}} \quad (1)$$

$$\varepsilon_2 = \frac{1}{2} \sqrt{-\text{tr}(CJ)^2 + \sqrt{\text{tr}^2(CJ)^2 - 16|C|}} \quad (2)$$

The four-dimensional matrix J is the skew-symmetric matrix with non-zero entries on the block diagonal of form. Eigen-emittances are invariant under symplectic transformations, and the eigen-emittances are equal to rms-emittances when the inter-plane correlations are zero.

BEAM TO BE STRIPPED

Multi-particle beam dynamics simulations have been done using the TRACK code [4]. The uncoupled particle distribution at the entrance of this beam line is concluded from beam experiments and plotted in Fig. 2.

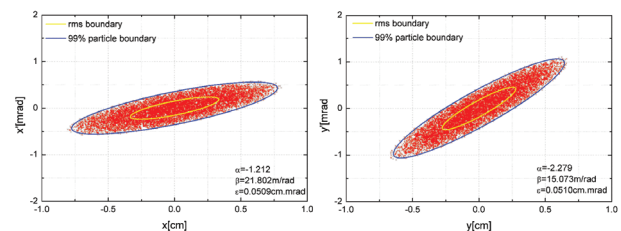


Figure 2: The particle distributions at the entrance of beam line.

The subroutines of the stripper in the TRACK code are based on the SRIM code [5]. The three-dimensional field

STATUS OF THE IFMIF-EVEDA 9 MeV 125 MA DEUTERON LINAC

A. Mosnier, Fusion for Energy, BFD Department, Garching, Germany

Abstract

The scope of IFMIF/EVEDA has been recently revised to set priority on the validation activities, especially on the Accelerator Prototype (LIPAc) extending the duration up to mid 2017 in order to better fit the development of the challenging components and the commissioning of the whole accelerator. The present status of LIPAc, currently under construction at Rokkasho in Japan, outlines of the engineering design and of the developments of the major components will be reported. In conclusion, the expected outcomes of the engineering work, associated with the experimental program will be presented.

INTRODUCTION

The International Fusion Materials Irradiation Facility (IFMIF) aiming at generating materials irradiation test data for DEMO and future fusion power plants is based on an accelerator-driven, D-Li neutron source to produce high energy neutrons at sufficient intensity and irradiation volume. IFMIF Engineering Validation and Engineering Design Activities (EVEDA) have been conducted since mid 2007 in the framework of the Broader Approach Agreement.

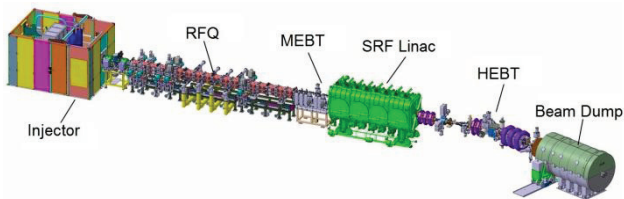


Figure 1: LIPAc layout

In order to demonstrate the feasibility and to develop the technology, a representative portion of one of the two IFMIF accelerators, up to the first section of the SRF Linac, is being designed and built. This high intensity linear accelerator prototype, called LIPAc (Fig. 1), will be assembled and commissioned at Rokkasho in Japan, with the objective to reach a stable 125 mA, 9 MeV continuous deuteron beam. These engineering validation activities are conducted since mid-2007 under the framework of the Broader Approach Agreement and are shared as follows:

- The accelerator components are designed, manufactured and tested by European institutions (CEA, CIEMAT, INFN, SCK-CEN): Injector, Radio Frequency Quadrupole (RFQ), Medium and High Energy Beam Transport lines, Superconducting RF Linac, Beam Dump, 175 MHz RF Systems, Local Control Systems, Beam Instrumentation;
- The conventional facilities (building and auxiliaries), the Central Control System, as well as the RFQ couplers, are provided by JAEA;

- The design integration and the interface management are coordinated by Fusion for Energy (F4E);
- The coordination and the integration on site are provided by the Project Team hosted in Rokkasho.

In 2010, the priority was set on the validation of the Accelerator Prototype [1] extending the duration up to mid 2017 in order to better fit the time required for the development of the challenging components and for the installation and sequential commissioning of the accelerator at Rokkasho.

ACCELERATOR COMPONENTS

Accelerator components [2] are designed, manufactured and individually tested in Europe, and then transported to Rokkasho for installation in the accelerator building.

Injector

The injector has to deliver a continuous low emittance deuteron beam (140 mA, 100 keV) with high reliability. The ion source is based on an electron cyclotron resonance cavity, excited by a 2.45 GHz magnetron [3]. The extracted beam is matched to the RFQ entrance by means of a dual solenoid focusing scheme in the LEBT. In order to meet emittance and matching requirements, the space charge must be highly compensated by injection of krypton gas and up to the RFQ entrance thanks to an electron repeller electrode. In addition, an electrostatic chopper will be implemented between the two solenoids to enable the operation of LIPAc with short pulses of very sharp rise/fall times.

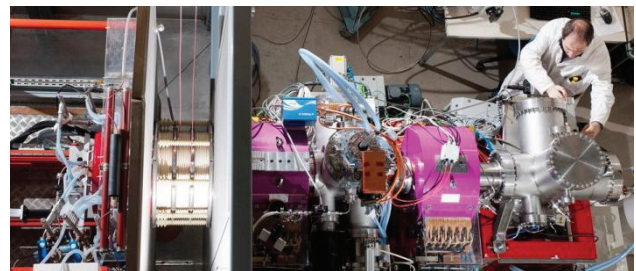


Figure 2: Top view of the Injector (P. Stroppa/cea credit).

The injector was assembled at CEA-Saclay in order to test the components in Europe before the shipment to Japan scheduled at the beginning of 2013 (Fig. 2). After the first H⁺ beam produced in May 2011, a test campaign was carried out in pulsed and continuous operation. Pulsed beams of 150 mA at 100 kV and continuous beams of 100 mA at 75 kV were routinely produced. The first D⁺ beam was extracted in April 2012, first in pulsed mode and then in continuous mode for a short period in order to limit the activation of the elements. However, as the continuous operation at 100 kV was limited by HV discharges in the extraction system, a new 5 electrode

CHINESE ADS PROJECT AND PROTON ACCELERATOR DEVELOPMENT*

W.M. Pan[#], Y.L. Chi, S.N. Fu, P. Sha, IHEP, Beijing, P.R.China
Q.Z. Xing, Tsinghua University, Beijing, P.R.China

Abstract

Significance of proton accelerator on the science and application has been widely recognized in the 21st century. The high-current proton accelerator can be utilized to drive the sub-critical nuclear reactor to build the clean nuclear power system. Moreover, it can serve in the field of high-energy physics, such as the neutrino factory and muon collider. For the spallation neutron source, the high-current proton accelerator provides the important platform for the multidisciplinary development of condensed matter physics, radiation physics, material science, aerospace science and life science. So proton accelerator is developing very fast in China nowadays. There're many proton accelerators under construction over China, which includes Accelerator Driven Sub-critical System (ADS), China Spallation Neutron Source

(CSNS), Compact Pulsed Hadron Source (CPHS). These three projects will be introduced in this paper.

INTRODUCTION

ADS [1], CSNS [2] and CPHS have common ground, but are applied in different fields. They're all ongoing in China at present.

ADS ACCELERATOR

ADS project is a strategic plan to solve the nuclear waste problem and the resource problem for nuclear power plants in China [3]. It's supported financially by the central government and administrated by the Chinese Academy of sciences (CAS). With its long-term planning lasting until 2032, the project will be carried out in three major phases, see Figure 1.

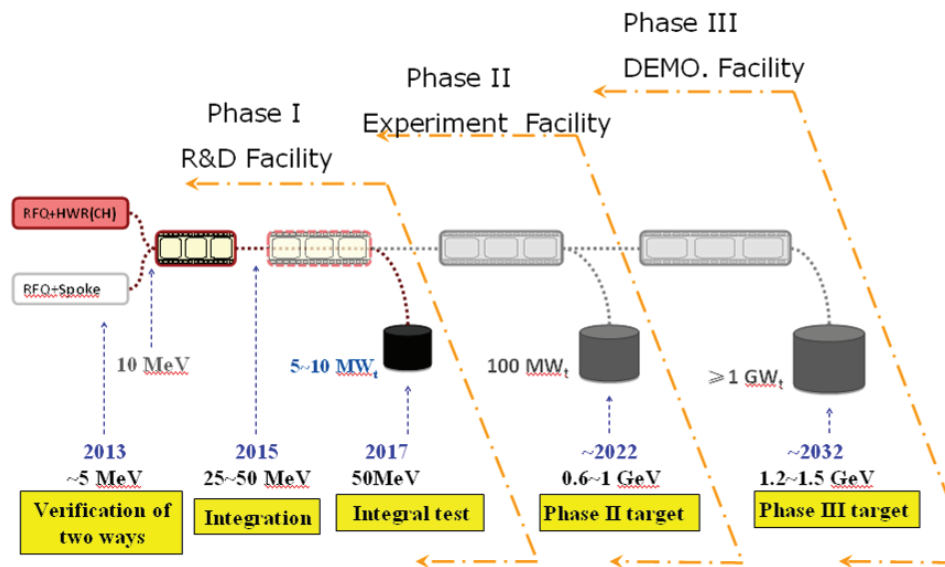


Figure 1: Road map of ADS

ADS accelerator will be built by two institutes of CAS: Institute of High Energy Physics (IHEP) and Institute of Modern Physics (IMP). It's a CW proton linac and uses superconducting acceleration structures except RFQ, the design specifications for the proton beam are shown in Table 1. For Phase I, the goal is to build a CW proton linac of 50 MeV and 10 mA by about 2015. Phase I will be executed progressively in several steps, with the 1st step to build two 5-MeV test stands of different front-end designs.

*Work supported by CAS
#panwm@ihep.ac.cn

Table 1: ADS Proton Beam Specifications

Parameters	Value	Units
Energy	1.5	GeV
Current	10	mA
Beam power	15	MW
Frequency	162.5/325/650	MHz
Duty factor	100%	
Beam Loss	<1 (0.3)	W/m
Beam trips/year [4]	<25000	1s<t<10s
	<2500	10s<t<5m
	<25	t>5m

FRIB ACCELERATOR STATUS AND CHALLENGES*

J. Wei^{#1}, D. Arenius², E. Bernard¹, N. Bultman¹, F. Casagrande¹, S. Chouhan¹, C. Compton¹, K. Davidson¹, A. Facco^{1,4}, V. Ganni², P. Gibson¹, T. Glasmacher¹, K. Holland¹, M. Johnson¹, S. Jones¹, D. Leitner¹, M. Leitner¹, G. Machicoane¹, F. Marti¹, D. Morris¹, J. Nolen^{1,3}, J. Ozelis¹, S. Peng¹, J. Popielarski¹, L. Popielarski¹, E. Pozdeyev¹, T. Russo¹, K. Saito¹, R. Webber¹, M. Williams¹, Y. Yamazaki¹, A. Zeller¹, Y. Zhang¹, Q. Zhao¹

¹ Facility for Rare Isotope Beams, Michigan State University, East Lansing, MI 48824, USA

² Thomas Jefferson National Laboratory, Newport News, VA 23606, USA

³ Physics Division, Argonne National Laboratory, Argonne, IL 60439, USA

⁴ INFN - Laboratori Nazionali di Legnaro, Legnaro (Padova), Italy

Abstract

The Facility for Rare Isotope Beams (FRIB) at MSU includes a driver linac that can accelerate all stable isotopes to energies beyond 200 MeV/u at beam powers up to 400 kW. The linac consists of 330 superconducting quarter- and half-wave resonators operating at 2 K temperature. Physical challenges include acceleration of multiple charge states of beams to meet beam-on-target requirements, efficient production and acceleration of intense heavy-ion beams from low to intermediate energies, accommodation of multiple charge stripping scenarios (liquid lithium, helium gas, and carbon foil) and ion species, designs for both baseline in-flight fragmentation and ISOL upgrade options, and design considerations of machine availability, tunability, reliability, maintainability, and upgradability. We report on the FRIB accelerator design and developments with emphasis on technical challenges and progress.

INTRODUCTION

The Facility for Rare Isotope Beams (FRIB), baselined as a 7-year, US\$680 million construction project, is to be built at the Michigan State University under a corporate agreement with the US DOE [1]. FRIB driver accelerator is designed to accelerate all stable ions to energies above 200 MeV/u with beam power on the target up to 400 kW (Table 1). As shown in Figure 1, the driver accelerator consists of Electron Cyclotron Resonance (ECR) ion sources, a low energy beam transport containing a pre-buncher and electrostatic deflectors for machine protection, a Radiofrequency Quadrupole (RFQ) linac, linac segment 1 (with Quarter-wave Resonators (QWR) of $\beta=0.041$ and 0.085) accelerating the beam up to 20 MeV/u where the beam is stripped to higher charge states, linac segments 2 and 3 (with Half-wave Resonators (HWR) of $\beta=0.29$ and 0.53) accelerating the beam above 200 MeV/u, folding segments to confine the footprint and facilitate beam collimation, and a beam delivery system to transport to the target a tightly focused beam. The reaccelerator (ReA) consists of similar $\beta=0.041$ and 0.085 accelerating structures [2].

*Work supported by the U.S. Department of Energy Office of Science under Cooperative Agreement DE-SC0000661
#wei@frib.msu.edu

Table 1: FRIB Driver Accelerator Primary Parameters

Parameter	Value	Unit
Primary beam ion species	H to ²³⁸ U	
Beam kinetic energy on target	> 200	MeV/u
Maximum beam power on target	400	kW
Macropulse duty factor	100	%
Beam current on target (²³⁸ U)	0.7	emA
Beam radius on target (90%)	0.5	mm
Driver linac beam-path length	517	m
Average uncontrolled beam loss	< 1	W/m

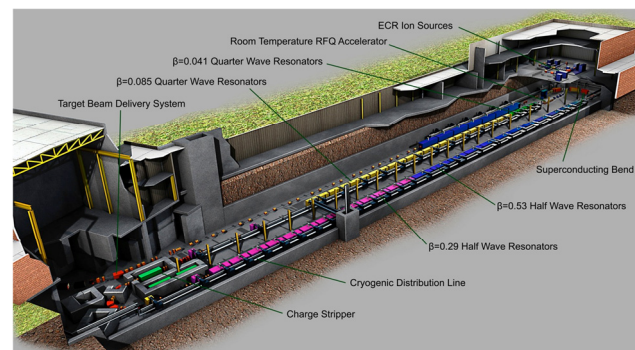


Figure 1: Layout of the FRIB driver accelerator.

DESIGN PHILOSOPHY

Full-energy linac technology is chosen to deliver primary beam that can meet the FRIB requirements of rare-isotope productivity and separation accuracy. Up to 400 kW of beams are focused to a diameter of 1 mm (90%), energy spread of 1% (95% peak-to-peak), and bunch length of < 3 ns (95%) on the target.

Superconducting (SC) technology is the energy-efficient choice for the CW linac. SC acceleration of heavy-ion beams is feasible from very low energy (500 keV/u) with practically sized cavity bores by housing both the cavities and solenoids in a cryomodule. A two-cell scheme is chosen throughout the entire linac providing both efficient acceleration and focusing. Developments of digital low-level RF control and solid-

STATUS AND COMMISSIONING PLAN OF PEFP 100-MEV LINEAR ACCELERATOR*

Hyeok-Jung Kwon#, Yong-Sub Cho, Ji-Ho Jang, Han-Sung Kim, Kyung-Tae Seol, Young-Gi Song, Dae-Il Kim, Bum-Sik Park, Sang-Pil Yun, Jin-Yeong Ryu, PEFP/KAERI, Daejeon, Korea

Abstract

One of the goals of the Proton Engineering Frontier Project (PEFP) is to develop a 100-MeV proton linear accelerator, which consists of 50-keV proton injector, 3-MeV radio frequency quadrupole (RFQ), 20-MeV / 100-MeV drift tube linac (DTL) and 20-MeV / 100-MeV beam lines. The 100-MeV linear accelerator and beam line components have been installed in the tunnel and experimental hall. After the completion of the utility commissioning, the commissioning of the accelerator starts with a goal of the beam delivery to the 100-MeV target room located at the end of the beam line. The proton beams will be supplied to users from March 2013. In this paper, the status and commissioning plan of the PEFP 100-MeV linear accelerator are presented.

INTRODUCTION

The PEFP was launched by the Korean Government at 2002 as a 21st century Frontier R&D program. It has three main objectives; to develop a high power proton linac, to develop proton beam utilization and accelerator application technology, to industrialize developed technologies.

The specifications and schematics of the 100-MeV, 20mA proton accelerator developed by PEFP are shown in Table 1 and Figure 1 respectively. The PEFP proton accelerator has its own characteristics; to supply high duty & high average current beam to users, to supply proton beam with wide range in beam energy and current, to supply proton beam into 3 beam lines simultaneously, and to supply beam with large area up to 300mm in diameter. The main application fields of the accelerator are such that; industrial field with ion cut, semiconductor switch application, radio isotope production, medical field with proton therapy research, biological field with mutation of plants & micro-organism, space technology field with research on radiation effect on materials, and basic science field with neutron application.

The project host city is Gyeongju who supplies land and supporting buildings such as main office building, regional cooperation centre and dormitory and so on. The main buildings for accelerator and experimental hall, utility and substation are provided by the central government. The construction of the main buildings will be completed in October, 2012.

The development of 100-MeV DTL was completed in

2010. The main accelerator components such as RFQ and DTL were designed by PEFP, fabricated by the 17 Korean domestic industries, assembled and tested by PEFP. As a front end, a 20-MeV linac was developed, installed and operated since 2007 at KAERI Daejeon site waiting for the PEFP site preparation at Gyeongju. [1][2] The operation of 20-MeV linac at Daejeon was finished at November 2011. Since then, the machine was disassembled and delivered to Gyeongju site at February 2012 when the accelerator tunnel was prepared. The 100-MeV accelerator and two beam lines were installed inside the accelerator tunnel and the experimental hall, respectively. The commissioning of the accelerator will start at the end of 2012 after the klystron gallery, modulator room and utility are prepared.

Table 1: Specifications of the PEFP Proton Accelerator

Parameter	DTL-I	DTL-II
Output Energy (MeV)	20	100
Max. Peak Beam Current (mA)	20	20
Max. Beam Duty (%)	24	8
Average Beam Current (mA)	4.8	1.6
Max. Pulse Length (ms)	2	1.33
Max. Repetition Rate (Hz)	120	60
Max. Avg. Beam Power (kW)	96	160

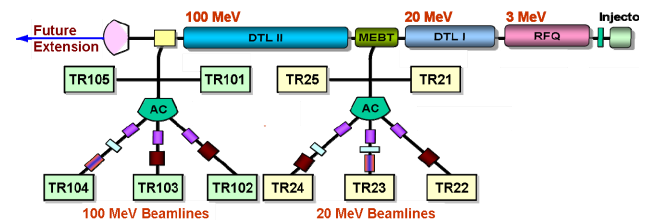


Figure 1: Schematic of the PEFP proton accelerator and beam lines

ACCELERATOR DEVELOPMENT

20-MeV Linac Operation

The 20-MeV linac was installed at Daejeon site temporarily in 2005 waiting for site preparation at Gyeongju. The 20-MeV linac got an operation license in 2007, since then the machine was used to study the machine itself and to test 100-MeV accelerator components in addition to supply proton beams to users. The key technologies developed during 20-MeV linac operation are as follows.

*Work supported by the MEST in Korean Government

#hjkwon@kaeri.re.kr

OVERVIEW OF SACLA MACHINE STATUS

Y. Otake[#], on behalf of the members of XFEL division, XFEL Research and Development Division, RIKEN SPring-8 Center, Harima Institute, RIKEN, 1-1-1, Kouto, Sayo-cho, Sayo-gun, Hyogo JAPAN 679-5148
XFEL Division, JASRI, 1-1-1, Kouto, Sayo-cho, Sayo-gun, Hyogo JAPAN 679-5198

Abstract

SACLA, part of an X-ray free-electron laser, has been constructed, and was successfully lased at 0.06 nm in 2011. SACLA mainly comprises a low-emittance thermionic electron gun, an 8-GeV linear accelerator using C-band (5712 MHz) cavities and 18 in-vacuum undulators. A concept used to develop this machine involves compactness compared with the other machine, such as LCLS with a length of more than 1 km. Stable X-ray lasing of up to 0.06 nm to also be a concept demands extremely stable accelerator components, such as a 50 fs temporal stability of an rf phase at a cavity in an injector. We have now realized a 700 m compact machine by using low-emittance at an electron gun, an accelerating gradient of more than 35 MV/m by a C-band accelerator, and short-period undulators. Continuous lasing for more than several days is strongly supported by these stable components and small operator's trimming, and has also been established by reducing perturbation sources to laser instability. SACLA is regularly operated for user experiments, such as material imaging with an extreme amount of data.

INTRODUCTION

SACLA has been constructed in order to generate an X-ray laser of up to a wavelength of around 0.06 nm, and is now under operation for user experiments [1]. We can explore new science, such as revealing protein membrane structures, by this machine.

SACLA was designed in accordance with the following two concepts, called SCSS concepts [2]. One is a short machine length, like compactness, which is associated with low construction costs. Next, is an ultra stable machine, which guarantees stable laser intensity, contributing to reliable experiments. In order to realize this concept, we employ a method using a high-brightness, low-emittance thermionic electron gun operated at a 500 kV high-voltage pulse [3], a C-band accelerator with a high-gradient acceleration of more than 35 MeV/m [4] and an in-vacuum undulator with a short period and a narrow gap [5]. Their high-brightness electron beam and narrow gap as well as short period, λ_u , associated with a large undulator parameter, K , and a short radiation wavelength, λ , allow us to reduce the gain length of self-amplified spontaneous emission (SASE) along the undulator beam line. High-gradient acceleration is also effective to make a short accelerator. Hence, the machine length becomes shorter than other X-ray free electron laser (XFEL) machines of over 1 km, such as the

linac coherent light source (LCLS) at SLAC [6] and Euro-XFEL at DESY [7]. This SCSS concept is the most prominent characteristic of our SACLA.

Ultimate stability of an X-ray laser, which is guided by ultra-stable accelerator components, is also a crucial part of SACLA. As examples to realize stable X-ray lasing conditions, it is necessary that the electron beams and related undulator radiation should spatially overlap within 4 μm in STD along the undulator line [8], if we allow for reduction of the SASE intensity up to half of the peak intensity (design value). The demanded rf phase (temporal) stability at cavities in an injector is around 100 fs in STD, if we also accept a peak electron-intensity fluctuation of 10% in STD, corresponding to a peak X-ray laser intensity fluctuation of 10% in STD [9], which is almost the intrinsic intensity jitter of statistical SASE generation. The amplitude of the Pierce gain parameter, ρ , for FEL amplification along an undulator section directly reflects the overlap factor, OF , between the electron beam and its radiation [10], and also the charge density of the electron beam [2]. For example, these component stabilities mean a stable low-emittance value and electron beam energy stability established by the emission stability of the electron beams form the thermionic electron gun, the rf phase and amplitude stabilities of acceleration cavities, the magnetic field stabilities of beam-transport magnets, undulator magnetic field stability, and components alignment in order to secure the interaction between the electron beams and the beam radiated field along the undulator line.

We must realize these required values to secure stable X-ray laser radiation, as well as the concept. This paper introduces accelerator components and their performances, X-ray lasing performance, and the present issues to deteriorate the lasing performance of SACLA.

SACLA'S MACHINE LAYOUT, ITS FUNCTION AND COMPONENTS

Layout and Function

Figure 1 shows the machine configuration of SACLA, which mainly comprises a 500 kV thermionic electron gun, a 238, 476, 1428 MHz multi-sub harmonic bunching and accelerating system as an injector, 8 S-band detuned-accelerating structures, 128 C-band choke-mode accelerating structures, 18 in-vacuum undulators and an X-ray beam line. The individual components of SACLA work as follows. At first, the electron gun emits electron beams with a low emittance of 0.6 $\pi\text{mm-mrad}$ in rms, a pulse width of 3 μs in FWHM and a 1A peak current.

[#]otake@spring8.o.jp

LCLS OPERATIONAL EXPERIENCE AND LCLS-II DESIGN*

Tor O. Raubenheimer[#], for the LCLS/LCLS-II Team, SLAC, Menlo Park, U.S.A.

Abstract

Five months after first lasing in April 2009, the Linac Coherent Light Source (LCLS) began its first round of x-ray experiments. The facility has rapidly attained and surpassed its design goals in terms of spectral tuning range, peak power, energy per pulse and pulse duration. There is an ongoing effort to further expand capabilities while supporting a heavily subscribed user program. The facility continues to work toward new capabilities such as fs-scale pulses, self-seeding, synchronized THz for pump-probe, and multiple-bunch operation. Future upgrades will include polarization control as well as hard and soft x-ray self-seeded operation. The facility is already starting to construct a major expansion, with two new undulator sources and space for four new experiment stations referred to as the LCLS-II.

LCLS FACILITY

The Linac Coherent Light Source Facility (LCLS) at SLAC National Accelerator Laboratory is based on the last third of the SLAC linac where a high brightness beam is generated in an off-axis injector and then accelerated to ~14 GeV [1,2]. The concept for the facility was laid out in 1992 at the Workshop on 4th Generation Light Sources at SLAC [3]. Now, the LCLS is well on its way to realizing all the scientific capabilities envisioned in *LCLS – the First Experiments* [4], which described six broad areas of opportunity for research with an x-ray laser.

The facility achieved its design goals during the first weeks of operation [5] and is developing new capabilities on an almost weekly basis. Essentially all the experiment techniques envisioned for LCLS are being tested and proven in operation and the full suite of three experimental stations in each of two experiment halls have been commissioned as indicated in Table 1.

Table 1: LCLS Experimental Stations

Experimental Station	Start of User Operations
Atomic, Molecular & Optical Science (AMO)	October, 2009
Soft X-ray Materials Science (SXR)	June, 2010
X-ray Pump-Probe (XPP)	October, 2010
Coherent X-ray Imaging (CXI)	February, 2011
X-ray Correlation Spectroscopy (XCS)	November, 2011
Matter in Extreme Conditions (MEC)	April, 2012

* Work supported in part by the DOE Contract DE-AC02-76SF00515.
tor@slac.stanford.edu

The principal performance goals of LCLS-I were to produce:

- X-ray pulses of 230 femtoseconds duration or shorter
- Photon energies ranging from 800 eV to 8,000 eV
- 10^{12} photons per pulse at 8 keV

As noted, these goals were achieved or exceeded promptly at the outset of commissioning, in April- May 2009; a list of the present operating parameters can be found in Table 2. A rapid and productive research program commenced with a 1,300 hour operation run, October-December 2009, during which 152 experimenters participated in 11 experiments. Productivity has continued to increase; in FY2010, 359 experimenters participated in LCLS experiments. Demand for access to LCLS continues to grow as illustrated in Fig. 1 where the proposals for each the experimental stations is plotted versus run number; each run is roughly 5 months in duration. However, as shown in Fig. 1, the LCLS productivity is already limited by capacity; only one in four proposals receive beam time.

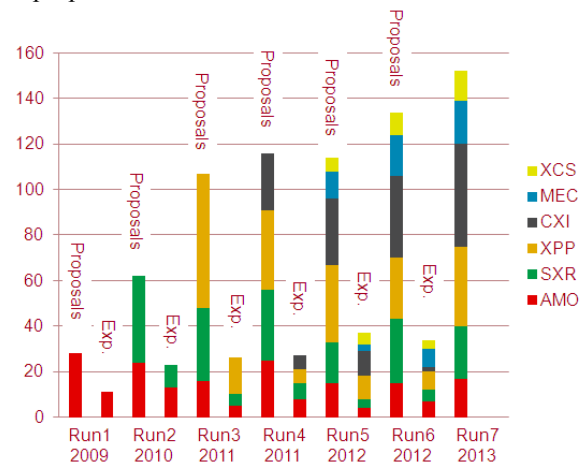


Figure 1: LCLS proposals and experiments receiving beam time by experimental station and run number.

OPERATIONAL EXPERIENCE EXTENDED LCLS CAPABILITIES

Rapid progress in accelerator research and accelerator commissioning has made it possible to expand LCLS capabilities well beyond the LCLS the goals listed in the previous section. The energy produced in a single x-ray pulse has reached 6 mJ. The operating range of photon energies, originally specified at 800-8,000 eV, has been expanded to 480-10,000 eV, limited by the electron beam energy and the fixed period and magnetic field in the undulator. The pulse duration can be varied between a few femtosecond (fs) and 500 fs with soft x-rays and a few fs to ~100 fs for hard x-rays.

THE HIGH-CURRENT ERL AT BNL*

I. Ben-Zvi[#], BNL, Upton NY, USA

Abstract

The electron hadron collider eRHIC will collide polarized or non-polarized electrons with a current of 50 mA and energy in the range of 5 GeV to 30 GeV with hadron beams, including heavy ions or polarized light ions of the RHIC storage ring. The electron beam will be generated in an Energy Recovery Linac (ERL) contained inside the RHIC tunnel, comprising six passes through two linac sections of about 2.5 GeV each. The electron ERL poses many challenges in term of a high-current high-polarization electron gun, HOM damping in the linac, crab cavities, harmonic cavities and beam stability. Three R&D projects are underway to provide experience with the eRHIC ERL components. A prototype high-current ERL is under commissioning to test performance at up to 300 mA of the ERL. A prototype polarized-electron gun based on funneling of 20 separate cathodes, providing 3.5 nC per bunch, is under construction and a Coherent electron Cooling (CeC) proof-of-principle experiment is under construction.

INTRODUCTION

RHIC, the Relativistic Heavy Ion Collider at Brookhaven Lab, found it first: a “perfect” liquid of strongly interacting quarks and gluons — a quark-gluon plasma (QGP) — produced by slamming heavy ions together at close to the speed of light. The fact that the QGP produced in these particle smashups was a liquid and not the expected gas, and that it flowed like a nearly frictionless fluid, took the physics world by surprise. Similarly, searches for the source of “missing” proton spin at RHIC have opened a deeper mystery: So far, it’s nowhere to be found. To probe these and other puzzles, nuclear physicists would like to build a new machine: an electron-ion collider (EIC) designed to probe structures with extreme precision, at the scale of 10^{-15} meters, both protons and heavy ions to reveal their inner secrets.

The use of an Energy Recovery Linac (ERL) for the electron accelerator of eRHIC was suggested [1] as means to achieve high-luminosity, outstanding polarization and convenient upgradability features. Given a hadron machine design, a linac-ring configuration allows a 10- to 50-fold higher luminosity than an optimized ring-ring design. ERLs combine the advantages of linear accelerators, like beam quality, immunity to resonances, high degree of polarization and beam disruption with those of storage rings, such as high beam power and stability.

* Work supported by Brookhaven Science Associates, LLC under Contract No. DE-AC02-98CH10886 with the U.S. DOE

[#]benzvi@bnl.gov

A polarized electron beam with an energy up to 30 GeV would collide with a number of ion species accelerated in the existing RHIC accelerator complex, from polarized protons with a top energy of 250 GeV to fully-stripped uranium ions with energies up to 100 GeV/u covering a C.M. energy range from 45 to 175 GeV for polarized e-p, and from 32 to 110 GeV for electron heavy-ion-collisions. Using the present significant margin of the RHIC superconducting magnets the maximum beam energy could be increased by 10 or more percent.

The eRHIC design is based on using one of the two RHIC hadron rings and a multi-pass ERL. Using an ERL as the electron accelerator assures high luminosity in the range of $10^{33}\sim 10^{34}\text{cm}^2\text{s}^{-1}$. Locating the ERL inside the RHIC tunnel allows for significant cost savings and natural staging: the energy can be increased from the initial 5 - 10 GeV of the first stage to the final 30 GeV by incrementally adding additional accelerating cavities to the two main linacs. eRHIC will be able to provide electron-hadron collisions in up to three interaction regions. [2]

Polarized electrons will be generated in a high-current 20 photocathode funneling electron gun. The ion beams of the RHIC component will be cooled by a novel Coherent electron Cooling (CeC) system. The machine will heavily rely on SRF technology for production and acceleration of electrons, cooling of hadron beams and realizing crab crossing collision scheme.

In this paper we will describe the layout of the multi-pass eRHIC electron ERL, and describe R&D projects carried out in the Accelerator R&D Division of the BNL Collider-Accelerator Department (C-AD) towards the realization of eRHIC, including the polarized electron source, the SRF cavities (5-cell accelerating cavities, crab cavities), the R&D high-current ERL and the CeC Proof-of-Principle (PoP) experiment.

LAYOUT OF THE ACCELERATOR

eRHIC General Layout

Figure 1 presents a layout of the collider with locations of various systems in the existing RHIC tunnel. The injection system consists of an electron gun, 10 MeV SRF injector linac (with no energy recovery) and 600-MeV single-pass SRF ERL. Two 2.45 GeV SRF linacs in combination with six passes make the main ERL. In addition to the main SRF linacs, eRHIC will have energy loss and energy spread compensation linacs (not shown in the figure). The CeC accelerator will consist of a low frequency SRF gun and buncher and a 136 MeV ERL. Finally, there will be SRF crab cavities for both hadrons and electrons (not shown in figure). The lattice provides separation of the electron orbits to individual arcs in the

THE SWISS FEL RF GUN: RF DESIGN AND THERMAL ANALYSIS

J.-Y. Raguin, M. Bopp, A. Citterio, A. Scherer
PSI, CH-5232 Villigen, Switzerland

Abstract

We report here on the design of a dual-feed S-band 2.5-cell RF gun, developed in the framework of SwissFEL, capable of operating at 100 Hz repetition rate. As in the LCLS RF gun, z-coupling, to reduce the pulsed surface heating, and a racetrack coupling cell shape, to minimize the quadrupolar component of the fields, have been adopted. The cell lengths and the iris thicknesses are as in the PHIN gun operating at CERN. However the iris aperture has been enlarged to obtain a frequency separation between the operating π mode and the $\pi/2$ mode higher than 15 MHz. An amplitude modulation scheme of the RF power, which allows one to obtain a flat plateau of 150 ns for multibunch operation and a reduced average power is presented as well. With an RF pulse duration of 1 μ s it is shown that operation at 100 MV/m and 100 Hz repetition rate is feasible with very reasonable thermal stresses.

INTRODUCTION

Paul Scherrer Institut is completing the study of the accelerating systems of SwissFEL, a Free Electron Laser which targets a maximum electron beam energy of 5.8 GeV. SwissFEL is designed for two standard electron beam operation modes, one with a 200 pC charge per bunch and a core slice emittance of 0.43 mm-mrad and the second with a 10 pC charge per bunch and a core slice emittance of 0.18 mm-mrad. SwissFEL, the main linac frequency being the C-band American frequency 5712 MHz, operates with a repetition rate of 100 Hz and two electron bunches, with a spacing of 28 ns, are accelerated at each RF pulse.

The proposed 2.5-cell RF gun operates with a nominal body temperature of 40 °C in the π mode at the S-band frequency of 2998.8 MHz, such a frequency having a common sub-harmonic with the SwissFEL C-band main linac frequency. The beam energy at the exit of the RF gun is about 7 MeV. The two full cell lengths and the iris thicknesses of the RF gun are identical to the ones of the CTF3 PHIN RF gun [1]. The upstream cell, shorter than the two full cells, has a longitudinally adjustable backplane. The middle cell is coupled to two rectangular waveguides symmetrically arranged to cancel the dipolar component of the field. The racetrack interior shape of this coupling cell is optimized to minimize the quadrupolar field component, as in the LCLS RF gun [2]. Long lifetime and reliable operation with the targeted peak on-axis electric field of 100 MV/m requires the optimization of the two RF coupling port dimensions to reduce the dynamic thermal stress due to pulsed heating. With the high 100 Hz repetition rate, mechanical stresses caused by thermal loading have to be thoroughly addressed.

ISBN 978-3-95450-122-9

SWISSFEL RF GUN DESIGN

Design with 2D RF Simulations

Ignoring at this stage the middle cell coupling ports, RF simulations performed with the 2D electromagnetic code SUPERFISH [3] are used to determine the radius and the elliptical shape of the irises between the cells compatible with reduced surface electric fields and large frequency separation between the operating π mode ($TM_{010-\pi}$ mode) and the $\pi/2$ next lower mode ($TM_{010-\pi/2}$ mode). The radius of the upstream cell and of the two full cells are adjusted to reach a balanced on-axis field at the operating frequency. The 2D RF design was then guided by the requirements that the mode separation between the operating π mode and the $\pi/2$ mode be higher than 15 MHz and that the peak surface electric field is not higher than the electric field on the cathode. The large mode separation between the operating mode and the next lower mode reduces the impact of the lower mode on the electron bunch energy spread and projected emittance. It is also expected to make the field balance less sensitive to thermal expansion under operational conditions and to manufacturing dimension deviations that may occur during production [4].

Fig. 1 shows the electric field contour lines of the π mode. The cell radii are optimized to obtain field flatness at the operating frequency. The dimensions of some geometrical parameters, used also for the final 3D design, are specified in Table 1. The elliptical profile of the irises is characterized by an aspect ratio of 1.7:1 so that the maximum surface electric field is lower than the peak field on the cathode.

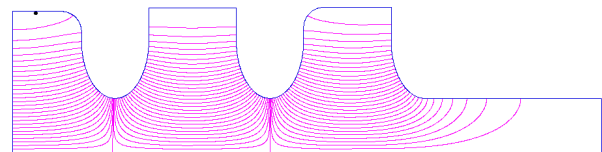


Figure 1: Electric field contour lines of the operating π mode

Table 1: Geometrical parameters of the SwissFEL RF gun

Parameter	Value		
Cell length	20.5 mm	26 mm	26 mm
Iris thickness	20 mm		
Iris radius	16 mm		
Drift radius	16 mm		

Final Design with 3D RF Simulations

The dimensions obtained with the 2D code SUPERFISH are used as input to complete the RF design of the gun with the 3D electromagnetic code HFSS [5], in particular the

DEFLECTING STRUCTURES WITH MINIMIZED LEVEL OF ABERRATIONS*

V. Paramonov †, INR of the RAS, Moscow, 117312, Russia

Abstract

Deflecting structures are now widely used for bunch phase space manipulations either in special bunch diagnostic or in emittance exchange experiments. As a tool for manipulation, the structure itself should provide the minimal phase space perturbations due to non linear additives in the field distribution. Criterion of the field quality estimation is developed and deflecting structures are considered for minimization of non linear additives.

INTRODUCTION

The Deflecting Structures (DS) - periodical structures with transverse components of the electromagnetic field - initially were introduced for charged particle deflection and separation. The bunch cross DS synchronously with the deflecting field E_d , corresponding the phase $\phi = 0$ in the structure and particles get the increment in the transverse momentum p_t . There are a lot of papers, see for example [1], describing DS design and application for such purpose. At present for short and bright electron bunches DS found another applications, either for bunch special diagnostic, [2], or emittance exchange experiments. Both directions are related to the transformation of particle distributions in the six dimensional phase space and DS operates in another mode - the bunch center cross DS at zero E_d value, $\phi = 90^\circ$. There are also a lot of papers, describing it in more details. Application for Particles Distributions Transformation (PDT) provide additional requirements - a tool for transformation should provide the minimal, as possible, own distortions to the original distributions.

FIELD DISTRIBUTION QUALITY

For deflecting field E_d description the widely used basis of $TM - TE$ waves can not be used due to degeneration into TEM at $\beta = 1$. A basis of hybrid waves $HE - HM$ was introduced, [3], [4] to avoid this methodical problem. The common representation for the field distribution in the DS aperture is

$$\vec{E} = C\vec{E}_{HE} + D\vec{E}_{HM}, \quad \vec{H} = C\vec{H}_{HE} + D\vec{H}_{HM}, \quad (1)$$

with the weighting coefficient C, D depending both on supporting structure and on operating mode. It is the method of description and results treatment. The physical object - the deflecting force - is the transverse component of the Lorenz force

$$\vec{F}^L = e(\vec{E} + [\vec{v}, \vec{B}]), \quad F_x = eE_d = e(E_x - \beta Z_0 H_y), \quad (2)$$

where $Z_0 = \sqrt{\frac{\mu_0}{\epsilon_0}}$, expressed in (2) through the transverse E_x and H_y components in Cartesian coordinates. In any periodical structure for Traveling Wave (TW) operating mode each field component $E_j(r, z)$ in the beam aperture can be represented in the complex form as the set over spatial harmonics:

$$\begin{aligned} E_j(r, z) &= E_j(\widehat{r}, z)e^{i\psi_j(z)} = \\ &= \sum_{n \rightarrow -\infty}^{n \rightarrow +\infty} a_{jn}(r)e^{\frac{-i(\Theta_0 + 2n\pi)z}{d}}, \end{aligned} \quad (3)$$

where $E_j(\widehat{r}, z)$ and $\psi_j(z)$ are the amplitude and the phase distributions, d is the structure period and $a_{jn}(r)$ is the transverse distribution for the n -th spatial harmonics. The period length is defined from synchronism with the main a_{j0} harmonic, $d = \frac{\Theta_0 \beta \lambda}{2\pi}$.

The bunch emittance deterioration during PDT take place due to non linear additions both in transverse and longitudinal distributions of the field. There is inevitable nonlinearity at $\beta < 1$ even in main harmonic distribution, vanishing for $\beta \rightarrow 1$, [3], [5]. But the main source of additions are higher spatial harmonics. For each harmonic the transverse and longitudinal distributions are rigidly coupled and are proportional to harmonic amplitude. To estimate field quality, we have to estimate the level of spatial harmonics, [5]. Spatial harmonics are essential at the aperture radius $r = a$ and higher harmonics attenuate to the axis as

$$a_{jn}(0) \sim a_{jn}(a) \cdot \exp\left(-\frac{4\pi^2 n}{\beta \Theta_0} \cdot \frac{a}{\lambda}\right), \quad |n| \gg 1, \quad (4)$$

where λ is the operating wave length. At the axis $r = 0$ just lower harmonics $n = \pm 1, \pm 2, \pm 3$ are really presented. For harmonics estimations in details and 'in total', let us introduce parameters $\delta\psi_j(z)$ and Ψ_j at the axis $0 \leq z \leq d, r = 0$

$$\delta\psi_j(z) = \psi_j(z) + \frac{\Theta_0 z}{d}, \quad \Psi_j = \max(|\delta\psi_j(z)|), \quad (5)$$

with the physical sense as the deviation and the maximal phase deviation of the real wave component from the synchronous harmonic. The qualitative estimation and correct value for $a_{jn}(0)$ one can get as

$$\begin{aligned} |a_{jn}(0)| &< \frac{(E_j(\widehat{0}, z)_{max} + E_j(\widehat{0}, z)_{min})\Psi_j}{2n}, \quad (6) \\ a_{jn}(0) &= \frac{\int_0^d E_j(\widehat{0}, z) \sin(\delta\psi_j(z)) \sin(\frac{2\pi n z}{d}) dz}{d}. \end{aligned}$$

From linearity, we can apply $\delta\psi_j(z)$ and Ψ_j for quality

ISBN 978-3-95450-122-9

* Work supported in part by RBFR N12-02-00654-a

† paramono@inr.ru

RESULTS OF TESTING OF MULTI-BEAM KLYSTRONS FOR THE EUROPEAN XFEL

V. Vogel, L. Butkowski, A. Cherepenko, S. Choroba, I Harders and J. Hartung,
DESY, 22607 Hamburg, Germany

Abstract

For the European XFEL multi-beam klystrons, which can produce RF power of 10 MW at an RF frequency of 1.3 GHz, at 1.5ms pulse length and 10 Hz repetition rate, were chosen as RF power sources. Twenty-seven of horizontal multi-beam klystrons (MBK) together with connection modules (CM) will be installed in the XFEL underground tunnel. The CM will be installed on the MBK and connects the MBK to the pulse transformer with only one HV cable, because the CM has a filament transformer inside as well as all diagnostics for HV and cathode current measurements. MBK prototypes together with CM prototypes have been tested for long time at a test stand at DESY, about 4600 hours of operation for each of horizontal MBK with full RF output power, full pulse length and repetition rate of 10 Hz. Testing of first MBKs from series production has been started. In this paper we will give an overview of the test procedure, summarize the current test results and we will give a comparison of the most important parameters.

INTRODUCTION

For the XFEL project [1] as a source of RF power for 27 RF station were chosen the horizontal MBK made by two companies: MBK TH1802 from “Thales” [3] and MBK E3736H from “Toshiba” [4]. The main parameters of MBK are given in Table 1.

Table 1: Main parameters of L-band MBK for XFEL

Parameters	Design value	Test value
Output power (MW)	10	10.3
RF pulse length (ms)	1.5	1.5
Efficiency (%)	> 63	64
Repetition rate (Hz)	up to 30	10
Max average RF power (kW)	150	155
Max average power in collector (kW)	300	270
Max drive power (W)	<200	<150
Bandwidth (MHz)	3	>3

Both prototypes of MBK were tested on DESY MBK test stands [2], a total time of testing exceed of 4600 hours for both of tubes. The test was done with full RF power of 10 MW, full RF pulse length of 1.5 ms and with repetition rate of 10 Hz. Fig. 1 shows the top view of the test stands. Because the all of RF station will be located in the

underground tunnel it is very important do not have the open oil during installation of MBK. It was proposed and tested the connection between MBK and HV pulse transformer through connection module (CM) [5, 6 and 7] and HV cable. Several types of HV cables and connectors as well as CM prototypes were tested. Big advances of using CM are that CM has inside a high voltage high frequency filament transformer and monitors for measurement of klystron voltage and cathode current. Fig. 2 shows the one of klystrons with CM and HV cable.



Figure 1: MBK test stands in DESY Hamburg



Figure 2: MBK with CM and HV cable “PFISTERER 3S”

RESULTS OF MBK PROTOTYPES TEST

Since February 2008 we started the test of the first of horizontal MBK prototype on DESY site. For the test of MBK it was specially developed two radiation protected

COMPUTATIONAL MODEL ANALYSIS FOR EXPERIMENTAL OBSERVATION OF OPTICAL CURRENT NOISE SUPPRESSION BELOW THE SHOT-NOISE LIMIT

A. Nause, E. Gover, Tel Aviv University, Israel

Abstract

In this paper we present simulation analysis of experimental results which demonstrate noise suppression in the optical regime, for a relativistic e-beam, below the classical shot-noise limit. Shot-noise is a noise resulting from the granular nature of the space-charge in an e-beam. It is linear to the beam current due to its Poissonic distribution in the emission process. Plasma oscillations driven by collective Coulomb interaction during beam drift between the electrons of a cold intense beam are the source of the effect of current noise suppression. The effect was experimentally demonstrated [1] by measuring Optical Transition Radiation (OTR) power per unit e-beam pulse charge. The interpretation of these results is that the beam charge homogenizes due to the collective interaction (sub-Poissonian distribution) and therefore the spontaneous radiation emission from such a beam would also be suppressed (Dicke's sub-radiance [2]). Analysis of the experimental results using GPT simulations will demonstrate the suppression effect. For the simulation results we used a full 3D GPT model of the ATF section in which the experiment took place at.

INTRODUCTION

Shot-noise is a noise resulting from the granular nature of the space-charge in an e-beam. The discreteness of the particles and the randomness of electrons emission from the cathode causes time dependent fluctuations of the charge and current density at any cross section along the beam transport line. This noise was first reported in 1918 by Schottky who made experiments in vacuum tubes.

Noise is best characterized in terms of the Fourier transform of the time-varying fluctuations in electric current, namely, by its spectral density. Gover and Dyunin showed in a 1D model [3] that it is possible to observe and control optical frequency energy and current (shot noise) fluctuations in a dense relativistic charged particles beam. GPT simulations were used to demonstrate this effect for a real-like beam starting from Shot-noise [4]. Moreover, at certain conditions, when the dominant noise in the beam is current shot noise (density fluctuations), it is possible to reduce significantly the beam noise by virtue of a collective interaction process along an interaction length corresponding to a quarter period longitudinal plasma oscillation in the beam. This means that the charge distribution in the beam can be homogenized in this process.

First experimental observation of this phenomenon using OTR from a metallic foil was presented last year [1]. Noise suppression using a dispersive section (dog-leg bend) was demonstrated in SLAC [5]. TR is proportional to the

current-noise amplitude [6], and therefore can be used in order to estimate the suppression in the current noise. In this paper we press analysis of the experimental results and demonstrate this effect using full 3D GPT simulations that were carried out for this purpose.

1D Model of Noise Dynamics in Charged Electron Beams

In electron-beam transport under appreciable space-charge conditions, the microdynamic noise evolution process may be viewed as the stochastic oscillations of Langmuir plasma waves [3]. In the linear regime, the evolution of longitudinal current and velocity modulations of a beam of average current I_b , velocity βc and energy $E = (\gamma - 1)mc^2$, can be described in the laboratory frame by [7]:

$$\frac{d}{d\phi_p} \check{i}(z, \omega) = -\frac{i}{W(z)\check{v}(z, \omega)} \quad (1)$$

$$\frac{d}{d\phi_p} \check{v}(z, \omega) = -iW(z)\check{i}(z, \omega) \quad (2)$$

where $\check{i}(\omega) = \check{I}(\omega)e^{i\omega z/\beta c}$, $\check{v}(\omega) = \check{V}(\omega)e^{i\omega z/\beta c}$. $\check{I}(\omega)$, $\check{V}(\omega)$ are the respective Fourier components of the beam current and kinetic-voltage modulations. The kinetic-voltage modulation is related to energy and longitudinal velocity modulations: $\check{V}(\omega) = -(mc^2/e)\check{\gamma} = -(mc^2/e)\gamma^3\beta\check{\beta}$, $\phi_p(z) = \int_0^z \theta_{pr}(z')dz'$ is the accumulated plasma phase, $W(z) = r_p^2/(\omega A_e \theta_{pr} \epsilon_0)$ is the beam wave-impedance. A_e is the effective beam cross-section area, $\theta_{pr} = r_p \omega_{pl}/\beta c$ is the plasma wavenumber of the Langmuir mode, $r_p < 1$ is the plasma reduction factor, $\omega_{pl} = \omega_{p0}/\gamma^{3/2}$ is the longitudinal plasma frequency in the laboratory frame. The single-frequency Langmuir plasma wave model expressions [3] can be solved straightforwardly in the case of uniform drift transport. After employing an averaging process, this results in a simple expression for the spectral parameters of stochastic current and velocity fluctuations (noise) in the beam assuming that they are initially uncorrelated[]:

$$\check{i}(L, \omega) = \cos \phi_p(L)\check{i}(0, \omega) + (\sin \phi_p(L)/W_d)\check{v}(0, \omega) \quad (3)$$

where $\phi_p = \theta_{pr}z$, $\theta_{pr} = r_p \frac{\omega'_p}{v_0}$, $\omega'_p = (\frac{e^2 n_0}{m \epsilon_0 \gamma^3})$, $W_d = \sqrt{\mu_0/\epsilon_0}/k\theta_{pr}A_e$.

The beam current noise evolution is affected by the initial axial velocity noise through the parameter

$$N^2 = |\check{v}(0, \omega)|^2/W^2|\check{i}(0, \omega)|^2 = (\omega/c\beta k_D)^2 \quad (4)$$

STATUS OF THE RARE ISOTOPE SCIENCE PROJECT IN KOREA*

J. W. Kim for the RISP, Institute for Basic Science, Daejeon, Korea

Abstract

A heavy-ion accelerator facility has been designed in Korea for the production of rare isotope beams under the rare isotope science project (RISP). The project is funded and officially started in the end of 2011. The accelerator complex is composed of three main accelerators: a superconducting linac to use the in-flight fragmentation (IF) method to generate isotope beams, a 70 MeV proton cyclotron for the ISOL method, and a superconducting post accelerator for re-acceleration of rare isotope beams produced by ISOL to the energy range of 18 MeV/u. Minimum energy of a U beam requested for the IF driver is 200 MeV/u at the beam power of 400 kW. This facility will be unique in the aspect that the IF and ISOL systems can be combined to produce extreme exotic beams. In addition, standalone operation of each accelerator will accommodate diverse users in the beam application fields as well as in nuclear physics.

INTRODUCTION

A heavy ion accelerator facility is being designed in Korea to produce rare isotope beams by using both in-flight fragmentation (IF) and ISOL methods. The project is named as rare isotope science project (RISP), and was started from the end of 2011 after a period of conceptual design [1]. A conceptual layout of the facility is shown in Fig. 1.

The main accelerator is a superconducting linac, which can accelerate a ^{238}U beam to 200 MeV/u and protons to 600 MeV. It is divided into two sections, SCL1 before charge stripping at the energy of 18.5 MeV/u and SCL2 after the stripping. These parameters of the primary beam are similar to those of the FRIB project in the US [2]. A major difference from the planned FRIB facility is the use of an independent ISOL driver. A 70-MeV H⁻ cyclotron will be employed to drive a 70-kW ISOL target system. The radioisotope beam extracted from the target will be further ionized in EBIS [3] or ECR ion sources to achieve a higher charge state before beam injection to the post accelerator (SLC3), which is also a superconducting linac to accelerate a beam up to the energy of around 18 MeV/u. Furthermore this isotope beam produced by ISOL can be accelerated using the SCL2 for the IF system to produce more exotic isotope beams.

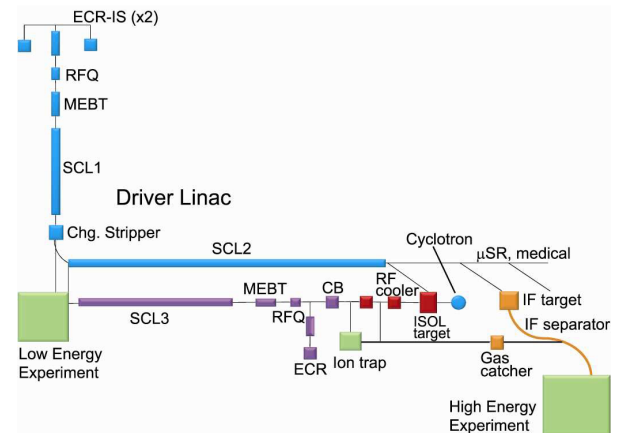


Figure 1: Conceptual layout of the heavy-ion accelerator complex of the RISP.

When the primary beam passes through a thin target, fast radioisotope beams are produced by the projectile fragmentation and fission mechanisms. Then the following isotope-beam selection system utilizes $B\rho$ -energy loss- $B\rho$ analysis to separate and identify an isotope beam of interest. This fast isotope beam can be stopped using a gas stopper, and the charge state of the beam extracted from the gas stopper can be boosted like in the ISOL method before being injected into the post accelerator. A main advantage of the IF method is that it is not subject to chemistry of the ions unlike in the ISOL. Hence rare isotope beams in a wider range can be produced.

The experimental areas are divided depending on the energy of the beam delivered as shown in Fig. 1. Different kinds of spectrometers are planned to be facilitated for nuclear reaction and structural studies [4]. In addition, the facility will accommodate beam users in various application fields including biomedical and material sciences using both stable and isotope beams. The stopping location of an isotope beam can be accurately traced by radiation measurement, which is a notable advantage of radioactive beam and is to be explored in some applications.

ACCELERATOR COMPLEX

To produce highly charged ion beams, a superconducting ECR ion source similar to the VENUS source of the LBL [5] is to be developed. To meet the goal of 400-kW beam power for U beam, envisioned scheme was to accelerate a beam in two charge states of 34+ and

*Work supported by the Rare Isotope Science Project of the MEST and National Research Foundation of Korea.
jwkim@ibs.re.kr

REDUCED-BETA CAVITIES FOR HIGH-INTENSITY COMPACT ACCELERATORS*

Z.A. Conway[#], S. Gerbick, M.J. Kedzie, M.P. Kelly, J. Morgan, R. Murphy, P.N. Ostroumov, and T. Reid, ANL, Argonne, IL 60439, USA

Abstract

This paper reports on the development and testing of a superconducting quarter-wave and a superconducting half-wave resonator. The quarter-wave resonator is designed for $\beta = 0.077$ ions, operates at 72 MHz and can provide more than 7.4 MV of accelerating voltage at the design beta, with peak surface fields of 165 mT and 117 MV/m. Operation was limited to this level not by RF surface defects but by our administrative limits on x-ray production. A similar goal is being pursued in the development of a half-wave resonator designed for $\beta = 0.29$ ions and operating at 325 MHz.

INTRODUCTION

The length and cost of the low-velocity portion ($\beta = v/c < 0.6$) of superconducting proton and heavy-ion linacs are dominated by the accelerator cavity performance. Accelerator cavities used in this velocity region, reduced-beta cavities, have not performed at the same peak-surface fields which are regularly achieved in elliptical-cell cavities optimized for velocity-of-light electrons [1], 160 mT and 80 MV/m peak surface fields. This performance disparity has been blamed on the greater complexity of the reduced-beta cavity fabrication and processing. Several advances at Argonne National Laboratory in cavity design [2]; fabrication and processing have disproved this hypothesis.

First, the results locating a defect which limited the performance of a prototype 72 MHz quarter-wave cavity (QWR) optimized for $\beta = 0.077$ ions for the ATLAS intensity upgrade will be presented. Second, the fabrication and processing of a subsequent geometrically identical quarter-wave cavity will be outlined. Finally, the impact of these results and future plans for a similarly constructed half-wave cavity will be discussed.

INITIAL PROTOTYPE PERFORMANCE

The QWR prototype fabrication and test results were presented in [3]. Since these papers were published we have refined our electromagnetic simulations of the cavity surface fields and the results used in this paper are given in table 1. This cavity was limited to peak surface fields of 96 mT and 70 MV/m by a surface defect which initiated a cavity quench. Figure 1, shows the cavity with the location of the defect highlighted in red along with a single channel record of the quench.

The defect was located by measuring the time-of-flight of second sound waves propagating from the cavity

quenching defect to an array of oscillating superleak transducers [4]. The distance the second sound wave travelled was calculated with the wave velocity. This combined with the known location of the detectors allowed us to determine the defect location. Our detector array was 1-dimensional in nature and located the height of the defect in the quarter-wave cavity center conductor.

This defect was located at the same height as an electron beam weld blow-out which occurred during final welding of the center conductor. The center conductor is formed from two halves which are welded together. The center conductor halves were tack welded, but the final electron beam welds could not be finished within the desired 24-hour etch window between pre-weld etching and welding. The parts were etched again after tacking and the very small-gap joint between the two parts could not be properly cleaned. Some foreign debris was trapped in this joint which caused a blow-out during the final electron beam welding which was repaired.

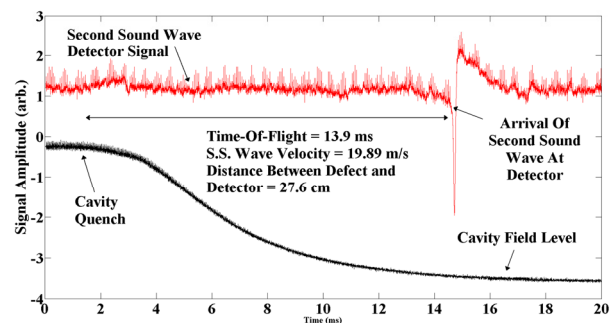
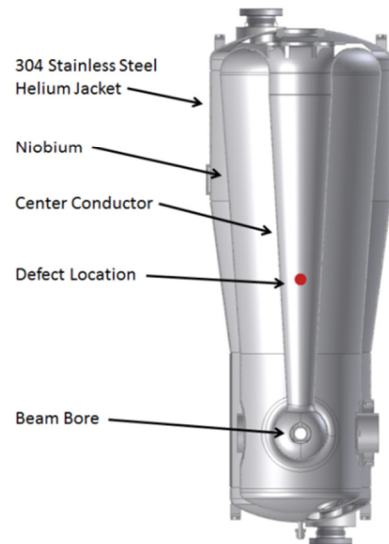


Figure 1: (Top) The cavity with a red dot placed at the height of the defect in the center conductor, the cavity is 53 inches from top to bottom. (Bottom) A single quench event with an oscillating superleak transducer signal and the cavity transmitted power.

* This work was supported by the U.S. Department of Energy, Office of Nuclear Physics, under Contract DE-AC02-06CH11357 and ANILWFO 8R268 supported by DTRA.

[#] zconway@anl.gov

R&D TOWARDS CW ION LINACS AT ANL*

P.N. Ostroumov[#], A. Barcikowski, Z. Conway, S. Gerbick, M. Kedzie, M.P. Kelly, S. Kutsaev, J. Morgan, R. Murphy, B. Mustapha, D. Paskvan, T. Reid, D. Schrage, S. Sharamentov, K. Shepard, G. Zinkann,
Argonne, IL 60439, U.S.A ANL, Argonne, IL 60439, U.S.A.

Abstract

The accelerator development group in ANL's Physics Division has engaged in substantial R&D related to CW proton and ion accelerators. Particularly, a 4-meter long 60.625-MHz CW RFQ has been developed, built and commissioned with beam. Development and fabrication of a cryomodule with seven 72.75-MHz quarter-wave resonators (QWR) is complete and it is being assembled. Off-line testing of several QWRs has demonstrated outstanding performance in terms of both accelerating voltage and surface resistance. Both the RFQ and cryomodule were developed and built to upgrade ATLAS to higher efficiency and beam intensities. Another cryomodule with eight 162.5-MHz SC HWRs and eight superconducting SC solenoids is being developed and built for Project X at FNAL. We are also developing both an RFQ and cryomodules (housing 176-MHz HWRs) for proton & deuteron acceleration at SNRC (Soreq, Israel). In this paper we discuss ANL-developed technologies for normal-conducting and SC accelerating structures for medium- and high-power CW accelerators, including the projects mentioned above and other developments for applications such as transmutation of spent reactor fuel.

INTRODUCTION

Technologies for CW RFQ and SC RF successfully developed for ATLAS upgrade for higher efficiency and beam intensities [1,2] can be applied in future high-power CW accelerators. Particularly, we are developing a CW RFQ and two cryomodules with different β_{OPT} for the SARAF accelerator facility at SNRC [3]. Similar SC RF technology is being used for the development and construction of the HWR cryomodule for Project X [4]. Below we discuss beam commissioning of the RFQ and results of QWRs testing and cryomodule assembly for the ATLAS upgrade project. Status of the SARAF and PXIE cryomodule development is presented.

CW RFQ

This summer we commissioned a CW RFQ designed and built for the ATLAS Facility [5]. Several innovative ideas were implemented in this CW RFQ. By selecting a multi-segment split-coaxial structure we have achieved moderate transverse dimensions for a 60.625 MHz resonator. For the design of the RFQ resonator and vane tip modulations we have developed a full 3D approach which includes MW-Studio and TRACK simulations of

the entire structure. A novel trapezoidal vane tip modulation is used in the acceleration section of the RFQ which resulted in increased shunt impedance. To form an axially symmetric beam exiting the RFQ, a very short output radial matcher, only $0.75\beta\lambda$ long, was developed.

An advanced fabrication technology was applied for the construction of the RFQ which includes precise machining and two-step high temperature brazing. Thanks to the high accuracy of the overall fabrication, the assembly of the 5-segment RFQ was straightforward and resulted in excellent alignment. The resonance frequency control system based on water temperature regulation showed excellent performance. The RF measurements show excellent RF properties for the resonator, with a measured intrinsic Q equal to 94% of the simulated value for OFE copper. The multi-segment split-coaxial structure creates strong coupling between the quadrants and individual RFQ segments which reduces the effect of local frequency deviations on electromagnetic field distortions. Therefore, no bead-pull measurements were required for tuning of the accelerating field. Figure 1 shows the complete RFQ assembly after installation of

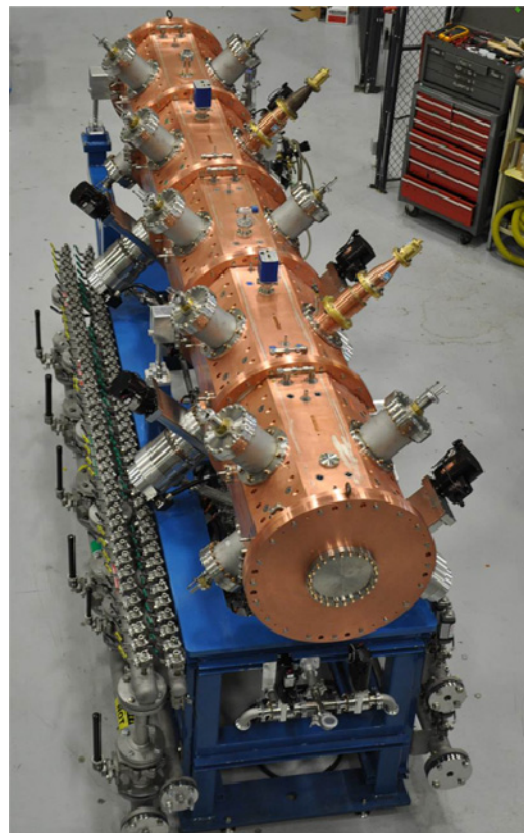


Figure 1: Completed RFQ assembly.

* This work was supported by the U.S. Department of Energy, Office of High Energy Physics and Nuclear Physics, under Contract DE-AC02-76CH03000, DE-AC02-06CH11357 and ANL WFO 85Y47
[#]ostroumov@anl.gov

DESIGN AND BEAM TEST OF SIX-ELECTRODE BPMS FOR SECOND-ORDER MOMENT MEASUREMENT

K. Yanagida*, S. Suzuki, and H. Hanaki, JASRI/SPring-8, Sayo Hyogo, Japan

Abstract

To enhance a beam observation system during top-up operation, we developed in the SPring-8 linear accelerator non-destructive beam position monitors (BPMS) that can detect second-order moments of electron beams. BPMS have six stripline-type electrodes with circular or quasi-elliptical cross-sections. We tested a BPM with a circular cross-section using electron beams, and our results showed that its normalized moments were determined accurately by electrostatic field calculation. We studied a precise calibration method to determine the relative attenuation factors between the electrode channels based on the principle that the relative moments must not vary with a change of the beam position using a steering magnet in drift space.

INTRODUCTION

The SPring-8 linear accelerator provides electron beams toward a storage ring about every twenty seconds because of the top-up operation of the storage ring. To enhance the beam observation system during the top-up operation, a non-destructive BPM system is being upgraded to a six-electrode BPM system that can detect the second-order moments of electron beams because the second-order moments are physical quantities related to beam sizes, which can be deduced by measuring second-order moments at more than six locations in FODO magnetic lattices [1].

Therefore, we developed the major components of a six-electrode BPM system: BPMS, a signal processor, and a digital input board. We installed our developed six-electrode BPMS with a circular cross-section in the beam transport line and tested them using electron beams. This paper describes the BPM designs as the parts of the six-electrode BPM system, the principle of multipole moment measurement, and the beam test results.

SIX-ELECTRODE BPMS

This section describes the designs of six-electrode BPMS and the principle of absolute moment measurement.

BPM designs

We developed two kinds of six-electrode BPMS for second-order moment measurement. One is a BPM with a circular cross-section for the non-dispersive section, and the other is a BPM with a quasi-elliptical cross-section for the dispersive section (Fig. 1). In the figure the numbers represent electrode number d . Both BPMS have stripline-type electrodes as signal pick-ups. The stripline length is

27 mm, which corresponds to $\lambda/4$ of the acceleration radio frequency. The characteristic impedance is designed as 50Ω . One electrode of both BPMS shares 30° with respect to the duct center. The aperture radius of a BPM with a circular cross-section is 16 mm, and the long and short radii of a BPM with a quasi-elliptical cross-section are 14 mm and 28 mm. These BPMS were or will be installed instead of the existing four-electrode BPMS with circular and quasi-elliptical cross-sections [2][3].

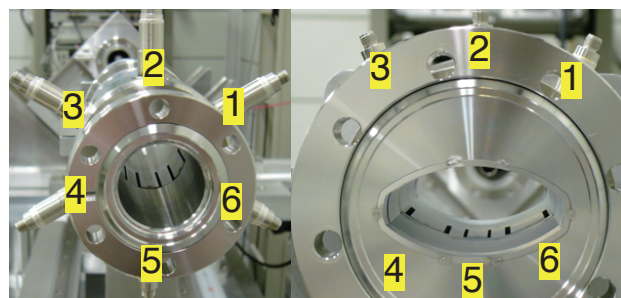


Figure 1: Six-electrode BPMS with circular and quasi-elliptical cross-sections. Numbers represent electrode number d .

Absolute Moment Measurement

A BPM with symmetrical arranged electrodes can detect multipole moments with respect to the duct center. These are called absolute moments P_n and Q_n , where n is the order of the multipole moment. For example, first-order absolute moments represent the transverse positions of beam centroid P_1 (horizontal position) and Q_1 (vertical position). The two-dimensional position (P_1, Q_1) is generally called the beam position.

Our developed six-electrode BPMS have two electrodes in the vertical direction, but none horizontally. This configuration enables us to measure three higher-order ($n \geq 2$) absolute moments: P_2 , Q_2 , and Q_3 .

Because the signal voltage of each electrode V_d is proportional to the integral of the electric field strength on the electrode, we can obtain the absolute moments with normalized moments $R_{P_n}^n/2$, $R_{Q_n}^n/2$ and geometrical factors k , K , as described in Eq. (1). In the equation, R_{P_n} or R_{Q_n} is called an effective aperture radius. The effective aperture radii and the geometrical factors are calculated analytically, especially for a BPM with circular cross-section, or numerically [4].

The calculation result is summarized in Table 1. A smaller effective aperture radius is preferable for accurate

*ken@spring8.or.jp

NON-DESTRUCTIVE REAL-TIME MONITOR TO MEASURE 3D-BUNCH CHARGE DISTRIBUTION WITH ARRIVAL TIMING TO MAXIMIZE 3D OVERLAPPING FOR HHG-SEEDED EUV-FEL

H. Tomizawa, K. Ogawa, T. Sato, and M. Yabashi

RIKEN Hariama Institute, 1-1-1 Kouto, Sayo-cho, Sayo-gun, Hyogo, Japan

Y. Okayasu, S. Matsubara, and T. Togashi

JASRI/SPring-8, 1-1-1 Kouto, Sayo-cho, Sayo-gun, Hyogo, Japan

E. J. Takahashi

RIKEN Advanced Science Institute, Hirosawa 2-1, Wako, Saitama 351-0198, Japan

M. Aoyama

Kansai Photon Science Institute, Japan Atomic Energy Agency,

8-1-7 Umemidai, Kizukawa-shi, Kyoto 619-0215, Japan

A. Iwasaki and S. Owada

Department of Chemistry, The School of Science, The University of Tokyo,

7-3-1 Hongo, Bunkyo-ku, Tokyo 113-0033, Japan

H. Minamide and T. Matsukawa

RIKEN 519-1399, Aramaki-aza, Aoba, Aoba-ku, Sendai, Miyagi, 980-0845, Japan

Abstract

We have developed a three-dimensional bunch charge distribution (3D-BCD) monitor with arrival timing for an FEL seeded with a high-order harmonic (HH) pulse. A 3D-BCD monitor is based on an Electro-Optic sampling (EOS) technique with multiple EO crystal detectors in spectral decoding. Utilizing this EO-multiplexing technique, we obtained the relative positioning in the transverse and the timing in the longitudinal of the electron bunch with respect to arriving timing of a seeding HH pulse at the undulator in real-time with non-destructive measurements. In our EUV-FEL accelerator, we prepared a seeded FEL with an EOS-based feedback system for user experiments. For obtaining a higher seeding hit rate, 3D overlapping between the electron bunch and the seeding pulse must be maximized at the optimal point. Keeping the peak wavelength of EO signals at the same wavelength with our feedback system, we provided seeded FEL pulses (intensity $>4\sigma$ of SASE) with a 20-30% hit rate during pilot user experiments. For achieving the upper limit of temporal resolution, we are planning to combine high-temporal-response EO-detector crystals and an octave broadband probe laser pulse with a linear chirp rate of 1 fs/nm. We are developing an EO-probe laser pulse with ~ 10 μ J pulse energy and bandwidth over 300 nm (FWHM). In 2011, we successfully demonstrated the first bunch measurement with an organic EO crystal in the FEL accelerator at SPring-8.

INTRODUCTION

Since 2010 at SPring-8, we have been demonstrating a seeded free-electron laser (FEL) in the extreme ultra violet (EUV) region by high-order harmonics (HH) generation from an external laser source in a prototype test accelerator (EUV-FEL) [1]. In FEL seeding as a full-coherent high-intensive light source for EUV user

experiments, a high hit rate of successfully seeded FEL pulses is required. Precise measurements of the electron bunch charge distribution (BCD) and its arrival timing are crucial keys to maximize and keep 3D (spatial and temporal) overlapping between the high-order harmonics (HH) laser pulse and the electron bunch. We constructed a timing drift monitor based on Electro-Optic (EO) sampling, which simultaneously measures the timing differences between the seeding laser pulse and the electron bunch using a common external pulsed laser source (Ti: Sapphire) of both the HH driving and EO-probing pulses (Fig. 1). The EO-sampling system can use timing feedback for continuous (without interruption) operation of HH-seeded FELs.

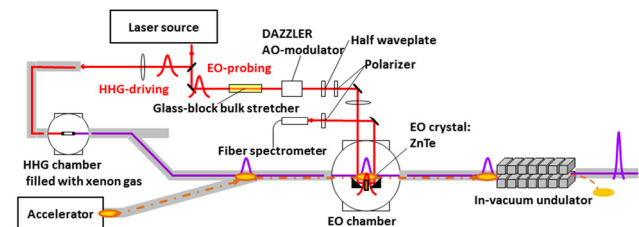


Figure 1: Experimental setup of seeded FEL with EO-sampling feedback at EUV-FEL accelerator: relative positioning in transverse and timing in longitudinal of electron bunch with respect to arriving timing of a seeding HH pulse are monitored at entrance of the first in-vacuum undulator to keep in a best seeding condition.

The R&D of a non-destructive 3D-BCD monitor (proposed in 2006 [2]) with bunch-by-bunch detection and real-time reconstructions has been extensively investigated at SPring-8. This ambitious monitor is based on an EO-multiplexing technique that resembles real-time spectral decoding and enables simultaneous non-destructive measurements of longitudinal and transverse BCDs. This part of the monitor was simultaneously materialized for probing eight EO crystals that surround

DEVELOPMENT OF PERMANENT MAGNET FOCUSING SYSTEM FOR KLYSTRONS

Y. Fuwa, Y. Iwashita, H. Tongu, Institute for Chemical Research, Kyoto University, Kyoto, Japan
S. Fukuda, S. Michizono, High Energy Accelerator Research Organization, Ibaraki, Japan

Abstract

A permanent magnet focusing system for klystrons is under development to improve reliability of RF supply system and reduce power consumption. To save production cost, anisotropic ferrite magnets are used in this system. A test model has been fabricated and the power test of a 750 kW klystron with this focusing magnet is carried out. 60 % of the nominal output power has been achieved at a preliminary power test so far.

INTRODUCTION

Distributed Klystron Scheme (DKS) is proposed as one of the RF supply scheme for International Linear Collider (ILC) to reduce the cost and the down time by raising the reliability [1]. Because thousands of relatively small modulating anode (MA) klystrons were required in DRFS scheme, the failure rate of each component must be reduced. Especially thousands units of electromagnet for klystron beam focusing would cause maintenance problems. Replacing the electromagnets by permanent magnets can eliminate their power supplies and cooling system. Hence the failure rate of the RF supply system can be reduced and cut down the operation cost. A klystron beam focusing system with ferrite magnets is under development is described.

FABRICATION OF FOCUSING MAGNET

Magnetic Materials

There have been precedents for electron beam focusing in klystrons with permanent magnets such as ALNICO, the rare earth (RE) [2,3,4]. Figure 1 shows the B-H curves for these magnet materials and anisotropic ferrite magnets. ALNICO magnets, which have high remanence, shows less coercivity and easily demagnetize. Although RE magnets such as NdFeB has high remanence and coercivity, they are rather expensive and have the resource problem. The anisotropic ferrite magnets have less remanence but higher coercivity than ALNICO. The required magnetic field for beam focusing in klystrons is less than 1 kGauss, therefore the remanence of the anisotropic ferrite magnets is enough high. And the material costs are not expensive, because anisotropic ferrite magnets are composed of iron oxide.

Magnet Field Distributions

Periodic Permanent Magnet (PPM) focusing scheme has relatively well-known magnetic field distribution. In a focusing system with permanent magnet, the alternating magnetic field can be easily generated because an integrated value of magnetic field vector along closed

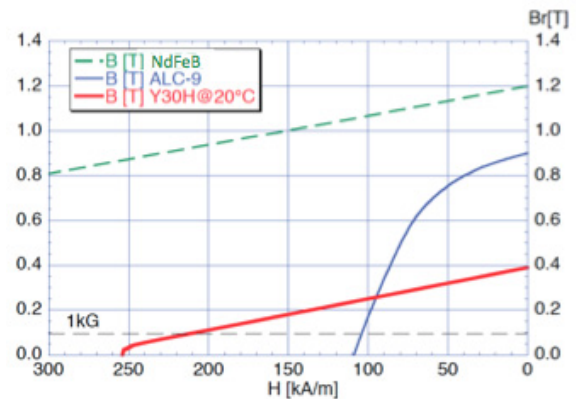


Figure 1: B-H curves of rare earth, ALNICO and ferrite magnets.

curve or infinitely-long axis is zero by the Ampere's law. However, periodicity cause stop bands. For pulse operations, the operating point always crosses such region during pulse rising time and the beam loss causes wall heating and prevents stable operation.

For safe operation, unidirectional magnetic field distribution is applied. Because the required magnet field is not high, anisotropic ferrite magnets can be used. RADIA 4.29[5,6] is used for the magnetic field design. Applied design is shown in Figure 2. Magnets shown in Figure 2 are categorized into two groups. The one group consists of magnets surrounding the klystron body

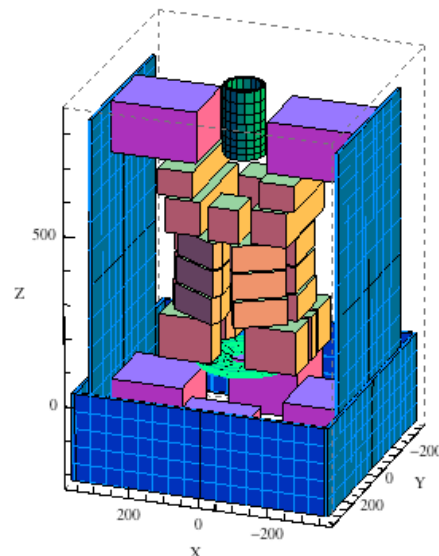


Figure 2: Layout of magnet and iron yoke.

THE FINE STRUCTURE FOR THE ZONE OF PARTICLE INTERACTION WITH A FINITE LENGTH PERIODIC STRUCTURE

V. Paramonov*, INR of the RAS, 117312, Moscow, Russia

Abstract

Interaction of the charged particle with finite length periodic structure is considered to estimate the long range wakefield effects in the constant impedance periodic deflecting structure for the special bunch diagnostic. In each structure passband there is a narrow zone with three modes, effectively interacting with the particles. To separate these modes, both frequency domain and time domain simulations are considered and compared.

INTRODUCTION

To describe long range wakefield effects for the m -th mode of the cavity, both longitudinal and transversal, loss factor k_m^l and kick factor k_m^t are used.

$$k_m^l = \frac{|\int_0^L E_{zm}(r=0, z) e^{\frac{i\omega_m z}{c}} dz|^2}{4U_m}, \quad (1)$$

$$k_m^t = \frac{|\int_0^L E_{zm}(r=r_e, z) e^{\frac{i\omega_m z}{c}} dz|^2}{4r_e^2 U_m}$$

where $E_{zm}(r, z)$, ω_m and U_m are the distribution of z component, the frequency and the stored field energy of the m -th mode. For more details and explanations one can see [1], for example.

To estimate effects in a wide frequency range, one should either simulate frequencies and fields distributions in the structure, or directly simulate wakefields of the short bunch in the long structure. Below we consider some particularities of the long range wakefields in the periodic structure with finite number of periods.

PARTICLE INTERACTION WITH FINITE LENGTH PERIODIC STRUCTURE

For the traveling wave in the infinite periodic structure each field component can be represented in complex form and expanded in a series of spatial harmonics:

$$E_{fj}(r, z) = \Re E_j(r, z) - i\Im E_j(r, z) = \quad (2)$$

$$= \sum_{p \rightarrow -\infty}^{p \rightarrow +\infty} a_{jp}(r) e^{\frac{-i(\Theta_0 + 2p\pi)z}{d}}, \quad 0 \leq \Theta_0 \leq \pi.$$

where d is the structure period, Θ_0 is the phase advance per period. Suppose the structure has a finite number of periods N and appropriate (half cells) terminations. For the standing wave a discrete set of possible phase advance

$\Theta_m = \frac{m\pi}{N}$, $m = 0, 1, \dots, N$ is possible and the field distribution can be described, [2], as:

$$E_{sjm}(r, z) = \sum_{p \rightarrow -\infty}^{p \rightarrow +\infty} 2a_{jp}(r) \cos\left(\frac{\Theta_m + 2p\pi}{d}z\right) \quad (3)$$

with the same coefficients $a_{jp}(r)$ as in appropriate traveling wave representation (2). For such field representation of the standing wave let us consider the weighting function $S(\Theta_{mp})$, $\Theta_{mp} = \Theta_m + 2p\pi$, which describes interaction of relativistic $\beta = 1$ particle with p -th spatial harmonics in the field expansion (3):

$$S(\Theta_{mp}) = \int_0^L \cos\left(\frac{\Theta_{mp}z}{d}\right) e^{\frac{i\omega_m z}{c}} dz = \quad (4)$$

$$= \frac{1}{2} \left\{ \frac{e^{iL(\frac{\omega_m}{c} + \frac{\Theta_{mp}}{d})} - 1}{i(\frac{\omega_m}{c} + \frac{\Theta_{mp}}{d})} + \frac{e^{iL(\frac{\omega_m}{c} - \frac{\Theta_{mp}}{d})} - 1}{i(\frac{\omega_m}{c} - \frac{\Theta_{mp}}{d})} \right\}.$$

The functions $\Re S(\Theta)$, $\Im S(\Theta)$ and $|S(\Theta)|$ are plotted in

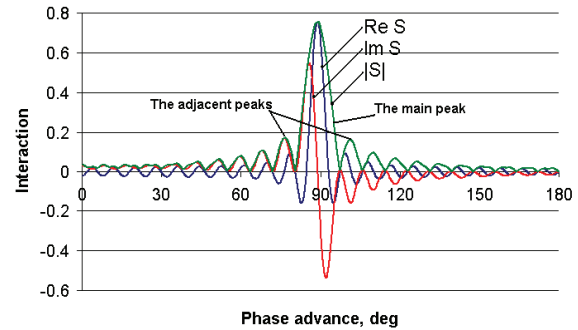


Figure 1: The functions $\Re S(\Theta)$, $\Im S(\Theta)$ and $|S(\Theta)|$ for the first monopole passband of the LOLA IV deflecting structure, $N = 46$

Fig. 1 for the first monopole passband of the LOLA IV [3] deflecting structure.

The maximal value $\Re S(\Theta_s)_{max} = |S(\Theta_s)|_{max} = \frac{L}{2} = \frac{Nd}{2}$ corresponds to the synchronous interaction $\frac{\omega_m}{c} = \frac{\Theta_s}{d}$ and linearly increases with the increasing number of cells in the structure. The width of the main peak $|S(\Theta)|$ (the distance in Θ between points $|S(\Theta)| = 0$ is $d\Theta = \frac{4\pi}{N}$ and for longer structure the main peak is narrowed. Because the separation between standing wave modes at Θ axis is of $\frac{\pi}{N}$, all time three or four modes belong to the main peak. The adjacent peaks in $|S(\Theta)|$, see Fig. 1, are placed at the distance $\delta\Theta = \pm \frac{3\pi}{N}$ with respect to the main peak $\Theta = \Theta_s$. The width of adjacent peaks is $\frac{2\pi}{N}$ - twice less, as compared to the width of the main peak. The maximal values of the

*paramono@inr.ru

DEFLECTING STRUCTURES WITH MINIMIZED LEVEL OF ABERRATIONS*

V. Paramonov[†], INR of the RAS, Moscow, 117312, Russia

Abstract

Deflecting structures are now widely used for bunch phase space manipulations either in special bunch diagnostic or in emittance exchange experiments. As a tool for manipulation, the structure itself should provide the minimal phase space perturbations due to non linear additives in the field distribution. Criterion of the field quality estimation is developed and deflecting structures are considered for minimization of non linear additives.

INTRODUCTION

The Deflecting Structures (DS) - periodical structures with transverse components of the electromagnetic field - initially were introduced for charged particle deflection and separation. The bunch cross DS synchronously with the deflecting field E_d , corresponding the phase $\phi = 0$ in the structure and particles get the increment in the transverse momentum p_t . There are a lot of papers, see for example [1], describing DS design and application for such purpose. At present for short and bright electron bunches DS found another applications, either for bunch special diagnostic, [2], or emittance exchange experiments. Both directions are related to the transformation of particle distributions in the six dimensional phase space and DS operates in another mode - the bunch center cross DS at zero E_d value, $\phi = 90^\circ$. There are also a lot of papers, describing it in more details. Application for Particles Distributions Transformation (PDT) provide additional requirements - a tool for transformation should provide the minimal, as possible, own distortions to the original distributions.

FIELD DISTRIBUTION QUALITY

For deflecting field E_d description the widely used basis of $TM - TE$ waves can not be used due to degeneration into TEM at $\beta = 1$. A basis of hybrid waves $HE - HM$ was introduced, [3], [4] to avoid this methodical problem. The common representation for the field distribution in the DS aperture is

$$\vec{E} = C\vec{E}_{HE} + D\vec{E}_{HM}, \quad \vec{H} = C\vec{H}_{HE} + D\vec{H}_{HM}, \quad (1)$$

with the weighting coefficient C, D depending both on supporting structure and on operating mode. It is the method of description and results treatment. The physical object - the deflecting force - is the transverse component of the Lorenz force

$$\vec{F}^L = e(\vec{E} + [\vec{v}, \vec{B}]), \quad F_x = eE_d = e(E_x - \beta Z_0 H_y), \quad (2)$$

where $Z_0 = \sqrt{\frac{\mu_0}{\epsilon_0}}$, expressed in (2) through the transverse E_x and H_y components in Cartesian coordinates. In any periodical structure for Traveling Wave (TW) operating mode each field component $E_j(r, z)$ in the beam aperture can be represented in the complex form as the set over spatial harmonics:

$$E_j(r, z) = E_j(\widehat{r}, z)e^{i\psi_j(z)} = \sum_{n \rightarrow -\infty}^{n \rightarrow +\infty} a_{jn}(r)e^{-\frac{i(\Theta_0 + 2n\pi)z}{d}}, \quad (3)$$

where $E_j(\widehat{r}, z)$ and $\psi_j(z)$ are the amplitude and the phase distributions, d is the structure period and $a_{jn}(r)$ is the transverse distribution for the n -th spatial harmonics. The period length is defined from synchronism with the main a_{j0} harmonic, $d = \frac{\Theta_0 \beta \lambda}{2\pi}$.

The bunch emittance deterioration during PDT take place due to non linear additions both in transverse and longitudinal distributions of the field. There is inevitable nonlinearity at $\beta < 1$ even in main harmonic distribution, vanishing for $\beta \rightarrow 1$, [3], [5]. But the main source of additions are higher spatial harmonics. For each harmonic the transverse and longitudinal distributions are rigidly coupled and are proportional to harmonic amplitude. To estimate field quality, we have to estimate the level of spatial harmonics, [5]. Spatial harmonics are essential at the aperture radius $r = a$ and higher harmonics attenuate to the axis as

$$a_{jn}(0) \sim a_{jn}(a) \cdot \exp\left(-\frac{4\pi^2 n}{\beta \Theta_0} \cdot \frac{a}{\lambda}\right), \quad |n| \gg 1, \quad (4)$$

where λ is the operating wave length. At the axis $r = 0$ just lower harmonics $n = \pm 1, \pm 2, \pm 3$ are really presented. For harmonics estimations in details and 'in total', let us introduce parameters $\delta\psi_j(z)$ and Ψ_j at the axis $0 \leq z \leq d, r = 0$

$$\delta\psi_j(z) = \psi_j(z) + \frac{\Theta_0 z}{d}, \quad \Psi_j = \max(|\delta\psi_j(z)|), \quad (5)$$

with the physical sense as the deviation and the maximal phase deviation of the real wave component from the synchronous harmonic. The qualitative estimation and correct value for $a_{jn}(0)$ one can get as

$$|a_{jn}(0)| < \frac{(E_j(0, z)_{max} + E_j(0, z)_{min})\Psi_j}{2n}, \quad (6)$$

$$a_{jn}(0) = \frac{\int_0^d E_j(\widehat{0}, z) \sin(\delta\psi_j(z)) \sin(\frac{2\pi n z}{d}) dz}{d}.$$

From linearity, we can apply $\delta\psi_j(z)$ and Ψ_j for quality

* Work supported in part by RBFR N12-02-00654-a

[†] paramono@inr.ru

RESULTS OF TESTING OF MULTI-BEAM KLYSTRONS FOR THE EUROPEAN XFEL

V. Vogel, L. Butkowski, A. Cherepenko, S. Choroba, I Harders and J. Hartung,
 DESY, 22607 Hamburg, Germany

Abstract

For the European XFEL multi-beam klystrons, which can produce RF power of 10 MW at an RF frequency of 1.3 GHz, at 1.5ms pulse length and 10 Hz repetition rate, were chosen as RF power sources. Twenty-seven of horizontal multi-beam klystrons (MBK) together with connection modules (CM) will be installed in the XFEL underground tunnel. The CM will be installed on the MBK and connects the MBK to the pulse transformer with only one HV cable, because the CM has a filament transformer inside as well as all diagnostics for HV and cathode current measurements. MBK prototypes together with CM prototypes have been tested for long time at a test stand at DESY, about 4600 hours of operation for each of horizontal MBK with full RF output power, full pulse length and repetition rate of 10 Hz. Testing of first MBKs from series production has been started. In this paper we will give an overview of the test procedure, summarize the current test results and we will give a comparison of the most important parameters.

INTRODUCTION

For the XFEL project [1] as a source of RF power for 27 RF station were chosen the horizontal MBK made by two companies: MBK TH1802 from “Thales” [3] and MBK E3736H from “Toshiba” [4]. The main parameters of MBK are given in Table 1.

Table 1: Main parameters of L-band MBK for XFEL

Parameters	Design value	Test value
Output power (MW)	10	10.3
RF pulse length (ms)	1.5	1.5
Efficiency (%)	> 63	64
Repetition rate (Hz)	up to 30	10
Max average RF power (kW)	150	155
Max average power in collector (kW)	300	270
Max drive power (W)	<200	<150
Bandwidth (MHz)	3	>3

Both prototypes of MBK were tested on DESY MBK test stands [2], a total time of testing exceed of 4600 hours for both of tubes. The test was done with full RF power of 10 MW, full RF pulse length of 1.5 ms and with repetition rate of 10 Hz. Fig. 1 shows the top view of the test stands. Because the all of RF station will be located in the

underground tunnel it is very important do not have the open oil during installation of MBK. It was proposed and tested the connection between MBK and HV pulse transformer through connection module (CM) [5, 6 and 7] and HV cable. Several types of HV cables and connectors as well as CM prototypes were tested. Big advances of using CM are that CM has inside a high voltage high frequency filament transformer and monitors for measurement of klystron voltage and cathode current. Fig. 2 shows the one of klystrons with CM and HV cable.



Figure 1: MBK test stands in DESY Hamburg



Figure 2: MBK with CM and HV cable “PFISTERER 3S”

RESULTS OF MBK PROTOTYPES TEST

Since February 2008 we started the test of the first of horizontal MBK prototype on DESY site. For the test of MBK it was specially developed two radiation protected

COMPUTATIONAL MODEL ANALYSIS FOR EXPERIMENTAL OBSERVATION OF OPTICAL CURRENT NOISE SUPPRESSION BELOW THE SHOT-NOISE LIMIT

A. Nause, E. Gover, Tel Aviv University, Israel

Abstract

In this paper we present simulation analysis of experimental results which demonstrate noise suppression in the optical regime, for a relativistic e-beam, below the classical shot-noise limit. Shot-noise is a noise resulting from the granular nature of the space-charge in an e-beam. It is linear to the beam current due to its Poissonic distribution in the emission process. Plasma oscillations driven by collective Coulomb interaction during beam drift between the electrons of a cold intense beam are the source of the effect of current noise suppression. The effect was experimentally demonstrated [1] by measuring Optical Transition Radiation (OTR) power per unit e-beam pulse charge. The interpretation of these results is that the beam charge homogenizes due to the collective interaction (sub-Poissonian distribution) and therefore the spontaneous radiation emission from such a beam would also be suppressed (Dicke's sub-radiance [2]). Analysis of the experimental results using GPT simulations will demonstrate the suppression effect. For the simulation results we used a full 3D GPT model of the ATF section in which the experiment took place at.

INTRODUCTION

Shot-noise is a noise resulting from the granular nature of the space-charge in an e-beam. The discreteness of the particles and the randomness of electrons emission from the cathode causes time dependent fluctuations of the charge and current density at any cross section along the beam transport line. This noise was first reported in 1918 by Schottky who made experiments in vacuum tubes.

Noise is best characterized in terms of the Fourier transform of the time-varying fluctuations in electric current, namely, by its spectral density. Gover and Dyunin showed in a 1D model [3] that it is possible to observe and control optical frequency energy and current (shot noise) fluctuations in a dense relativistic charged particles beam. GPT simulations were used to demonstrate this effect for a real-like beam starting from Shot-noise [4]. Moreover, at certain conditions, when the dominant noise in the beam is current shot noise (density fluctuations), it is possible to reduce significantly the beam noise by virtue of a collective interaction process along an interaction length corresponding to a quarter period longitudinal plasma oscillation in the beam. This means that the charge distribution in the beam can be homogenized in this process.

First experimental observation of this phenomenon using OTR from a metallic foil was presented last year [1]. Noise suppression using a dispersive section (dog-leg bend) was demonstrated in SLAC [5]. TR is proportional to the

current-noise amplitude [6], and therefore can be used in order to estimate the suppression in the current noise. In this paper we press analysis of the experimental results and demonstrate this effect using full 3D GPT simulations that were carried out for this purpose.

1D Model of Noise Dynamics in Charged Electron Beams

In electron-beam transport under appreciable space-charge conditions, the microdynamic noise evolution process may be viewed as the stochastic oscillations of Langmuir plasma waves [3]. In the linear regime, the evolution of longitudinal current and velocity modulations of a beam of average current I_b , velocity βc and energy $E = (\gamma - 1)mc^2$, can be described in the laboratory frame by [7]:

$$\frac{d}{d\phi_p} \check{i}(z, \omega) = -\frac{i}{W(z)\check{v}(z, \omega)} \quad (1)$$

$$\frac{d}{d\phi_p} \check{v}(z, \omega) = -iW(z)\check{i}(z, \omega) \quad (2)$$

where $\check{i}(\omega) = \check{I}(\omega)e^{i\omega z/\beta c}$, $\check{v}(\omega) = \check{V}(\omega)e^{i\omega z/\beta c}$. $\check{I}(\omega)$, $\check{V}(\omega)$ are the respective Fourier components of the beam current and kinetic-voltage modulations. The kinetic-voltage modulation is related to energy and longitudinal velocity modulations: $\check{V}(\omega) = -(mc^2/e)\check{\gamma} = -(mc^2/e)\gamma^3\beta\check{\beta}$, $\phi_p(z) = \int_0^z \theta_{pr}(z')dz'$ is the accumulated plasma phase, $W(z) = r_p^2/(\omega A_e \theta_{pr} \epsilon_0)$ is the beam wave-impedance. A_e is the effective beam cross-section area, $\theta_{pr} = r_p \omega_{pl}/\beta c$ is the plasma wavenumber of the Langmuir mode, $r_p < 1$ is the plasma reduction factor, $\omega_{pl} = \omega_{po}/\gamma^{3/2}$ is the longitudinal plasma frequency in the laboratory frame. The single-frequency Langmuir plasma wave model expressions [3] can be solved straightforwardly in the case of uniform drift transport. After employing an averaging process, this results in a simple expression for the spectral parameters of stochastic current and velocity fluctuations (noise) in the beam assuming that they are initially uncorrelated[]:

$$\check{i}(L, \omega) = \cos \phi_p(L)\check{i}(0, \omega) + (\sin \phi_p(L)/W_d)\check{v}(0, \omega) \quad (3)$$

where $\phi_p = \theta_{pr}z$, $\theta_{pr} = r_p \frac{\omega'_p}{v_0}$, $\omega'_p = (\frac{e^2 n_0}{m \epsilon_0 \gamma^3})$, $W_d = \sqrt{\mu_0/\epsilon_0}/k\theta_{pr}A_e$.

The beam current noise evolution is affected by the initial axial velocity noise through the parameter

$$N^2 = \frac{|\check{v}(0, \omega)|^2/W^2}{|\check{i}(0, \omega)|^2} = (\omega/c\beta k_D)^2 \quad (4)$$

STABILITY PERFORMANCE OF THE INJECTOR FOR SACLA/XFEL AT SPRING-8

T. Asaka[#], T. Hasegawa, T. Inagaki, H. Maesaka, T. Ohshima, S. Takahashi, K. Togawa, Y. Otake,
RIKEN SPring-8 Center, Hyogo 679-5148, Japan

Abstract

To realize stable lasing of an X-ray free electron laser, it is required to obtain more stability of more than one or two figures compared with a conventional accelerator technology. At SACLA, stabilities of 100 ppm and 50 fs in the amplitude and timing of the accelerating RF field, respectively, have been attained, resulting in an achievement of a beam energy stability of 0.02% (std.) or less at 8-GeV. However, two variations with different cycle periods were found in the laser power. One was a long-term variation over several hours, which was in agreement with the phase drift of a 238 MHz/SHB. The other was caused by a variation of the beam position in a 30-MeV injector section. A periodically changed beam position of 30 μm (std.) was found out at a cycle of 0.5 Hz by a fast Fourier transform method using BPM data. The temperatures of all the injector RF cavities are kept within $28 \pm 0.04^\circ\text{C}$ by controlling the cooling water temperature. The AC power supply of the controller to heat the cooling water is operated at 0.5 Hz by a pulse width modulation control with alternatively turning on and off. A strong correlation between the laser intensity fluctuation and the modulation frequency of the AC power supply was found out. We are planning to improve the RF cavity temperature variation to an order of less than 0.01 K by establishing a new temperature regulation system using a continuous level control with a DC power supply. This plan will reduce the XFEL power fluctuation.

INTRODUCTION

User experiment at SACLA started in March of this year after beam commissioning for one year [1]. Toward increasing laser intensity, an accurate beam adjustment of a linear accelerator was carried out during the beam commissioning. At the same time, we have conducted some research and analysis aiming at high-level laser stability.

In order to realize a stable X-ray Free Electron Laser (XFEL) at SACLA, the peak current of an electron beam, passing through a 90-m long undulator section, should reach 3 kA with a normalized emittance of 1π mm mrad or less. In addition, it is important to maintain this beam performance with a high-level stability. Because even a slight beam orbit variation of without 4 μm (rms) in the accelerator end causes unstable laser oscillation, which measures decreasing half of the peak laser intensity, in the undulator, RF equipment has to be very carefully designed so as to minimize its variation in the RF

amplitude and phase [2]. We took thorough stabilization countermeasures against all of the RF equipment, such as controlling a cooling water temperature for each RF cavity by using a precise temperature regulation system, employing a low-noise power supply and the suppressing of a mechanical vibration. As a results, stability performances of the RF cavities were improved to almost satisfy the target values, that is the RF amplitude and time jitter were <100 ppm and <50 fs, respectively. Accordingly, the beam energy stability of 0.02% (std.) or less has been achieved at the end of the 8-GeV accelerator because of the highly stabilized RF system.

However, it was observed that the laser power with an optimized lasing parameter decreased in a few hours. We were forced to spend about one hour in readjustment of the lasing parameter for recovering the laser power. To make the user experiment more efficient, it was urgent to investigate the cause of the laser power variation and fix it. The possible causes are as follows: (1) a variation of the beam arrival time with the velocity bunching process in the injector section, (2) RF phase drift due to a low level RF system of the injector section, which depends on the environment temperature, and (3) RF phase fluctuation of the cavities, which depends on the cooling water temperature. To clarify the causes, the correlations between each apparatus and surrounding factors were investigated. Consequently, the dominant factors were clarified, and a readjustment procedure for recovery of the laser power was established. The laser power is kept stable during user experiment at present, as shown in Fig. 1. This report presents details of the analysis of beam fluctuation and improvement of laser performance.

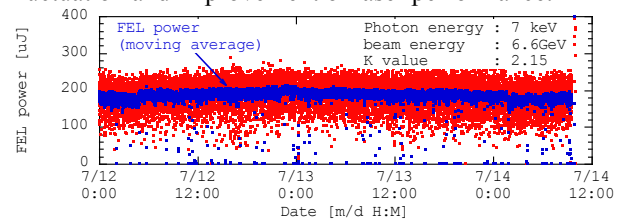


Figure 1: Stability of laser power in user experiment measured using photo detectors.

LONG-TERM VARIATION

Measurement of Laser Power Stability, Beam Arrival Time and Beam Energy

Accelerator operation was performed during three days to reveal which part of the accelerator caused beam variation. First, the condition of the lasing parameter was optimized for 10-keV photon energy at 7-GeV. The laser power immediately after the optimization reached 0.13 mJ.

[#]asaka@spring8.or.jp

MAJOR TRENDS IN LINAC DESIGN FOR X-RAY FELS*

A.A. Zholents[#], ANL, Argonne, IL 60439, USA

Abstract

Major trends in the contemporary linac designs for x-ray free-electron lasers (XFELs) are outlined starting with identification of the key performance parameters, continuing with considerations of the design options for the electron gun and linac, and finishing with electron beam manipulation in the phase space.

KEY PERFORMANCE PARAMETERS

Pursuit of the XFEL demands improvements in accelerator technology for producing and accelerating high-brightness electron beams. The brightness of the electron beam $B_n = N_e (\lambda_c)^3 / \varepsilon_x \varepsilon_y \varepsilon_z$, where N_e is the number of electrons in the electron bunch; $\varepsilon_x, \varepsilon_y, \varepsilon_z$ are the normalized horizontal, vertical, and longitudinal emittances; and $\lambda_c \approx 3.86 \cdot 10^{-11}$ cm is the Compton wavelength, plays the most important role in the FEL process. It was shown in [1, 2] that in the best possible scenario when electron beam and FEL parameters are optimized to yield the fastest growth rate of the microbunching, the inverse gain length in the FEL scales linearly with brightness and quadratically with the electron beam energy (a typo in [1] shows linear dependence), i.e.,

$$\frac{\lambda_u}{L_g} \propto \frac{K^2}{2 + K^2} \left(\frac{E_b}{\hbar \omega_s} \right)^2 B_n, \quad (1)$$

where L_g is the gain length, $\hbar \omega_s$ is the x-ray photon energy, E_b is the electron beam energy, λ_u is the undulator period, and K is the undulator parameter.

The electron beam energy is the next most important parameter (after brightness) that strongly affects FEL performance. Besides Eq. (1), E_b appears in the optimization of FEL performance in a few other places. The first is a constraint on the geometrical emittance $\varepsilon_{x,y} / \gamma \leq \lambda_s / 4\pi$, providing that the electron beam size matches the light beam and electrons do not de-phase over the FEL gain length due to betatron oscillations. Here the relativistic factor γ was used instead of E_b . The second is a constraint on the relative energy spread σ_E / E_b , which is basically driven by the same de-phasing concern. The third is the FEL resonance condition $\lambda_s = \lambda_u / 2\gamma^2 \times (1 + K^2 / 2)$. Finally, the electron beam energy almost solely defines the cost of the electron beam delivery system. According to these listed constraints, the next-generation FELs should rely on the increased brightness of the electron beam and undulators with short periods in order to lower E_b and, thus, the cost of the FEL. Although, clearly, the undulator technology is extremely important, it is out of the scope of this review and, thus, we refer the reader to a recent publication [3].

*Work supported by the U.S. Department of Energy, Office of Science, under Contract No. DE-AC02-06CH11357.
#azholents@aps.anl.gov

ELECTRON GUN

Production and acceleration of high-brightness electron beams are the two most challenging tasks for the electron gun and linac. The brightness is largely defined by the ability of the electron gun to produce a small emittance, and at present, the rf photocathode guns yield the brightest electron beams. Any advances in this area will allow for lowering the linac energy, thus saving on the construction cost of the facility, and also on the operation cost, as a smaller linac can be used. The ultimate brightness is defined by a so-called “intrinsic emittance” (IE), which is solely dependent on the cathode material work function ϕ_0 and an electron extraction mechanism. For example, measurements of the IE in the case of the photoemission from a Cu cathode shown in Figure 1 [4] demonstrate that it depends on the difference between photon energy $\hbar \omega$ and the effective work function $\phi_{eff} = \phi_0 - (e^3 E_c)^{1/2}$ (in CGS units), where e is the electron charge, and E_c is the applied electric field on the cathode

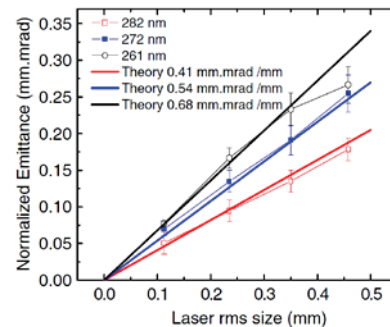


Figure 1: Normalized projected emittance versus laser spot size for three different laser wave lengths as shown in Ref [4]. Measurements were carried out for a copper cathode using a low charge less than 1 pC and $E_c = 25$ MV/m. Theoretical fit assumes $\phi_0 = 4.3$ eV. Thermal effects are not included.

surface responsible for reduction of the potential barrier due to the work function ϕ_0 . Here one can see that the smaller the excess energy $\hbar \omega - \phi_{eff}$, the smaller the IE [5]:

$$\varepsilon_{intrinsic} = \sigma_r \sqrt{\frac{\hbar \omega - \phi_{eff}}{3mc^2}}, \quad (2)$$

where σ_r is the rms size of the laser beam on the cathode, and m is the electron mass. This trend was also observed with Mo, Nb, Al, and bronze cathodes [4] and is expected in semiconductor cathodes such as Cs_2Te and SbK_2Cs [6]. Thus, matching the work function of the cathode material to laser photon energy is expected to yield better IE. Some ideas aimed at production of the photocathode materials with desirable work function were proposed recently [6, 7]. For example, it was found that ternary alkali metal transition metal acetylides (Cs_2TeC_2) [8]

C-BAND ACCELERATOR STRUCTURE DEVELOPMENT AND TESTS FOR THE SWISSFEL

R. Zennaro, J. Alex, H. Blumer, M. Bopp, A. Citterio, T. Kleeb, L. Paly, J.-Y. Raguin
Paul Scherrer Institute, Villigen

Abstract

The SwissFEL requires a 5.8 GeV beam provided by a C-band linac consisting of 104 two-meter accelerating structures [1]. Each structure is of the constant-gradient type and is composed of 113 cups [2]. The cup shape is double-rounded to increase the quality factor. No tuning feature is implemented. For this reason ultra-precise turning is exploited. A strong R&D program has been launched on structure fabrication, which will be followed by a future technology transfer to a commercial company. The program includes the production and test of short structures that can be brazed in the existing PSI vacuum oven and will be completed with the production of the full two-meter prototype once the new full scale brazing oven, presently under construction, is operational. The status of the R&D program, including the production and power test results of the first two test structures, is reported here.

INTRODUCTION

The baseline of the R&D program includes the production and test of four short constant-impedance structures. The first and the second test structures are composed of eleven regular cells and two matching cells. Each cell geometry and volume are defined by two joined half cups. The dimensions of the regular cells are close to the one of the first regular cell of the two-meter structure prototype [2] whereas the regular cells of the third structure have a geometry close to the one of the last regular cell. The connection to the input waveguides and output loads is provided by removable mode launchers which are mechanically connected to the structure via two flanges and two RF chokes [3]; see Figure 1.

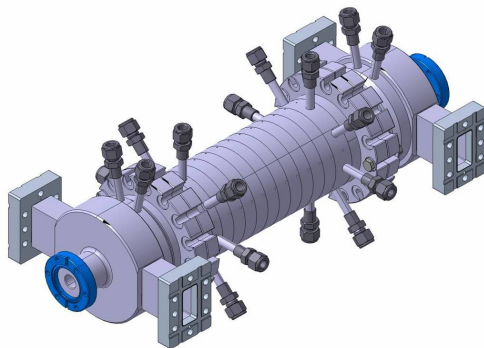


Figure 1: Short test structure.

The fourth test structure is under construction and will be equipped with an RF J-type coupler, the same type than the ones of the two-meter structure [2].

The main parameters of the test structures are summarized in Table 1.

Table 1: Main parameters of the test structures

Test Structure	Structure 1,2	Structure 3, 4
Type	Constant impedance	Constant impedance
Number of regular cells	11	11
Frequency	5.712 GHz	5.712 GHz
Phase advance/cell	$2\pi/3$	$2\pi/3$
Iris aperture radius /thickness	7.267/2.5 mm	5.478/2.5 mm
Group velocity	3.1 % c	1.4 % c
Q	10400	10350
R/Q	7214 Ohm/m	8522 Ohm/m
Nominal gradient (MV/m)	28 MV/m at 28 MW	28 MV/m at 10.84 MW

CUP PRODUCTION AND CONTROL

Extremely high accuracy in structure production is required to avoid tuning. The specified tolerance for the cup diameter is $\pm 4 \mu\text{m}$. In order to verify the cup size all the cups had metrology control. The histogram in Figure 2 shows the metrology results for the inner diameters of the cups produced for structure 3 and 4: the cups have a systematic error of $-0.9 \mu\text{m}$, the error distribution has a standard deviation of $0.4 \mu\text{m}$ and a peak to peak difference of $2.0 \mu\text{m}$.

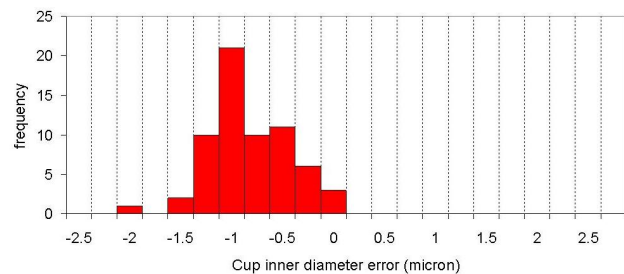


Figure 2: Histogram of the errors on the inner cup diameter for cups produced for structure 3 and 4.

To have a cheap and quick system to verify the cup dimensions we developed a single cup resonant frequency measurement tool. A resonating volume is defined by closing a half cup with a copper plate by applying a pressure of 14 MPa and by detuning the opposite half cup. The repeatability of the measurements in constant temperature conditions is excellent, with a standard deviation of the frequency of less than 5 kHz.

THE SWISS FEL RF GUN: RF DESIGN AND THERMAL ANALYSIS

J.-Y. Raguin, M. Bopp, A. Citterio, A. Scherer
 PSI, CH-5232 Villigen, Switzerland

Abstract

We report here on the design of a dual-feed S-band 2.5-cell RF gun, developed in the framework of SwissFEL, capable of operating at 100 Hz repetition rate. As in the LCLS RF gun, z-coupling, to reduce the pulsed surface heating, and a racetrack coupling cell shape, to minimize the quadrupolar component of the fields, have been adopted. The cell lengths and the iris thicknesses are as in the PHIN gun operating at CERN. However the iris aperture has been enlarged to obtain a frequency separation between the operating π mode and the $\pi/2$ mode higher than 15 MHz. An amplitude modulation scheme of the RF power, which allows one to obtain a flat plateau of 150 ns for multibunch operation and a reduced average power is presented as well. With an RF pulse duration of 1 μ s it is shown that operation at 100 MV/m and 100 Hz repetition rate is feasible with very reasonable thermal stresses.

INTRODUCTION

Paul Scherrer Institut is completing the study of the accelerating systems of SwissFEL, a Free Electron Laser which targets a maximum electron beam energy of 5.8 GeV. SwissFEL is designed for two standard electron beam operation modes, one with a 200 pC charge per bunch and a core slice emittance of 0.43 mm-mrad and the second with a 10 pC charge per bunch and a core slice emittance of 0.18 mm-mrad. SwissFEL, the main linac frequency being the C-band American frequency 5712 MHz, operates with a repetition rate of 100 Hz and two electron bunches, with a spacing of 28 ns, are accelerated at each RF pulse.

The proposed 2.5-cell RF gun operates with a nominal body temperature of 40 °C in the π mode at the S-band frequency of 2998.8 MHz, such a frequency having a common sub-harmonic with the SwissFEL C-band main linac frequency. The beam energy at the exit of the RF gun is about 7 MeV. The two full cell lengths and the iris thicknesses of the RF gun are identical to the ones of the CTF3 PHIN RF gun [1]. The upstream cell, shorter than the two full cells, has a longitudinally adjustable backplane. The middle cell is coupled to two rectangular waveguides symmetrically arranged to cancel the dipolar component of the field. The racetrack interior shape of this coupling cell is optimized to minimize the quadrupolar field component, as in the LCLS RF gun [2]. Long lifetime and reliable operation with the targeted peak on-axis electric field of 100 MV/m requires the optimization of the two RF coupling port dimensions to reduce the dynamic thermal stress due to pulsed heating. With the high 100 Hz repetition rate, mechanical stresses caused by thermal loading have to be thoroughly addressed.

SWISSFEL RF GUN DESIGN

Design with 2D RF Simulations

Ignoring at this stage the middle cell coupling ports, RF simulations performed with the 2D electromagnetic code SUPERFISH [3] are used to determine the radius and the elliptical shape of the irises between the cells compatible with reduced surface electric fields and large frequency separation between the operating π mode ($TM_{010-\pi}$ mode) and the $\pi/2$ next lower mode ($TM_{010-\pi/2}$ mode). The radius of the upstream cell and of the two full cells are adjusted to reach a balanced on-axis field at the operating frequency. The 2D RF design was then guided by the requirements that the mode separation between the operating π mode and the $\pi/2$ mode be higher than 15 MHz and that the peak surface electric field is not higher than the electric field on the cathode. The large mode separation between the operating mode and the next lower mode reduces the impact of the lower mode on the electron bunch energy spread and projected emittance. It is also expected to make the field balance less sensitive to thermal expansion under operational conditions and to manufacturing dimension deviations that may occur during production [4].

Fig. 1 shows the electric field contour lines of the π mode. The cell radii are optimized to obtain field flatness at the operating frequency. The dimensions of some geometrical parameters, used also for the final 3D design, are specified in Table 1. The elliptical profile of the irises is characterized by an aspect ratio of 1.7:1 so that the maximum surface electric field is lower than the peak field on the cathode.

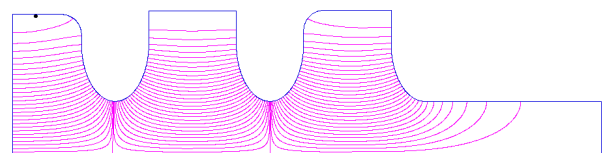


Figure 1: Electric field contour lines of the operating π mode

Table 1: Geometrical parameters of the SwissFEL RF gun

Parameter	Value		
Cell length	20.5 mm	26 mm	26 mm
Iris thickness	20 mm		
Iris radius	16 mm		
Drift radius	16 mm		

Final Design with 3D RF Simulations

The dimensions obtained with the 2D code SUPERFISH are used as input to complete the RF design of the gun with the 3D electromagnetic code HFSS [5], in particular the

THE SWISS FEL S-BAND ACCELERATING STRUCTURE: RF DESIGN

J.-Y. Raguin, PSI, CH-5232 Villigen, Switzerland

Abstract

The Swiss FEL accelerator concept consists of a 330 MeV S-band injector linac at 2998.8 GHz followed by the main linac at the C-band frequency aiming at a final energy of 5.8 GeV. The injector has six four-meter long S-band accelerating structures that shall operate with gradients up to 20 MV/m and with a 100 Hz repetition rate. Each structure has 122 cells, including the two coupler cells and operates with a $2\pi/3$ phase advance. The design presented is such that the average dissipated RF power is constant over the whole length of the structure. The cells consist of cups and the cell irises have an elliptical profile to minimize the peak surface electric field. The coupler cells are of the double-feed type with a racetrack cross-section to cancel the dipolar components of the fields and to minimize its quadrupolar components.

INTRODUCTION

The injector linac foreseen for SwissFEL at the Paul Scherrer Institut (PSI) [1] consists of two boosters, one with two S-band accelerating structures located between the PSI-designed RF gun [2] and the laser heater, the second with four S-band structures positioned between the laser heater and the two X-band structures used to complete the linearization of the longitudinal phase space. These accelerating structures are designed to operate at 40 °C with a pulse repetition frequency of 100 Hz and at 2998.8 MHz, an S-band frequency identical to the design frequency of the RF gun and which has a common sub-harmonic with the C-band main linac.

The presented S-band structure is of the travelling-wave type and operates with a $2\pi/3$ phase advance per cell. With a flange-to-flange length of 4.15 m, it consists of 122 cells - 120 regular cells and two coupler cells. Two cells, located upstream and downstream of the structure, are equipped with an RF pickup for monitoring and controlling the amplitude of the RF fields during operation. Since the energy of the electron bunches accelerated in the RF gun is about 7 MeV, any RF field distortion in the vicinity of the longitudinal axis of the structure may severely deteriorate the bunch emittance. In conventional travelling-wave structures, these field distortions are caused by the breaking of the azimuthal symmetry of the structure due to the topology of RF input and output ports. The remedies against these field distortions are to equip the coupler cells with symmetrically arranged double feeds and to adopt a racetrack shape of these cells [3]. These two geometrical features are selected for designing the coupler cells.

The peculiarity of the presented S-band structure is the optimized cell-to-cell iris and cell radii to obtain an RF

dissipated power per cell *constant* all along the structure. In addition, the cell-to-cell irises have an elliptical cross-section. Such a profile allows to reduce the ratio of the peak surface electric field to the accelerating gradient E_{peak}/E_{acc} and is expected to inhibit the generation of dark current. The accelerating gradient of the structure is 20 MV/m. Table 1 summarizes some main parameters of the designed S-band structure.

Table 1: Main parameters of the SwissFEL S-band structure

Parameter	Value
Operating frequency	2998.8 MHz
Phase advance per cell	$2\pi/3$
Total number of cells	122
Accelerating gradient	20 MV/m
Maximum pulse repetition frequency	100 Hz
Operating temperature	40 °C

DESIGN OF THE REGULAR CELLS

The regular cells of the designed structure have a cup-like shape with a curvature radius of 10 mm at the manufacturing temperature (see Fig. 1). The cell-to-cell iris thickness is 5 mm and is constant all along the structure. These irises have all the same elliptical cross-section with an aspect ratio of 1.5:1. Due the difficulty to tune and to match coupler cells with low group velocity, the radius of the last iris of the structure has been chosen to be 9.31 mm. The length of each cell is 33.324 mm at 40 °C to operate the structure in the TM_{010} -like mode with a $2\pi/3$ phase advance per cell,

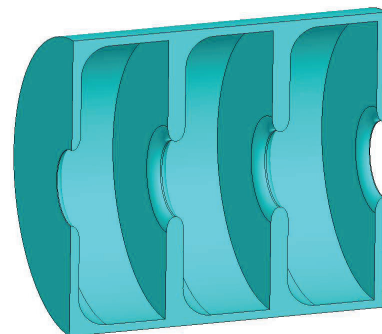


Figure 1: 3D model of the S-band structure cells.

The RF design of the regular cells is performed with the 2D electromagnetic code SUPERFISH [4]. By modelling three identical cells and by applying the appropriate boundary conditions, one obtains the standing-wave field map and the eigenfrequency from which the travelling-wave fundamental RF mode parameters characterizing the

THE SWISS FEL C-BAND ACCELERATING STRUCTURE: RF DESIGN AND THERMAL ANALYSIS

J.-Y. Raguin, M. Bopp, PSI, CH-5232 Villigen, Switzerland

Abstract

The Swiss FEL accelerator concept consists of a 330 MeV S-band injector linac followed by the main linac in C-band aiming at a final energy of 5.8 GeV. The two-meter long C-band accelerating structures have 113 cells, including the two coupler cells, and operate with a $2\pi/3$ phase advance. The structure is of the constant-gradient type with rounded wall cells and has an average iris radius of 6.44 mm, a radius compatible with the impact of the short-range wakefields on the whole linac beam dynamics. The cell irises have an elliptical profile to minimize the peak surface electric fields and the coupler cells are of the J-type. We report here on the RF design of the structure, as well as on its thermal analysis, to target operational conditions with an accelerating gradient of about 28 MV/m and a repetition rate of 100 Hz.

INTRODUCTION

The main linac of SwissFEL at the Paul Scherrer Institut (PSI) is designed to consist of 28 RF modules operating at the C-band American frequency 5712 MHz with a pulse repetition frequency of 100 Hz. Each module is composed of one solid-state modulator, one 50-MW klystron, one PSI-designed C-band pulse compressor - a barrel-open cavity (BOC) - and four accelerating structures. Since SwissFEL aims for two-bunch operation with a 28 ns spacing, it is crucial that the acceleration through the structures is identical for *both* bunches. Such a feature can be achieved by performing phase modulation on the klystron drive signal. With a 3 μ s, 40 MW klystron RF pulse, and taking into account the RF losses along the waveguide network of the module, the RF pulse, compressed by the BOC to 350 ns, is tailored so that *both* bunches gain an energy per accelerating structure as high as 56 MeV.

A 56 MeV energy gain per structure is achievable with a constant-gradient travelling-wave structure having in total 113 cells - 111 regular cells and two coupler cells. The length of each regular cell is fixed by the imposed $2\pi/3$ phase advance per cell. It can indeed be shown that the resulting energy gain is nearly optimal with such a choice of phase advance and the adopted pulse compression scheme. The accelerating gradient is then about 28 MV/m, a smaller - and safer - gradient than the 35 MV/m gradient corresponding to the state of the art [1].

One peculiarity of the designed C-band structure is the optimized cell-to-cell iris and cell radii theoretically resulting in *identical* accelerating gradient for each regular cell of the structure. In addition, J-type coupler cells [2] are selected since this type is mechanically the least complex to

manufacture. Table 1 summarizes some main parameters of the designed C-band structure.

Table 1: Main parameters of the SwissFEL C-band structure

Parameter	Value
Operating frequency	5712.0 MHz
Phase advance per cell	$2\pi/3$
Total number of cells	113
Accelerating gradient	28 MV/m
Maximum pulse repetition frequency	100 Hz
Operating temperature	40 °C

DESIGN OF THE REGULAR CELLS

The regular cells of the designed structure have rounded outer walls to reduce the RF losses. For a defined cell-to-cell iris geometry, the quality factor of such cells is typically 10 % higher than the cells of a disk-loaded structure. At the manufacturing temperature of 20 °C, the length of each cell is 17.489 mm so as to operate the structure at 40 °C on the TM_{010} -like mode with a $2\pi/3$ phase advance per cell. The cell-to-cell iris thickness is 2.5 mm at 20 °C, a compromise between the desired high *effective* shunt impedance and the high mechanical rigidity, and is constant all along the structure. These irises have an elliptical cross-section with an aspect ratio of 1.375:1. Due to the impact of the longitudinal short-range wakefields on the whole linac beam dynamics, the average iris radius of the structure is required to be about 6.44 mm.

Since the regular cells that composed the accelerating structure are axisymmetric, their RF design can be performed with the 2D electromagnetic code SUPERFISH [3]. SUPERFISH provides modal standing-wave eigenfrequencies and field maps from which the travelling-wave fundamental RF mode parameters of a cell under design can be calculated: the group velocity v_g , the effective shunt impedance per unit length r and the quality factor Q . The 3D electromagnetic code HFSS [4] is used for cross-checking the cell design.

The design of a tapered structure, such as a constant-gradient type, can be performed by modelling at first a set of single cells with different iris radius, the cell radii being optimized to have the required phase advance at the design frequency. The upstream and downstream iris radii of each of these individual cells are equal. With the mode parameters of these sample cells and with fitting procedures, a *pure* constant-gradient travelling-wave structure can be synthesized with an average iris radius of 6.436 mm at 40 °C.

Let us consider the gradient $E_{acc,n}$ in the n th cell and

UPDATE ON THE COMMISSIONING EFFORT AT THE SwissFEL INJECTOR TEST FACILITY

T. Schietinger for the SwissFEL team,
Paul Scherrer Institut, CH-5232 Villigen PSI, Switzerland

Abstract

The SwissFEL Injector Test Facility at the Paul Scherrer Institute is the principal test bed and demonstration plant for the SwissFEL project, which aims at realizing a hard-X-ray Free Electron Laser by 2017. Since the spring of 2012 the photoinjector facility has been running with all RF cavities in full operation, allowing beam characterization at energies around 230 MeV with bunch charges between 10 and 200 pC. We give an overview of recent commissioning efforts with particular emphasis on efforts to optimize the emittance of the uncompressed beam.

INTRODUCTION AND MOTIVATION

The Paul Scherrer Institute (PSI) is planning an X-ray Free Electron Laser (FEL) user facility, which is to deliver ultrashort coherent photon pulses with wavelengths ranging between 0.1 and 0.7 nm by the year 2017 [1]. For cost and space reasons the driving linac is foreseen to feature a relatively modest end energy, thus calling for very low emittance to still achieve lasing at the target wavelengths. In preparation of SwissFEL, PSI is commissioning a 250 MeV photo-injector, which allows gaining experience with high-brightness electron beams and serves as a realistic test bed for crucial components in development for SwissFEL.

The SwissFEL Injector Test Facility [2] has been in operation in various configurations since 2010 [3]. Only recently the RF system was completed and the design energy of 250 MeV could be reached. At the same time, a flexible magnetic chicane, designed to compress the electron bunch longitudinally, was put into operation. The results of the first beam characterization around this energy as well as the first experience with the bunch compressor were reported in an earlier note [4]. In this paper we report on the ensuing work on emittance optimization with uncompressed beam, performed in a high-charge (about 200 pC) and low-charge (about 10 pC) mode.

MACHINE SETUP

Electrons are extracted from a copper cathode by a TW class drive laser, which is based on a frequency tripled Ti:sapphire chirped-pulse amplifier [5]. A pulse-stacking method, where the laser beam is sent through several birefringent BBO-crystals, is applied to approximate a flat-top longitudinal intensity profile. In the high-charge mode (typically 200 pC), the FWHM pulse length is 10.3 ps, in the low-charge mode (10 pC) it is 3.6 ps. Figure 1 shows a comparison of the two pulse shapes, as measured with a

cross-correlation method. Transverse pulse shaping is performed with an aperture mask. The laser spot diameter on the cathode is about 0.84 mm for the high-charge mode and about 0.38 mm for the low-charge mode. A smaller back up laser system based on a Nd:YLF amplifier is used for simple tasks not requiring high beam quality.

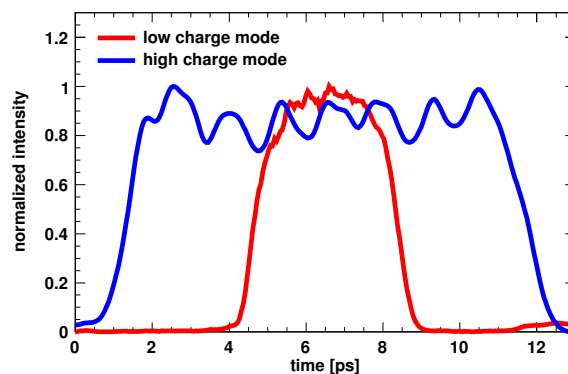


Figure 1: Laser longitudinal profile measurement for the two charge modes.

The first acceleration of the electrons to 7.1 MeV/c momentum is provided by the CTF3 Gun Nr. 5, an S-band RF gun originally built for the CLIC test facility at CERN [6].

A movable gun solenoid is used for initial focusing and optimization of the projected emittance. Energy and energy spread of the electrons emitted by the gun can be measured with a small dispersive beamline upstream of the booster.

The booster consists of four S-band travelling-wave structures, each surrounded by four solenoids for additional focusing. A fifth accelerating structure, operating at a harmonic frequency (X-band), was recently installed. Its purpose will be the approximate linearization of the longitudinal electron phase space for optimal bunch compression in the magnetic chicane following the booster. The bunch compressor was not in use (left in the straight position) during the measurements presented here, i.e., all results shown were obtained with uncompressed bunches.

An extensive diagnostic section equipped with a series of quadrupoles allows various kinds of optics-based emittance measurements. A transverse-deflecting RF cavity (S-band, five cells) is used for bunch length and slice-resolved measurements (resolution 20 fs). Transverse beam profiles are obtained by imaging the beam with either, for overview images, scintillating crystal screens (YAG or LuAG) or, for precision measurements, OTR screens (thin metal foils

COMPARATIVE DESIGN OF SINGLE PASS, PHOTO-CATHODE RF-LINAC FEL FOR THE THz FREQUENCY RANGE: SELF AMPLIFICATION vs. ENHANCED SUPER-RADIANCE

Yu. Lurie*, Y. Pinhasi, Ariel University Center of Samaria, Ariel, Israel

Abstract

Self amplified spontaneous emission and enhanced super-radiance are discussed and compared as possible configurations in the construction of a single-pass, photo-cathode RF-LINAC FEL source for THz radiation, being developed in Ariel University Center of Samaria. Numerical simulations carried out using 3D, space-frequency approach demonstrate the charge squared dependence of the radiation power in both cases, the characteristic typical to super-radiant emission. The comparison reveals a high efficiency of an enhanced super-radiance FEL, which however can only be achieved with ultra-short (the radiation wavelength long or shorter) drive electron beam bunches at a proper energy chirping.

INTRODUCTION

Tera-Hertz radiation is of interest for a basic science, medical and biological applications, spectrometry, remote detection, and etc. Free-electron lasers (FELs), which often can fit on or scale to the size of a table-top, are able to provide intense coherent electromagnetic radiation over a wide range of THz frequencies. In the present work, we consider a *single pass* FEL (without any oscillator resonant cavity) for production of such radiation. The FEL is designed to be driven by trains of short electron pulses, produced by a photo-injector RF-LINAC. The Israeli RF-LINAC FEL project under development is considered here as an example of such a radiation source [1]. Basic operational parameters of the FEL are given in table 1. Two possible configurations of the FEL are considered and compared in the work: a self amplified spontaneous emission (SASE) FEL, and an enhanced super-radiance (ESR) FEL [2]. The following discussion is concentrated just on the processes taking place in the FEL radiator section (wiggler), leaving aside any consideration of other FEL components.

SASE is a well-known FEL configuration, which is widely used at the far ultra-violet and X-ray wavelengths but also at the infra-red and THz frequencies. An initial spontaneous emission of electron beam is self amplified in SASE FELs, giving rise to a non-linear beam-radiation interaction which results in an exponential growth of the emission up to a saturation. ESR FEL [2] is supposed to utilize a constructive energy-phase correlation [3], what enhances the undulator super-radiant emission of short (a radiation wavelength long or shorter) electron pulses. Energy chirping is a well-known technique used in accelerator physics for density compression of electron pulses. In an

Table 1: Operational parameters of the THz FEL.

<u>Accelerator</u>	
Type:	Photo-injector RF-LINAC
Electron beam energy:	$E_k=3\div 6$ MeV
Pulse duration:	$T_b \gtrsim 0.1$ pS
Bunch charge:	$Q_b=30\text{-}500$ pC
<u>Wiggler</u>	
Magnetic induction:	$B_w=2$ kGauss
Period:	$\lambda_w=25$ mm
<u>Waveguide</u>	
Rectangular waveguide:	15×10 mm ²

ESR FEL, it is suggested to cause a longitudinal density compression of short electron pulses just inside the FEL interaction region, i.e. inside the wiggler.

THE MODEL

To simulate and compare between both FEL configurations, 3D space-frequency approach [4] was applied. The method is based on an expansion of the high-frequency electromagnetic field in terms of transverse eigen modes of the medium (free-space or a waveguide) in which the field is excited and propagates. The interaction between the electromagnetic field and the gain medium is fully described by a set of coupled equations, expressing the evolution of mode amplitudes along the interaction region. The model was realized in a numerical code WB3D and has been successfully applied to the analysis of various effects in FEL devices [5]-[11].

A drive electron beam pulse is considered in the model as a consisting of charged electron “macro-clusters” distributed over the beam. An initial distribution of the clusters in the beam is of great importance in simulations of radiation emission processes. Random Gauss longitudinal distribution of a fixed number ($N_q=300$) of equal charges was considered in the present work. Unfortunately this approach produces an artificial level of spontaneous emission, what prevents from a correct description of radiation build-up process. However this model seems to be adequate enough in description of a coherent emission of ultra-short (much shorter than the radiation wavelength) or highly-bunched electron beam pulses. To improve the description of spontaneous emission and of transition effects, the unified model of electron beam short noise from Ref. [12] was also applied to simulate the initial electron beam short noise in a wide frequency range.

*ylurie@ariel.ac.il

WARM BEAMLINES AND INFRASTRUCTURE IN THE EUROPEAN XFEL

M. Hüning, DESY, Hamburg, Germany

Abstract

The European XFEL is driven by a superconducting linear accelerator. In the main accelerator tunnel the accelerator modules will be suspended from the tunnel ceiling. The warm sections like bunch compressors will be installed on girders supported from the floor. The accelerator infrastructure like klystrons and electronic racks will be installed in the accelerator tunnel in close proximity to the electron beam line.

INTRODUCTION

The layout of the European XFEL [1] is depicted in figure 1. There are two injector linacs, each consisting of a normalconducting RF gun, one accelerating module with 8 superconducting cavities, one 3rd harmonic module with 8 superconducting cavities as well, and a warm beam line with laser heater and extensive beam diagnostics.

Two dogleg chicanes guide the beam onto the axis of the main linac. To transport the beam with relatively large energy spread, the chicanes consist of a large number of narrowly spaced dipoles, quadrupoles and sextupoles. At the entrance of the main linac tunnel follows the first bunch compressor chicane (B0). The chicane is C-shaped and deflects vertically. Subsequently the beam is matched into a string of four accelerator modules (L1) which is followed by the second bunch compressor (B1) and a diagnostic section for transverse and longitudinal beam diagnostics. This scheme is repeated once (L2, B2) before the beam is boosted to the final energy in the main linac. There is space reserved for an extension of the main linac. Still in the main linac tunnel the collimation section is located to limit the energy deviation and the maximum transverse excursions the beam might develop coming out of the main linac. Afterwards the beam is distributed to the undulator beam lines necessary for the SASE process.

and the fixture on the tunnel wall. The specifications for the tunnel straightness were comparatively relaxed, so that the ceiling frames have to allow for ± 50 mm adjustment both horizontally and vertically. This is achieved by making them out of two parts which are cut to length and shifted against each other before they are welded together in situ. The whole setup is welded to steel bands which were cast in the tubings of the tunnel wall at the time of manufacture. Including the suspension frames and the modules inner structure the beam axis is located 2.2 m from the tunnel ceiling.

Under the modules there is room for klystrons, high voltage pulse transformers, pumps, electronic racks, and other equipment. To protect the electronics from radiation caused by beam loss or dark current in the cavities the racks are shielded by concrete blocks. Two blocks are located in front of and behind the racks along the direction of the beam. A layer of blocks is put on top of the racks. The maximum top load on the racks needed to be increased to support the weight of the concrete. There is no shielding to the sides where the electronics are accessed. An assessment of the expected dose rate was done and a sideways shielding appeared unnecessary. The radiation dose in the racks however is monitored and should additional shielding be required additional shielding plates can be attached.

Short distance cable connections within one RF section comprised of 4 cryo modules are made on a cable tray on top of the shielding. Long distance connections are reduced to the absolute minimum and consist of fibre cables wherever possible. These connections are traced in a compartment below the tunnel floor.

The room under the tunnel floor is used for water supply lines, high voltage pulse cables for the klystrons, main lines of the electric supplies, and fibre cables.

COLD LINAC SECTIONS

The superconducting RF cryo modules in the main linac are suspended from the ceiling of the tunnel. This provides the shortest connection between the cavity axes

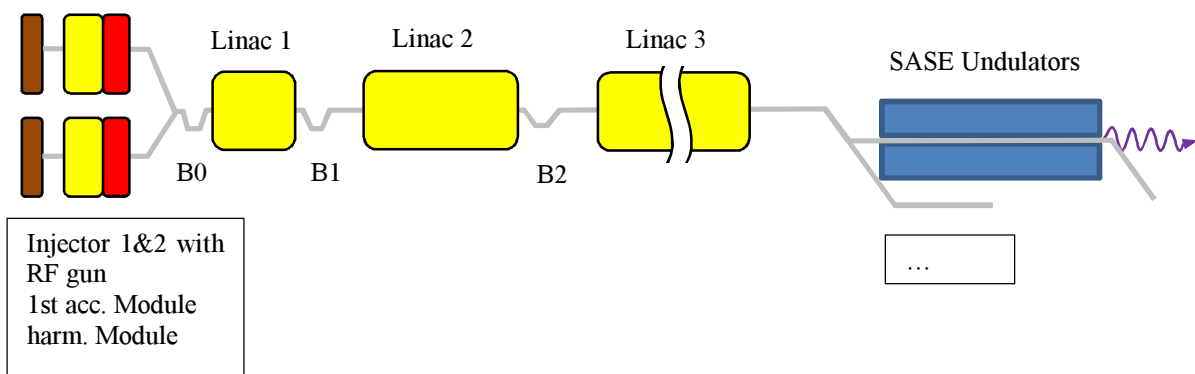


Figure 1: Layout of the European XFEL.

STUDY OF BEAM-BASED ALIGNMENT FOR SHANGHAI SOFT X-RAY FEL FACILITY

Duan Gu[#], D.Z.Huang, Meng Zhang, Qiang Gu, M.H.Zhao
 Shanghai Institute of Applied Physics, Shanghai 201800, China

Abstract

In linear accelerators, dispersion and transverse wakefield from alignment errors will lead to a significant emittance growth. The performance of the Free Electron Laser (FEL) process imposes stringent demands on the transverse trajectory, dispersion and emittance of the electron beam. So finding an effective Beam-Based Alignment(BBA) procedure is crucial for the success of Shanghai X-Ray FEL facility. This paper presents the preliminary study of different BBA method performances in SXFEL Linac. In addition, a MATLAB based simulation including quadrupole misalignment, dipole field errors and beam position monitor errors have been used to predict the orbit and emittance growth along the beamline and the required corrector current. Comparison with other codes is also presented.

INTRUDUCTION

As a critical development step towards constructing a hard X-ray FEL in China, a soft X-ray FEL facility (SXFEL) was proposed and will be constructed to verify the cascaded HGHG scheme and carry out the research on key technologies for X-Ray FEL. The SXFEL facility will be working at 9 nm soft X-ray band which consists of a 130MeV photo cathode injector, a main linac accelerating the beam to an energy of 840MeV, an undulator section with two stages of HGHG scheme and a diagnostic beamline. The local energy spread is 0.1%-0.15%, the peak current is about 600A and the normalized emittance is 2 mm·mrad[1].

In FEL facilities, misalignments between Quadrupoles and Beam Position Monitors(BPM) cause an increase of the transverse beam size and emittance which turns into an increase of normalized emittance. To keep the normalized emittance due to misalignment below 2 mm·rad, the average Quad-BPM misalignment in the linac must be smaller than 100um.

The traditional optical alignment can no longer meet such strict requirements, but a lot of analytical and numerical studies have been done and proved that Beam-Based Alignment technology can simultaneously eliminate the misalignment and dispersion in linac and undulator section, which obviously will leads to a much smaller emittance growth and transverse beam size. With the method above, a software based on MATLAB has been designed and simulation results have been compared with other software.

[#] gudian@sinap.ac.cn

BBA TECHNOLOGY OVERVIEW

Over past decade, a number of different realizations have been developed to measure the offset of magnetic center of quadrupole magnet[2][4]. Most techniques are based on a common approach, which is to change the quadrupole strength and measure the resulting deflection.

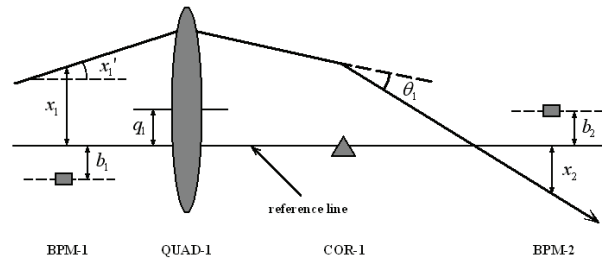


Figure 1: Common approach of BBA.

With respect to the reference line, m_i is the BPM reading at BPM-i. According to Linear optics theory (regardless wakefield effect and Quad-tilt), the transverse misalignment of upstream Quadrupole can be calculated using orbit response matrices, corrector values and inject parameters:

$$m_i = x_i - b_i = (x_i)_1 - b_i$$

$$x_i = R^{(B,i)} x_1 + \sum_j^{N_{C_i}} R^{(C_j,i)} c_j + \sum_j^{N_Q} R^{(Q_j,i)} (I - R^{(Q_j)}) q_j \quad (1)$$

Where b_i is BPM reading error due to off-axis between electronic center and geometric center. R is the 2×2 transport matrix from BPM-1 or corrector c_j or Q_j to BPM-i.

x_1 is initial incoming parameters, the unknown c_j the corrector strength and Q_j is Quadrupole misalignments, which are defined as:

$$x_1 = \begin{bmatrix} x_1 \\ x_1' \end{bmatrix}; c_j = \begin{bmatrix} 0 \\ \theta_j \end{bmatrix}; q_j = \begin{bmatrix} q_j \\ 0 \end{bmatrix} \quad (2)$$

Further more, we can simultaneously correct both orbit and dispersion using so called “Dispersion Free Steering” method. The optimal settings are calculated using the orbit and dispersion response matrices, which are defined as the shift of the orbit or dispersion due to corrector strength change:

$$R_{i,j} = \frac{\Delta x_i}{\Delta \theta_j}; D_{i,j} = \frac{\Delta d_i}{\Delta \theta_j} \quad (3)$$

SECOND CW AND LP OPERATION TEST OF XFEL PROTOTYPE CRYOMODULE

J. Sekutowicz, V. Ayvazyan, J. Branlard, M. Ebert, J. Eschke, A. Gössel, D. Kostin, F. Mittag, W. Merz, R. Onken, DESY, 22607 Hamburg, Germany
 W. Cichalewski, W. Jałmużna, A. Piotrowski, K. Przygoda, TUL, 90-924 Łódź, Poland
 K. Czuba, Ł. Zembala, WUT, 00-665 Warsaw, Poland
 I. Kudla, J. Szewiński, NCNR, 05-400 Świerk-Otwock, Poland

Abstract

In summer 2011, we performed the first test of continuous wave and long pulse operation of the XFEL prototype cryomodule [1], which originally has been designed for a short pulse operation. In April and June 2012, the second test took place, with the next prototype. For that test, cooling in the cryomodule was improved and new LLRF system has been implemented. In this contribution we discuss results of the second test of these new types of operation, which can in the future extend flexibility in the time structure of the electron and photon beams of the European XFEL facility.

INTRODUCTION

The XFEL cryomodules are based on TESLA collider cryomodules [2] and as such, they still have many features of that original design from early 90's. The TESLA cryomodules have been compromised to keep the cost possibly low. In these 8-cavity containers, unlike for example, in 2-cavity HERA cryomodules, only cells of cavities are immersed in the superfluid liquid helium (LHe). The energy dissipated in their superconducting surface is transferred to the LHe bath thru ~3 mm thick high purity Nb wall. The situation is very different for so-called end-groups, the end-beam tubes with attached input couplers and/or HOM couplers, located outside the LHe vessels. Energy dissipated in the end-groups is transported to the helium bath via much longer distance and much higher thermal resistance, which depends on the heat conductivity of niobium the end-groups are made of. The losses are often enhanced on the HOM antennae, which are made of niobium and should stay superconducting for an operation. The TESLA cavity and cryomodule designs prove to operate very successfully in the XFEL nominal short pulse mode, when the duty factor (DF) does not exceed 1.3 %, RF-pulses are ca. 1.3 ms long and their rep-rate is 10 Hz. This operation is demonstrated since many years at FLASH, which linac comprises 56 TESLA cavities.

A continuous improvement in the performance of superconducting 9-cell TESLA cavities, especially the remarkable increase of the intrinsic quality factor, and minor cooling improvements for the end-groups, should make possible operation of the XFEL cryomodules in continuous wave (cw) mode at gradients up to ~7.5 MV/m and in the long pulse (lp) mode up to the XFEL nominal gradient $E_{acc} = 23.4$ MV/m. These estimated gradients result from splitting of the XFEL linac in to 12-

cryomodule long cryogenic strings, which leads to the maximum allowed total 2K (1.8 K) heat load (HL) per cryomodule of 20 W. For the nominal operation, the estimated maximum 2 K heat load is ca. 11 W. The maximum gradient of 23.4 MV/m in the lp-mode seems to be achievable for up to 100 ms long RF-pulses.

The new operation modes will allow for more flexibility in the time structure of both the electron and photon beam. In the nominal operation, the intra RF-pulse bunch-to-bunch spacing is 220 ns. The new operation modes will offer significantly larger bunch spacing, of the order of few microseconds, keeping the average XFEL brilliance superior to other facilities. The enlarged spacing is advantageous. For example, it allows for less expensive detectors. Further, in the new operation modes, the photon burst rep-rate can be in the kHz range. This will make optical lasers for pump-and-probe experiments less technically challenging, still providing ca. 1000 photon-bursts in the cw operation and ca. 100 at the maximum electron beam energy in the lp runs. For the nominal short pulse operation, one will have only 10 bursts /s.

PREPARATION OF THE SECOND TEST

Thermal improvements in cryomodule

Two thermal improvements were done in cryomodule PXFEL3_1, which was foreseen for the tests in 2012. Each made cooling of the HOM antennae more effective. At first, five cavities could be equipped with prototypes of the high conduction HOM feedthrough, in which low conduction standard alumina window was replaced with the sapphire window and the niobium antenna was brazed to the inner-conductor pin. Secondly, all sixteen HOM feedthroughs were thermally connected, with copper strips, directly to the 2 K tube.

Cavity performance and Q_{ext} of input couplers

Prior to the cw/lp studies, the cryomodule was tested in the nominal mode. For that test, Q_{ext} of all input couplers had been set to $3 \cdot 10^6$. The test showed malfunctioning of two cavities. Cavity No 7 had strongly detuned HOM coupler and could be operated cw up to 4 MV/m. At this gradient, the out-coupled power was already 24 W, from which 20 % was dissipated in the cable, contributing significantly to the total HL at 2 K. Cavity No 8 showed strong electron emission, leading in the cw operation to enhanced HL and to quenching already at 9.3 MV/m.

For the cw/lp tests Q_{ext} of all cavities was set to $1.5 \cdot 10^7$, which corresponds to the 3 dB resonance width of 87 Hz.

STATUS OF THE EUROPEAN XFEL 3.9 GHZ SYSTEM

P. Pierini[#], A. Bosotti, P. Michelato, L. Monaco, C. Pagani, R. Paparella, D. Sertore,
INFN Milano/LASA, Italy
E. Vogel, DESY, Germany
E. Harms, FNAL, USA

Abstract

The third harmonic system at 3.9 GHz of the European XFEL injector section will linearize the bunch RF curvature, induced by first accelerating module, before the first compression stage. This paper presents qualification tests on cavity prototypes and the on-going activities towards the realization of the third harmonic section of the European XFEL in view of its commissioning in 2014.

INTRODUCTION

The European XFEL injector foresees a third harmonic section after the RF photocathode gun and the first 1.3 GHz accelerating module [1-3], just before the first bunch compression stage. The 3rd harmonic system is similar to the ACC39 module built by FNAL [4-7] and nowadays operated at FLASH in DESY Hamburg.

The XFEL 8-cavity module will provide a maximum voltage of 40 MV, with gradients well within the cavity performances already achieved by the FLASH experience.

This paper reports on the status of the main on-going activities related to different components of the 3.9 GHz section, namely testing of prototype cavities, procurement of components and finalization of the 3rd harmonic system design.

CAVITY PROTOTYPES

The baseline fabrication process for the 3.9 GHz resonators is based on the experience earned by the production of the 1.3 GHz TTF cavities. Moreover, since the maximum gradient required for these kinds of resonators is 20 MV/m, we chose a standard chemical processing (BCP) as bulk treatment. Minor adaptations were performed to the FLASH FNAL cavity design, mainly in order to conform to the different module design or to adapt them to standard XFEL components (e.g. flanged HOM/PU feedthroughs). In preparation for the realization of the final system, three full dressed prototype cavities (3HZ01-3) have been tendered for fabrication and processing at E. Zanon SpA, one of the qualified vendors for the XFEL main linac resonators [2].

To finalize the production phase, Cu and Nb mockups were used. After the mechanical fabrication, a bulk BCP etched 150 μm from the inner surface and an 800 °C UHV oven treatment (at DESY) was performed to remove the hydrogen content. The cavities were tuned to a final Field Flatness to > 95 %, with a length spread of ± 0.4 mm from

the nominal dimensions, well within the structure length specifications. Each cavity has then undergone the final light BCP chemistry (10-30 μm), HPRs and final preparation for cold vertical test.

After fabrication and processing, vertical testing of the cavities has been performed at INFN Milano - LASA, where the cavity preparation area and vertical RF test station was refurbished, adapted for the 1.3/3.9 GHz XFEL workprogram and qualified through test of 1.3 GHz single cells of proven performances provided by DESY.

TEST RESULTS

3HZ01

This was the first 3.9 GHz cavity tested at LASA with the upgraded infrastructure. Besides few glitches due the infrastructure commissioning, an error in the variable coupler setup prevented a consistent RF characterization of the cavity. We had indications of high losses, possibly located in the antenna region, but the absence of a complete temperature mapping of the cavity prevent its confirmation.

Moreover, due to the new changes in the cryogenic system and as a measure to limit LHe consumption, we performed LN₂ precooling, resulting in a long permanence of the cavity between 77 K and 150 K, possibly driving “Q-disease” effects that were concurrent, in our interpretation, with antenna losses.

To rule this effect out in preparation for a new test, the cavity has been newly heat-treated after warmup and it is now waiting the final chemistry and further testing.

Although the first test was not fully successful, it was a very important step for the final commissioning of the 3.9 GHz test infrastructure and highlighted the need for improved diagnostics. During the cryogenic operation, the overall static losses of the test stand were measured at values lower than 1 W. The lesson learned in this first cooldown and low He consumption required for operation allowed avoiding LN₂ precooling in the successive tests.

3HZ02

After the commissioning of the facility with the 3HZ01 test, the RF power feed was changed to a fix coupling scheme through the cavity main coupler port. Cavity 3HZ02 was therefore sent to measurement after a light final BCP chemistry of 10 μm . For this test temperature sensors were installed on the cavity.

After the subcooling from 4.2 K to 2.0 K the surface resistance reached a final value of about 320 n Ω . The cavity reached a maximum field of 15 MV/m with a Q₀ of

[#]paolo.pierini@mi.infn.it

STUDY OF PLASMA EFFECT IN LONGITUDINAL SPACE CHARGE INDUCED MICROBUNCHING INSTABILITY*

Dazhang Huang[†], Qiang Gu, SINAP, Shanghai, 201800, China, P. R.
King-Yuen Ng[‡], Fermilab, Batavia, IL 60616, USA

Abstract

Microbunching instability (μ BI) usually exists in the LINAC of a free electron laser facility. If it is not well-controlled, the beam quality will be seriously damaged and the machine will not operate properly. In many cases, the longitudinal space charge (LSC) is a dominant factor that generates the instability; therefore its contribution must be studied in details. The current model of the LSC impedance [1] derived from the fundamental electromagnetic theory [2] has been widely used to explain the physics of the LSC-induced μ BI. [3] However, in the case of highly bright electron beams, the plasma effect may also play a role. In this article, the basic model of the LSC impedance including the plasma effect is constructed by solving Vlasov and Poisson equations in the 6-D phase space, and preliminary investigation is carried out to study the modification to the instability gain. The solution indicates that the μ BI gain depends not only on the spatial information of the beam, but also on the velocity (momentum) and time information. The comparison of the gains of the μ BI in the LINAC of Shanghai soft X-ray Free Electron Laser Facility (SXFEL) computed by various methods is given and the discrepancy is illustrated.

INTRODUCTION

The possibility of oscillation in a plasma due to local separation of charges and the consequent restoring forces was discussed by J. D. Jackson long time ago. [4] The theory is based on a neutral plasma, which has both the positively (ion) and negatively (electron) charged components. For a charged particle beam in an accelerator, although it is not neutral in terms of charges, there is still density fluctuation due to the graininess of the individual particles — in our case, the individual electrons. Such graininess is usually smoothed out in the fluid model and ignored in most computations. In a highly intensive beam, however, it may introduce the “plasma-like” oscillation (for convenience, “plasma oscillation” is used hereafter), and must be investigated in details in order to reveal its magnitude and to discover its physics. Similar discussions in the 2-D phase space for this effects on the free electron laser have been addressed by Kim, et. al. [5]

In this article, we start our discussions in the 6-D phase space by employing Vlasov and Poisson (Gauss) equations,

* Work supported by National Science Foundation of China (NSFC), Project No. 11275253, and US DOE, contract DE-FG02-92ER40747.

[†] huangdazhang@sinap.ac.cn

[‡] ng@final.gov

which describe the evolution of the distribution function of the electron bunch and the electric field induced by the charge distribution. We then use a method similar to Jackson's [4] to linearize the Vlasov equation and obtain the solution of the initial-value problem. The solution includes the contributions from both the perturbed and unperturbed parts of the initial distribution. As the result, the contribution from the velocity distribution is also included. From the solution, we see that the plasma oscillation introduces a “relative dielectric factor (permittivity)” ϵ_r , and also an extra factor coming from the initial velocity distribution.

SOLUTION OF INITIAL-VALUE PROBLEM

We carry out the investigations with the equations describing the evolution of beam distribution under the influence of the electromagnetic force. The discussion is in laboratory frame hereafter. In cylindrical coordinates system, the linearized Vlasov-Poisson equation and the Poisson (Gauss) equation can be written:

$$\frac{\partial f_1}{\partial t} + v_z \frac{\partial f_1}{\partial z} + v_\perp \frac{\partial f_1}{\partial r} - \frac{eE_z}{\gamma m} \frac{\partial f_0}{\partial v_z} + \frac{F_\perp}{\gamma m} \frac{\partial f_0}{\partial v_\perp} = 0, \quad (1)$$

$$\frac{\partial E_z}{\partial z} + \frac{1}{r} \frac{\partial}{\partial r}(rE_r) = -\frac{e}{\epsilon_0} \int f_1 dv_z, \quad (2)$$

where $-e$ is charge of an electron, $f(t, \vec{r}, \vec{v}) = f_0(t, \vec{r}, \vec{v}) + f_1(t, \vec{r}, \vec{v})$, with f_0 being the unperturbed background of the beam and f_1 the density perturbation due to plasma oscillation. We assume that f_0 , f_1 and \vec{E} have no azimuthal dependence, which is reasonable. The Gauss's law or Poisson equation, Eq. (2), will be solved in the particles' rest frame and then Lorentz transformed to the lab frame in the next section.

Since the transverse velocity v_\perp is small, we can assume $v_z \approx v$ and $F_\perp \ll F_z$. Then Eq. (1) simplifies to

$$\frac{\partial f_1}{\partial t} + v \frac{\partial f_1}{\partial z} - \frac{eE_z}{\gamma m} \frac{\partial f_0}{\partial v} = 0. \quad (3)$$

Let us focus on Eqs. (3) and (2). Following Jackson, [4] we perform Fourier transform in t and Laplace transform in z on Eq. (3), and integrate by parts to obtain

$$\int dz \left[e^{-ikz+i\omega t} f_1(v, z, t) \right]_{t=0}^{t=\infty} + \int_{-\infty}^{\infty} dz \int_0^{\infty} e^{-ikz+i\omega t} dt \times \left[(-i\omega + ikv)f_1 - \frac{e}{\gamma m} \frac{\partial f_0}{\partial v} E \right] = 0. \quad (4)$$

A PASSIVE LINEARIZER FOR BUNCH COMPRESSION

Q. Gu#, M. Zhang, M. H. Zhao, SINAP, Shanghai, China

Abstract

In high gain free electron laser (FEL) facility design and operation, a high bunch current is required to get lasing with a reasonable gain length. Because of the current limitation of the electron source due to the space charge effect, a compression system is used to compress the electron beam to the exact current needed. Before the bunch compression, the nonlinear energy spread due to the finite bunch length should be compensated; otherwise the longitudinal profile of bunch will be badly distorted. Usually an X band accelerating structure is used to compensate the nonlinear energy spread while decelerating the beam. But for UV FEL facility, the X band system is too expensive comparing to other system. In this paper, we present a corrugated structure as a passive linearizer, and the preliminary study of the beam dynamics is also shown.

INTRODUCTION

In a high gain free electron laser facility, the electron beam will be accelerated and compressed before lasing. Because of the finite length of the electron beam and the sinusoidal accelerating voltage of the RF field, a nonlinear energy chirp has been induced. With this energy chirp, a ramped or a spiky [1] [2] current profile will be generated after the compressor, which will cause the partial lasing to the whole bunch and prevent getting higher peak current. To correct the nonlinear energy chirp, a higher harmonic RF linearizer was proposed and successfully used [2] [3] [4].

The corrugated structure is a metallic, cylindrical tube with periodic, shallow corrugations (see Figure 1). This structure was used for a model of roughness wake, a source of the THz radiation [5] and a dechirper for the high gain FELs [6]. By choosing the parameters of the structure, one can change both the wake length and the amplitude of the wake. With these two wake function parameters, one can easily match the duration (bunch length) and the amplitude of the nonlinear energy chirp.

In this paper, we will report the principle to setup a passive linearizer and the application to the Dalian UV FEL facility.

THE CORRUGATED STRUCTURE AS AN ENERGY CHIRP LINEARIZER

The structure of the corrugated cylindrical pipe is shown in Figure 1. The pipe radius is a , the corrugation period is p , the corrugation gap is g , and the corrugation depth is δ , while $p, \delta \ll a$, and $\delta \gg p$. The earlier work on corrugated structure [7] [8] [9] has shown that when a short, ultra-relativistic charged beam passes through the structure, a strong fundamental mode with a frequency

above the cut-off frequency of the cylindrical pipe will be excited. The longitudinal point charge wakefield of this mode is approximately written as,

$$W(s) = 2 \cdot \chi \cdot H(s) \cdot \cos(k \cdot s). \quad (1)$$

The χ is the loss fact by

$$\chi = \frac{Z_0 \cdot c}{2 \cdot \pi \cdot a'} \quad (2)$$

the $H(s)$ is a unit step function by,

$$H(s) = \begin{cases} 1, & s \geq 0 \\ 0, & s < 0 \end{cases} \quad (3)$$

and the k is the wave number of the fundamental mode by

$$k = \sqrt{\frac{2 \cdot p}{a \cdot \delta \cdot g}} \quad (4)$$

The wake potential is given by the convolution

$$W_\lambda(s) = \int W(s') \cdot \lambda(s - s') ds', \quad (5)$$

the $\lambda(s)$ is the line charge density of the charged beam. And the energy loss along the beam can be easily calculated as

$$E_{loss}(s) = W(s) \cdot \lambda(s). \quad (6)$$

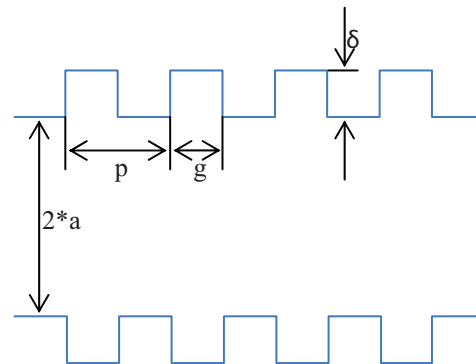


Figure 1: The drawing of the corrugated structure

Considering a beam with infinitesimal rising time and falling time, and with a length of l without any current fluctuation, we choose the wave length of the point charge wake potential twice as the bunch length. We simplify the calculation by only considering the field within the beam. The result is written as

$$E_{loss}(s) = -2 \cdot \chi \cdot \lambda \cdot \frac{l}{\pi} \cdot \sin\left(\frac{\pi}{l} \cdot s\right). \quad (7)$$

#guqiang@sinap.ac.cn

THE OPTIMIZATION OF RF DEFLECTOR INPUT POWER COUPLER

A. Smirnov, O. Adonev, P. Binyukov, N. Sobenin,
NRNU MEPhI, Moscow, 115409, Kashirskoe sh., 31, Russia

Abstract

This paper concerns the investigation of different types of input power cell for S-band RF electron deflector. This device serving for slice emittance diagnostics is a disc-loaded waveguide which operates with TE₁₁-like wave in travelling wave regime with 120 deg phase shift per cell. Since this deflector meets the restriction on its length and has to provide high enough deflecting potential to a particle during its flight time it is significant to increase the transversal field strength in coupling cell or to shorten it so that the deflecting potential remains constant. The total structure consists of 14 regular cells and two couplers. As it is now all cells have the same length equal to D=33.34 mm and the field in couplers is lower than that of regular cells. In this paper different lengths are considered and numerically simulated in order to choose the best one.

INTRODUCTION

A deflecting voltage seen by a particle travelling along the axis of a disc-loaded waveguide driven with dipole TE₁₁ (Fig. 1) mode can be calculated using transversal values of on-axis electric and magnetic fields or using longitudinal value of the electric field at some offset from the axis (Panofsky-Wenzel theorem) [1].

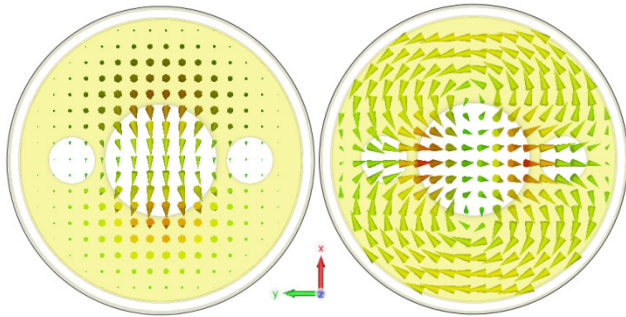


Figure 1: Electric (left) and magnetic (right) fields of TE₁₁ mode.

In the first method, we can use x -component (vertical) of E-field and y -component (horizontal) of H-field distributions along the axis z , since the particle experiences actions from both fields. Electric and magnetic fields are orthogonal to each other. The equivalent transversal deflecting field can be derived from the expression of Lorentz force $F_L = eE_d = e(E_x \pm vB_y)$:

$$\dot{E}_d(z) = \dot{E}_x(z) \pm \mu_0 \beta c \dot{H}_y(z), \quad (1)$$

where (and further on) the sign ‘ \pm ’ refers to the interplay of the particle and the wave propagation directions.

According to time dependence of field components as $\exp(i[\omega t + \theta])$, this gives the equation for the transversal potential that is gathered by electron on a path from $z=0$ to $z=L$ (structure length):

$$V_d(\theta) = \int_0^L \Re(\dot{E}_d(z)) dz = \int_0^L |\dot{E}_d(z)| \cos\left(\varphi_{E_d}(z) \pm \frac{2\pi}{\lambda} z + \theta\right) dz, \quad (2)$$

where $\lambda=c/f$ is the wavelength and θ is the initial phase of the deflecting voltage with respect to particle. Now by varying θ through the range from 0 to 2π one can find the maximal value of the deflecting voltage V_{dmax} .

An approach through Panofsky-Wenzel theorem requires longitudinal component of the electric field only, which is taken at some small enough vertical offset from the structure axis $a - E_z(z, x=a)$. The transverse deflecting field in this case is

$$\dot{E}^{PW}(\theta) = \frac{\lambda}{2\pi} \frac{\partial \dot{E}_z(z)}{\partial x} \Big|_{x=0} \approx \frac{\lambda \dot{E}_z(z, x=a)}{2\pi a} \quad (3)$$

due to the fact that longitudinal on-axis field $E_z(x=0)$ is nil for hybrid waves. And the corresponding potential V_{dmax} can be found from the following expression by varying θ from 0 to 2π :

$$V_d(\theta) = \frac{\lambda}{2\pi a} \times \int_0^L |\dot{E}_z(z, x=a)| \cos\left(\varphi_{E_z}(z, x=a) \pm \frac{2\pi}{\lambda} z + \theta\right) dz. \quad (4)$$

Both dependencies (2) and (4) are sin-shaped and shifted with 90° , which is result of Maxwell equations.

TRANSVERSE DEFLECTING STRUCTURE

The structure layout [2] is presented in Fig.2. Cell irises have two additional holes used both for coupling between the cells and for stabilization of the mode polarization plane. The deflector consists of 14 regular cells with length of D=33.34mm (required for a phase shift of 120° per cell) and two power couplers, therefore total length is $16D=533.44$ mm. It operates at frequency of 3 GHz. The input power is 2.5 MW, which provides total deflecting

MEASUREMENTS OF A REDUCED ENERGY SPREAD OF A RECIRCULATING LINAC BY NON-ISOCRONOUS BEAM DYNAMICS*

F. Hug[#], C. Burandt, M. Konrad, N. Pietralla, TU Darmstadt, Darmstadt, Germany
 R. Eichhorn, Cornell University, Ithaca, NY, USA

Abstract

The Superconducting Linear Accelerator S-DALINAC at the University of Darmstadt (Germany) is a recirculating linac with two recirculations providing beams for measurements in nuclear physics at small momentum transfers. For these experiments an energy spread of better than 10^{-4} (rms) is needed. Currently acceleration in the linac section is done on crest of the accelerating field. The recirculation path is operated achromatic and isochronous. In this recirculation scheme the energy spread of the resulting beam in the ideal case is determined by the electron bunch length. Taking into account the stability of the RF system the energy spread increases drastically to more than 10^{-3} (rms).

We will present a new non-isochronous recirculation scheme which helps cancelling out these errors coming from the RF-jitters. This scheme uses longitudinal dispersion in the recirculation paths and an acceleration off-crest on a certain phase with respect to the maximum. We will present results of the commissioning of the new system including measurements of the longitudinal dispersion in the recirculation arcs as well as measurements of the resulting energy spread using an electron spectrometer.

INTRODUCTION

Operating since 1987 the Superconducting DArmstadt LINear Accelerator (S-DALINAC) is used as a source for nuclear- and astrophysical experiments at the university of Darmstadt [1]. It can accelerate beams of either unpolarized or polarized electrons [2] to beam energies of 1 up to 130 MeV with beam currents from several pA up to 60 μ A. The layout of the S-DALINAC is shown in Fig. 1.

Acceleration in the injector and main linac is done by superconducting elliptical cavities with a quality factor of $Q_0 \approx 10^9$. These cavities are operating at a frequency of 3 GHz with a maximum accelerating gradient of 5 MV/m.

The main linac consists of 8 standard 20-cell cavities and can provide an energy gain of 40 MeV. By recirculating the beam two times the maximum energy of 130 MeV can be achieved. In the adjacent experimental hall this beam can be used for different experiments such as electron scattering in two electron spectrometers or experiments with tagged photons. For these experiments an energy spread of $\pm 1 \cdot 10^{-4}$ is required.

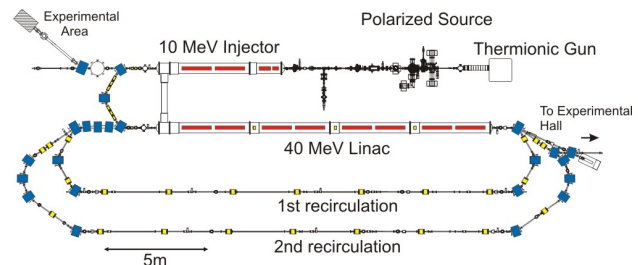


Figure 1: Floor plan of the S-DALINAC.

LONGITUDINAL BEAM DYNAMICS

The S-DALINAC is designed to use an isochronous recirculation scheme originally. On an isochronous working point the electrons are accelerated in the maximum of the accelerating field (on crest) in every turn and the bunch length is kept constantly small ($\pm 1^\circ$) using achromatic and isochronous recirculation paths. Isochronicity is a property of beam optics and can be described as $dl/dE = 0$ meaning that the length of the flight path of all electrons is independent from their energy. Acceleration on crest of the RF-field is the common mode for linear accelerators. Usually amplitude and phase jitters of the cavities are not correlated and the resulting energy spread is mainly determined by the short bunch length. In a recirculating linac the errors can add up coherently throughout the linac passages in a way that every electron sees the same errors in all passes through the linac due to the large time constant of field variations in the superconducting cavities compared to the short time of flight of the ultra relativistic electrons through the linac.

A way to overcome these correlated errors is changing the longitudinal working point to a non-isochronous one. This is the common operation mode for synchrotrons or microtrons. In a non-isochronous recirculation scheme the recirculation paths provide a longitudinal dispersion $dl/dE = D_L \neq 0$ while the accelerating field is operated at a certain synchrotron phase $\Phi_S \neq 0$ (on edge). The electrons then perform synchrotron oscillations in the longitudinal phase space. Compared to synchrotrons a quite large phase advance per turn is needed to cancel out the RF jitters. In fact a half or full integer number of synchrotron oscillations leads to the best energy resolution of the extracted beam in a way that the resulting energy spread at extraction is only determined by the energy spread at injection while the errors caused by the RF jitters of the main linac are cancelled out. [3,4]

The usability of such a non-isochronous recirculation scheme at the S-DALINAC has been verified already by numerical simulations (see Fig. 2). The new longitudinal

* Work supported by DFG through SFB 634
[#] hug@ikp.tu-darmstadt.de

STATUS OF THE RARE ISOTOPE SCIENCE PROJECT IN KOREA*

J. W. Kim for the RISP, Institute for Basic Science, Daejeon, Korea

Abstract

A heavy-ion accelerator facility has been designed in Korea for the production of rare isotope beams under the rare isotope science project (RISP). The project is funded and officially started in the end of 2011. The accelerator complex is composed of three main accelerators: a superconducting linac to use the in-flight fragmentation (IF) method to generate isotope beams, a 70 MeV proton cyclotron for the ISOL method, and a superconducting post accelerator for re-acceleration of rare isotope beams produced by ISOL to the energy range of 18 MeV/u. Minimum energy of a U beam requested for the IF driver is 200 MeV/u at the beam power of 400 kW. This facility will be unique in the aspect that the IF and ISOL systems can be combined to produce extreme exotic beams. In addition, standalone operation of each accelerator will accommodate diverse users in the beam application fields as well as in nuclear physics.

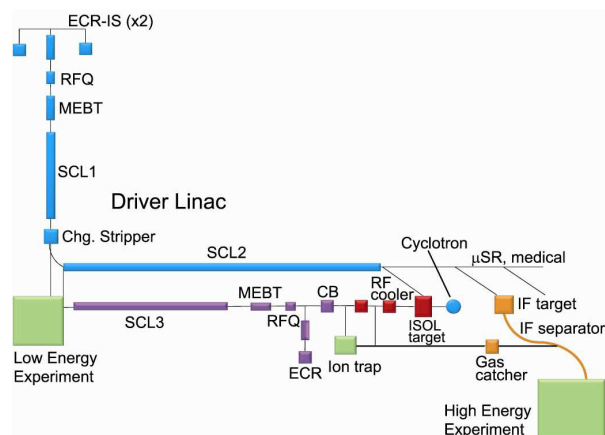


Figure 1: Conceptual layout of the heavy-ion accelerator complex of the RISP.

INTRODUCTION

A heavy ion accelerator facility is being designed in Korea to produce rare isotope beams by using both in-flight fragmentation (IF) and ISOL methods. The project is named as rare isotope science project (RISP), and was started from the end of 2011 after a period of conceptual design [1]. A conceptual layout of the facility is shown in Fig. 1.

The main accelerator is a superconducting linac, which can accelerate a ^{238}U beam to 200 MeV/u and protons to 600 MeV. It is divided into two sections, SCL1 before charge stripping at the energy of 18.5 MeV/u and SCL2 after the stripping. These parameters of the primary beam are similar to those of the FRIB project in the US [2]. A major difference from the planned FRIB facility is the use of an independent ISOL driver. A 70-MeV H⁻ cyclotron will be employed to drive a 70-kW ISOL target system. The radioisotope beam extracted from the target will be further ionized in EBIS [3] or ECR ion sources to achieve a higher charge state before beam injection to the post accelerator (SLC3), which is also a superconducting linac to accelerate a beam up to the energy of around 18 MeV/u. Furthermore this isotope beam produced by ISOL can be accelerated using the SCL2 for the IF system to produce more exotic isotope beams.

When the primary beam passes through a thin target, fast radioisotope beams are produced by the projectile fragmentation and fission mechanisms. Then the following isotope-beam selection system utilizes $B\rho$ -energy loss- $B\rho$ analysis to separate and identify an isotope beam of interest. This fast isotope beam can be stopped using a gas stopper, and the charge state of the beam extracted from the gas stopper can be boosted like in the ISOL method before being injected into the post accelerator. A main advantage of the IF method is that it is not subject to chemistry of the ions unlike in the ISOL. Hence rare isotope beams in a wider range can be produced.

The experimental areas are divided depending on the energy of the beam delivered as shown in Fig. 1. Different kinds of spectrometers are planned to be facilitated for nuclear reaction and structural studies [4]. In addition, the facility will accommodate beam users in various application fields including biomedical and material sciences using both stable and isotope beams. The stopping location of an isotope beam can be accurately traced by radiation measurement, which is a notable advantage of radioactive beam and is to be explored in some applications.

ACCELERATOR COMPLEX

To produce highly charged ion beams, a superconducting ECR ion source similar to the VENUS source of the LBL [5] is to be developed. To meet the goal of 400-kW beam power for U beam, envisioned scheme was to accelerate a beam in two charge states of 34+ and

*Work supported by the Rare Isotope Science Project of the MEST and National Research Foundation of Korea.
jwkim@ibs.re.kr

BEAM INTENSITY AND ENERGY CONTROL FOR THE SPIRAL2 FACILITY

C. Jamet, T. Andre, B. Ducoudret, C. Doutressoulles, W. Le Coz, G. Ledu, S. Leloir, S. Loret,
GANIL, Caen, France

Abstract

The first part of the SPIRAL2 facility, which entered last year in the construction phase at GANIL in France, consists of an ion source, a deuteron and a proton source, a RFQ and a superconducting linear accelerator delivering high intensities, up to 5 mA and 40 MeV for the deuteron beams.

Diagnostic developments have been done to control both beam intensity and energy by non-interceptive methods at the linac exit. The beam current is measured by using couples of ACCT-DCCT installed along the lines and the beam energy by using a time of flight device.

This paper gives explanations about the technical solutions, the results and resolutions for measuring and controlling the beam.

ACCELERATOR CHARACTERISTICS

The SPIRAL2 accelerator, an extension of the GANIL laboratory is under construction at CAEN in France [1].

The beams accelerated by the Linac will range in intensity from a few 10 μ A to 1mA for ions, up to 5 mA for deuterons, and in energy from 0.75 up to 14.5 MeV/A for ions, 20 MeV/A for deuterons and 33 MeV for protons.

BEAM CONTROLS

In order to control these beam characteristics, measuring chains and controlling devices are under development by the Electronic Machine Group at GANIL.

Controls of the beam intensity, efficiency, energy and beam power, will be necessary for the kick-off authorization issue by the French Nuclear Safety Authority (ASN).

These surveillances are part of the Machine Protection System (MPS) [2] and have to bring:

- A thermal protection, against direct beam damages, requiring a fast response time (few 10 μ s)
- An enlarged protection which controls the operation domain from the safety point of view.

Characteristics of the Beam Intensity

Intensity range:

- Few 10 μ A to 5mA

Duty cycle of the slow chopper:

- From 1/10000 to 1/1 (frequency of 1Hz from 1/10000 to 1/2000 and a frequency of 5Hz from 1/2000 to 1/1)

Duty cycle of the fast chopper:

- From 1/1000 to 1/100 (repetition frequency from 8,88 kHz to 880 kHz)

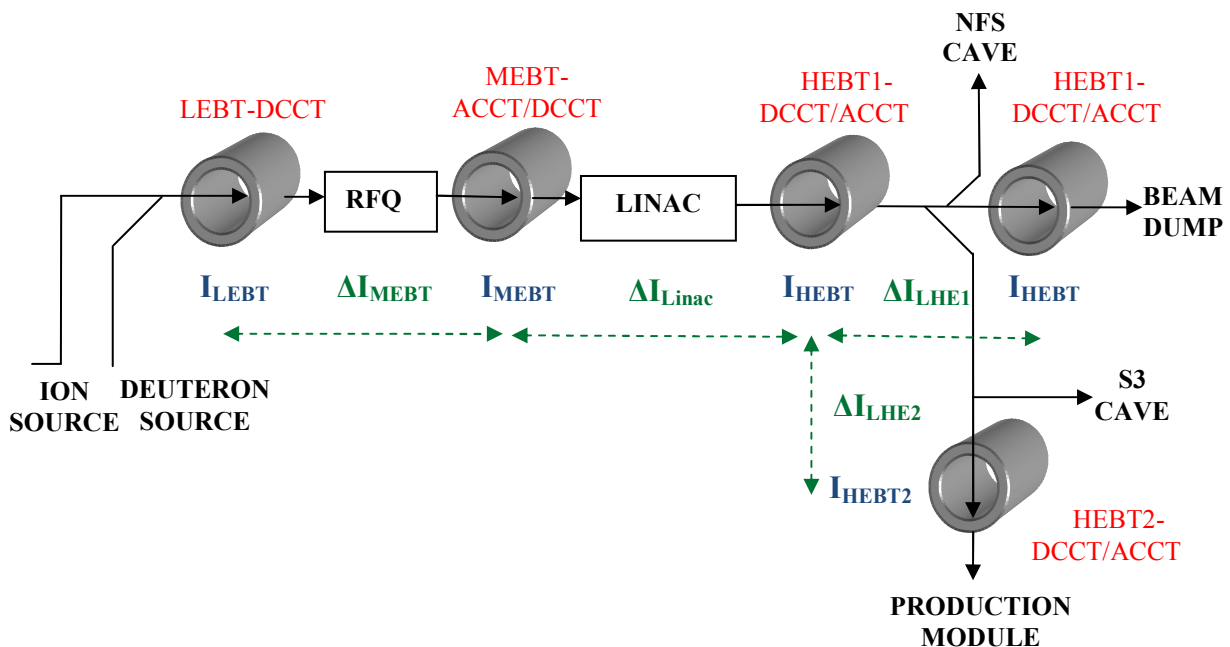


Figure 1: Scheme of the beam intensity and the beam efficiency control.

OVERVIEW OF THE RISP SUPERCONDUCTING LINAC

D. Jeon[#], H.J. Kim, H.C. Jung, S.K. Kim, Y.Y. Lee, S. Matlabjon, H.J. Kim, C.J. Choi, J. Joo, J.H. Lee, Y. Kim, G.T. Park, J. Song, RISP, Institute for Basic Science, Daejeon, Republic of Korea

Abstract

The Rare Isotope Science Project (RISP) is launched in Korea to build the IF and ISOL facilities to support researches in various science fields. Superconducting linac with 200 MeV/u, 400 kW is the driver for the IF (In-flight Fragmentation) facility and the 70 MeV, 70 kW cyclotron is the driver for the ISOL (Isotope Separation On-Line) facility. These facilities are to produce high intensity RI beams with high purity near the neutron-rich drip line. Design aspects of the driver SCL is presented.

INTRODUCTION

The International Science and Business Belt (ISBB) was initiated by the Republic of Korea government to promote the research in the forefront basic science and to seamlessly couple science and business. As the core institute of the International Science and Business Belt plan, the Institute for Basic Science was founded in November 2011 and under the IBS the Rare Isotope Science Project (RISP) was launched. The RISP is to construct a world-class multi-purpose facility to support a wide range of cutting edge science programs in but not limited to nuclear science, material science, bio & medical science, astrophysics, and atomic physics as well as interdisciplinary science programs. To meet the diverse demands, the RISP design is optimized to provide various high intensity stable ion beams and radioactive isotope (RI) beams from proton to uranium for domestic and international users. The RISP facility includes the In-Flight Fragmentation (IFF) facility and the Isotope Separator On-Line (ISOL) facility. The driver accelerator for the IFF facility is a superconducting linac that can accelerate to 200 MeV/u in case of uranium beam and that for the ISOL facility is a 70-MeV cyclotron. The IFF superconducting linac can deliver 400 kW beam power to the IFF target and the 70-MeV cyclotron can deliver 70 kW beam power to the ISOL target.

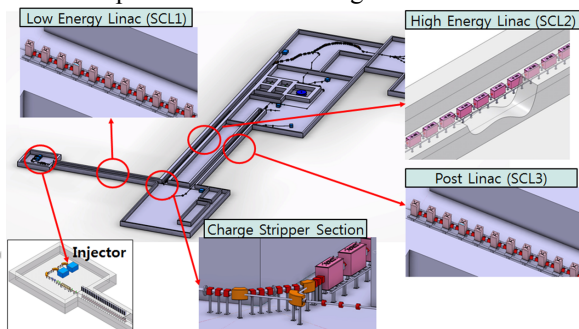


Figure 1: Schematic plot of the RISP facility layout phase.

[#]jeond@ibs.re.kr

The assessment of conceptual design is done and design changes are introduced [1].

THE DRIVER SCL DESIGN

Superconducting Cavities

The driver SCL for the IF facility is designed to accelerate high intensity heavy ion beams and to meet the needs of various users. Large cavity apertures (4 and 5 cm) are chosen to reduce uncontrolled beam loss on the superconducting cavities because beam loss is a serious issue for heavy ion beams. Cavity types are chosen and optimization of the geometric betas of SC cavities is done and an optimum set of $\beta_g = [0.047, 0.12, 0.30, 0.53]$ is obtained. Its results are shown in Fig. 2. The Half Wave Resonator (HWR) is chosen to minimize the asymmetric field effects and to improve the quality. And for each type of SC cavities, optimization of the cavity geometry was conducted with respect to R/Q , QR_s , $E_{\text{peak}}/E_{\text{acc}}$ and $B_{\text{peak}}/E_{\text{acc}}$ etc. Table 1 lists the cavity parameters. Figs. 3 and 4 show the electromagnetic fields of the optimized SC cavities.

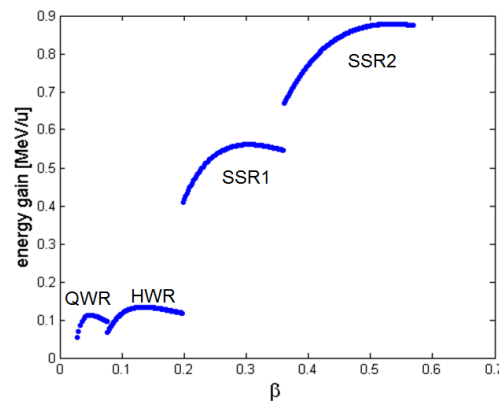


Figure 2: Plots of the optimized geometric betas of the superconducting cavities employed by the RISP.

Table I: Cavity Parameters

Parameters	Unit	QWR	HWR	SSR1	SSR2
β_g	-	0.047	0.12	0.30	0.53
Resonant frequency	MHz	81.25	162.5	325	325
No of cavities	-	24	138	88	136
Aperture diameter	mm	40	40	50	50
QR_s	Ohm	17.5	41.2	86.1	104.7
R/Q	Ohm	472.3	264.8	237.0	298.0
V_{acc}	MV	1.02	1.07	2.04	3.53
E_{peak}	MV/m	30	30	30	30
B_{peak}	mT	54.1	40.8	52.2	62.3
Operating temp	K	2	2	2	2
P_0	W	2.7	2.0	4.8	8.4
Beam current (U)	pA	9.5	9.5	8	8

BEAM ENVELOPE ANALYSIS AND SIMULATION

V.S. Dyubkov*, A.S. Plastun, NRNU MEPhI, Moscow, Russian Federation

Abstract

Forming the charge particle beams with small cross-sections and low energies is an actual problem for linac design. That beams are used actively for isotope therapy, ion implantation, etc. Beam emittance is its quality factor, and it should be matched with a facility channel acceptance. The method for beam dynamics analysis at linac is developed in terms of non-coherent particle oscillation study. Nonlinear beam dynamics is investigated by using this method. It is shown that this technique allows one to realize effective beam handling and emittance control. Analytical results obtained are verified by means of numerical simulation.

INTRODUCTION

One of the most interesting problems of accelerator engineering to date are the design and development of high-performance high-current compact systems for an injection and acceleration of low-velocity heavy-ion beams. This problem as well as others cannot be solved without taking into account problem solution on beam emittance matching with an acceptance of an accelerator channel. Effective acceptance evaluation for the resonance accelerator channel depends on a mathematical model used for describing a beam dynamics. Effective acceptance evaluation of the resonance accelerator channel was performed previously on basis of charged particle beam oscillation as a whole [1] – [4], that is under the assumption of coherent oscillations of individual particles. It is of particular interest to consider a model, which is taking into account non-coherent particle oscillations in the beam, and analyse results based on it.

BEAM DYNAMICS

It is difficult to analyse a beam dynamics in a high frequency polyharmonic field. Therefore, we will use one of methods of an averaging over a rapid oscillations period, following the formalism presented in [1] – [4]. One first expresses RF field in an axisymmetric periodic resonant structure as Fourier's representation by spatial harmonics of a standing wave assuming that the structure period is a slowly varying function of a longitudinal coordinate z

$$E_z = \sum_{n=0}^{\infty} E_n I_0(k_n r) \cos\left(\int k_n dz\right) \cos \omega t,$$

$$E_r = \sum_{n=0}^{\infty} E_n I_1(k_n r) \sin\left(\int k_n dz\right) \cos \omega t,$$

where E_n is the n th harmonic amplitude of RF field on the axis; $k_n = (1 + 2n)\pi/D$ is the propagation wave number for the n th RF field spatial harmonic; D is the resonant structure geometric period; ω is the RF frequency; I_0, I_1 are modified Bessel functions of the first kind.

As it was stated above, we will take into account non-coherent particle oscillations in the beam being accelerated. To this end, one introduces a notion of a reference particle, i.e. a particle moving on the channel axis. A magnetic force can be neglected for low-energy ions. We will assume that $dr/dz \ll 1$. Then, one passes into the reference particle rest frame. There is a differentiation over longitudinal coordinate in the beam motion equation. Thus, the motion equation together with an equation of particle phase variation can be presented in a view of a system of the first order differential equations as follows

$$\begin{cases} \frac{d\Gamma}{d\xi} = e_z(\xi, 0, \tau^*) - e_z(\xi, \rho, \tau), \\ \frac{d\beta_r}{d\xi} = \beta_z^{-1} e_r(\xi, \rho, \tau). \end{cases} \quad (1)$$

Here we introduced the following dimensionless variables: $\Gamma = \gamma^* - \gamma$; γ^* and γ are the Lorentz factors for the reference and given particles respectively; $\xi = 2\pi z/\lambda$ is dimensionless longitudinal coordinate; $e_{z,r} = eE_{z,r}Z\lambda/2\pi m_0 c^2$; e is the elementary charge; Z is a charge state of an ion; λ is a wave length of RF field; m_0 is an ion rest mass; c is the light velocity in free space; $\beta_{z,r}$ is normalized velocity component.

Let us introduce a new dynamical variable $\psi = \tau - \tau^*$ ($\tau = \omega t$, τ^* is a normalized motion time of the reference particle at the laboratory coordinate system). Note, that

$$\frac{d\psi}{d\xi} = \beta_s^{-3} \Gamma, \quad (2)$$

β_s is normalized synchronous particle velocity, s is the field harmonic number.

Suppose that $|\beta_z - \beta_s| \ll 1$ one can obtain

$$\frac{d^2\psi}{d\xi^2} + 3\kappa \frac{d\psi}{d\xi} = \frac{1}{\beta_s^3} \frac{d\Gamma}{d\xi} \quad (3)$$

upon differentiation of Eq. 2. The second equation of Eq. 1 can be rewritten as

$$\frac{d^2\delta}{d\xi^2} + \kappa \frac{d\delta}{d\xi} = \frac{e_r}{\beta_s^3}, \quad (4)$$

where $\delta = \rho/\beta_s$, $\rho = 2\pi r/\lambda$, $\kappa = \ln' \beta_s$.

* vsdyubkov@mephi.ru

BEAM DYNAMICS OF THE LINAC ALPI-PIAVE IN VIEW OF POSSIBLE UPGRADES SCENARIO FOR THE SPES PROJECT

M. Comunian, C. Roncolato, INFN/LNL, Legnaro,
B. Chalykh, ITEP, Moscow

Abstract

At the Legnaro National Laboratories it is operating a Super Conducting linac for nuclear studies named ALPI. The ALPI linac is injected either by a XTU tandem, up to 14 MV, or by the s-c PIAVE injector, made with 2 SC-RFQ. In this article will be report the beam dynamics simulations for some possible scenario upgrade of the linac operate by a new injector, made with a new RFQ.

INTRODUCTION

The SPES strategy is to develop a facility for Nuclear Physics research together with a facility for applied Physics based on the same technology and infrastructure.

SPES [1] is designed to provide neutron-rich radioactive nuclear beams (RIB) of final energies in the order of 10 MeV/A for nuclei in the $A=9-160$ mass region. The radioactive ions will be produced with the ISOL technique using the proton induced fission on a Direct Target of UCx [2] and subsequently reaccelerated using the PIAVE-ALPI accelerator complex. A Uranium fission rate of 10^{13} fission/s is foreseen.

Fig. 1 shows schematically the SPES main elements located at underground level, a second floor at ground level hosting laboratories and services is not shown.

The driver is the proton cyclotron delivering beam on different targets. Two production ISOL targets are planned to be installed. The production target and the first mass selection element will be housed in a high radiation bunker. Before the High Resolution Mass Spectrometer

(HRMS) a cryopanel will be installed to prevent the beam line to be contaminated by radioactive gasses and a RFQ cooler to reduce the input emittance of the HRMS. After passing through the HRMS, the selected isotopes will be stopped inside the Charge Breeder and extracted with increased charge ($n+$). A final mass selector will be installed before reaching the PIAVE-ALPI accelerator, to clean the beam from the contaminations introduced by the Charge Breeder itself.

THE NEW RFQ INJECTOR

The injection to the ALPI Linac is based on the use of a new Radio Frequency Quadrupole, with the adiabatic bunching inside. In this way a high voltage platform can be avoided, and a higher overall transmission could be achieved.

The new RFQ will operate in a CW mode (100% duty factor) at a resonant frequency of 80MHz. This frequency is the same as that of the lowest energy ALPI superconducting structures. The injection energy of ions was set to 5.7 keV/u. This choice is a compromise between the desire to reduce the ion energy to simplify the LEBT and RFQ bunching section design and the need to increase the injection energy to reduce space charge effects. The extraction energy was set to 727 keV/u, higher than the output of PIAVE RFQ, to optimize the beam dynamics of the SRF linac. Table 1 summarizes main new RFQ parameters [3].

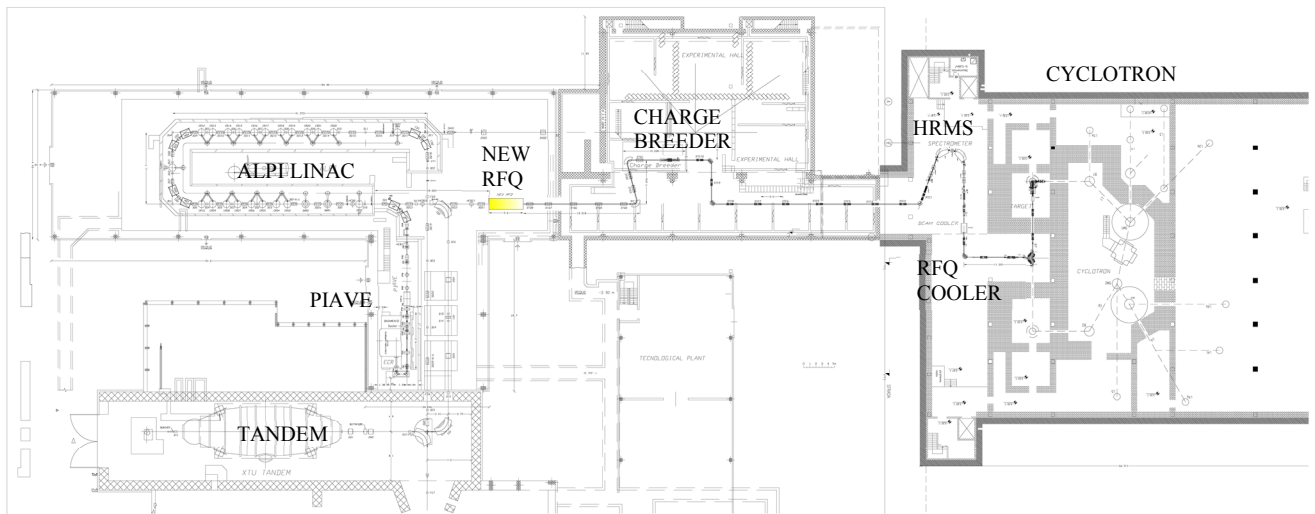


Figure 1: Layout of the SPES and ALPI facility; the dark black part on right is the new Cyclotron area. In yellow the new RFQ as ALPI injector.

PIEZOELECTRIC ACTUATOR BASED PHASE LOCKING SYSTEM FOR IUAC LINAC

B.K.Sahu, R. Ahuja, Rajesh Kumar, S.K. Suman, A.Rai, P.Patra, A.Pandey, J Karamkar, G.K.Chowdhury, Mukesh Kumar, R.N. Dutt, D.S.Mathuria, S. Ghosh, D.Kanjilal and A.Roy, Inter University Accelerator Centre (IUAC), Aruna Asaf Ali Marg, New Delhi – 110067, India

Abstract

The linac of IUAC consists of five cryostats having a superbuncher(SB), three accelerating modules, having eight quarter wave resonators (QWR) each, and a rebuncher(RB). At present SB, two accelerating modules and RB are operational and testing of the last linac module is being carried out. In the operational linac modules the phase locking is achieved by a combination of fast I-Q based electronic tuner and helium gas flow based mechanical tuner. Microphonics measurement on the resonators confirms the presence of low frequency vibrations along with main mechanical mode of the resonator. The existing gas flow based mechanical tuner working in the time scale of seconds can't arrest these vibrations, In a parallel development we have tested a piezoelectric actuator based fast tuner operating in the time scale of milli seconds. The test results showed that the piezoelectric based tuner can arrest all low frequency vibrations and reduce a substantial load from the electronic tuner to improve the dynamics of the phase locking scheme. The implementation of this scheme along with test result is presented in this paper.

The phase locking of the SC QWR consists of fast I-Q based dynamic phase control along with the helium gas flow based mechanical tuner [2]. The vibration related fluctuations around master frequency (microphonics) are mainly controlled by the fast I-Q based electronic tuner and the slow drifts of the central frequency are arrested by closed loop helium gas flow based mechanical tuner, to reduce the load on the electronic tuner. The gas flow based tuner operates in the time scale of seconds. Thus it can control frequency drifts less than a Hz. All the faster component of frequency jitter put an extra load on the electronic tuning mechanism of the resonator. An alternate piezoelectric actuator based tuner along with stepper motor based coarse tuner is successfully developed and tested with one of the QWRs in the test cryostat [3].

INTRODUCTION

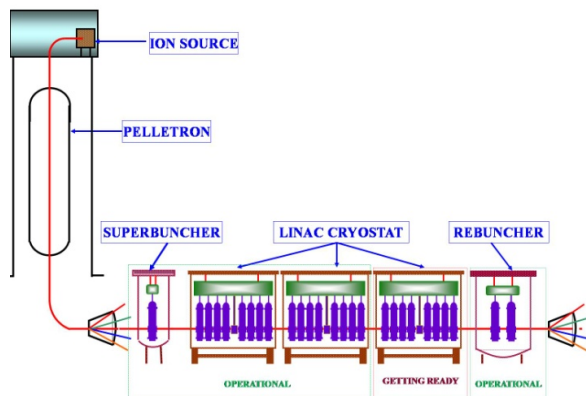


Figure 1: The schematic of IUAC linac.

At Present, the first two accelerating modules of IUAC superconducting (SC) linear accelerator (linac) are operational with superbuncher and rebuncher to provide accelerated heavy ion beams to conduct experiments in nuclear physics and materials science [1]. The third linac module is almost ready for beam acceleration. Each module has eight SC niobium Quarter Wave Resonators (QWR) operating at a resonance frequency of 97MHz and are independently phase locked with the master oscillator.

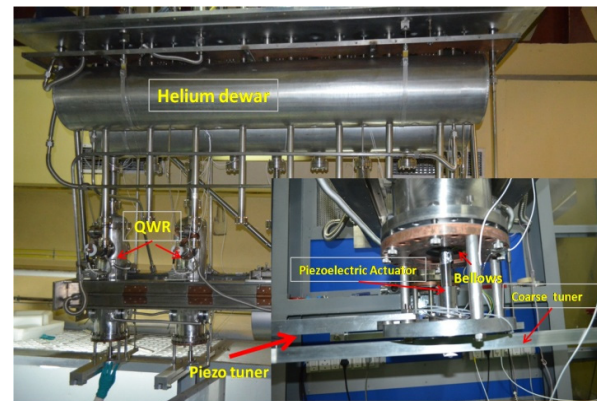


Figure 2: The piezoelectric actuator based mechanical tuner in third linac cryo module along with close view.

The stepper motor based coarse tuner brings frequency close to the master frequency and then the control is given to the piezoelectric actuator based tuner. The piezoelectric tuner operates in the time scale of tens of milli seconds and thus takes considerable load away from the fast tuner to reduce the average power during operation. After the successful operation of piezoelectric based tuner in test cryostat it is decided to optimise the tuner performance for linac operation and the new piezoelectric actuator based mechanical tuners are installed in two of the resonators in third linac module. The control scheme is tested with conditions similar to actual operation.

A HELIUM INJECTOR FOR COUPLED RFQ AND SFRFQ CAVITY PROJECT AT PEKING UNIVERSITY

Haitao Ren, Shixiang Peng*, Pengnan Lu, Jia Chen, Jie Zhao, Yuan XU, Shuli Gao, Zhi Wang, Zhiyu Guo and Jia'er Chen

INST, KLNPT & IHIP, School of Physics, Peking University, Beijing 100871, China

Abstract

A new acceleration structure named as coupled radio frequency quadrupole and separated function radio frequency quadrupole cavity (Coupled RFQ & SFRFQ) is under design at Peking University (PKU). A pulsed or CW He⁺ beam injector will be needed to transport 30 keV 20 mA He⁺ beam and normalized rms emittance less than 0.15 π .mm.mrad for this composited type cavity. For pulsed mode, the factor is 1/6, the pulse width is 1 ms. Based on the experimental results obtained on the PKU LEBT test bench, an injector with a 2.45GHz permanent magnet ECR ion source and a 1.16 m long two-solenoid type low energy beam transport (LEBT) line was developed. In this paper we will address the 30 keV He⁺ ion beam transportation experimental results on the test bench as well as the specific design on the helium injector.

INTRODUCTION

The development of advanced materials is a key to the achievement of nuclear fusion as a safe, environmentally attractive and economically competitive energy source [1]. Therefore, the study of material irradiation damage effects is increasingly important for advanced nuclear energy systems. An accelerator-based material irradiation facility with beam energy of MeV is a good choice to address the challenges presented by fusion wall materials and to study the form of the resulting waste. A coupled RFQ-SFRFQ accelerator for materials irradiation has been developed at Peking University [2]. It is a new acceleration structure that couples RFQ and SFRFQ electrodes in a single cavity. This material irradiation project is designed to accelerate the helium beam to 0.8 MeV with the peak current of 5 mA. In this paper we will address the general description of the He⁺ injector design in part 2. In part 3, we will present the bench experimental results on He⁺ ion beam production and transmission efficiency on the space charge compensation with Ar gas. In part 4, we will give out the concept and specific design of the helium injector. A summary will follow at the end of this paper.

GENERAL DESCRIPTION

A helium injector is used to generate plasma, to create an expected ion beam and to transport it into an accelerator. It consists of an ion source and a low energy beam transport part (LEBT).

* Corresponding author Email: sxpeng@pku.edu.cn

Among sorts of ion source we choose a permanent magnet 2.45 GHz Electron Cyclotron Resonance Ion Source (PKU PMECRIS) for this coupled RFQ and SFRFQ accelerator at PKU. One reason is that this type of ion source has very unique features, such as high ion beam density, high reliability, ability to operate both in CW mode and in pulsed mode, good reproducibility and low maintenance and long lifetime. And those outstanding characteristics make 2.45 GHz ECRIS popular as a High Current Ion Source in the world [3-7]. Another reason of our choice is that researchers at PKU are skilful on this kind of ECRIS [5,7]. By replacing the solenoid with permanent magnet, the ECR ion source body is more compact.

LEBT is used to transport and to match the beam created and extracted from the ion source to accelerator. Beam focus can be done with electrostatic or magnetic elements [8] within LEBT. Compared with electrostatic type LEBT, the advantage of magnetic LEBT is obvious on the neutralization of space charge, on the emittance growth suppressing and on the improvement of beam transmission efficiency within the injector [8]. When the injector dimension is not the limitation, magnetic type LEBT is a good choice for a high intensity low energy ion beam. Based on the above understanding and our experience on D⁺ injector design for PKUNIFTY [5], a magnetic low energy beam transport (LEBT) line with two solenoids is chosen to transport the He⁺ beam into the coupled RFQ-SFRFQ. This injector must produce and transport at least 20 mA (peak current) of helium beam with energy of 30 keV to the entrance of RFQ, and the normalized rms emittance of the beam should be less than 0.15 π mm.mrad. Parameters of the injector are listed in table 1.

Table 1: Parameters of the Helium Injector

He+ beam current	mA	20
Energy	keV	30
Duty cycle	Hz	166
Pulse length	ms	1
Emittance(norm rms)	π mm.mrad	0.15

BENCH EXPERIMENTS

Nonlinear space charge force for low energy intense beam is a main reason of beam divergence and emittance growth, which leads to low transmission efficiency [4]. In LEBT line, the space charge effect is more obvious,

A NEW DESIGN OF THE RFQ CHANNEL FOR GSI HITRAP FACILITY

S. Yaramyshev[#], W. Barth, G. Clemente, L. Dahl, V. Gettmann, F. Herfurth, M. Kaiser, M. Maier, D. Neidherr, A. Orzhekhovskaya, H. Vormann, G. Vorobjev, GSI, Darmstadt, Germany
 R. Repnow, MPI-K, Heidelberg, Germany

Abstract

The HITRAP linac at GSI is designed to decelerate ions with mass to charge ratio of $A/Z < 3$ from 4 MeV/u to 6 keV/u for experiments with ion traps. The particles are decelerated to 500 keV/u with an IH-DTL structure and finally to 6 keV/u with a 4-rod RFQ. During commissioning stage the deceleration to approx. 500 keV/u was successfully demonstrated, while no particles behind the RFQ with an energy of 6 keV/u were observed. Dedicated simulations with DYNAMION code, based on 3D-fotometrie of the fabricated RFQ electrodes were successfully performed comprehending the commissioning results. In a second step the simulations have been experimentally confirmed at a test-stand (MPI-K, Heidelberg). An input energy, accepted by the RFQ is significantly higher than design value. For this reason the longitudinal beam emittance after deceleration with IH structure does not fit to the longitudinal RFQ acceptance. To solve this problem a new design of the RFQ channel with a correct input energy has been started. New RFQ parameters and the results of the beam dynamics simulations are presented in this paper.

to 6 keV/u failed. Therefore a beam dynamics study for the RFQ by means of the advanced multiparticle code DYNAMION [4] has been carried out. As a basis for precise and reliable simulations the RFQ electrodes have been disassembled from the tank and measured by Sigma3D Company (Aachen, Germany). The photometric data has been used to build a 3D surface of the electrodes "as fabricated" (Fig. 2). Detailed distribution of the electrical potential inside an RFQ channel was calculated by means of a relaxation scheme. Obtained 3D electrical field mapping was used as an input data.

INTRODUCTION

The **Heavy Ion Trap** (HITRAP) facility of the GSI Helmholtzcenter for Heavy Ion Research at Darmstadt has been built to decelerate highly charged heavy ions to an energy of 6 keV/u. Then ions can be captured in a Penning trap, cooled further to cryogenic temperatures, extracted and transported to the experiments for atomic, nuclear and solid state physics [1-2].

The HITRAP linac (Fig. 1) is foreseen to decelerate heavy ions with an energy of 4 MeV/u down to 500 keV/u by IH-DTL section and to 6 keV/u by a 108 MHz RFQ [3], designed by Prof. A. Schempp (IAP Frankfurt, Germany) and fabricated by NTG Company (Gelnhausen, Germany). A deceleration of the beam to 500 keV/u at HITRAP facility was successfully demonstrated, while until now all efforts providing for complete deceleration

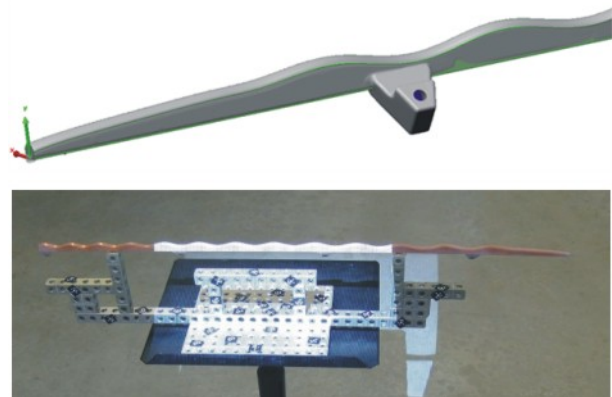


Figure 2: 3D surface of the rods (top) used for the simulations and created from the measurements (bottom)

The results of DYNAMION simulations for the HITRAP-RFQ demonstrated significantly higher (approx. 525 keV/u) beam energy than the design value of 500 keV/u. This fact can be the most probable explanation of the not reached deceleration of the beam to the design energy of 6 keV/u at HITRAP facility.

HITRAP-RFQ EXTERNAL TESTS

In 2011 the HITRAP-RFQ was transported to MPI-K (Heidelberg, Germany), installed at Pelletron accelerator and tested with H_2^+ beam (Fig. 3).

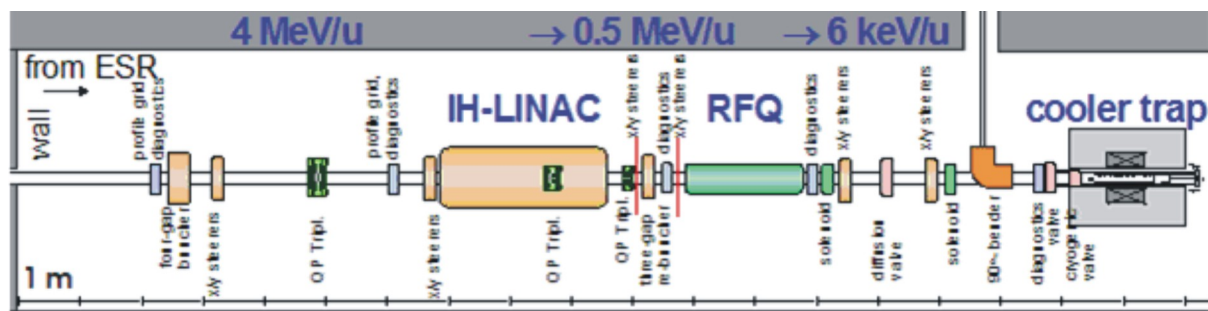


Figure 1. Schematic layout of the HITRAP facility

[#]S.Yaramyshev@gsi.de

DESIGN OF RE-BUNCHER CAVITY FOR HEAVY-ION LINAC IN IMP

L. Sun[#], Y. He, A. Shi, X. Du, Z. Zhang, C. Zhang

Institute of Modern Physics, Chinese Academy of Sciences, Lanzhou 730000, China

Abstract

A re-buncher with spiral arms for a heavy ion linear accelerator named as SSC-LNAC at HIRFL (the heavy ion research facility of Lanzhou) has been constructed. The re-buncher, which is used for beam longitudinal modulation and match between the RFQ and DTL, is designed to be operated in continuous wave (CW) mode at the Medium-Energy Beam-Transport (MEBT) line to maintain the beam intensity and quality.

Because of the longitudinal space limitation, the re-buncher has to be very compact and will be built with four gaps. We determined the key parameters of the re-buncher cavity from the simulations using Microwave Studio software, such as the resonant frequency, the quality factor Q and the shunt impedance. The detailed design of a 53.667 MHz spiral cavity and measurement results of its prototype will be presented.

INTRODUCTION

The spiral cavity shown in Fig.1 is a kind of characteristic RF structure other than QWR (Quarter Wave Resonator) cavity, whose remarkable properties are attributed to a high efficiency, compact design and a big variety of possible fields. In comparison to other available designs, the advantage of this structure lies in its small size. Furthermore it can easily be tuned to expected frequency point by varying the length of the spiral. Of course, due to the small size the required budget can also be kept low. This re-buncher resonator, having four gaps in it, operates at a fixed frequency of 53.667MHz to provide the longitudinal focusing of 7.12MeV heavy ion beam. To reduce the risk of sparking, the voltage of gaps

is well optimized at 30kV. The bunching voltage, which is defined as the sum of the four gap voltages, has reached 120kV at a power consumption of 0.95kW.

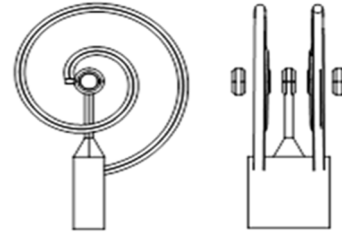


Figure 1: Schematic drawing

DYNAMICS DESIGN

According to the design for LINAC [1] which are presented in Fig.2, the re-buncher is located between the RFQ and the IH-DTL cavities, and it can be used to provide adjustable longitudinal focusing force to guarantee that most particles do not exceed the longitudinal acceptance of the DTL. The longitudinal emittance of the main bunch and the longitudinal acceptance of the DTL at its entrance are illustrated in Fig.3. The void region is the longitudinal acceptance of the whole DTL. The area occupied by black dots is the matched longitudinal particle distribution at the entrance of the DTL. Obviously, without bunching function, the majority of particles will be lost, only 23.2% particles can be accelerated by the DTL. When the re-buncher is turned on, a satisfying result can be acquired by optimizing the re-buncher structure and its bunching voltages

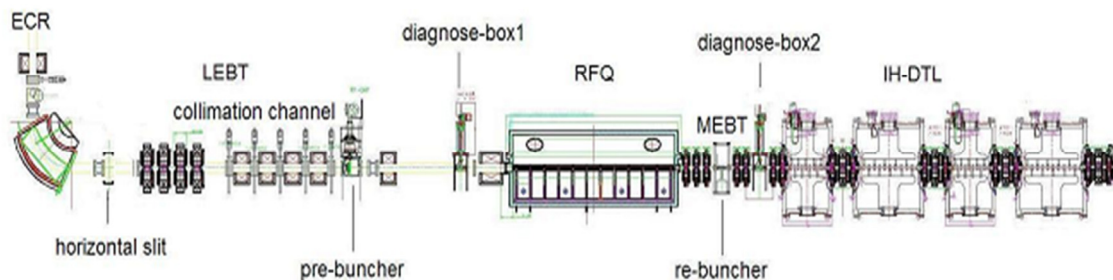


Figure 2: The layout of the SSC-LINAC

#sunlp@impcas.ac.cn

CONCEPTUAL DESIGN OF SUPERCONDUCTING HEAVY ION LINEAR INJECTOR FOR HIAF*

Z.J. Wang, Y. He, H. Jia, S.H. Liu, C. Li, X.B. Xu, B. Zhang,
W. Wu, H.W. Zhao IMP, Lanzhou,730000,China

Abstract

A heavy ion accelerator facility, High Intensity Heavy Ion Accelerator Facility (HIAF), has been promoted by Institute of Modern Physics IMP of Chinese Academy of Sciences (CAS). The injector of the accelerator facility is a superconducting linac(HIAF-linac). It is a high intensity heavy ion linac and works on pulse mode. The final energy is 100 MeV/u. The accelerated species are from Prton to Uranium. The linac works with both laser and ECR ion source. The designed current is 1.0 emA. The general concept of HIAF and the preliminary design of linear injector are presented in the paper.

INTRODUCTION

High Intensity Heavy Ion Accelerator Facility (HIAF) will be a national user facility. The proposed HIAF facility is based on a heavy-ion linac with a minimum energy of 100 MeV/u for all ions at a beam current 1.0emA. This advanced facility will provide high intensive ion beam for high energy nuclear science to understand the fundamental forces and particles of nature as manifested in nuclear matter. The HIAF project will include three parts, ion linac injector, the rings and experiments facility. The concept HIAF-linac design will be introduced as following.

The proposed linac design is based on the goal of constructing a reliable, low-maintenance, state-of-the-art accelerator with proven technology and robust operating stability that will minimize downtime and ensure production of intense beams for world-class experiments. The design of the driver linac is largely determined by the requirement of a 100 MeV/u, 1.0 mA uranium beam, and the need to accelerate a wide range of ions while limiting the uncontrolled beam loss below 1 W/m, high power SC machine to facilitate hands-on maintenance. The accelerator lattice design must provide adequate transverse and longitudinal acceptance.

Fig. 1. shows a concept schematic layout of the linac facility.

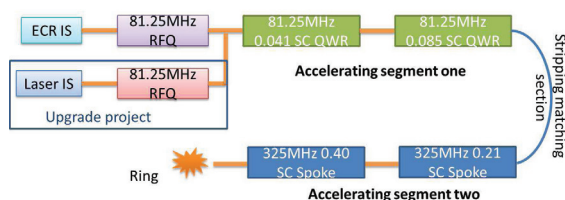


Figure 1: The concept layout of HIAF-linac.

*Supported by the National Natural Science Foundation of China (Grant No.11079001)

As shown in the Fig.1, HIAF-linac will be consisted of front end, superconducting(SC) accelerating segment one, stripping and matching section and superconducting accelerating segment two.

In this paper, concept design of each section are presented.

FRONT END DESIGN

Front end section includes ECR, LEBT and RFQ. The ECR will provide high charge ions beam at both CW and pulse mode. LEBT has two functions, one is to select the charge state from hybrid charge beam, the other is to match the beam to RFQ entrance. The RFQ will accelerator ion beam from 0.02MeV/u to 0.4MeV/u. The layout of the front is shown in Fig. 2 shows the schematic layout of front end. As shown in the figure, one prebuncher is located in

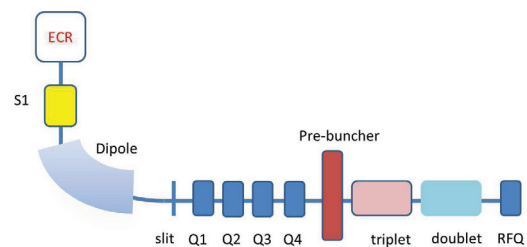


Figure 2: The schematic layout of front end.

the LEBT to decrease the longitudinal emittance to meet the requirement of the acceptance in superconducting section.

The design goals were to minimize the longitudinal emittance and transverse emittance, the RF power, and the structure length. After several optimizations, the parameters of RFQ were found to minimize output longitudinal emittance and maximum transmission. The RFQ was designed using DESRFQ[1] code. The final design structure parameters will be simulated by Track code[2]. RFQ cell profile at different section are shown in the Fig. 3

SUPERCONDUCTING ACCELERATING SEGMENT ONE

Beam from the front end will be injected into the SC linac. Two types of accelerating structures in fourteen cryomodules are used to achieve energy of 15MeV/u for uranium in segment one. Segment one will be approximately 80.2m long and will accelerate the uranium beam from 0.4 to 15 MeV/u when the beam current is 1mA. Segment one includes two periodic structures. Three cryomodules, each containing six $\beta_{opt}=0.041 \lambda/4$ cavities op-

STATUS OF THE LINAC SRF ACQUISITION FOR FRIB*

M. Leitner[#], E. Bernard, J. Binkowski, B. Bird, S. Bricker, S. Chouhan, C. Compton, K. Elliot, B. Enkhabat, A. Fox, L. Harle, M. Hodek, M. Johnson, I. Malloch, D. Miller, S. Miller, T. Nellis, D. Norton, R. Oweiss, J. Ozelis, J. Popielarski, L. Popielarski, K. Saito, M. Shuptar, G. Velianoff, J. Wei, M. Williams, K. Witgen, Y. Xu, Y. Yamazaki, Y. Zhang
 FRIB, Michigan State University, East Lansing, MI 48824, U.S.A.
 A. Facco, INFN-Laboratori Nazionali di Legnaro, I-35020 Legnaro, Padova, Italy

Abstract

The Facility for Rare Isotope Beams (FRIB) will utilize a high-intensity, superconducting heavy-ion driver linac to provide stable ion beams from protons to uranium up to energies of >200 MeV/u and at a beam power of up to 400 kW. The ions are accelerated to about 0.5 MeV/u using a room-temperature 80.5 MHz RFQ and injected into a superconducting cw linac consisting of 330 individual low-beta cavities in 49 cryomodules operating at 2 K. This paper discusses the current status of the linac SRF acquisition strategy as the project phases into construction mode.

INTRODUCTION

Due to the heavy mass and correspondingly low velocity of the accelerated ions the FRIB driver linac [1] utilizes four different low-beta SRF resonator designs as shown in figure 1 and figure 2. The status of SRF system designs and overall acquisition strategies have been summarized in [2]. For high-beta applications superconducting RF has become an established technology with a history of industrial optimization efforts. However, for low-beta structures, FRIB will most likely be the first facility requiring industrially produced components on a larger scale.

FRIB is a US\$ 680 million construction project with an 8-year timetable: According to the current FRIB baseline schedule fabrication and procurement of linac components will start mid-2014. Actual linac installation will begin end of 2016 after completion of conventional facilities and cryoplant construction. Accelerator commissioning is scheduled to initially proceed in parallel with installation and to conclude at the earliest by end of 2019 (beginning of 2021 if schedule contingency is included). 2015 to 2018 will be the peak period for industrial SRF cavity and cryomodule production.

The FRIB project plans to place approximately 450 procurements above US\$ 50,000 each. The sum of all technical equipment procurements (excluding conventional facility construction) issued to industry amounts to US\$ 217 million. Roughly 30% of that procurement value will be spent on cryomodule components not including RF amplifier equipment.

* This material is based upon work supported by the U.S. Department of Energy Office of Science under Cooperative Agreement DE-SC0000661.

[#] LeitnerM@frib.msu.edu

SRF PROCUREMENT SPECIFICS

A major challenge for the FRIB project is the need to develop, qualify, and industrialize four independent cryomodule and cavity types before start of construction. Optimization of the linac resulted in a design with 49 cryomodules incorporating 106 quarter-wave (QWR) and 224 half-wave (HWR) resonators (330 total) with four different optimum velocities as shown in figure 2. A detailed cavity count table can be found in [2].

Unlike prior superconducting low- β linacs, the large size of FRIB has required optimization of the resonator designs for both maximum performance and for low cost in the view of a large production. This requirement guided the choice of the resonator geometries, materials and mechanical solutions avoiding complicated shapes, minimizing the amount of electron beam welds, eliminating bellows, as well as optimizing construction and surface treatment procedures. The history of the resonator development and detailed FRIB cavity specifications are summarized in [3].

Cavity Procurement Status

Including development, pre-production, spare, and 10% excess cavities FRIB will procure more than 400 cavities within the next six years. FRIB can select from a highly qualified cavity supplier base due to world-wide strong, industrial interest in SRF cavity fabrication. Six vendors have consistently bid for FRIB cavity production: AES, Niowave, Roark, and Pavac on the American continent; Research Instruments and Zanon on the European continent. So far AES, Niowave, and Roark have produced physical cavity prototypes for FRIB.

$\beta=0.53$ Cavities:

The first and largest (several M\$) FRIB cavity production contract (for a total of 160 undressed $\beta=0.53$ cavities: 2 development, 10 pre-production, 148 linac cavities) has been awarded to Roark, Inc. as a firm price contract. For FRIB procurement quantities the cost reduction between development cavities and mass-produced cavities falls around 3. The $\beta=0.53$ cavities are the largest and most expensive cavities used in the driver linac.

$\beta=0.29$ Cavities:

Due to federal funding delays FRIB has slowed down the procurement of the other cavity types. At present two

SCATTERING OF H^- STRIPPED ELECTRONS FROM SEM GRIDS AND WIRE SCANNERS AT THE CERN LINAC4

B.Cheymol*, E. Chevally, M. Duraffourg, G.J. Focker, C. Hessler, U. Raich, F. Roncarolo†, C. Vuitton, F. Zocca, CERN, Geneva, Switzerland

Abstract

At the CERN LINAC4, wire grids and scanners will be used to characterize the H^- beam transverse profiles from 45 keV to 160 MeV. The wire signal will be determined by the balance between secondary emission and number of charges stopped in the wire, which will depend on the wire material and diameter, the wire polarization and the beam energy. The outermost electrons of H^- ions impinging on a wire are stripped in the first nanometers of material. A portion of such electrons are scattered away from the wire and can reach the neighboring wires. In addition, scattered electrons hitting the surrounding beam pipe generate secondary electrons that can also perturb the measurement. Monte Carlo simulations, analytical calculations and a laboratory experiment allowed quantifying the amount of scattering and the scattered particles distributions. The experiment was based on 70 keV electrons, well reproducing the case of 128 MeV H^- ions. For all the LINAC4 simulated cases the predicted effect on the beam size reconstruction results in a relative error of less than 5%.

INTRODUCTION

When H^- ions interact with matter the outer electron is stripped almost immediately. These electrons can be considered free with an energy of: $E_e = E/1836$ where E is the energy of the H^- beam. For LINAC4 the stripped electrons energy ranges from about 25 eV at the source exit to about 87 keV. Some data about electron scattering can be found in literature [1, 2, 3] for the energy range and materials considered for LINAC4. For electron energies below the MeV range, the proportion of backscattered electrons is around 10 % for low Z materials and up to 50 % in case of materials with higher density.

TWO WIRE SIMULATIONS

The Monte Carlo code FLUKA [4] code was used to simulate an electron beam hitting two parallel wires of the same material and diameter separated of $500 \mu m$. This was done for H^- energies above 50 MeV. Below such energy, the corresponding electron energy is not properly simulated by FLUKA. A beam composed of 10^6 electrons, with a rectangular shape of width equal to the wire diameter was sent to one wire in order to investigate the amount of scattered particles reaching the second wire. The simulation was repeated for 27 keV and 87 keV electrons (cor-

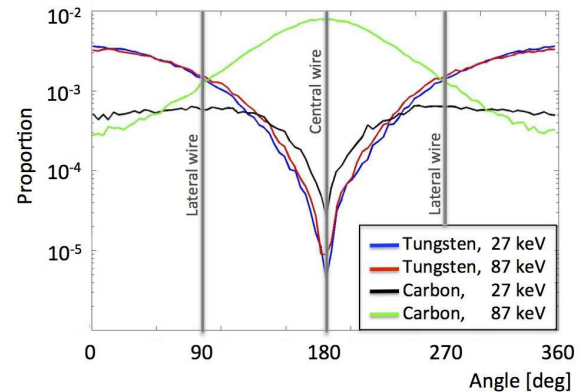


Figure 1: Angular distribution of particles emerging the wire, normalized to the number of primary electrons.

responding to 50 MeV and 160 MeV H^- energy respectively) and $33 \mu m$ Carbon wires or $40 \mu m$ Tungsten wires. Fig 1 shows the angular distribution of the particles emerging from the first wire for the four simulated settings. At the position of the second wire (i.e. 90° or symmetrically 270°), the ratio of particles varies from 2×10^{-4} to 3×10^{-3} . It drops for angles between 90° and 270° and reaches its minimum for an angle equal to 180° . For Tungsten the angular distribution is independent of the beam energy and at 180° the flux is less than 10^{-5} for both energies. For Carbon, at the lowest energy, the flux is around 10^{-5} at 180° . At 87 keV some electrons have enough energy to cross the wire and 44 % of the particles exiting the wire have angles between 150° and 210° . Table 1 shows the percentage of scattered electrons emerging from the first wire and how many of them reach the second wire. At both energies, about 55 % of incident electrons are scattered on a Tungsten wire and in the worst case less than 0.7 % reach the side wire. For a Carbon wire and 27 keV electrons, about 17 % of the impinging particles are scattered, while at 87 keV the amount of scattered electrons is hardly distinguishable from the ones traversing the wire. At both energies, it can be estimated that the percentage of scattered electrons reaching the second wire is below 0.3 %. Even if these results (wire cross talk below 1 %) arise from a simplified case not considering Secondary Emission (SE) electrons, the scattering coefficients determined with the FLUKA simulations agree very well with the data found in literature [3]. Both the scattering coefficients and the scattering angles are also in agreement with similar studies performed at INR with GEANT4 [5].

* Now at ESS, Lund, Sweden

† federico.roncarolo@cern.ch

PROGRESS ON RFQIII FABRICATION IN J-PARC LINAC

T. Morishita, Y. Kondo, K. Hasegawa, JAEA, Tokai, Japan
H. Kawamata, T. Sugimura, F. Naito, KEK, Tsukuba, Japan

Abstract

For the beam current upgrade in J-PARC linac, the fabrication of a new RFQ, which is designed for 50mA beam acceleration, has been started. The engineering design and the fabrication technologies were carefully chosen to reduce the discharge risk during the operation. For good vacuum pumping, vanes and ports are brazed for the direct pumping through slits at the tuners. Also, we tried a chemical polishing to improve the smoothness of the vane surface.

INTRODUCTION

The J-PARC accelerator comprises an injector linac, a 3-GeV Rapid-Cycling Synchrotron and a 50-GeV Main Ring. The J-PARC linear accelerator consists of an ion source, an RFQ, DTLs, separated DTLs (SDTL), and the beam transport line to the RCS synchrotron [1].

The J-PARC linac has been operating for users with the beam energy of 181 MeV. The currently operating RFQ is a four-vane type cavity used to accelerate a negative hydrogen beam from 50 keV to 3 MeV with peak current of 30mA. The RF duty factor is 3% (600 μ s at 50 Hz). For the quick replacement in case of the RFQ trouble, we fabricated a spare RFQ (RFQII) as a backup machine. [2, 3, 4]

The energy (to 400MeV) and current (to 50mA) upgrade of the linac is scheduled for 1MW operation at RCS. The beam dynamics of an RFQ is newly designed for beam current upgrade to 50 mA operation. [4, 5] Then, we started a fabrication of RFQIII last year.

In this paper, we present the fabrication progress of an RFQIII for J-PARC linac.

ENGINEERING DESIGN

Table 1 shows the RFQ III parameters. For the beam current upgrade, the vane length is longer than RFQII about 0.5 m. The RFQ cavity is divided into three unit tanks. Each tank (about 1.2 m long) will be integrated together on a platform after the brazing of the major and the minor vanes.

Engineering design topics are listed in Table 2. The high-power test of the RFQII has been done successfully at April 2012. Basically the mechanical design and the fabrication procedure are the same as RFQII. Followings are the points which are changed from RFQII

Drilled Hole Plugging

The drilled hole plugging technique was changed from electron beam welding to the brazing. In the fabrication of RFQII, there was a vacuum leak at the welding spot after

the brazing (one of seventy-two welding points). Then we changed it to brazing along with the vane brazing in the RFQIII fabrication.

Table 1: Main Parameters of RFQIII

parameter	RFQ III
Beam current [mA]	50
Frequency [MHz]	324
Acceleration energy [MeV]	0.05 to 3
Vane length [m]	3.6
Inter-vane voltage[kV]	81
Maximum surface field [MV/m]	30.7 (1.72 Kilpatrick)
Average bore radius [mm]	3.5
Vane-tip curvature [mm]	0.75r0(2.617)

Table 2: Mechanical Design Features

Material	High-purity oxygen-free copper with HIP(Hot Isostatic Pressing)
Drilled hole plugging	RFQII : Electron beam welding RFQIII : Brazing
Annealing	600 degree C in vacuum furnace
Vane machining	Numerical-controlled machining with ball-end mill RFQIII: Introduced non-contact measurement [6]
Surface treatment	Chemical polishing (3-5 μ m)
Integration method	Vanes and ports are jointed in one step brazing
Unit cavities connection	RFQII : Welding for vacuum sealing, bolting for mechanical alignment RFQIII : bolting for mechanical alignment and vacuum sealing

Dry Cutting for the Fitting of End Flanges

Figure 1 shows a schematic drawing of the unit cavity components to be assembled for brazing. After the final cutting of vanes, those are assembled and machined for a flange fitting at each ends. In the RFQII, vanes were disassembled for the surface treatment to remove cutting oil, then, reassembled for brazing. In the RFQIII, to reduce costs and production period, dry-machining for a flange fitting is adopted after the surface treatment. Then we can reduce the disassemble-reassemble process.

#takatoshi.morishita@j-parc.jp

ONE DESIGN OF HEAVY ION LINAC INJECTOR FOR CSRm

X.H. Zhang, Y.J. Yuan, J.W. Xia

Institute of Modern Physics, Chinese Academy of Sciences, CHINA

Abstract

The design of heavy ion linac as one new injector of the main Cooling Storage Ring (CSRm) has been discussed. The linac design is based on interdigital H mode drift tube with KONUS (Kombinierte Null Grad Struktur). A high acceleration rate with zero degree synchronous particle phase acceleration reduces the length of IH-KONUS linac and the cost in comparison with conventional linac based on Alvarez structure. To reduce the effect of emittance growth, the RFQ structure is used in front of the IH-KONUS linac. In this linac, the design particle $^{238}\text{U}^{28+}$ will be accelerated to 7 AMeV, and the transmission of Uranium beam can reach up to 80%. In this report, the initial physics design of the main linac is presented.

INTRODUCTION

HIRFL-CSR (Heavy Ion research Facility in Lanzhou-Cooling storage Ring) has been built and supplied 7000 hours operation time. As the user number increasing and the experimental requirement improved, the injection linac is proposed, which will make the operation time to improve by 2000 hours. The whole HIRFL-CSR Layout with CSR-LINAC injector is shown in figure.1.

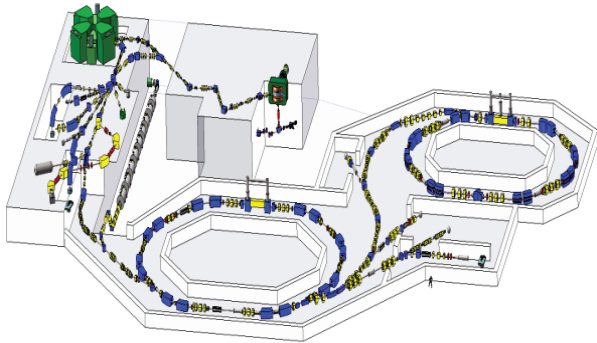


Figure 1: The whole HIRFL-CSR Layout with CSR-LINAC injector.

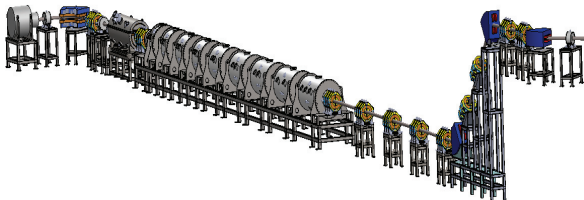


Figure 2: The 3-Dimensional Map of the heavy ion linac for CSRm.

The new linac injector will accelerate $^{238}\text{U}^{28+}$ to

7AMeV and the operation frequency is chosen to 108.48 MHz [1] [2]. The main parameters are summarized in table.1. The heavy ion linac consists of electron cyclotron resonance ion source, low energy beam transport, radio frequency quadrupole linac, medium energy beam transport and drift tube linac. The 3-Dimensional Map of the heavy ion linac injector for CSRm is shown in figure.2.

Table 1: Heavy Ion Injection Linac Main Parameters

Ion source	parameter
Particles	C, Ar, Xe, Pb, U
Superconducting ECRIS	$^{208}\text{Pb}^{35+}$, $^{238}\text{U}^{28+}$
Beam current (emA)	0.05-0.15 (pulsed)
Emittance (pi.mm.mrad)	0.4 (normalized, 90%)
Voltage (KV)	25-40
RFQ	parameter
Input energy (AkeV)	4
Exact energy (AkeV)	300
q/A	1/8.5
Frequency (MHz)	108.48
maximum power (kW)	250
Duration (ms)	10
Repetition (Hz)	10
Duty factor	2%
Transmission (design)	>90%
emittance (pi.mm.mrad)	<0.8 (normalized, 90%)
IH-DTL	Parameter
Input energy (AkeV)	300
Exact energy (AMeV)	7
q/A	1/8.5
Frequency (MHz)	108.48/216.96
Duration (ms)	10
Repetition (Hz)	10
Duty factor	2%
emittance (pi.mm.mrad)	0.8 (normalized, 90%)
Output momentum spread	< ±0.15%
Transmission (design)	> 90%

Copyright © 2012 by the respective authors — cc Creative Commons Attribution 3.0 (CC BY 3.0)

zhangxiaohu@impcas.ac.cn

CRYOGENIC SYSTEM FOR THE ADS INJECTOR II IN IMP, CAS*

X. H. Guo¹, T. Jin¹, H. L. Su¹, X. F. Niu¹, Y. N. Han¹, J.H.Zhang¹
N. Peng², L. Y. Xiong², L. Q. Liu²

¹Institute of Modern Physics, Chinese Academy of Sciences, Lanzhou, 730000, China

²Key Laboratory of Cryogenics, Technical Institute of Physics and Chemistry
Chinese Academy of Sciences, Beijing, 100190, China

Abstract

In order to meet the requirements of ADS Injector II project which is now designing and building in IMP, CAS, a liquid helium cryogenic system with 4.5K&850W cooling power is building. This paper presents the primary design and the status of this cryogenic system with deferent operation models according to the need of superconducting tests.

INTRODUCTION

In order to produce energy and transmute radioactive wastes in a possibly, cleaner and safer way, the Accelerator Driven Sub-critical (ADS) program has been officially started under the coordination of Chinese Academy of Sciences (CAS). The final aim of this program is to build a 1000 MW demo facility in 2032. The road map of this program is shown in Figure 1. There are two beam lines will be built before 2015, which respectively called ADS injector I and II with deferent design idea. The upper line is ADS injector II (RFQ + HWR) [1], will build by Institute of Modern Physics (IMP), Chinese Academy of Sciences (CAS). It has three cryomodules, two of them are on-line operation and the other one is off-line test module. Each of them includes 8 superconducting HWR cavities and 9 superconducting solenoids [2]. The superconducting solenoids are bath-cooled with saturated liquid helium near the atmospheric pressure and the superconducting cavities are bath-cooled with 2 K saturated liquid helium. For the steady operation, the pressure fluctuation of the liquid helium in the cryomodules of cavities should be less than ± 0.3 mbar, while the liquid level should be kept in a small band of $\pm 1\%$.

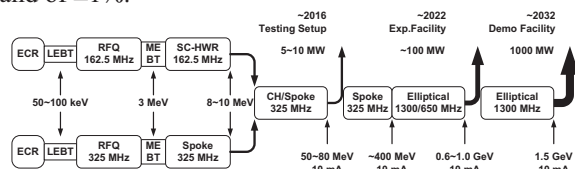


Figure 1: Road map of ADS program.

CRYOGENIC SYSTEM

The flow diagram of the cryogenic system is shown as Figure 2. It consists of a helium refrigerator, a 2000 L helium storage dewar, a purification system, three identical valve boxes, three cryomodules, four 100 m³

pure helium gas buffer tanks and several cryogenic lines. The helium refrigerator system, a standard helium refrigerator LR280 developed by LINDE, is based on 2-turbine-in-series and 1 additional JT turbine Claude cycle. It consists of a compressor module, an oil removal system, gas management panel, a cold box. An oil lubricated screw compressor (FSD 571 made by KAESER Ltd.) is used to compress 95 g/s helium gas from 105 kPa to 1.4 MPa. The oil remove system comprises a bulk oil separator, two coalescing filters mounted in series and a final activated charcoal absorber. The gas management system consists of two by-pass recycle valves (for roughly and finely adjusting, respectively) to automatically recycle excess flow from compressor discharge to suction line and two control valves to automatically adjust the helium inventory in the refrigeration system. The cold box is a vertical cylinder consisting of 5 stages of brazed aluminium plate-fin heat exchangers, two gas-bearing turbo-expanders arranged in series, one additional JT turbine, valves, one 80 K absorber and one 20 K absorber furnished to remove contaminants from the helium stream. The three valve boxes are used to distribute and control the helium flow and nitrogen flow in different operation models such as cool-down, warm-up, 4.3 K bath-cooled mode, 2 K bath-cooled mode and to protect the cryomodules against any possible damages. The cryogenic transfer lines used for delivering LHe, GHe and LN₂ include a coaxial transfer line, a multi-channel transfer line and several single channel transfer lines.

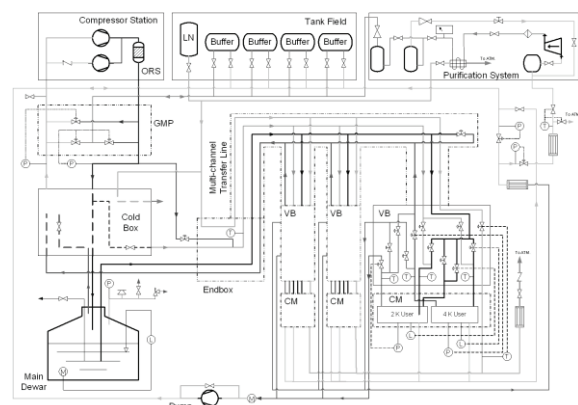


Figure 2: Flow diagram of the ADS Injector II cryogenic system.

*Work supported by Accelerator Driven Sub-critical (ADS) program of CAS, China. guoxh@imp.ac.cn

R&D TOWARDS CW ION LINACS AT ANL*

P.N. Ostroumov[#], A. Barcikowski, Z. Conway, S. Gerbick, M. Kedzie, M.P. Kelly, S. Kutsaev, J. Morgan, R. Murphy, B. Mustapha, D. Paskvan, T. Reid, D. Schrage, S. Sharamentov, K. Shepard, G. Zinkann,
Argonne, IL 60439, U.S.A ANL, Argonne, IL 60439, U.S.A.

Abstract

The accelerator development group in ANL's Physics Division has engaged in substantial R&D related to CW proton and ion accelerators. Particularly, a 4-meter long 60.625-MHz CW RFQ has been developed, built and commissioned with beam. Development and fabrication of a cryomodule with seven 72.75-MHz quarter-wave resonators (QWR) is complete and it is being assembled. Off-line testing of several QWRs has demonstrated outstanding performance in terms of both accelerating voltage and surface resistance. Both the RFQ and cryomodule were developed and built to upgrade ATLAS to higher efficiency and beam intensities. Another cryomodule with eight 162.5-MHz SC HWRs and eight superconducting SC solenoids is being developed and built for Project X at FNAL. We are also developing both an RFQ and cryomodules (housing 176-MHz HWRs) for proton & deuteron acceleration at SNRC (Soreq, Israel). In this paper we discuss ANL-developed technologies for normal-conducting and SC accelerating structures for medium- and high-power CW accelerators, including the projects mentioned above and other developments for applications such as transmutation of spent reactor fuel.

INTRODUCTION

Technologies for CW RFQ and SC RF successfully developed for ATLAS upgrade for higher efficiency and beam intensities [1,2] can be applied in future high-power CW accelerators. Particularly, we are developing a CW RFQ and two cryomodules with different β_{OPT} for the SARAF accelerator facility at SNRC [3]. Similar SC RF technology is being used for the development and construction of the HWR cryomodule for Project X [4]. Below we discuss beam commissioning of the RFQ and results of QWRs testing and cryomodule assembly for the ATLAS upgrade project. Status of the SARAF and PXIE cryomodule development is presented.

CW RFQ

This summer we commissioned a CW RFQ designed and built for the ATLAS Facility [5]. Several innovative ideas were implemented in this CW RFQ. By selecting a multi-segment split-coaxial structure we have achieved moderate transverse dimensions for a 60.625 MHz resonator. For the design of the RFQ resonator and vane tip modulations we have developed a full 3D approach which includes MW-Studio and TRACK simulations of

the entire structure. A novel trapezoidal vane tip modulation is used in the acceleration section of the RFQ which resulted in increased shunt impedance. To form an axially symmetric beam exiting the RFQ, a very short output radial matcher, only $0.75\beta\lambda$ long, was developed.

An advanced fabrication technology was applied for the construction of the RFQ which includes precise machining and two-step high temperature brazing. Thanks to the high accuracy of the overall fabrication, the assembly of the 5-segment RFQ was straightforward and resulted in excellent alignment. The resonance frequency control system based on water temperature regulation showed excellent performance. The RF measurements show excellent RF properties for the resonator, with a measured intrinsic Q equal to 94% of the simulated value for OFE copper. The multi-segment split-coaxial structure creates strong coupling between the quadrants and individual RFQ segments which reduces the effect of local frequency deviations on electromagnetic field distortions. Therefore, no bead-pull measurements were required for tuning of the accelerating field. Figure 1 shows the complete RFQ assembly after installation of

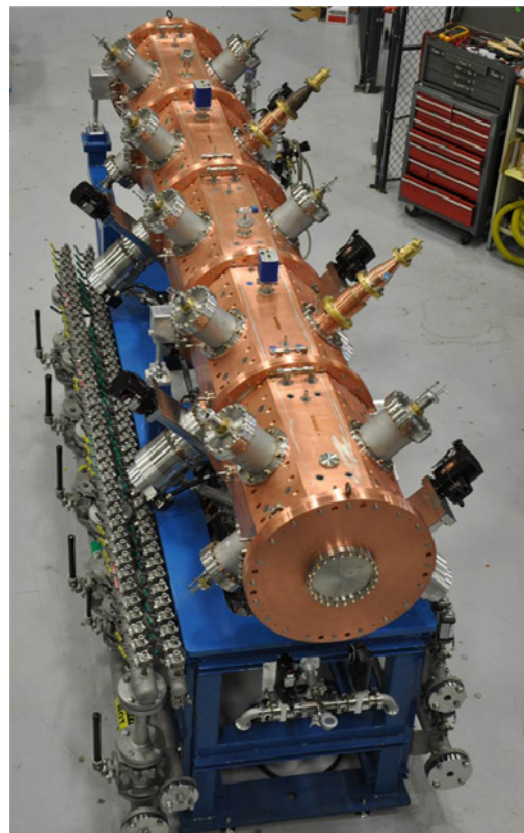


Figure 1: Completed RFQ assembly.

* This work was supported by the U.S. Department of Energy, Office of High Energy Physics and Nuclear Physics, under Contract DE-AC02-76CH03000, DE-AC02-06CH11357 and ANL WFO 85Y47
[#]ostroumov@anl.gov

STATUS OF THE SUPERCONDUCTING RF ACTIVITIES FOR THE HIE-ISOLDE PROJECT

W. Venturini Delsolaro, L. Alberty Vieira, S. Calatroni, O. Capatina, B. Delaup, A. D'Elia*,
I. Mondino, E. Montesinos, M.A. Fraser, P. Maesen, Y. Kadi, N. Jecklin, M. Therasse, D. Valuch.
CERN, Geneva, Switzerland; *Manchester University and Cockcroft Institute

Abstract

The planned upgrade of the REX ISOLDE facility at CERN will boost the energy of the machine from 3 MeV/u up to 10 MeV/u with beams of mass-to-charge ratio $2.5 < A/q < 4$. For this purpose, a new superconducting post accelerator based on independently phased 101.28 MHz Quarter Wave Resonators (QWR) will replace part of the normal conducting Linac. The QWRs make use of the Niobium sputtering on Copper technology which was successfully applied to LEP2, LHC and to the energy upgrade of the ALPI Linac at INFN-LNL. The status of advancement of the project will be detailed, limited to the SRF activities.

INTRODUCTION

The upgrade of the REX ISOLDE facility [1] relies on a new superconducting Linac to bring the energy of the radioactive beams from 3 MeV/u up to 10 MeV/u with beams of mass-to-charge ratio $2.5 < A/q < 4$.

The project is staged in three phases in order to optimize the beam delivery to the physicists and to take advantage of the scheduled shut down periods of the CERN accelerator complex. The first phase will consist in the installation of two cryomodules, each housing 5 high beta Quarter Wave Resonators (QWR) and a superconducting solenoid for beam focusing.

The core element of the HIE ISOLDE Linac is the QWR, which will make use of the sputtered Nb/Cu technology pioneered at CERN for LEP2 [2], and subsequently developed for the complex QWR shape in INFN-LNL for the energy upgrade of ALPI [3], [4]. The elliptical cavities in use at CERN were coated by magnetron sputtering at relatively low temperatures, whereas the QWR for ALPI were realized by bias diode sputtering at higher temperatures.

The design of the high beta cavity is reported in [5], the main parameters are listed in Table 1.

Work to set up a production chain for sputtered QWR started in CERN in 2008 and the early reached milestones are reported in [6], [7]. The most recent project schedule requires series production of the cavities to start at CERN in early 2013.

Besides the cavity itself, ancillaries like the power coupler and tuning system are being developed. This paper reports on the latest developments in the SRF frame, while a recent and detailed update on the whole HIE ISOLDE project is given in [8]

Table 1: Parameters of the high β HIE ISOLDE QWR

Frequency (MHz)	101.28
β (%)	10.3
Active length (m)	0.3
$\Gamma = R_s Q$ [Ω]	30.34
E_{acc} (MV/m)	6
$Q_0 @ E_{acc}=6$ MV/m	$5 \cdot 10^8$
E_{apk} / E_{acc}	5.4
B_{apk} / E_{acc} (Gauss/MV/m)	96

STUDY OF CAVITY MECHANICAL TOLERANCES

The high substrate temperatures reached during the sputtering process called for a reconsideration of the mechanical tolerances for the manufacture of the cavity. Indeed, it was not clear to what extent the induced mechanical deformations would affect the beam quality. A study was launched in early 2012 to understand the effect of the misalignment of the internal conductor of the quarter-wave resonator on the beam. In previous error studies only misalignments of the ideal cavity were considered, see [9]. In the new study, the outer conductor of the cavity was assumed as ideal but the internal conductor was misaligned in each independent mode: Δx , Δy , Δz and $\Delta \theta_y$, where the magnitude of each error was parameterized at the beam ports. The misalignments were implemented by pivoting the internal conductor about its point of attachment at the top of the cavity. In fact, the field perturbation seen by the beam is dominated by the fringing electric fields in the vicinity of the beam ports. Moving the position of the drift-tube on the inner conductor could attain analogous results. Systematic RF simulations were performed with CST-MWS: many cavities were generated with regular increments in each independent type of misalignment; the field profiles on the axis were extracted and kick factors calculated. An example of these results is shown in Fig. 1.

DISCUSSION OF THE OPTIMISATION OF A LINAC LATTICE TO MINIMISE DISRUPTION BY A CLASS OF PARASITIC MODES

S. Molloy*, ESS, Lund, Sweden

R. Ainsworth, Royal Holloway, University of London, Egham, UK

Abstract

It is well known that each resonant mode in the RF spectrum of multi-cell accelerating cavities will split into a passband containing a number of modes, and that the coupling of these modes to the beam is dependent on the velocity of the accelerated particles. If these modes are found to degrade the quality of the beam, it is possible to take various measures to damp them, and thus keep their effect below some critical threshold. In the case of the parasitic modes within the same passband as the fundamental accelerating mode, their frequency is typically too close to that of the fundamental to allow their power to be safely extracted, and so cavity designers must rely on the natural damping of the cavity itself. This note contains a theoretical discussion of the coupling of the beam to these passband modes for a large class of accelerating cavities, and provides a mathematical model for use during the design and optimisation of linacs.

INTRODUCTION

In general, π -mode accelerating cavities act as several coupled cells, each of which resonates at almost the same frequency. The cell-cell coupling splits each of the resonances into a passband containing the same number of modes as there are coupled cells. Each of these will have the same character (i.e. TM_{mnp} , TE_{mnp} , etc.) as the single cell resonance, but may be differentiated by their frequency and cell-cell phase difference.

Modes lying within the same passband as the accelerating mode will be referred to as Same Order Modes (SOMs), while others will be called Higher Order Modes (HOMs).

Various schemes are used to damp the power in these parasitic modes so that their amplitude has fallen below some threshold value by the time a subsequent beam pulse arrives at the cavity, however the SOMs remain problematic since the similarity of their frequency and structure with the desired fundamental mode mean that it is normally not possible to damp their power sufficiently.

In storage rings or CW linacs, the pulses last long enough that modes whose frequency, f_m , does not lie within a very small region around an integer multiple of the bunch repetition frequency, $n \cdot f_b \pm \Delta f$, will be “washed out”, and will not obtain an amplitude large enough to cause problems. In other words, these modes will be excited at all phases, thus resulting in almost complete cancellation.

In the case of pulsed machines, the shortness of the pulse

will increase the window, Δf , in which damaging parasitic modes might exist. Equivalently, decreasing the pulse length will increase the proportion of the bunch train that will experience high field amplitudes for the parasitic modes before their phase slip with respect to the bunch frequency begins to damp them. Therefore, studies of these modes are important for pulsed machines such as the European Spallation Source (ESS).

Velocity range

In machines that accelerate “heavy” particles such as protons or ions, the accelerating cavities must be designed so as to handle the changing velocity of the beam. Often, linacs are divided into various families of cavities, each of which is optimised for a particular beam velocity. These cavities will have a velocity range over which the efficiency of the acceleration is considered to be acceptable, and so optimisation of the linac design proceeds while taking these boundaries into account.

Just as the efficiency of the accelerating mode (i.e. the coupling of the mode to the beam) is a function of the beam velocity, so is the coupling to the SOMs, and there may be a velocity range where the coupling to a SOM exceeds that of the accelerating mode. In this case, it is likely that this mode will cause significant deterioration of the quality of the beam pulse.

Therefore, the function of the beam’s coupling to the SOMs may provide a tighter limit on the acceptable velocity range of the cavity than would otherwise be expected.

CAVITY MODEL

The cavity model used here follows the derivation used in [1], although note that there are several typos in that paper that make the quantitative conclusions unreliable. Much of the calculation may also be extrapolated from [2].

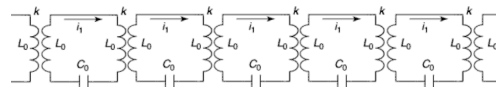


Figure 1: Lumped circuit model of a five-cell cavity connected at both ends to a beam-pipe.

Figure 1 shows the lumped circuit used to model a five-cell cavity coupled to a beam-pipe.

The coupling, k , between each cell, and between the end cells and the beam pipe, is modeled as a transformer, and the cells are modelled as resonant circuits. The values of k , L_0 , & C_0 , may be derived from the desired response of the circuit (i.e. resonant frequency, etc.).

*stephen.molloy@ess.se

SUPERCONDUCTING LOW BETA NIOBIUM RESONATOR FOR HEAVY IONS

Prakash N. Potukuchi, Amit Roy, K.K. Mistri, J. Sacharias and S.S.K. Sonti
Inter-University Accelerator Centre, Aruna Asaf Ali Marg, New Delhi - 110067, India

Abstract

A High Current Injector, as an alternate injector for the superconducting linac, is currently under development at Inter-University Accelerator Centre. To provide some cushion for velocity matching of the beams from HCI, a superconducting low beta module is also being planned for which a new niobium resonator optimized for $\beta=0.05$ operating at 97 MHz, has been designed. This resonator has the highest frequency in its class among the superconducting structures designed for such low velocity particles. The resonator has been carefully modeled to optimize its parameters. Even though the frequency of the resonator is high, its physical dimensions are large enough to allow processing of the superconducting surface effectively. The first niobium prototype has been built and bead pull measurements have been done. It will be tested at 4.2 K shortly. This paper briefly presents the resonator design and fabrication; results from bead pull measurement and expected beam energy from the system.

INTRODUCTION

Presently the 15 UD Pelletron accelerator injects heavy ion beams into the superconducting booster linac at Inter-University Accelerator Centre (IUAC) [1]. In order to provide larger beam currents at high charge states than are currently available from the Pelletron accelerator, a high current injector (HCI) is being developed. In figure 1, a block diagram of the HCI system is shown. The high temperature superconducting electron cyclotron resonance (HTS-ECR) ion source [2] will inject heavy ion beams of mass to charge ratio (A/q) = 6 at an energy of ~ 8 keV/u into a room temperature radio frequency quadrupole (RFQ) [3] which will accelerate it to ~ 180 keV/u. The beam would be further accelerated through a drift tube linac (DTL) section [4] which will have half a dozen tanks, the maximum number that can be accommodated in the new HCI-hall. The expected maximum energy at the end of the DTL section is around 1.8 MeV/u. However, long term stable operation may require restricting its operation to ~ 1.5 MeV/u only. This corresponds to a velocity β ($=v/c$) = 0.056, which is very close to the lower velocity cut off of the quarter wave resonators employed in the linac [5]. In order to provide some cushion for velocity matching of the beams from HCI into the linac, a superconducting low beta module (LBM) is being planned after the DTL section. The low beta module, however, will be positioned in such a way that it can accelerate beams from HCI as well as the Pelletron accelerator. A new superconducting niobium quarter wave resonator optimized for $\beta_0=0.05$ operating at 97 MHz has been designed for this module.

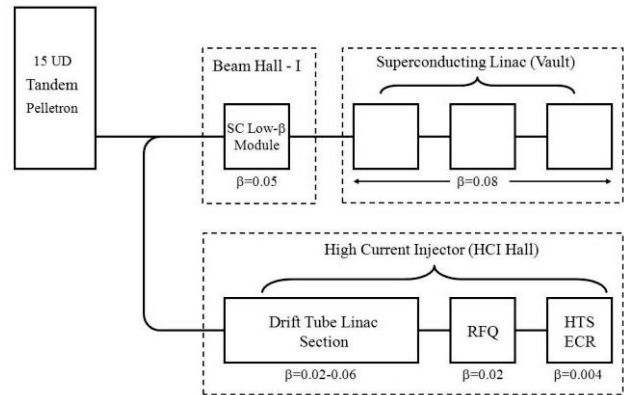


Figure 1: Block diagram of the HCI system. The dashed boxes indicate the location of the various components.

LOW β RESONATOR

Design

TEM class superconducting niobium resonators are used in linacs for accelerating heavy ions. Several variants of this class of structure have been designed and developed around the world [6]. Among them, the two gap quarter wave co-axial line resonator (QWR) is characterized by its excellent mechanical stability and broad velocity acceptance. In addition, QWRs are simpler to fabricate compared to other structures, although more number of resonators are required to reach the final beam energy. Over the past two decades many techniques have been developed to effectively address the extrinsic effects that limit the achievable accelerating gradient in niobium resonators and these have helped in pushing the gradients up [7]. Besides, it is well known that quarter wave resonators achieve higher gradients as compared to, say half wave structures [8]. Overall the QWR structure therefore offered a very good choice for the low beta resonator design.

The LBM will be located in beam hall-I (figure 1) where the ceiling height is slightly less than that in the linac vault. The overall height of the resonator was therefore an important design parameter. In order to restrict it we decided to keep the frequency high and chose 97 MHz, which is also the frequency of the quarter wave resonators used in the linac. The electromagnetic parameters of the low beta resonator were carefully optimized using Microwave Studio code [9]. The main goal in the optimization was to reduce the peak magnetic and electric fields in the resonator while maintaining high values for the shunt impedance and geometric factor, and a small value of stored energy. To achieve these, the drift tube length and accelerating gaps were chosen to obtain

STUDIES OF PARASITIC CAVITY MODES FOR PROPOSED ESS LINAC LATTICES

R. Ainsworth*, Royal Holloway University of London, UK
 S. Molloy, European Spallation Source AB, Lund, Sweden

Abstract

The European Spallation Source (ESS) planned for construction in Lund, Sweden, will be the worlds most intense source of pulsed neutrons. The neutrons will be generated by the collision of a 2.5 GeV proton beam with a heavy-metal target. The superconducting section of the proton linac is split into three different types of cavities, and a question for the lattice designers is at which points in the beamline these splits should occur. This note studies various proposed designs for the ESS lattice from the point of view of the effect on the beam dynamics of the parasitic cavity modes lying close in frequency to the fundamental accelerating mode. Each linac design is characterised by the initial kinetic energy of the beam, as well as by the velocity of the beam at each of the points at which the cavity style changes. The scale of the phase-space disruption of the proton pulse is discussed, and some general conclusions for lattice designers are stated.

INTRODUCTION

The European Spallation Source is a facility, currently in its design phase [1], for the generation of intense pulses of neutrons for studies in applied science. The neutrons are generated through the spallation process when a 5 MW (average) proton pulse is made to impact a heavy metal target.

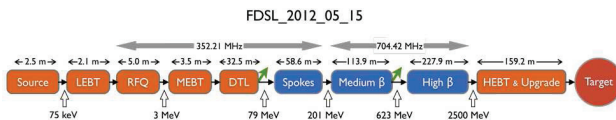


Figure 1: Block diagram of the ESS linac.

	Value	Unit
Final kinetic energy	2.5	GeV
Macropulse current	50	mA
Macropulse repetition rate	14	Hz
Bunch frequency	352.21	MHz

Table 1: Main ESS linac parameters.

A cartoon of the ESS linac is shown in Figure 1, and the main parameters of the proton beam are given in Table 1.

*rob.ainsworth.2009@live.rhul.ac.uk

This note concerns the beam dynamics within the superconducting sections of the machine:

Spokes: Two–spoke cavities operating at 352.21 MHz.

This section accelerates the beam from the exit of the DTL at 79 MeV to 201 MeV.

Medium β : Five–cell elliptical cavities operating at 704.42 MHz. The geometrical beta of this section is still under discussion, but is likely to be set at a value close to, $\beta_g = 0.65$. In this section, the beam is accelerated from 201 MeV to 623 MeV.

High β : Five–cell elliptical cavities operating at 704.42 MHz. As with the previous section, the geometrical beta is still under discussion, but the likely value is close to, $\beta_g = 0.92$. This section accelerates the beam to its final energy of 2.5 GeV

Given the high intensity of the beam, one major concern is that strong resonances will be excited in the superconducting cavities that will then act to disrupt subsequent bunches. In particular parasitic modes that lie close in frequency to that of the accelerating mode. They are of concern due to there small frequency spread and high R/Q relative to the accelerating mode. If they are found to be a problem, the geometric beta of the cavity may need to be altered or the velocity partitioning between the cavity families may need to be shifted.

LINACS

For the studies into Same Order Modes (SOMs), that is, modes that are part of the same passband as the fundamental accelerating mode, four linacs are investigated as shown in Table 2 where cavities per family denotes the number of cavities in the spoke, medium β and high β sections.

Linacs	Cavities per family	Energy In [MeV]
HS_2011_11_23	36-64-12	50
FD_SL_2012_04_13	32-60-120	79
FD_SSCL_2012_04_16	32-52-128	80
FD_SL_2012_05_15	28- 60-120	79

Table 2: Linacs investigated for SOM simulations.

MAIN COUPLER DESIGN FOR PROJECT X*

S. Kazakov, O. Pronitchev, S. Cheban, M. Kramp, V. Poloubotko,
V. P. Yakovlev, T. N. Khabiboulline, Y. Orlov, FNAL, Batavia, IL 60510, USA
M. S. Champion, ORNL, Oak Ridge, Tennessee, USA

Abstract

325MHz and 650MHz multi-kilowatt CW main couplers for superconducting linac of Project X and their design parameters are presented. Experimentally measured effectiveness of antenna air cooling is introduced.

INTRODUCTION

A multi-megawatt proton/ H^- source, Project X, is under development at Fermi National Accelerator Laboratory [1]. Main element of it is 3 GeV superconducting proton linac which includes 5 families of superconducting cavities of three frequencies: 162.5, 325 and 650 MHz. 162.5 MHz cavities and main couplers are under developing in Argonne National Laboratory. Scope of this paper is development of power couplers for 325 and 650 MHz at FNAL. Superconducting linac of Project X is supposed to accelerate 1 mA average proton beam and it is considered a possibility to increase beam current up to 5mA in the future. This upgraded version of accelerator will require two types of couplers, which reliably can operate at CW power level ~ 25 kW at 325MHz and ~ 100 kW at 650MHz respectively. In this paper we are describing current design of these couplers.

COUPLERS DESIGN AND PARAMETERS

Recent Changes in the Design

There were several earlier publication on subject of Project X couplers [2,3]. Since the last publication, several changes were made in the design, which resulted in a change of some coupler parameters.

In the previous design there was a large bellows, which is housed outside the cryomodule. The purpose of the bellows was compensation an accelerating cavity shift and thermal shrink/expansion of coupler parts during cool down/warming up. Due to the bellows location outside of cryomodule, a sufficiently large force (~ 200 kg) due to the atmospheric pressure was applied to the accelerating cavity. It had to be compensated by special springs. In this design a coupler had to be rigidly fixed to cryomodule body after completion of the cooling down/warming up and had to be unfixed during these procedures. It was deemed inconvenient and potential reason of accidents.

A large bellows was replaced by four bellows. Two of them are located on the outer conductor of coaxial coupler, two - in the internal conductor. Bellows are located inside the cryomodule and coupler does not require to be fixing/unfixing during cooling down and

warming up. The atmospheric pressure difference driven force is reduced to 40 kg. The bellows are still located on the non-vacuum side of the coupler and requirements are not as high as if they were located in vacuum close to an accelerating cavity. Current set of bellows can accommodate ± 3 mm displacement in any direction.

The second important change: a copper plating was removed from coaxial outer conductor of vacuum side of 350 MHz coupler. It decreases static and increases dynamic cryo-loadings, but improves the reliability of the coupler. Previous experience shows that the copper coating often is a source of many problems. Dynamic cryo-loading still is in an acceptable range.

The third change: the temperatures of thermal interceptors were increased. Now temperature of interseptor nearest to 2 K cavity flange is considered as 15 K instead of 5 K and temperature of second interseptor is considered to be 125 K instead of 80 K. We think these values are more realistic, though perhaps are too conservative. It increases calculated static cryo-loading of the coupler.

The fourth change: in order to decrease a static cryo-loading, the thickness of stainless outer conductor of vacuum part of couplers was changed from 0.8mm to 0.4mm

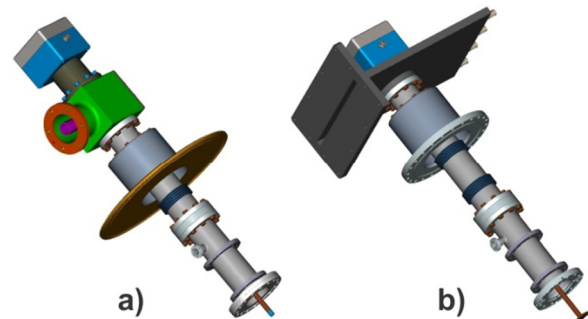


Figure 1: General view of a) 325MHz and b) 650 MHz couplers

Current Design and Electrical Parameters

General views of 325 MHz and 650 MHz couplers are presented in Figure1. Couplers have similar structures and have many common parts and technologies. Cut view of 325 MHz coupler with details is shown in Figure 2. 650 MHz coupler has the same internal structure but waveguide input port instead of coaxial one. We would like to remind the design approach: to keep a geometry of vacuum part of couplers, which connected to superconducting cavity, as simple as possible. We think it should increase reliability. All complicated elements like a bellows and matching elements are moved to the air part of devices. Main features of the design: single RF

*Work supported by DOE

COHERENT EFFECTS OF HIGH CURRENT BEAM IN PROJECT-X LINAC

A. Sukhanov*, A. Lunin, V. Yakovlev, I. Gonin, T. Khabiboulline, A. Saini,
N. Solyak, and A. Vostrikov, Fermilab[†], Batavia, IL 60510, USA

Abstract

Resonance excitation of longitudinal high order modes in superconducting RF structures of Project-X continuous wave linac is studied. We analyze regimes of operation of the linac with high beam current, which can be used to provide an intense muon source for the future Neutrino Factory or Muon Collider, and also important for the Accelerator-Driven Subcritical systems. We calculate power loss and associated heat load to the cryogenic system. Longitudinal emittance growth is estimated. We consider an alternative design of the elliptical cavity for the high energy part of the linac, which is more suitable for high current operation.

INTRODUCTION

A multi-megawatt proton source, Project-X (PX) is now under development at Fermilab [1]. PX will provide high quality muon, kaon and neutrino beam, unavailable at existing facilities, and support physics program at the intensity frontier. Eventually, PX may become a driver for a future Neutrino Factory and/or Muon Collider at Fermilab.

Technology, which is being developed for Project-X, may be directly applied to Accelerator-Driven Subcritical systems (ADS) for energy generation and transmutation of nuclear waste [2]. ADS applications require continuous wave (CW) multi-MW proton beam with high average current and high availability. Thus, exploration of the capability of PX technology to deliver beam of ≥ 10 mA is important.

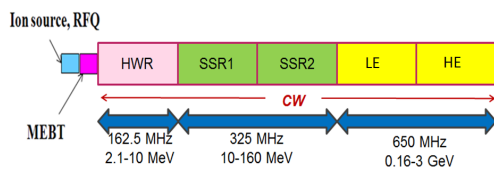


Figure 1: Project-X linac layout.

A key component of Project-X is the CW superconducting RF linear accelerator. It accelerates bunches of H^- ions from 2.1 MeV to 3 GeV. Layout of the linac is shown in Fig. 1. The high energy (HE) section of the linac uses 650 MHz 5-cell elliptical cavities. Coherent excitation of monopole high order modes (HOMs) in these cavities may affect stable operation of the linac due to rise of cryogenic losses and deterioration of beam quality. Our study [3]

shows, that it is not a problem for the present PX parameters, CW regime, and 1 mA average beam current. However, HE cavities have a potential problem, when monopole HOMs of the 5th passband may become trapped in the internal cells of a cavity [4]. This, together with the fact that cryogenic losses increase as square of an average beam current, $P_{loss} \sim I_{beam}^2$, may lead to losses up to hundred Watt for 10 mA beam.

In this paper we calculate cryogenic heat load and estimate growth of the longitudinal beam emittance due to coherent excitation of monopole HOMs during operation of PX CW linac with an average beam current up to 10 mA. We compare results of these calculations for the present and alternative [4] designs of the HE elliptical cavities.

COHERENT HOM EXCITATION

A bunched continuous beam passing through a superconducting cavity may coherently excite one of the cavity HOM with a high quality factor, Q . The bunch sequence frequency in PX linac is 162.5 MHz. A broad-band chopper provides the beam structure needed for experiments. A typical bunch timing structure required for muon, kaon and nuclear experiments running in parallel at 3 GeV is shown in Fig. 2. Average beam current in this mode is 1 mA. Fig. 3 shows the spectrum for the idealized 3 GeV beam structure, assuming very short bunches of equal charge and in the absence of timing jitter.

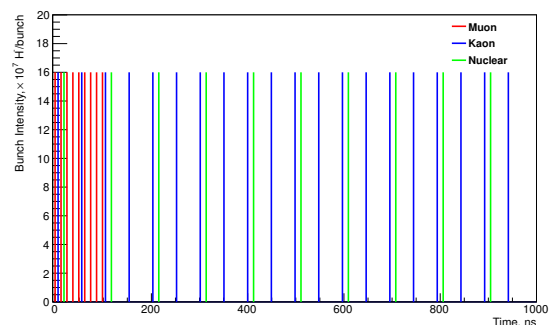


Figure 2: Beam structure for 3 GeV program.

Spectrum and (R/Q) values of PX HE structure are shown in Fig. 4. Amplitude of an excited monopole HOM depends on the amplitude of the nearest beam spectrum line, \tilde{I} , and detuning δf , the distance between the HOM frequency f and the beam spectrum line frequency, and

* ais@fnal.gov

[†] Operated by Fermi Research Alliance, LLC under Contract No. De-AC02-07CH11359 with the United States Department of Energy.

R&D OF IMP SUPERCONDUCTING HWR FOR CHINA ADS

Weiming Yue, Yuan He, Shenghu Zhang, Bin Zhang, Shoubo He, Cong Zhang, Mengxin Xu, Pingran Xiong, Shengxue Zhang, Ruoxu Wang, Xueliang Guo, Hongwei Zhao, Institute of Modern Physics, Chinese Academy of Sciences Lanzhou 730000, China

Abstract

The R&D program of IMP superconducting HWR is based on the China ADS, The aim is to build and test a HWR prototype on December 2012. We have designed a 162.5 MHz $\beta=0.09$ half-wave resonator (HWR), and a copper HWR has been fabricated in January 2012. The fabrication of a Nb HWR will be completed by September 2012, and the fabrication of a slow tuner and a high power coupler for this HWR will be completed then. In this poster, we present the HWR electromagnetic design, mechanical design, fabrication arts, copper HWR RF test result, the design of the slow tuner and the power coupler.

INTRODUCTION

At present, many energy researchers agree that nuclear energy is the best way to solve the issue of an energy shortage. In order to apply nuclear energy in a safe and clear way, the accelerator and nuclear scientists obtained a reasonable way to apply nuclear energy and dispose the nuclear wastes, this is an accelerator-driven system (ADS). IMP and IHEP are developing a high-intensity CW H- ion linac for China ADS (Accelerator Driven Sub-critical System), The main design parameters of linac are listed in Table1 [1]. Two injectors are being constructed by IMP and IHEP to demonstrate the most critical R&D issue related to the front-end of a CW high-power and proton linac. Injector I chose Superconducting spoke cavity to accelerate H- from 3.2MeV to 10MeV, which is being constructed by IHEP. Inject II chose Superconducting Half-wave Resonator to accelerate H- from 2.1MeV to 10MeV, which is being constructed by IMP. HWR is a well built superconducting cavity international, there are many labs in the world have designed and constructed HWR cavities.

Table 1: China ADS Linac Main Design Parameters

Parameters	Value	Unit
Particle	Proton	
Frequency	162.5/325/650	MHz
Energy	1.5	GeV
Current	10	mA
Beam power	15	MW
Duty factor	100	%

ELECTROMAGNETIC DESIGN

The design of the HWR consists in reaching a reasonable compromise between optimal electromagnetic performances, acceptable mechanical characteristics, and ease of fabricating and preparation [2]. The first step in this HWR design is to optimize the RF properties of the HWR.

The goal of the RF properties is to get a lower heat load and a higher accelerating gradient, which are determined by a higher R/Q0 (R is the shunt impedance and Q0 is the quality factor) and lower peak surface fields (Bpk/Eacc and Epk/Eacc). There are four electron beams welding in the cavity high magnetic region when welding our HWR, and we can't grinding this region, so the performance limitation in the HWR is the thermal-magnetic quench, which leads us to put more care to minimize Bpk/Eacc.

RF Optimization

The most important design parameters to optimize were: Bpk/Eacc, Epk/Eacc, R/Q0 and G [3]. A selected number of cavity geometry parameters were used during this optimization. They are shown on Fig. 1.

In order to optimize the HWR geometry parameters, CST-MWS is used to conduct the RF simulation. Starting from a initial HWR model showed in Fig. 1 and varying the geometry parameters one at a time we were able to establish the general dependence of the important design parameters on the geometry parameters, Fig. 2 shows the quantitative dependence in %.

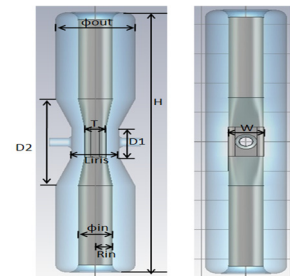


Figure 1: Parameters of the cavity geometry used in the RF optimization.

We notice that the design parameters to optimize are more sensitive to the parameters, namely, Rout, Rin, T, Liris, W and Rblend2. Increasing the HWR outer conductor radius (Rout), a significant improvement in all parameters of interest. Beyond 92 mm we begin to sacrifice real-estate gradient. We choose Rout as 92 mm. By decreasing the inner conductor radius (Rin) while

THE MULTIPACTING SIMULATION FOR THE NEW-SHAPED QWR USING TRACK3P*

C. Zhang[#], S. He, Y. He, S. Huang, Y. Huang, T. Jiang, R. Wang, M. Xu, Y. Yang, W. Yue, S.H. Zhang, S. Zhang, H. Zhao
 Institute of Modern Physics, Lanzhou, Gansu 730000, China

Abstract

In order to improve the electro-magnetic performance of the quarter wave resonator, a new-shaped cavity with an elliptical cylinder outer conductor has been proposed [1]. This novel cavity design can provide much lower peak surface magnetic field and much higher R_a/Q_0 and G. The multipacting simulation has been done for this new QWR cavity using ACE3P/TRACK3P code, in this paper the simulation results will be presented and analyzed.

INTRODUCTION

In the Heavy Ion Accelerating Facility (HIAF) of IMP, superconducting quarter wave resonators (QWRs) with frequency of 81.25 MHz and β of 0.041, 0.085 will be applied to accelerate the ion beams from 0.3 MeV/u to 17 MeV/u. Because of the extremely high design voltage for the $\beta = 0.085$ QWR cavity, an elliptical cylinder outer conductor shape has been proposed for it (see Fig. 1).

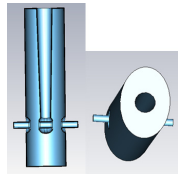


Figure 1: The elliptical cylinder outer conductor QWR model for multipacting simulation.

MULTIPACTING SIMULATION

Parallel codes Omega3P and Track3P which are developed at SLAC have been used, to obtain the field maps and then to analyse the multipacting barriers [2, 3]. When doing the multipacting simulation, one half of the QWR cavity was used taking advantage of the symmetry. Seed particles were initiated on all the RF surfaces. The accelerating gradient was scanned up to 6 MV/m firstly to locate the multipacting band, and then much finer scan interval was used in order to study the multipacting band in detail. 2 eV was used as the initial energy for primary and secondary emissions to study its effect on multipacting and typical niobium secondary electron yield (SEY) was applied to estimate the multipacting strength (see Fig. 2). At each field level, 50 RF cycles were used as total running time to obtain resonant trajectories.

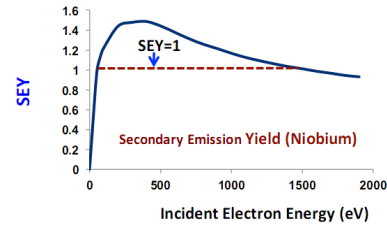


Figure 2: Secondary electron yield (SEY) for Niobium on the dependence of impact energy. The impact energy range relevant to the peak SEY is 150~700 eV. Resonant electrons with impact energies in this range are most dangerous to lead to hard multipacting.

MULTIPACTING SIMULATION RESULTS

Multipacting Band at Low Field Level

The distribution of resonant particles identified by Track3P presented the multipacting bands occurred at low field levels, Figure 3, 4 show the expanded plot around this multipacting band and impact positions.

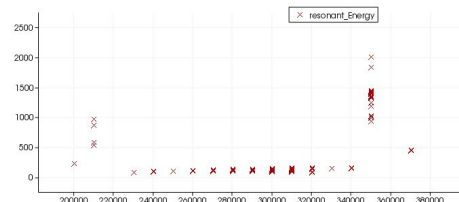


Figure 3: Impact energy vs. accelerating gradient at low field level.

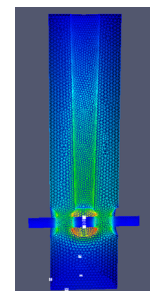


Figure 4: Impact positions at all field levels.

There are two multipacting bands, one at field levels of 0.2 ~0.34 MV/m with impact energies 80~160 eV in the beampipe region (see Fig. 5, 6); the other at around the accelerating gradient of 0.35 MV/m with impact energies 700~2000 eV in the bottom part of the cavity. In consideration of the peak SEY energy for Nb (see Fig. 2), such two bands are expected to be a soft barrier.

* Work supported by 91026001 Nature Science Foundation
[#] claire335@gmail.com

STRUCTURAL ANALYSIS OF THE NEW-SHAPED QWR FOR HIAF IN IMP*

C. Zhang[#], S. He, R. Wang, M. Xu, W. Yue, S. Zhang, S. Huang, Y. Yang, Y. Huang
T. Jiang, S. Zhang, Y. He, H. Zhao

Institute of Modern Physics, Lanzhou, Gansu 730000, China

Abstract

Since the QWR cavity is very successful for the operation with frequency of 48 to 160 MHz and beta value of 0.001 to 0.2, a new-shaped QWR is being designed for the low energy superconducting section of HIAF in the Institute of Modern Physics [1]. The cavity will work at 81.25 MHz and beta of 0.085, with an elliptical cylinder outer conductor to better its electro-magnetic performance and keep limited accelerating space. Structural design is an important aspect of the overall cavity implementation, and in order to minimize the frequency shift of the cavity due to the helium bath pressure fluctuations, the Lorentz force and microphonics excitation, stiffening elements have to be applied. In this paper, structural analyses of the new-shaped QWR are presented and stiffening methods are explored.

INTRODUCTION

A stable resonant frequency for the superconducting cavity is desired, because excessive frequency fluctuations require extra power to control the RF amplitude and phase. The reasons that lead to frequency fluctuations include the fluctuations in the liquid helium pressure, Lorentz force detuning, mechanical vibration modes and the etching effect from the cavity surface treatment. Since the operating temperature for the QWR cavities is 4.5 K, the helium pressure stability will be determined by the extent to which the cryogenic plant can be controlled. The stiffening measures were intended primarily to reduce the pressure sensitivity.

MECHANICAL SIMULATION

When the EM design has been completed, the mechanical performance of the cavity should be evaluated. We tried to figure out the cavity's helium pressure sensitivity, severity of Lorentz Force Detuning plus the vibration frequency of mechanical modes, and further, to minimize the instabilities using different stiffening measures. Simulations and optimizations have been done by the 3D Multiphysics solver ANSYS-APDL [2]. In the simulation, niobium sheet of 3 mm thickness was firstly used, with the mechanical properties of Young

modulus of 105000 N/mm², Poisson ratio of 0.38 (see Fig. 1) .

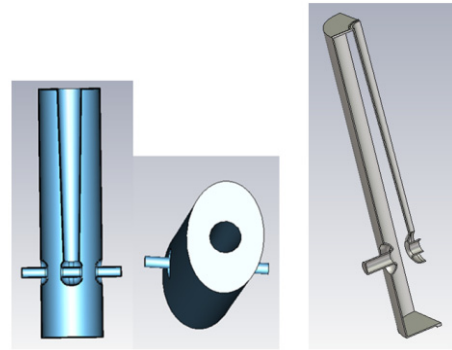


Figure 1: Mechanical model of the elliptical cylinder outer conductor QWR for the structural analysis.

Etching Effects

Surface processing is very important in order to achieve good performance of the superconducting cavity. Either the BCP or the EP is to etch proper thickness of the inner surface, which will change the frequency. According to Slater's perturbation theory, a small deformation in the cavity boundary will lead to a frequency shift.

Using the ANSYS-APDL code, the change in the frequency because of the etching can be calculated. Firstly, you have to get the electro-magnetic field distribution, and then the frequency change caused by the cavity wall's deformation can be obtained. The simulation results show that 1 μm etching thickness will lead to 27Hz increase in the frequency.

Lorentz Force Detuning

The Lorentz force on the cavity surface results from the interaction of the surface electromagnetic fields with the induced surface currents, which will exert pressure to the cavity wall, and the resulting cavity shape deformation ΔV will cause the change in the resonant frequency. The frequency shift caused by Lorentz force is often quantified by K_L which is defined as: $K_L = \Delta f / (E_{acc})^2$.

If the cavity works at the continuous wave mode, then the frequency change will be invariant, it is the static Lorentz force detuning; otherwise, when the cavity works at the pulsed wave mode, the dynamic Lorentz force detuning will be caused. In this paper, only the static situation was considered and 2.5 MV accelerating voltage was to be scaled for the naked cavity whose

*Work supported by 91026001 Nature Science Foundation
#claire335@gmail.com

AN ANALYTICAL CAVITY MODEL FOR FAST LINAC-BEAM TUNING*

Zhengqi He[#], Zhihong Zheng (FRIB, East Lansing, Michigan; TUB, Beijing),
Zhengzheng Liu, Yan Zhang, Jie Wei, (FRIB, East Lansing, Michigan)

Abstract

Non-axisymmetric RF cavities can produce axially asymmetric acceleration fields. Conventional method using numerical 3-D field tracking to address this feature is time-consuming and thus not appropriate for on-line beam tuning applications. In this paper, we develop analytical treatment of non-axisymmetric RF cavities. Multipole models of cavities are derived using realistic 3-D field in both longitudinal and transverse dimensions. Then, beam dynamics formalism is established. Finally, special case of FRIB quarter-wave resonators are calculated by the model and benchmarked against 3-D field tracking to ensure the efficiency and accuracy of the model.

INTRODUCTION

Non-axisymmetric RF cavities, such as quarter-wave resonators (QWR), half-wave resonators (HWR) and spoke cavity, can produce dipole and quadrupole terms in transverse direction, and can cause beam steering and deformation. Up to now, no model can handle this problem except for multi-particle tracking. So, we aim at building longitudinal and transverse model for non-axisymmetric RF cavities to solve this problem. The model will be implemented into on-line beam tuning application^[1], therefore the basic requirement is accuracy and efficiency.

LONGITUDINAL DYNAMICS

For linac acceleration, keeping track of kinetic energy and phase evolution would be important. Particle tracking by iteration is the traditional way, while revealing lack of efficiency when applying to online beam tuning. To solve the problem, the thin lens model is implemented, describing the energy gain and phase advance after a RF cavity, which can be considered as a drift-kick-drift model as below^{[2][3]}:

$$\begin{cases} W_f = W_i + qV_0T(k)\cos\phi_i - qV_0S(k)\sin\phi_i \\ \phi_f = \phi_i + \frac{qV_0}{2W_i}k[T'(k)\sin\phi_i + S'(k)\cos\phi_i] \end{cases} \quad (1)$$

where W_i and W_f stands for initial and final kinetic energy and ϕ_i and ϕ_f are initial and final particle phase. V_0 are the static electric voltage. T , T' , S and S' are the transit-time factors calculated from numerical electric field data. In order to analyse the error introduced by constant beta assumption during drift section, two kinds of thin lens model is developed comparatively for multi-gap cavities. 1) One gap kick model treats the whole cavity as one thin

accelerating gap. 2) Multi-gap kick model treats each accelerating gap separately.

Comparison with Simulation

Facility of Rare Isotope Beams (FRIB)^[4] linac segment is implemented for comparison between model and numerical calculation. FRIB linac segment one, which consists of three $\beta=0.041$ QWR cryomodules and eleven $\beta=0.085$ QWR cryomodules, accelerates ions from 0.5MeV/u to 16.6MeV/u. By adding cavity driven phase onto absolute particle phase, we obtain the initial phase of the certain particle, which can be described as: $\phi_i = \phi_{abs} + \phi_{drive}$; The driven phase is set so that the synchrotron phase is -30 deg. After setting the driven phase, linac segment acceleration simulation is performed via 4 different methods, namely, IMPACT^[5] tracking (used as reference), particle tracking, 2-gap kick model, 1-gap kick model. For 2-gap kick model, we can achieve the phase precision of 0.31% when divided by 2π , and kinetic energy gain prediction precision of 0.042% of the 16.1MeV/u kinetic energy gain (figure 1). The numerical electric field data comes from CST^[6] simulation.

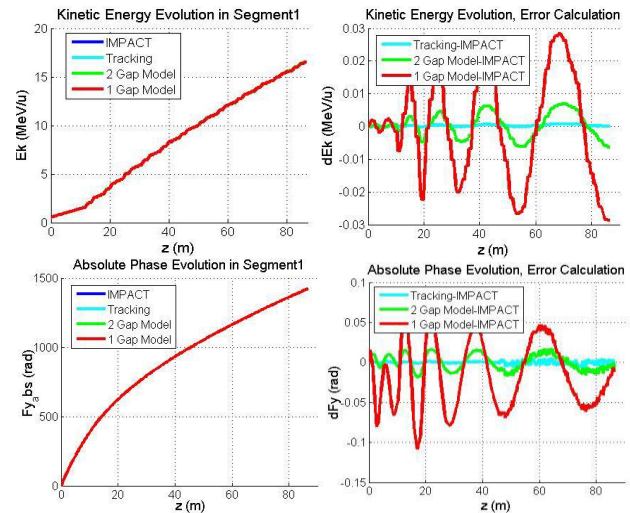


Figure 1, Kinetic energy and Absolute phase evolution and error calculation; a) Kinetic Energy evolution; b) Difference between different models and IMPACT simulation in Kinetic energy prediction; c) Absolute phase evolution; d) Difference between different models and IMPACT simulation in absolute phase prediction.

TRANSVERSE DYNAMICS

Traditional treatment of transverse RF cavity field usually only consists of focusing electric field terms. However, early studies already show that field dipole terms and quadrupole terms exist in non-axisymmetric RF

* Work supported by the U.S. Department of Energy Office of Science under Cooperative Agreement DE-SC0000661

MULTIPACTING SUPPRESSION MODELING FOR HALF WAVE RESONATOR AND RF COUPLER *

Z. Zheng^{1,2}, A. Facco^{1,3}, Z. Liu¹, J. Popielarski¹, K. Saito¹, J. Wei¹, Y. Xu¹, Y. Zhang¹

¹ FRIB, East Lansing 48824, Michigan, USA

² TUB, Beijing, China

³ INFN - Laboratori Nazionali di Legnaro, Padova, Italy

Abstract

In prototype cryomodule test of Facility of Rare Isotope Beam (FRIB) $\beta=0.53$ half-wave-resonators (HWRs) severe multipacting barriers, prevented RF measurement at the full field specified. The multipacting could not be removed by several hours of RF conditioning. To better understand and to eliminate multipacting, physics models and CST simulations have been developed for both cavity and RF coupler. The simulations have good agreement with the multipacting discovered in coupler and cavity testing. Proposed cavity and coupler geometric optimizations are discussed in this paper.

INTRODUCTION

While the multipacting can be categorized by different physics features, the 1st order multipacting with electrons bouncing between two points is significantly stronger than other kinds of multipacting. First order two point multipacting is related primarily to the geometric structures. During the prototype cryomodule test with the final cavity coupler, multipacting barriers which did not show up or that could be easily conditioned in the vertical test prevented us from reaching full gradient. RF conditioning had very little effect. Since the only significant change from the successful vertical test was the coupler, we attributed these new barriers to the change of geometry in the coupler region. The fact that MP could be suppressed by magnetic field around the coupler confirmed our hypothesis. We developed physics models to help simplify the coupler geometry optimization to eliminate MP. Simulations done with CST [1] reassured the physics models. In this paper, Section 1 gives the physics model and CST simulation results of FRIB $\beta=0.53$ HWR 1st generation prototype; Section 2 discusses the physics model and optimization scheme for the RF coupler.

MULTIPACTING IN HWR

Multipacting Conditions in the HWR

From CST simulation, multipacting in the HWR cavity mainly locates at the short plate as shown in Figure 1 (green semi-circle). The two-point, 1st order multipacting can thus be described with a cyclotron model, as shown in Figure 2.

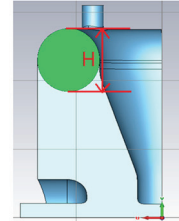


Figure 1: 1/8 structure of FRIB $\beta=0.53$ cavity, the short plate is marked as green semi-circle, which is the conjunction between cavity inner and outer conductor.

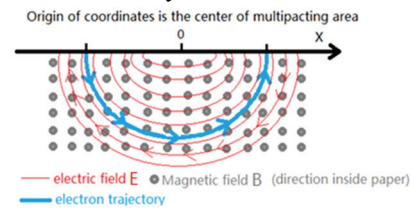


Figure 2: Physics picture of two point 1st order multipacting at a short plate. The flat is the infinitesimal approximation of the semi-circle short plate.

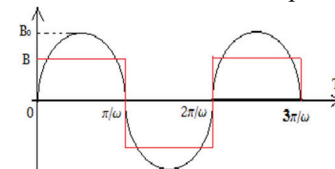


Figure 3: Assumption of B field (red line) as an approximation of the real field B_0 .

The magnitude of B is assumed to be $1/\sqrt{2}$ of B_0 to simplify the analytical model, as the red step function shown in Figure 3. Electric field has the same assumption.

According to this cyclotron model, conditions of two-point 1st order multipacting are:

$$E_0(-x) = -E_0(x) \quad (1)$$

$$T = T_{rf} = \frac{2\pi}{\omega} \quad (2)$$

$$W_1 < K_{impact} < W_2 \quad (3)$$

B_0 and E_0 are the magnetic and electric field amplitudes on the plate surface, ω is the cavity's circular frequency, T is the cyclotron period of electron and T_{rf} is the RF period, $[W_1, W_2]$ is the region of impact energy corresponding to $SEY > 1$.

To further interpret Eq. (3) of K_{impact} in terms of electric and magnetic field, we obtain:

$$r \approx \sqrt{\frac{K_{impact} m}{B_0 e}} \quad (4)$$

*Work supported by the U.S. Department of Energy Office of Science under Cooperative Agreement DE-SC0000661

ADRC CONTROL FOR BEAM LOADING AND MICROPHONICS *

Z. Zheng[#] (FRIB, East Lansing, Michigan; TUB, Beijing)

Z. Liu, J. Wei, S. Zhao, Y. Zhang (FRIB, East Lansing 48824, Michigan, USA)

Abstract

Superconducting RF (SRF) cavities are subject to many disturbances such as beam loading and microphonics. Although we implemented Proportional Integral (PI) control and Active Disturbance Rejection Control (ADRC) in the Low Level RF (LLRF) system at FRIB to stabilize the RF field, the control loop gains are inadequate in the presence of beam loading and microphonics. An improved scheme is proposed and simulated with much higher gains are achieved. The feasibility to include piezo tuner in ADRC and PI circuit is also presented in this paper.

INTRODUCTION

For a SRF cavity, there exist many disturbances, either external or self-induced, in which beam loading and microphonics are two most important ones. While beam loading disturbs the cavity voltage and RF phase with beam induced voltage, microphonics detunes cavity by mechanical perturbations. To reject the disturbances, PI control strategy and ADRC method have been considered. PI handles disturbances in a passive way, reacting to tracking errors caused by the disturbances, while ADRC rejects the disturbances actively by estimating the disturbances directly.

In the original LLRF system of FRIB cavities, both PI and ADRC solutions are implemented to control the amplitude and phase separately, because it was assumed that independent amplitude and phase control will benefit more to operation. Simulation shows that such a scheme presents potential difficulties in phase control, with both ADRC and PI, where the loop gain can be inadequate to reject microphonics. Figure 1 shows the phase fluctuation of ADRC exceeds the cavity phase stability limit of 0.5 degree. PI control performs worse than ADRC with much larger phase and amplitude fluctuations with separated phase and amplitude controllers.

According to SNS LLRF control experience [1], we proposed a new scheme to process and control the cavity voltage as a vector instead of separating amplitude and phase. Section 1 explains the new model of ADRC control. Section 2 shows the comparison of ADRC and PI with the new scheme, from which one can see the stable loop gain increased significantly and rejected beam loading and microphonics effectively. Section 3 discusses the feasibility to reject microphonics by a piezo-tuner.

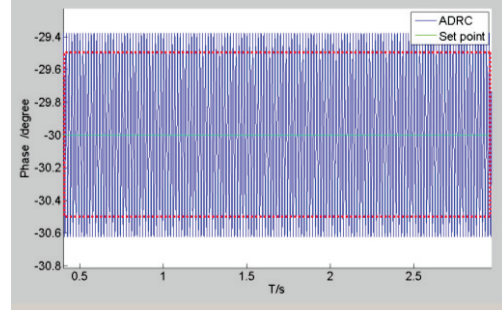


Figure 1: Phase fluctuation to reject microphonics by the original ADRC scheme. The red line marks the fluctuation limit due to stability concern of cavity phase. Microphonics amplitude is assumed to be 20Hz in this calculation.

MODEL OF ADRC CONTROL

The cavity dynamics is represented by a parallel RLC circuit as shown in Figure 2. According to Kirchhoff's law, we have:

$$\frac{d^2\hat{V}_c}{dt^2} + \frac{\omega_0}{Q} \frac{d\hat{V}_c}{dt} + \omega_0^2 \hat{V}_c = \frac{R\omega_0}{Q} \frac{d\hat{I}_c}{dt} \quad (1)$$

$$\hat{I}_c = \frac{(\hat{I}_g + \hat{I}_b)Z_{ext}}{Z_{ext} + Z_{cav}}, \quad Z_{ext} = \frac{R}{\beta} \quad (2)$$

$$\hat{V}_c(t) = \vec{V}(t)e^{j\omega_g t} = V_c(t)e^{j\phi_s(t)}e^{j\omega_g t} \quad (3)$$

$$\hat{I}_c(t) = \vec{I}(t)e^{j\omega_g t} = I_c(t)e^{j\theta(t)}e^{j\omega_g t} \quad (4)$$

Since $\dot{\vec{V}}_c \ll \omega_g \vec{V}_c$ and $\dot{\vec{I}}_c \ll \omega_g \vec{I}_c$, Eq. (1) can be simplified to first-order differential equation as:

$$\dot{\vec{V}}_c + \omega_{1/2}(\vec{V}_c - \frac{\hat{I}_b Z_{ext}}{Z_{ext} + Z_{cav}} R) + \frac{\Delta\omega}{j} \vec{V}_c = \omega_{1/2} \frac{\hat{I}_g Z_{ext}}{Z_{ext} + Z_{cav}} R \quad (5)$$

where ω_0 is cavity resonant frequency and Q is quality factor, β is coupling factor, \hat{I}_g is generated current, \hat{I}_b is beam induced current due to beam loading effect, \hat{I}_c is total current of cavity, \hat{V}_c is cavity voltage, ω_g is generator circular frequency, $\Delta\omega = \omega_0 - \omega_g$ is the total cavity detuning by microphonics and tuner, $\omega_{1/2} = \omega_0 / 2Q$ is cavity half bandwidth, Z_{cav} and Z_{ext} is cavity and external impedance.

According to the model, we can define the output of cavity system as $y = \alpha \vec{V}_c$, cavity input as $u = I_g / A$. Eq.

(5) can be simplified as $\dot{y} = f + bu$, where

$$f = -\alpha\omega_{1/2}(\vec{V}_c - \frac{\hat{I}_b Z_{ext}}{Z_{ext} + Z_{cav}} R) - \alpha \frac{\Delta\omega}{j} \vec{V}_c \quad (6)$$

*Work supported by the U.S. Department of Energy Office of Science under Cooperative Agreement DE-SC0000661

[#]zhzheng@msu.edu

LONGITUDINAL DYNAMIC ANALYSIS FOR THE PROJECT X 3-8 GeV PULSED LINAC

G. Cancelo, B. Chase, Nikolay Solyak, Yury Eidelman, Sergei Nagaitsev
 Fermi National Accelerator Laboratory, Batavia, IL 60510, U.S.A.

Abstract

The Pulsed Linac requires over 200 9-cell, 1300 MHz cavities packed in 26 ILC type cryomodules to accelerate 1 mA average beam current from 3GeV to 8 GeV. The architecture of the RF must optimize RF power, beam emittance, and energy gain amid a large number of requirement and constraints. The pulse length is a critical issue. Ideally, a 26 ms pulse would allow direct injection into the Fermilab’s Main Injector, bypassing the need of the Fermilab’s Recicler. High loaded quality factors (QL) are also desirable to minimize RF power. These requirements demand an accurate control of the cavity resonant frequency disturbed by Lorentz Force Detuning and microphonics. Also the LLRF control system must regulate the RF amplitude and phase within tight bounds amid a long list of dynamic disturbances.

INTRODUCTION

The H⁺ 3-8 GeV LINAC for Project X [1] is optimized for accelerating the synchronous particle at a small negative phase close to the RF peak voltage. At 3 GeV beam β 's and transit time factors (TTF) along the 200+ cavity LINAC are near 1 and monotonically increasing along z. Although TTF and β_0 impact in the longitudinal dynamics most longitudinal problems arise from the fact that, to cut costs, modern accelerators are being designed powering a string of cavities from one klystron. As multiple cavities are connected to a single klystron the setting and control of RF system parameters becomes more complex. A low level RF (LLRF) control loop controls the amplitude and the phase of the klystron’s RF power. However, the loop cannot dynamically control individual cavity amplitude and phases. This is further complicated due to Lorentz forces (LFD) and microphonics that severely detune superconducting cavities. One more problem arises from the fact that to achieve the maximum possible acceleration cavities are operated at their maximum operating gradient, close to their quenching limit. Since some disturbances are pulse to pulse repetitive we can use some feedforward compensation. For instance LFD can be minimized at the single cavity level using piezoelectric tuners. The setting of RF cavity parameters such as synchronous phases (Φ_s), predetuning ($\Delta\omega$) and RF power P_{for_i} and fill time t_0 are very important.

LONGITUDINAL DYNAMICS SIMULATIONS

For small phase-energy oscillations the stability of the longitudinal dynamics can be studied using a Hamiltonian equation (1) relating the phase and energy stability [2] (Figure 1).

$$H_{\phi} = \frac{Aw^2}{2} + B(\sin\phi - \phi\cos\phi_s) \quad (1)$$

where the first term represents the kinetic energy of the particle and the second term the potential energy. A and B are constants:

$$A = \frac{2\pi}{\beta_s^3 \gamma_s^3 \lambda}, \quad B = \frac{qE_0 T}{mc^2}$$

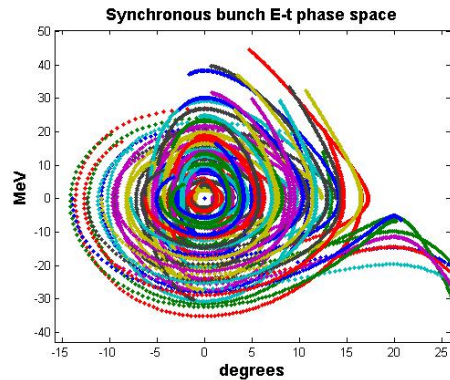


Figure 1: Synchronous bunch E-T phase space.

As shown in Figure 2, at 3 GeV the small amplitude oscillation frequency is 1.24 MHz (i.e. 0.8μs period). The oscillation frequency slows down as energy increases.

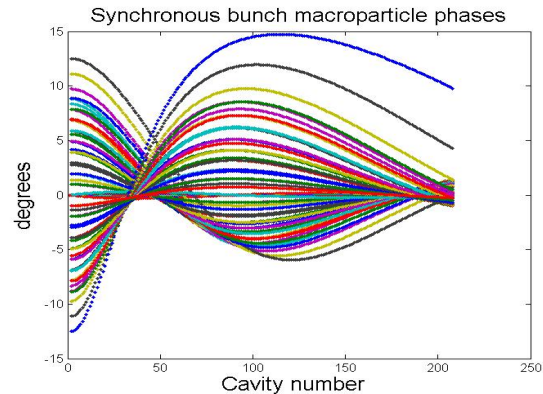


Figure 2: Synchronous bunch macroparticle phases.

$$\omega_{osc} = \sqrt{\frac{\omega_0 E_0 TTF \sin(\phi_s) c}{m c^2 \beta_s^3 \gamma_s^3}}$$

$\phi_s = -10^\circ$	<i>sync_phase</i>
$TTF = 0.97$	<i>TransitTimeFactor</i>
$E_0 = 3\text{GeV}$	<i>InitEnage</i>
$\beta_s = 0.95$	<i>syncbeta</i>
$\omega_0 = 2\pi \cdot 1.3\text{GHz}$	<i>RFfreq</i>

These simulations are performed using a bunched beam represented by 73 macroparticles and a Gaussian profile in E and t. The total number of particles is $6.24 \cdot 10^{12}$ per mA of current.

The simulated conditions are:

*Work supported by Fermi Research Alliance, LLC. under Contract No. DE-AC02-07CH11359 with the United States Department of Energy.
 #cancelo@fnal.gov

REDUCED-BETA CAVITIES FOR HIGH-INTENSITY COMPACT ACCELERATORS*

Z.A. Conway[#], S. Gerbick, M.J. Kedzie, M.P. Kelly, J. Morgan, R. Murphy, P.N. Ostroumov, and T. Reid, ANL, Argonne, IL 60439, USA

Abstract

This paper reports on the development and testing of a superconducting quarter-wave and a superconducting half-wave resonator. The quarter-wave resonator is designed for $\beta = 0.077$ ions, operates at 72 MHz and can provide more than 7.4 MV of accelerating voltage at the design beta, with peak surface fields of 165 mT and 117 MV/m. Operation was limited to this level not by RF surface defects but by our administrative limits on x-ray production. A similar goal is being pursued in the development of a half-wave resonator designed for $\beta = 0.29$ ions and operating at 325 MHz.

INTRODUCTION

The length and cost of the low-velocity portion ($\beta = v/c < 0.6$) of superconducting proton and heavy-ion linacs are dominated by the accelerator cavity performance. Accelerator cavities used in this velocity region, reduced-beta cavities, have not performed at the same peak-surface fields which are regularly achieved in elliptical-cell cavities optimized for velocity-of-light electrons [1], 160 mT and 80 MV/m peak surface fields. This performance disparity has been blamed on the greater complexity of the reduced-beta cavity fabrication and processing. Several advances at Argonne National Laboratory in cavity design [2]; fabrication and processing have disproved this hypothesis.

First, the results locating a defect which limited the performance of a prototype 72 MHz quarter-wave cavity (QWR) optimized for $\beta = 0.077$ ions for the ATLAS intensity upgrade will be presented. Second, the fabrication and processing of a subsequent geometrically identical quarter-wave cavity will be outlined. Finally, the impact of these results and future plans for a similarly constructed half-wave cavity will be discussed.

INITIAL PROTOTYPE PERFORMANCE

The QWR prototype fabrication and test results were presented in [3]. Since these papers were published we have refined our electromagnetic simulations of the cavity surface fields and the results used in this paper are given in table 1. This cavity was limited to peak surface fields of 96 mT and 70 MV/m by a surface defect which initiated a cavity quench. Figure 1, shows the cavity with the location of the defect highlighted in red along with a single channel record of the quench.

The defect was located by measuring the time-of-flight of second sound waves propagating from the cavity

quenching defect to an array of oscillating superleak transducers [4]. The distance the second sound wave travelled was calculated with the wave velocity. This combined with the known location of the detectors allowed us to determine the defect location. Our detector array was 1-dimensional in nature and located the height of the defect in the quarter-wave cavity center conductor.

This defect was located at the same height as an electron beam weld blow-out which occurred during final welding of the center conductor. The center conductor is formed from two halves which are welded together. The center conductor halves were tack welded, but the final electron beam welds could not be finished within the desired 24-hour etch window between pre-weld etching and welding. The parts were etched again after tacking and the very small-gap joint between the two parts could not be properly cleaned. Some foreign debris was trapped in this joint which caused a blow-out during the final electron beam welding which was repaired.

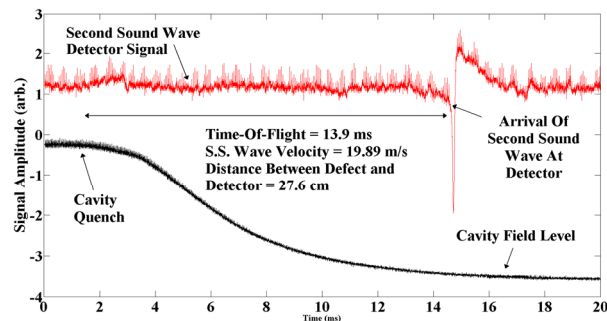
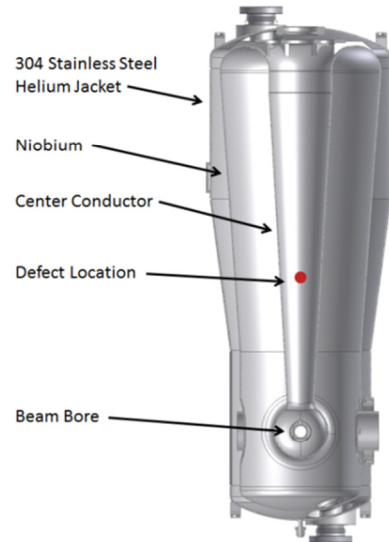


Figure 1: (Top) The cavity with a red dot placed at the height of the defect in the center conductor, the cavity is 53 inches from top to bottom. (Bottom) A single quench event with an oscillating superleak transducer signal and the cavity transmitted power.

* This work was supported by the U.S. Department of Energy, Office of Nuclear Physics, under Contract DE-AC02-06CH11357 and ANILWFO 8R268 supported by DTRA.

[#] zconway@anl.gov

DEVELOPMENT OF A SUPERCONDUCTING HALF-WAVE RESONATOR FOR PXIE *

Z.A. Conway[#], R.L. Fischer, S.M. Gerbick, M.J. Kedzie, M.P. Kelly, S.V. Kutsaev, B. Mustapha, P.N. Ostroumov and K.W. Shepard, ANL, Argonne, IL 60439, USA

I.G. Gonin, A. Lunin and V.P. Yakovlev, FNAL, Batavia, IL 60510, USA

Abstract

An ambitious upgrade to the FNAL accelerator complex is progressing in the Project-X Injector Experiment (PXIE). The PXIE accelerator requires 8 superconducting half-wave resonators optimized for the acceleration of 1 mA $\beta = 0.11$ H⁻ ion beams. Here we present the status of the half-wave resonator development, focusing particularly on cavity design, with a brief update on prototype fabrication.

INTRODUCTION

Project-X is based upon a 1-5 mA H⁻ linear accelerator to be constructed at FNAL to support advanced intensity frontier physics over the next several decades in the US [1]. The Project-X Injector Experiment (PXIE), is being designed, built and commissioned as a demonstration of the most critical R&D issues related to the front-end of the driver linac [2].

The PXIE project will include the beam source, LEBT, RFQ, MEBT, and two superconducting cavity cryomodules. The first superconducting cavity cryomodule will house 8 half-wave resonators, 8 magnets which integrate the focusing solenoids with x-y steering coils [3], and all of the necessary peripherals for operation, e.g., power couplers, slow tuners, etc. This half-wave cryomodule is being designed and built at Argonne National Laboratory.

The initial half-wave resonator design was presented in [4, 5], which contains the main cavity RF performance parameters. In this paper we update the status of the half-wave resonator design. We address methods of minimizing cavity frequency dependence on changes in external pressure (df/dP), simulations of the slow-tuner performance and the pressure safety analysis of the cavity.

MINIMIZING df/dP

The half-wave resonators in PXIE will be operated at 2 K. While this greatly reduces the external fluctuations in helium pressure relative to a 4 K cryogenic system, variations of 1-2 mbar are expected. To accommodate this, the cavities were designed to have a $df/dP = 6$ Hz/mbar. This enables operation with RF amplifiers of ~ 4 kW, requiring no mechanical fast tuner, at the desired accelerating gradient of 8.2 MV/m for a 1 mA beam current.

* This work was supported by the U.S. Department of Energy, Office of High Energy Physics and Nuclear Physics, under contract DE-AC02-76CH03000 and DE-AC02-06CH11357

[#] zconway@anl.gov

$df/dP \sim 6$ Hz/mbar is a good compromise minimizing the fabrication cost and complexity simultaneously with the df/dP , which results in a more stable and reliable accelerator system and smaller RF amplifiers. A 0.125 inch helium jacket with a $df/dP = 6$ Hz/mbar satisfies our design requirements, but we spent a little additional time to determine how we may zero df/dP if it proves necessary after prototyping or in future projects.

The cavity Nb design is the results of detailed electromagnetic studies and was taken as the starting point for our design [4, 5]. The cavity is formed from 0.125 inch thick Nb sheet. We have recent experience with using 0.125" and 0.187" thick stainless steel helium jackets on superconducting cavities. We prefer to use 0.125 inch thick stainless steel but were unsure of its effect on df/dP . The cavity is shown in figure 1. Table 1 gives the results of varying the stainless steel material thickness of this model.

A novel technique to reduce df/dP is to add a flat or a dish to the side of the cavity in the high-electric field region. This increases the negative frequency shift due to deformations resulting from increases in the external pressure. Figure 2 shows a dish geometry in a half-symmetry cavity model and its displacement, please note that the helium jacket is not shown in this picture. Table 2 gives the results of varying the dish depth, where the depth is measured inward from the cavity surface. The peak surface electric field was not increased by more than 2% in these simulations.

Notice that df/dP may be controlled in finished cavities by choosing a dish which yields $df/dP < 0$. The dish may then be stiffened with a small gusset which may be subsequently weakened via machining to tune df/dP to zero. A similar gusset weakening procedure was employed in [6].

SLOW-TUNER PERFORMANCE

Our half-wave resonator design is highly re-entrant at the beam ports. This breaks the cylindrical symmetry in the high-electric field region which, in the past, has limited the slow-tuning range of half-wave cavities squeezed at the beam ports. We will employ the pneumatic ANL slow-tuner design discussed in [4]. Our simulations found that the tuning sensitivity for an applied force will be 84 kHz/kN for the 0.187 inch thick and 93 kHz/kN for the 0.125 inch thick helium jackets. The later sensitivity will be verified with the prototype cavity which is under construction.

CRYOMODULE DESIGNS FOR SUPERCONDUCTING HALF-WAVE RESONATORS*

Z.A. Conway[#], G.L. Cherry, R.L. Fischer, S.M. Gerbick, M.J. Kedzie, M.P. Kelly, S.H. Kim, J.W. Morgan, P.N. Ostroumov and K.W. Shepard, ANL, Argonne, IL 60439, USA

Abstract

In this paper we present advanced techniques for the construction of half-wave resonator cryomodules. Recent advances in superconducting low-beta cavity design and processing have yielded dramatically improved cavity performance which reduces accelerator cost and improves operational reliability. This improvement has led to the proposal and construction of half-wave resonators by ANL for the acceleration of $0.1 < \beta < 0.5$ ions, e.g., the SARAF Phase-II project at SNRC (SOREQ, Israel) and Project-X at Fermilab. These cryomodules build and improve upon designs and techniques recently implemented in upgrades to ATLAS at ANL. Design issues include the ease of assembly/maintenance, resonator cleanliness, operating at 2 or 4 Kelvin, and ancillary system interfacing.

INTRODUCTION

We are developing three separate cryomodules for two distinct projects: one for Project-X at FNAL [1] and two for SARAF Phase-II at SOREQ [2]. The cryomodules for these projects will house superconducting half-wave resonators [3, 4] which require similar layouts but differ in operation modes and dimensions. To reduce risk and optimize the cost of the cryomodule fabrication we are developing the three designs together. All designs are modifications and improvements on box-cryomodules fabricated at ANL in the past 5 years [5, 6].

In this paper several aspects of the designs and their differences will be presented. First, the cryomodule requirements will be discussed. This is followed by a discussion of a few select aspects of the cryomodule designs, differences and plans for addressing these differences. Finally, this paper concludes with a short statement of our future plans.

CRYOMODULE REQUIREMENTS

Project-X is a high intensity, 1 mA, H⁻ linear accelerator facility being developed at FNAL. A single half-wave resonator cryomodule will house 8 $\beta = 0.11$ 162.5 MHz superconducting cavities, 8 superconducting magnets and will operate at 2 K.

The SARAF Phase-II project is an upgrade of the current SARAF accelerator to accelerate >5 mA, 40 MeV/u, proton/deuteron beams. Four cryomodules are required of two types, all of which will operate at 4 K. The first type, the low-beta cryomodule, contains 7 $\beta = 0.09$ 176 MHz superconducting cavities and 7

superconducting magnets. The second type, two high-beta cryomodules, each housing 7 $\beta = 0.16$ 176 MHz superconducting cavities and 4 superconducting magnets [7].

While the accelerator lattice and operating temperature differ between the cryomodules enough similarities exist such that we see significant cost savings in designing a cryomodule which may be adapted to each case, with minor modifications.

CRYOMODULE DESIGN

Vacuum Vessel

The cryomodule designs all build upon past ANL experience with box-cryomodules (see for example [5]). Here the cryomodules are much wider due to the half-wave cavities being mounted on their sides. To keep the half-cylinder bottom would make the vacuum vessels unacceptably tall. We have arrived at making the vacuum vessel a box which appears to be a good compromise between fabrication cost, structural integrity and minimizing cryostat height. The radii of the rounded corners were chosen to fit the contents of the box minimizing overall height including the depth of the required gussets.

Figure 1 shows the results from ANSYS calculations of the structural deformations due to vacuum being pulled on the inside. Notice that the structure pulls in about 0.25" on average due to evacuation, the maxima are between 0.5" and 0.67". We are currently evaluating whether or not to stay with this or reinforce the box further. Motion of the vacuum vessel wall moves the internal magnetic shielding and stresses the baton points which may degrade performance. Reducing the maximum displacement to less than 0.25" will avoid this but it adds the cost of additional gusseting. Future tests are planned here to evaluate the magnetic shielding.

With the rounded corners the vacuum vessel dimensions may be scaled between the three different sizes required by varying the length of the straight sections. Other designs we considered included straight sides (too mechanically compliant), angled corners (more expensive to fabricate), and a half-cylinder bottom (makes the cryomodule too tall). All of these designs were discarded for the mentioned reasons.

Beam-Line Component Support and Alignment

While the required accelerator lattice varies between the cryomodules the same support scheme may be used. All of the cryomodules require the solenoids to be aligned to better than ± 1.0 mm_{peak} transversely with $\pm 0.1^\circ$ for all of the rotation angles with similar constraints on the cavities. The beam-line string length varies from 4 to 6

* This work was supported by the U.S. Department of Energy, Office of High Energy Physics under contract DE-AC02-76CH03000 and by SOREQ-NRC under work for others agreement 85Y47.

[#] zconway@anl.gov

BEAMDULAC-SCL CODE FOR COMPLEX APPROACH OF BEAM DYNAMIC INVESTIGATION IN SC LINAC

A.V. Samoshin

National Research Nuclear University “MEPhI”, Moscow, Russian Federation

Abstract

Periodic sequences of independently phased accelerating cavities and focusing solenoids are used in MeV and GeV energy range linacs. The beam dynamic investigation is difficult for such superconducting linear accelerator. The matrix calculation was preferably used for primary choused of accelerating structure parameters. This method does not allows properly investigate the longitudinal motion. The smooth approximation can be used to investigate the nonlinear ion beam dynamics in such accelerating structure and to calculate longitudinal and transverse acceptances. The advantages and disadvantages of each method will describe, the results of investigation will compare. The user friendly software BEAMDULAC-SCL for ion beam dynamic analysis was created. A numerical simulation of beam dynamics in the real field are carried out for the different variants of the accelerator structure based on previously analytically obtained results.

INTRODUCTION

High-current accelerators have great perspectives for problems of thermonuclear fusion, safe nuclear reactors, transmutation of radioactive wastes and free electron lasers. A large number of low energy particle accelerators are applied in micro- and nanoelectronics, material science, including the study of new construction materials for nuclear industry, in medical physics, in particular for cancer treatment by using of the accelerators of protons and light ions, in radiation technology. It is proposed to use one universal accelerator, consisting of independently phased cavities and solenoids sequence to solve these problems.

An ion superconducting linac is usually based on the superconducting (SC) independently phased cavities. This linac consists of the niobium cavities which can provide typically 1 MV or more of accelerating potential per cavity. Such structures can be used for ion acceleration with different charge-to-mass ratio in the low energy region [1] and for proton linac in the high-energy region (SNS, JHF, ESS project). It is desirable to have a constant geometry of the accelerating cavity in order to simplify manufacturing and to decrease the linac cost. Such geometry leads to a non-synchronism but a stable longitudinal particle motion can be provided by proper RF cavities phasing. The beam can be both longitudinally stable and accelerated in the whole system by control of the accelerating structure driven phase and the distance between the cavities. In this paper two methods of the beam dynamics investigation are compared for low ion velocities and for the charge-to-mass ratio $Z/A = 1/66$.

This comparison can be demonstrated as an example of a post-accelerator of radioactive ion beams (FRIB) linac, where beam velocity increases from $\beta = 0.01$ to $\beta = 0.06$ [1].

The beam transverse focusing can be provided with the help of SC solenoid lenses, following each cavity and with the help of special RF fields. As it was shown early the beam focusing can be realized for the solenoid field near $B \sim 20$ T. The value of magnetic field B can be reduced by using of addition alternating phase focusing (APF). The smooth approximation has been applied to study the APF in RIB linac. By adjusting the drive phase (φ_1 and φ_2) of the two cavities, we can achieve the acceleration and the focusing by less magnitude of the magnetic field B [2]. Adding a solenoid into focusing period will also allow the separate control of the transverse and longitudinal beam dynamics. A schematic plot of one period of the accelerator structure is shown in Figure 1. The low-charge-state low velocity beams require stronger transverse focusing than one is used in existing SC ion linac. Early investigation of beam dynamics shows that with the initial normalized transverse emittance $\varepsilon_T = 0.1\pi$ -mm-mrad and the longitudinal emittance $\varepsilon_V = 0.3\pi$ -keV/u-nsec the connection between the longitudinal and transverse motion can be neglected if maximum beam envelop $X_m < 3$ -4 mm and inner radius of drift tubes $a = 15$ mm.

Beam dynamics in such systems cannot be studied by means of analytical methods only. The initial setup of the system consisting of different types superconducting resonators and focusing solenoids or quadrupoles, can be performed using the transfer matrix calculation and the method of smooth approximation, and then refined the beam dynamics simulation in polyharmonic field.

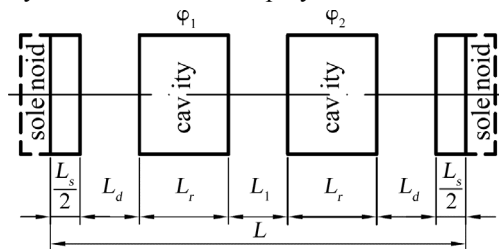


Figure 1: Layout of structure period.

The BEAMDULAC-SCL code is developed in the laboratory DINUS and allows to do the comprehensive research of ion beam dynamics in a different structures that satisfy the acceleration of many methods. To evaluate the accelerator parameters implemented transfer matrix calculation method. Using a smooth averaging technique we can to determine the stability region and to calculate

DEVELOPMENT OF PROTON THERAPY AT THE SC LINAC WITH BEAMDULAC-SCL CODE

S.M. Polozov, A.V. Samoshin

National Research Nuclear University “MEPhI”, Moscow, Russian Federation

Abstract

Proton cancer therapy complexes are conventionally developing based on synchrotrons and cyclotrons. High electrical power consumption and especial devices necessary to energy variation (as slow extraction systems and degraders) are the main problems of such complexes. At once SC linacs based on short independently phased cavities have a serious progress at present. Linear accelerator consumes less power comparably with cyclic and the energy variation can be easily realized by means of RF field amplitude and phase variation in a number of cavities. The accelerator’s modular configuration which is now widely used in FRIB’s or SNS’s can be applied for therapy linac also. It is possible to choose the SC linac parameters and to do the proton and ion beams stability study with help of the BEAMDULAC-SCL code. This software also allows providing of the structure optimization and the beam dynamics control.

INTRODUCTION

Development of a simple in operation and cost-effective cancer treatment proton accelerator is very important now. Normal conducting cyclotrons and synchrotrons are conventionally uses for treatment. A number of comparatively compact SC synchrocyclotrons are under development. But contemporary progress in SC linacs development, construction and operation experience let to propose their using for medical application. Such linacs have a very high rate of energy gain and can by compact thus, need low RF power feeding and large scale and power-intensive magnets are not necessary for it. But the possibility of easily beam energy variation by means of a number of the resonator turn-off (deeply variation) or RF field phase in last resonators (slow variation) can be the main advantage of SC linac.

A number of cancer therapy linacs projects as TOP [1], LIBO [2], TOP-IMPLART [3] are under R&D at present. The novel CYCLINAC concept combines compact low energy cyclotron and short linac is also discussed [4].

Contemporary SC linac technologies are used for development of spallation neutron sources (SNS) and facilities for radioactive ion beams (FRIB). High-gradient quarter- and half-wave, elliptical and side-coupled cavities are used for beam acceleration and SC solenoids of quadrupoles for transverse focusing. The average rate of energy gain in SNS linac is about 4 MeV/m for example. It can be proposed that 200 MeV low intensity linac can be compact that 50 m.

The optimization of linac structure will done in this paper using BEAMDULAC-SCL code with was developed for heavy ion beam dynamics simulation in

FRIB’s. The possibility of permanent magnet using for transverse beam focusing will discussed, the limit gradient for different energy ranges will defined. The beam quality (beam envelope control in main) preservation is one of the main goals.

PERIOD LAYOUT

Let’s we consider the linear accelerator, consisting of independently phased cavities and solenoids sequence first (fig. 1).

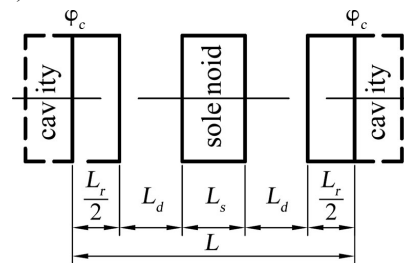


Figure 1: Layout of structure period.

For low-velocity ion beams the quarter- and half-wave resonators with few amounts of gaps are commonly used as accelerating structures. If SC resonators are used they should be the same, otherwise the cost of facility rapidly increase. This means that the phase velocity of the wave should be constant in each cavity. With a large number of resonators is economically advantageous to divide them into several groups, consists of identical resonators. Obviously, in this acceleration system will always violate the principle of synchronicity, when the synchronous particle velocity equal to the phase velocity of the accelerating wave at any time. I.e. in this case, appear a slipping of the particles relative to the accelerating wave. The slipping value must not exceed acceptable value, if not acceleration rate and rapidly reduced and beam longitudinal and transverse stability worse, and the transmission coefficient decreases. Therefore the number of identical resonators should be limited, and the number of groups consisting of identical geometry should be minimal.

Ions are accelerated and slipping relative to the RF field in dependence of the ratio between the particle velocity β and the phase velocity of the wave in cavity β_G .

The beam motion can be both longitudinally stable and accelerated in the whole system by control the driven phase of the accelerating structure and the distance between the cavities [5]. The beam focusing can be provided by solenoids or permanent magnet lenses (PML) which follow each of the cavity [6].

The conditions of longitudinal and transverse beam stability for the structure consisting from the periodic

FIRST MEASUREMENTS ON THE 325 MHz SUPERCONDUCTING CH CAVITY*

M. Busch^{†,1}, F. Dziuba¹, H. Podlech¹, U. Ratzinger¹, W. Barth^{2,3},
S. Mickat^{2,3}, M. Amberg³, M. Pekeler⁴

¹IAP Frankfurt University, 60438 Frankfurt am Main, Germany

²GSI Helmholtzzentrum, 64291 Darmstadt, Germany

³Helmholtz-Institut Mainz (HIM), 55099 Mainz, Germany

⁴RI Research Instruments, Bergisch Gladbach, Germany

Abstract

At the Institute for Applied Physics (IAP), Frankfurt University, a superconducting 325 MHz CH-Cavity has been designed and built. This 7-cell cavity has a geometrical β of 0.16 corresponding to a beam energy of 11.4 AMeV. The design gradient is 5 MV/m. Novel features of this resonator are a compact design, low peak fields, easy surface processing and power coupling. Furthermore a new tuning system based on bellow tuners inside the resonator will control the frequency during operation. After successful rf tests in Frankfurt the cavity will be tested with a 10 mA, 11.4 AMeV beam delivered by the GSI UNILAC. In this paper first measurements and corresponding simulations will be presented.

CAVITY LAYOUT

Worldwide there is a growing interest in applications demanding high beam power and quality (e.g. MYRRHA (Multi Purpose HYbrid Research Reactor for High-Tech Applications) [1]). The superconducting CH-cavity is an appropriate structure for these specifications being characterized by a small number of drift spaces between adjacent cavities compared to conventional low- β ion linacs [2]. Applying KONUS beam dynamics, which decreases the transverse rf defocusing and allows the development of long lens free sections, this results in high real estate gradients with moderate electric and magnetic peak fields. In the past a 19-cell, superconducting 360 MHz CH-prototype has been developed and successfully tested [3]. For future operations a new design proposal for high power applications has been investigated. Presently a new cavity operating at 325.224 MHz, consisting of 7 cells, $\beta = 0.16$ and an effective length of 505 mm (see table 1) is undergoing first measurements. Referring to the previous structure this cavity utilizes some novel features (see fig. 1):

- inclined end stems
- additional flanges at the end caps for cleaning procedures
- two bellow tuners inside the cavity
- two ports for large power couplers through the girders

* Work supported by GSI, BMBF Contr. No. 06FY7102, 06FY9089I

[†] busch@iap.uni-frankfurt.de

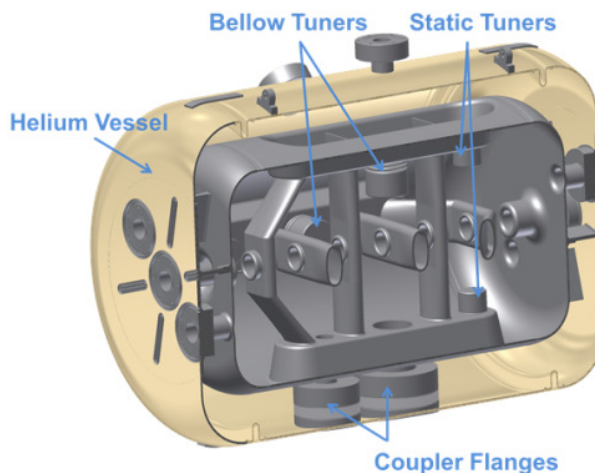


Figure 1: Layout of the superconducting 7-cell CH-Cavity (325.224 MHz, $\beta = 0.16$) [4].

Table 1: Specifications of the 325 MHz CH-Cavity.

β	0.16
frequency [MHz]	325.224
no. of cells	7
length ($\beta\lambda$ -def.) [mm]	505
diameter [mm]	352
E_a [MV/m]	5
E_p/E_a	5
B_p/E_a [mT/(MV/m)]	13
G [Ω]	64
R_a/Q_0	1248
$R_a R_s$ [$k\Omega^2$]	80

SCOPE FOR THE DYNAMIC BELLOW TUNERS

Rf, mechanical properties as well as Multipacting studies of the novel bellow tuner system can be reviewed in [5], [6], [7].

STATUS OF THE SUPERCONDUCTING CW DEMONSTRATOR FOR GSI*

F. Dziuba^{†,1}, M. Amberg^{1,3}, K. Aulenbacher^{3,4}, W. Barth^{2,3}, M. Busch¹,
H. Podlech¹, U. Ratzinger¹, S. Mickat^{2,3}

¹IAP University of Frankfurt, 60438 Frankfurt am Main, Germany

²GSI Helmholtzzentrum, 64291 Darmstadt, Germany

³Helmholtz Institut Mainz (HIM), 55099 Mainz, Germany

⁴KPH Mainz University, 55128 Mainz, Germany

Abstract

Since the existing UNILAC at GSI will be used as an injector for the FAIR facility a new superconducting (sc) continuous wave (cw) LINAC is highly requested by a broad community of future users to fulfill the requirements of nuclear chemistry, especially in the research field of Super Heavy Elements (SHE). This LINAC is under design in collaboration with the Institute for Applied Physics (IAP) of Frankfurt University, GSI and the Helmholtz Institut Mainz (HIM). It will consist of 9 sc Crossbar-H-mode (CH) [1] cavities operated at 217 MHz which provide an energy up to 7.3 AMeV. Currently, a prototype of the cw LINAC is under development. This demonstrator comprises the first sc CH cavity of the LINAC embedded between two sc solenoids mounted in a horizontal cryomodule. One important milestone of the project will be a full performance test of the demonstrator by injecting and accelerating a beam from the GSI High Charge State Injector (HLI) in 2014. The status of the demonstrator is presented.

The demonstrator will be the first section of the new sc cw LINAC at GSI. It will be operated at 217 MHz which is the second harmonic of the existing 1.4 AMeV GSI HLI. A test of the sc 217 MHz CH cavity, which is the key component of the project, under real operational conditions is the main aim of the demonstrator [2, 3]. It is planned to run a full performance test by injecting and accelerating a beam from the HLI in 2014. Figure 1 shows the cw demonstrator setup and the HLI.

STATUS OF THE SC 217 MHz CH CAVITY

The sc 217 MHz CH cavity for the cw LINAC demonstrator (see fig. 2) will consist of 15 accelerating cells at a total length of 690 mm while the maximum gradient is 5.1 MV/m. Furthermore, the cavity is designed with the special EQUUS (EQUidistant mUlti-gap Structure) beam dynamics [4].

THE SUPERCONDUCTING CW LINAC DEMONSTRATOR

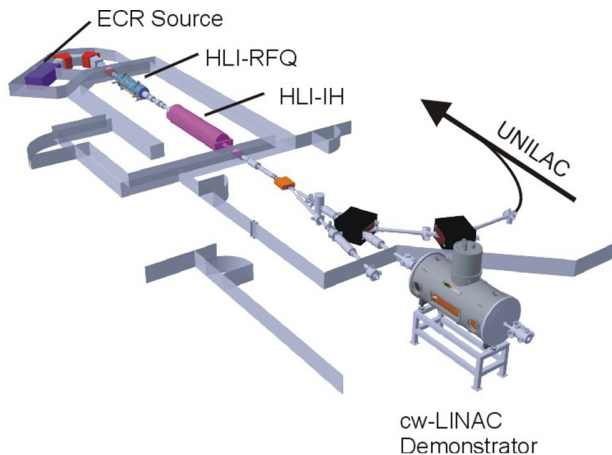


Figure 1: Demonstrator setup with the High Charge Injector at GSI.

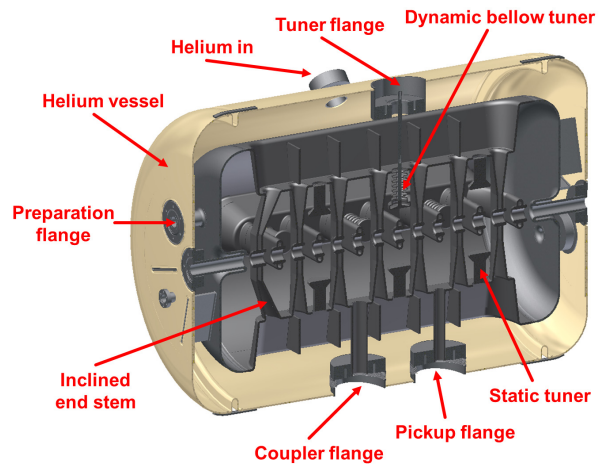


Figure 2: Side view of the sc 217 MHz CH cavity for the cw demonstrator at GSI.

The rf design of the cavity is finished. All main parameters of the cavity are shown in table 1. In June 2012 the production of the cavity has started at Research Instruments (RI) GmbH, Bergisch Gladbach, Germany. It is scheduled to be delivered to the IAP in 2013.

The cavity will be equipped with all necessary auxiliaries like a 10 kW cw power coupler, a titanium helium

* Work supported by HIM, GSI, BMBF Contr. No. 06FY7102
† dziuba@iap.uni-frankfurt.de

DESIGN AND SIMULATION OF A TEST MODEL FOR A TRI-SPOKE CAVITY AT RIKEN *

L. LU, N. Sakamoto, K. Suda, K. Yamada, O. Kamigaito,
RIKEN Nishina Center for Accelerator-Based Science,
RIKEN, 2-1, Hirosawa, Wako, Saitama 351-0198, JAPAN

Abstract

A design for a tri-spoke-type superconducting cavity for uranium beams with $\beta = 0.303$ and a 219 MHz operational frequency is presented. And a test model designed and assembled by two end-wall flanges and one triparted part of the designed tri-spoke cavity, was expected to be built using the same fabrication technology that is supposed for Nb cavity manufacture. The designs and simulations of the tri-spoke cavity and the test model will be reported in this paper.

INTRODUCTION

Very heavy ions such as uranium can be accelerated to very high energy using an accelerator chain, which consists of a new linear injector named RILAC2 with a powerful superconducting ECR ion source and four booster cyclotrons in the RIKEN RI-beam factory (RIBF) [1-4]. However, two charge-stripping sections cause an increase in the phase width of the beam in subsequent cyclotrons. Thus, we aim to design a tri-spoke type superconducting cavity as a rebuncher in order to focus the beam in the longitudinal direction. This tri-spoke cavity would be placed between fRC and IRC. The frequency of the tri-spoke cavity was chosen to be 219 MHz, which is the 12th harmonic of the fundamental frequency of 18.25 MHz. This frequency yields a cell length of $\beta\lambda/2 = 207$ mm at $\beta = 0.303$ [5]. The total voltage is estimated to be a few megavolts at this frequency.

We have not experiences and facilities of fabrication of superconducting cavity. Thus, the novelty of SC rf

technology, the complexity of mechanical construction, and use of electron beam welding, a substantial effort should first be invested and researched in fabricating a test model from oxygen-free copper. The test model is assembled from two end-wall flanges and a triparted tri-spoke cavity, as shown in Fig. 1 [6]. The parameters of the tri-spoke cavity and the fabrication model are listed in Table 1.

Table 1: Parameters of tri-spoke cavity model and fabrication model

Parameter	Tri-spoke	Test model
Frequency (MHz)	219	228
Length (mm)	828.8	346.4
Cavity Dia. (mm)	580	580
Beam Bore (mm)	15	15
R/Q (Ω)	241.21	155.6
E_{pk}/E_{acc}	2.75	2.04
H_{pk}/E_{acc} (Oe/MV/m)	58.21	
G (Ω)	81.17	79.4
R_{res} @ 4.2K (n Ω)	25	25
Q @ 4.2K (Ω)	3.25E+09	3.17E+09
Power@ 4.2K (W)	0.42	0.45

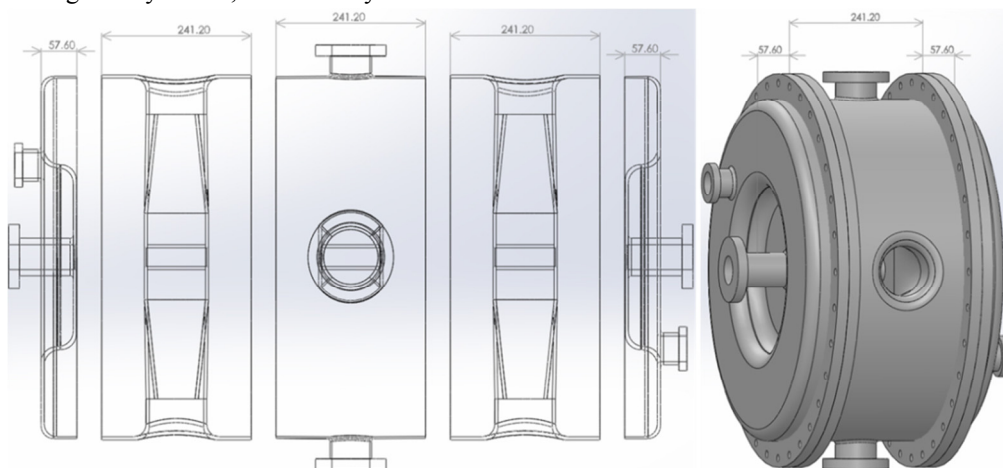


Figure 1: Images of wall flanges and triparted cavity parts (left) and the assembled image of the test model (right).

*luliang@riken.jp

*Work supported by Foreign Postdoctoral Researcher

ISBN 978-3-95450-122-9

SUPERCONDUCTING CW HEAVY ION LINAC AT GSI

Winfried Barth, Peter Gerhard, Viktor Gettmann, Sascha Mickat
HIM, Mainz

Gesellschaft für Schwerionenforschung, D-64291 Darmstadt, Germany

Abstract

An upgrade program has to be realized in the next years, such that enhanced primary beam intensities at the experiment target are available. For this a new sc 28 GHz full performance ECR ion source is under development. Via a new low energy beam line an already installed new RFQ and an IH-DTL will provide for cw-heavy ion beams with high average beam intensity. It is planned to build a new cw-heavy ion-linac behind this high charge state injector. In preparation an R&D program is still ongoing: The first linac section comprising a sc CH-cavity embedded by two sc solenoids (financed by HIM and partly by HGF-ARD-initiative) as a demonstrator will be tested with beam at the GSI High Charge Injector (HLI). The new linac should feed the GSI flagship experiments SHIP and TASCA, as well as material research, biophysics and plasma physics experiments in the MeV/u-area. The linac will be integrated in the GSI-UNILAC-environment; it is housed by the existing constructions. Different layout scenarios of a multipurpose high intensity heavy ion facility will be presented as well as the schedule for preparation and integration of the new cw-linac.

a new 28 GHz ECR source and a new cw capable RFQ [1,2]. As a result of a long term cost-benefit analysis a standalone sc cw-LINAC in combination with the upgraded HLI is assumed to fit the requirements of SHE best. Significant higher beam intensities will be provided and lead to an increase of the SHE production rate.

The technical design and the realisation of such a sc cw-LINAC in parallel to the existing UNILAC at GSI is assigned to a collaboration of GSI, the IAP, and the Helmholtz-Institute Mainz (HIM), which was founded in 2009. A conceptual layout [3] of a sc cw-LINAC was worked out, which allows the acceleration of highly charged ions with a mass to charge ratio of 6 at 1.4 MeV/u from the upgraded HLI. Nine superconducting CH-cavities [4] operated at 217 MHz accelerate the ions to energies between 3.5 MeV/u and 7.3 MeV/u, while the energy spread should be kept smaller than $\pm 3\text{keV/u}$. As beam focusing elements seven superconducting solenoids are applied. The general parameters are listed in table 1. The commissioning of the cw-LINAC is scheduled in 2019 at earliest.

INTRODUCTION

Table 1: Design Parameters of the cw-LINAC

Mass/Charge		6
Frequency	MHz	217
Max. beam current	mA	1
Injection Energy	MeV/u	1.4
Output energy	MeV/u	3.5 – 7.5
Output energy spread	keV/u	+ - 3
Length of acceleration	m	12.7
Sc CH-cavities		9
Sc solenoids		7

The HLI in combination with the Universal Linear Accelerator (UNILAC) is a powerful high duty factor (25%) accelerator to provide heavy ion beams for the ambitious SHE-research program at GSI. In future the UNILAC is designated as an injector for FAIR (Facility for Antiproton and Ion Research). Beam time availability for SHE-research will be decreased due to the limitation of the UNILAC in providing a proper beam for SHE and in fulfilling the requirements for FAIR simultaneously. To keep the SHE program at GSI competitive on a high level, an upgrade program of the HLI was initialized comprising

CW-LINAC-DEMONSTRATOR

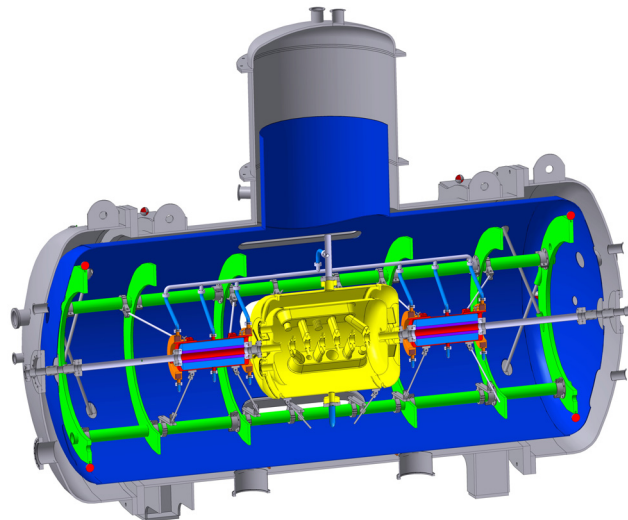


Figure 1: Scheme of the cw-LINAC Demonstrator; CH-cavity (yellow) in its centre embedded by two sc solenoids (red-orange).

The first section of the cw-LINAC comprising a sc CH-cavity embedded by two sc solenoids (financed by HIM and ARD) as a demonstrator (see fig. 1) will be tested with beam at the HLI (see fig. 2).

BEAM DYNAMICS DESIGN OF CHINA ADS PROTON LINAC*

Z.H. Li, F. Yan, P. Cheng, H.P. Geng, Z. Guo, C. Meng, B. Sun, J.Y. Tang, IHEP, Beijing, China

Abstract

It is widely accepted that the Accelerator Driven System (ADS) is one of the most promising technical approach to solve the problem of the nuclear wastes, a potential threaten to the sustainable development of the nuclear fission energy. An ADS study program was approved by Chinese Academy of Sciences at 2011, which aims to design and built an ADS demonstration facility with the capacity of more than 1000 MW thermal power within the following 20 years. The 15 MW driver accelerator will be designed and constructed by the Institute of High Energy Physics (IHEP) and Institute of Modern Physics (IMP) of China Academy of Sciences. This linac is characterized by the 1.5 GeV energy, 10mA current and CW operation. It is composed by two parallel 10 MeV injectors and a main linac integrated with fault tolerance design. The superconducting acceleration structures are employed except the RFQ. In this paper the general considerations and the beam dynamics design of the driver accelerator will be presented.

INTRODUCTION

The C-ADS project is a strategic plan to solve the nuclear waste and resource problems for nuclear power plants in China. It is supported financially by the central government and administrated by the Chinese Academy of Sciences. With its long-term planning lasting until 2032 aiming at construction of an ADS demonstration facility with 1000MW thermal power, the project will be conducted in three major phases.

As part of the whole project, the C-ADS driver accelerator is a CW proton linac and uses superconducting acceleration structures except the RFQs. The design specifications for the proton beams are shown in Table 1. For the first phase, the project goal is to build a CW proton linac of 50 MeV and 10 mA by about 2015.

The first phase itself will be executed progressively in several steps, with the first step to build two 5-MeV test stands of different designs.

Table 1: Specifications for C-ADS Accelerator

Energy	1.5 GeV
Current	10 mA
Beam Power	15 MW
Frequency	(162.5)325/650MHz
Duty factor	100%
Beam loss	<1 W/m
Beam Trips/Year[1]	<25000 1s<t<10s <2500 10s<t<5min <25 t>5min

GENERAL

The C-ADS accelerator is a CW proton linac characterised by the properties of very high beam power and stringent requirements for reliability and availability that are not possessed by any of the existing proton linac. Therefore, the linac design had to integrate the stringent requirements from the very beginning [2]. The C-ADS linac is composed by two parallel 10 MeV injectors, main linac and a section of beam line (MEBT2) used to transfer and match beams from injectors to the main linac. The total length of the linac is about 450 m and the layout of the C-ADS driver linac is show in Figure 1.

Injectors

Two parallel 10MeV Injectors are designed working at “hot spare” mode to satisfy the stringent requirements on reliability and availability. This is the most difficult part of the whole linac. At present different technical

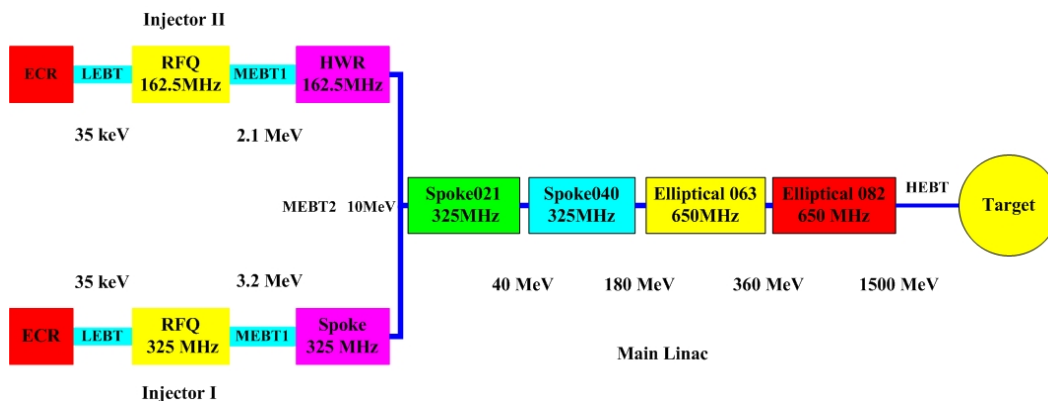


Figure 1: Layout of China ADS linac.

*Work supported by NSFC (10875099, 91126003), the China ADS Project (XDA03020000), IHEP special funding (Y0515550U1) #lizhihui@ihep.ac.cn

THORIUM ENERGY

S. Peggs, BNL, USA and ESS, Sweden

R. Seviour, ESS, Sweden and Huddersfield U., UK and Lund U., Sweden

R. Cywinski, Huddersfield U., UK

SAFETY, PROLIFERATION, AND WASTE

Uranium-based nuclear fission technologies are an important energy source for many industrialised nations, although use has been limited by: high cost; perceived adverse safety; the potential for proliferation; and the management of nuclear waste. A thorium fuel cycle, combined with alternative technologies, presents numerous potential advantages [1]. Thorium fuel cycles are intrinsically more proliferation-resistant, reduce plutonium production, and can consume legacy plutonium and waste actinides. The different characteristics of the thorium cycle options arise not only from the different system designs, but also from the physical properties of the fuels themselves [2, 3].

Safety: Molten salt reactor (MSR) and high-temperature gas-cooled reactor (HTGR) thorium reactors have safety advantages over conventional light water reactors (LWR) [2, 3, 4]. The liquid fuel in an MSR may provide improved reactivity feedback and can be removed from the reactor core [4]. HTGRs can withstand very high temperatures in excess of 2000 K without fuel failure [5]. As demonstrated at the German AVR, these designs may survive a complete loss of power event [2]. The use of thorium in LWR fuel can have advantages over solely U-Pu systems because of its better thermal, physical, and irradiation performance [5].

Proliferation: Thorium occurs in nature as a single fertile isotope. In itself, it cannot be enriched to produce weapons grade material. Consequently it has been argued that thorium is “proliferation resistant” [6, 7]. Additionally, production of Pu-239 is extremely small in most proposed thorium cycles, due to the different actinide distribution, thereby posing a significantly lower proliferation risk. However, thorium cycles do generate U-233 as the fissile isotope, rather than the Pu-239 bred from U-238 in the U-Pu cycle. U-233 is in principle useable in nuclear weapons, but the inherent co-generation of U-232 provides significant protection due to the steady growth of hard-gamma emitting Tl-208 in its decay chain. This makes non-state weapons manufacture difficult, and easily detectable.

Waste: Thorium systems have the ability to burn actinides, and provide several routes to plutonium stockpile disposal [6]. Waste forms for thorium-bearing fuels have been studied and shown to have advantages based on their physical and chemical properties [3, 5, 8, 9].

SOLID FUEL REACTORS

Thorium can in principle be used as a solid fuel component in all the main reactor types that have operated to date: boiling and pressurised light water reactors (BWRs and PWRs), heavy water reactors (HWRs), HTGRs, and sodium-cooled fast reactors. Thorium based fuels offer

higher operational safety margins and accident tolerance due to various favourable, robust, properties: a very high melting point; non-oxidizability; general chemical inertness; reasonable thermal conductivity; and a strong ability to retain fission products within its crystal lattice.

Reactors without accelerators: Thorium cycles have been investigated in a variety of reactors, including Gas-Cooled Reactors (GCRs), BWRs, and PWRs [10, 11, 12]. These studies demonstrated good performance of thorium in oxide form in LWRs and in carbide form in GCRs [13]. The Light Water Breeder Reactor programme in a PWR [14] demonstrated the feasibility of a closed Th-U-233 fuel cycle, confirming that U-233 breeding is achievable using a heterogeneous epi-thermal spectrum U-Th core. Near-complete transuranic waste incineration has been suggested in a thorium-fuelled PWR [15]. India has operated thorium-fuelled research reactors for many years: first the Purnima-II reactor (1984-6) and, since 1997, in the 30 kW Kamini research reactor [16], which uses U-233 bred from thorium in another reactor.

Accelerator-driven subcritical cores: The accelerator provides a controlled external source of fast neutrons in the reactor core, to breed fissile material at the same rate or faster than it is consumed. Some neutrons maintain a chain reaction while others breed Th-232 to U-233. Eventually the U-233 becomes the fissile fuel, with fertile thorium being added to the mix as necessary.

Proton-driven spallation is the usual choice (especially for GW-scale reactors), although other particles including electrons have also been proposed. Heavier nuclei bring little advantage at considerable cost. The required beam current I is given by

$$I = e \frac{(1-k)P}{nfE_f} \quad (1)$$

where $k < 1$ is the “criticality” factor of the reactor, P is the thermal power, n is the number of neutrons produced per incident proton, of which a fraction f induce fission, and E_f is the mean energy release per fission. A typical 1 GWe reactor requires average currents of about 10 mA and a beam power of about 10 MW, beyond today’s most powerful accelerators.

In 1996 the Indian Atomic Energy Commission initiated design studies for a 200 MWe PHWR ADS system fuelled by uranium and thorium [17]. Jacobs Engineering Group Inc. (Jacobs) have produced a conceptual design of an Accelerator-Driven Thorium Reactor (ADTR™) 600 MWe power station, based on the lead-cooled fast reactor illustrated in Figure 1 [18, 19]. The ADTR™ challenges previously established criticality margins, with a proposed k value of 0.995 [20].

DESIGN AND BEAM TEST OF SIX-ELECTRODE BPMS FOR SECOND-ORDER MOMENT MEASUREMENT

K. Yanagida*, S. Suzuki, and H. Hanaki, JASRI/SPring-8, Sayo Hyogo, Japan

Abstract

To enhance a beam observation system during top-up operation, we developed in the SPring-8 linear accelerator non-destructive beam position monitors (BPMS) that can detect second-order moments of electron beams. BPMS have six stripline-type electrodes with circular or quasi-elliptical cross-sections. We tested a BPM with a circular cross-section using electron beams, and our results showed that its normalized moments were determined accurately by electrostatic field calculation. We studied a precise calibration method to determine the relative attenuation factors between the electrode channels based on the principle that the relative moments must not vary with a change of the beam position using a steering magnet in drift space.

INTRODUCTION

The SPring-8 linear accelerator provides electron beams toward a storage ring about every twenty seconds because of the top-up operation of the storage ring. To enhance the beam observation system during the top-up operation, a non-destructive BPM system is being upgraded to a six-electrode BPM system that can detect the second-order moments of electron beams because the second-order moments are physical quantities related to beam sizes, which can be deduced by measuring second-order moments at more than six locations in FODO magnetic lattices [1].

Therefore, we developed the major components of a six-electrode BPM system: BPMS, a signal processor, and a digital input board. We installed our developed six-electrode BPMS with a circular cross-section in the beam transport line and tested them using electron beams. This paper describes the BPM designs as the parts of the six-electrode BPM system, the principle of multipole moment measurement, and the beam test results.

SIX-ELECTRODE BPMS

This section describes the designs of six-electrode BPMS and the principle of absolute moment measurement.

BPM designs

We developed two kinds of six-electrode BPMS for second-order moment measurement. One is a BPM with a circular cross-section for the non-dispersive section, and the other is a BPM with a quasi-elliptical cross-section for the dispersive section (Fig. 1). In the figure the numbers represent electrode number d . Both BPMS have stripline-type electrodes as signal pick-ups. The stripline length is

27 mm, which corresponds to $\lambda/4$ of the acceleration radio frequency. The characteristic impedance is designed as 50Ω . One electrode of both BPMS shares 30° with respect to the duct center. The aperture radius of a BPM with a circular cross-section is 16 mm, and the long and short radii of a BPM with a quasi-elliptical cross-section are 14 mm and 28 mm. These BPMS were or will be installed instead of the existing four-electrode BPMS with circular and quasi-elliptical cross-sections [2][3].

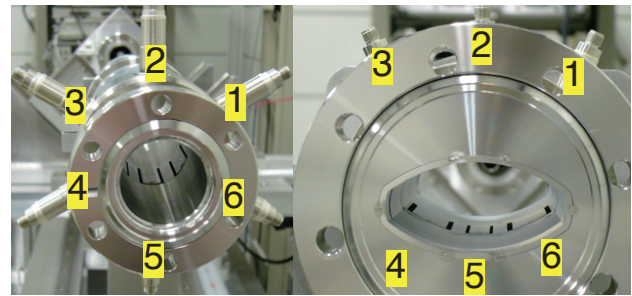


Figure 1: Six-electrode BPMS with circular and quasi-elliptical cross-sections. Numbers represent electrode number d .

Absolute Moment Measurement

A BPM with symmetrical arranged electrodes can detect multipole moments with respect to the duct center. These are called absolute moments P_n and Q_n , where n is the order of the multipole moment. For example, first-order absolute moments represent the transverse positions of beam centroid P_1 (horizontal position) and Q_1 (vertical position). The two-dimensional position (P_1, Q_1) is generally called the beam position.

Our developed six-electrode BPMS have two electrodes in the vertical direction, but none horizontally. This configuration enables us to measure three higher-order ($n \geq 2$) absolute moments: P_2 , Q_2 , and Q_3 .

Because the signal voltage of each electrode V_d is proportional to the integral of the electric field strength on the electrode, we can obtain the absolute moments with normalized moments $R_{P_n}^n/2$, $R_{Q_n}^n/2$ and geometrical factors k , K , as described in Eq. (1). In the equation, R_{P_n} or R_{Q_n} is called an effective aperture radius. The effective aperture radii and the geometrical factors are calculated analytically, especially for a BPM with circular cross-section, or numerically [4].

The calculation result is summarized in Table 1. A smaller effective aperture radius is preferable for accurate

*ken@spring8.or.jp

NON-DESTRUCTIVE REAL-TIME MONITOR TO MEASURE 3D-BUNCH CHARGE DISTRIBUTION WITH ARRIVAL TIMING TO MAXIMIZE 3D OVERLAPPING FOR HHG-SEEDED EUV-FEL

H. Tomizawa, K. Ogawa, T. Sato, and M. Yabashi

RIKEN Hariama Institute, 1-1-1 Kouto, Sayo-cho, Sayo-gun, Hyogo, Japan

Y. Okayasu, S. Matsubara, and T. Togashi

JASRI/SPring-8, 1-1-1 Kouto, Sayo-cho, Sayo-gun, Hyogo, Japan

E. J. Takahashi

RIKEN Advanced Science Institute, Hirosawa 2-1, Wako, Saitama 351-0198, Japan

M. Aoyama

Kansai Photon Science Institute, Japan Atomic Energy Agency,

8-1-7 Umemidai, Kizukawa-shi, Kyoto 619-0215, Japan

A. Iwasaki and S. Owada

Department of Chemistry, The School of Science, The University of Tokyo,

7-3-1 Hongo, Bunkyo-ku, Tokyo 113-0033, Japan

H. Minamide and T. Matsukawa

RIKEN 519-1399, Aramaki-aza, Aoba, Aoba-ku, Sendai, Miyagi, 980-0845, Japan

Abstract

We have developed a three-dimensional bunch charge distribution (3D-BCD) monitor with arrival timing for an FEL seeded with a high-order harmonic (HH) pulse. A 3D-BCD monitor is based on an Electro-Optic sampling (EOS) technique with multiple EO crystal detectors in spectral decoding. Utilizing this EO-multiplexing technique, we obtained the relative positioning in the transverse and the timing in the longitudinal of the electron bunch with respect to arriving timing of a seeding HH pulse at the undulator in real-time with non-destructive measurements. In our EUV-FEL accelerator, we prepared a seeded FEL with an EOS-based feedback system for user experiments. For obtaining a higher seeding hit rate, 3D overlapping between the electron bunch and the seeding pulse must be maximized at the optimal point. Keeping the peak wavelength of EO signals at the same wavelength with our feedback system, we provided seeded FEL pulses (intensity $>4\sigma$ of SASE) with a 20-30% hit rate during pilot user experiments. For achieving the upper limit of temporal resolution, we are planning to combine high-temporal-response EO-detector crystals and an octave broadband probe laser pulse with a linear chirp rate of 1 fs/nm. We are developing an EO-probe laser pulse with ~ 10 μ J pulse energy and bandwidth over 300 nm (FWHM). In 2011, we successfully demonstrated the first bunch measurement with an organic EO crystal in the FEL accelerator at SPring-8.

INTRODUCTION

Since 2010 at SPring-8, we have been demonstrating a seeded free-electron laser (FEL) in the extreme ultra violet (EUV) region by high-order harmonics (HH) generation from an external laser source in a prototype test accelerator (EUV-FEL) [1]. In FEL seeding as a full-coherent high-intensive light source for EUV user

experiments, a high hit rate of successfully seeded FEL pulses is required. Precise measurements of the electron bunch charge distribution (BCD) and its arrival timing are crucial keys to maximize and keep 3D (spatial and temporal) overlapping between the high-order harmonics (HH) laser pulse and the electron bunch. We constructed a timing drift monitor based on Electro-Optic (EO) sampling, which simultaneously measures the timing differences between the seeding laser pulse and the electron bunch using a common external pulsed laser source (Ti: Sapphire) of both the HH driving and EO-probing pulses (Fig. 1). The EO-sampling system can use timing feedback for continuous (without interruption) operation of HH-seeded FELs.

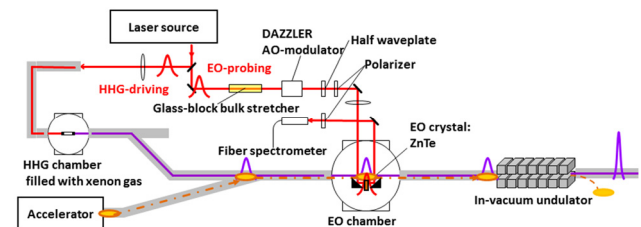


Figure 1: Experimental setup of seeded FEL with EO-sampling feedback at EUV-FEL accelerator: relative positioning in transverse and timing in longitudinal of electron bunch with respect to arriving timing of a seeding HH pulse are monitored at entrance of the first in-vacuum undulator to keep in a best seeding condition.

The R&D of a non-destructive 3D-BCD monitor (proposed in 2006 [2]) with bunch-by-bunch detection and real-time reconstructions has been extensively investigated at SPring-8. This ambitious monitor is based on an EO-multiplexing technique that resembles real-time spectral decoding and enables simultaneous non-destructive measurements of longitudinal and transverse BCDs. This part of the monitor was simultaneously materialized for probing eight EO crystals that surround

BEAM DIAGNOSTICS DEVELOPMENT FOR TRIUMF E-LINAC*

V.A. Verzilov[#], P. Birney, D.P. Cameron, J. Van Holec, S.Y. Kajioka, S. Kellogg, M. Lenckowski, B. Minato, W.R. Rawnsley, TRIUMF, Vancouver, Canada
J.M. Abernathy, D. Karlen, D.W. Storey, Victoria University, Victoria, Canada

Abstract

TRIUMF is currently in a phase of the construction of a superconducting 50 MeV 10 mA CW electron linear accelerator (e-linac) to support the photo-fission based rare radioactive isotope beam production program. The project imposes certain technical challenges to various accelerator systems including beam diagnostics. In the first place these are a high beam power and widely varying beam operating modes: from very short beam pulses to the CW regime. A number of development projects have been started with the aim to construct the diagnostic instrumentation required for commissioning and operation of the facility. The paper reports the present status of the projects.

INTRODUCTION

As a part of the effort to expand the Rare Radioactive Isotope Beam (RIB) program, TRIUMF has started the construction of a 50 MeV 10mA CW superconducting electron linac as a driver for production of neutron-rich isotopes via photo-fission reactions [1]. The facility will comprise a gridded 300 keV thermionic electron gun operated at 650 MHz, a 1.3 MHz superconducting linac, a 70 m long transfer line and the Target Stations for RIB production. Future expansion foresees a recirculation ring to bust the beam energy up to 75 MeV. While civil construction works are carried on, chosen design and operation strategies can be proved at the injector test facility that produced the first beam in November of 2011.

Design challenges are largely associated with a substantial (half a Megawatt) beam power in the CW mode. Clearly, commissioning and tune-up modes are necessary to safely deliver the beam all the way to the targets or dedicated beam dumps. It is presently seen that the beam tuning may require beam pulses of a few microseconds short. A number of development projects were launched about two years ago in order to design the diagnostics capable of supporting all the variety of beam modes. As for today all these projects are either close to completion and moving into production phase or at least reached the maturity state.

DIAGNOSTICS SYSTEMS

Not all the e-linac diagnostics devices are presented and discussed below. Some were reported elsewhere [2]. The beam loss monitoring and machine protection, which are both critical for the operation of the facility are subjects for a dedicated paper.

Beam Position Monitors (BPM)

The general absolute accuracy of beam position measurements is expected to be better than 500 μm . The required relative position resolution of 50 μm is not very high and should be easily achievable. Both button and stripline BPM monitors have been designed for the project. The stripline BPM provides a higher signal strength and better absolute accuracy. The button BPM, which is substantially smaller in dimensions, was demanded for locations with tight space constraints.

Each button electrode, that is 12 mm in diameter, is mounted at the pin tip of a SMA vacuum feedthrough welded to a NW16 flange (see Fig. 1). A special alignment groove is machined to improve the position accuracy. The required absolute accuracy is expected to be achieved by a torque adjustment in situ of the fastening bolts to balance the calibration signal strength delivered by individual pickups composing a BPM. The button pickups are manufactured by Kyocera Corporation according to TRIUMF drawings. Three complete BPM were installed at the injector test facility. First beam data are available.

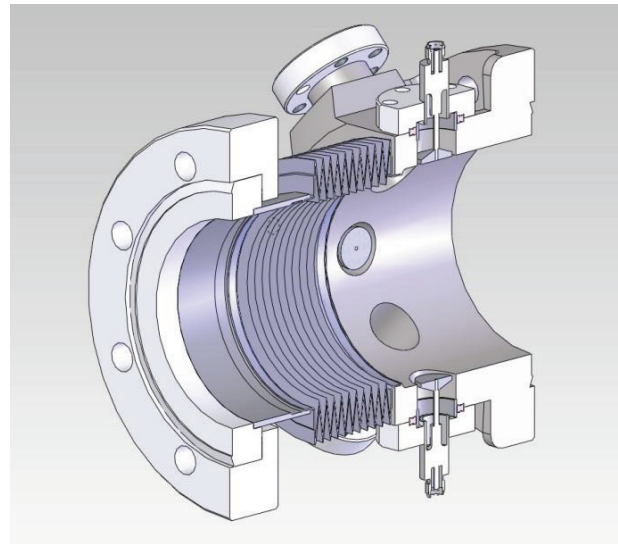


Figure 1: A cross-section view of the button BPM.

The stripline BPM (see Fig. 2) was developed based on work done at Cornell. The Cornell design was adjusted to comply with the 650 MHz bunch repetition frequency and a smaller diameter (50 mm) of the beam pipe. The prototype unit is currently being assembled. Position sensitivity of both button and stripline BPMs is 1.4 dB/mm. The estimated signal strength of the button BPM is about -30 dBm (confirmed by measurements) at the

*Funding is received from National Research Council of Canada
#verzilov@triumf.ca

BEAM LOSS TRACK MEASUREMENTS BY A FAST TRIGGER SCHEME IN J-PARC LINAC*

H. Sako[#], T. Maruta, and A. Miura, Japan Atomic Energy Agency, Tokai, Japan

Abstract

In J-PARC Linac, highest beam loss has been observed at the ACS (Annular-Coupled Structure linac) section. The primary source of the beam loss is considered to be H^0 produced by an interaction of H^- beams with remnant gas. The H^0 hits the beam duct, converted to H^+ , and escapes from the beam duct.

To detect the H^+ s and estimate the absolute magnitude of the beam loss, we constructed a detector system, which consists of 6 planes of hodoscopes made of 16 scintillation fibers with $64 \times 64 \text{ mm}^2$ area. The scintillation light is measured by multi-anode photomultipliers. In the ACS section, two planes to measure horizontal positions are installed, and at about 1 m downstream positions, two planes for horizontal measurements and two for vertical measurements are placed. We will reconstruct charged particles passing through all the 6 planes, and measure the velocity by time-of-flight and energy loss to identify particle species.

We present new measurements since the recovery of the J-PARC after the earthquake started in April 2012 by a new fast trigger scheme using dynode signals of photomultipliers in order to improve signal-to-noise ratios.

INTRODUCTION

The H^0 ion produced by a beam H^- interacted with a remnant gas atom is considered to be the main source of the beam loss in the J-PARC ACS section. The primary goal of this work is to measure H^+ s converted from the H^0 s through the beam duct. For this measurement, we constructed 6 planes of scintillating fiber detectors. Each plane consists of $16 \times 4 \times 4 \times 64 \text{ mm}^3$ plastic scintillating fibers. There are 2 upstream horizontal-measuring planes (H0, H1), 2 downstream horizontal-measuring planes (H2, H3) 1130 mm apart from H0/H1, and 2 downstream vertical-measuring planes (V0, V1) 58 mm apart from H2/H3. 32 fibers in each pair of planes are connected to a multi-anode photo-multipliers (PMT's) Hamamatsu H8500C. This pairing is to reduce inefficiency when a charged particle passes through a boundary between adjacent fibers in a plane and also to suppress accidental background.

Charged particle tracks are reconstructed by combining hits at the fiber planes. Energy of each track is measured with the time-of-flight, and energy loss in each plane is measured by the amplitude of the signal. The energy and the amplitude are used to identify protons and reject other particle species such as electrons, X ray, gamma ray, and neutrons.

The second goal of this work is to measure beam loss source positions along the beam duct and identify hot spots, by projecting each track to the beam axis.

Since 2010, we have measured beam loss with these detectors in ACS section, where we already observed charged particle tracks by beam loss. Detailed description of the scintillating fiber counters and data acquisition system, see [1,2].

FAST TRIGGER SCHEME

In 2012 measurements, the trigger scheme was improved significantly. Until 2011, we used a scheduled timing of the beginning of the macro pulse as the start signal for TDC (Time-to-Digital Converter) CAEN V785 and the gate signal for QDC (charge (Q)-to-Digital Converter) CAEN V792. There were two serious problems with this scheme. First, since the TDC cannot record multiple hits, in case there is another hit before the interesting signal, a wrong timing was recorded, and therefore signal-to-background (S/N) ratio was significantly deteriorated. To solve this problem, we utilized final-stage dynode signals (DY) which are available for PMT H8500C. The polarity of DY signals is opposite to the negative anode signals. Since the PMT has multiple anodes, the DY signal serves as analog sum signal over all the anode channels. We discriminate the DY signals of the three PMT's (DY1 for H0/H1, DY2 for H2/H3, and DY3 for V0/V1), and form coincidence signal from discriminated signals of DY1 and DY3 for the start timing of TDC's and the timing gate of QDC's. The DY1 and DY3 coincidence signal (DY1&DY3) is used as a trigger of a charged particle track penetrating from H0 to V1. Timing and charge of individual anode signal can be measured with low accidental background by narrowing the duration from the start timing to the anode signals for TDC's, and the gate width for QDC's. We also formed a time gate (TG) from the scheduled beam start timing to define the timing within the macro pulse. The coincidence DY1&DY3&TG is used for the data taking. The timing offset and time interval per TDC channel for each fiber was calibrated by injecting a pulse generator signal split to all the detector signal cables end and measuring the timing with the data acquisition system.

RESULTS

The analysis shown here is based on the data taken from Apr. to Jun. 2012. The fiber geometry for H0, H1, H2, and H3 is shown in Fig. 1. By moving H2 and H3, we cover three different track angles, 3.6° - 5.0° , 6.0° - 7.0° , and 9.0° - 11.0° .

*Work supported by JSPS KAKENHI Grant Numbers 23656063, 24510134.

[#]hiroyuki.sako@j-parc.jp

HIGH DYNAMIC-RANGE HIGH SPEED LINAC CURRENT MEASUREMENTS *

C. Deibele, D. Curry, R. Dickson, ORNL, Oak Ridge, TN 37831 USA

Abstract

It is desired to measure the linac current of a charged particle beam with a consistent accuracy over a dynamic range of over 120 dB. Conventional current transformers suffer from droop, can be susceptible to electromagnetic interference (EMI), and can be bandwidth limited. A novel detector and electronics were designed to maximize dynamic range of about 120 dB and measure rise-times on the order of 10 nanoseconds.

BACKGROUND/GENERAL THEORY

An ideal beam of current in a linac can be expressed as a series of Gaussian pulses of current separated by a unit of time, t_o , as described $I(t) = \sum_{n=-\infty}^{\infty} I_m(t - nt_o)$, where $I_m(t) = \frac{1}{\sigma\sqrt{2\pi}} e^{-\frac{t^2}{2\sigma^2}}$. Since the current, $I(t)$, is periodic, the current can be realized as a Fourier series $I(t) = \sum_{n=0}^{\infty} a_n \cos(n\omega_o t)$, $\omega_o = \frac{2\pi}{t_o}$. Many linac beam measurement systems make use of this spectral analysis technique and rely on a measurement of a particular harmonic. For example, beam position and phase measurement systems measure the first and/or second harmonic component, and draw various conclusions about the beam position within the beampipe or beam phase relative to some rf source.

Measurements of a beam harmonic have an inherent advantage that baseband noise, interference, or EMI can be easily filtered and therefore not contaminate the intended spectral measurement. For example, switched power supplies can easily inject parasitic baseband signals into the intended measurement signal and therefore reduce the signal-to-noise ratio. It is desired, therefore, that thermal noise be the limiting factor in many of the linac beam measurements.

To measure the beam current, a measurement of a signal that can be calibrated to an individual harmonic of the beam and is directly proportional to beam harmonic is desired. Many BPM (Beam Position Monitoring) systems rely on this technique, and a signal that is proportional to beam current is reported. Unfortunately, output signals from BPM electrodes by its design are strongly dependent on beam position, and therefore the design of the BPM electrodes can produce a nonlinear calibration of the reported current. Also, many linac BPM systems use an IQ under-sampled/down converted signal processing technique which may not adequately measure the sharp rise/fall times of linac beam, which is essential in any chopped linac current.

A detector is sought that:

- can successfully measure a signal that is proportional to a beam harmonic,
- does not intercept the beam and can support high intensity operation,
- has an output signal that is independent of beam position as beam traverses through it,
- has a low quality factor (or “Q”), so that accurate rise-times and fall-times can be measured,
- is optimized for measuring high dynamic range.

SYSTEM DESIGN

A description of the overall beam current measurement system is described. Particular and practical design issues are discussed.

Detector Design

The detector design was inspired by a stripline BPM, as it possesses most of the design criteria in the preceding section. A stripline can be optimized for beam response for a particular harmonic, and thereby is optimal for high dynamic range. The output of most BPM designs, however, is dependent on beam position. This effect can be reduced by placing the BPM striplines outside of the beampipe diameter. A schematic of the envisioned detector is depicted in Fig. 1.

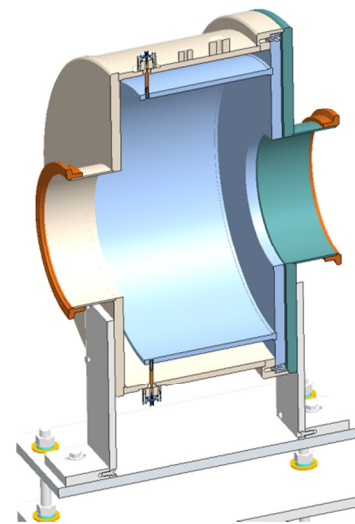


Figure 1: Schematic of the beamline detector.

A circumferentially continuous electrode that is $\lambda/4$ in length is short circuited to the wall of the vacuum vessel. Two of the four feed-thrus are shown.

* Work performed at (or work supported by) Oak Ridge National Laboratory, which is managed by UT-Battelle, LLC, under contract DE-AC05-00OR22725 for the U.S. Department of Energy.

DEVELOPMENT OF PERMANENT MAGNET FOCUSING SYSTEM FOR KLYSTRONS

Y. Fuwa, Y. Iwashita, H. Tongu, Institute for Chemical Research, Kyoto University, Kyoto, Japan
S. Fukuda, S. Michizono, High Energy Accelerator Research Organization, Ibaraki, Japan

Abstract

A permanent magnet focusing system for klystrons is under development to improve reliability of RF supply system and reduce power consumption. To save production cost, anisotropic ferrite magnets are used in this system. A test model has been fabricated and the power test of a 750 kW klystron with this focusing magnet is carried out. 60 % of the nominal output power has been achieved at a preliminary power test so far.

INTRODUCTION

Distributed Klystron Scheme (DKS) is proposed as one of the RF supply scheme for International Linear Collider (ILC) to reduce the cost and the down time by raising the reliability [1]. Because thousands of relatively small modulating anode (MA) klystrons were required in DRFS scheme, the failure rate of each component must be reduced. Especially thousands units of electromagnet for klystron beam focusing would cause maintenance problems. Replacing the electromagnets by permanent magnets can eliminate their power supplies and cooling system. Hence the failure rate of the RF supply system can be reduced and cut down the operation cost. A klystron beam focusing system with ferrite magnets is under development is described.

FABRICATION OF FOCUSING MAGNET

Magnetic Materials

There have been precedents for electron beam focusing in klystrons with permanent magnets such as ALNICO, the rare earth (RE) [2,3,4]. Figure 1 shows the B-H curves for these magnet materials and anisotropic ferrite magnets. ALNICO magnets, which have high remanence, shows less coercivity and easily demagnetize. Although RE magnets such as NdFeB has high remanence and coercivity, they are rather expensive and have the resource problem. The anisotropic ferrite magnets have less remanence but higher coercivity than ALNICO. The required magnetic field for beam focusing in klystrons is less than 1 kGauss, therefore the remanence of the anisotropic ferrite magnets is enough high. And the material costs are not expensive, because anisotropic ferrite magnets are composed of iron oxide.

Magnet Field Distributions

Periodic Permanent Magnet (PPM) focusing scheme has relatively well-known magnetic field distribution. In a focusing system with permanent magnet, the alternating magnetic field can be easily generated because an integrated value of magnetic field vector along closed

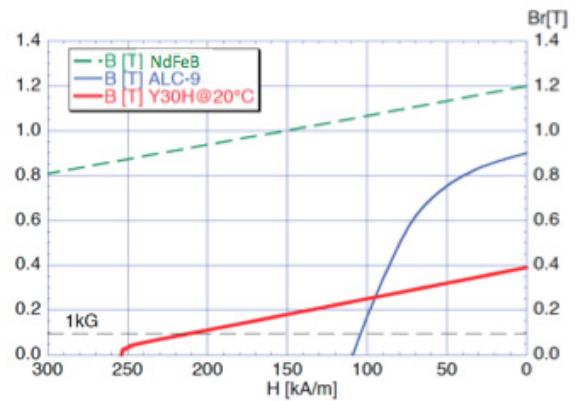


Figure 1: B-H curves of rare earth, ALNICO and ferrite magnets.

curve or infinitely-long axis is zero by the Ampere's law. However, periodicity cause stop bands. For pulse operations, the operating point always crosses such region during pulse rising time and the beam loss causes wall heating and prevents stable operation.

For safe operation, unidirectional magnetic field distribution is applied. Because the required magnet field is not high, anisotropic ferrite magnets can be used. RADIA 4.29[5,6] is used for the magnetic field design. Applied design is shown in Figure 2. Magnets shown in Figure 2 are categorized into two groups. The one group consists of magnets surrounding the klystron body

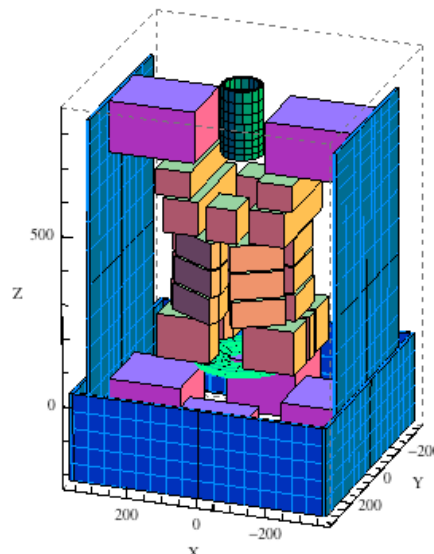


Figure 2: Layout of magnet and iron yoke.

176 MHz SOLID STATE MICROWAVE GENERATOR DESIGN

A. Smirnov, A. Krasnov, K. Nikolskiy, N. Tikhomirova, E. Ivanov,
Siemens Research Center, Moscow, Russia
O. Heid, T. Hughes, Siemens AG, Erlangen, Germany

Abstract

This paper concerns the R&D work upon design of a compact RF amplifier to be used for linear accelerators. The machine under development will operate at 176 MHz with output power of 25 kW in continuous wave regime. It consists of 50 push-pull PCB modules (approx. 500W output power each), connected in parallel to several radial filter rings, which both allow class-F operation and combine the power from the modules, delivering it to a single 50 Ohm coax cable. The CST simulations and the design of 324 MHz test prototype are presented.

INTRODUCTION

High power RF sources are important elements for most of linear accelerators that have found growing number of applications in physics and medicine.

The main benefits of the generator under development will be its smaller size, perspective of lower cost, better reliability and higher efficiency, achieved with class-F operation, compared to conventional RF power sources like klystrons. The solid-state microwave power modules based on SiC vJFET transistors arranged in parallel push-pull circuits, will be designed on PCB boards.

All modules will be connected to a power combiner with common output 50 Ohm coaxial cable.

This generator is planned to be a predecessor to the 'big' 324 MHz machine with pulsed RF output power of 3 MW.

RF POWER MODULES

We have designed and manufactured compact RF power modules with one pair of SiC transistors arranged in circlotron topology [1] as shown on Fig.1.

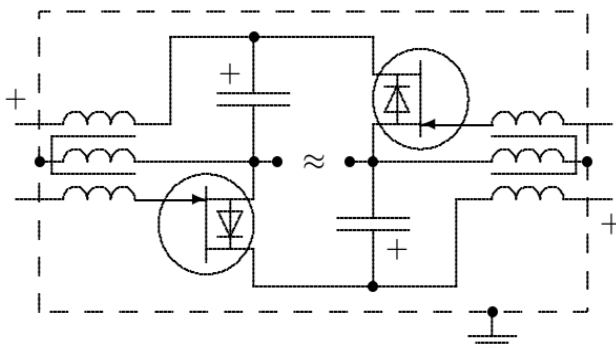


Figure 1: Parallel push-pull circuit.

The manufactured module layout is presented on Fig.2. We used Rogers 4003C with $\epsilon=3.55$ as a substrate material. The transistors are fed with 180° phaseshift,

provided with external balun. The module provides maximum available gain of 18.9 dB at output power of 2.0 kW and with supply voltage of 150 V.

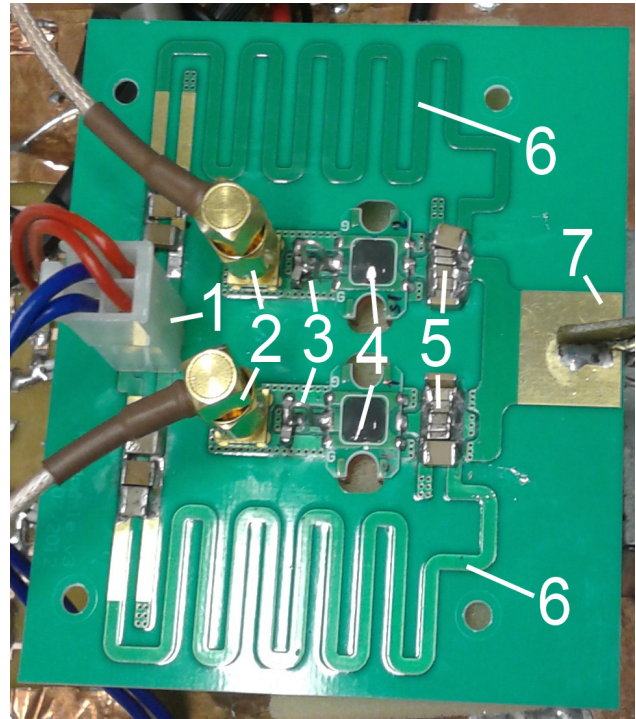


Figure 2: RF power module (heat sink is not shown): 1 – DC supply voltage; 2 – RF inputs; 3 – input matching circuit; 4 – SiC transistors; 5 – DC-blocking capacitors; 6 – quarter-wavelength lines; 7 – symmetric output stripline.

Each transistor will be mounted on a water-cooled heat-sink with a sinter paste, as shown on Fig. 3, which can dissipate up to 300 W average thermal power.

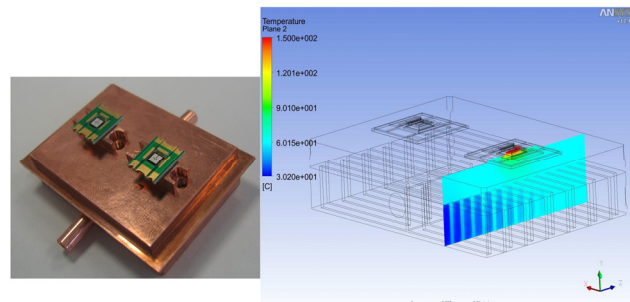


Figure 3: Transistor package mounted on a water-cooling module with temperature distribution.

HIGH POWER AMPLIFIER SYSTEMS FOR SARAF PHASE II

I. Fishman, I. Gertz, B. Kaizer, D. Har-Even, Soreq NRC, Yavne, Israel

Abstract

Soreq NRC initiated the establishment of SARAF- Soreq Applied Research Accelerator Facility. SARAF is based on continuous wave (CW), proton/deuteron RF superconducting linear accelerator with variable energy (5-40 MeV) and current (0.04-5 mA). RF power to each cavity is driven by a High Power Solid State Amplifier. The paper outlines the design concept of 10 and 15 kW at 176 MHz power amplifiers. 10 kW amplifier was successfully tested at the beginning of 2012. 15 kW system is now under final design stage. The amplifiers are combined from basic 5.5 kW compact 19" 7U water cooled drawers.

INTRODUCTION

The paper describes the basic 5.5 kW amplifier drawer and method of building and construction of High Power amplifier systems. The need of High Power Amplifiers appears when the 6 exiting 2 kW 176 MHz amplifier built by "Accel" for Prototype Cryogenic cavities limits to rise the current of the accelerator. The 4 kW amplifiers were designed and built to exchange the 2 kW.

The 5.5 kW is designed and built for future design of high energy cavities for the Phase II project.

BASIC 5.5 kW RF POWER AMPLIFIER

The 5.5 kW High Power Amplifier (HPA) consists of following sub modules and components:

- 4 double 800 W water cooled RF modules.
- 8 ways 100 W RF Power Splitter.
- 8 ways 5.5 kW RF Power Combiner.

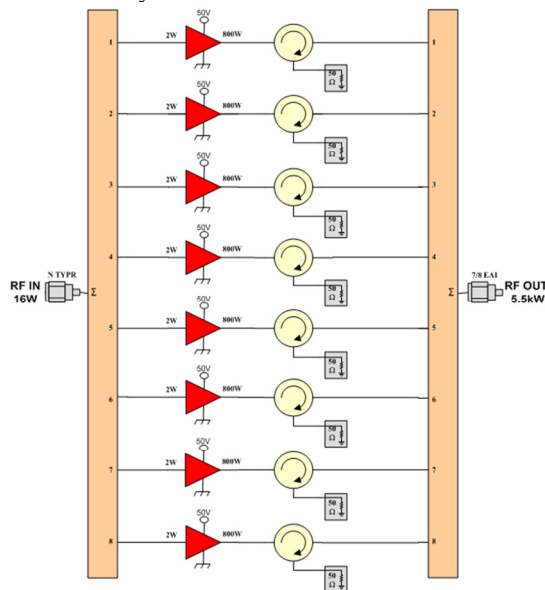


Figure 1: 5.5 kW block diagram.

800 W RF Power Module

The power amplifiers are attached to opposite sides of a joint heat sink to reduce separate water cooling and optimize the design. This permits to enter in very small volume 100x200x350 mm. Each amplifier delivers 800 Watt P1dB CW RF power. The amplifiers are protected by two circulators and two 800 Watt RF resistors. This permits safe operation with full reflected RF power.

The following control signals are available from each amplifier:

- C max, normally high, low in case overheat.
- Temperature measurements, 10 mV / deg C.
- REF Power Detector Pout@800W 40°C-1.5v.
- FWR Power Detector Pout@800W40°C-1.5v.

This signals permits to monitor the status of each amplifier in the drawer.



Figure 2: The double 800 W amplifier module view.

8 way 100 W RF Power Splitter

The splitter divides the driver's RF power into 8 equal signals to drive each of eight Power Amplifier modules up to 800 Watt. The splitter is designed by micro strip line technology and is mounted in aluminium milled case. The splitter was computer simulated and has very low loss and good matching. The RFin connector is N-type and 8 output connectors are SMA type.



Figure 3: 8 way 100 W splitter (divider) view.

COMPACT 4 kW VARIABLE RF POWER COUPLER FOR FRIB QUARTER-WAVE CAVITIES *

M.P. Kelly[#], S.V. Kutsaev, Z.A. Conway, M. Kedzie,
ANL, Argonne, IL 60439, U.S.A.

J.L. Crisp, L.L. Harle, FRIB, East Lansing, Michigan, USA

Abstract

A new compact 4 kW power coupler has been designed and prototyped at Argonne National Laboratory in collaboration with Michigan State University. The coupler is intended for use on the $\beta=0.085$ 80.5 MHz superconducting quarter-wave cavities for the FRIB driver linac and also for the ReA6 cryomodule using the same quarter wave cavity design. The coupler has a cold RF window and a 3 cm variable bellows section. The short 16 cm length of the RF window plus bellows facilitates a simple and compact clean room installation onto the cavity coupling port. A prototype has been fabricated in collaboration with U.S. industry and cold tested at 3 kW forward power under realistic operating conditions at Argonne. Simulation and test results are presented.

INTRODUCTION

The front-end of the superconducting linac for the Facility for Rare Isotope Beams (FRIB) at Michigan State University includes two different types of 80.5 MHz quarter-wave resonators (QWR's) operating with $\beta=0.041$ and $\beta=0.085$. [1] The rf power coupler will be the primary means of locking the cavity rf phase to a master oscillator in the presence of microphonics and, at the same time, will provide the required beam power. The proposed full $\beta=0.085$ cavity rf bandwidth is 40 Hz, with a corresponding total rf power of 2.5 kW. In order to provide reasonable margin, coupler specifications call for reliable coupler operation at 4 kW CW power under all conditions of reflection angle.

DESIGN APPROACH

As always, a coupler should reliably deliver rf power to the beam at the nominal Q_{ext} and also be suitable for other modes of operation such as cavity rf (pulse) conditioning. The coupler should not adversely impact cleanliness of the high-gradient SC cavities either in assembly or long-term operation. Considerations for the previously tested ANL 4 kW, 72 MHz coupler are similar [2], and the early 4 kW design served as the starting point for the new coupler. RF parameters are given in Table 1.

The modular design has four separate components. These include a variable bellows, a 'cold' rf window, a 55-to-300 K transition and a room temperature rf window. Both window assemblies are built around a donut-shaped alumina disc with a hole for the center conductor. The

* This work was supported by the U.S. Department of Energy, Office of High Energy Physics and Nuclear Physics, under Contract DE-AC02-76CH03000 and DE-AC02-06CH11357.

[#]mkelly@anl.gov

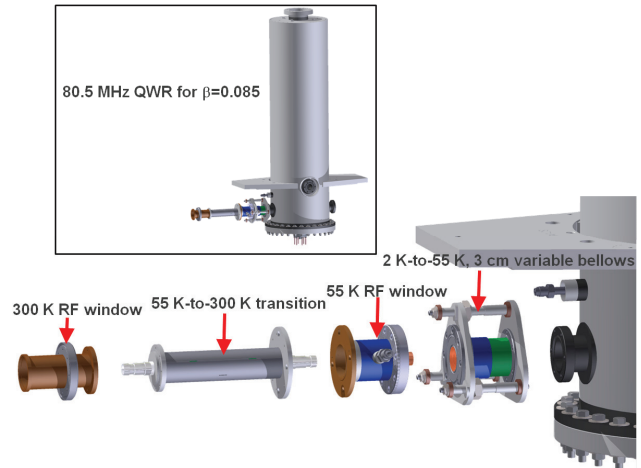


Figure 1: Prototype 4 kW coupler for FRIB quarter-wave cavity.

discs have been fabricated from alumina ceramic and brazed between the copper inner and outer conductors at MPF Products Inc.. The ceramic material was chosen for its good combination reliable brazing characteristics and good rf performance.

Adjustability of the center conductor by 3 cm into or out of the cavity coupling port is performed by compressing a cold bellows, formed from thin-walled stainless steel with 20 μm of copper deposited on the inner (rf) surface. The cold window is anchored to 55 K by circulating cold He

Table 1: Coupler Design Parameters

Parameter	Value
Nominal design power (kW)	4
Type	Coaxial capacitive
Outer diameter (cm)	4.1
Length (cm)	37
Impedance, nominal (Ω)	50
S11 @ 80.5 MHz (dB)	-31
Static load to 2K (W)	0.36
Static load to 55K (W)	4.1
Dynamic load to 2K (W)	0.15
Dynamic load to 55K (W)	8.4

HIGH POWER TESTS OF TRASCO RFQ COUPLERS

E. Fagotti, F. Grespan, L. Antoniazzi, A. Palmieri, F. Scarpa, INFN/LNL, Legnaro, Italy
 M. Desmons, CEA, Saclay, France
 O. Brunasso Cattarello, R. Panero, INFN, Torino, Italy

Abstract

The TRASCO RFQ is powered by eight coaxial power couplers, magnetically coupled to the cavity by a loop-antenna. Couplers were designed to support up to 140 kW in cw operation. After a test-stand validation with a 10 kW power amplifier in Legnaro, the system was tested up to full power at CEA-Saclay. This paper covers the main steps of the coupler validation and conditioning results.

INTRODUCTION AND LOW POWER TESTS AT LNL

Two RF couplers were constructed based on the design developed in [1]. The RF coupler consists of the drive loop, the coaxial transmission line (inner diameter 19.4 mm, outer diameter 38 mm) and its associated cooling channels, and the coaxial alumina window (Figure 1).

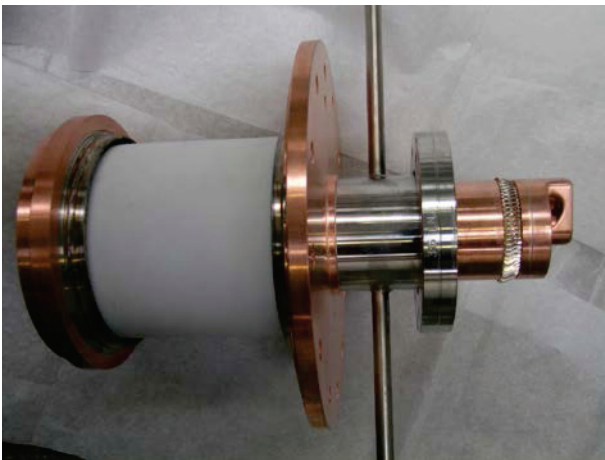


Figure 1: RF coupler system with loop, coaxial transmission line and coaxial alumina window.

In order to match the impedance of the coaxial line with the WR2300 waveguide used for the RF distribution, a “half doorknob” matching device is employed. The relatively small dimension of the coupler is determined by the 57 mm diameter of the RFQ port, in turn due to the small cross-sectional construction of the RFQ structure. The inner conductor of the loop is cooled via a coaxial SS tube and the outer conductor with a cooling SS sleeve. In particular, the CU OFE (inner coaxial, outer coaxial and drive loop) and the LN316 (flange and cooling sleeves) sub-assemblies were constructed and cleaned separately and then brazed together in a single brazing step. Prior to the brazing, the dimensions of the loop were determined after a set of measurements performed on the first two modules of the RFQ with on-purpose built aluminium dummy couplers. Finally, the cylindrical RF alumina windows were TIG welded on the coupler body. Such

windows are the same used for the NC LEP couplers and can withstand up to 140 kW CW RF power.

In order to allow the RF processing of the couplers a bridge waveguide cavity was employed. Such cavity is made with aluminium and is water cooled through the cooling sleeves on its walls. An aluminium strip acts both as RF joint and vacuum seal. The cavity has two ports in order to allow the conditioning of two couplers, one connected to the RF source and the other connected to the load, with minimum reflection ($RL = -15$ dB). HFSS simulations showed that about 30% of the input power is dissipated on the cavity walls. Figure 2 shows the couplers connected with the bridge cavity.

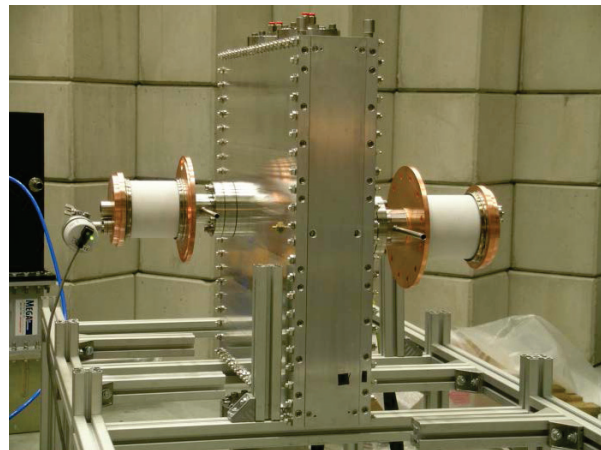


Figure 2: View of the two couplers connected with the bridge cavity. It is possible to notice the cooling channels and the RF windows.

A dedicated low power test-stand was installed at LNL for system validation, in which the RF source was provided by a 10 kW solid state amplifier. Before the final assembly, the coupler components were cleaned; the two couplers were inserted in the bridge cavity and baked out under vacuum with a maximum temperature of 150°C. During this baking process, one of the O-rings used to close the interface SS flange on the bridge cavity experienced problems at high temperature and started melting. The problem was not discovered during this test, because no vacuum analysis was available at the time and the O-ring melting had no impact on the vacuum level (later, it came out that the O-ring was not made of Viton®, as requested, but of NBR). However, after baking, a vacuum level of 1.9×10^{-8} mbar at the ceramic window location was measured.

The test in pulsed mode with 20 μ s pulse length and a 500 ms repetition period started in March 2011. The power was increased from 100 W up to 9.5 kW playing

DESIGN OF COUPLER FOR DIRECT COUPLED AMPLIFIER TO DRIFT TUBE LINAC CAVITIES OF THE INJECTOR RILAC2 FOR RIKEN RI BEAM FACTORY

K. Suda*, S. Arai, Y. Chiba, O. Kamigaito, M. Kase, H. Okuno, N. Sakamoto, Y. Watanabe, K. Yamada
RIKEN Nishina Center for Accelerator-Based Science, Wako-shi, Saitama, Japan

Abstract

Drift Tube Linac cavities for the new injector RILAC2 for RIKEN RI-Beam Factory were designed and constructed. To reduce an installation area and cost, we adopted a direct coupling method for a power amplifier to the cavity without using a long transmission line. A change of resonant frequency of the cavity caused by the coupler and amplifier must be accurately taken into account. The lumped element circuit model was not sufficient to estimate such a change. A complicated design procedure for the coupler and cavity was performed using a three-dimensional electromagnetic calculation software. The required input impedance seen from the amplifier was successfully achieved.

INTRODUCTION

The new heavy-ion linac RILAC2 was successfully constructed and commissioned at RIKEN RI Beam Factory [1, 2]. The main part of the accelerating cavity consists of three drift tube linac (DTL) cavities, operate in continuous wave mode at a fixed frequency of 36.5 MHz. Their structure is a quarter wavelength resonator because the size of the resonator is the smallest available in this frequency range. In order to reduce an installation area further, and to save a construction cost, we adopted a direct coupling method for a power amplifier to each DTL cavity without using a long transmission line. However, the direct coupling of the power amplifier changes the resonant frequency of the coupled system considerably from that of the cavity itself. Thus, the cavity design is dependent on that for the amplifier. Therefore, a detailed cavity and coupler design was carried out by using the three-dimensional electromagnetic calculation software, CST Microwave Studio (MWS).

REQUIRED PERFORMANCES FOR DTL CAVITIES

The design parameters of DTL cavities as determined by beam dynamics calculations [3] are listed in Table 1. The required gap voltages were 110, 210, and 260 kV for DTL1, DTL2, and DTL3, respectively. The height and diameter of the cavity to be used were required to be less than 3 m and 1.3 m, respectively, due to space restrictions in the AVF cyclotron hall. Each cavity consists of an outer and inner conductor, drift tubes, a capacitive coupler, and a capacitive tuner. The amplifiers for the three DTLs were based on the tetrode 4CW50,000E (Eimac). Their maximum output powers were 25, 40, and 40 kW for the respec-

tive DTLs. The required gap voltages were obtained when the parallel shunt impedances of each cavity are higher than 1.1 M Ω . The first two cavities (DTL1 and DTL2)

Table 1: Design Parameters for DTL Cavities

Cavity	DTL1	DTL2	DTL3
Frequency (MHz)	36.5	36.5	36.5
Duty (%)	100	100	100
Mass-to-charge ratio	7	7	7
Input energy (keV/u)	100	220	450
Output energy (keV/u)	220	450	670
Diameter (m)	0.8	1.1	1.3
Height (m)	1.32	1.429	1.890
Gap number	10	10	8
Gap length (mm)	20	50	65
Gap Voltage (kV)	110	210	260
Drift tube aperture radius (mm)	17.5	17.5	17.5
Peak surface field (MV/m)	8.9	12.3	13.7
Synchronous phase ($^{\circ}$)	-25	-25	-25
Power amp. (Maximum: kW)	25	40	40

were newly constructed, while the DTL3 cavity was modified from the decelerating cavity of the Charge State Multiplier (CSM) [4]. The design of the cavity without a coupler and amplifier was performed by MWS [5].

AMPLIFIER DIRECT COUPLING

Figure 1 shows images of the amplifiers and coupler, coupled to the DTL3 cavity. The RF coupler consists of

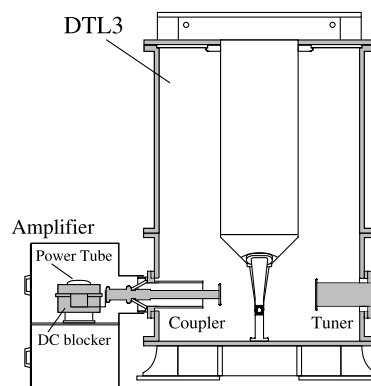


Figure 1: Schematic of the amplifiers coupled to cavity of DTL3. The output from the amplifier is directly connected to the coupler through a capacitor (DC blocker).

*ksuda@ribf.riken.jp

THE C-BAND RF PULSE COMPRESSION FOR SOFT XFEL AT SINAP

W.C. Wang, Z.T. Zhao, Q. Gu, SINAP, Shanghai, China

Abstract

A compact soft X-ray free electron laser facility is presently being constructed at Shanghai Institute of Applied Physics Chinese Academy of Science (SINAP) in 2012 and will be accomplished in 2014. This facility will be located to the shanghai synchrotron radiation facility (SSRF) which is a third generation light source in china. It requires a compact linac with a high-gradient accelerating structure for a limited overall length less than 230m. The c-band technology which is already used in KEK/Spring-8 linear accelerator is a good compromise for this compact facility and a c-band traveling-wave accelerating structure was already fabricated and tested at SINAP[1], and a c-band pulse compression will be required. There are some reasons, why RF pulse compression devices are quite useful to be applied in RF power supply of the soft XFEL. For it can enhance the peak RF power by expense of RF pulse length, so it will not increase the average power and at the same time reduce the total number of the klystron, it also increases the gradient of the accelerating structure, so we need the c-band pulse compressor. AND a SLED type RF pulse compression scheme is proposed for the C-band RF system of the soft XFEL and this scheme uses TE0.1.15 mode energy storage cavity for high Q-energy storage.

The C-band pulse compression under development at SINAP has a high power gain about 3.1 and it is designed to compress the pulse width from 2.5μs to 0.5μs and multiply the input RF power of 50MW to generate 160MW peak RF power, and the coupling coefficient will be 8.5. It has three components: 3-dB coupler, mode convertors and the resonant cavities. In this paper C-band pulse compression and some components for the c-band pulse compression will be described.

INTRODUCTION

The future c-band accelerator structure of SXFEL is supposed to operate at high acceleration gradient about 40MeV per meter, this requires very high peak RF power about 160MW at frequencies 5712MHz. So as to reduce the total number of the klystron and enhance the peak RF power, the RF pulse compression is needed.

RF pulse compression is one of the methods to compress the RF pulse length and at the same time increase the peak RF power that klystron deliver. RF pulse compression is based on the principle that the RF pulse is stored in a resonance cavity or a delay line and emitted within a short time to create the short RF pulse with high peak power and then deliver it into accelerating section. At present, several RF pulse compressions systems have been already utilized successfully in the s-band or c-band linear accelerator, such RF pulse compression, the SLAC

Energy Double (SLED) was the first, it was successfully applied in SLC operation, and now SLED-I, SLED-II, SLED-III (coupled cavities), BPC, DLDS and VPM (BOC) were already developed.

BPC, SLED-II and DLDS use the delay line as the energy storage cavity, have the flat output, high power gain and high efficiency, but the delay line is long and not economical. SLED-III (coupled cavities) use coupled cavities as the energy storage cavity, reduce the length of the delay line, but the output power irregular. It is applied a complex amplitude modulation on the input RF power, it is hard to control the accuracy and the stable. SLED-I has the simple structure and work stable, but it has the low power gain and less efficiency and a decaying exponential output pulse shape, so the technology AM-PM is applied for the flat output pulse shape.

In the soft XFEL, the design goal of the pulse compression is to compress the pulse width from 2.5μs to 0.5μs and to multiply the input RF power of 50MW to generate 160MW peak RF power. To satisfy this requirement for the soft XFEL, we adopted a SLED type pulse compression as the c-band pulse compressor. This scheme use TE0.1.15 mode for the storage cavity to compress an RF pulse into a short square high peak-power pulse for the course of R&D study of the soft XFEL. Figure 1 shows the schematic diagram. This scheme consists of one 3-dB coupler, two mode convertors, and a pair of high-Q resonant cavities.

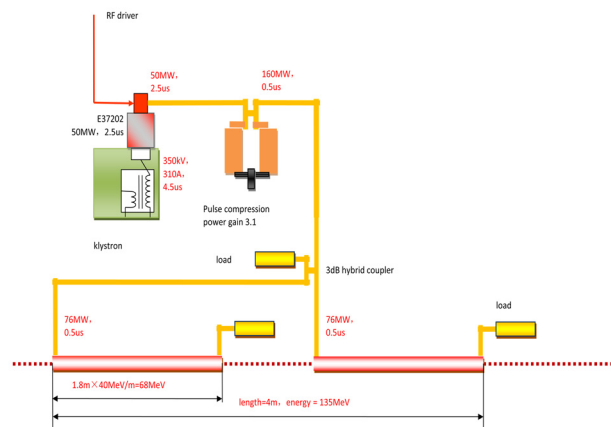


Figure 1: C-band 50WM RF Scheme.

C-BAND PULSE COMPRESSOR

C-band Pulse Compressor

For the SLED type RF pulse compression, the expression of the power for the resonant cavity is[2]

$$T_c \frac{dE_e}{dt} + E_e = -\alpha E_K \quad (1)$$

INPUT COUPLER OF THE J-PARC DTL

Fujio Naito*, Hirokazu Tanaka, Kesao Nanmo, KEK, Japan
Takashi Ito, Koichiro Hirano, JAEA, Japan

Abstract

DTL of the J-PARC has two input couplers in one tank. The coupler has a movable coupling loop with a capacitive element which increase the coupling with the tank. The loop position is the outside of the tank, where is in the atmosphere. The tank vacuum is kept by the ceramic window on the wall in the coupler port. The rf properties and the mechanical structure of the coupler were designed to achieve the larger coupling constant. Features of the coupler design for J-PARC DTL is described.

INTRODUCTION

Japan Proton Accelerator Research Complex (J-PARC) is a high-intensity proton accelerator facility constructed in the Tokai campus of Japan Atomic Energy Agency (JAEA) under the collaboration between KEK and JAEA. The accelerator consists of a 181-MeV linac, a 3-GeV rapid cycle synchrotron and a 30-GeV synchrotron main ring. The 181-MeV injection linac comprised of the an H⁻ ion source, RFQ linac, DTLs, and separated type DTLs (SDTLs). The resonant frequency of whole rf cavities in operation is 324MHz. The beam energy of linac will be increased to 400MeV by adding the annular-ring coupled structure (ACS) linac at the end of 2013[1].

The DTL section is composed of three long tanks. The length of each tank is approximately 9m. Each drift tube in the tank accommodates the compact electric quadrupole magnet. The beam is accelerated to approximately 50-MeV by the three DTL tanks.

The SDTL is a short DTL which has 5 gaps in a tank. Drift tubes in the SDTL do not accommodate the quadrupole magnet but the quadrupole doublet is set between the tanks. J-PARC has 30 SDTL tanks for the beam acceleration and two SDTL tanks as a debuncher.

The input coupler of the DTL has a different design from that of the SDTL. In the following sections the different points are mainly described.

REQUIREMENT ON THE COUPLER

The high-power rf is provided to each DTL tank independently. Each DTL tank has two input couplers so that the rf power which one coupler should transfer is reduced by half compared to the case that one tank has one coupler. However it is not simple to tune the coupling constant for both couplers adequately. In order to simplify the tuning procedure, the coupling constant of the coupler must be changed easily keeping the vacuum in the tank.

Rf coupling method we usually use is a loop coupling for DTL because it is much easier to adjust the coupling constant than an iris coupling. The coupling constant of the loop coupler is tuned by changing the tilt of the loop to the tank or changing the distance from the cavity.

The input coupler has a ceramic window to keep the vacuum in the tank. If the coupling loop of the coupler is in the vacuum side, the vacuum is usually broken when the loop tilt or the loop position is changed. Of course it is possible in principle to make a certain mechanical structure to move the loop in vacuum. However it is not reliable because the structure is probably too complicated.

For the DTL of J-PARC the coupling loop is set outside of the tank, where is in the atmosphere. The tank vacuum is kept by the ceramic window on the wall in the coupler port. The schematic view of the coupler design is shown in figure 1. The distance between the loop and the window is changeable by sliding the inside cylinder of the coaxial waveguide on which the loop is brazed. The loop is not fixed on the outer cylinder of the coaxial waveguide but the loop is contacted to the outer by the finger type rf contact.

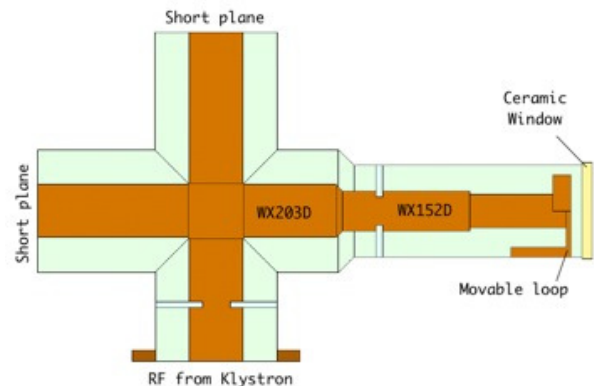


Figure 1: Coupler design.

As the loop is located outside of the tank, it is hard to have the large coupling constant with the tank. As the result, the coupling strength achieved by the loop is not enough for the DTL in spite of the fact that one DTL tank has two couplers as mentioned before.

Consequently the movable loop of the coupler has been put an capacitive element as shown in figure 2, which increase the coupling with the tank. In the figure 2 the rectangle plate on the right of the coaxial waveguide is the coupling loop. The half circle on the left is the capacitive element. Figure 3 shows the loop of the coupler for the SDTL. It is the simple loop. It is described that how we fixed the radius and thickness of the element in the next section.

* fujio.naito@kek.jp

RECOVERY AND STATUS REPORT OF DTL/SDTL FOR THE J-PARC AFTER EARTHQUAKE

T. Ito[#], K. Hirano, Japan Atomic Energy Agency, Tokai, Japan
 K. Nanmo, F. Naito KEK, Tsukuba, Japan

Abstract

The Japan Proton Accelerator Research Complex (J-PARC) facilities had big damages because of an earthquake on March 11, 2011. A DTL and an SDTL that were installed at the linac area had also damages. The alignment of the cavity was deformed more than 40mm and there had been observed about 0.2mm misalignment of the DT position in the DTL, and so on. However the result of the recovery work over eight months, we restarted proton beam acceleration at the linac section. As is the case with before earthquake, the DTL and the SDTL are operating with a few trips per day, as of April 2012. In this paper, we will present the recovery works from the earthquake and the operating status of the DTL and the SDTL.

DAMAGES OF THE DTL AND THE SDTL

By the earthquake, the Drift Tube Linac (DTL), Separated type DTL (SDTL) and various equipment of the cavity had damages [1] [2]. The situation damage is described below.

Drift Tube Alignment

Fortunately there were no damages, like a dent and a crack, on the outside of cavity and focusing magnets between SDTL tanks by the visual inspection. A movable Tuner and an RF coupler attached on the cavity was also no damage. However, it was observed that the alignment of the all tanks of DTL and SDTL was broken by the deformation of the floor of the tunnel. Furthermore a few misaligned drift tubes in the DTL were also observed.

First, we check the DT position by using a digital camera and the alignment telescope. Figure 1 shows the pictures of the DT bore of the DTL and the SDTL.

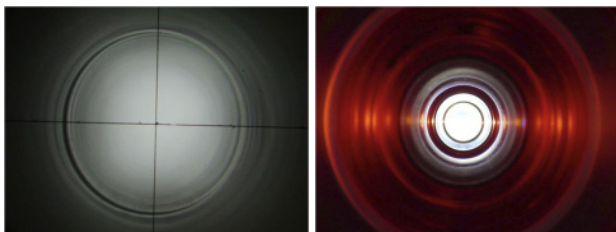


Figure 1: Pictures of the DT bore. Left:DTL, Right:SDTL

For the DTL bore picture (left picture), the black circular arc of the left side is broader than right side. This means that the DT bore center or DT position is decidedly sifted in a horizontal direction. On the other hand, the circles in the SDTL picture (right picture) were nearly

arranged in a concentric pattern. Therefore we judged that there was no clear displacement of the alignment of the DT position for the SDTL.

Next we measured the center position of the DT bore of the DTL by using alignment telescope. Figure 2 is a schematic view of the measurement system and the measured center position of the DT bore for a D1-1 (unit tank #1 of the DTL1).

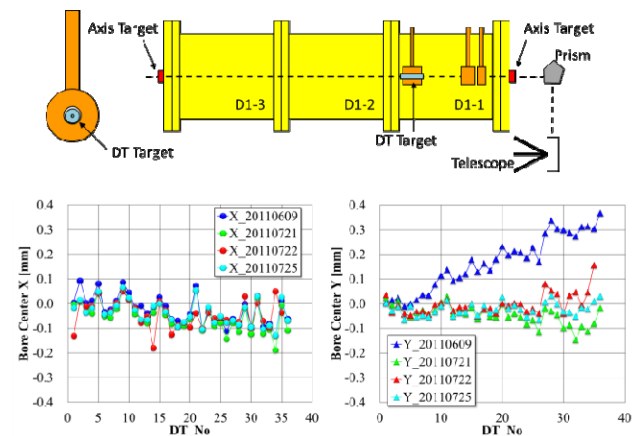


Figure 2: Schematic view of the measurement system and the measured center position of the DT bore.

The telescope axis was set on a line defined by the two axis targets and the DT target center position from the telescope axis was measured.

The graph shows the measured displacement of the DT bore center for the unit tank D1-1. The abscissa is DT number and the ordinate is the displacement of the bore center from the telescope axis.

There is about 0.2mm misalignment of bore center for X direction. The displacement for Y direction is less than X displacement except for the large DT number with large reading error. The reason is that the DT is swung like pendulum by horizontal vibration of earthquake because the DT is fixed at the top of the cavity.

There is a line with large tilt for Y measurement. This means that the unit tank D1-1 is inclined with respect to the telescope axis. This tilt line was measured before re-alignment of the DTL unit tank. Namely, the accelerator tunnel was deformed by the earthquake and the DTL was deformed along a floor of the tunnel. After re-alignment of the unit tank, the deformation of the DTL for Y direction is resolved (i.e. other three lines).

We did not measure the DT bore center of other cavities, because we could not prepare the target for DTL2 and the DTL3 soon. However, a drift of a resonant frequency of the cavity and an abnormal Q value were not observed. Therefore we concluded that there was no serious displacement of the DT.

[#]itou.takashi@jaea.go.jp

BEAM LOSS OCCURRED AT DTL CAVITY IN J-PARC LINAC*

A. Miura[#], T. Ito, K. Hirano, T. Maruta

J-PARC Linac, Japan Atomic Energy Agency, Tokai, Ibaraki, Japan

T. Miyao, K. Nanmo, M. Ikegami, F. Naito

J-PARC Linac, High Energy Accelerator Organization, Oho, Tsukuba, Japan

Abstract

We measured the residual radiation along the beam line during short operation intervals. Because the dependence on the operational condition of higher residual radiation was recognized at the surface of drift tube linac (DTL) cavity by radiation survey, we installed scintillation beam loss monitors at some points with particularly high radiation to investigate the cause of the radiation. Although the DTL section is low energy part of the linac, fine structure of the beam loss was observed by the scintillation BLM. We also measured the beam loss occurred at the DTL varying the beam orbit. In this paper, the result of the radiation measurement and beam loss signals obtained by the scintillation BLM's are presented.

INTRODUCTION

There was big damage in J-PARC caused by the Tohoku earthquake in March 2011^[1-3]. And the beam operation of J-PARC linac was suspended. We resumed the beam operation and delivered to the laboratory from December. After resuming the operation, we measured the residual radiation along the beam line during short intervals. Because the dependence on the operation condition and history of higher residual radiation was recognized at the surface of drift tube linac (DTL) cavity by radiation survey, we installed scintillation beam loss monitors (BLM's) at some points with particularly high radiation to investigate the cause of the radiation. We also measured the beam loss occurred at the DTL varying the beam orbit.

RESIDUAL RADIATION IN DTL SECTION

DTL (Drift Tube Linac) in Linac

J-PARC linac consists of the IS (ion source), RFQ (Radiofrequency Quadrupole), DTL (Drift Tube Linac), SDTL (Separated type DTL) and the beam transport to downstream RCS (Rapid Cycling Synchrotron) as fig. 1. Negative hydrogen ion beam is accelerated up to 50 keV in the ion source chamber. After the beam is accelerated up to 3 MeV by RFQ and had matching by the quadrupole magnets in MEBT (middle energy beam transport) section, it is injected to DTL through SDTL to be accelerated.

J-PARC linac has three DTL cavities, and each cavity consists of connected 3 unit tanks. Length of a unit tank reaches 3 m, then a DTL cavity reaches about 9 m. The first DTL cavity consists of 75 drift tubes (DTs) and quadrupoles. All DTs are aligned within 50 μm to the center of the magnetic fields^[4].

[#]miura.akhiko@jaea.go.jp

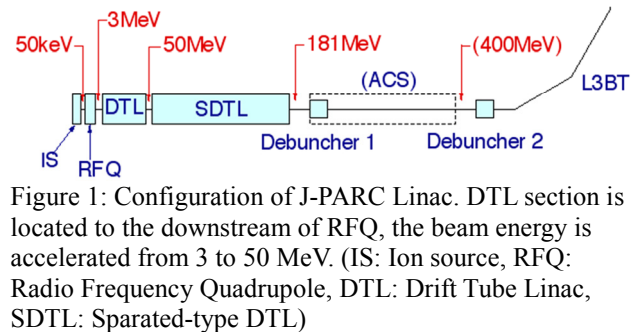


Figure 1: Configuration of J-PARC Linac. DTL section is located to the downstream of RFQ, the beam energy is accelerated from 3 to 50 MeV. (IS: Ion source, RFQ: Radio Frequency Quadrupole, DTL: Drift Tube Linac, SDTL: Separated-type DTL)

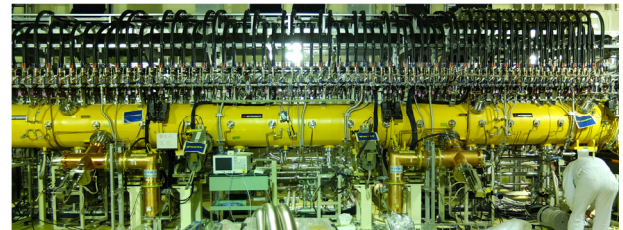


Figure 2: Overview of DTL Cavity. One DTL cavity consists of 3 unit tanks.

Residual Radiation in DTL Section

Intervals of the first operation after resuming the operation, residual radiation at the surface of DTL cavities was measured using Geiger-Muller counter. Most of all points are measured under 1.0 $\mu\text{Sv/h}$, but higher residual radiation was recognized at DT25 (the 25th DT) and DT55 (the 55th DT) of 1st DTL cavity. Measured points are described in fig. 3 and measured values are listed in table 1.

Based on these results, we measured the residual radiation every interval of beam operation. As described in fig. 4, dependences on the operational conditions and

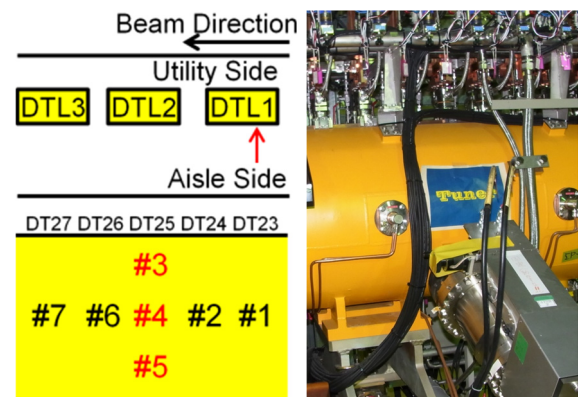


Figure 3. Measurement Points of 1st DTL1 Cavity. Axis is defined to the x-y-z coordination, +y as a top of vertical, +z as a beam direction, +x as a inevitably defined for aisle direction.

DESIGN AND PERFORMANCES OF PHASE MONITOR IN J-PARC LINAC

A. Miura^{*},

J-PARC Linac, Japan Atomic Energy Agency, Tokai, Ibaraki, 319-1195, Japan

T. Miyao, Z. Igarashi,

J-PARC Linac, High Energy Accelerator Organization, Oho, Tsukuba, 305-0801, Japan

Abstract

J-PARC linac employs a fast current transformer (FCT) as a beam phase monitor to calculate the beam energy by time-of-flight method, and the 4-stripline beam position monitors (BPMs) for the beam position measurement. We designed, fabricated and have been used them to the beam operation. Performances of fabricated monitors and their calibration data have been measured. Here, we will discuss the structure and frequency performance of the FCT monitor. At the great earthquake occurred off the Pacific coast of Tohoku, some CT monitors, such as a phase monitor and beam current monitor had damage and the vacuum leakage was observed. But no damage of BPMs was found. It has been considered that the signals from striplines of BPM would be useful for a phase measurement. A phase measurement using a BPM has been successfully conducted. Above the lessons learnt from the damage by the quake, we consider to employ the BPM for the FCT backups after evaluation of the performances of BPM as the phase measurement device. Finally, these performances of BPM are compared with those of FCT. Based on the results of the evaluations, we will discuss the performance to measure the beam phase both FCT and BPM.

INTRODUCTION

Energy upgrade project is now progressed in J-PARC linac. Currently, J-PARC linac accelerates the negative hydrogen beam up to 181 MeV, but 400 MeV accelerated beam can be obtained with 21 ACS cavities^[1]. We designed and fabricated the beam monitors, such as BPM (beam position monitor), SCT (slow current transfer) as the beam current monitor, FCT (fast current transfer) as the beam phase monitor, WSM (wire scanner monitor) as the beam profile monitor) for this project^[2]. After fabricated BPM and CT monitors, the performance of each monitor had been obtained to confirm the design parameters and for calibration^[3].

There was big damage in J-PARC caused by the Tohoku earthquake in March 2011^[4-5]. As for the beam monitors in J-PARC Linac, there was no damage of BPMs and WSMs, but deformation of CT monitors (SCT and FCT) was found and vacuum leak occurred. Damage was mainly observed at the part where the ceramics and metal parts were brazed. BPM has a strong structure for shaking by quakes, on the other hand, FCT monitor has a such structural weak point for shaking. Because the BPM also can measure the beam phase using an electrical

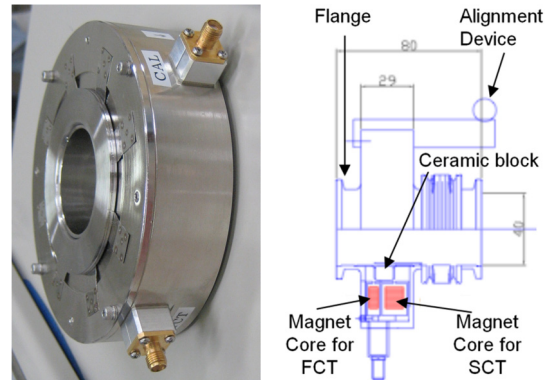


Figure 1: Overview and drawing of FCT and SCT monitor. In the drawing figure, cross-section is described in the bottom half.

circuit for phase detection, it has been considered to use the BPM for the backup of FCT.

FCT is well calibrated to detect the beam phase for 324 MHz acceleration frequency. If the BPM is employed for phase measurement, it is thought that it also needs to calibrate to 324 MHz. Then, we obtained the performance of BPM as the phase monitor. And the data are compared with the data obtained from FCT monitor.

In this paper, we describe the design parameters and performances of FCT and compared results obtained from BPM.

DESIGN OF FCT MONITOR

The beam phase monitor is the other kind of beam current monitor, which is specially designed for high frequency response. The beam phase measurement related to the RF signal provides key information in order to tune the acceleration RF phase. So that the most important information should be extracted from the fundamental RF component, 324MHz. The beam phase monitor has to have an efficient response to this RF fundamental component.

The conventional current transformer is difficult to extend its high frequency cut-off, $1/CR=\omega_H$, because of the stray-capacitance. Using crystallized magnetic alloy makes the beam phase monitor transformer, and a single winding is taken to reduce the stray-capacitance. The frequency response of the Fast-Current-Transformer (FCT) has been sufficiently extended up to GHz region.

FinemetTM core (Hitachi Metals, Ltd.) with high magnetic permeability is employed for the FCT, a single turn coil is combined with the Finemet core with 5 mm thickness is for a coil (fig. 1). Except for MEBT and DTL subsection, each current transformer has its inductive core

^{*}miura.akihiko@jaea.go.jp

CSNS DTL PROTOTYPING AND RF TUNING

H.C. Liu, X.J. Yin, J. Peng, A.H. Li, K.Y. Gong, Y.C. Xiao, Q. Chen, S.N. Fu
Institute of High Energy Physics, Beijing, China

Abstract

The 324MHz Alvarez-type Drift Tube Linac (DTL) for the China spallation neutron source will be used to accelerate the H^- ion beam of up to 15mA peak current from 3 to 80MeV. It consists of four independent tanks, of which the average length is about 8.6 m. Each tank is divided into three short unit tanks about 2.8 m in length for easy manufacture. A full-scale prototype of the first unit tank with 28 drift tubes containing electromagnetic quadrupoles has been constructed to validate the design and to demonstrate the technology. The overall features of the prototype in both key technology and RF tuning are presented. In particular, the influence of the post couplers was studied in the ramped field DTL.

INTRODUCTION

The China Spallation Neutron Source (CSNS) Linac mainly consists of an H^- ion source, a LEBT, a 3 MeV RFQ, a MEBT and an Alvarez-type Drift Tube Linac (DTL) as shown in Figure 1[1]. The DTL will accelerate H^- ion beam of up to 15mA peak current from 3 to 80 MeV in 4 accelerating cavities over a length of 35m. These four RF cavities operating at 324MHz and at 1.05 duty cycles are 560mm in diameter. Several new features have been incorporated in the basic design, leading to many technical difficulties, especially in the low energy section. A 2.8m long full-scale prototype thus has been built to validate the design principles. RF low-power measurements were performed to verify the electromagnetic properties of the cavity and to define the most appropriate tuning strategy.



Figure 1: CSNS Linac layout

RF STRUCTURE

The Prototype RF structure includes a single tank, 28 drift tubes accommodated with electromagnetic quadrupoles, end walls, slug tuners, and post couplers. See Figure 2 for a general layout of the prototype Model.

Tank Fabrication

The tank is a vacuum vessel that provides a RF envelope and a mechanically stable platform for the array of drift-tube assemblies, post couplers, and slug tuners. It is made of a carbon steel tube with copper plated in the inner surface to increase its electrical conductivity. It

contains 9 large ports for tuners, vacuum, and approximately 60 small ports for drift-tubes, post couplers and pickups. Tank inner surface and all ports were coated with Oxygen-Free Copper (OFC) applying successfully the Periodic Reverse (PR) copper electroforming technology.

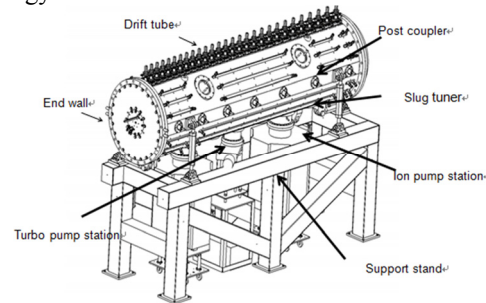


Figure 2: CSNS prototype DTL

Figure 3 shows the tank prototype module after electroforming. The inner copper surface has been polished and the ports have been finish machined for high accuracy and high flatness. The measured inner surface roughness is between 0.26 and 0.29 μ m. The average copper thickness is 0.2 mm (design 0.15 mm).



Figure 3: Internal view of DTL prototype

Drift tube

Each drift tube assembly is comprised of a body and stem, see Figure 4. One of the main features of the CSNS DTL is the use of OFC in all parts of DTs. Long-term deformation test has been done which convinced us of the material selection and design.

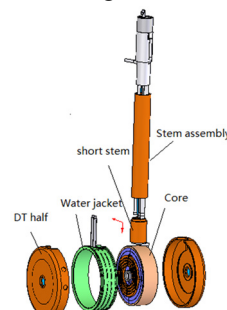


Figure 4: View of a typical Drift tube

liuhc@mail.ihep.ac.cn

ISBN 978-3-95450-122-9

702

STUDY ON THE BEAM DYNAMICS IN THE RISP DRIVER LINAC

H. J. Kim, J.-G. Hwang, and D. Jeon, RISP, Deajeon, Korea

Abstract

Rare Isotope Science Project (RISP) has been proposed as a multi-purpose accelerator facility for providing beams of exotic rare isotopes of various energies. The RISP driver linac which is used to accelerate the beam, for an example, Uranium ions from 0.3 MeV/u to 200 MeV/u consists of superconducting RF cavities and warm quadrupole magnets for focusing heavy ion beams. Requirement of the linac design is especially high for acceleration of multiple charge beams. In this paper, we present the RISP linac design and the requirements of dynamic errors to minimize the beam centroid oscillation and preserve beam losses under control.

INTRODUCTION

The RISP (Rare Isotope Science Project) accelerator has been planned to study heavy ion of nuclear, material and medical science at the Institute for Basic Science (IBS). It can deliver ions from proton to Uranium with a final beam energy, for an example, 200 MeV/u for Uranium and 600 MeV for proton, and with a beam current range from 8.3 pμA (Uranium) to 660 pμA (proton) [1, 2]. The facility consists of three superconducting linacs of which superconducting cavities are independently phased and operating at three different frequencies, namely 81.25, 162.5 and 325 MHz.

The layout of the RISP accelerator is shown in Fig. 1. The Uranium ions produced in an electron cyclotron resonance ion source are preaccelerated to an energy of 300 keV/u by a radio frequency quadrupole and transported to the superconducting cavities by a medium energy beam transport. The driver linac is divided into three different sections: low energy superconducting linac (SCL1), charge stripper section and high energy superconducting linac (SCL2). Figure 2 shows a conceptual structure of SCL1 and SCL2. The SCL1 uses the two different families of superconducting resonators, i.e., quarter wave resonator (QWR) and half wave resonator (HWR). The SCL11 consists of 24 QWR's whose geometrical β is 0.047 and 24 doublets. The resonance frequency of QWR is 81.25 MHz. The cryomodule of the SCL11 hosts one superconducting cavity. The SCL12 consists of 138 HWR's whose geometrical β is 0.12 and 36 doublets. The resonance frequency of HWR is 162.5 MHz. This segment has the two families of cryomodules: one type of cryomodule hosts three superconducting cavities and the other hosts six superconducting cavities.

The SCL2 consists of the SCL21 and the SCL22, each consisting of geometric β 0.30, resonance frequency 325 MHz Single Spoke Resonators (SSR) and geometric β

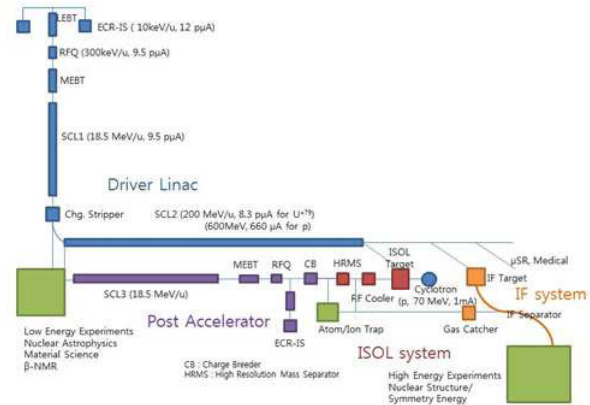


Figure 1: Layout of the RISP accelerator.

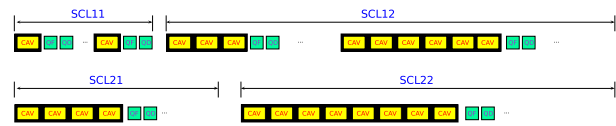


Figure 2: Layout of the SCL: SCL1 (top) and SCL2 (bottom).

0.53, resonance frequency 325 MHz SSR. Single Spoke Resonator type is chosen mainly because it can have a larger bore radius compared with the Half Wave Resonator type, which is very essential to reduce the uncontrolled beam loss in the high energy linac section. The number of cavities in the SCL21 and SCL22 is 88 and 138 respectively. The cryomodule of the SCL21 and SCL22 hosts 4 and 8 cavities respectively. Table 1 summarizes the parameter of four different superconducting cavities. The charge stripper section is located between SCL1 and SCL2. The charge stripper strips electrons from heavy ion

Table 1: Superconducting cavity parameters.

Parameter	unit	QWR	HWR	SSR 1	SSR 2
β_g		0.047	0.12	0.30	0.53
Frequency	MHz	81.25	162.5	325	325
Aperture	mm	40	40	50	50
V_{acc}	MV	1.02	1.07	2.04	3.53
E_{peak}/E_{acc}		5.08	6.2	4.06	4.15
B_{peak}/E_{acc}	mT/(MV/m)	9.16	8.4	7.07	8.6
QR_s	Ohm	37	47	86	108
R/Q	Ohm	480	319	242	304
Temperature	K	2	2	2	2
Q_0	10^9	3.6	4.6	8.1	10

AMPLITUDE AND PHASE CONTROL OF THE ACCELERATING FIELD IN THE ESS SPOKE CAVITY

V.A. Goryashko *, V. Ziemann, R. Yogi, R. Ruber, Uppsala University

Abstract

We report about numerical simulations of the accelerating field dynamics in the ESS spoke cavity in the presence of the beam loading and Lorentz detuning. A slow feedforward is used to cure the Lorentz detuning whereas a fast feedback through a signal oscillator and cavity pre-tuning technique are applied to eliminate the beam loading effect. An analysis performed with a Simulink model shows that a combination of feedforward, feedback and cavity pre-detuning result in a substantially shorter stabilization time of the field voltage and phase on a required level as compared to a control method using only the feedforward and feedback. The latter allows one to obtain smaller magnitude but longer duration deviations of the instantaneous voltage and phase from the required nominal values. As a result, a series of cavities only with feedforward and feedback needs an extra control technique to mitigate a cumulative systematic error rising in each cavity. In addition, a technique of adiabatic turning off of the RF power in order to prevent a high reflected power in the case of a sudden beam loss is studied.

INTRODUCTION

To obtain the beam of a high quality in terms of the energy spread and emittance the cavity voltage magnitude and phase should be controlled very accurately. According to the ESS design [1], the voltage magnitude deviation must be below 0.1% of the total value and its phase deviation must not exceed 0.5 degrees. This can be achieved by means of an appropriate control. The most widely used control technique is the negative feedback based on a PID controller. The idea is to control a system's output by comparing it to a desired setpoint and feeding the error back to the input dynamically. At the same time, when a perturbation can be foreseen like the Lorentz detuning, it is useful to use a feed-forward technique to prevent such a perturbation. Combined feedback and feed-forward control can significantly improve performance over simple feedback architectures when there is a major disturbance to the system that can be measured beforehand [2]. In the present paper we apply aforementioned techniques of the control to stabilize the spoke cavity voltage magnitude and phase.

THE BEAM-CAVITY INTERACTION: FEEDBACK AND FEED-FORWARD

To study the evolution of the accelerating field in a spoke cavity we will adopt the traditional model [3], in which the cavity is presented by the lumped RLC circuit, the coupler

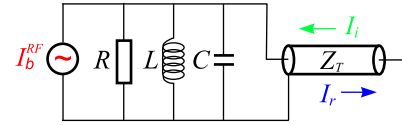


Figure 1: The lumped model: cavity modeled by an RLC circuit, the coupler by a connected transmission line of impedance Z_T and the beam by a current source.

by the transmission line with impedance Z_T on which we have the incident (generator) wave current I_i and the reflected wave current I_r . The latter is assumed to disappear without re-reflection. The beam is modeled as a current source I_b^{RF} , where I_b^{RF} is the RF beam current that is twice of the DC beam current, $I_b^{RF} = 2I_b^{DC}$. The cavity characterized by the resonant frequency ω_0 is excited to voltage V_c under these conditions.

We will assume that variations of the generator and beam currents as well as external perturbations are slow as compared to the RF period such that a dynamic quantity may be represented as a product of a slow varying envelope multiplied by $\exp(i\omega t)$ (in general case ω is not identical to ω_0), e.g. $V_c(t) = \text{Re}\{A(t) \exp(i\omega t)\}$ and $\omega^{-1} d \ln A/dt \ll 1$. Impedances of the loaded cavity and transmission line can be expressed in terms of the shunt cavity resistance R , and three quality factors: Q_0 is the quality factor of the bare cavity, Q_{ext} is the quality factor of the cavity with the coupler, $Q_L = (Q_0^{-1} + Q_{ext}^{-1})^{-1}$ is the total quality factor. For a superconducting cavity the loaded quality factor is mainly determined by the external Q -factor, $Q_L \approx Q_{ext}$. Then, using the slow varying approximation we arrive at a first order differential equation for the complex cavity voltage amplitude [3]

$$t_F \frac{dA}{dt} + A(1 - 2i\delta Q_L) = 2Q_L \frac{R}{Q} [I_i(t) - I_b^{DC}(t) F_b e^{-i\phi_e}], \quad (1)$$

where $\delta = (\omega_0 - \omega)/\omega$ is the normalized detuning, ϕ_e is the synchronous phase defined according to the electron linac convention (the energy transfer from the field to the beam is maximal when $\phi_e = 0$), F_b is the beam form-factor, t and $t_F = 2Q_L/\omega$ are the observation and filling time, respectively.

The current reflected by the cavity reads

$$I_r(t) = \frac{1}{2Q_L(R/Q)} \left[A(1 + 2i\delta Q_L) - t_F \frac{dA}{dt} \right] - I_b^{DC}(t) F_b e^{-i\phi_e}. \quad (2)$$

and the power coming to the cavity from the coupler (incident power) and the power reflected by the cavity to the

* vitaliy.goryashko@physics.uu.se

UPPSALA HIGH POWER TEST STAND FOR ESS SPOKE CAVITIES

R.A. Yogi, A. Rydberg, D. Dancila, K. Gajewski, L. Hermansson, M. Noor, R. Wedberg, R. Santiago-Kern, T. Ekelöf, T. Lofnes, V. Ziemann, V. Goryashko, R. Ruber, Uppsala University, Uppsala, Sweden

Abstract

The European Spallation Source (ESS) is one of the world’s most powerful neutron source. The ESS linac will accelerate 50mA pulse current of protons to 2.5GeV in 2.86 ms long pulses at a repetition rate of 14 Hz. It produces a beam with 5MW average power and 125MW peak power. ESS Spoke Linac consist of 28 superconducting spoke cavities, which will be developed by IPN Orsay, France. These Spoke Cavities will be tested at low power at IPN Orsay and high power testing will be performed in a high power test stand at Uppsala University.

The test stand consists of tetrode based RF amplifier chain (352MHz, 350 kW) power and related RF distribution. Outputs of two tetrodes shall be combined with the hybrid coupler to produce 350 kW power. Pre-amplifier for a tetrode shall be solid state amplifier. As the spoke cavities are superconducting, the test stand also includes horizontal cryostat, Helium liquefier, test bunker etc. The paper describes features of the test stand in details.

INTRODUCTION

The European Spallation Source (ESS) is the world’s most powerful neutron source. The ESS linac will accelerate 50mA pulse current of protons to 2.5GeV in 2.86ms long pulses at a repetition rate of 14 Hz [1].

ESS Linac has twenty eight superconducting Spoke cavities. The power coupled to the beam ranges from 162 kW to 239 kW per coupler for beam current of 50mA. The RF amplifier for Spoke will power the spoke cavities via RF distribution system. Considering 5% loss overhead in RF distribution system and 25% power overhead for LLRF, the power for RF amplifier will range from 225 kW upto 350 kW.

ESS Specifications for Spoke Linac amplifier:

- Frequency = 352.21 MHz
- Power = 350 kW
- 3 dB Band-width = 200 kHz.
- Pulse width = 3.5 ms
- Pulse repetition rate = 14 Hz

RF amplifier at ESS specifications doesn’t exist. Hence there is a need for prototyping it.

Also the superconducting spoke cavity for ESS Spoke Linac is being developed at IPN Orsay. It needs to be tested for high power.

Hence there is a need for High Power Test Stand. The ESS spoke cryomodule consists of two spoke cavities. Hence the test stand shall consist of two high power RF chains. A facility called FREIA is being built at Uppsala University to serve these purposes.

FREIA FACILITIES RELATED TO ESS

FREIA (Facility for Research and Instrumentation for Accelerators) is a facility being developed at Uppsala. First project of FREIA is High Power Test Stand for ESS superconducting Spoke Cavities (fig.1).

High Power Amplifier:

The various technologies of RF sources like tetrodes, solid state, IOTs and klystrons are compared [2] and Tetrode is finalized as the first high power amplifier for the first chain at FREIA.

Three Thales tetrodes TH781, TH391 and TH595 can serve the purpose.

Table 1: Comparison of Tetrodes

Specification	TH781	TH391	TH595
Maximum power at 352MHz	350kW	200kW	200kW
Efficiency	50 – 55%	> 65 %	> 65 %
Gain	11 dB	15 dB	15 dB
Cavity	Doesn’t exist	Exist	Exist
Cooling	Water	Air	Water

The calculations show that TH781 can produce 350 kW at 352 MHz but at reduced gain and efficiency. Though TH391 offers improved gain and efficiency, it is air cooled, which allows anode dissipation of only 12 kW. Type of cooling will also affect the size of the system. Air cooling may lead to system with bigger size. TH595 is water cooled and hence it has higher anode dissipation of 40 kW, in addition the system will also be compact.

So 350kW power will be generated by combining outputs from the two tetrodes (TH595) which produce 175 kW each. Power combining will be achieved with help with the 3dB Hybrid coupler.

The specifications for Tetrode amplifier are:

- Frequency = 352.21 MHz
- Power = 175 kW
- 3 dB Band-width = 200 kHz.
- Pulse width = 3.5 ms
- Pulse repetition rate = 14 Hz
- Gain > 15 dB
- Efficiency > 65%

It is well known that gain of the tetrode reduces with aging. While calculating power needed from the pre-driver, this fact was taken into consideration, so gain of 13 dB is assumed and output power of pre-driver is 10 kW.

ERL-BASED LIGHT SOURCE CHALLENGES

Yukinori Kobayashi[#], KEK, Oho 1-1 Tsukuba, Ibaraki 305-0801, Japan

Abstract

The challenges of the design and technology for the future Energy Recovery Linac (ERL) based light source are reviewed. The developments of a high-brightness electron source, including the drive laser, and the CW high gradient superconducting cavities for both injector and main linac as key components of the accelerator are described. In addition, the status of the compact ERL (cERL) for R&D which is going to be constructed at KEK is presented.

INTRODUCTION

The Energy Recovery Linac (ERL) is a future X-ray light source based on state-of-the-art superconducting linear accelerator technology, which will offer far higher performance than the existing storage ring. The high repetition rate, short pulse, high spatial coherence and high brightness will enable the filming of ultrafast atomic-scale movies and determination of the structure of heterogeneous systems on the nano-scale. These unique capabilities of ERL will lead to a distinct paradigm shift in X-ray science from static and homogeneous systems to dynamic and heterogeneous systems, in other words, from time- and space-averaged analysis to time- and space-resolved analysis. In short, ERL will be an unprecedented tool that will bridge the critical gaps in our understanding of material science and technology [1].

In addition, continuous improvements in linear accelerator technology may result in dramatic progress in X-ray science in the future, such as the realization of a fully coherent X-ray free-electron laser. Although self-amplified spontaneous emission X-ray free-electron lasers (SASE-XFELs) are in use around the world, the X-ray beam from SASE-XFEL is essentially not fully coherent in the temporal domain. By configuring a Bragg diamond cavity for lasing in the X-ray region, it may be possible to create an X-ray free-electron laser oscillator (XFEL-O) by taking full advantage of the unprecedented electron beam quality of ERL [2-4]. Construction of the XFEL-O is planned in the second stage of the ERL project.

KEK established the ERL Project Office in April 2006. Because a GeV-class ERL machine has not been constructed anywhere in the world, it is first necessary to construct a compact ERL (cERL) with an energy of 35 MeV that can be used for developing several key accelerator components such as a high-brilliance DC photocathode electron gun and superconducting cavities for the injector and main linac. During 2011, such main accelerator components were successfully developed and operation of the beam will start at the end of March 2013.

In this conference, the development of high-brightness electron sources and superconducting cavities, which are key accelerator components for the ERL, and construction of the compact ERL for R&D at KEK, will be mainly presented.

DESIGN CONCEPT OF THE 3-GEV ERL AT KEK

For the future project of the KEK Photon Factory, we propose constructing a 3-GeV ERL that can be upgraded to become the XFEL-O [5-7]. A conceptual layout of the 3-GeV ERL is shown in Fig. 1. In the first stage of the project, a 3-GeV ERL which comprises an injector linac, a superconducting main linac, and a return loop will be constructed. In the return loop, 20–30 insertion devices which are used to emit synchrotron radiation will be installed. Using state-of-the-art undulator technology, a broad spectrum of synchrotron radiation from vacuum ultra-violet (VUV) to hard X-rays will be covered.

In the second stage of the project, an XFEL-O system which comprises a long undulator and an X-ray resonator will be built. To deliver high-energy beams for the XFEL-O system, the path length in the return loop by a half rf wavelength of 115.3 mm will be adjusted. Under this configuration, the beams are firstly accelerated to 3 GeV through the main linac and pass through the return loop. The beams are then accelerated again (without energy recovery) through the main linac up to 6 GeV. Finally, the beams are used to drive the XFEL-O, and dumped without energy recovery.

Target parameters of the 3-GeV ERL are given in Table 1. Since the ERL is a very flexible light source, this table shows some typical operational modes. For the major users requiring highly brilliant SR, we provide high-coherence or high-flux modes of operation. Among these modes, the high-flux mode imposes a greater challenge for the lifetime of the photocathodes. The “ultimate” mode requires both very-low emittance and high currents; this imposes much greater challenges for the accelerator physics and engineering, and thus is a long-term goal. In the ultra-short-pulse mode, we compress the electron bunches down to a hundred femtoseconds or shorter. In this mode, the beam emittances are largely influenced by the coherent synchrotron-radiation in the return loop. Then, bunch charges in this mode will be chosen by balancing the SR intensity and the beam emittance.

[#]yukinori.kobayashi@kek.jp

STATUS AND FUTURE OF THE CLIC STUDY

R. Corsini*, CERN, Geneva, Switzerland

Abstract

The Compact Linear Collider (CLIC) International Collaboration is carrying out an extensive R&D program towards a multi-TeV electron-positron collider.

The CLIC concept is based on the use of high-gradient normal-conducting accelerating structures in conjunction with a novel two-beam acceleration scheme, where the RF power needed to accelerate the colliding beams is extracted from a high-current drive beam running parallel to the main linac. In order to establish the feasibility of such concept a number of key issues were addressed, both experimentally and theoretically, and the results of the study were documented in the recently completed CLIC Conceptual Design Report (CDR). The conclusions reached in the CDR constitute also an important contribution to the European strategy group. A short summary of the present status will be given, together with an outlook on the program for the next period, aimed at the preparation of an implementation plan.

INTRODUCTION

CLIC is a high-energy linear e^+e^- collider with the potential to operate at centre-of-mass energies ranging from a few hundred GeV up to 3 TeV and with luminosities of a few $10^{34} \text{ cm}^{-2}\text{s}^{-1}$.

In CLIC the colliding beams are produced in conventional electron and positron sources and accelerated to about 2.8 GeV. The beam emittances are reduced in a pre-damping ring followed by a damping ring. In the ring-to-main-linac transport system (RTML) the beams are compressed longitudinally and accelerated to 9 GeV. The main linac uses 100 MV/m, 12 GHz, normal conducting accelerating structures to achieve the final beam energy. In the beam delivery system (BDS) the beams are cleaned by collimation and compressed to their final sizes at the collision point. The main challenges for the CLIC main beam are the accelerating gradient needed to get to the high centre-of-mass energy and the good beam quality (i.e., the ultra low beam emittances and sizes) needed to reach high luminosity.

The RF power used to accelerate the electron and positron beams is extracted from a high-current, low-energy drive beam running in parallel to them. The drive beam is generated in a dedicated accelerator complex located in the central area. The other challenges for CLIC are related to the two-beam concept: the efficient generation of the drive beam, the power production in special RF structures called PETS (power extraction and transfer structures) and the stable drive beam deceleration. The fundamental CLIC parameters and its conceptual layout can be found in Table 1 and in Fig. 1. More details about the CLIC machine are given in the recently completed Conceptual Design Report.

*On behalf of the CLIC Collaboration

Table 1: Fundamental CLIC parameters at 3 TeV centre-of-mass. The luminosity quoted is within 1% of the nominal energy.

Centre-of-mass energy	3	TeV
Luminosity	2×10^{34}	$\text{cm}^{-2}\text{s}^{-1}$
Particles per bunch	3.72×10^9	
Horizontal beam size at IP	≈ 40	nm
Vertical beam size at IP	≈ 1	nm
Bunches per pulse	312	
Bunch separation	0.5	ns
Repetition rate	50	s^{-1}

The CLIC accelerator complex and the CLIC physics and detector studies are described in separate documents. The CLIC accelerator CDR [1] provides detailed descriptions of the accelerator layout, its components and the expected performance of CLIC. In particular, it describes technical solutions to the key feasibility issues, thus proving the validity of the CLIC concept. In this framework, prototypes of many of the technical subsystems have been successfully tested at the CLIC test facility CTF3 at CERN and at other facilities around the world. The test results are reported in detail in the CDR.

This paper gives a status update on the most important design challenges of CLIC, namely:

- The main linac gradient and issues related to the accelerating structures.
- The experimental verification of the two beam concept, which is essential to provide the main linac RF power.
- The ultra low beam emittances and sizes to reach high luminosity. In particular alignment and stabilization of the main linac and BDS components.

In order to have energy flexibility a possible staged implementation of the machine is being studied. The future program of the studies is focused on an implementation plan by 2016, at the same time as results from LHC running at full energy are expected to provide results guiding the way for a possible implementation. The main elements of the future program are also briefly discussed at the end of the paper.

ACCELERATING STRUCTURES

Each main linac contains about 70000 23 cm long accelerating structures. The total ratio of active length to total linac length reaches almost 80%, resulting in an extremely high “real estate” gradient. The structure design has been carefully optimized using empirical constraints to achieve a gradient of 100 MV/m, as described in [1].

APPLICATION OF X-BAND LINACS

G. D'Auria

Sincrotrone Trieste, Trieste, Italy

Abstract

Since the late 80's the development of Normal Conducting (NC) X-band technology for particle accelerators has made significant progress and has witnessed tremendous growth. The driving force behind this technological development, has been, and is, the interest of the scientific community in the construction of a Multi-TeV e^+e^- Linear Collider at a reasonable size and cost. The use of the X-band frequency allows for a much higher accelerating gradient per meter, when compared to the S and C bands. SLAC, with a major contribution from KEK, has been pioneering this development since the late 80's in the framework of the NLC/JLC projects. Later, in 2007, the same technology was chosen by CERN for CLIC, the 12 GHz Linear Collider based on the Two-Beam Acceleration (TBA) concept. In addition to these applications, X-band technology is also rapidly expanding in the field of X-ray FELs and other photon sources where it shows great potential. Here, a selection of X-band projects as well as the main applications of this technology at different international laboratories, is reported. The paper also includes a brief report on X-band medical and industrial applications.

INTRODUCTION

In radar engineering the X-band is specified as frequencies in the range of 8-12 GHz. Already by the mid 60's, the SLAC "Blue Book" reported a clear interest for X-band technology in the process of selecting the best frequency for the SLAC Linac [1]. From the late 80's up to 2004, groups from SLAC, KEK, and later Fermilab, began a dedicated development of accelerating structures and components at 11.4 GHz (four times the frequency of the SLAC Linac), for a TeV-scale e^+e^- Linear Collider. A slowdown of these activities occurred in 2004, after the decision of the International Technology Review Panel (ITRP) to select L-band superconducting technology for the International Linear Collider (ILC). However, in 2007 CERN decided to lower the frequency of the Compact Linear Collider (CLIC) to 12 GHz (previously at 30 GHz), resulting in a renewed, and more vigorous, interest in X-band. Significant progress has been made in the last decade to raise the achievable accelerating gradients from the 65-70 MV/m declared at the end of the NLC/JLC program [2], up to the 100 MV/m reached on CLIC test structures [3], values far beyond those reached with the present S and C band technology. Today X-band developments are rapidly expanding due to their demonstrated potential in different segments of accelerator technology. X-band structures are currently used for very accurate beam diagnostics and e-bunch manipulations at many X-ray FEL facilities worldwide

[4,5,6]. Very ambitious projects using X-band Linacs, and based on Inverse Compton Scattering (ICS) for "extreme light" sources, are under construction or have been proposed [7,8]. Moreover, with the low bunch charge option currently considered for future X-ray FELs, X-band technology offers a low cost, compact solution for generating multi-GeV low emittance bunches. With the accelerating gradients mentioned above, an entire 1 GeV Linac can be easily housed in less than 20 m, representing a very cost effective solution for application with limited space [9].

HIGH ENERGY COLLIDER

CERN's decision to lower the CLIC frequency to 12 GHz, has been a key factor in the revival of X-band work. The intense activity carried out in the framework of the CLIC international collaboration has led to important developments. At present the CLIC CDR has been completed [10] and the project is moving into the technical design of the main components. Concerning the high gradient X-band structures, two different modules, called T24 and TD24 (Dumped), have been successfully tested, with the CLIC RF pulse shape, to the CDR specifications of 100 MV/m (unloaded average gradient), $\tau_{RF} > 170$ ns flat-top and a BDR/m $< 3 \times 10^{-7}$. Moreover, the measured RF breakdown rate (BDR) has shown good agreement with theory [11]. The baseline design of the CLIC structure, named TD26, has been completed and is very similar to TD24 [12]. The structure is designed for a $2/3\pi$, quasi-constant gradient, operating mode, with an average iris radius of 2.75 mm ($r_{av}/\lambda_{rf}=0.11$). Four damping waveguides, with SiC absorbers, are integrated in each cell to provide for adequate HOM damping. Each structure is composed of 26 cells plus two couplers.

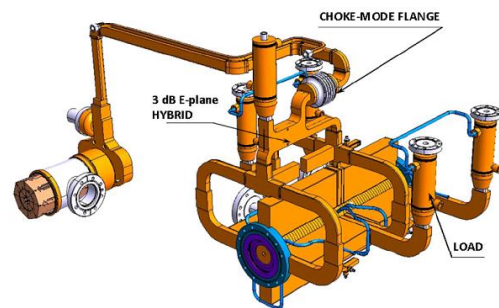


Figure 1: CLIC RF module

Two TD26, assembled together, make up what is called a "Superstructure" (SAS). Wakefield monitors, used for beam-based alignment, and accurate trajectory correction, are integrated into the first cell of every second structure of a SAS. To achieve the CLIC luminosity, the accelerating structures must be aligned to an accuracy of $5 \mu\text{m}$ with respect to the beam. Figure 1 shows one CLIC

ARIEL SUPERCONDUCTING ELECTRON LINAC

S. Koscielniak, F. Ames, R. Baartman, I. Bylinskii, Y. Chao, D. Dale, R. Dawson, E. Guetre, N. Khan, A. Koveshnikov, A. Laxdal, R. Laxdal, F. Mammarella, M. Marchetto, L. Merminga, A. Mitra, T. Planche, A. Sitnikov, Y.N. Rao, V. Verzilov, D. Yosifov, V. Zvyagintsev, TRIUMF*, 4004 Wesbrook Mall, Vancouver, B.C. Canada;
D. Karlen, R. Langstaff, University of Victoria, Victoria, B.C. Canada

Abstract

The TRIUMF Advanced Rare Isotope Laboratory (ARIEL) is funded since 2010 June by federal and BC Provincial governments. In collaboration with the University of Victoria, TRIUMF is proceeding with construction of a new target building, connecting tunnel, rehabilitation of an existing vault to contain the electron linear accelerator, and a cryogenic compressor building. TRIUMF starts construction of a 300 keV thermionic gun, and 10 MeV Injector cryomodule (EINJ) in 2012; the designs being complete. The 25 MeV Accelerator Cryomodule (EACA) follows in autumn 2013. TRIUMF is embarking on major equipment purchases and has signed contracts for 4K cryogenic plant and four sub-atmospheric pumps, a 290 kW c.w. klystron and high-voltage power supply, 80 quadrupole magnets, EINJ tank and lid, and four 1.3 GHz niobium 9-cell cavities from a local Canadian supplier. The low energy beam transport and beam diagnostics are being installed at the ISAC-II/VECC test facility. Procurement is anticipated October 2012 for the liquid He distribution system.

CONVENTIONAL INFRASTRUCTURE

The ARIEL project is described in Refs. [1,4]. The conventional infrastructure consists of four contracts: the main ARIEL construction, demolition and excavation, and the Stores and Badge buildings replacements. The latter are necessitated by site congestion. The new Compressor Building (CB), for gaseous helium management, forms part of the ARIEL package. In addition there are major renovations that will transform the former Proton Hall to the Electron Hall (e-hall).

Chernoff-Thompson Architects led a successful bid for the overall architecture and engineering contract, awarded October 2010. The Stores and Badge building construction is complete and occupancy was taken Sept 2011 and Dec 2011, respectively.

The demolition and excavation work started October 2011, and completed April 2012. The ARIEL main construction package was awarded Feb 2012. There is substantial completion of the tunnel and B2 level of the actinide target preparation labs, target hall and Rare Isotope Beams annexe. The annexe will contain mass separators and front-end accelerators. The CB is well advanced: roofing and envelope cladding, mechanical and electrical rough-in, are all proceeding on-track for occupancy in December 2012.

*TRIUMF is funded under a contribution agreement with the National Research Council of Canada.

The e-hall was emptied of legacy proton spectrometers in March 2012. The e-hall shielding, south wall upgrade and new north wall (that will protect e-hall from the future BL4N proton beam), is complete. The 10T full-coverage crane, and egress stairway are installed. Sealing of the concrete roof beams is pending final shield block moves. E-hall occupancy is anticipated October 2012.



Figure 1: ARIEL construction site, view north.

To accommodate the power requirements of e-linac systems a new 12.5 kV, 5 MW switchgear will be installed atop the e-hall roof. The gear will be close to the klystron power supplies and other local loads including a 0.5 MW emergency power bus. Further, the gear will feed north to the ARIEL building (2 MW) and south to the He CB (1 MW) housing the compressors and SA pumps.

The contract was awarded to Siemens Electric Canada April 2012. Fabrication is complete, and factory tests satisfactory. Delivery and installation will occur Sept-December, followed by connection to the TRIUMF grid, commissioning and energization.

ELECTRON GUN

The thermionic gun provides 300 keV kinetic energy electron bunches with charge up to 16 pC at a repetition frequency of 650 MHz. Aspects of the gun design were reported [2] previously. The main components are a gridded gun in a 2 bar SF₆ filled vessel, and in-air HV power supply. Unique features of the gun are its inverted cathode/anode geometry to reduce dark current, and transmission of RF modulation via a dielectric (ceramic) waveguide and chokes through the SF₆. The latter obviates the need for an HV platform inside the vessel to carry the RF transmitter, and results in a significantly smaller/simpler vessel. The modulation is applied to a CPI Y-845 gridded dispenser cathode via a stepped

LINAC-BASED LASER COMPTON SCATTERING X-RAY AND GAMMA-RAY SOURCES

R. Hajima*, JAEA, Ibaraki 3191195, Japan

Abstract

Laser Compton scattering (LCS) light sources can provide high-energy photons from keV to MeV range. Many research and development projects of linac-based LCS sources are carried on. For the photon energies of tens keV, linac-based LCS sources realize laboratory-size X-ray sources, of which performance is potentially comparable to 2nd generation synchrotron light sources. Linac-based LCS also realizes unparalleled γ -ray sources of high-brightness and narrow bandwidth. In the present paper, status and perspectives of linac-based LCS X-ray and γ -ray sources are reviewed.

LASER COMPTON SCATTERED PHOTON SOURCES

The combination of a high-energy electron accelerator and a laser realizes high-energy photon sources based on laser Compton scattering (LCS) [1].

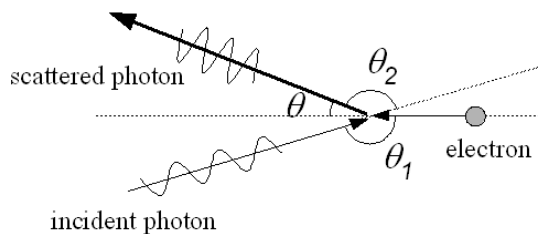


Figure 1: Laser Compton scattering.

Figure 1 shows a schematic representation of laser Compton scattering, where a high-energy photon (X-ray or γ -ray) is generated via the Compton back-scattering of an incident laser photon with a relativistic electron. The energy of the scattered photon, E_x , is a function of the incident photon energy, $E_L = hc/\lambda$, electron energy $E_e = \gamma mc^2$, and scattering geometry, and approximated for a head-on collision:

$$E_x \approx \frac{4 \gamma^2 E_L}{1 + (\gamma \theta)^2 + 4 \gamma E_L / (mc^2)} \quad (1)$$

The above equation shows that the LCS photon energy is tunable by changing electron beam energy, laser wavelength or collision angle. The LCS photon energy also has a correlation to the scattered angle. Therefore, monochromatic photon beam can be obtained by putting a collimator to restrict the LCS beam divergence at the downstream. We can produce linear- and circular-polarized high-energy photons by using polarized lasers. The electron energy necessary for generation of hard X-

ray (20 keV, for example) is only 30 MeV, which is much smaller than the electron energy to produce hard X-ray via synchrotron radiation.

Owing to the above features of LCS photon source, energy tunability, monochromatic and polarized photon generation, compactness, LCS sources have been developed by using various types of accelerators such as storage rings, linacs and microtron [2-6]. In the present review, we focus on linac-based LCS photon sources in X-ray and γ -ray energies.

A photon flux from laser Compton scattering at an ideal head-on geometry integrated over the entire scattering angle is given by

$$F_{total} = \frac{16}{3} N_e N_L f \frac{r_0^2}{w_0^2} \quad (2)$$

where N_e and N_L are the number of electrons and laser photons at the collision, respectively, f is the collision frequency, r_0 is the electron classical radius and w_0 is the collision spot size.

Spectral brightness of laser Compton scattered photon sources can be calculated as

$$B \approx F_{total} \frac{\gamma^2}{\epsilon_n^2} \times 0.1\% \quad (3)$$

where ϵ_n is normalized emittance and the factor 0.1% is for the conventional unit of spectral brightness, (photons/sec/mm²/mrad²/0.1%BW).

In order to obtain a high-flux and high-brightness photon beam from laser Compton scattering, it is necessary to increase the density of both electrons and photons at the collision point and to reduce normalized emittance. An electron beam of small emittance and high-average current is, thus, essential to high-flux and high-brightness photon generation via laser Compton scattering.

LINAC-BASED LCS X-RAY SOURCES

Linac-based LCS X-ray source enable us to produce energy-tunable X-ray beams with a laboratory-size apparatus, of which flux and brilliance is potentially comparable to synchrotron radiation from a bending magnet of GeV-class storage rings. There are many R&D programs carried out for realizing LCS X-ray sources. Here, we see research activities on-going in Japan.

A LCS X-ray source has been developed at AIST (National Institute of Advanced Industrial Science and Technology) [7]. They employed a 42-MeV S-band linac equipped with a photocathode RF gun. For the laser Compton scattering, they use a Ti:Sapphire laser. Two

*hajima.ryoichi@jaea.go.jp

RF POWER PRODUCTION AT THE TWO BEAM TEST STAND AT CERN

I. Syratchev, CERN, Geneva, Switzerland.

Abstract

The generation of short (250 ns) high peak power (135 MW) RF pulses by decelerating a high current (100 A) bunched (12 GHz) drive beam is one of the key components in the CLIC two beam acceleration scheme. Recent tests with drive beam deceleration at CERN's CTF3, using specially developed 1 m long CLIC Power Extraction and Transfer Structure (PETS) operated in a re-circulation regime have successfully demonstrated this concept. The results of these tests are presented.

INTRODUCTION

The CLIC PETS is a low impedance, high group velocity iris loaded 0.213 m long structure with a relatively large ($2a/\lambda = 0.92$) beam aperture. Each PETS is comprised of eight octants separated by damping slots. Each slot is equipped with damping loads in order to provide the strong damping of the transverse higher order modes [1]. In operation, the high peak power RF pulses (135 MW \times 240 ns) are generated in the PETS via interaction with a high current (100 A) bunched (12 GHz) drive beam. These pulses are extracted at the downstream end of the PETS using a special high power coupler and are distributed to the two CLIC accelerating structures using an RF waveguide network. The snapshot of such a process simulated with computer code T3P [2] is shown in Fig. 1.

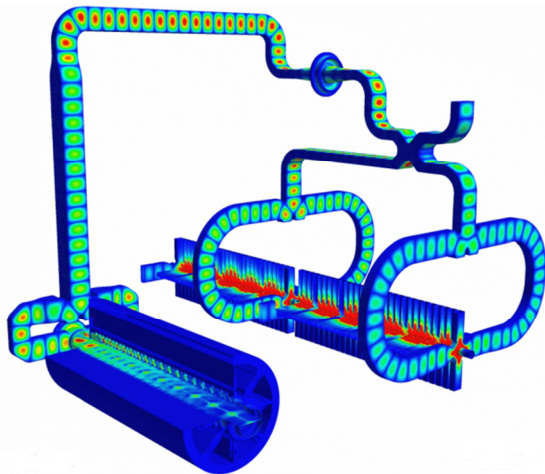


Figure 1: Electric field plot in the CLIC two-beam accelerator unit. Here the PETS (shown left) is driven by the steady state drive beam current (courtesy SLAC).

During the period of 2008-2012, a thorough high RF power testing program was conducted at CERN in order to demonstrate experimentally the feasibility of all the issues associated with high RF power generation using the drive beam. In parallel, complimentary tests using X-band high power klystrons as a RF power source were

done at ASTA (SLAC). Operated at a repetition rate of 60 Hz, such experiments provided high enough statistics to quantify the RF breakdown trip rate. To do these tests, an 11.424 GHz scaled version of the 12 GHz PETS was designed and fabricated, see Fig. 2. The feasibility of the PETS operation at a peak RF power level $\sim 7\%$ higher and with RF pulses $\sim 10\%$ longer compared to CLIC requirements was successfully demonstrated in these experiments [3]. The tests at a fixed power level (see Fig. 3) were ended when the measured breakdown trip rate was close enough to the CLIC specification of $1.0E-7/\text{pulse/m}$. In the ASTA test, it occurred after 80 hours of operation without breakdown ($\text{BDR} < 2.4E-7/\text{pulse/m}$).

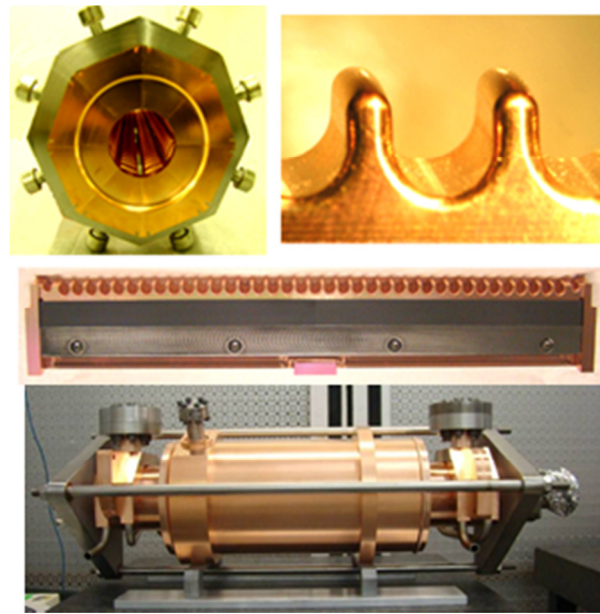


Figure 2: The front view of the assembled PETS body (top left), zoom of the PETS single bar period (top right), the single bar equipped with damping loads (centre) and fully assembled structure (bottom).

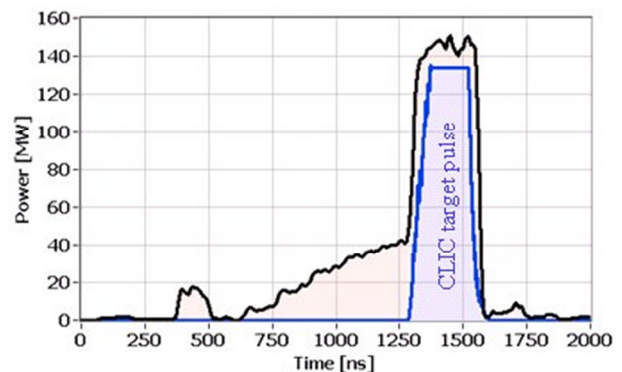


Figure 3: Typical RF pulse shape in ASTA. Here, for convenience, we also have plotted the shape of the CLIC target pulse.

SOLID STATE MARX MODULATORS FOR EMERGING APPLICATIONS*

M.A. Kemp[#], SLAC National Accelerator Laboratory, Menlo Park, CA, USA

Abstract

Emerging linear accelerator applications increasingly push the boundaries of RF system performance and economics. The power modulator is an integral part of RF systems whose characteristics play a key role in the determining parameters such as efficiency, footprint, cost, stability, and availability. Particularly within the past decade, solid-state switch based modulators have become the standard in high-performance, high power modulators. One topology, the Marx modulator, has characteristics which make it particularly attractive for several emerging applications. This paper is an overview of the Marx topology, some recent developments, and a case study of how this architecture can be applied to a few proposed linear accelerators.

THE MARX TOPOLOGY

It is a futile task to completely capture all the implementations of Marx which have been developed. However, presented in this section is one way in which to describe a Marx and highlights several particular implementations which embody many of the strengths of the topology.

The Ideal Modulator

In the context of RF sources, the modulator is typically defined as the power converter interfacing the AC mains with the RF tube. In CW systems, it is common to refer to this interface simply as the power supply. Hence, the modulator is usually a pulsed supply.

The desired characteristics of a modulator are most effectively optimized in view of a specific implementation. However, some general positive attributes are common. First, the pulse quality of a modulator must be appropriate for the RF system. Output voltage, output current, pulse width, and pulse repetition frequency broadly classify the modulator. However, especially in linacs for light sources, secondary parameters such as timing jitter, pulsed amplitude stability, and flat-top droop are increasingly important.

The power input to the modulator is most commonly the AC mains. While it is possible to further sub-divide some modulators into a power supply and a pulse shaping unit, the view is typically most straightforward considering these to be one system. A consideration for the modulator is to draw a constant power with near-unity power factor from the mains. Some facilities are bound by regulatory requirements which dictate harmonic content at the point of common coupling with the utility, such as IEEE 519. An ideal modulator is lossless. Short of this,

waste heat is most typically rejected to the facility water cooling system or the ambient atmosphere.

The availability, A , of a system is typically defined in terms of the mean time to repair (MTTR) and the mean time between failures (MTBF),

$$A = \frac{MTBF}{MTBF + MTTR} \quad (1)$$

To enable very high availability numbers, redundant architectures can be used. This allows a component to fail without bringing down the system.

The cost of a modulator might be divided into three categories: the procurement costs, the maintenance costs, and the operation costs. The maintenance costs might include the manpower and replacement parts to repair and refurbish the system. Operation costs include utility needs and system configuration adjustments.

Secondary characteristics of interest include the ability of a modulator to operating into different impedance loads. During commissioning or operation of an accelerator at different configurations, the modulator may most efficiently interface with the RF source at a lower or higher output voltage. In the case, for example, of the klystron, this would necessitate modulator operation into a different effective impedance. The pulse shape characteristics must be appropriately preserved at these varying load conditions.

In addition, it is critical that the system is appropriately protected in the case of a load short. Both the modulator should remain undamaged and the modulator must prevent excess energy transfer to the load arc. This is one of the more challenging parameters for a modulator to produce.

General Marx Description

The Marx bank has been used as a high voltage generator since the patent from Erwin Marx in 1923. While there have been demonstrations utilizing inductive elements and opening switches, the most common embodiment uses capacitors and closing switches to construct the output pulse. Specifically: *A Marx modulator is a topology in which capacitors are charged in parallel during the recharge period and discharged in series during the output pulse.* A generic Marx circuit is shown in Fig. 1. In the case of modulators for linac applications, the pulse is repetitive, has a flat or shaped output, and can be terminated in the event of a detected fault. Therefore, turn-on and turn-off switching is necessary, and hence so is solid-state switching.

*Work supported by Department of Energy contract DE-AC02-76SF00515.

[#]mkemp@slac.stanford.edu

RESULTS ACHIEVED BY THE S1-GLOBAL COLLABORATION FOR ILC

H. Hayano, M. Akemoto, S. Fukuda, K. Hara, N. Higashi, E. Kako, H. Katagiri, Y. Kojima, Y. Kondo, T. Matsumoto, S. Michizono, T. Miura, H. Nakai, H. Nakajima, K. Nakanishi, S. Noguchi, N. Ohuchi, T. Saeki, M. Satoh, T. Shidara, T. Shishido, T. Takenaka, A. Terashima, N. Toge, K. Tsuchiya, K. Watanabe, S. Yamaguchi, A. Yamamoto, Y. Yamamoto, K. Yokoya,
KEK, Tsukuba, Japan

K. Jensch, D. Kostin, L. Lilje, A. Matheisen, W. -D. Moeller, M. Schmoekel, P. Schilling,
N. Walker, H. Weise, DESY, Hamburg, Germany

T. Arkan, S. Barbanotti*, M. Battistoni, H. Carter, M. Champion, A. Hocker, R. Kephart, J. Kerby,
D. Mitchell, Y. Pischalnikov, M. Ross, T. J. Peterson, W. Schappert, B. Smith,
FNAL, Chicago, USA

A. Bosotti, C. Pagani, R. Paparella, P. Pierini, INFN, Milano, Italy

C. Adolphsen, C. Nantista, SLAC, Menlo Park, USA

Abstract

The S1-Global cryomodule experiment [1] by ILC-GDE (International Linear Collider, Global Design Effort) was planned to achieve “S1” goal, which is to operate at least one of cryomodule with 31.5MV/m ILC average gradient. The design, fabrication, assembly, experiment, and disassembly were done by the international collaboration based on ILC-GDE. The experiment hosted by KEK STF (Superconducting RF Test Facility at KEK) was performed from June 2010 to February 2011. The achieved gradient performance of the contributed cavities was average 30.0MV/m before installation, 27.7MV/m for single cavity operation after installation, and 26.0MV/m for 7 cavities simultaneous operation [2, 3].

The other goal of the S1-Global is to perform plug-compatibility concept by building one set of cryomodule from brought-in cavities and couplers of each laboratories. The half-size cryomodule-C was its demonstration built from INFN cryostat, two set of DESY cavities and couplers, and two set of FNAL cavities and couplers. The connection of cryomodule-C and KEK cryomodule-A was also another aspect of plug-compatibility.

The S1-Global program was the truly international cryomodule experiment by the effort of GDE members and GDE participation laboratories. The program has demonstrated to realize the international cryomodule and their performance close to ILC specification. The issues of the current cryomodule technologies and what we need to solve in the next were identified.

INTRODUCTION

The S1 is one of the identified tasks by the GDE R&D board, where an RF operation of a cryomodule with an average accelerating gradient of 31.5MV/m is to be demonstrated. The S1-global experiment was the world’s first program of building a segment of a superconducting linac system and testing a string of superconducting RF

cavities by a global collaboration in the Technical Design phase of the ILC project. The proposal was to bring eight 9-cell superconducting cavities and associate hardware components from institutions in the world, install them in common cryomodules, and demonstrate their operation by a global collaboration. The participating institutions contributed their hardware and human resources on an equal footing. The picture of the cryomodules is shown in Fig.1. While the S1-Global program lacked beam operation, it involved all the essential steps that are required prior to beam acceleration. The program successfully addressed numerous critical issues such as the plug-compatibility (i.e. compatible but not identical) of hardware components, as well as single- and multiple-cavity operation with pulsed microwave power and associated LLRF controls. While the tests were all completed by the end of February 2011, disassembly of the S1-Global cryomodules was started on May 2011 toward the end of the year 2011, practically all of the contributed cavity components were brought back to their home institutions for post-mortem diagnosis studies.

CAVITY PACKAGE

A new half-length cryomodule (Cryomodule-C) was designed and prepared by INFN, while the other half cryomodule (Cryomodule-A) was built by modifying an existing 6-m STF cryomodule at KEK.

The upstream module, Cryomodule-C, has 2 FNAL cavities, TB9AES004 for slot C1 and TB9ACC0112 for slot C2, and two DESY cavities; Z108 for slot C3 and Z109 for slot C4. Four cavities are equipped with TTF3 type main input couplers. In Fig.2, the illustrations of their cavity packages are shown. TB9AES004 was last tested in the horizontal test stand at FNAL before shipment, while TB9ACC011 was last tested in the vertical test stand. They are processed and tested at JLAB, ANL and FNAL. DESY cavities were processed with the DESY EP treatment and had been previously installed in the module 8 and tested on the CMTB at DESY. Before shipment to KEK, Z108 and Z109 underwent 6 HPR cycles and were tested in the DESY vertical cryostat.

*Current affiliation: DESY

COMPACT SUPERCONDUCTING CRABBING AND DEFLECTING CAVITIES*

S. U. De Silva^{1,2#}

¹Center for Accelerator Science, Old Dominion University, Norfolk, VA 23529, USA.

²Thomas Jefferson National Accelerator Facility, Newport News, VA 23606, USA.

Abstract

Recently, new geometries for superconducting crabbing and deflecting cavities have been developed that have significantly improved properties over those of the standard TM_{110} cavities. They are smaller, have low surface fields, high shunt impedance and, more importantly for some of them, no lower-order-mode with a well-separated fundamental mode. This talk will present the status of the development of these cavities.

INTRODUCTION

Primarily the crabbing and deflecting structures are used to restore luminosity in particle colliders or in separating a single beam into multiple beams. The crabbing concept was initially proposed by R.B. Palmer for collider rings [1] and was later proven for linear colliders [2] as well. The applications of crabbing and deflecting cavities are not limited to the above-mentioned applications but also can be used in many applications for beam diagnostics, emittance exchange, in generating compressed x-ray beams etc. Some of the potential applications at present are the deflecting cavity needed for the Jefferson Lab 12 GeV upgrade [3] to separate the maximum energy beam into the three experimental halls and the deflecting cavity system required for the multi experimental project under Project-X [4]. One of the crabbing applications is the LHC luminosity upgrade that requires a crabbing system for vertical and horizontal crossing at the integrations regions of IP_1 and IP_5 [5].

The stringent dimensional constraints set by these current applications especially operating at low frequencies demands the design and development of compact crabbing and deflecting cavities. Compared to the crabbing and deflecting cavities operating in TM_{110} these compact designs that has been developed have improved properties with low surface fields, high shunt impedance. Most of the designs have no lower order modes (LOMs) with a widely separated higher order mode (HOM) spectrum.

The First Superconducting Deflecting Cavity

The early research in superconducting crabbing and deflecting structures was done in 1970s where the first superconducting rf deflecting cavity as shown in Fig. 1

* Authored by Jefferson Science Associates, LLC under U.S. DOE Contract No. DE-AC05-06OR23177. The U.S. Government retains a non-exclusive, paid-up, irrevocable, world-wide license to publish or reproduce this manuscript for U.S. Government purposes.

Part of this work was done in collaboration with and supported by Niowave Inc. under the DOE STTR program.

#sdesilva@jlab.org

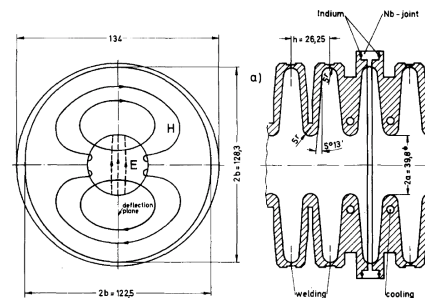
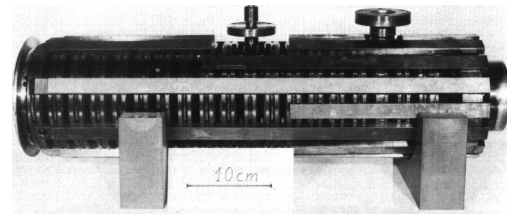


Figure 1: 19-cell end section of the 2.865 GHz rf separator cavity (top) and bi-periodic TM_{110} operating mode (bottom).

was designed and developed in KfK, Karlsruhe in collaboration with CERN [6]. The 2.865 GHz, 104-cell cylindrical-shaped standing wave rf particle separator shown in Fig. 1 installed at CERN in 1977 was capable of delivering a deflection in the vertical plane. The rf separator driven at 1.8 K, in a bi-periodic TM_{110} -type mode (Fig. 1) was in operation until 1981.

The First Superconducting Crabbing Cavity

The first crabbing cavity system was developed and installed in 2007 at KEK [7] for the KEKB electron-positron collider. The crabbing cavity shown in Fig. 2, operating in TM_{110} mode at 508.9 MHz was the only crabbing cavity system that has been in operation in a particle collider until 2010 after the installation in 2007.

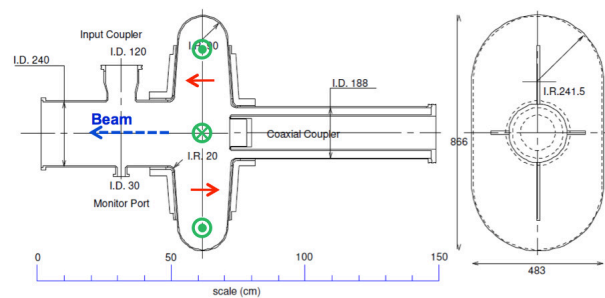


Figure 2: Superconducting 508.9 MHz KEK crabbing cavity.

SUPERCONDUCTING SPOKE CAVITIES FOR ELECTRONS AND HIGH-VELOCITY PROTON LINACS*

J. R Delayen[#]

Center for Accelerator Science, Old Dominion University, Norfolk, VA 23529, U.S.A
Thomas Jefferson National Accelerator Facility, Newport News, VA 23606, USA

Abstract

Over the last two decades, spoke resonators have been developed for the medium-velocity range of many proton and ion machines. These structures are now being considered and developed for electron linacs and high velocity proton linacs. The status of these developments and the properties of high-velocities spoke cavities are presented.

FEATURES OF THE SPOKE CAVITY

The spoke cavity, shown in Fig. 1, is a variant of the coaxial half-wave geometry. In its fundamental mode of operation, the spoke sustains a TEM mode where the length of the spoke is approximately half the wavelength. The current (and magnetic field) is large where the spoke meets the outer conductor, and the voltage (and electric field) is large in the middle of the spoke.

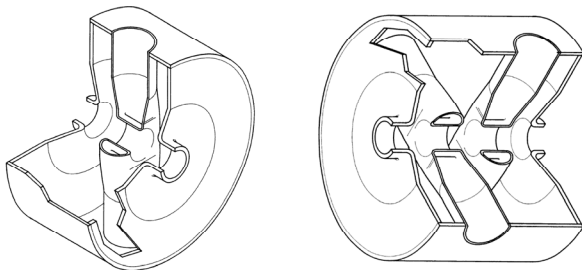


Figure 1: Single-spoke and double-spoke cavity [1].

In multi-spoke cavities, shown in Fig. 2, each spoke operates 180° out of phase with the nearest ones and is usually perpendicularly oriented with respect to them.

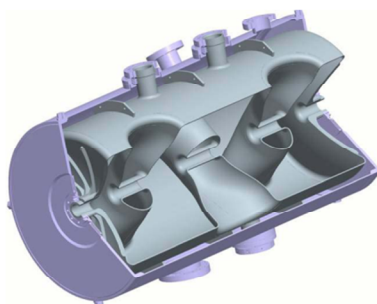


Figure 2: triple-spoke cavity [2].

The spoke cavity was initially developed for the mid-velocity range because of a number of attractive features [3, 4].

Size

For the same frequency and in the medium-velocity region, spoke cavities are smaller than TM-class cavities. The transverse size of a spoke cavity is in the range $0.5-0.55 \lambda$ while that of a TM cavity is about 0.95λ . As a result accelerators can be designed for low frequency where 4.2K operation is practical, while maintaining cavities of a reasonable size. At half the frequency of a TM cavity of the same β , a multi-spoke cavity of the same length would have half the number of cells. Therefore its velocity acceptance is broader and the cavity is useful over a wider range of velocities. Lower frequency would also result in a higher longitudinal acceptance, which might be beneficial in high current applications.

As will be shown later, the size difference is not as dramatic with spoke cavity designs that maximize the shunt impedance and minimize the surface fields. These optimizations lead to geometries of the spoke themselves which deviate substantially from cylinders; as a consequence, in order to maintain the frequency, the spokes have to be longer and the diameter of the cavity larger.

Cell-to-cell Coupling

Unlike TM cavities where the cell-to-cell coupling occurs through the iris opening, a multi-spoke cavity is much more open and magnetic field lines couple all the cells. The cell-to-cell coupling is much higher in multi-spoke cavities than in multi-cell TM cavities and they are much more robust with respect to manufacturing inaccuracies. Tuning to achieve field profile balance is probably unnecessary while it is an important and necessary step for TM cavities.

The strong cell-to-cell coupling, together with the fact that multi-spoke cavities have only a relatively small number of spokes, implies that the accelerating mode will be well separated from the nearest mode. In addition, unlike multi-cell TM cavities, the fundamental accelerating mode in multi-spoke cavities is the lowest frequency mode, and there are no lower-order modes. This was known to be true in the medium-velocity regime and it has been confirmed in all the high-velocity spoke cavities designed to-date.

* Work supported by U.S. DOE Award No. DE-SC0004094

[#] jdelayen@odu.edu

SUPERCONDUCTING LINAC AND ASSOCIATED DEVELOPMENTS AT IUAC DELHI

A. Roy, Inter-University Accelerator Centre, Aruna Asaf Ali Marg, New Delhi – 110067, India

Abstract

A superconducting linear accelerator system has been developed as a booster of heavy ion beams available from the existing 15UD Pelletron accelerator. Two linac modules having eight niobium quarter wave resonators (QWRs) each have been installed and are fully operational for regular scheduled experiments. The third module is being added to the system. A new high current injector has been planned to couple to the superconducting linac. For this a high temperature superconducting electron cyclotron resonance ion source (HTS-ECRIS) was designed, fabricated and installed successfully. A radio frequency quadrupole (RFQ) accelerator is being developed for accelerating accelerate ions from the ECR ($A/Q \sim 6$) to an energy to of about 180 keV/A. The beams will then be accelerated further by drift tube linacs (DTL) to the required velocity to inject them to the existing superconducting linac booster. Prototypes of both these have been tested for power and thermal studies. Details of these developments and associated systems are presented in this paper.

INTRODUCTION

A superconducting linac boosters for increasing the energy of heavy ions from the Pelletron accelerator at Inter-University Accelerator Centre (IUAC), New Delhi is in operation for the past four years [1,2,3]. Heavy ions from the 15 UD Pelletron Accelerator have been accelerated through two modules, each with eight Nb quarter wave cavity resonators and used for many experiments in Nuclear Physics and Materials Science. The third module is in the process of installation and testing. The layout of the accelerator is shown in figure 1.

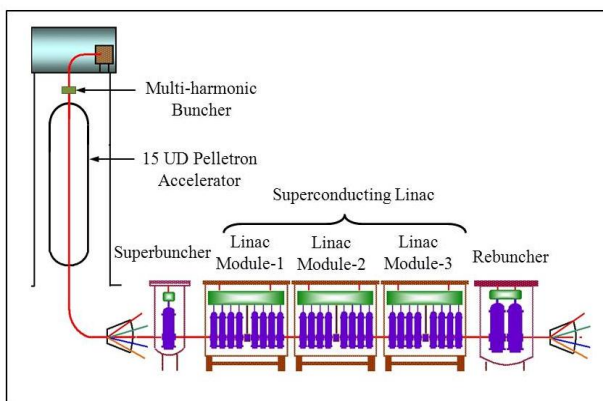


Figure 1: Sketch of the Pelletron – Linac accelerator system at IUAC, New Delhi.

Improvements were made in cooling the drive couplers of the resonators and an alternate frequency tuning mechanism based on piezo tuners has been developed. The novel method of reducing the microphonic noise in the cavity using steel balls to reduce the power required to amplitude and phase lock the cavities has been improved further. Automation of the phase tuning of the resonators was successfully tested out.

The High Current Injector planned to increase the ion flux has been designed and prototype of a suitable low beta Nb resonator with $\beta = 0.05$ has been fabricated. Prototypes of room temperature radio frequency quadrupole and drift tube linac have been built and tested for design validation.

IUAC is fabricating two $\beta = 0.22$, 325 MHz Single Spoke Resonators for the Project X of Fermi National Accelerator Lab (FNAL), USA. Several single cell 1.3 GHz TESLA type cavities and a 5-Cell cavity have been built in collaboration with RRCAT, Indore.

SUPERCONDUCTING LINAC

The complete linear accelerator (Linac) of Inter University Accelerator Centre (IUAC) will consist of five cryostats, the first one acting as superbuncher (SB) consists of a single quarter wave resonator (QWR), the next three linac cryomodules house eight QWRs each, and the last one has two QWRs used as rebuncher (RB).

In recent past, with the help of superbuncher, the first linac accelerating module and the rebuncher, Pelletron ion beams from ^{12}C to ^{107}Ag were further accelerated and delivered to conduct experiments in Nuclear Physics and Material Science. In 2011 another eight niobium resonators were installed in the linac cryostat-2 and a couple of off-line cold tests were conducted followed by beam acceleration through linac without the last accelerating module. During the beam acceleration, all sixteen resonators of cryostat 1 and 2 took part along with the single resonator operated each in superbuncher and rebuncher cryostat. During this entire period of beam acceleration extending for more than a month, three different beam species: ^{19}F , ^{28}Si and ^{31}P were accelerated and beam was delivered in the beam line of HYRA (Hybrid Recoil mass Analyzer) and NAND (National Array of Neutron Detectors). The results of the beam acceleration, in brief, are given in Table 1.

THE ESS LINAC DESIGN

M. Lindroos*, S. Molloy, D. McGinnis, C. Darve, H. Danared, ESS AB, Lund, Sweden
and the ESS Accelerator Collaboration

Abstract

The European Spallation Source (ESS) is a 5 MW, 2.5 MeV long pulse proton machine. It represents a big jump in power compare to the existing spallation facilities. The design phase is well under way, with the delivery of a Conceptual Design Report published in the beginning of 2012, and a Technical Design Report in December 2012. Why and how the 5 MW goal influences the parameter choices will be described.

INTRODUCTION

Spallation is a nuclear process in which neutrons of different energies are emitted in several stages following the bombardment of heavy nuclei with highly energetic particles. The spallation process is the most practical and feasible way of producing neutrons for a reasonable effort (or cost) of the neutron source cooling system. Spallation sources come in at least three types: short pulse sources (a few μs), long pulse sources (a few ms) and continuous sources. The future European Spallation Source (ESS) will be a long pulse source and the first spallation source with a time average neutron flux as high as that of the most intense research reactors.

The highest power spallation source currently in operation – the Spallation Neutron Source (SNS) in Oak Ridge – combines a full energy SC linear accelerator with an accumulator ring to provide very high intensity short pulses of neutrons to the instruments. The European Spallation (ESS) source will provide even higher intensities, but is developing instruments able to use longer linac pulses directly for spallation, avoiding the need for a costly and performance-limiting accumulator ring [1].

The obvious advantage of a linac is that beam passes only once through the accelerating structures, enabling it to accelerate a high current beam with a minimum of constraints. The current limit is mainly set by space charge effects at low energy, as well as the power that can be delivered to the beam in each accelerating cavity at medium and high energies, and by beam losses.

The spallation cross section for protons on heavy nuclei increases as a function of proton energy up to several tens of GeV [2]. Nonetheless it is generally agreed that a kinetic proton energy between 1-3 GeV is optimal for practical target and moderator designs, and in order to keep the shielding requirements reasonable.

The ESS has the ambitious goal of becoming a sustainable research facility with zero release of carbon dioxide. This will be achieved through a combination of actions, but

with the linac being the most energy hungry part of ESS, the energy efficient design of the RF power sources and the cryogenics systems and high-Q cavities are important issues.

THE ESS BASELINE

The ESS accelerator high level requirements are to provide a 2.86 ms long proton pulse at 2.5 GeV at repetition rate of 14 Hz, with 5 MW of average beam power on target. The configuration of the current, May 2012 Baseline linac is shown schematically in Fig. 1, and selected linac parameters are listed in Tab. 1 [3]. The warm linac has contributions from INFN Catania, CEA Saclay, ESS-Bilbao and INFN Legnaro, the superconducting cavities and their cryomodules are designed at IPN Orsay and CEA Saclay, and the HEBT will come from ISA in Aarhus. The 50-mA proton beam is produced in a pulsed microwave-discharge source on a platform at 75 kV. A low-energy beam transport, LEBT, with two solenoid magnets as focusing elements brings the beam to the entrance of the RFQ. The LEBT has a chopper that cuts away the beam while the proton pulses from the ion source stabilize, preventing a beam with off-nominal parameters from being accelerated in the RFQ and lost at high energy. The 4-vane RFQ accelerates the beam to 3 MeV with small losses and a minimal emittance growth. It is designed specifically for ESS but it is based on the IPHI RFQ at Saclay. The RF frequency of the RFQ and the warm linac is 352.21 MHz. After the RFQ there is a medium-energy beam transport, MEBT, with three buncher cavities and 10 quadrupole magnets. The MEBT has several different functions: it has optics to match and steer the beam from the RFQ into the drift-tube linac, it has a comprehensive set of beam-instrumentation devices, it has a chopper which acts faster than the LEBT chopper since space-charge neutralization is not an issue in the MEBT, and it allows collimation of the transverse particle distribution. A drift-tube linac, DTL, with four tanks takes the beam from 3 MeV to 79 MeV. It has a FODO structure with permanent-magnet quadrupoles. Every second drift tube is empty or used for steering magnets and beam-position monitors. The superconducting linac has three types of cavities: double-spoke resonators, five-cell medium-beta elliptical cavities and five-cell high-beta elliptical cavities. The May 2012 linac has 14 spoke cryomodules with two double-spoke resonators in each, and between the cryomodules there are warm quadrupole doublets. The spoke resonators operate at 352.21 MHz like the warm linac, but then there is a frequency doubling to the 704.42 MHz of the elliptical cavities. There are 15 medium-beta cryomodules with four cavities in each and

02 Proton and Ion Accelerators and Applications

2A Proton Linac Projects

* E-mail: mats.lindroos@ess.se

SPIRAL2 ACCELERATOR CONSTRUCTION PROGRESS

P. Bertrand, R. Ferdinand, GANIL, Caen France,
on behalf of the SPIRAL2 team and partners.

Abstract

The installation of the SPIRAL2 superconducting accelerator at GANIL is almost started. All the major components have been tested in the various partner laboratories, and the building construction is now well engaged. The management of the interfaces between the process and the buildings is a strategic point in an underground accelerator, with strong space constraints. This paper describes the performances of the various components.

INTRODUCTION

Officially approved in May 2005, the SPIRAL2 radioactive ion beam facility at GANIL (Caen-Normandy) has been launched in July 2005, with the participation of many French laboratories (CEA, CNRS) and international partners. Figure 1 describes the project layout. In 2008, an important decision has been taken to build the SPIRAL2 complex in two phases:

- *Phase one* includes the complete accelerator and two new experimental halls, the Super Separator Spectrometer (S3) and the Neutron-based research area (NFS), all to be installed in a new dedicated building.
- *Phase two* includes the RIB production process and building, the low energy RIB experimental hall (DESIR) and the transfer line connection to the present GANIL facility for RIBs post-acceleration by means of the existing SPIRAL1 cyclotron called CIME.

The planning objective of the first phase is to have installed and tested the whole accelerator in order to start the experiments with NFS and S3 in 2014-2015. A complete presentation of the SPIRAL2 scientific case can be found in the White Book of SPIRAL2, and through the large number of Letters of Intent for physics [1] [2] [3].

Recalled in table 1, the SPIRAL2 accelerated beams will include protons, deuterons, $A/q < 3$ ions, and optionally $A/q < 6$ ions in the future. As indicated, a maximum beam power of 200kW is expected for deuterons in CW mode.

Table 1: Beam Specifications

beam	P+	D+	ions	ions
Q/A	1	1/2	1/3	1/6
Max. I (mA)	5	5	1	1
Min. output E (MeV/A)	2	2	2	2
Max output E (MeV/A)	33	20	14.5	8
Max. beam power (kW)	165	200	44	48

During the last years, our strategy for the accelerator itself was the following:

We decided a few years ago to install the low energy

02 Proton and Ion Accelerators and Applications

2G Other Proton/Ion

heavy ion transfer line and ECR source at LPSC laboratory (Grenoble), and the Deuteron/proton ones at IFRFU/Saclay, in order to operate a maximum of technical and beam tests, to check the validity of our design, and to improve with all partner laboratories our knowledge and collaboration. This will also gain time for the definitive installation and tests at GANIL.

Thanks to our partnership with existing accelerators (SARAF, INFN-HH, GANIL...), we were also able to test various components like diagnostics in presence of existing beams, and to have some irradiation tests on samples to check their resistance to radiations and to validate the activation codes.

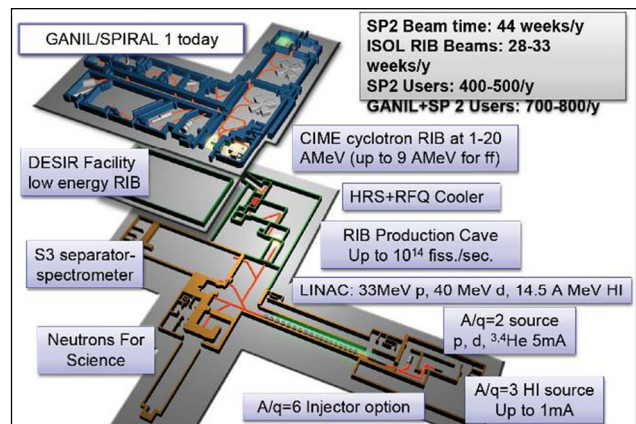


Figure 1: SPIRAL2 project layout, with experimental areas and connexion to the existing GANIL.

In the next paragraphs, we will focus essentially on the first phase of the project, providing the status of the main parts of the accelerator, the progress of construction of its building, and some scheduling.

SPIRAL2 INJECTOR STATUS

The Spiral2 injector, dedicated to protons, deuterons and heavy ions of $q/A > 1/3$, is mainly composed of two ECR ion sources with their associated LEBT lines, a warm RFQ and the MEBT line connected to the LINAC.

Heavy ECR ion source, and LBET1

The 18GHz ECR heavy ion source, called Phoenix-V2, and its analysis beam line LBET1 have been installed at the LPSC/Grenoble for a few years (Figure 2). The ECR source was updated these last years, in particular to host metallic ovens developed at GANIL.

Here are summarised the main results obtained: (see also [4] and [5] for more details) :

- Using automated optimization algorithms developed

ISBN 978-3-95450-122-9

DESIGN AND CONSTRUCTION OF THE LINAC4 ACCELERATING STRUCTURES

F. Gerigk, Y. Cuvet, A. Dallochio, G. Favre, L. Gentini, J.M. Geisser, J.M. Guiguet, S. Mathot
 M. Polini, S. Ramberger, B. Riffaud, C. Rossi, P. Ugena Tirado, R. Wegner, M. Vretenar,
 CERN, Geneva, Switzerland M. Naumenko, VNIITF, Snezhinsk, Russia
 E. Kendjebulatov, Ya. Kryuchkov, A. Tribendis, BINP, Novosibirsk, Russia

Abstract

The Linac4 project at CERN is at an advanced state of construction. Prototypes and/or operational modules of the different types of accelerating structures (RFQ, buncher, DTL, CCDTL, and PIMS) have been built and are presently tested. This paper gives the status of the cavity production and reviews the RF and mechanical design of the various structure types. Furthermore the production experience and the first test results shall be presented.

INTRODUCTION

Linac4 [1] consists of four sections, which accelerate the beam up to its final energy of 160 MeV. The recently completed Radio Frequency Quadrupole (RFQ) [2] creates the 352.2 MHz bunch structure and raises the beam energy from 45 keV to 3 MeV. It is further accelerated by three Drift Tube Linac (DTL) tanks up to 50 MeV, followed by seven Cell-Coupled Drift Tube Linac (CCDTL) modules up to 103 MeV and 12 Pi-Mode Structures (PIMS) up to 160 MeV. Figure 1 shows a block diagram of Linac4 and the general parameters of each structure are summarized in Table 1.

Table 1: General Structure Parameters

Parameter	DTL	CCDTL	PIMS
f [MHz]	352.2	352.2	352.2
$E_{in/out}$ [MeV]	3-50.3	50.3-102.9	102.9-160
E_0T [MV/m]	2.65 - 2.95	3.6 - 2.7	3.74
ϕ_s [deg]	-35 \rightarrow -24	-20	-20
ZT^2 [M Ω] †	44-52	40-33	24.6-26.2
av. Q_0 ‡	41000	42500	21600
P_{peak} [MW]	1.0/2.0/2.0	0.95-1.0	0.92-1.0
cav. length [m]	3.9/7.3/7.3	0.7-1.04	1.3-1.54
$N_{cavities}$	3	21	12
$N_{cav./module}$	n.a.	3	n.a.
$N_{gaps/cavity}$	39/42/30	3	7

† linac definition, operational value ‡ operational value



Figure 1: Linac4 block diagram.

The Linac4 accelerating structures are designed, constructed and tested under the supervision of the CERN RF group, supported by the CERN purchasing office, the vacuum group, the mechanical design office and by the CERN workshops for prototyping and qualification of construction procedures at the contractors. In general the prototyping and mechanical development was done at CERN and then exported for external construction. However, for certain critical construction processes – as outlined in the following – it was decided to “in-source” them.

All accelerating structures are designed for a maximum duty cycle of 10%, having in mind a future intensity upgrade of Linac4 as an injector to a high (average) power proton linac [3]. Linac4 itself will operate at a duty cycle of 0.04%, limited by the 1 Hz repetition rate of the PS Booster (PSB) into which the Linac4 beam is injected.

Due to LHC operational constraints the connection of Linac4 to the PSB is now foreseen to take place during the 2nd long LHC shutdown, which is expected for 2017/18 [1]. Commissioning with beam will take place in 2014/15 to leave sufficient time for improving reliability prior to operation in the LHC injection chain. The planning for the construction and commissioning of the accelerating structures has been adapted to this target date and is shown in Table 2.

Table 2: Key Dates for Linac4 RF Structures

date	status
10/12 - 11/13	RFQ, DTL, CCDTL assembly, tuning and testing
10/12 - 10/14	PIMS assembly, tuning and testing
09/13 - 04/14	DTL installation and commissioning
09/14	ready for 50 MeV protons
05/14 - 12/14	CCDTL commissioning
01/15 - 06/15	PIMS commissioning
07/15 - 12/15	160 MeV beam tests
01/16 - 11/16	reliability run
11/16	ready for 160 MeV H- operation
2017 - 2018	foreseen connection to PSB

RFQ

The RFQ is the only Linac4 accelerating structure which was completely constructed at CERN. Its design was elaborated in collaboration with CEA Saclay making use of experience with the IPHI RFQ [4]. In August 2012 the

COMPUTATIONAL MODEL ANALYSIS FOR EXPERIMENTAL OBSERVATION OF OPTICAL CURRENT NOISE SUPPRESSION BELOW THE SHOT-NOISE LIMIT

A. Nause, E. Gover, Tel Aviv University, Israel

Abstract

In this paper we present simulation analysis of experimental results which demonstrate noise suppression in the optical regime, for a relativistic e-beam, below the classical shot-noise limit. Shot-noise is a noise resulting from the granular nature of the space-charge in an e-beam. It is linear to the beam current due to its Poissonic distribution in the emission process. Plasma oscillations driven by collective Coulomb interaction during beam drift between the electrons of a cold intense beam are the source of the effect of current noise suppression. The effect was experimentally demonstrated [1] by measuring Optical Transition Radiation (OTR) power per unit e-beam pulse charge. The interpretation of these results is that the beam charge homogenizes due to the collective interaction (sub-Poissonian distribution) and therefore the spontaneous radiation emission from such a beam would also be suppressed (Dicke's sub-radiance [2]). Analysis of the experimental results using GPT simulations will demonstrate the suppression effect. For the simulation results we used a full 3D GPT model of the ATF section in which the experiment took place at.

INTRODUCTION

Shot-noise is a noise resulting from the granular nature of the space-charge in an e-beam. The discreteness of the particles and the randomness of electrons emission from the cathode causes time dependent fluctuations of the charge and current density at any cross section along the beam transport line. This noise was first reported in 1918 by Schottky who made experiments in vacuum tubes.

Noise is best characterized in terms of the Fourier transform of the time-varying fluctuations in electric current, namely, by its spectral density. Gover and Dyunin showed in a 1D model [3] that it is possible to observe and control optical frequency energy and current (shot noise) fluctuations in a dense relativistic charged particles beam. GPT simulations were used to demonstrate this effect for a real-like beam starting from Shot-noise [4]. Moreover, at certain conditions, when the dominant noise in the beam is current shot noise (density fluctuations), it is possible to reduce significantly the beam noise by virtue of a collective interaction process along an interaction length corresponding to a quarter period longitudinal plasma oscillation in the beam. This means that the charge distribution in the beam can be homogenized in this process.

First experimental observation of this phenomenon using OTR from a metallic foil was presented last year [1]. Noise suppression using a dispersive section (dog-leg bend) was demonstrated in SLAC [5]. TR is proportional to the

current-noise amplitude [6], and therefore can be used in order to estimate the suppression in the current noise. In this paper we press analysis of the experimental results and demonstrate this effect using full 3D GPT simulations that were carried out for this purpose.

1D Model of Noise Dynamics in Charged Electron Beams

In electron-beam transport under appreciable space-charge conditions, the microdynamic noise evolution process may be viewed as the stochastic oscillations of Langmuir plasma waves [3]. In the linear regime, the evolution of longitudinal current and velocity modulations of a beam of average current I_b , velocity βc and energy $E = (\gamma - 1)mc^2$, can be described in the laboratory frame by [7]:

$$\frac{d}{d\phi_p} \check{i}(z, \omega) = -\frac{i}{W(z)\check{v}(z, \omega)} \quad (1)$$

$$\frac{d}{d\phi_p} \check{v}(z, \omega) = -iW(z)\check{i}(z, \omega) \quad (2)$$

where $\check{i}(\omega) = \check{I}(\omega)e^{i\omega z/\beta c}$, $\check{v}(\omega) = \check{V}(\omega)e^{i\omega z/\beta c}$. $\check{I}(\omega)$, $\check{V}(\omega)$ are the respective Fourier components of the beam current and kinetic-voltage modulations. The kinetic-voltage modulation is related to energy and longitudinal velocity modulations: $\check{V}(\omega) = -(mc^2/e)\check{\gamma} = -(mc^2/e)\gamma^3\beta\check{\beta}$, $\phi_p(z) = \int_0^z \theta_{pr}(z')dz'$ is the accumulated plasma phase, $W(z) = r_p^2/(\omega A_e \theta_{pr} \epsilon_0)$ is the beam wave-impedance. A_e is the effective beam cross-section area, $\theta_{pr} = r_p \omega_{pl}/\beta c$ is the plasma wavenumber of the Langmuir mode, $r_p < 1$ is the plasma reduction factor, $\omega_{pl} = \omega_{p0}/\gamma^{3/2}$ is the longitudinal plasma frequency in the laboratory frame. The single-frequency Langmuir plasma wave model expressions [3] can be solved straightforwardly in the case of uniform drift transport. After employing an averaging process, this results in a simple expression for the spectral parameters of stochastic current and velocity fluctuations (noise) in the beam assuming that they are initially uncorrelated[]:

$$\check{i}(L, \omega) = \cos \phi_p(L)\check{i}(0, \omega) + (\sin \phi_p(L)/W_d)\check{v}(0, \omega) \quad (3)$$

where $\phi_p = \theta_{pr}z$, $\theta_{pr} = r_p \frac{\omega'_p}{v_0}$, $\omega'_p = (\frac{e^2 n_0}{m \epsilon_0 \gamma^3})$, $W_d = \sqrt{\mu_0/\epsilon_0}/k\theta_{pr}A_e$.

The beam current noise evolution is affected by the initial axial velocity noise through the parameter

$$N^2 = |\check{v}(0, \omega)|^2/W^2|\check{i}(0, \omega)|^2 = (\omega/c\beta k_D)^2 \quad (4)$$

STATUS OF ILC

A. Yamamoto*, High Energy Accelerator Research Organization (KEK), Tsukuba, Japan,
 M. Ross*, SLAC National Accelerator Laboratory, Menlo Park, CA, USA
 N. Walker*, DESY, Hamburg, Germany
 * Project Managers of ILC Global Design Effort

Abstract

The International Linear Collider (ILC) is anticipated to be the next energy-frontier electron-positron accelerator based on superconducting radio-frequency (SCRF) technology, and to accelerate electron and positron beams up to 250 GeV each with having extend-ability up to 500 GeV each. This paper describes the progress of the technical design and R&D efforts progressed in the ILC Technical Design phase since 2007 and includes further effort after the completion of Technical Design Report (TDR) in 2012.

INTRODUCTION

The International Linear Collider (ILC) is proposed as the next energy-frontier electron-positron accelerator to be built with a global effort [1 - 3]. The ILC accelerator is based on SCRF accelerator technology, as recommended by the International Technology Recommendation Panel [4] and endorsed by the International Committee for Future Accelerators. The ILC Global Design Effort (ILC-GDE) was launched to advance the accelerator design and R&D efforts. It published the Reference Design Report (RDR) in 2007 [2]. The ILC design assumes an averaged cavity field gradient of 31.5 MV/m to achieve a center-of-mass energy of 500 (=2 x 250) GeV with two 11-km long main linacs. The technical design work and R&D efforts have significantly progressed during the Technical Design (TD) phase started in 2007 and are completed with the Technical Design Report (TDR) in 2012.

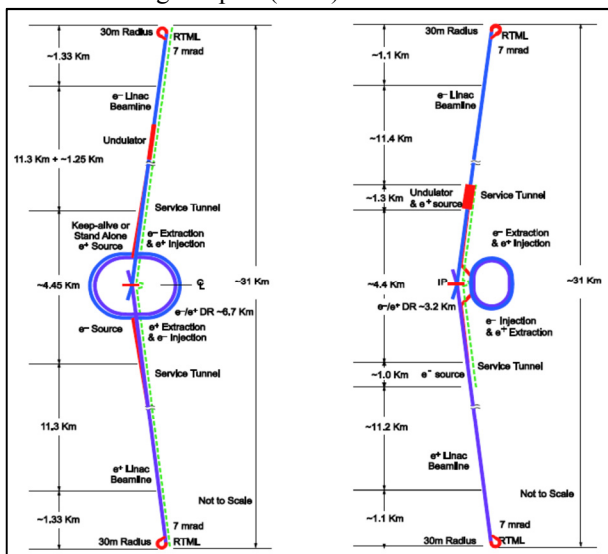


Figure 1: Layouts of ILC in RDR (left) and TDR (right).

A major update of the accelerator design has been made for TDR, seeking for the best cost-effective design with a ‘cost-containment’ guideline [5]. Figure 1 shows the TDR accelerator layout with the RDR accelerator layout, and Table 1 summarizes the main parameters.

Table 1: ILC accelerator and SCRF requirement.

Parameter	RDR	TDR
Energy (cms: GeV)	500	500
L (cm ² s ⁻¹)	2 x 10 ³⁴	1.5 x 10 ³⁴
Beam current (mA)	9	5.8
Beam Rep. (Hz)	5	5
Bunch spacing (ns)	369	554
Bunch train length (μs)	1.000	0.727
Numbers of bunches	2625	1312
Cav. Grad. (MV/m)	31.5	31.5
# 1.3-GHz, 9-cell cavity	15,941	16,024
# 1.3-GHz, Cryomodule	1,824	1,855
# 10-MW Klystron	646	413+α / 378+β (KCS/DKS)

GENERAL DESIGN UPDATES

The ILC accelerator design has been updated in the middle of the Technical Design Phase [5]. It has been motivated by i) overall cost containment and balancing among sub-system, ii) improved understanding of system functionality, iii) more complete and robust design, and iv) re-optimized R&D plans. The major design update includes:

- A Main Linac length consistent with an *average* accelerating gradient of 31.5 MV/m with a spread within +/-20%, and maximum operational beam energy of 250 GeV,
- A single-tunnel solution for the Main Linac and RTML, with two possible variants for the High-Level RF (HLRF) configuration:
 - Klystron cluster scheme (KCS):
 - Distributed Klystron scheme (DKS).
- Undulator-based positron source located at the end of the electron Main Linac (250 GeV),
- A lower beam-power parameter set with the number of bunches per pulse reduced by a factor of two,
- Reduced circumference Damping Rings (~3.2 km) at 5 GeV with a 6 mm bunch length,

THE 12 GeV ENERGY UPGRADE AT JEFFERSON LABORATORY

F. Pilat

Thomas Jefferson National Accelerator Facility, Newport News, VA 23606, USA

Abstract

Jefferson Laboratory has undertaken a major upgrade of its flagship facility, the CW re-circulating CEBAF linac, with the goal of doubling the linac energy to 12 GeV. I will discuss here the main scope and timeline of the upgrade and report on recent accomplishments and the present status. I will then discuss in more detail the core of the upgrade, the new additional C100 cryomodules, their production, tests and recent successful performance. I will then conclude by looking at the future plans of Jefferson Laboratory, from the commissioning and operations of the 12 GeV CEBAF to the design of the MEIC electron ion collider.

INTRODUCTION AND OVERVIEW

The CEBAF (Continuous Electron Beam Accelerator Facility) started operations in 1995 as the first CW re-circulating linac and first large accelerator based on superconducting RF technology. Designed for a maximum energy of 6 GeV, CEBAF has operated continuously serving a large nuclear physics community of more than 1400 users for 17 years, its last run at 6 GeV successfully completed in the spring 2012. With 5 recirculation passes and an injector able to tailor different beam characteristics (energy, intensity and polarization) independently for 3 experimental Halls capable to run concurrently, the linac has been a flexible and reliable source that has sustained a rich and successful nuclear physics program.

In the late 1990's the concept for an energy doubling to 12 GeV was defined, and the plan was approved and funded starting in 2004.

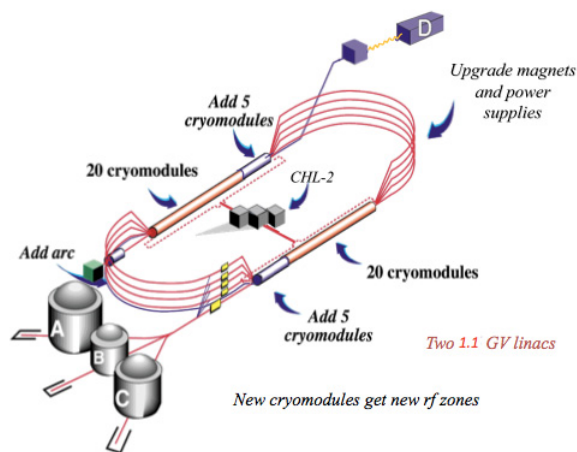


Figure 1: The main components of the CEBAF upgrade to 12 GeV.

The energy doubling is achieved by adding 10 new C100 to the existing 40 CEBAF cryomodules in free

space at the end of each linac and by upgrading the magnets in the original 9 arcs to higher fields. The higher cryogenic load necessitates the doubling of the cryogenics capability with the addition of a second cryogenics plant, CHL-2 to the existing CHL-1. In addition, a new arc (Arc 10) provides an additional pass to deliver 12 GeV beam to the new Hall D. Beam for the existing Halls A, B and C is extracted at 11 GeV. The design is for a maximum of 3 Halls operating at the same time. The new Hall D adds the capability of a photon beam dedicated to the new Glue-X experiment. Included in the scope of the upgrade are new experimental detectors for the Halls B and C and infrastructure upgrades for Hall A. The injection line also needs to double the energy to match the linac.

A comparison of the high-level machine parameters between the 6 and 12 GeV CEBAF is given in Table 1.

Table 1: High-level parameters for the 6 and 12 GeV CEBAF.

Parameter	Unit	6 GeV	12 GeV
Max Energy to Halls	GeV	6	12
Passes for Hall ABC/D		5	5/5.5
Max current Hall A,C/B	μA	200 / 5	85/5
Emittance at max E H/V	nm-rad	1 / 1	10 / 2
Energy spread at max E	10^{-5}	2.5	50 at 11 GeV 500 at 12 GeV
Bunch length (rms)	ps	0.2	~ 1
Polarization	%	80	80

TIMELINE AND STATUS

The 12 GeV Upgrade is being managed as the 12 GeV Project, with project management structure and practices in place. The total Project cost is 310 M\$ (excluding the injector upgrade, the path-length adjusters, the 5-pass RF separators and necessary machine maintenance, that are funded and managed off Project) and the Project is at the time of writing 68% complete and 79% obligated. The overall Project timeline is shown in Figure 2.

While procurement and subsystem work as well as civil construction have been in progress since FY04, the bulk of the construction and installation work has been planned during 2 operations shut-downs, the 6 month shutdown, May-November 2011 and the ongoing 16 month long shut-down, May 2012 to September 2013.

The present timeline has machine commissioning at 12 GeV starting in the fall of 2013, beam to Hall A in February 2014, followed by Hall D commissioning in October 2014, and Hall B and C in April 2015. Project completion, assuming the planned funding, is foreseen in June 2015.

The rationale of distributing the installation for the upgrade over 2 separate shutdowns in lieu of one was mainly motivated by two objectives: concluding the 6

ERL-BASED LEPTON-HADRON COLLIDERS: eRHIC AND LHeC

F. Zimmermann, CERN, Geneva, Switzerland

Abstract

Two hadron-ERL colliders are being proposed. The Large Hadron electron Collider (LHeC) plans to collide the high-energy protons and heavy ions in the Large Hadron Collider (LHC) at CERN with 60-GeV polarized electrons or positrons. The baseline scheme for this facility adds to the LHC a separate recirculating superconducting (SC) lepton linac with energy recovery, delivering a lepton current of 6.4 mA. The electron-hadron collider project eRHIC aims to collide polarized (and unpolarized) electrons with a current of 50 (220) mA and energies in the range 5–30 GeV with a variety of hadron beams — heavy ions as well as polarized light ions — stored in the existing Relativistic Heavy Ion Collider (RHIC) at BNL. The eRHIC electron beam will be generated in an energy recovery linac (ERL) installed inside the RHIC tunnel.

INTRODUCTION

The LHeC and eRHIC projects would involve one of the proton or ion beams of the LHC and RHIC, respectively. They, therefore, represent interesting possibilities for further efficient exploitation of the LHC and RHIC infrastructure investments. These and other (non-linac) lepton-hadron colliders, e.g. MEIC at TJNAF, are reviewed in [1].

For the LHeC [2], with 60-GeV lepton beam energy and using the 7 TeV proton (and few TeV / nucleon ion) beam, centre-of-mass collision (CM) energies in the TeV range are attained, significantly exceeding the CM energy of HERA, the first (ring-ring) ep collider built. The LHeC ep target luminosity is $10^{33} \text{ cm}^{-2}\text{s}^{-1}$. Extensions to $10^{34} \text{ cm}^{-2}\text{s}^{-1}$ are being considered. In order to keep the power consumption of the LHeC facility at a realistic level, the total electrical power for the LHeC lepton branch has been limited to 100 MW. A Conceptual Design Report (CDR) has been published [3]. The LHeC physics program comprises precision QCD, electroweak physics, high parton densities, and new physics at high energy.

The LHeC CDR considered both ERL-ring and ring-ring options for the LHeC. Recently [4] the ERL-ring design was chosen as the baseline scheme for several reasons: (1) the installation of the ring-ring machine would interrupt the ongoing and planned LHC program as well as imply extended tunnel work and interference with the existing LHC, and (2) the development of a CW SC recirculating energy-recovery linac for LHeC would prepare for many possible future projects, e.g., for an International Linear Collider, for a neutrino factory, for a proton-driven plasma wake field accelerator, or for a muon collider. With some additional arcs, using 4 instead of 3 passes through the linacs, a machine like the LHeC ERL (without energy recovery) could also operate as Higgs factory $\gamma\gamma$ collider [5].

The eRHIC [6] will collide 5–30 GeV polarized electron beams with 250–325 GeV polarized protons or 100–130 GeV / nucleon heavy-ion beams. The ultimate eRHIC luminosity per nucleon, achieved with lower hadron-beam emittances and with larger electron-beam currents than for the LHeC, is a factor 100–400 higher. In particular, eRHIC will employ a novel system of Coherent Electron Cooling (CEC) [7] to reduce the transverse and longitudinal emittances of the RHIC hadron beams, so that the normalized transverse emittances are about a factor 10 lower than those of the LHC. The enhanced space-charge tune shift requires a dedicated compensation by another electron beam [8]. For eRHIC, the total beam power loss, mainly due to synchrotron radiation, has been limited to about 10 MW. The ERL design offers a natural staging of the eRHIC facility where the beam energy is planned to be raised in steps as progressively additional SC cavities are installed and powered in the linac straights. The eRHIC physics program includes unraveling the origin of the proton spin, quantum phase space tomography of the nucleon, and the physics of strong color fields [9].

The luminosity of an ERL-ring collider can be written as

$$L = \frac{1}{4\pi e} \frac{N_{b,h}}{\varepsilon_h} \frac{1}{\beta_h^*} I_e H_{hg} H_D, \quad (1)$$

where e denotes the elementary charge, H_D the disruption enhancement factor ($H_D \approx 1.3$ for e^-p/A and $H_D \approx 0.3$ for e^+p/A collisions), and matched round colliding beams are considered. To obtain the maximum luminosity one aims for a large hadron bunch population $N_{b,h}$, a small geometric hadron-beam emittance ε (or large hadron-beam brightness $N_{b,h}/\varepsilon_h$), a small hadron beam interaction-point (IP) beta function β_h^* , a high geometric overlap factor H_{hg} (head-on collision, and small lepton beam emittance), and, provided by the ERL, a large lepton beam current I_e .

Table 1 compares parameters for the two projects. In case of the LHC the geometric emittances for proton and ion beams are the same, and correspond to the values available in present operation. The projected eRHIC hadron beam emittances are determined from the expected performance of the CEC system and from imposing consistent requirements for the space-charge compensation system. As a result, in the case of eRHIC it is the normalized, not the geometric emittances, which is the same for heavy-ion and proton beams.

LINACS, ARCS AND BEAM DYNAMICS

Both LHeC and eRHIC ERLs comprise two linacs. Their parameters are compared in Table 2. The LHeC linac is about 5 times longer and provides 4 times the energy gain, at comparable cavity voltage. The lower cavity filling factor for LHeC is partly due to the presence of about

PLASMAS, DIELECTRICS AND THE ULTRAFAS: FIRST SCIENCE AND OPERATIONAL EXPERIENCE AT FACET*

C.I. Clarke[†], E. Adli, S. Corde, F.J. Decker, R.J. England, R. Erickson, A. Fisher, S. Gessner, C. Hast, M.J. Hogan, S.Z. Li, N. Lipkowitz, M. Litos, Y. Nosochkov, J. Seeman, J.C. Sheppard, I. Tudosa, G. White, U. Wienands, M. Woodley, Z. Wu, G. Yocky, SLAC, Menlo Park, CA 94025, USA
C. Clayton, C. Joshi, W. Lu, K.A. Marsh, N. Vafaei, University of California, Los Angeles, USA

Abstract

FACET (Facility for Advanced Accelerator and Experimental Tests) is an accelerator R&D test facility that has been recently constructed at SLAC National Accelerator Laboratory. The facility provides 20 GeV, 3 nC electron beams, short (20 μm) bunches and small (20 μm wide) spot sizes, producing uniquely high power beams. FACET supports studies from many fields but in particular those of Plasma Wakefield Acceleration and Dielectric Wakefield Acceleration. FACET is also a source of THz radiation for material studies. We present the FACET design, initial operating experience and first science from the facility.

INTRODUCTION

Accelerators are our primary tool for discovering the fundamental laws to the universe. Each new frontier we probe requires a new, more powerful machine. Accelerators using conventional technologies are therefore increasing in size and cost. The future of this field will require new accelerating techniques that can reach the high energies required over shorter distances. New concepts for high gradient acceleration include utilizing the wakes in plasma and dielectric and metallic structures. FACET was built to provide a test bed for novel accelerating concepts with its high charge, highly compressed beams. As a test facility unlike any other, it has also attracted groups interested in beam diagnostic techniques and studies using terahertz radiation. In addition, the SLAC linac continues to offer opportunities to study conventional acceleration structures and accelerator physics.

FACET construction was completed in May 2011 and it became a United States Department of Energy User Facility for High Energy Physics in January 2012. FACET was commissioned and the first User Run took place over 12 weeks in 2012.

FACET has a five year program, operating four to five months every year through to 2016. Proposals are solicited every year and peer reviewed with the highest ranked experiments gaining beam time.

THE FACILITY

FACET delivers electron bunches to experiments with tightly focused transverse beam sizes and ultra-short bunch

*Work supported by the U.S. Department of Energy under contract number DE-AC02-76SF00515.

[†]cclarke@slac.stanford.edu

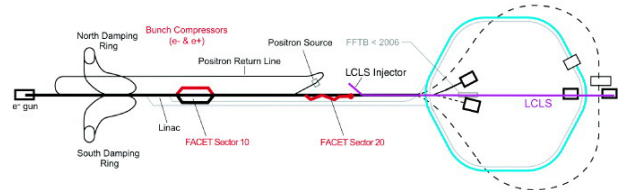


Figure 1: The SLAC linear accelerator and associated facilities. Two kilometers of s-band accelerating structures lead into FACET's final focus section. FACET's dump separates the first 20 sectors of the linac from the final 10 which are used by LCLS.

lengths. Positron bunches will be commissioned in 2013 for delivery to FACET experiments in 2014.

Multiple experiments share the same beam line and the waist of the beam is shifted according to the location of the experiment. The design parameters are given in Table 1 along with the best beam parameters that have been achieved during the 2012 user run and typical parameters that were delivered regularly.

Linear Accelerator

FACET uses the first two-thirds of the SLAC linac to accelerate electrons up to 20 GeV (Fig. 1). An extraction kicker after the accelerating structures can direct the electrons to either the FACET experimental area and dump or into a positron target. Positrons are generated at the target and boosted to 200 MeV. They are then transported to the start of the linac and accelerated such that they enter the positron damping ring at 1.2 GeV. The positrons are then accelerated to an energy above 20 GeV using the same beamline as the electrons.

Bunch Compression

Three stages of bunch compression deliver the ultra-short bunches (with a design value of σ_z of 17 μm or 57 fs) to FACET experiments.

The first stage of compression occurs on injection from the damping ring to the linac. The bunches are compressed from 5.5 mm in the damping ring to 1.5 mm in the linac.

The next stage was built in 2002 for the Sub-Picosecond Pulse Source (SPPS) to compress electron bunches further to $\sim 50 \mu\text{m}$. This is a magnetic chicane in Sector 10 of the linac. The positron arm of the chicane was built in March 2012 and is exactly symmetric to the electron chicane.

LINAC CONSTRUCTION FOR CHINA SPALLATION NEUTRON SOURCE

Shinian Fu, Jian Li, Huachang Liu, Huaifu Ouyang, Xuejun Yin, IHEP, Beijing 100049, China

Abstract

Construction of China Spallation Neutron Source (CSNS) has been launched in September 2011. CSNS accelerator will provide 100kW proton beam on a target at beam energy of 1.6GeV. It consists of an 80MeV H⁺ linac and 1.6GeV rapid cycling synchrotron. Based on the prototyping experience, CSNS linac, including the front end and four DTL tanks, has finalized the design and started procurement. In this paper, we will first present an outline of the CSNS accelerator in its design and construction plan. Then the some prototyping results of the linac will be presented. Finally the linac construction progress in recent will be updated.

foil, the RCS accumulates and accelerates the proton beam to 1.6 GeV before extracting it to the target.

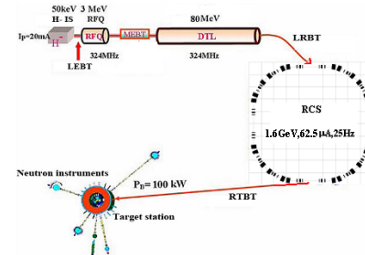


Figure 2: Schematics of the CSNS complex

INTRODUCTION

China Spallation Neutron Source(CSNS) project was approved by the Chinese central government in 2008[1-2]. It has been launched in September 2011. Figure 1 shows the linac tunnel construction status up to now. It is planed to provide neutrons to the users in the first half of 2018. CSNS has a total budget of \$260 M for construction of the accelerator, the spallation neutron target and 3 neutron spectrometers. Its site is at Dongguan, south part of China. The local government will support free land, additional budget of \$57M, infrastructure, dedicated high-way and power transformer station.



Figure 1: Civil construction status of the linac tunnel.

CSNS accelerator is the first large-scale, high-power accelerator project to be constructed in China. The CSNS is designed to accelerate proton beam pulses to 1.6 GeV kinetic energy at 25 Hz repetition rate, striking a solid metal target to produce spallation neutrons. The accelerator provides a beam power of 100 kW on the target in the first phase and then 500 kW in the second phase by increasing the average beam intensity 5 times while raising the linac output energy to 250 MeV. A schematic layout of CSNS phase-I complex is shown in Figure 2. The major design parameters of the CSNS accelerator complex for the two phases are listed in Table 1. In the phase-I, an H⁺ ion source produces a peak current of 25 mA H⁺ beam. RFQ linac bunches and accelerates it to 3 MeV. DTL linac raises the beam energy to 80 MeV. After H⁺ beam is converted to proton beam via a stripping

Table 1: CSNS Design Parameters

Project Phase	I	II
Beam power on target [kW]	100	500
Proton energy [GeV]	1.6	1.6
Average beam current [μ A]	62.5	312.5
Pulse repetition rate [Hz]	25	25
Linac energy [MeV]	80	250
Linac type	DTL	+SC Spoke
Linac RF frequency [MHz]	324	324
Macropulse. ave current [mA]	15	40
Macropulse duty factor	1.0	1.7
RCS circumference [m]	228	228
RCS harmonic number	2	2
RCS acceptance [π mm-mrad]	540	540

LINAC DESIGN AND DEVELOPMENT^[3]

Penning H⁺ ion source is adopted for CSNS linac. The source provides 25 mA peak current, 0.5 ms long, $0.2\pi\mu$ m normalized emittance (rms) pulses at 50 kV and 25 Hz repetition rate for Phase-I.

The LEBT is for matching and transporting the H⁺ beam from ion source to RFQ accelerator, and pre-chopping the beam according to the requested time structure by the RCS with a chopping rate of 50%. Three-solenoid focusing structure is adopted for space charge neutralization, as shown in Figure 3. An electrostatic deflector is chosen as pre-chopper, positioned at the end of the LEBT. A prototype pre-chopper was installed at the entrance of the 352MHz proton RFQ, and it reached a fast rise time of 15 ns in the beam measurement at the exit of the RFQ[4].

PERFORMANCE OF FERRITE VECTOR MODULATORS IN THE LLRF SYSTEM OF THE FERMILAB HINS 6-CAVITY TEST*

P. Varghese[†], B. Chase, E. Cullerton, C. Tan, B. Barnes
Fermi National Accelerator Laboratory (FNAL), Batavia, IL 60510, USA

Abstract

The High Intensity Neutrino Source (HINS) 6-cavity test is a part of the Fermilab HINS Linac R&D program for a low energy, high intensity proton/H- linear accelerator. One of the objectives of the 6-cavity test is to demonstrate the use of high power RF Ferrite Vector Modulators (FVM) for independent control of multiple cavities driven by a single klystron. The beamline includes an RFQ and six cavities. The LLRF system provides a primary feedback loop around the RFQ and the distribution of the regulated klystron output is controlled by secondary learning feed-forward loops on the FVMs for each of the six cavities. The feed-forward loops provide pulse to pulse correction to the current waveform profiles of the FVM power supplies to compensate for beam-loading and other disturbances. The learning feed-forward loops are shown to successfully control the amplitude and phase settings for the cavities well within the 1% and 1° requirements specified for the system.

INTRODUCTION

The use of FVMs to regulate the phase and amplitude of individual cavities in a multi-cavity system driven by a single klystron helps to reduce the cost of the RF system for linear accelerators[1]. High power waveguide FVMs have been developed and the dynamic range of their phase shifting and amplitude attenuating capabilities have been studied[2]. Modeling and simulation of RF control systems with FVMs have shown their potential for field control of individual cavities in a multi-cavity system[3]. A learning feed-forward[LFF] control for the HINS six cavity test accelerator was integrated into the LLRF system. All RF components are driven by a single 325 MHz, 2.5MW pulsed klystron. The LFF algorithm is described and the results of its performance with beam are presented.

LLRF SYSTEM

The RF control block diagram for the 6-cavity test is shown in Fig.1. The LLRF control system regulates the phase and amplitude of the RF field vectors of the RFQ and the six room temperature copper cavities. There is a traditional wide-band proportional and integral feedback control loop around the klystron and the RFQ. Because the RFQ is a low Q device, it behaves much like a resistive load. Therefore, by regulating the RFQ field, the klystron output to the six cavities is effectively regulated as well.

*Work supported by Fermi Research Alliance LLC. Under DE-AC02-07CH11359 with U.S. DOE.

[†]varghese@fnal.gov

This RFQ control loop greatly reduces errors from klystron modulator voltage variations and from changing beam current. There are several disturbances to the six cavities that must be corrected by the FVM controllers. These are static amplitude and phase errors, drifts in cavity resonance frequency, differences in cavity Qs, and variations in cavity beam loading. Field errors in the cavities are corrected by an adaptive feed-forward system.

The primary feed-back loop is implemented as a PI controller in a FPGA with a sampling frequency of 56 MHz. The 325MHz RF is downconverted to a 13 MHz IF which is sampled and downconverted to baseband. A 2.1 MSPS DAQ system acquires baseband I,Q signals for pulses up to 4ms wide. The data from all channels is uploaded to the slot0 controller between pulses and is available for processing in the CPU or for transmittal through an ethernet port to both the Fermilab ACNET control system and Labview user interfaces, for waveform display and parameter control.

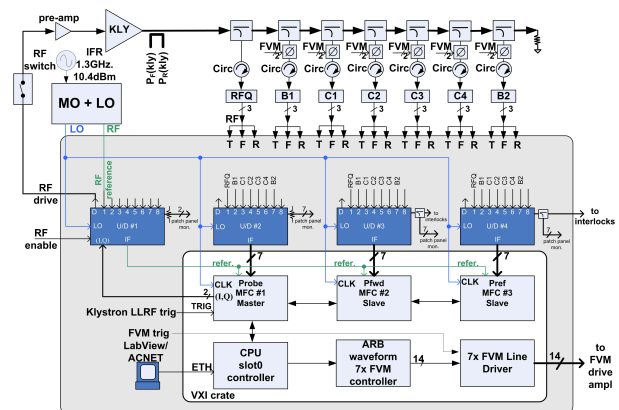


Figure 1: LLRF system configuration

LEARNING ALGORITHM

The learning feed-forward algorithm implementation for one cavity is shown in Fig.2. The wideband RFQ/klystron primary control loop is processed at the full 56 MHz sample rate of A/D converters, while the FVM control loops decimate the data to a 100 kHz rate, where it is processed and the feed-forward controller output is written to a VXI 16 channel arbitrary waveform generator module. Regulation waveforms are recalculated at the machine repetition rate of 0.5 Hz. Decimating the DAQ data by 21 brings the sample rate close to the 100 kHz sampling rate of the output DACs to the FVM. With 1024 points in the FVM waveform, the maximum width of the FVM profile is 10ms

FRONT-END LINAC DESIGN AND BEAM DYNAMICS SIMULATIONS FOR MYRRHA *

C. Zhang[#], H. Klein, D. Mäder, H. Podlech, U. Ratzinger, A. Schempp, R. Tiede, M. Vossberg
 Institut für Angewandte Physik, Goethe-Universität, D-60438 Frankfurt a. M., Germany

Abstract

A 17MeV, 176MHz, and CW (Continuous Wave) proton linac is being developed as the front end of the driver accelerator for the MYRRHA facility in Mol, Belgium. Based on the promising preliminary design, further simulation and optimization studies have been performed with respect to code benchmarking, RFQ simulation using realistic LEBT output distributions, and an updated CH-DTL design with more detailed inter-tank configurations. This paper summarizes the new results.

the Kilpatrick factor to $\leq 30\text{kW/m}$ and 1, respectively, for all warm cavities, even shortened the whole layout from 11.4m to 10.6m, and kept the beam dynamics performance satisfying. Being very conservative for CW operation and more cost-saving, this design has been taken as the baseline for further studies [5].

PRELIMINARY DESIGN

Following the EUROTRANS project [1], MAX [2] (MYRRHA Accelerator eXperiment research and development programme) is the ongoing European ADS (Accelerator-Driven System) project. For the front end of the driver linac, the EUROTRANS-style injector [3] that consists of one RFQ (Radio-Frequency Quadrupole), two RT (room-temperature) and four SC (superconducting) CH (Cross-bar H-mode)-DTL (Drift-Tube Linac) cavities will be still adopted, but with many new concepts [4].

The most important idea is to halve the RF frequency from 352MHz to 176MHz, which improves the RFQ shunt impedance significantly (see Fig. 1), enlarges the minimum gap between electrodes, and allows replacing the 4-vane RFQ structure by the simple 4-rod one. Consequently, for keeping the RFQ length at $\sim 4\text{m}$ and the warm part still compact, the RFQ-DTL and RT-SC transition energies are reduced from 3MeV and 5MeV to 1.5MeV and 3.5MeV, respectively, which indeed brings more difficulties to the beam dynamics design but helps improving the RT-CH shunt impedance.

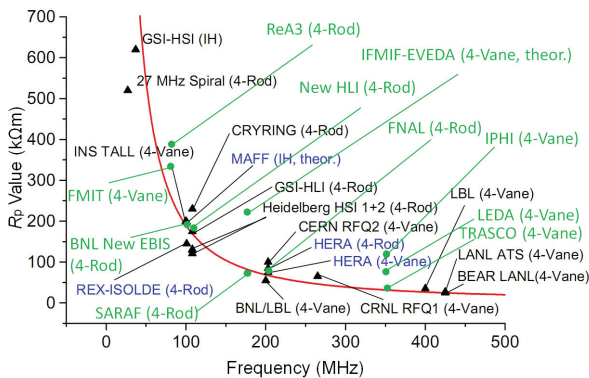


Figure 1: A survey of R_p values for RFQs [5].

From EUROTRANS to MAX, the injector design has lowered the RF power consumption per unit length and

* Funded by the European Atomic Energy Community's (Euratom) 7th Framework Programme under Grant Agreement n°269565.

[#] Chuan Zhang: zhang@iap.uni-frankfurt.de

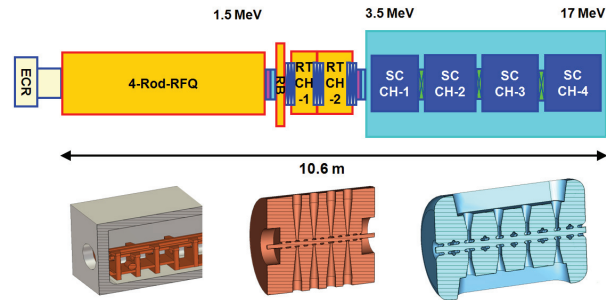


Figure 2: Preliminary layout for the MAX injector.

CODE BENCHMARKING

For the preliminary design of the MAX injector, the ParmteqM [6] and Lorasz [7] codes were used to simulate the beam transport in the RFQ and CH-DTL parts, respectively. Recently, the Toutatis [8] and TraceWin [8] codes have been introduced for benchmarking.

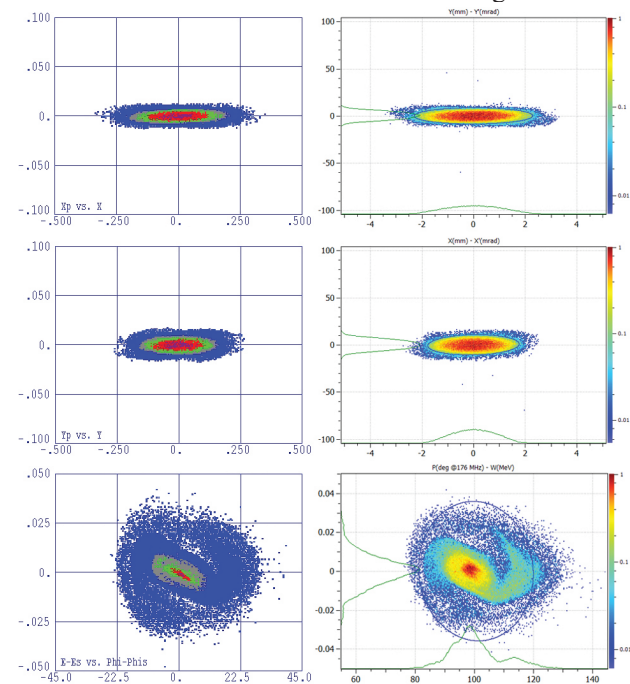


Figure 3: RFQ output particle distributions given by the ParmteqM (L) and Toutatis (R) codes.

Fig. 3 shows the RFQ output beams simulated by the ParmteqM and Toutatis codes. It's clear that the shape,

PRELIMINARY STUDY OF PROTON BEAM TRANSPORT IN A 10 MeV DIELECTRIC WALL ACCELERATOR*

J. Zhu[#], L.S. Xia, Y. Shen, W. Wang, H. Zhang, Y. Liu, S.F. Chen, W.D. Wang, J.S. Shi,
L.W. Zhang, J.J. Deng

Institute of Fluid Physics, CAEP, Mianyang, Sichuan, 621900, China

Abstract

A novel proton accelerator based on Dielectric Wall Accelerator (DWA) technology is being developed at Institute of Fluid Physics (IFP). The accelerating gradient will be 25 MV/m or even higher based on current high gradient insulator (HIG) performance. Theoretical study and numerical simulation of accelerating the proton beam to 10 MeV by virtual travelling wave method are presented in this paper. The beam injection at the DWA entrance is also discussed.

INTRODUCTION

The proton dielectric wall accelerator is being developed at Institute of Fluid Physics. The DWA system is a block structure which is similar to the linear induction accelerator. Each block of cell is consist of a ring-shape high gradient insulator, parallel-plate Blumlein pulse forming lines and photon conductive switches. To obtain the highest accelerating gradient, the DWA will be operated in the “virtual” travelling wave mode with the accelerating pulse as short as no more than 2 nanoseconds in the majority of the HGI tube [1]. These technologies are now being tested individually and will soon be tested integrally. The proton bunch will first be accelerated to 1 MeV with the accelerating gradient of about 20 MV/m and then upgraded to higher energy by adding more DWA cells. The accelerating gradient is also expected to be 25 MV/m or even higher, which is mainly determined by the performance of the HGI tube.

The major advantageous of a DWA system used for cancer treatment is that the total length of the system will be less than 3 meters so that it can be equipped in a single treatment room and the large and costly gantry can be neglected. Moreover, the energy, spot size of the proton bunch can be changed from shot-to-shot by adjusting the pulsed power system.

ION SOURCE AND LEBT

The layout of a 10-MeV DWA system is shown in Fig.1. It will start with a proton beam generated in an ECR ion source and extracted at about 40 keV. The main purpose of the LEBT is to transport the beam to the entrance of the DWA and match the injection requirements. Since a DWA system should be short and light enough to be rotated for intensity modulated proton therapy (IMPT), a two Einzel lens structure was chosen as

the LEBT system. The pulse width of the proton bunch generated by the ion source is expected to be much longer than the DWA requirement. A fast kicker system will be mounted at the exit of the LEBT. Most of the protons will be deflected and hit on the metal wall at the DWA entrance, and only a small part of protons is allowed to enter the DWA. Design and fabrication of the ion source and LEBT is performed by Institute of Heavy Ion Physics, Peking University.

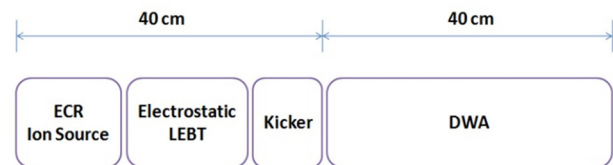


Figure 1: Layout of a 10 MeV DWA.

BEAM INJECTION

Generally, there is no any external focusing element or grid in the DWA system. The proton bunch is supposed to be focused to the downstream of the DWA by the radial electric field produced by the field gradient at the entrance [2]. The focusing effect is generally determined by the beam parameters, the accelerating gradient, the electric field and the time sequence. Chen [3] has demonstrated transporting a 2-MeV (injection energy) proton bunch in a 120-MeV DWA system at the accelerating gradient of 60 MV/m. For a 40-keV proton bunch, the radial electric field can easily cause the bunch pinching at the front of the DWA first and then defocusing. To demonstrate the focusing effect of the radial electric field at the entrance, the envelop equation

$$R'' = -\frac{\gamma'}{\gamma\beta^2} R' - \frac{\gamma''}{2\gamma\beta^2} R + \frac{K}{R} + \frac{\varepsilon_n^2}{\beta^2 \gamma^2 R^3} \quad (1)$$

for a 40-keV, 20-mA, 1-mm-mrad proton bunch at its waist is solved, where R , β , γ , ε_n and K is the beam's radius, velocity relative to the speed of light, Lorentz factor, normalized edge emittance and generalized perveance, respectively. We consider the case that the length of the DWA is 40 cm and the proton bunch rides on the flattop of the electric field (25 MV/m) except that there is a constant field gradient at the beginning 5 cm of the DWA. The proton bunch envelop as a function of the proton energy is plotted in Fig.2 (a). It is obvious that the focal spot of the beam will move upstream as the proton energy decreases. The focal spot of proton bunch with 2-MeV injection energy just locates at the end of the drift

*Work supported by National Natural Science Foundation of China (11035004) and Nuclear Energy Development Project of State Administration of Science, Technology and Industry for National Defence

#zhujun98@tsinghua.org.cn

ISBN 978-3-95450-122-9

R&D ACTIVITIES ON HIGH INTENSITY SUPERCONDUCTING PROTON LINAC AT RRCAT

S.C. Joshi, S.B. Roy, P.R. Hannurkar, P. Kush, A. Puntambekar, P. Shrivastava, G. Mundra, J. Dwivedi, P. Khare, P.D. Gupta, Raja Ramanna Centre for Advanced Technology, Indore, India

Abstract

Raja Ramanna Centre for Advanced Technology (RRCAT), Indore has taken up a program on R&D activities of 1 GeV, high intensity superconducting proton linac for Spallation Neutron Source. This will require several multi-cell superconducting cavities operating at different RF frequencies. To start with, a number of single-cell prototype cavities at 1.3 GHz have been developed in high RRR bulk niobium. These single-cell cavities have exhibited high quality factor and accelerating gradients. Superconducting properties of niobium are being studied for varying composition of impurities and different processing conditions. Physics design of linac configuration and various accelerating structures have been initiated. Development activities on cryomodules, cavity test facilities and solid state RF amplifiers to power the SRF cavities at various RF frequencies are being pursued. Infrastructure setup required for SRF cavity fabrication, processing and testing is under progress at RRCAT.

INTRODUCTION

A programme is envisaged to develop a pulsed, MW range Spallation Neutron Source based on 1 GeV, 1 MW superconducting RF H- Ion linac, a full-energy injector for a 1GeV Accumulator Ring. The pulsed Spallation Neutron Source will be used for applications in the field of condensed matter physics, material sciences, chemistry, biology and engineering. In addition to setting up of SNS facility, it will enhance capacity building in the area of high intensity proton accelerators in India.

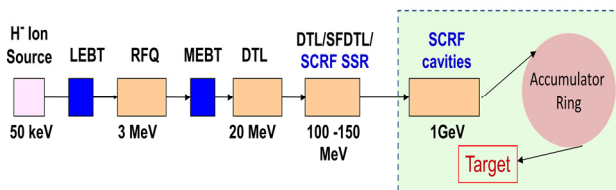


Figure 1. Schematic of Pulsed Proton Linac for Indian Spallation Neutron Source.

R&D ACTIVITIES

R&D activities for a SRF linac and accumulator ring for SNS would include prototype development of various sub-systems and setting up of infrastructure in the following areas:

- Ion source and front end component
- Materials R&D, cavity & cryomodule development

- Niobium cavity fabrication and processing facility
- Test facility for large number of SRF cavities and cryomodules
- Cryogenics setup for large size LHe Plant & supply network
- RF power sources and control electronics
- Sub-systems for 1 GeV accumulator ring including magnets, power supplies, RF cavity, UHV system and controls
- Manpower development and training

Ion Source and Front End

Development of a 3 MeV H- ion linac front end has been initiated for 1 GeV proton accelerators for a pulsed Spallation Neutron Source [1]. The front-end system will comprise of a filament driven multi-cusp H- ion source, Low Energy Beam Transport (LEBT) system, Radio Frequency Quadrupole (RFQ), RF power sources, Controls, Beam dump and Beam diagnostics.

H- Ion Source: In order to meet the requirement of H- ion front end linac system, a multicusp filament based 50 keV, 30 mA, low emittance H- ion-source operating in pulsed mode with a repetition rate of 25 Hz has been initiated. Physics design of the multicusp source was carried out analytically and also using computer simulations based on finite element method. This system has recently been tested for extraction of hydrogen ion current of 1.0 mA at 15 kV accelerating field. Figure 2, shows the multi-cusp H- ion source system.

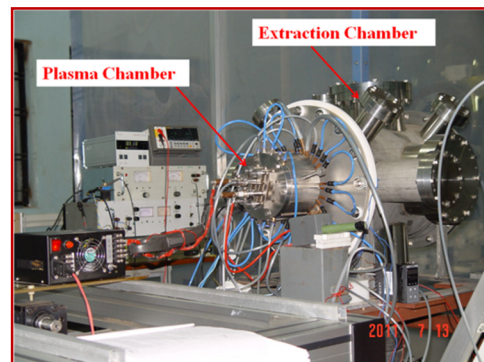


Figure 2. Prototype multi-cusp filament based source pulsed H- ion source.

LEBT and RFQ: For prototype studies, design has been carried out for a suitable LEBT for beam transport from Ion Source to RFQ and a 3 MeV, 352 MHz RFQ. A Low Energy Beam Transport (LEBT) line, consisting of solenoid magnets of maximum strength 3.5 kG and steering coils having a maximum field of 100 G has been

THE NEW OPTION OF FRONT END OF ION LINAC

A. Kovalenko, JINR, Dubna, Russia

A. Kolomiets, ITEP, Moscow, Russia

Abstract

The standard set of elements consisting of RFQ, two tanks of accelerating IH-structures, external matching and focusing sections is modified to achieve better performances. Special insertions corresponding to buncher and quadrupole triplet are combined within the RFQ tank, whereas superconducting focusing elements are installed between the DTL - structure tanks. Simulation of the system parameters was performed to provide the output beam energy of 5 MeV/u for the ions with charge - to - mass ratio of $0.33 \leq Z/A \leq 1$. Possible application of the considered scheme for the NICA facility at JINR (Dubna, Russia) is discussed.

INTRODUCTION

The work was motivated by our desire to find optimal way of the constructing linear accelerator chain aimed at injection of light ions and protons for the NICA complex at JINR [1] and also for other applications, in particular for the future carbon/proton superconducting (SC) medical synchrotrons [2].

The physics research program at NICA [3] requests the beams of heavy and light ions, protons, polarized deuterons and protons as well. The facility is based on the existing SC synchrotron - Nuclotron that is in operation since 1993 [4] and that was upgraded in 2008-2010[5]. The accelerator complex will include also two separate injection chains, 25 T-m SC booster synchrotron, the collider SC rings, beam transfer channels. The collider will provide heavy ion collisions of average luminosity of $10^{27} \text{cm}^{-2} \text{s}^{-1}$ at the energies of $\sqrt{s_{NN}} \sim (4 - 11) \text{ GeV}$. The collider detector MPD is scheduled for starting data taken in 2017. The fixed target experiment Baryonic Matter at Nuclotron (BM@N) is planned to start data taking in 2015 in the beam of gold ions extracted from the Nuclotron. The NICA will provide polarized proton and deuteron collisions up to $\sqrt{s} = 26 \text{ GeV}$ and 12.5 GeV/u , respectively, with the average luminosity of $10^{31} \text{cm}^{-2} \text{s}^{-1}$.

The two injection chains aimed at heavy ions and protons/light ions (including polarized ones) injection contain respectively the following: high charge state heavy ion source → the new heavy ion linac → SC booster → Nuclotron → collider and the sources of protons, deuterons (including polarized) and light ions → upgraded existing linac LU-20 → Nuclotron → Collider.

The Alvarez type proton linac LU-20 was commissioned in 1974. At the present time LU-20 provides proton beam with energy 20 MeV and light ions ($Z/A \geq 1/3$) up to 5 MeV/u. The LU-20 planned upgrade includes, at the first stage, replacement of old high voltage preinjector by the new one having much lower voltage of the ion source platform ($U = 100 \text{ kV}$) and the

use of RFQ to provide the ion energy required for injection to LU-20.

It is clear, however, that use of LU-20 for acceleration of ions heavier than protons is not very efficient. Moreover it would be very risky to expect reliable operation of the old linac in the coming decades even in the case of complete and very expensive replacement of the drift tubes containing quadrupoles inside.

The main goal of the work is design of compact and efficient linac that can be considered as an option of light ion injector for NICA project.

LIGHT ION INJECTOR

General Layout

Particles that will be accelerated in this device are protons, deuterons (including polarized) and other ions with charge - to - mass ratio of $1/3 \leq Z/A \leq 1/2$, in particular $^{12}\text{C}^{6+}$ and $^{12}\text{C}^{4+}$ as well. The specified values of the beam currents and the expected transverse emittance define the choice of the injector layout and basic parameters of its accelerating structures. After analysis of different possibilities, the scheme shown in Figure 1 is proposed.



Figure 1: Structural scheme of the NICA injector of light and polarized ions. (IS – ion sources)/

Initial part is a combination of RFQ and the DTL that was designed following the idea proposed in [6]. This combination allows to form at output of initial part beam parameters required for injection to DTL 1 and to exclude MEFT with focusing and rf elements for beam matching between RFQ and DTL 1.

DTL 1 and DTL 2 are designed for acceleration of ions with $Z/A = 0.33$ up to final energy 5 MeV/u. DTL 3 is aimed only for proton acceleration and has to be switched off in the other cases.

Superconducting solenoids are used for beam focusing between DTL sections. It allows reducing drift space between cavities and improving longitudinal beam dynamics. Application of superconducting elements in the proposed new injector is logically follows from the NICA basic technology concept and the advanced level of cryogenics in the Laboratory of High Energy Physics.

RFQ

The RFQ is based on a resonant structure with coupling windows developed in ITEP for TWAC facility injector [7]. The main attention at the design stage was devoted to

EXPERIENCE WITH A 4-ROD CW RADIO FREQUENCY QUADRUPOLE

P. Gerhard*, W. Barth, L. Dahl, W. Hartmann, G. Schreiber, W. Vinzenz, H. Vormann
 GSI Helmholtzzentrum f. Schwerionenforschung mbH (GSI), 64291 Darmstadt, Germany

Abstract

The High Charge State Injector (HLI) provides heavy ion beams for the linear accelerator UNILAC at GSI [1]. After 20 years of successful operation its four-rod Radio Frequency Quadrupole (RFQ) was replaced in 2010 [2]. Besides higher beam transmission, the principal intention of this upgrade was to raise the duty factor up to 100%. Commissioning and operational experience from the first years revealed that this goal could not be reached easily. After serious problems with melting of rf contacts were overcome, operation is still restricted. There is strong, modulated rf power reflection, most likely due to mechanical instabilities of the structure. In this paper we present the RFQ design, commissioning results, operational experience and future activities.

INTRODUCTION

The HLI is equipped with an ECR ion source and an RFQ-IH linac which accelerates highly charged ion beams with high duty factor of up to 30% to 1.4 MeV/u for further acceleration in the Alvarez DTL of the UNILAC. Since 1991 main user of these beams is the Super Heavy Element (SHE) research, one of the outstanding projects at GSI [3]. Experiments like TASCAs and SHIP strongly benefit from the high average beam intensities. A dedicated cw linac for SHE research at GSI is seriously proposed, with the HLI as its injector. The existing HLI is not designed for cw operation. The replacement of the RFQ in 2010 was the first step towards a cw capable injector.

DESIGN & COMMISSIONING

Due to the high average rf power caused by the cw operation, all parts of the new 4-rod RFQ (electrodes, stems, tuning plates, plungers and coupling loop) had to be directly water cooled. This results in 72 connections and vacuum feedthroughs for cooling water, equipped with pre-vacuum sealing, making the mechanical engineering rather complex. More design properties are given in Tab. 1.

Table 1: Design properties of the new HLI RFQ.

Injection / extraction energy [keV/u]	2.5 / 300
RF frequency [MHz]	108.408
A/q (cw / max.)	6.0 / 8.5
Power (max. avg. / max. pulse) [kW]	60 / 120
Intervane voltage (cw / max.) [kV]	55 / 78
RMS emittance in / out [π mm mrad]	0.1 / 0.1009
Electrode length [m]	2.0

* p.gerhard@gsi.de

The new RFQ was delivered to GSI in autumn 2009. RF and beam commissioning was finished in spring 2010. Achievement of the design beam parameters (transmission, energy, emittance) could be demonstrated (Fig. 1 and [4]). Extensive beam measurements at different locations of the HLI beam line were performed.

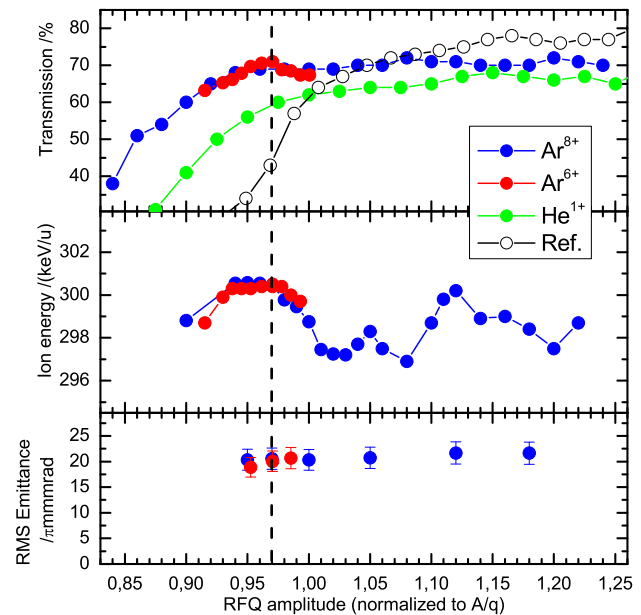


Figure 1: Beam commissioning results (top to bottom): Transmission, ion energy and beam emittance for different ions as a function of the rf amplitude, normalized to the mass-to-charge ratio. Reference data: Old RFQ; dashed line: Derived working point.

THERMAL ASPECTS

During rf commissioning two issues were discovered:

- Insufficient rf contact springs and
- the thermal instability of the 4-rod structure.

Rf contact springs

Several breakdowns of contact springs between the tuning plates and the stems occurred at rf power levels far below the design (s. Fig. 2). The first burning occurred at 16 kW avg. power, possibly due to incorrect mounting of the springs. After two breakdowns, complete renewal with more robust contacts and careful mounting was employed. Nevertheless, damages were found after operation at 24 and 30 kW. Obviously this type of contacts could not handle enough power safely in routine operation. Therefore it was decided to introduce a different contact mechanism using

HIGH-POWER RF CONDITIONING OF THE TRASCO RFQ

E. Fagotti, L. Antoniazzi, A. Palmieri, F. Grespan, , INFN-LNL, Legnaro, ITALY
M. Desmons, CEA, Saclay, FRANCE

Abstract

The TRASCO RFQ is designed to accelerate a 40 mA proton beam up to 5 MeV. It is a CW machine which has to show stable operation and provide the requested availability. It is composed of three electromagnetic segment coupled via two coupling cells. Each segment is divided into two 1.2 m long OFE copper modules. The RFQ is fed through eight loop-based power couplers to deliver RF to the cavity from a 352.2 MHz, 1.3 MW klystron. After couplers conditioning, the first electromagnetic segment was successfully tested at full power. RFQ cavity reached the nominal 68 kV inter-vane voltage (1.8 Kilp.) in CW operation. Moreover, during conditioning in pulsed operation, it was possible to reach 83 kV inter-vane voltage (2.2 Kilp.) with a 0.1% duty cycle. The description of the experimental setup and procedure, as well as the main results of the conditioning procedure will be reported in this paper.

EXPERIMENTAL SETUP

The test was performed at CEA Saclay in January, February and March 2012.

The systems involved in the test are:

- RFQ cavity
- RFQ power system
- Vacuum system
- Cooling system
- Control system

The cavity under test is the first electromagnetic segment of the TRASCO RFQ [1], composed by two 1.2 m long OFE copper modules. The first module accommodates 12 gridded vacuum ports, the second one the 2 coupler ports. The RFQ end plates are equipped with dipole stabilizers [2, 3]. RFQ power level and field flatness are monitored by 16 pick-up loops, located inside the tuners along the 4 quadrants. The preservation of field flatness was verified looking at the pick-up signals, after transportation and positioning inside the CEA tunnel (Figure 1).

The core of the RF power system is the CEA 1.3 MW klystron, protected from the reverse power by a 1 MW circulator. The RF power is led into the RFQ tunnel through full-height WR2300 waveguide and then it is tapered to half-height WR2300 for the final distribution to the RFQ. Just upstream the RFQ, the RF power is split by a magic-TEE: two waveguide arms are coupled into the RFQ through 2 coupling loops, the 4th arm goes to a 100 kW water load. Forward and reverse powers are measured by directional couplers in the two waveguide arms before power couplers.

The vacuum system is composed by a dry primary pump, a turbo pump and two cryogenic pumps. The

system was designed to maintain a pressure level $P \leq 1.3 \times 10^{-6}$ mbar under proton gas load. In particular, cryogenic pumps are unnecessary in absence of proton beam and they have not been used for this test. Vacuum gauges are located above couplers and on the vacuum manifold. Gate valves and nitrogen filling channel allow keeping the cavity in inert atmosphere during transports.

Cooling system is designed to remove 300 kW of power and to finely tune the resonant frequency by temperature regulation. For this purpose, it is necessary to have two independent water loops with two regulating temperatures. In the cooling skid, the temperature of each water circuit can be regulated by mixing the cold inlet water with part of the warm water coming from the cavity. Furthermore, the global temperature of the system can be adjusted by regulating the amount of warm water circulating in the heat exchanger. Water flow inside RFQ cooling channel is finely set by flow regulating valves located on each cooling channel. These valves maintain the required flow within $\pm 2\%$ when input pressure varies in the range 1-10 bar. Water flows and input/output temperatures of both water loops are monitored.

Control system [4] is connected to the other subsystems in order to monitor their characteristic parameters (temperature, powers, water flows, pressures), to command their actuators (valves, pumps) and set-up variables (interlock thresholds, water temperatures). In particular, interlocks on temperature, pressure, water flow, forward power are processed by PLC (response time = 10 ms), while arc detectors and reflected power are directly sent to klystron to interrupt power in a few μ s.

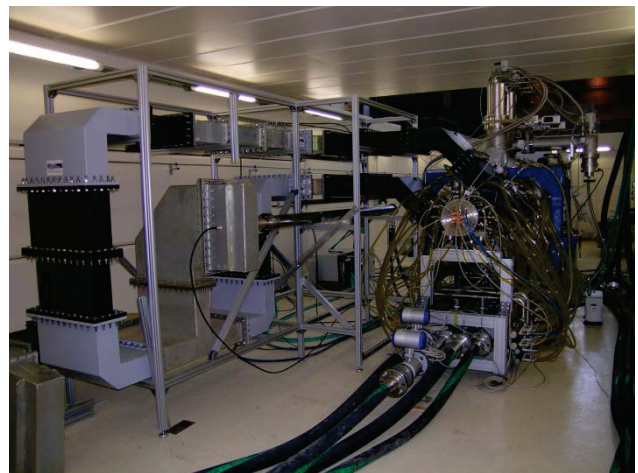


Figure 1: A view of TRASCO RFQ test in the IFMIF tunnel at CEA.

STATUS OF E-XFEL STRING AND CRYOMODULE ASSEMBLY AT CEA-SACLAY

C. Madec, S. Berry, P. Charon, J.-P. Charrier, C. Cloué, A. Daël, M. Fontaine, O. Napoly, N. Sacépé, C. Simon, B. Visentin, A. Brasseur, Y. Gasser, S. Langlois, R. Legros, G. Monnereau, J.-L. Perrin, D. Roudier, Y. Sauce, T. Vacher, CEA/Irfu, Gif-sur-Yvette, France

Abstract

As In-Kind contributor to the E-XFEL project, CEA is committed to the integration on the Saclay site of the 100 cryomodules (CM) of the superconducting linac as well as to the procurement of the magnetic shieldings, superinsulation blankets and 31 cold beam position monitors (BPM) of the re-entrant type. The assembly infrastructure has been renovated from the previous Saturne Synchrotron Laboratory facility: it includes a 200 m² clean room complex with 112 m² under ISO4, 1325 m² of assembly platforms and 400 m² of storage area. In parallel, CEA has conducted industrial studies and three cryomodule assembly prototyping both aiming at preparing the industrial file, the quality management system and the commissioning of the assembly plant, tooling and control equipment. In 2012, the contract of the integration has been awarded to ALSYOM. The paper will summarize the outputs of the preparation and prototyping phases and the status of the up-coming industrial phase.

INTRODUCTION

The 17.5 GeV superconducting RF linac of the E-XFEL project [1] will comprise 100 cryomodules (cf fig.1), after the injector module. These twelve-meter long cryomodules, deriving from the FLASH technology, include a string of eight 1.3 GHz RF cavities with an average gradient of 24 MV/m, followed by a BPM and a superconducting quadrupole.

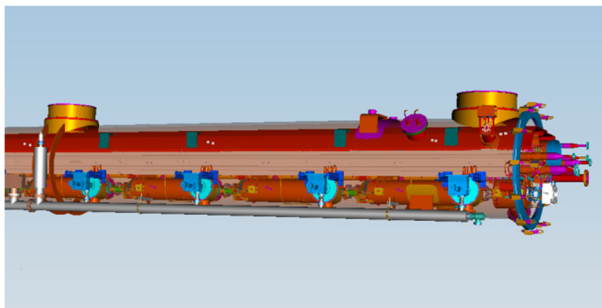


Figure 1: XFEL Cryomodule 3D-model

This string is closed by two gate valves at both ends. Within the Accelerator Consortium (AC), CEA is committed to the assembly of the 103 cryomodules over 2013 to mid-2015 with the goal to deliver one cryomodule per week to DESY for RF acceptance. Strategic decisions, shared by the AC, were taken in 2008 first to host the assembly plant on CEA premises at Saclay, using the former Saturne Synchrotron Laboratory

accelerator and experimental halls, second to subcontract the 103 modules, assembly work, including 3 pre-series modules, to an industrial company for. The layout of the assembly plant (see Fig. 2), was optimized by breaking down the assembly work in seven successive blocks of one-week procedures, leading to one clean room complex for coupler and string assembly, and five cryostating workstations for the remaining cryostating work, including alignment and control operations. To allow for a fluid circulation of the cryomodules along the assembly chain even when a repair is needed at one workstation, each workstation, but the vacuum vessel cantilever (see Fig. 3), has been doubled to offer module parking possibilities.

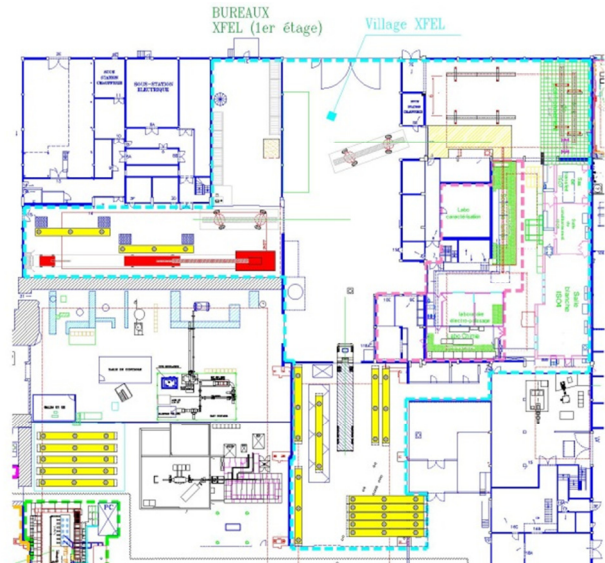


Figure 2: Layout of the XFEL infrastructure



Figure 3: Vacuum vessel and cold mass on the cantilever

OUTPUTS FROM THE PREPARATION PHASE

To ensure the integration of 103 CM at the rate of one cryomodule per week, CEA has set up a program to form

EXPERIMENTAL AND SIMULATION STUDY OF THE LONG-PATH-LENGTH DYNAMICS OF A SPACE-CHARGE-DOMINATED BUNCH*

I. Haber, B. L. Beaudoin, S. Bernal, R. A. Kishek, T. W. Koeth, Y. C. Mo
University of Maryland, College Park, MD 20742, USA

Abstract

The University of Maryland Electron Ring (UMER) is a low-energy (10 KeV) electron facility built to study, on a scaled machine, the long-propagation-length evolution of a space-charge-dominated beam. Though constructed in a ring geometry to achieve a long path length at modest cost, UMER has observed important space-charge physics directly relevant to linear machines. Examples are presented that emphasize studies of the longitudinal dynamics and comparisons to axisymmetric simulations. The detailed agreement obtained between axisymmetric simulation and experiment is presented as evidence that the longitudinal physics observed is not strongly influenced by the ring geometry. Novel phenomena such as soliton formation, unimpeded bunch-end interpenetration, and an instability that occurs after this interpenetration, are discussed.

BACKGROUND

The University of Maryland has had a long-standing program, inspired and nurtured by the late Prof. Martin Reiser, of using electron beams to conduct research, on a scaled basis, into the fundamental physics of intense charged particle beams when the beam evolution is dominated by the influence of space charge. An important and continuing element of this research has been its emphasis on comparison of theory and simulation to experiment. The early successes achieved are a strong motivation for the current research.

During the early years, the primary experimental facility was a 240 mA, 5 KeV electron beam injected into a transport system that consisted of 38 discrete iron core solenoid magnets, placed 13.6 cm apart [1]. Particle-in-cell (PIC) simulations [2] that carefully modelled the iron core solenoids [3] were successful in reproducing, in detail, experimentally observed behavior. The influence of space charge on beam characteristics such as emittance growth in the presence of misalignments and small errors in the initial match [4] were quantitatively reproduced and explained.

A significant milestone in simulation/experiment benchmarking [5] was achieved in an experiment where a mask was placed immediately downstream of the electron gun to produce a five beamlet pattern. This experiment was performed to test the theory that a nonuniform transverse current profile will relax to the lowest-potential-energy uniform profile. The excess energy would be converted to kinetic energy, causing the beam

emittance to grow [6]. Agreement was obtained on the emittance growth between experiment and simulation and theory.

An unexpected downstream re-emergence of the initial five-beamlet pattern was observed on a series of downstream phosphor screen images. Furthermore, the image evolution was reproduced in striking detail in simulation. The simulations assumed uniform emission from the gun with the intrinsic emittance calculated from the cathode temperature and employed no adjustable free parameters. In addition, evolution of the current cross-section was sufficiently sensitive to the initial emittance that only a few percent variation in the initial emittance assumed in the simulation resulted in a noticeable deviation from the experimentally observed patterns. Comparison between simulation and experiment could therefore be used to deduce beam emittance.

To study conversion of the space charge potential energy in a mismatch to kinetic energy, an additional series of experiments was performed where the beam was purposely mismatched. Theoretical predictions of the energy exchange were verified. However, unlike the matched beamlet case where a final distribution with a uniform cross section was observed, the extra kinetic energy was transferred mostly to a beam halo [7].

Additional experiments were also conducted to test longitudinal beam dynamics. Generally good agreement between theory and experiment was also obtained [8]. In investigating both transverse and longitudinal dynamics, many experiments were conducted that validated both theoretical predictions of the physics of the evolution of space-charge dominated beams, as well as, the ability of simulations to predict the observed behavior. However, because of the limited length of the linear transport line, it was not possible to address many significant questions about the physics of space-charge-dominated beams. For example, what are the characteristic of the equilibrium distribution that is reached after long time relaxation of a space-charge-dominated beam? In addition, many questions concerning the longitudinal dynamics, which have a much slower evolution time than the transverse dynamics are inaccessible in a short linear transport system.

UNIVERSITY OF MARYLAND ELECTRON RING (UMER)

Ring Description

In order to address the long pathlength physics of a space charge dominated beam, while remaining within the available space and budgetary limits, the University of Maryland Electron Ring (UMER) was constructed. A

*Work supported by the United States Department of Energy and the Office of Naval Research.

PHOTOINJECTOR SRF CAVITY DEVELOPMENT FOR BERLinPro *

A. Neumann[†], W. Anders, T. Kamps,
 J. Knobloch - Helmholtz-Zentrum Berlin, Berlin, Germany
 E. Zaplatin - FZJ Jülich, Jülich, Germany

Abstract

In 2010 HZB has received approval to build BERLinPro, an ERL project to demonstrate energy recovery at 100 mA beam current by perturbing a high quality beam. These goals place stringent requirements on the SRF cavity for the photoinjector which has to deliver a small emittance 100 mA beam with at least 1.8 MeV kinetic energy while limited by fundamental power coupler performance to about 230 kW forward power. In order to achieve these goals the injector cavity is being developed in a three stage approach. The current design studies focus on implementing a normal conducting cathode insert into a newly developed superconducting photoinjector cavity. In this paper the fundamental RF design calculations concerning cell shape for optimized beam dynamics as well as SRF performance will be presented. Further studies concentrate on HOM properties, the field-flatness and tuning mechanism for that design.

REQUIREMENTS TO THE CAVITY DESIGN

The BERLinPro ERL will be a prototype facility demonstrating energy recovery with a 100 mA beam at 50 MeV beam energy while preserving a normalized emittance of better than 1 mm mrad at a pulse length of 2 ps or less [1]. This machine will make fully use of superconducting RF technology operated in continuous wave (CW). The injec-

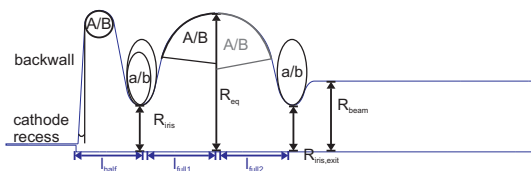


Figure 1: Geometry design parameters used for the cavity optimization scheme.

tor has to deliver a high brightness beam at a high repetition rate, filling every RF bucket, a low emittance allowing for emittance compensation and a compression of the longitudinal phase space in the ps regime. At this high average current also higher order mode excitation and damping have to be considered as well as coupling strongly to the fundamental. The high beam brightness will be achieved by inserting a high quantum efficiency normal conducting semi-conductor cathode within the SC environment of the

cavity. This cathode insert will mainly rely on the design by HZDR used in the ELBE SC 3.5 cell injector cavity [2]. As these are demanding goals, the injector and cavity are developed in a three stage approach. First results of an all superconducting gun cavity with a SC lead cathode were published in [5][6].

RF DESIGN STUDIES

The gun cavity has to fulfill several objectives while limited by some fundamental boundary conditions. The available total power will be limited to about 230 kW by using two KEK-style [3] fundamental power couplers (FPC), whereas the maximum electric peak field E_{peak} was recently demonstrated to reach 45 MV/m [4]. To name a few, regarding SRF and beam based properties the injector cavity has to be designed regarding the following aspects:

- Minimize E_{peak}/E_0 with $E_{cathode} < E_0$: This maximizes the field during beam extraction $E_{launch} = E_{cathode} \cdot \sin \Phi$ compared to the field anywhere on the surface E_{peak} , while it might be helpful to have the maximum on-axis field E_0 away from the cathode to reduce the probability of dark current.
- Minimize H_{peak}/E_{peak} and maximize R/Q to minimize losses. Consider the cutoff of the beam tube and iris diameter for a compromise between R/Q and HOM propagation and cell-to-cell coupling.
- The resonators length determines the launch phase Φ and field level during emission and thus energy gain and emittance. Thereby it also defines the field level for the field emitted dark current at about $\Phi = 90 \pm 20$ degrees.
- Transverse beam properties are influenced by the field during emission (>10 MV/m [7]) as by the transverse focussing due to e.g. retraction of the cathode, back-wall inclination and the transverse field component when the bunch leaves the RF structure.

Figure 1 shows the geometric parameters used in this work to run different optimization steps to converge to a suitable design. The design iteration was done by implementing different optimization schemes, like golden section search and Nead-Melder Simplex algorithms within a MATLABTM wrapper to run the 2-D RF field solver Superfish [8]. The obtained fields were used in the same loop to perform a first field-phase scan of the longitudinal phase space using a simple self written tracking code. Following, a set of candidates were included in ASTRA-based [9] beam dynamics simulations including the solenoid or the whole injector

* Work supported by Bundesministerium für Bildung und Forschung and Land Berlin

[†] Axel.Neumann@helmholtz-berlin.de

PRELIMINARY STUDY OF PROTON BEAM TRANSPORT IN A 10 MeV DIELECTRIC WALL ACCELERATOR*

J. Zhu[#], L.S. Xia, Y. Shen, W. Wang, H. Zhang, Y. Liu, S.F. Chen, W.D. Wang, J.S. Shi,
L.W. Zhang, J.J. Deng

Institute of Fluid Physics, CAEP, Mianyang, Sichuan, 621900, China

Abstract

A novel proton accelerator based on Dielectric Wall Accelerator (DWA) technology is being developed at Institute of Fluid Physics (IFP). The accelerating gradient will be 25 MV/m or even higher based on current high gradient insulator (HIG) performance. Theoretical study and numerical simulation of accelerating the proton beam to 10 MeV by virtual travelling wave method are presented in this paper. The beam injection at the DWA entrance is also discussed.

INTRODUCTION

The proton dielectric wall accelerator is being developed at Institute of Fluid Physics. The DWA system is a block structure which is similar to the linear induction accelerator. Each block of cell is consist of a ring-shape high gradient insulator, parallel-plate Blumlein pulse forming lines and photon conductive switches. To obtain the highest accelerating gradient, the DWA will be operated in the “virtual” travelling wave mode with the accelerating pulse as short as no more than 2 nanoseconds in the majority of the HGI tube [1]. These technologies are now being tested individually and will soon be tested integrally. The proton bunch will first be accelerated to 1 MeV with the accelerating gradient of about 20 MV/m and then upgraded to higher energy by adding more DWA cells. The accelerating gradient is also expected to be 25 MV/m or even higher, which is mainly determined by the performance of the HGI tube.

The major advantageous of a DWA system used for cancer treatment is that the total length of the system will be less than 3 meters so that it can be equipped in a single treatment room and the large and costly gantry can be neglected. Moreover, the energy, spot size of the proton bunch can be changed from shot-to-shot by adjusting the pulsed power system.

ION SOURCE AND LEBT

The layout of a 10-MeV DWA system is shown in Fig.1. It will start with a proton beam generated in an ECR ion source and extracted at about 40 keV. The main purpose of the LEBT is to transport the beam to the entrance of the DWA and match the injection requirements. Since a DWA system should be short and light enough to be rotated for intensity modulated proton therapy (IMPT), a two Einzel lens structure was chosen as

the LEBT system. The pulse width of the proton bunch generated by the ion source is expected to be much longer than the DWA requirement. A fast kicker system will be mounted at the exit of the LEBT. Most of the protons will be deflected and hit on the metal wall at the DWA entrance, and only a small part of protons is allowed to enter the DWA. Design and fabrication of the ion source and LEBT is performed by Institute of Heavy Ion Physics, Peking University.

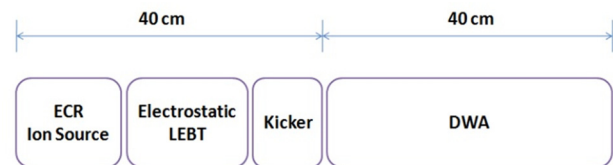


Figure 1: Layout of a 10 MeV DWA.

BEAM INJECTION

Generally, there is no any external focusing element or grid in the DWA system. The proton bunch is supposed to be focused to the downstream of the DWA by the radial electric field produced by the field gradient at the entrance [2]. The focusing effect is generally determined by the beam parameters, the accelerating gradient, the electric field and the time sequence. Chen [3] has demonstrated transporting a 2-MeV (injection energy) proton bunch in a 120-MeV DWA system at the accelerating gradient of 60 MV/m. For a 40-keV proton bunch, the radial electric field can easily cause the bunch pinching at the front of the DWA first and then defocusing. To demonstrate the focusing effect of the radial electric field at the entrance, the envelop equation

$$R'' = -\frac{\gamma'}{\gamma\beta^2} R' - \frac{\gamma''}{2\gamma\beta^2} R + \frac{K}{R} + \frac{\varepsilon_n^2}{\beta^2 \gamma^2 R^3} \quad (1)$$

for a 40-keV, 20-mA, 1-mm-mrad proton bunch at its waist is solved, where R , β , γ , ε_n and K is the beam's radius, velocity relative to the speed of light, Lorentz factor, normalized edge emittance and generalized perveance, respectively. We consider the case that the length of the DWA is 40 cm and the proton bunch rides on the flattop of the electric field (25 MV/m) except that there is a constant field gradient at the beginning 5 cm of the DWA. The proton bunch envelop as a function of the proton energy is plotted in Fig.2 (a). It is obvious that the focal spot of the beam will move upstream as the proton energy decreases. The focal spot of proton bunch with 2-MeV injection energy just locates at the end of the drift

*Work supported by National Natural Science Foundation of China (11035004) and Nuclear Energy Development Project of State Administration of Science, Technology and Industry for National Defence

#zhujun98@tsinghua.org.cn

ISBN 978-3-95450-122-9

R&D ACTIVITIES ON HIGH INTENSITY SUPERCONDUCTING PROTON LINAC AT RRCAT

S.C. Joshi, S.B. Roy, P.R. Hannurkar, P. Kush, A. Puntambekar, P. Shrivastava, G. Mundra, J. Dwivedi, P. Khare, P.D. Gupta, Raja Ramanna Centre for Advanced Technology, Indore, INDIA

Abstract

Raja Ramanna Centre for Advanced Technology (RRCAT), Indore has taken up a program on R&D activities of 1 GeV, high intensity superconducting proton linac for Spallation Neutron Source. This will require several multi-cell superconducting cavities operating at different RF frequencies. To start with, a number of single-cell prototype cavities at 1.3 GHz have been developed in high RRR bulk niobium. These single-cell cavities have exhibited high quality factor and accelerating gradients. Superconducting properties of niobium are being studied for varying composition of impurities and different processing conditions. Physics design of linac configuration and various accelerating structures have been initiated. Development activities on cryomodules, cavity test facilities and solid state RF amplifiers to power the SRF cavities at various RF frequencies are being pursued. Infrastructure setup required for SRF cavity fabrication, processing and testing is under progress at RRCAT.

INTRODUCTION

A programme is envisaged to develop a pulsed, MW range Spallation Neutron Source based on 1 GeV, 1 MW superconducting RF H- Ion linac, a full-energy injector for a 1GeV Accumulator Ring. The pulsed Spallation Neutron Source will be used for applications in the field of condensed matter physics, material sciences, chemistry, biology and engineering. In addition to setting up of SNS facility, it will enhance capacity building in the area of high intensity proton accelerators in India.

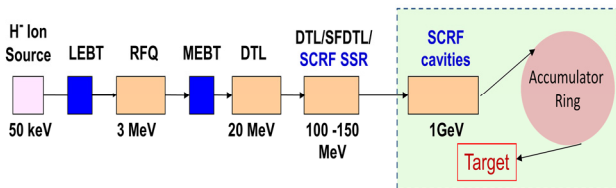


Figure 1. Schematic of Pulsed Proton Linac for Indian Spallation Neutron Source.

R&D ACTIVITIES

R&D activities for a SRF linac and accumulator ring for SNS would include prototype development of various sub-systems and setting up of infrastructure in the following areas:

- Ion source and front end component
- Materials R&D, cavity & cryomodule development

- Niobium cavity fabrication and processing facility
- Test facility for large number of SRF cavities and cryomodules
- Cryogenics setup for large size LHe Plant & supply network
- RF power sources and control electronics
- Sub-systems for 1 GeV accumulator ring including magnets, power supplies, RF cavity, UHV system and controls
- Manpower development and training

Ion Source and Front End

Development of a 3 MeV H- ion linac front end has been initiated for 1 GeV proton accelerators for a pulsed Spallation Neutron Source [1]. The front-end system will comprise of a filament driven multi-cusp H- ion source, Low Energy Beam Transport (LEBT) system, Radio Frequency Quadrupole (RFQ), RF power sources, Controls, Beam dump and Beam diagnostics.

H- Ion Source: In order to meet the requirement of H- ion front end linac system, a multicusp filament based 50 keV, 30 mA, low emittance H- ion-source operating in pulsed mode with a repetition rate of 25 Hz has been initiated. Physics design of the multicusp source was carried out analytically and also using computer simulations based on finite element method. This system has recently been tested for extraction of hydrogen ion current of 1.0 mA at 15 kV accelerating field. Figure 2, shows the multi-cusp H- ion source system.

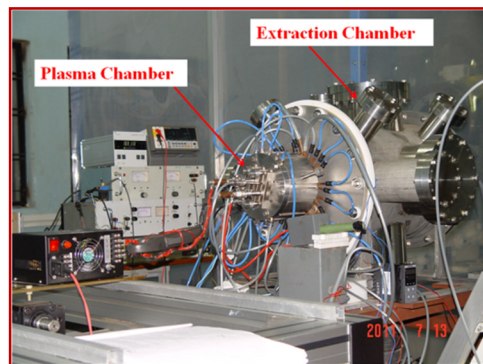


Figure 2. Prototype multi-cusp filament based source pulsed H- ion source.

LEBT and RFQ: For prototype studies, design has been carried out for a suitable LEBT for beam transport from Ion Source to RFQ and a 3 MeV, 352 MHz RFQ. A Low Energy Beam Transport (LEBT) line, consisting of solenoid magnets of maximum strength 3.5 kG and steering coils having a maximum field of 100 G has been

CURRENT STATUS OF THE RAL FRONT END TEST STAND (FETS) PROJECT

A. Letchford, M. Clarke-Gayther, D. Faircloth, S. Lawrie, STFC/ISIS, Rutherford Appleton Laboratory, Harwell, UK

S. Alsari, M. Aslaninejad, A. Kurup, J. Pozimski, P. Savage, Imperial College of Science and Technology, London, UK

C. Gabor, C. Plostinar, STFC/ASTeC, Rutherford Appleton Laboratory, Harwell, UK

G. Boorman, A. Bosco, Royal Holloway University of London, London, UK

S. Jolly, University College London, London, UK

J. Back, University of Warwick, Coventry, UK

A. Garbayo, AVS, Eibar, Gipuzkoa, Spain

Abstract

The UK proton accelerator strategy aims to develop a viable high power proton driver with applications including spallation neutrons, the neutrino factory and ADSR. An essential first ingredient, identified as one of the main UK R&D accelerator projects, is the Front End Test Stand (FETS) at the Rutherford Appleton Laboratory (RAL), aimed at producing a high quality, high current, cleanly chopped H⁺ beam. Through its component parts, FETS has triggered development of a high brightness, 60 mA H⁺ ion source, a three-solenoid Low Energy Beam Transport line (LEBT), a 3 MeV four-vane Radio-Frequency Quadrupole (RFQ) and a Medium Energy Beam Transport line (MEBT) with a high speed chopper. The project is well advanced and when operational should be sufficiently versatile to explore a range of operating conditions. In this paper we present the current status of the construction, and plans for operation, experiments and future development.

THE FRONT END TEST STAND

The Front End Test Stand was first proposed nearly a decade ago [1], as a demonstrator for fast, high quality beam chopping. Since then, FETS has become the main proton R&D project in the UK, being a collaborative effort between Rutherford Appleton Laboratory where it is being built, and several universities as well as international partners [2]. FETS is of high relevance for the next generation of high power proton accelerators that are aiming to deliver beam powers in the megawatt range, in particular, the ISIS upgrade plans [3] and the UK neutrino factory design efforts [4].

A schematic FETS layout can be seen in Figure 1. It consists of five main components: an H⁺ ion source, a LEBT based on three solenoids, a 3 MeV RFQ, a MEBT with a fast chopping system and a wide-ranging set of

diagnostics. When completed it will deliver a 60 mA, 2 ms, 50 Hz chopped beam at 3 MeV [5]. With the commissioning efforts in full swing, in this paper we will briefly present the current status of each section, highlighting recent progress as well as future plans.

ION SOURCE

A Penning surface plasma H⁺ ion source is used in FETS. The source is a modified version of the existing ISIS ion source that has successfully been used in routine operation for nearly 30 years. To meet the FETS requirements, a systematic development programme was started several years ago. This has led to a number of modifications including: geometry changes, transport optimisations, cooling improvements, power supply upgrades and operating parameter investigations.

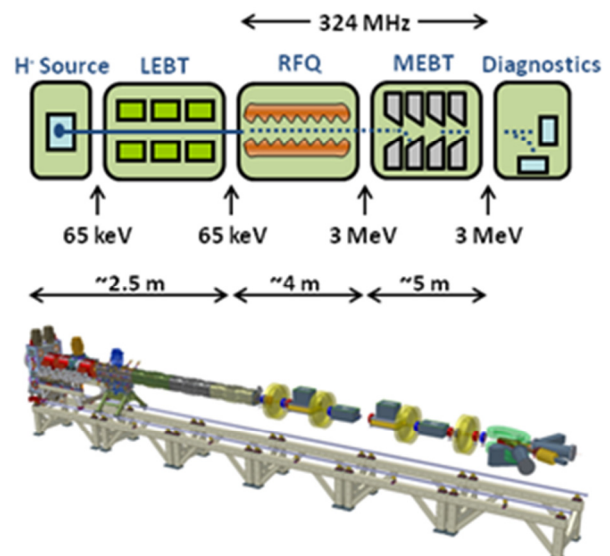


Figure 1: Schematic FETS layout.

FRONT-END LINAC DESIGN AND BEAM DYNAMICS SIMULATIONS FOR MYRRHA *

C. Zhang[#], H. Klein, D. Mäder, H. Podlech, U. Ratzinger, A. Schempp, R. Tiede, M. Vossberg
 Institut für Angewandte Physik, Goethe-Universität, D-60438 Frankfurt a. M., Germany

Abstract

A 17MeV, 176MHz, and CW (Continuous Wave) proton linac is being developed as the front end of the driver accelerator for the MYRRHA facility in Mol, Belgium. Based on the promising preliminary design, further simulation and optimization studies have been performed with respect to code benchmarking, RFQ simulation using realistic LEBT output distributions, and an updated CH-DTL design with more detailed inter-tank configurations. This paper summarizes the new results.

the Kilpatrick factor to $\leq 30\text{kW/m}$ and 1, respectively, for all warm cavities, even shortened the whole layout from 11.4m to 10.6m, and kept the beam dynamics performance satisfying. Being very conservative for CW operation and more cost-saving, this design has been taken as the baseline for further studies [5].

PRELIMINARY DESIGN

Following the EUROTRANS project [1], MAX [2] (MYRRHA Accelerator eXperiment research and development programme) is the ongoing European ADS (Accelerator-Driven System) project. For the front end of the driver linac, the EUROTRANS-style injector [3] that consists of one RFQ (Radio-Frequency Quadrupole), two RT (room-temperature) and four SC (superconducting) CH (Cross-bar H-mode)-DTL (Drift-Tube Linac) cavities will be still adopted, but with many new concepts [4].

The most important idea is to halve the RF frequency from 352MHz to 176MHz, which improves the RFQ shunt impedance significantly (see Fig. 1), enlarges the minimum gap between electrodes, and allows replacing the 4-vane RFQ structure by the simple 4-rod one. Consequently, for keeping the RFQ length at $\sim 4\text{m}$ and the warm part still compact, the RFQ-DTL and RT-SC transition energies are reduced from 3MeV and 5MeV to 1.5MeV and 3.5MeV, respectively, which indeed brings more difficulties to the beam dynamics design but helps improving the RT-CH shunt impedance.

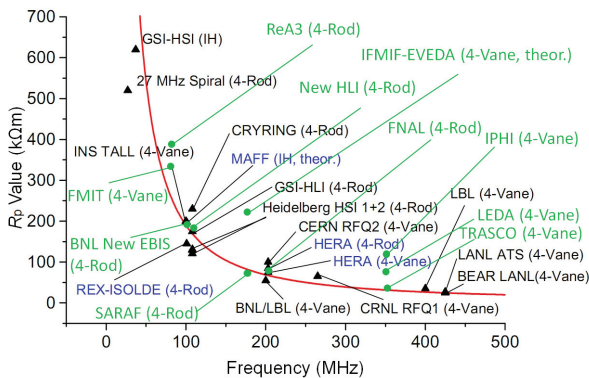


Figure 1: A survey of R_p values for RFQs [5].

From EUROTRANS to MAX, the injector design has lowered the RF power consumption per unit length and

* Funded by the European Atomic Energy Community's (Euratom) 7th Framework Programme under Grant Agreement n°269565.

[#] Chuan Zhang: zhang@iap.uni-frankfurt.de

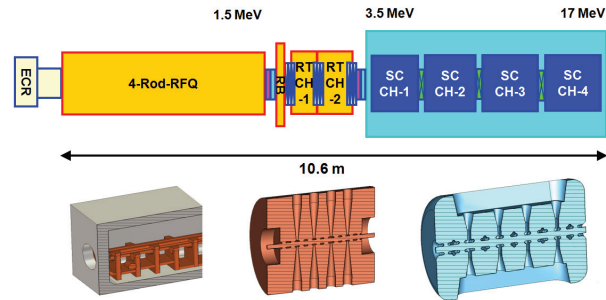


Figure 2: Preliminary layout for the MAX injector.

CODE BENCHMARKING

For the preliminary design of the MAX injector, the ParmteqM [6] and Lorasz [7] codes were used to simulate the beam transport in the RFQ and CH-DTL parts, respectively. Recently, the Toutatis [8] and TraceWin [8] codes have been introduced for benchmarking.

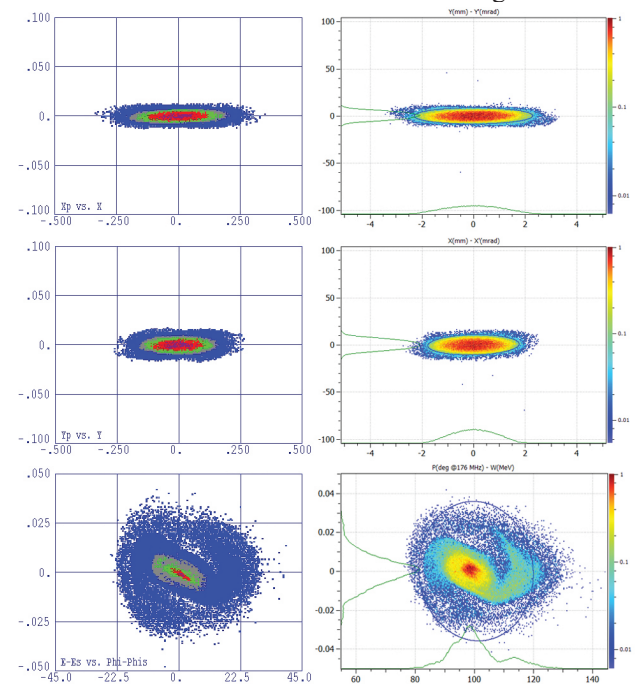


Figure 3: RFQ output particle distributions given by the ParmteqM (L) and Toutatis (R) codes.

Fig. 3 shows the RFQ output beams simulated by the ParmteqM and Toutatis codes. It's clear that the shape,

POST ACCELERATION OF LASER GENERATED PROTON BUNCHES BY A CH-DTL*

Ali Almomani, Martin Droba, Ulrich Ratzinger, Ingo Hofmann, IAP-Frankfurt University, Germany

Abstract

Laser driven proton beam sources applying the TNSA process show interesting features in terms of energy and proton number per bunch. This makes them attractive as injectors into RF linacs at energies as high as 10 MeV or beyond. The combination shows attractive features like a very high particle number in a single bunch from the source and the flexibility and reliability of an RF linac by one pulsed magnetic solenoid lens only. A Crossbar H-type CH – structure is suggested because of its high acceleration gradient and efficiency at these beam energies. It is intended to realize the first cavity of the proposed linac and to demonstrate the acceleration of a laser generated proton bunch within the LIGHT collaboration at GSI Darmstadt. Detailed beam and field simulations will be presented.

INTRODUCTION

With advanced lasers like PHELIX (Petawatt High Energy Laser for Heavy Ion eXperiments), one can achieve focused intensities approaching 10^{20} W/cm². Under these conditions, intense protons with energies of ten to several tens on MeV are accelerated normally from the rear surface of the target by quasistatic electric fields of the order TV/m [1-2]. This process is called Target Normal Sheath Acceleration (TNSA) [2].

An interesting application for these proton beams is the matching into the acceptance of a succeeding RF accelerator for further post acceleration.

The LIGHT (Laser Ion Generation, Handling and Transport) collaboration aims to inject the laser accelerated protons into a conventional accelerator structure [3-4]. Due to the available energies, drift tube linacs are the most adequate choice. A CH – DTL is suggested as the linac structure [5-6].

This work is intended to realize the first cavity of the proposed CH-DTL and to demonstrate the acceleration of a laser generated proton bunch within the LIGHT project.

HYBRID RF ACCELERATOR OF THE LASER GENERATED PROTON PULSE

In PHELIX experiments protons with energies up to 30 MeV and with a total yield of 10^{13} protons per bunch were observed [7]. For the reference energy of 10 MeV, the yield within ± 0.5 MeV was exceeding 10^{10} protons. To compare this number with the conventional currents, the equivalent current of these bunches might add up to 500 mA beam current if every bucket would be filled with that proton number at 325 MHz.

The matching of laser – accelerated protons into a conventional RF linac is difficult due to the high particle

* This work is supported by HIC for FAIR and by BMBF: Contract number. 06FY71041.

number at large energy spread and large beam divergence. The coupling will be done by a pulsed magnetic solenoid. Figure 1 shows a schematic view for the hybrid accelerator.

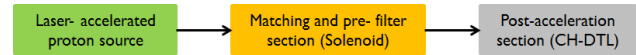


Figure 1: Scheme of the hybrid configuration.

Magnetic Solenoid

In order to collimate the laser – accelerated protons, a pulsed magnetic solenoid was chosen [5]. The 10 MeV p bunch in this lens layout (Figure 2) affords a magnetic field level of about 18 T in order to focus directly into a CH-DTL at a distance of about 210 mm from the target.

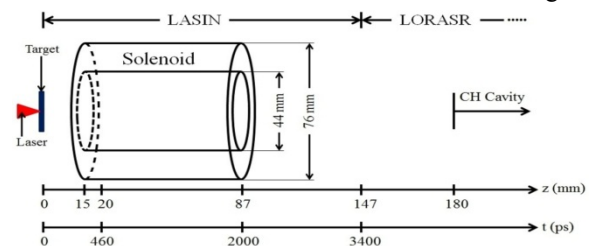


Figure 2: Schematic view on the laser target, the focusing solenoid and the drift to the rf linac. The longitudinal axis is marked in mm and in ps time of flight for a 10 MeV proton beam.

The output distributions, 60 mm behind the solenoid, are shown in Figure 3. The beam dynamics studies including the effect of co-moving electrons is described in Ref. 5.

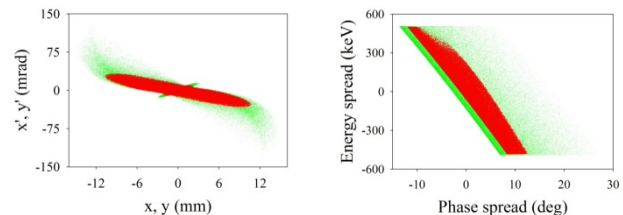


Figure 3: Particle distribution in transversal (left) and longitudinal (right) planes at the DTL – entrance within the energy range $10 \text{ MeV} \pm 0.5 \text{ MeV}$ (green). The red 72% subsets of the particle distribution fall within the CH – DTL acceptance area and are used for DTL beam dynamics simulations.

Dedicated 40 MeV CH - DTL

The layout of the CH-DTL [5] was performed in two main steps. At first a 500 mA equivalent beam current design was developed by using a waterbag - type input distribution. In a second step, this linac layout was used to simulate the acceleration of the laser – accelerated bunch,

A PULSED LINAC FRONT-END FOR ADS APPLICATIONS

U. Ratzinger, H. Podlech, A. Schempp, K. Volk, IAP, Goethe Universität Frankfurt am Main, Germany
 O. Heid, T. Hughes, U. Hagen, SIEMENS AG
 H. Höltermann, BEVATECH, Frankfurt*

Abstract

Quite a number of projects worldwide develop proton driver linacs for neutron sources and for other Accelerator Driven Systems. One trend is to use a high duty factor and superconducting cavities as much as possible. Alternatively, one can aim on short duty factor and count on a continuing rapid development of pulsed rf amplifiers based on power transistor technology. A 500 mA, 5% duty factor layout of a proton injector is presented, consisting of a filament driven volume ion source, of a 150 keV transport section and of a 4.5 m long 162.5 MHz RFQ up to 2 MeV beam energy. Results of beam dynamics and technical designs will be presented.

INTRODUCTION

Worldwide there is an increasing interest in high power ADS (Accelerator Driven System) applications in the multi-MW range. Most of the planned facilities are using low to moderate beam currents (2-50 mA) with cw operation like MYRRHA [1] or the Chinese ADS [2]. The concept described in this paper is based on a pulsed linac with a duty factor of about 5% with very high beam currents of up to 500 mA of protons. The average beam current on the target should be larger than 20 mA. The advantage of lower duty factors is the economic use of room temperature RF structures alternatively to superconducting cavities.

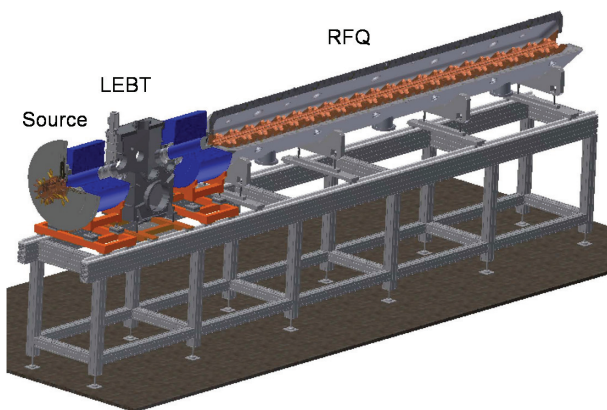


Figure 1: Schematic view of the high current 2 MeV front-end.

Of course, the required RF peak power is significantly larger because of the high beam load. But ongoing developments in pulsed solid state amplifiers will lead to a further reduction of the costs for RF power sources. Alternatively

Table 1: Main parameters of the 500 mA front-end

Parameter	Value	Unit
Particles	protons	NA
Current	500	mA
Platform voltage	150	kV
Source	volume type	NA
LEBT	magnetic	NA
RFQ	4-Rod	NA
Frequency	162.5	MHz
Energy	2	MeV
Duty factor	5	%

it may be possible to use Solid State Direct DriveTM technology [3] in the future.

The 500 mA front-end consists of a high current proton volume source, a short LEBT-section and a 2 MeV 162.5 MHz 4-Rod-RFQ. Figure 1 shows schematically the layout and table 1 summarizes the main parameters.

PROTON SOURCE

The proton source is a filament driven volume source which is based on the 220 mA proton source for the FRANZ project [4]. The extraction voltage has been set to 150 kV to keep emittance growth due to space charge small and to limit the technical effort as much as possible. A single hole extraction will be used to minimize the emittance. Numerical simulations have been performed to optimize the triode-extraction system. The other two beam species H_2^+ or H_3^+ can be reduced by source tuning and the proton content will be around 90% of the total beam current. Figure 2 shows schematically the 500 mA proton source.

LEBT

To optimize the beam parameters for injection into the RFQ a very compact LEBT-section consisting of two solenoids and a diagnostic chamber has been chosen. This enables the space charge compensated beam transport of high proton currents with only modest emittance growth. The space charge compensation in the simulations was 90%. Beam transport simulations have been performed with a simplified solenoid model. The solenoid aberrations can be kept small by designing for low aperture filling factor below 0.5. The transmission for the different ion species along the LEBT has been simulated to 100% for protons, 40% for H_2^+ and 24% for H_3^+ . Figure 3 shows the loss profile for the two last mentioned species. The unwanted

* bevatech.com

A COUPLED RFQ-IH CAVITY FOR THE NEUTRON SOURCE FRANZ*

M. Heilmann, D. Mäder, O. Meusel, U. Ratzinger[†], A. Schempp, M. Schwarz
IAP, Frankfurt University, 60438 Frankfurt am Main, Germany

Abstract

The Frankfurt neutron source FRANZ [1] will deliver neutrons in the energy range up to 500 keV with high pulsed intensities. A 2 MeV proton beam will produce protons via the ${}^7\text{Li}(p, n){}^7\text{Be}$ reaction. The 175 MHz accelerator cavity (Table 1) consists of a 4-rod-RFQ [2] coupled with an 8 gap interdigital H-type drift tube [3] section, the total cavity length being 2.3 m. The combined cavity will be powered by one RF amplifier to reduce investments and operation costs. The inductive power coupler will be at the RFQ part. The coupling into the IH-section is provided through a large aperture - mainly inductively. By CST-MWS-simulations [4] as well as by an RF model (Fig. 1) the voltage tuning along the cavity was investigated, and with special care the balance between both cavity sections. A first set of RFQ electrodes should allow to reach beam currents up to 50 mA in cw operation. The beam is pulsed with 100 ns, 250 kHz, while the cavity has to be operated cw due to the high repetition rate. The layout of the cavity cooling is adequate for a maximum heat load of 200 kW.



Figure 1: Coupled 1:2 RFD-DTL model for investigation of the coupling between two different accelerator structures. The RF-dipole (RFD)-model shows a capacity load per meter which is equivalent to the RFQ structure.

INTRODUCTION

The coupling of RF components is beneficial in many cases to reduce the RF amplifier costs and to profit from short drifts between accelerator sections - usually an advantage in high current beam dynamics. A IH-RFQ IH-DTL combination was suggested in ref. [5]. Such a combination was realized for the first time recently [6]. One difficulty in this case is the large diameter difference between RFQ and IH-section, due to the high capacitive load of an RFQ. The coupled structure for FRANZ consists of a 4-rod-RFQ and an IH-DTL. The resonance frequency is the same in both structures and can be driven in 0 and π -mode. It's possible to switch between these two modes after adapting the drift between both sections. The FRANZ-combination is investigated for the 0-mode [7, 8, 9]. The coupling between RFD and IH-DTL is mainly inductive.

Table 1: Parameters of FRANZ-RFQ-IH combination at 140 mA beam current. Parameters in brackets are valid for the 50 mA electrode design.

Parameter	Unit	
Particle		Proton
Frequency	MHz	175
Current	mA	(50) 140
RFQ Input-Energy	keV	120
IH-DTL Input-Energy	keV	700
IH-DTL Output-Energy	MeV	2.03
RFQ Thermal Losses	kW	139
IH Thermal Losses	kW	75
RFQ $\epsilon_{in}^{trans.,norm.,rms}$	mm mrad	0.4
IH $\epsilon_{X,out}^{trans.,norm.,rms}$	mm mrad	0.9
IH $\epsilon_{Y,out}^{trans.,norm.,rms}$	mm mrad	1.09
IH $\epsilon_{Z,out}^{trans.,norm.,rms}$	keV ns	5.2
RFQ - # of Cells		(97) 95
IH - # of Cells		8
RFQ - # of Stems		18
IH - # of Stems		6
RFQ - Aperture	mm	4
IH - Aperture	mm	22-24
RFQ - Dimension	mm	300x340x1825
IH - Dimension	mm	412x642x560
Electrode voltage	kV	(61) 75
Coupling constant		0.03
Q - Factor		8000
Shunt impedance	M Ω /m	69

* Work supported by HIC for FAIR and DFG

[†] u.ratzinger@iap.uni-frankfurt.de

STATUS OF CH CAVITY AND SOLENOID DESIGN OF THE 17 MeV INJECTOR FOR MYRRHA*

D. Mäder[†], H. Klein, H. Podlech, U. Ratzinger,
C. Zhang, IAP, Goethe-Universität, Frankfurt am Main, Germany

Abstract

The multifunctional subcritical reactor MYRRHA (Multi-purpose hybrid research reactor for high-tech applications) will be an accelerator driven system (ADS) located in Mol (Belgium). The first accelerating section up to 17 MeV is operated at 176 MHz and consists of a 4-rod-RFQ followed by two room temperature CH cavities with intertank quadrupole triplet focusing and four superconducting CH structures with intertank solenoids. Each room temperature CH cavity provides about 1 MV effective voltage gain using less than 30 kW of RF power. The superconducting resonators have been optimized for electric peak fields below 30 MV/m and magnetic peak fields below 30 mT. For save operation of the superconducting resonators the magnetic field of the intertank solenoids has to be shielded towards the CH cavity walls. Different coil geometries have been compared to find the ideal solenoid layout.

INTRODUCTION

Transmutation of long-lived radioactive waste and advanced technologies for future power generation will be investigated with the MYRRHA ADS [1]. The IAP of Frankfurt University is responsible for the development of the 17 MeV injector, a 13 meter long front end of the 600 MeV MYRRHA linac. To achieve the extremely high reliability of the beam supply for the reactor, two injectors will be driven at the same time. With this parallel redundancy the beam can be provided even during a failure of one injector. Because of thermal stress in the reactor not more than 11 beam trips of $t > 3s$ per year are allowed. The following accelerating structures up to 60 MeV are using the concept of serial redundancy [2].

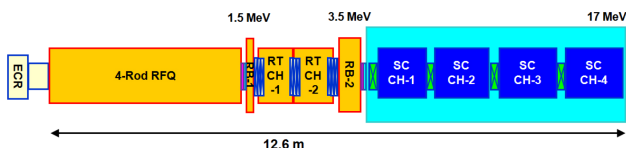


Figure 1: Overview of the MYRRHA injector.

A 4-rod-RFQ will bunch and accelerate the proton beam up to 1.5 MeV [3]. After a five gap CH rebuncher the proton bunches will be accelerated to 3.5 MeV with room temperature CH structures. Quadrupole triplets for focusing and

* Work supported by the EU, FP7 MAX contract number 269565

[†] d.maeder@iap.uni-frankfurt.de

phase probes for diagnostics are placed between the structures. 3 MV/m will be provided by the superconducting accelerators. Four bulk niobium CH cavities are assembled together with four 4.5 Tesla solenoids with coils made of NbTi in one cryomodule [Figure 1].

CH CAVITY DESIGN

Crossbar H-mode (CH) cavities are excellent candidates for acceleration of ions in the low and medium energy range. These resonators driven in the TE₂₁₁-Mode will be used for all accelerating and rebunching cavities after the 4-rod-RFQ from 1.5 to 17 MeV.

Room temperature CH cavities

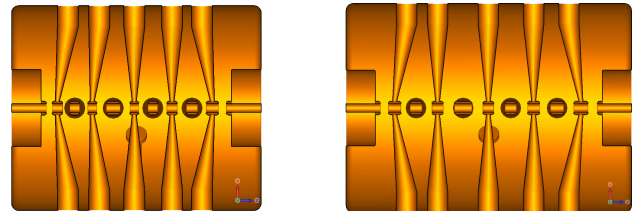


Figure 2: Scheme of the two room temperature CH structures.

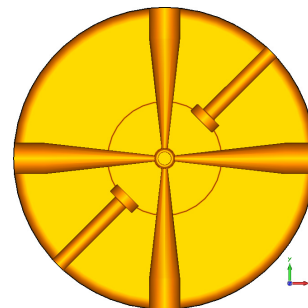


Figure 3: The diagonal tuners act mainly capacitively and provide a total frequency shift of 1 MHz.

CH-1 consists of three and CH-2 of two inclined stems [Figure 2]. Together with the extra volume around the vaults the inclination of the stems increases the induction on the outer stems. This flattens the gap voltage distribution and consequently the thermal load on the stems. The vaults at the resonator ends create additional space outside the cavity and are used for the quadrupole triplet lenses.

Each CH structure is tuned by two mainly capacitively acting tuners that provide a total frequency shift of 1 MHz.

PROGRESS IN THE CONSTRUCTION OF LINAC4 AT CERN

M. Vretenar, L. Arnaudon, P. Baudrenghien, C. Bertone, Y. Body, J. Broere, O. Brunner, G. Bellodi, M. Buzio, C. Carli, J.P. Corso, J. Coupard, A. Dallochio, N. Dos Santos, J.F. Fuchs, A. Funken, R. Garoby, F. Gerigk, L. Hammouti, K. Hanke, J. Hansen, I. Kozsar, J. Lettry, J.B. Lallement, A. Lombardi, L.A. Lopez-Hernandez, C. Maglioni, S. Mathot, B. Mikulec, D. Nisbet, M. Paoluzzi, B. Puccio, U. Raich, S. Ramberger, F. Roncarolo, C. Rossi, N. Schwerg, R. Scrivens, G. Vandoni, J. Vollaire, R. Wegner, S. Weisz, T. Zickler, CERN, CH1211 Geneva, Switzerland

Abstract

As first step of the LHC luminosity upgrade program CERN is building a new 160 MeV H^- linear accelerator, Linac4, to replace the ageing 50 MeV Linac2 as injector to the PS Booster (PSB). Linac4 is an 86-m long normal-conducting linac made of a 3 MeV injector followed by 22 accelerating cavities of three different types.

The general service infrastructure has been installed in the new tunnel and surface building and its commissioning is progressing; high power RF equipment is being installed in the hall and installations in the tunnel will start soon. Construction of the accelerator parts is in full swing involving industry, the CERN workshops and a network of international collaborations. The injector section including a newly designed and built H^- source, a 3-m long RFQ and a chopping line is being commissioned in a dedicated test stand. Beam commissioning of the linac will take place in steps of increasing energy between 2013 and 2015. From end of 2014 Linac4 could deliver 50 MeV protons in case of Linac2 failure, while 160 MeV H^- could be injected into the PSB from 2016; connection to the PSB will take place during a long LHC shut-down foreseen to begin end of 2017.

MOTIVATIONS AND PARAMETERS

The peak luminosity of the LHC has been constantly increased during its first years of operation and the nominal value of $10^{34} \text{ cm}^{-2}\text{s}^{-1}$ is now expected to be reached after the 2013-14 shut-down in parallel with the increase in energy. In this way, the LHC could provide to its experiments about $40 \text{ fb}^{-1}/\text{year}$, a value sufficient for Higgs physics but most likely too low for new physics discoveries. Extending the physics reach of the LHC during the next decade is therefore a priority for CERN: specific projects have been launched to overcome the present luminosity limitations, related both to the LHC interaction regions and to its injector chain, with the goal of achieving a levelled luminosity of $5 \times 10^{34} \text{ cm}^{-2}\text{s}^{-1}$ with integrated luminosities of $250 \text{ fb}^{-1}/\text{year}$.

In particular, the LHC Injectors Upgrade (LIU) project aims at increasing the beam brightness from the injectors, limited now by several factors of which the most severe are related to space charge tune shift at the injection into the low-energy synchrotrons in the chain, the PS Booster (PSB) and the Proton Synchrotron (PS) [1]. Increasing their injection energies is thus required to reduce tune shift permitting higher beam brightness; to reach the LIU

goals, injection energy from the linac into the PSB has hence to go up from 50 to 160 MeV and from the PSB into the PS from 1.4 to 2 GeV. For the PSB injection, an energy upgrade of the present 50 MeV Linac2 was ruled out because of the lack of space and of its obsolete technology; instead, the construction of the new 160 MeV Linac4 (the 4th hadron linac built at CERN) was approved by the CERN Council in 2007. The new linac will bring other advantages related to injecting into the PSB H^- instead of protons, to a modern construction technology exempt from the reliability concerns of Linac2, and to the possibility of increased beam intensity for non-LHC users [2]. Linac4 is being built in a location parallel to the present Linac2 (Fig. 1); a new surface building houses the RF and all other infrastructure and equipment.

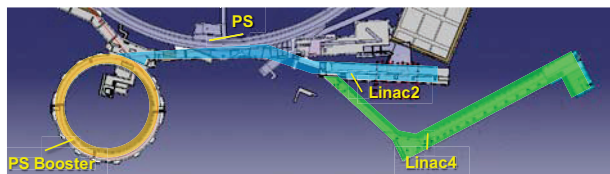


Figure 1: Linac4 and the other low-energy accelerators.

The new linac is dimensioned to double the maximum intensity from the PSB with the same transverse emittances, providing up to 10^{14} protons per pulse; this charge will be supplied by $400 \mu\text{s}$ long pulses at 40 mA current. The pulse repetition frequency is limited to a maximum of about 1 Hz by the PSB magnetic cycle. In case Linac4 would be used in a future high-intensity facility for neutrino physics, the accelerating structures have been designed for a maximum duty cycle of 10%; nevertheless, infrastructure and power supplies are dimensioned only for the duty cycle corresponding to PSB injection. Chopping of about 35% of the beam at 3 MeV is foreseen to allow low-loss injection in the PSB, bringing the required current out of the ion source to 80 mA. The accelerator (Fig. 2) is composed by a 3 MeV Front end (source, LEPT, RFQ and chopper line) followed by three normal-conducting accelerating structures all at 352 MHz, for a total length of 76 m. Adopting three different accelerating sections allows maximising the RF efficiency reducing at the same time the construction costs; using the same RF frequency as in the old LEP machine allowed to recover an important stock of klystrons, circulators and waveguides. A 70-m long transfer line connects to the existing Linac2 line.

LINAC4 45 keV PROTON BEAM MEASUREMENTS

G. Bellodi, V. A. Dimov, L. M. Hein, J-B. Lallement, A. M. Lombardi, O. Midttun, R. Scrivens,
CERN, Geneva, Switzerland

P. A. Posocco, Imperial College of Science and Technology, London, UK

Abstract

Linac4 is a 160 MeV normal-conducting H^- linear accelerator, which will replace the 50 MeV proton Linac2 as injector for the CERN proton complex.

Commissioning of the low energy part - comprising the H^- source, a 45 keV Low Energy Beam Transport line (LEBT), a 3 MeV Radiofrequency Quadrupole (RFQ) and a Medium Energy Beam Transport (MEBT) - will start in fall 2012 on a dedicated test stand installation.

In preparation to this, preliminary measurements were taken using a 45 keV proton source and a temporary LEBT setup, with the aim of characterising the output beam by comparison with the predictions of simulations. At the same time this allowed a first verification of the functionalities of diagnostics instrumentation and acquisition software tools.

Measurements of beam profile, emittance and intensity were taken in three different setups: right after the source, after the first and after the second LEBT solenoids respectively. Particle distributions were reconstructed from emittance scans and used as input to simulation studies of the beam transport through the line (forward and backward tracking). Comparison of the results with the measurements at different locations allowed an experimental validation of the LEBT (in terms of misalignments and calibration points) and qualification of the beam at the source output.

INTRODUCTION

The Linac4 [1] 3 MeV frontend is presently in the process of being assembled for the start of commissioning on a dedicated test stand in autumn 2012. While waiting for completion of the RFQ construction and final developments on the H^- ion source, a preliminary campaign of measurements was carried out in 2011 to characterise the performance of a prototype Low Energy Beam Transport (LEBT) section of Linac4 and provide first validation of the beam simulation models used in the design of Linac4 as well as of the beam diagnostics and software acquisition tools functionality.

The LEBT is a critical part of the machine in the control of beam emittance and parameters for optimised matching into the RFQ acceptance of the beam extracted from the source. It consists of two solenoids, two steerers, a beam current transformer (BCT) and a diagnostics box containing a Faraday cup, a profile monitor, a moveable iris device for the production of lower intensity beams [2] and a pre-chopper (not operational at the time of the measurements). The layout has been kept as compact as possible in its 1.8 m length, to minimise space charge effects, predominant at these low energies. Beam

dynamics simulations studies carried out with the PATH code [3] show that in the case of nominal beam parameters (45 keV, 80 mA, 90% space charge compensation, $\epsilon=0.25$ mm mrad), and using a uniform input particle distribution, we can achieve almost lossless transmission through the LEBT and good matching to the RFQ. The LEBT acceptance is largely determined by the distance between the source output plane and the first solenoid, together with the first solenoid aperture.

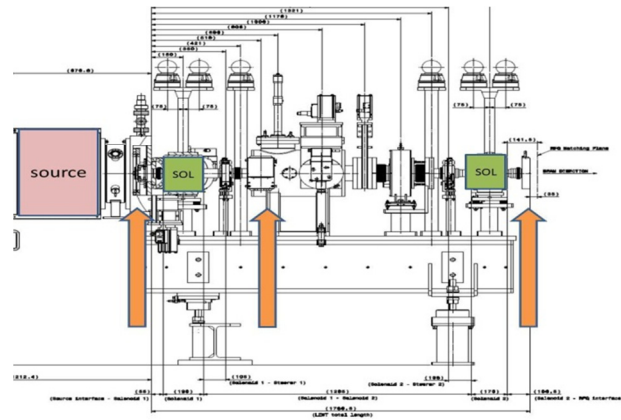


Figure 1: LEBT prototype setup (orange arrows indicate measurement positions).

MEASUREMENTS

A prototype version of the H^- ion source was used for the measurements, in proton operation mode. Different neutralisation effects have to be expected, but beam dynamics in the LEBT is overall charge state insensitive, making the results of this pre-commissioning still meaningful for the final setup of the machine. Goal of the campaign was to calibrate the response of solenoids and steerers in the LEBT layout, and study the dependence of beam transport conditions and final parameters on the source settings (extraction voltage, RF power and gas pressure). The output beam was characterised via beam current and emittance measurements taken with the aid of a Faraday cup and a slit-and-grid device respectively at three distinct locations along the LEBT: at the source exit, between the two solenoids and downstream of the RFQ matching plane (see Figure 1).

Source Exit

Figure 2 shows the measured total beam current at the exit of the source when varying the RF power at a constant pulsed hydrogen gas flux. The beam consists of protons (about 70% of the total), as well as H_2^+ and H_3^+ ions (15% each), overlapped at this point, and which will

HIGH RESOLUTION EMITTANCE MEASUREMENTS AT SNS FRONT END

A. Zhukov, A. Aleksandrov, ORNL, Oak Ridge, TN 37831, USA

Abstract

The Spallation Neutron Source (SNS) linac accelerates an H⁻ beam from 2.5MeV up to 1GeV. Recently the emittance scanner in the MEBT (2.5 MeV) was upgraded. In addition to the slit - harp measurement, we now can use a slit installed on the same actuator as the harp. In combination with a faraday cup located downstream in DTL part of the linac, it represents a classical slit-slit emittance measurement device. While a slit – slit scan takes much longer, it is immune to harp related problems such as wire cross talk, and thus looks promising for accurate halo measurements. Time resolution of the new device seems to be sufficient to estimate the amount of beam in the chopper gap (the scanner is downstream of the chopper), and probably to measure its emittance. This paper describes the initial measurements with the new device and some model validation data.

BEAM TIME STRUCTURE

The SNS runs a pulsed H⁻ beam at 60Hz. The pulse can be up to 1 mS long. It consists of a train of mini-pulses having a 945 nS period. The LEBT chopper creates such a train by periodically kicking the beam into a target to create gaps between the mini-pulses. In addition, the MEBT chopper cleans up the gap further downstream. The LEBT chopper cyclically kicks the beam in four different directions, effectively creating periodicity with a period of 4 mini-pulses. This can cause variation of emittance along the beam pulse due to mini-pulse on/off transients, improper MEBT chopper and other causes.

EMITTANCE SCANNER

The emittance scanner is a classical slit-harp device [1]. It was recently upgraded to have additional capabilities of a slit-slit scan. The harp actuator also holds a plate with a slit in it. A faraday cup located in the DTL part of accelerator is used as a collector for slit-slit scans. Table 1 shows the most important properties of the beam and emittance device.

Table 1: Scanner and Beam Parameters

Parameter	Value
Ion Energy (H ⁻)	2.5 MeV
$\beta = v/c$	0.073
Slit – harp distance	353 mm
Signal wires	16
Distance between wires	1 mm
HV Bias	+300 V
Macro pulse length	~ 40 μ S when using scanner

Beam current	~ 30 mA
Slit	0.1 mm carbon
Wire	0.1 mm tungsten
Second slit	0.15 mm
Harp Faraday Cup distance	24.45 m

Raw Signals

In order to measure signals from harp wires we use a custom-made transimpedance amplifier with 16 independent channels. A raw signal, digitized by a GE ICS-645 (5MS/s 16 bits) ADC, is shown on figure one.

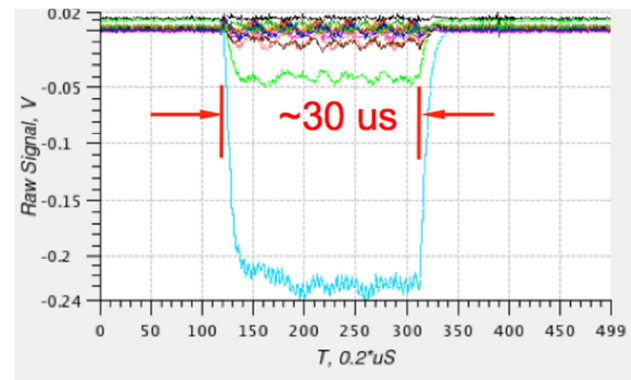


Figure 1: Raw signal from harp wires.

The time resolution of the harp signals is $\sim 1\mu$ s, and is a fundamentally limited by the current harp's design that introduces different coupling mechanisms [1].

The signal from a faraday cup is amplified by the commercially available SR445 wide-bandwidth amplifier and sampled with a 200MS/s 12 bit NI-5124 digitizer.

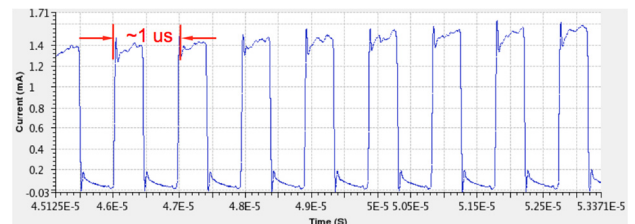


Figure 2: Raw signal from Faraday Cup.

The time resolution of the FC signal is at least 10 times better than from the harp. It clearly resolves the mini-pulse structure of SNS beam.

HIGH TIME RESOLUTION

In order to investigate the emittance variations along the beam pulse, we performed a slit-slit emittance scan and calculated emittance at different locations along the

DIAGNOSTIC TOOLS FOR BEAM HALO INVESTIGATION IN SNS LINAC

A. Aleksandrov, W. Blokland, Y. Liu, C. Long, A. Zhukov.
Oak Ridge National Laboratory, Oak Ridge, TN 37830 USA

Abstract

Uncontrolled beam loss is a major concern in the operation of a high intensity hadron linac. A low density cloud of particles with large oscillation amplitudes, so called halo, can form around the dense regular beam core. This halo can be a direct or indirect cause of beam loss. There is experimental evidence of halo growing in the SNS linac and limiting the further reduction of beam loss. A set of tools is being developed for detecting of the halo and investigating its origin and dynamics. The set includes high resolution emittance measurements in the injector, laser based emittance measurements at 1 GeV, and high resolution profile measurements along the linac. We will present our experience with useful measurement techniques and data analysis algorithms.

INTRODUCTION

The SNS linac is operating routinely at beam power of about 1 MW with typical levels of uncontrolled beam loss within the design limit of 1W/m. This small level of beam loss, while considered to be acceptable, still creates significant activation of the beam line equipment, which affects the lifetime and complicates maintenance. Moreover, the SNS power upgrade plan requires a 50% increase in beam intensity while keeping uncontrolled beam loss at the present level. The major area of beam loss reduction efforts at SNS is the Super Conducting Linac (SCL). The SCL has large transverse aperture, therefore it was expected to be essentially lossless. Nonetheless, a significant beam loss was observed during commissioning and initial operation. It was discovered later that an intra-beam stripping is the main mechanism of the observed losses [1].

Intra-beam stripping losses are proportional to charge density in the bunch and, therefore, are inversely proportional to the bunch size. Increasing the bunch size is the easiest way to reduce the losses caused by the intra-beam stripping. On the other hand, the direct losses on the vacuum pipe aperture increase proportionally to the bunch size. There is an optimal beam size that can be easily calculated for a Gaussian bunch distribution. Unfortunately, as our measurements show, the bunch distribution in the SCL is not Gaussian. It consists of a dense Gaussian-like core and a less dense cloud surrounding the core. We call this cloud a “halo” without giving it a formal definition. Our goal is to reduce the number of particles in the halo or extension of the halo to allow further increase of the bunch core size.

The halo can be created at several places along the SNS linac: In the process of forming the bunches in the injector, at the transitions between the linac sections due

to mismatch, and in the linac due to non-linear RF and space charge forces. Therefore, ideally, we need several measurement points to study the halo creation and propagation: at the exit of the injector, at the exit of the linac, and at as many points inside the linac as practical.

If, at this point of our study we do not understand the halo well and we do not define it quantitatively, then how do we measure it? We will use the “I know it when I see it” approach until we have sufficient understanding for developing a more sophisticated quantitative measure. In our experience, a 2-d emittance plot is a good halo visualization tool. An example of a comparison between measured emittance at 2.5MeV and at 1 GeV is shown in Fig.1. An ellipse drawn on the upper plot encloses 99% of the beam; an ellipse on the bottom plot has the same normalized area (area divided by $\beta \cdot \gamma$). If the normalized emittance was conserved than the ellipse on the bottom plot would enclose 99% of the beam as well. One can clearly see that in this case there is a significant amount of beam outside of the ellipse, which looks like a low density cloud. In other words, there is a halo at 1GeV, which was not present at 2.5MeV.

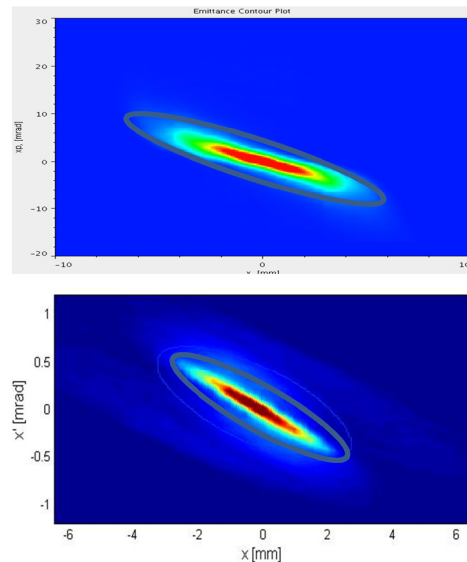


Figure 1: A comparison of two emittance measurements: one is measured at 2.5MeV (top) and the other at 1GeV (bottom). The ellipses superimposed on the images have same area in normalized coordinates.

In the next sections we will describe the tools we have or are developing to obtain the 2-d emittance plots along the SNS linac.

LATTICE DESIGN AND BEAM DYNAMICS STUDIES FOR PROJECT-X*

J.-F. Ostiguy[†], A. Saini, N. Solyak, J.-P. Carneiro, V. Lebedev
Fermilab, Batavia IL 60510, USA

Abstract

Project-X is a proposed proton accelerator complex at Fermilab to support a diversified experimental program at the intensity frontier. As currently envisioned, the complex would employ a CW superconducting linac to accelerate a 1 mA average, 5 mA peak H^- beam from 2.1 MeV to 3 GeV. A second superconducting linac –operating in pulsed mode– would ultimately accelerate a small fraction of this beam up to 8 GeV. The CW linac is based on five families of resonators operating at three frequencies: half-wave (1 family at 162.5 MHz), spoke (2 families at 325 MHz) and elliptical (2 families at 650 MHz). We discuss the latest iteration (v 6.0) of the CW linac baseline lattice.

INTRODUCTION

From 2.1 MeV up to 3 GeV, Project X employs SC linac technology operating in CW mode. The front-end MEBT incorporates a high bandwidth chopper with the ability to reject individual bunches. In conjunction with CW operation, this arrangement enables a variable and flexible bunch structure that can simultaneously accommodate a variety of experiments. The (multiplexed) beam structure can be quite complex; however, the average current over a time interval $T \sim \frac{Q_L}{2\omega_0}$ must remain 1 mA. While the overall concept is by now relatively mature, details are still evolving.

Some recent developments are worthy of mention. The first one is the decision to rely on 162.5 MHz half-wave resonator technology from Argonne National Laboratory to handle acceleration from 2.1 to 11 MeV. The considerations that led to this decision were many and include improved acceleration efficiency and longitudinal acceptance. It also allows the project to leverage ANL's expertise and infrastructure for fabrication. The second is the decision to build a test facility[1], dubbed PXIE (Project X Injector Experiment), to validate the concept of wide bandwidth chopping in the MEBT and to mitigate technical risks. PXIE comprises the ion source, LEBT and MEBT followed by one 162.5 MHz cryomodule (HWR) and one 325 MHz (SSR1) cryomodule. The intent is to maximally re-use the PXIE infrastructure for Project-X. In the interest of allowing PXIE to physically fit into existing available space and to minimize its cost – and eventually that of the Project-X CW linac itself – our recent lattice iterations strive to make maximum use of available cavity gradient even at the expense of some deviation from traditional design rules. Finally, it is becoming clear that in the current budgetary context the 3 GeV CW linac should be planned and build

in stages. The existence of a compelling nuclear physics experimental program at 1 GeV makes this energy a logical choice for a first stage. Our most recent lattice iterations therefore assume 1 GeV as output energy. The default option for acceleration from 1 to 3 GeV would be to continue with cryomodules based on $\beta_g = 0.9$, 650 MHz cavities, as described in [3]. Recently, a number of other projects including NGLS at LBNL and X-FEL at DESY have been seriously looking into CW operation with 1.3 GHz ILC-style cavities. Given the larger size and overall cost of 650 MHz cavities, standardized CW 1.3 GHz technology and power sources from 1 to 3 GeV might prove a better and more cost-effective choice. We intend to study this option at a later time.

LINAC LAYOUT

A high level block diagram of the latest linac layout (dubbed “v6.0”), starting for completeness, at the ion source, is shown in Fig. 1. Relevant details for each regular sections are summarized in Table 1. Overall transverse and longitudinal rms beam envelopes are shown in Fig. 2.

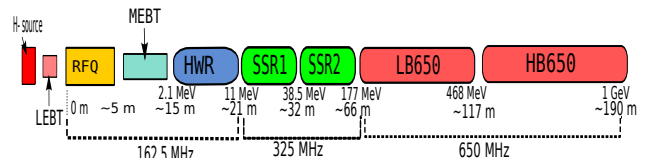


Figure 1: High Level Block Diagram for the (stage 1) 1 GeV CW Linac.

Table 1: Details of Linac Sections. Key: CM: cryomodule; D:doublet, S:solenoid, R:resonator, R^n : n -resonator sequence.

Section	f[MHz]	Cav/mag/CM	Period [m]	Cell
HWR	162.5	8/8/1	0.686	S-R
SSR1	325	16/8/2	1.250	R-S-R
SSR2	325	36/20/4	1.720	S-R ²
LB650	650	30/20/5	5.1	D-R ³
HB650	650	40/10/5	14.3	D-R ⁸

Ion source, LEBT, RFQ and MEBT

The ion source –which has been obtained from industry and tested– nominally supplies 5 mA of H^- at 30 keV continuously. It is followed by a LEBT section whose primary function is to match the beam into a RFQ operating at 162.5 MHz. Beam chopping is provided in the LEBT primarily to reduce beam power during machine commissioning and tuning. The 4.4 m RFQ, which is designed and ready for

* Work performed under US DOE contract DE-AC02-76CH03000.

[†] ostiguy@fnal.gov, solyak@fnal.gov

PERFORMANCE OF FERRITE VECTOR MODULATORS IN THE LLRF SYSTEM OF THE FERMILAB HINS 6-CAVITY TEST*

P. Varghese[†], B. Chase, E. Cullerton, C. Tan, B. Barnes
 Fermi National Accelerator Laboratory (FNAL), Batavia, IL 60510, USA

Abstract

The High Intensity Neutrino Source (HINS) 6-cavity test is a part of the Fermilab HINS Linac R&D program for a low energy, high intensity proton/H- linear accelerator. One of the objectives of the 6-cavity test is to demonstrate the use of high power RF Ferrite Vector Modulators(FVM) for independent control of multiple cavities driven by a single klystron. The beamline includes an RFQ and six cavities. The LLRF system provides a primary feedback loop around the RFQ and the distribution of the regulated klystron output is controlled by secondary learning feed-forward loops on the FVMs for each of the six cavities. The feed-forward loops provide pulse to pulse correction to the current waveform profiles of the FVM power supplies to compensate for beam-loading and other disturbances. The learning feed-forward loops are shown to successfully control the amplitude and phase settings for the cavities well within the 1% and 1° requirements specified for the system.

INTRODUCTION

The use of FVMs to regulate the phase and amplitude of individual cavities in a multi-cavity system driven by a single klystron helps to reduce the cost of the RF system for linear accelerators[1]. High power waveguide FVMs have been developed and the dynamic range of their phase shifting and amplitude attenuating capabilities have been studied[2]. Modeling and simulation of RF control systems with FVMs have shown their potential for field control of individual cavities in a multi-cavity system[3]. A learning feed-forward[LFF] control for the HINS six cavity test accelerator was integrated into the LLRF system. All RF components are driven by a single 325 MHz, 2.5MW pulsed klystron. The LFF algorithm is described and the results of its performance with beam are presented .

LLRF SYSTEM

The RF control block diagram for the 6-cavity test is shown in Fig.1. The LLRF control system regulates the phase and amplitude of the RF field vectors of the RFQ and the six room temperature copper cavities. There is a traditional wide-band proportional and integral feedback control loop around the klystron and the RFQ. Because the RFQ is a low Q device, it behaves much like a resistive load. Therefore, by regulating the RFQ field, the klystron output to the six cavities is effectively regulated as well.

This RFQ control loop greatly reduces errors from klystron modulator voltage variations and from changing beam current. There are several disturbances to the six cavities that must be corrected by the FVM controllers. These are static amplitude and phase errors, drifts in cavity resonance frequency, differences in cavity Qs, and variations in cavity beam loading. Field errors in the cavities are corrected by an adaptive feed-forward system.

The primary feed-back loop is implemented as a PI controller in a FPGA with a sampling frequency of 56 MHz. The 325Mhz RF is downconverted to a 13 MHz IF which is sampled and downconverted to baseband. A 2.1 MSPS DAQ system acquires baseband I,Q signals for pulses up to 4ms wide. The data from all channels is uploaded to the slot0 controller between pulses and is available for processing in the CPU or for transmittal through an ethernet port to both the Fermilab ACNET control system and Lab-view user interfaces, for waveform display and parameter control.

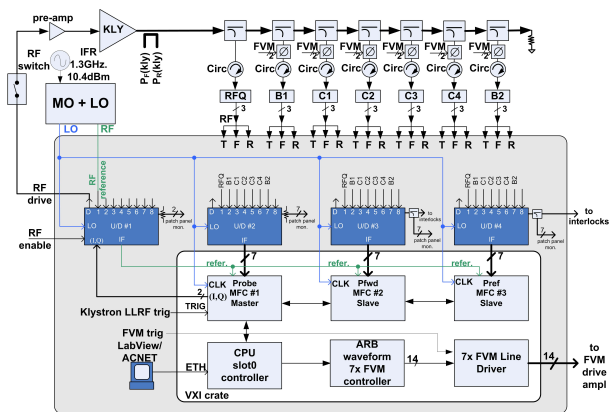


Figure 1: LLRF system configuration

LEARNING ALGORITHM

The learning feed-forward algorithm implementation for one cavity is shown in Fig.2. The wideband RFQ/klystron primary control loop is processed at the full 56 MHz sample rate of A/D converters, while the FVM control loops decimate the data to a 100 kHz rate, where it is processed and the feed-forward controller output is written to a VXI 16 channel arbitrary waveform generator module. Regulation waveforms are recalculated at the machine repetition rate of 0.5 Hz. Decimating the DAQ data by 21 brings the sample rate close to the 100 kHz sampling rate of the output DACs to the FVM. With 1024 points in the FVM waveform, the maximum width of the FVM profile is 10ms

*Work supported by Fermi Research Alliance LLC. Under DE-AC02-07CH11359 with U.S. DOE.

[†]varghese@fnal.gov

CONCEPT: LOW ENERGY, LOW INTENSITY NF FROM PROJECT X*

Milorad Popovic[#], FERMILAB, Batavia, IL 60510, USA

Abstract

This paper describes the concept of a Low Luminosity Low Energy Neutrino Factory (L^3 ENF) using a Project X pulsed, or CW, Linac at 8GeV. By collecting π and μ with energy ~ 1 GeV, and accelerating them to 10 GeV, it is possible to store $\sim 10^{20}$ μ per year. Most of the concepts suggested here can be tested using the Booster beam, Recycler, Antiproton Target Station, the Main Injector and the Tevatron. Once the VLENF Muon Storage Ring is built, components needed for L^3 ENF could be used in experiments before Project X completion.

INTRODUCTION

The beam from the Project-X Linac [1] has a 162.5 MHz structure, and the accumulation ring is a multiple of this frequency so that the beam is transferred bunch to bucket in the ring. There will be a gap of ~ 10 buckets, 61ns long, in the linac beam train to create a beam gap in the ring for extraction. Accumulation of protons is carried continuously for 100 ms for CW linac, or for 16 ms for a pulsed linac, and then beam is sent onto a Be target using a single turn extraction and accumulation is continued.

The Li lens is used to collect as many 1 GeV pions as possible, and that bunched pion beam is injected into the linac structure used as a 200 meter long decay/buncher channel. Finally, the 1 GeV muon beam with a bunch structure of 162 MHz is accelerated to 10 GeV using 325 MHz superconducting beta=1 cavities.

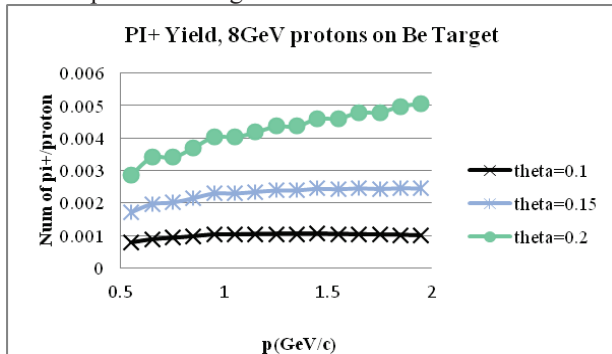


Figure 1: The pion yield curves above are produced using Striganov calculations.

Figure 1 shows number of positive pions produced with 8 GeV protons on a Be target with energy bins of ± 0.1 GeV for three different values of forward acceptance angle θ . Table 1 lists components and main parameters of each stage of L^3 ENF. Figure 2 shows a sketch of the whole complex.

*Work supported by Fermi Research Alliance, LLC, under contract No. DE-AC02-07CH11359 with the U.S. Department of Energy.
#popovic@fnal.gov

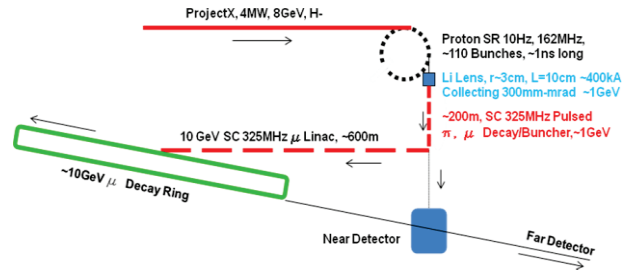


Figure 2: Protons are accelerated with ProjectX linac, then accumulated and targeted.

Table 1: Basic Beam Parameters

Protons	Parameters
Linac, H- Beam, 650MHz SC RF	BeamPower=4MW, CW I=0.5mA ~600ns on, ~60ns off, or 10Hz, 16ms Ekin=8GeV, Bunch Structure=162MHz
Proton Accumulation Ring	RingLength~200m, h=110, of 162MHz, 0.4MW stored per pulse, 100 bunches, $\sim 4 \cdot 10^{12}$ protons per bunch, bunch length \sim 1ns, emittance 50mm-mrad, SC tune shift ~ 0.005 LongLimit ~ 0.1 MW per bunch
Pions/Muons	Parameters
Target & Collection & Matching, at 1 GeV, energy spread of \pm 0.15GeV. Collecting E_un95%=300mm-mrad, L=3.5m, Yield $\sim 5 \cdot 10^{-3}$ pi+/proton	Target: Be or Hg, Li Lens, 15cm long, 3 cm radius, 10 Hz, Peak Current ~ 600 kA, Focal length \sim 20cm. Quad doublet, Q1 g=4.1T/m, l_q1=0.35m, Q2 g=9T/m l_q2=0.7m
Linac/Pi Decay Chanel from 1.0 to 1.2 GeV, SC, pulsed, 325MHz	~ 20 FODO cells, ~ 8 m, two 3-cell cavities beta=1, ~ 17 MV/m, Cavity bore radius 0.2m L_quad=0.35m, g ~ 3 T/m, Synch Phase ~ 0 degree, Bunching mode
Linac/Mu from 1.2 to 10 GeV, SC, pulsed, 325MHz	~ 100 FODO cells, ~ 8 m, two 3- cell cavities beta=1, ~ 17 MV/m, Cavity bore radius 0.2m L_quad=0.35m, g from 3T/m, rumped

In the rest of this note detailed descriptions of each stage and its building blocks are given. The assumption is that the Project X Linac accelerates H^- beam to 8 GeV with a bunch structure of 162.5 MHz and a programmable pulse width.

ACCUMULATION RING

The ring size is dictated by the space needed for RF, injection and extraction devices. The ring should be based on iron dominated magnets and be able to store an 8 GeV beam. The length of the ring should be a multiple of $\lambda_{rf}=1.845$ m.

A CONCEPT: 8 GeV CW LINAC, STAGED APPROACH*

Milorad Popovic[#], J-F. Ostiguy, FERMILAB, Batavia, IL 60510, USA

Abstract

This paper describes a concept for a CW Proton Linac on the Fermilab site. Except for the RFQ, the linac is based on superconducting technology. The linac has three segments that accelerate to 1 GeV, 3 GeV, and 8 GeV, respectively. It is located near the existing Fermilab Proton Source so that each section of the linac can be used as soon as it is commissioned. The whole design is based on the designs suggested for the Proton Driver and Project X. The suggested site and linac segmentation allow for the construction to start as soon as approval is granted. Additional benefits come from the fact that the present linac (the oldest machine in the Fermilab complex) is replaced, and the functionality of the existing Proton Source is preserved for the future.

INTRODUCTION

In order to create more opportunities for beam-based experiments using existing Fermilab infrastructure and in light of the expressed interest in a proton source capable of delivering multi-megawatt beam, a linac similar in design to Project X[1], but located near the existing linac, is proposed. The proposed linac, when completed, would be used to feed the existing 8 GeV program with increased intensity. Additionally, the proposed staged scenario would allow make use of some of the existing infrastructure.

The energy profile of the beam as suggested for Project X is shown in Figure 1.

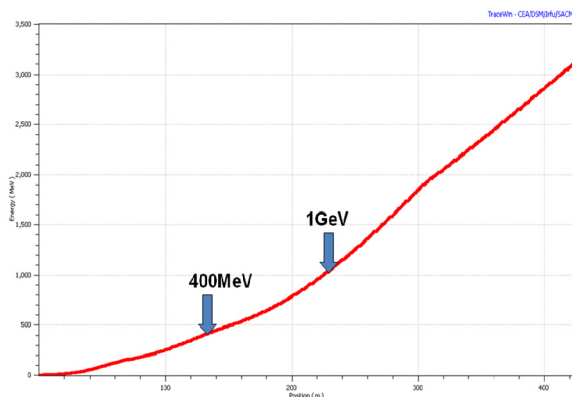


Figure 1: The arrows show the energies of the beam at the indicated distances from the ion source.

The proposed location of the new linac is indicated in Figure 2. The present 400-MeV linac (indicated by the blue line in Figure 2) is ~150 meters long and will be replaced with the new linac starting ~90 meters further upstream (as indicated by the red line in Figure 2). This

*Work supported by Fermi Research Alliance, LLC, under contract No. DE-AC02-07CH11359 with the U.S. Department of Energy.
#popovic@fnal.gov

will allow use of the existing tunnels for the linac and the beam transport line to inject 1-GeV beam into the Booster.

The injection can be bunch to bucket, as shown later. As in the case of the 400-MeV linac upgrade, the increase in injection energy will decrease the space charge tune shift in the Booster. For example, for typical present-day beam intensity and normalized transverse emittances, the space charge tune shift will decrease from 0.33 to 0.18. That in turn will allow more intense Booster beam at 8 GeV. This will also reduce the needed frequency swing of the RF cavities, allowing an increase of the total RF voltage per turn. The second blue line in Figure 2 indicates a CW linac from 1 to 3 GeV, and the long yellow line directed toward MI30 (the left side of Figure 2) shows the position of the 3 to 8 GeV linac.

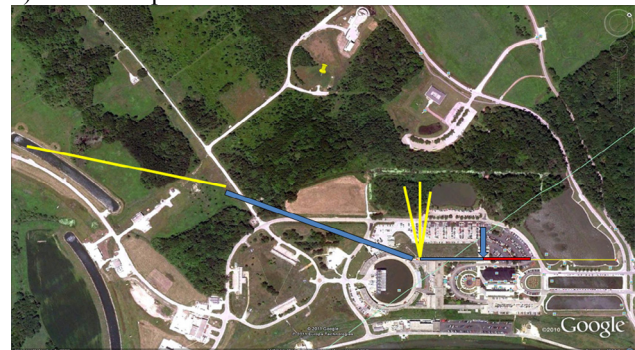


Figure 2: Proposed layout of the new linac on the Fermilab site.

In the rest of this note, a plan for staging of the new linac and the resultant effect on operation of the complex at each stage are described.

LOW ENERGY LINAC-CONCEPT

The low energy portion of the linac complex consists of ion source(s), LEBT, RFQ, MEBT, and linac up to some energy. For a high power CW machine with multiple users, redundancy in the form of multiple ion sources is needed. Also needed to provide the various required beam time structures is a wideband low energy beam chopping system. All these elements are indicated in Figure 3 and will be described in the following sections

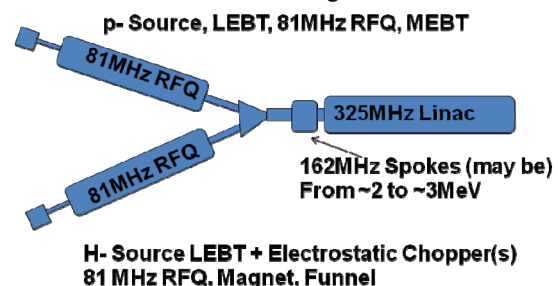


Figure 3: Low energy section of proposed linac. Details of components are described below.

ANNULAR-RING COUPLED STRUCTURE FOR THE ENERGY UPGRADE OF THE J-PARC LINAC

H. Ao*, H. Asano, J. Tamura, N. Ouchi, J-PARC, JAEA, Ibaraki, Japan
 F. Naito, K. Takata, J-PARC, KEK, Ibaraki, Japan

Abstract

The J-PARC linac is preparing to boost the beam energy from 181 to 400 MeV by using annular-ring coupled structures (ACS) for the 1-MW operation from the 3-GeV rapid cycle synchrotron. The mass-production of the ACS cavities started from March 2009 is proceeding on schedule and most of all the cavities have been fabricated until March 2012. The other cavities will be finished until March 2013. The first mass-produced ACS module was successfully conditioned up to 1.6 MW without any issues. For the installation schedule in 2013, the user operation has to be restarted after six months shutdown due to the strong requests from users. As yet, further work is necessary to arrange the schedule and the required manpower for the installation.

INTRODUCTION

The linac of Japan proton accelerator research complex (J-PARC), which is the injector of the 3-GeV rapid cycle synchrotron (RCS), is preparing to boost the beam energy from 181 to 400 MeV in order to raise the possible output power of the 3-GeV RCS from 0.6 to 1 MW. The output energy of the linac is upgraded by using annular-ring coupled structures (ACS). This energy upgrade will increase the limit on the number of particles due to a space charge effect $\Delta\nu \propto \beta^{-2}\gamma^{-3}$. Here, β and γ are Lorentz factors.

Figure 1 shows the schematic configuration of the linac. The downstream area where the ACS cavities will be in-

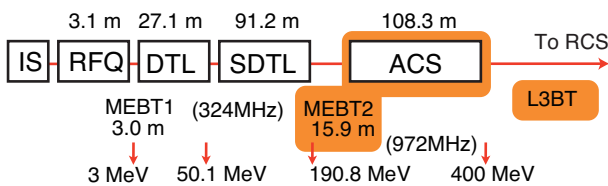


Figure 1: Schematic configuration of the linac.

stalled in the future is used as the beam transport line for 181 MeV at present. The energy upgrade requires 25 ACS modules in total, which include 21 ACS accelerating modules, two ACS bunchers and two ACS debunchers. The two bunchers and three accelerating modules already have been fabricated as a prototype of the common ACS module. All the other cavities have to be mass-produced within a three-year period from March 2009. The cell dimensions of these modules are varied from module to module, which means that the frequencies of many types of cells have to

be tuned within a short time. Thus, the iteration of a frequency tuning was reduced to only one step by using the results of the test cell measurement [1]. In the last of 2010, the first mass-produced ACS module was completed and its high-power test was successfully finished to confirm the stable operation at the required input power.

In the middle of the mass-production, the Great East Japan Earthquake occurred in March 2011 and it severely damaged the linac facility. Fortunately, the factory which were making the ACS cavities is about 1000 km from the epicenter and did not affected.

This paper describes the present status of the ACS cavity fabrication, the measurement result of the first mass-produced ACS module and the installation scenario of the energy upgrade in 2013.

CAVITY FABRICATION STATUS AND INSTALLATION SCHEDULE

Figure 2 shows the progress of the cavity fabrication. At first, all the cavities were schedule to be fabricated until March 2012 and installed in summer of that year. However, the installation was postponed to 2013 due to the earthquake. Most cavities were fabricated until March 2012 according to the first schedule. Of the required 20 ACS modules, 17 modules are completed at present. Of the other three modules, two modules were already brazed and will be finished after assembling an RF window and cooling pipes. The last one module will be done until March 2013¹.

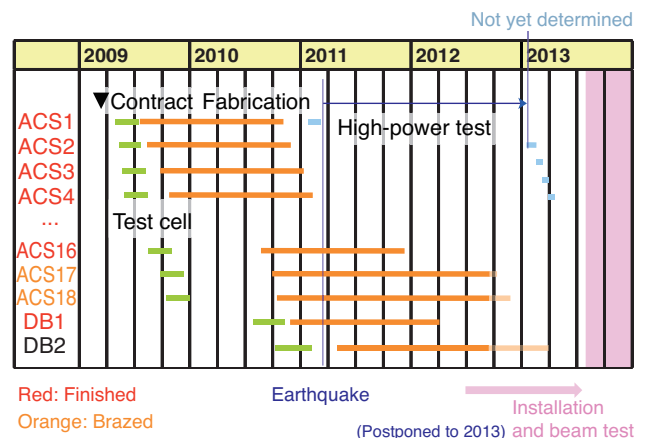


Figure 2: Current progress status of the ACS cavity fabrication.

¹The schedule of the last three modules is not delayed due to technical issues since it was rearranged after the earthquake.

Copyright © 2012 by the respective authors — cc Creative Commons Attribution 3.0 (CC BY 3.0)

* hiroyuki.ao@j-parc.jp

RECOVERY EFFORTS FROM THE TOHOKU EARTHQUAKE AND ENERGY UPGRADE PREPARATION OF THE BEAM TRANSPORT FROM J-PARC LINAC TO 3-GeV SYNCHROTRON

J. Tamura*, H. Ao, H. Asano, T. Morishita, N. Ouchi, JAEA/J-PARC, Ibaraki, Japan
 Y. Sawabe, Mitsubishi Electric System & Service Co., Ltd., Ibaraki, Japan

Abstract

In 2013, the beam energy of the Japan Proton Accelerator Research Complex (J-PARC) linac is going to be increased from 181 to 400 MeV. This energy upgrade is carried out by adding the Annular-ring Coupled Structure (ACS) linac to the beam transport at the downstream of the 191-MeV drift tube linac. To install and condition all the ACS cavities in only five months, we decided to replace and upgrade most of the related components of the beam line (cables, power supplies for magnets and vacuum control systems) for the 400-MeV operation, in the annual maintenance period in summer and the period of the recovery from the 2011 Tohoku Earthquake. The original 181-MeV beam line is operated by using some part of the 400-MeV components. In this paper, the recovery of the beam transport, the present status of the beam operation, and the future tasks of the beam energy upgrade will be presented.

INTRODUCTION

In the J-PARC linac, H- beams are accelerated by 3-MeV RFQ, 50-MeV DTL, and 181-MeV Separate-type DTL (SDTL). Then, the beams are transported to the 3-GeV synchrotron. To achieve the beam power of 1 MW after the 3-GeV synchrotron, we are planning to increase the injection energy into the synchrotron from 181 to 400 MeV. The beam energy upgrade is scheduled in 2013 and carried out by adding the ACS linac to the beam transport at the downstream of SDTL [1]. Figure 1 shows the diagram of the J-PARC linac. Twenty-one ACS accelerating modules are going to be installed in A0BT. Two ACS buncher modules are going to be installed in MEBT2, which is a matching section for the ACS accelerating section. Two ACS debuncher modules are going to be installed in L3BT, which is a beam transport from the linac to the 3-GeV synchrotron.

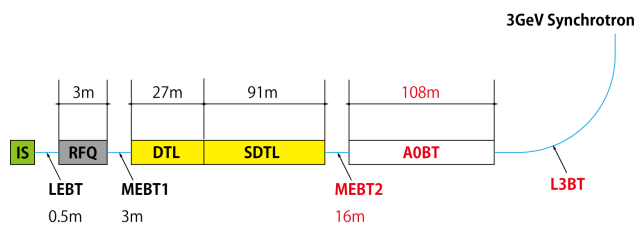


Figure 1: Diagram of the J-PARC linac.

*jtamura@post.j-parc.jp

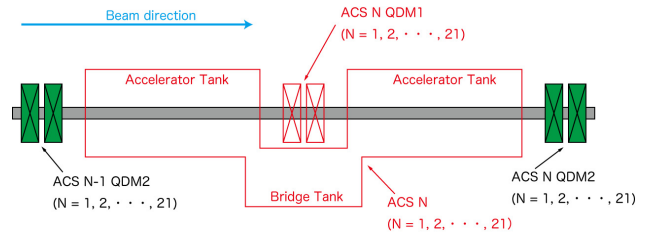


Figure 2: Layout of the quadrupole array in A0BT.

The ACS cavities are operated at 972 MHz, While the RFQ, DTLs and SDTLs are operated at 324 MHz.

MEBT2 and A0BT have 6 and 21 quadrupole doublets, respectively. The drift space length of MEBT2 and A0BT increase gradually from 2.5 to 3.4 m and from 4.6 to 5.7 m, respectively. Figure 2 shows the layout of the quadrupole array in A0BT. ACS accelerating modules and doublets over the ACS bridge tanks, which are drawn by red line in Fig. 2, are going to be installed in the 2013 energy upgrade shutdown.

Before the 2011 Tohoku Earthquake, the beam energy upgrade was scheduled to be completed in 2012. The earthquake caused a tremendous damage to the J-PARC accelerator facility. It made beam operation impossible for nine months and delayed the beam energy upgrade from 2012 to 2013. In this paper, the recovery of the beam transport, the present status of the beam operation, and the future tasks of the beam energy upgrade will be presented.

BEAM LOSS REDUCTION BY BEAM DUCT REALIGNMENT

In the J-PARC linac, almost all the cavities and magnets were precisely realigned because the accelerator tunnel had been deformed by the 2011 Tohoku Earthquake [2]. In MEBT2 and A0BT, the beam ducts have been roughly aligned after the precise alignment of the quadrupole doublets. The beam ducts are made up of titanium pipes with inner radius of 41 mm and branch ducts for vacuum pumps in the center of two doublets.

The beam study operation in the linac has been resumed on 9th of December 2011 [3]. During the first beam operation after the earthquake, remarkable beam loss and residual radiation have been observed at some parts of MEBT2 and A0BT. This beam loss had a strong correlation with the beam orbit. The beam loss has been reduced by adjusting the beam orbit using steering magnets, but it were

BEAM PHASE MEASUREMENT FOR PEFP LINEAR ACCELERATOR*

Han-Sung Kim[#], Hyeok-Jung Kwon, Jin-Yeong Ryu, Kyung-Tae Seol, Young-Gi Song,
Ji-Ho Jang, Yong-Sub Cho, PEFP/KAERI, Daejeon, Korea

Abstract

According to the commissioning plan of the PEFP proton linac, an accurate measurement of beam phase is essential, especially for setting up the RF operating parameters of DTL. Beam position monitors (BPMs) installed between DTL tanks can provide information about the beam phase as well as about the beam transverse position. By using a BPM as a beam phase monitor, beam phase can be measured without additional devices on the linac or the beam line. The signals from 4 electrodes in the BPM can be summed by using a 4-way RF combiner, by which the effect of the transverse beam offset on the phase measurement can be eliminated. The combined BPM signal (350 MHz) is mixed with LO signal (300 MHz) and down-converted to IF signal (50 MHz), then fed into the signal processing unit, where the phase information is extracted by using IQ demodulation method with a sampling frequency of 40 MHz. In this paper, the beam phase measurement system and signal processing scheme will be presented.

INTRODUCTION

The main facility of the PEFP is 100-MeV proton linac with a high duty factor [1]. Currently the installation of the accelerator is under-going. For the determination of RF set-point during the commissioning of the linac, the beam phase must be measured accurately. A strip-line type beam position monitor (BPM) will be used for the beam phase measurement. Figure 1 shows the layout of beam diagnostic devices along the linac [2]. Note that there is only one BPM between 20-MeV section of linac and MEBT. The 20-MeV section consists of 4 DTL tanks and is driven by single klystron. Therefore, 4 DTL tanks would be considered as single large tank from the view point of RF system [3]. To adjust RF phase of each tank

in 20-MeV section, we installed high power RF phase shifter in each RF waveguide branch to each tank.

A 100-MeV section is composed of 7 DTL tanks and one BPM is allocated right after each DTL tanks. One additional BPM is located in front of the beam dump and will be used for RF set-point determination. The initial goal of the linac commissioning is the beam power of 100W with the peak beam current of 20 mA, the pulse width of 50 μ s in 1 Hz operation [2].

BPM FOR PHASE MEASUREMENT

To measure the beam phase as well as the beam position, we designed and fabricated a strip-line type BPM. The design of the BPM is based on the beam parameters such that the beam energy ranges from 20 MeV to 100 MeV with minimum peak current of 1 mA. The minimum beam pulse width is 50 μ s, which was determined considering the LLRF control system.

One of the major constraints in BPM design was space limitation. The BPM should be installed between DTL tanks. The shortest gap is between the first and the second DTL tank and is less than 125 mm. The isolation vacuum gate valve and flexible bellows must be installed in that gap as well as the BPM, which leaves only about 50 mm of the net space for the BPM installation.

The electrode aperture is 20 mm in diameter, which is same as the inner diameter of the drift tube. The electrode angular span is 60 degree to increase the output signal amplitude. The electrode is made of stainless steel with thickness of 2 mm to give enough mechanical stability. For the proper operation of the strip-line type BPM, the characteristic impedance should be well matched and the gap was determined to be 3.5 mm based on the POISSON calculation. Figure 2 and 3 show the drawing of the designed BPM and fabricated one, respectively [4].

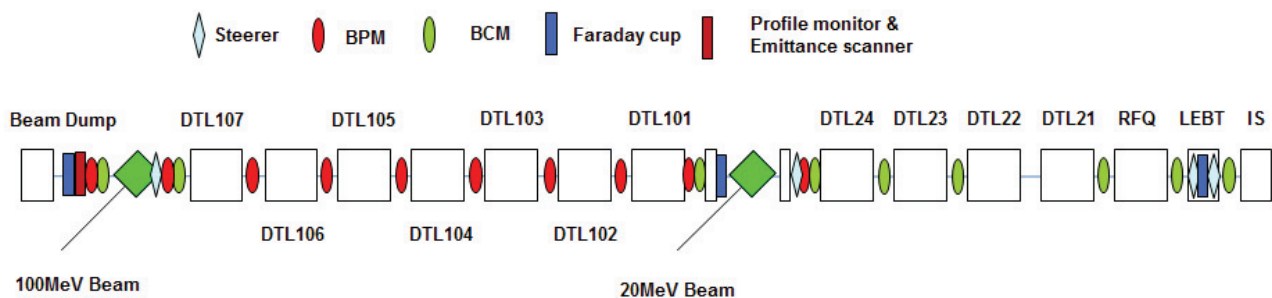


Figure 1: Layout of beam diagnostics in PEFP linac.

*Work supported by Ministry of Education, Science and Technology of the Korean government

[#] kimhs@kaeri.re.kr

LINAC CONSTRUCTION FOR CHINA SPALLATION NEUTRON SOURCE

Shinian Fu, Jian Li, Huachang Liu, Huaifu Ouyang, Xuejun Yin, IHEP, Beijing 100049, China

Abstract

Construction of China Spallation Neutron Source (CSNS) has been launched in September 2011. CSNS accelerator will provide 100kW proton beam on a target at beam energy of 1.6GeV. It consists of an 80MeV H⁺ linac and 1.6GeV rapid cycling synchrotron. Based on the prototyping experience, CSNS linac, including the front end and four DTL tanks, has finalized the design and started procurement. In this paper, we will first present an outline of the CSNS accelerator in its design and construction plan. Then the some prototyping results of the linac will be presented. Finally the linac construction progress in recent will be updated.

foil, the RCS accumulates and accelerates the proton beam to 1.6 GeV before extracting it to the target.

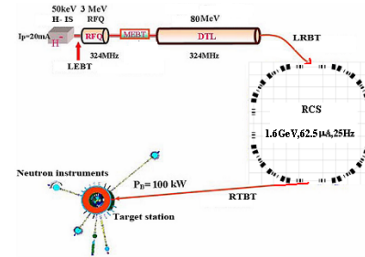


Figure 2: Schematics of the CSNS complex

INTRODUCTION

China Spallation Neutron Source(CSNS) project was approved by the Chinese central government in 2008[1-2]. It has been launched in September 2011. Figure 1 shows the linac tunnel construction status up to now. It is planed to provide neutrons to the users in the first half of 2018. CSNS has a total budget of \$260 M for construction of the accelerator, the spallation neutron target and 3 neutron spectrometers. Its site is at Dongguan, south part of China. The local government will support free land, additional budget of \$57M, infrastructure, dedicated high-way and power transformer station.



Figure 1: Civil construction status of the linac tunnel.

CSNS accelerator is the first large-scale, high-power accelerator project to be constructed in China. The CSNS is designed to accelerate proton beam pulses to 1.6 GeV kinetic energy at 25 Hz repetition rate, striking a solid metal target to produce spallation neutrons. The accelerator provides a beam power of 100 kW on the target in the first phase and then 500 kW in the second phase by increasing the average beam intensity 5 times while raising the linac output energy to 250 MeV. A schematic layout of CSNS phase-I complex is shown in Figure 2. The major design parameters of the CSNS accelerator complex for the two phases are listed in Table 1. In the phase-I, an H⁺ ion source produces a peak current of 25 mA H⁺ beam. RFQ linac bunches and accelerates it to 3 MeV. DTL linac raises the beam energy to 80 MeV. After H⁺ beam is converted to proton beam via a stripping

Table 1: CSNS Design Parameters

Project Phase	I	II
Beam power on target [kW]	100	500
Proton energy [GeV]	1.6	1.6
Average beam current [μ A]	62.5	312.5
Pulse repetition rate [Hz]	25	25
Linac energy [MeV]	80	250
Linac type	DTL	+SC Spoke
Linac RF frequency [MHz]	324	324
Macropulse. ave current [mA]	15	40
Macropulse duty factor	1.0	1.7
RCS circumference [m]	228	228
RCS harmonic number	2	2
RCS acceptance [π mm-mrad]	540	540

LINAC DESIGN AND DEVELOPMENT^[3]

Penning H⁺ ion source is adopted for CSNS linac. The source provides 25 mA peak current, 0.5 ms long, $0.2\pi\mu$ m normalized emittance (rms) pulses at 50 kV and 25 Hz repetition rate for Phase-I.

The LEBT is for matching and transporting the H⁺ beam from ion source to RFQ accelerator, and pre-chopping the beam according to the requested time structure by the RCS with a chopping rate of 50%. Three-solenoid focusing structure is adopted for space charge neutralization, as shown in Figure 3. An electrostatic deflector is chosen as pre-chopper, positioned at the end of the LEBT. A prototype pre-chopper was installed at the entrance of the 352MHz proton RFQ, and it reached a fast rise time of 15 ns in the beam measurement at the exit of the RFQ[4].

MAIN LINAC PHYSICS DESIGN STUDY OF THE C-ADS PROJECT*

Fang Yan, Zhihui Li, Cai Meng, Jingyu Tang

Institute of High Energy Physics, Chinese Academy of Science, Beijing, 100049, China

Abstract

The Chinese ADS (C-ADS) project is proposed to build a 1000MW Accelerator Driven sub-critical System before 2032. The accelerator will be operating on CW mode with 10mA average current and the final energy is 1.5GeV. The whole linac are composed of two major sections: the Injector section and the main linac section. There are two different schemes for the Injector section. Injector I is basing on 325MHz RFQ and superconducting spoke cavities and Injector II is basing on 162.5MHz RFQ and superconducting HWR cavities. The main linac design will be different for different Injector choice. If Injector II scheme is adopted, the main linac bunch current will be doubled. In this paper the main linac design basing on Injector II scheme is studied. The design principles and considerations are introduced; the base line design is presented.

INTRODUCTION

Along with the rapid economy growth, China is experiencing an increasing demanding on energy resources and in the mean while is facing an increasing prominent problem of energy resources shortage. In the next two decades, Chinese government will devote major efforts to developing nuclear power, as nuclear power is acknowledged as a clean, safe, economic energy resource in the international society. However the key roadblock to development of additional nuclear power capacity is the concern over management of nuclear waste and it is an open question not only in China. In China, the accumulated waste is estimated to be more than 10k ton in 2020, and it will be doubled in 2030. Worldwide, more than 250,000 tons of spent fuel from reactors currently operating will require disposal.[1,2] In the past two decades, the accelerator driven sub-critical systems (ADS) is raising more and more interest and is actively studied over the world, because it is recognized as the best option for reducing the radioactive toxicity by transmutation the long-life nuclear radioactive waste into short-life radioactive waste and in the mean while getting power production in a controllable way.[3,4] But until now, there are not any large scale ADS accelerator build yet.

The Chinese ADS project is proposed to build a 1000MW Accelerator Driven sub-critical System before 2032. The driven accelerator will be operating in CW mode and the final goal is 1.5GeV with average current of 10mA. The C-ADS linac includes two major sections: the Injector section and the main linac section. The Injector accelerate the proton up to 10MeV and the main linac boost the energy from 10MeV up to 1.5GeV. It is staged

in three phases. The first phase is aimed to accomplish two different schemes of the Injector designs (IHEP and IMP independently) by 2015 and in the mean time accomplish a part of the main linac up to the energy of 50MeV by 2016. The second phase is planned to extend the main linac energy up to 600MeV with 10mA average current by 2022 and the phase three is to achieve 1.5GeV 10mA final goal by 2032.

The main linac is a critical part of the whole driven accelerator as any design philosophy has to be considered to ensure the beam going through the whole linac and most of the design problems or defects may not appear until the beam is tracked through to the very end of the linac. This paper will present the design considerations of the main linac lattice basing on Injector II scheme.

LATTICE DESIGN AND BEAM DYNAMICS

For ADS applications, it has a rigorous demand on the accelerator stability and reliability. In order to ensure the availability of the ADS reactor and avoiding thermal stress causing damage to the subcritical reactor core, the number of unwanted "beam trips" should not exceed a few per year. This extremely high reliability specification is several orders of magnitude above usual accelerator performance. [5] To fulfill this strict reliability constrains, over-design, redundancy and fault tolerance strategies are implemented in the basic design.

In order to keep the beam in the stable area of Hofmann stability chart [6] and avoid energy change causing emittance growth and beam quality deterioration by thermal equilibrium between transverse and longitudinal planes. The approximately equipartitioning condition is applied on basis of formula (1) [7] and in the mean time to assure a current-independent lattice. According to this formula, once the normalized emittance ratio is fixed the zero current phase advance ratio is fixed accordingly.

$$\frac{\sigma_{0r}}{\sigma_{0z}} = \frac{k_{r0}}{k_{z0}} = \left(\frac{3}{2} \frac{\epsilon_{nz}}{\epsilon_{nr}} - \frac{1}{2} \right)^{1/2} \quad (1)$$

For conservative and especially avoiding any potential reasons which may cause the beam to be unstable such as envelope resonant, the zero current phase advances in all three planes remain below 90 degree.

One of the most critical characters of C-ADS accelerator is keeping the beam loss rate down to 10^{-8} . In order to meet this strict criterion, one has to control the halo growth as small as possible which means the mismatch factor has to be reduced to the maximum extent. Several methods are applied for approaching this goal. The focusing periods of the main linac are designed to have long drifts at both ends to accommodate the cryomodule warm to cold transition without destroying

*Work supported by Advanced Research Project of CAS

#yanfang@ihep.ac.cn

325 MHz CW ROOM TEMPERATURE HIGH POWER BUNCHING CAVITY FOR THE CHINA ADS MEBT1

S. Pei, H. Ouyang, J. Zhang, X. Li, IHEP, Beijing 100049, P. R. China

Abstract

Two room temperature high power bunching cavities are required to be located in the ADS MEBT1 section. Double re-entrant nose cone geometry has been adopted as the type of the bunching cavity for its simplicity, higher shunt impedance and lower risk of multipacting. SUPERFISH is used to optimize the internal dimensions of the bunching cavity, then the RF-thermal-structural-RF coupled analysis were carried out in ANSYS to obtain the preliminary mechanical design, the layout of the cooling channels is optimized to suppress the frequency shift as much as possible. The cavity was specially designed to have the capability to withstand the 1 atm air pressure effect. In addition, the main dimensions of the coupler and tuner are also estimated.

channels, so that the Von Mises stress induced by the high RF heating load can be fairly lower than the yield strength of the cavity material. To suppress the frequency shift caused by the air pressure, the cavity was designed to have double walls consisting of an inner copper wall and an outer stainless steel wall. HFSS and CST Microwave Studio have been used to match the power coupler and estimate the tuner tuning range.

INTRODUCTION

The ADS pilot project based on the proton linac is being developed at IHEP, Beijing, China [1]. In order to realize the matching in both transversal and longitudinal phase spaces, one Medium Energy Transport Line (MEBT1) is needed in the front end injector-injector-I [2], while bunching cavity is one of the key components. Two 325 MHz bunching cavities with a relatively large aperture of 34 mm and an effective voltage of 120 kV are required. In order to obtain high shunt impedance and low risk of multipacting, the nose-cone geometry shown in Fig. 1 has been selected as the cavity shape.

The China ADS accelerator will operate at the CW mode (100% duty factor), SUPERFISH was used to optimize the internal geometric dimensions of the cavity. The RF-thermal-structural-RF coupled analysis has been done in ANSYS to finalize the layout of the cooling

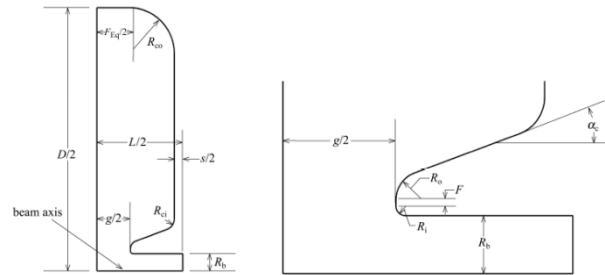


Figure 1: Cavity with nose-cone geometry.

CAVITY INTERNAL SHAPE OPTIMIZATION

The cavity internal geometric dimensions determine its RF characteristics, such as the shunt impedance R , the transit-time factor T , the Kilpatrick factor and so on. Cavity with higher R and T has lower RF heat load, and then the cooling design can be simplified to the largest extent. With the fixed effective cavity voltage, lower Kilpatrick factor will greatly reduce the possibility of electrical discharge (sparking). Fig. 2 shows the relationship between the effective impedance RTT , the Kilpatrick factor and the main cavity internal dimensions.

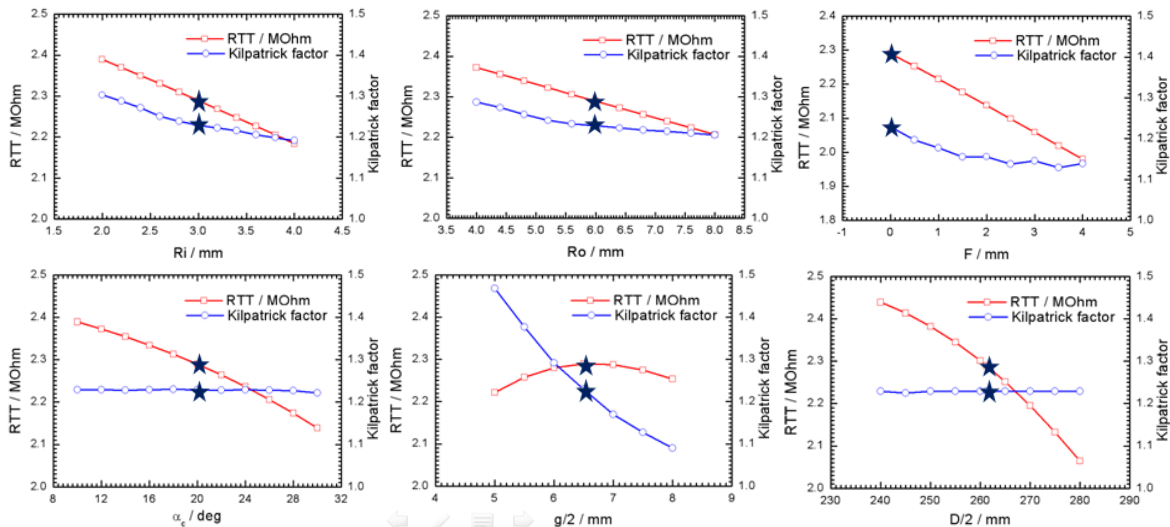


Figure 2: Relationship between the effective shunt impedance RTT , the Kilpatrick factor and R_i , R_o , F , α_c , $g/2$, $D/2$.

#peisl@ihep.ac.cn

THE BEAM COMMISSIONING PLAN OF INJECTOR II IN C-ADS*

Z.J. Wang, Y. He, H. Jia, S.H. Liu, C. Li, X.B. Xu, B. Zhang,
W. Wu, H.W. Zhao IMP, Lanzhou, 730000, China

Abstract

The design work of the Injector II, which is 10 MeV proton linac, in C-ADS project is being finished and some key hard wares are being fabricated. Now it is necessary to definite the operation mode of beam commissioning, including the selection of the beam current, pulse length and repetition frequency. Also the beam commissions plan should be specified. The beam commissions procedures is simulated with t-mode code GPT [1]. In this paper, the general beam commissioning plan of Injector II in C-ADS and simulation results of commissions procedures are presented.

INTRODUCTION

Nuclear energy as a kind of clean energy will be widely used in Chinese energy program in the future. But one of the serious problems is how to handle radioactive waste produced by nuclear plants. ADS, which is the effective tool for transmuting the long-lived transuranic radionuclides into shorter-lived radionuclides, is being studied in the Chinese Academy of Sciences. The road map of the project is shown in Fig. 1.

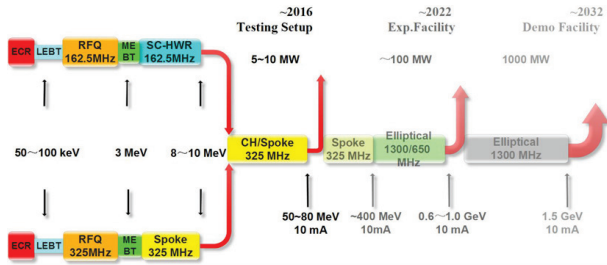


Figure 1: The roadmap of China CAS.

The linac will accelerate the proton with beam current 10mA to about 1.5GeV to produce high flux neutrons for transmutation of nuclear waste.

To ensure technical feasibility in the low energy section, two injectors for the superconduction linac are studied during the first step. One of the injectors, that is Injector II, is been designed and fabricated at Institute of Modern Physics of the Chinese Academy of Sciences. Injector II as part of the ADS is being designed and built at IMP. Injector II is composed of Low Energy Beam transport Line(LEBT), Radio Frequency Quadrupole(RFQ), Medium Energy Beam transport Line(MEBT) and the SC accelerating section. The layout of Injector II is shown in Fig. 2. The LEBT will match the proton beam with 0.035MeV from the ECR source to the RFQ by two solenoids. The RFQ will accelerate and focus the beam

from 0.035 MeV to 2.1 MeV simultaneously. The MEBT has two main functions, which are to match the proton beam from the RFQ to the superconducting accelerating section and to place some on line beam diagnostics devices. The superconducting accelerating section will accelerate proton from 2.1 MeV to 10 MeV with 16 superconducting half wave resonator(HWR) cavities. .

The basic parameters of Injector II are listed in Table. 1.

Table 1: The basic parameters of injector II.

Parameters	Value
Particle type	Proton
Operation frequency(MHz)	162.5
Operation mode	CW
Input beam energy(MeV)	0.035
Output beam energy(MeV)	10
Beam current(mA)	10

In this paper, the general beam commissioning plan of Injector II in C-ADS and simulation results of commissions procedures are presented.

THE BEAM DYNAMICS OF INJECTOR II

The MEBT and superconducting section are simulated by TRACK code. The particles distribution out from the RFQ [2] are transported as the initial distribution of the downstream lianc.

The results of the simulation with three-D field map are shown in Fig. 3. The RMS envelopes in both transverse and longitudinal direction are smooth and periodic in the superconducting section. This depicts that there is good matching between MEBT and the superconducting section.

COMMISSIONS BEAMS OF INJECTOR II

The commissions beams will be chopped for the commissioning of RFQ at first stage, then we plan to use unchopped beam for the bulk of the superconducting section commissioning studies. The beam will be consistent with the beam-handing capabilities of the beam diagnostics system in use at the time.

Beam current

The 0.5mA peak current beam will be chosen to be as the initial commissioning study. The reason is we want to reduce the space charge effect as weak as possible to simply the initial commissioning. At the same time the low limitation of measurement dynamics range of the beam diagnostics device should be considered. Also the low current is

*Supported by the National Natural Science Foundation of China (Grant No.11079001)

PROGRESS OF ONE OF 10 MeV SUPERCONDUCTING PROTON LINEAR INJECTORS FOR C-ADS*

Y. He, Z.J. Wang, B. Zhang, S.H. Zhang, Z. XU, W. Wu, J.X. Wu, Z.M. Zhang, J.H. Zhang, J. Meng, A.M. Shi, Z.Z. Zhou, H.W. Zhao, H.S. Xu, Institute of Modern Physics, Lanzhou, China
 D. Li, LBNL, Berkeley, California, USA

Abstract

A 10 MeV superconducting proton linac is being design and constructing at Institute of Modern Physics (IMP) of Chinese Academy of Sciences (CAS). This proton linac is one of two injectors for Chinese ADS project. It is to validate one of concepts technical baseline for C-ADS front end, to demonstrate the low beta acceleration, to minimize the risk of key technologies within the Reference Design. It consists of a 2.1 MeV RFQ and two cryomodules hosting 8 HWR cavities. The basic frequency is 162.5 MHz. The physical design of linac and the progress of prototypes for solid-state amplifiers, superconducting solenoids, superconducting HWRs, ion source, and RFQ are presented in the paper.

INTRODUCTION

The China ADS (C-ADS) project [1] is a strategic plan to solve the nuclear waste problem and the resource problem for nuclear power plants in China. The road map is shown in Figure 1. It is a long-term planning till 2032. In the first five years (phase I), the goal of the project is to do the research of key components. The prototypes of high stability proton source, RFQ [2], superconducting cavities and the relative hardware will be developed. A superconducting linac with ~30 MeV proton beam will be demonstrated. The accelerator for C-ADS is a superconducting proton linac. It consists of two injectors with energy of 10 MeV, and a main linac. The two injectors will be identical and hot spare during operation. It is the redundancy of low energy section of accelerator. Due to the technology on low energy superconducting linac is unqualified, the injectors of C-ADS will follow two concept designs. The injector I bases on spoke cavities and frequency of 325 MHz, and the injector II bases on HWR cavities [3] and the frequency of 162.5 MHz. The two injectors will be constructed in parallel by the Institute of High Energy Physics (IHEP) and Institute of Modern Physics (IMP) separately.

Table 1: Main Specifications of C-ADS

Item	Quantity	Unit
Energy	1.5	GeV
Current	10	mA
Beam power	15	MW
RF frequency	(162.5)/325/650	MHz
Duty factor	100	%
Beam loss	< 1	W/m

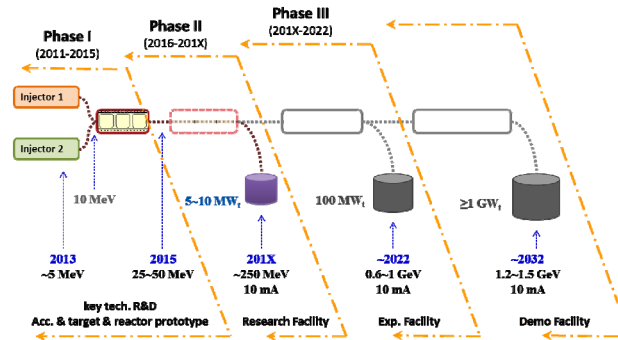


Figure 1: Road map of C-ADS.

PROGRESS OF PROTOTYPES

Conceptual Physics Design

The layout of injector II is shown in Figure 2. The accelerator for C-ADS will operate in CW mode. That is a challenge for RFQ design. Considering the possible thermal-problem of the RFQ, the basic frequency of injector II is selected as 162.5 MHz, the half of frequency of injector I. The main design parameters of injector II for C-ADS proton linear accelerator are listed in Table 2.

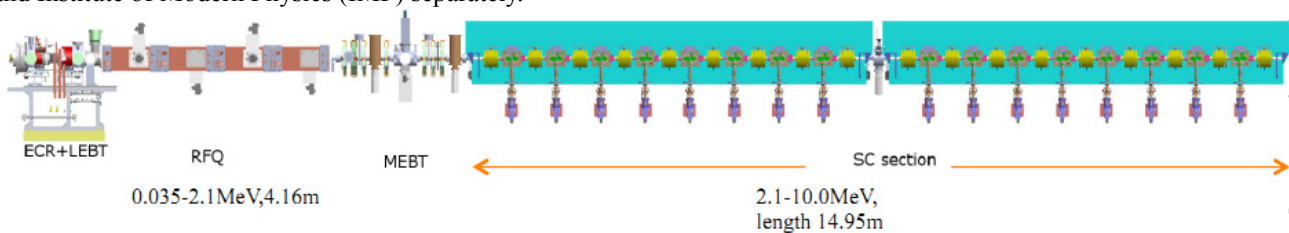


Figure 2: Layout of injector II for C-ADS.

*Work supported by the “Strategic Priority Research Program – Green Nuclear Energy: ADS Transmutation System” of the Chinese Academy of Sciences, Grant No. XDA03020102

THE ESS LOW ENERGY BEAM TRANSPORT LINE DESIGN

L. Neri[#], L. Celona, S. Gammino, D. Mascali, A. Caruso, A. Longhitano, L. Calabretta, INFN, Laboratori Nazionali del Sud, Catania, Italy
B. Cheymol, A. Ponton, European Spallation Source ESS AB, Lund, Sweden

Abstract

The linear accelerator of the European Spallation Source (ESS) will deliver proton beams of 50 mA and 2.5 GeV onto the 5 MW neutron production target. The Proton Source for ESS (PS-ESS) [1] is based on the experience of TRIPS and VIS developed at LNS Catania [2,3]. A two solenoid Low Energy Beam Transport (LEBT) is foreseen to match the beam into the first acceleration stage, the Radio-Frequency Quadrupole (RFQ) [4]. Beam production means also detailed characterization of produced beam, with this scope the LEBT houses many instrumentation devices and use different techniques that will be described in this work. The LEBT will be also equipped with an electrostatic chopper in order to remove the unwanted part of the beam pulse during the natural rise and fall times of the ion source. Beam dynamics calculations of the LEBT have been carried out considering also the Space Charge Compensation (SCC) produced by the interaction of the beam with the residual gas, and its effect on beam transport and chopping. Particular emphasis has been put on the evaluation of the beam transient behavior, due to the chopping process, at the entrance of the RFQ, results of the study are presented in this paper.

INTRODUCTION

The ESS, to be built in Lund, Sweden, will use a high current proton linac required for generating high flux of pulsed neutrons by the spallation process. The linac layout [5] is made of a warm section and a superconducting section. The warm linac is composed of an ion source (75 keV), a LEBT, a RFQ (3 MeV), a Medium Energy Beam Transport (MEBT) line and a 4-tank Drift Tube Linac (DTL) to accelerate the beam up to 80 MeV. Double-spoke resonators and five cell-elliptical cavities will accelerate the beam in the superconducting linac up to 2.5 GeV. This paper will focus on the LEBT line of the ESS project. The purpose of the LEBT is to transport and adapt the 50 mA beam from the ion source into the RFQ. The beam pulse duration will be 2.86 ms for a repetition rate of 14 Hz; and rise and fall time must be of around 100ns, for that purpose two electrostatic chopper will be used, one located in the LEBT and the other in the MEBT. Beam dynamics investigations have been performed to design the pre-chopper (LEBT) and to evaluate the performances of the latter.

LEBT LAYOUT

The beam focusing in the LEBT is performed by dual solenoid system. The design of the solenoids is similar to

[#] neri@lns.infn.it

the one of the IFMIF LEBT [6]. The deflecting plates of the chopper are inserted between the solenoids. The total length of the line from the plasma electrode to the RFQ entrance is 2.10 m. Two pumping system will be installed in the line, one before the first solenoid and one in between the magnetic elements. The position of the different optical and monitor components are still under discussion and they are subjected to modification. A preliminary layout is shown in Fig. 1.

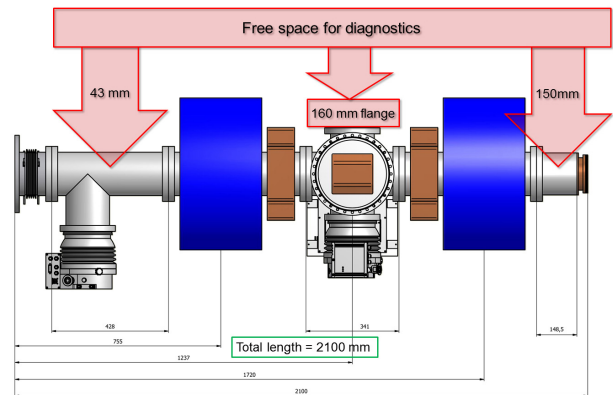


Figure 1: Diagram of the ESS LEBT with beam instrumentation

BEAM INSTRUMENTATION

Beam Profile Measurements

Beam profile measurement will be performed with SEM grids at two locations in the LEBT, between the two solenoids, and after the second solenoid. Each grids will be moved by a stepping motor in order to increase the resolution if it is needed. The profile measurements will be used for the beam steering strategy, and match the beam at the RFQ entrance. In LINAC4, using tungsten wire, the profile measurement was perturbed by thermoionic emission when the beam pulse is longer than 600 μ s at a current of 30 mA, the measurable pulse length can be increased by using a carbon wire.

Emittance Measurement

An emittance measurement is foreseen to characterize the ion source and the beam optics in order to optimize the beam injection in the RFQ entrance and provide beam distribution for end to end simulations. The measurements will be performed during commissioning phase and during operation for dedicated beam studies. For operation, the system will be installed between the two solenoid, the slit will be positioned as close as possible to the first solenoid, the SEM grids used for profile measurement will be reused for this measurements. For the commissioning the emittance meter will be positioned

THE ESS RFQ BEAM DYNAMICS DESIGN

A. Ponton*, European Spallation Source ESS AB, Lund, Sweden

Abstract

The European Spallation Source (ESS), to be built in Lund, Sweden, will use a high current proton linear accelerator (linac) required for generating high flux of pulsed neutrons by the spallation process. The linac will deliver proton beams of 50 mA and 2.5 GeV onto the 5 MW neutron production target. The Radio-Frequency Quadrupole (RFQ) will bunch the continuous beam, coming from the ion source [1] and transported through the dual solenoid Low Energy Beam Transfer (LEBT) line [2] at 352.21 MHz, focalize and accelerate it from 75 keV to 3 MeV. The current design is a 4-vane RFQ composed of 4 segments of 1 m each. This new RFQ is 1 m shorter than the previous 2011 design. However very similar performances are foreseen. The paper reports the motivations of such a change and presents also the beam dynamics study of the current 4 m RFQ.

MOTIVATIONS FOR A SHORTER RFQ

Previous and current performance requirements

The previous RFQ 2011 design was, in part, based on the following performance requirements:

- initial operation at peak current of 50 mA but upgradable to 75 mA;
- beam loss above 2 MeV is limited to 1 W/m;
- both transverse and longitudinal emittances are minimized to reduce the potential for subsequent halo development;
- there should be no longitudinal tails as they are known to translate into transverse halo.

Beam dynamics studies showed that a long structure was needed to fulfill these requirements. The 2010 RFQ was then composed of 5 one-meter segments [3]. Since the latter design has been achieved, the benefits of having such a long structure and the associated potential risks have been deeply analyzed. In particular, the proton beam induced activation of the linac has been evaluated [4] and the beam loss criterion has been relaxed consequently. Moreover the design intensity has been revised. The reflection has finally led to recommend the following updated requirements:

- peak operational beam current will not exceed 50 mA;
- no limit to allowable beam loss below 3 MeV;

- halo development and beam loss in the high energy linac section traceable to the RFQ are minimized;
- no longitudinal tails as they are known to translate into transverse halo;
- phase advances are matched to adjacent sections.

To reach the requirements a 4 m RFQ has been designed. The latter includes less cells in the bunching section and performs a better rate of acceleration while keeping high performance beam dynamics.

Consequences on the designs

Taking into account the above-mentioned relaxation of the performance requirements, the design study results in a 1 m shorter RFQ. We have shortened the *pure* bunching section¹ from 160 to 55 cells. More losses of high energy protons have then been observed but very similar performances in terms of transmission and emittances are foreseen. Particle tracking have also been performed through the linac from the RFQ output to the end of the superconducting (sc) section and no hazardous losses have occurred. Full integration of the RFQ in the ESS linac has also been improved by matching the phase advances to the subsequent Drift Tube Linac (DTL) [5]. Moreover, the RFQ output beam orientation and size have been selected in order to facilitate the transport and matching in the Medium Energy Beam Transport (MEBT) line.

Benefits of a shorter RFQ

Shortening the RFQ has reduced the potential fabrication and operational risks since less tuners and vacuum and RF seals as well as vacuum pumps are required. The construction cost will also be lower as machining and brazing are known to impact significantly the overall cost of the RFQ. Less power dissipated in copper will as well reduce the cost in operation. Removing one segment will finally ease the alignment procedure

BEAM DYNAMICS

Geometry

The main geometry parameters of the current 4 m RFQ are presented in Fig. 1. It can be observed that the minimal aperture is always greater than 3 mm and the modulation factor stays below 2.4. For more flexibility and in order to reduce sparking problems, the Kilpatrick limit [6] does

* aurelien.ponton@ess.se

¹Non accelerating section where the synchronous phase is set to zero.

DTL DESIGN FOR ESS

M. Comunian, F. Grespan, A. Pisent, INFN/LNL, Legnaro, Italy

M. Eshraqi, ESS, Lund, Sweden

R. De Prisco, ESS Lund University, Lund, Sweden and INFN-LNL, Italy

P. Mereu, INFN Torino, Torino, Italy

Abstract

In the present design of the European Spallation Source (ESS) accelerator, the Drift Tube Linac (DTL) will accelerate a proton beam of 50 mA pulse peak current from 3 to ~80 MeV. It is designed to operate at 352.21 MHz, with a duty cycle of 4% (2.86 ms pulse length, 14 Hz repetition period). Permanent magnet quadrupoles (PMQs) are used as focusing elements in a FODO lattice scheme, which leaves space for steerers and diagnostics. In this paper beam dynamics studies and preliminary RF design are shown, including constraints in terms of quadrupole dimensions, total length, field stability, RF power, and peak electric field.

INTRODUCTION

The ESS, going to be built at Lund, will require a high current linac to accelerate protons for the spallation process on which high flux of pulsed neutrons will be generated. The accelerator is 5 MW superconducting proton linac delivering beams of 2.5 GeV to the target in pulses of 2.86 ms long with a repetition rate of 14 Hz [1]. Beam current is 50 mA, which at 352.21 MHz is equivalent to $\sim 9 \times 10^8$ protons per bunch.

Both handling on maintenance and machine protection set a strict limit on beam losses and have been a concern in every high power linac: Therefore it is crucial, especially for high power accelerators, to design a linac which does not excite particles to beam halo and also minimizes emittance growth. The ESS linac is carefully designed to minimize such effects all along the linac and transfer lines.

INFN is in charge of the design of this DTL accelerator. This design is based on the mechanical design and prototyping of CERN Linac4 [2], to which INFN has participated in the last years. In this paper the Physical design of ESS DTL is shown.

DTL DESIGN

Table 1: Main DTL Parameters

Parameter	Value
Duty cycle (%)	4
Frequency (MHz)	352.21
Injection Energy (MeV)	3.0 ($\beta=0.008$)
Output Energy (MeV)	77.5 ($\beta=0.383$)
Accelerated beam current (mA)	50

The design is done by respecting practical technology limits and by avoiding losses along the DTL structure. The maximum RF power per tank is fixed at 2.15 MW. The surface electric field limit is 1.4 Kilpatrick, to avoid sparking, specially at the first DTL cells, due to the contemporaneity presence of electric and static magnetic fields.

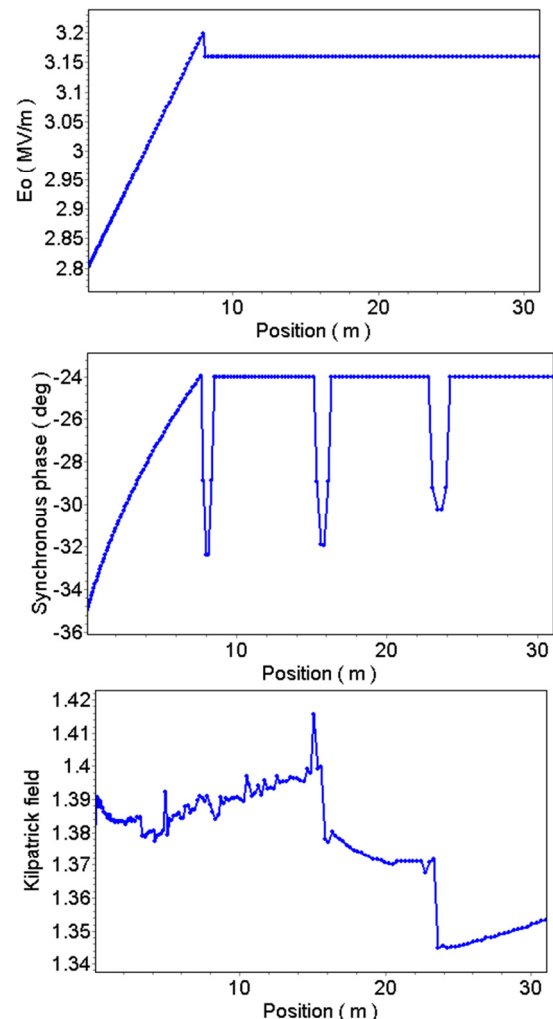


Figure 1: Design E0, synchronous phase and Surface field, along the DTL.

The tank length is limited at 8 meters (9.3λ), to avoid stability problem on the voltage RF design. The total number of tanks is 4, to reduce the global RF power needed. The DTL beam bore radius is increased along the DTL to avoid losses. The optimized solution has been found by using GenDTL, from the CEA suit of codes.

STATUS REPORT ON THE FRENCH HIGH-INTENSITY PROTON INJECTOR PROJECT AT SACLAY (IPHI)

B. Pottin, M. Desmons, A. France, R. Gobin and O. Piquet for the CEA and CNRS IPHI team, CEA Saclay, DSM/IRFU, Gif sur Yvette, France

Abstract

The construction of IPHI (High Power Proton Accelerator) is in its final step of installation. The high intensity light ion source (SILHI) has been built first to produce regularly CW high intensity (over 100 mA) proton beams. The low energy front end of IPHI is based on a 352 MHz, 6 m long Radiofrequency Quadrupole (RFQ) cavity. The RFQ will accelerate beam up to 100 mA with energy up to 3 MeV. A diagnostics line has been built to measure all the main characteristics of the beam at the RFQ output. In this paper we will present the status for the main components of the injector, in particularly the RF power facility, the RFQ fabrication, and the RF tuning.

STATUS OF THE INSTALLATION

Source and Diagnostics Line

The ECR source (2.45GHz, 100keV) is for some years producing routinely beam currents of 130 mA. The beam is used to optimize diagnostics for high energy and to develop new non interceptive diagnostics [1]. The beam diagnostics will allow the characterization of the beam accelerated by the RFQ. The diagnostics line is completely assembly and in vacuum. Every diagnostics were tested and operational.

RF Power Facility

The RFQ will be now powered through four RF ports (instead of three in the previous design). This power is provided by two equally loaded 1100kW klystrons. The two klystrons (1100 kW) have been conditioned (CW operation with matched water cooled load). The conditioning duration was two hours for High Voltage only and one day for Radiofrequency.

The four RF windows have been conditioned by pair in standing wave operation (full reflection) at a maximum 550kW 300 μ s square pulse (10Hz rep. rate) and 250kW CW direct power, the reflected power being dissipated into the circulator load.

RFQ

The IPHI RFQ, 4-vane RFQ, made up of 6, one-meter module assembled in three coupled segments by two coupling plates. Each module is machined in four parts (the vanes) which are brazed together. The final precision (10 μ m) required is close to the limit of what is possible to manufacture using the technology available today with machining and brazing. After different tests, the brazing in vertical position and in one step was chosen.



Figure 1 : Final machining of one RFQ's major vane

The method defined is: deep drilling for cooling channels (1 m long with a maximum deviation about 0.4 mm), rough machining (residual skin: 1 mm), annealing, semi-final machining (residual skin: 0.2 mm), RF control, final machining (Fig. 1), cleaning (chemical polishing), assembling, RF checking, brazing, RF control and vacuum test.

The brazing temperature is about 800°C. The required time for brazing is about 36 hours which include warming and cooling time. The RFQ ready for brazing inside the furnace is shown in Figure 2.



Figure 2: The RFQ in vertical position in the furnace

RF Control of RFQ Modules

RF properties of RFQ modules are carefully controlled after each fabrication step (assembly, 1st braze, etc.). Inter-vane voltages are deduced from bead-pull measurements, and the RFQ 4-wire transmission line model is used to estimate departure of electrical parameters from theoretical values. There are 10 such parameters: 4 parallel inductances, 4 parallel capacitances and 2 diagonal capacitances. However voltage and voltage-slope (the analogue of current for a transmission line) carried by a 4-wire system are dim. 3 vectors (one quadrupole component "Q" and two dipole components "S" and "T"), hence only three parameters may be estimated. Observing that voltage perturbations result primarily from axial region misalignments hence from capacitance errors, and using first-order perturbation analysis, these three parameters are $C_{QQ} = (C_1 + C_2 + C_3 + C_4)/4$, $C_{SQ} = (C_1 - C_3)/2$ and $C_{TQ} = (C_4 - C_2)/2$ (where the

BEAM DYNAMICS DESIGN ASPECTS FOR A PROPOSED 800 MEV H⁻ ISIS LINAC

C. Plostinar, C. Prior, G. Rees, STFC/ASTeC, Rutherford Appleton Laboratory, UK

Abstract

Several schemes have been proposed to upgrade the ISIS Spallation Neutron Source at Rutherford Appleton Laboratory (RAL) [1]. One scenario is to develop a new 800 MeV, H⁻ linac and a ~3 GeV synchrotron, opening the possibility of achieving several MW of beam power. In this paper the design of the 800 MeV linac is outlined with an emphasis on the beam dynamics design philosophy. The linac consists of a 3 MeV Front End similar to the one now under construction at RAL (the Front End Test Stand -FETS). Above 3 MeV, a 324 MHz DTL will be used to accelerate the beam up to ~75 MeV. At this stage a novel collimation system will be added to remove the halo and the far off-momentum particles. To achieve the final energy, a 648 MHz superconducting linac will be employed using three families of elliptical cavities with transition energies at ~196 MeV and ~412 MeV.

Table 1: General Linac Parameters

Ion Species	H ⁻
Output Energy	800 MeV
Accelerating Structures	DTL/SC Elliptical Cavities
Frequency	324/648 MHz
Beam Current	43 mA
Repetition Rate	30 Hz (Upgradeable to 50)
Pulse Length	0.75 ms
Duty Cycle	2.25 %
Average Beam Power	0.5 MW
Total Linac Length	243 m

beam between the linac and the ring. The main linac parameters are presented in Table 1 and a schematic overall layout in Figure 1 [2],[3],[4].

THE FRONT END

The linac front end will consist of an H⁻ ion source, a Low Energy Beam Transport Line (LEBT), an RFQ and a Medium Energy Beam Transport Line (MEBT) with a beam chopper [5].

The FETS Penning type surface plasma H⁻ ion source will be adopted for the new linac. This source is already operating at parameters exceeding those required for the new linac having been improved over many years in ISIS and FETS. A beam of 65 keV, 1 ms at 50 Hz with beam currents exceeding 60 mA is routinely extracted.

A three solenoid magnetic LEBT will transport and match the beam from the ion source to the RFQ. A 4 m long, 4-vane RFQ operating at 324 MHz will accelerate the beam up to 3 MeV making use of the available 2.5 MW Toshiba klystron used at J-PARC. An RMS emittance in the region of 0.27 π mm mrad transversally and 0.39 π mm mrad longitudinally is expected at the output of the RFQ.

DESIGN OVERVIEW

The design of the new linac follows the same overall guiding principles as several recent major proton/H⁻ linac projects (ESS, J-PARC, Linac4/SPL, SNS). It consists of a 3 MeV front end copying the FETS project currently under construction at RAL. After 3 MeV, a DTL will accelerate the beam up to 74.8 MeV at which stage an intermediate energy beam transport line (IEBT) with an innovative collimation system will be used to remove the halo and the far off-momentum beam. Although this adds ~7.5 m to the overall linac length, hence increasing its cost, it is imperative to control the beam loss of quality ahead of the superconducting stages. The superconducting linac (SCL) uses 648 MHz cavities to accelerate the beam to 800 MeV with three families of elliptical cavities and transition energies at ~196 and ~412 MeV. A beam line of with achromatic bending sections is used to transport the

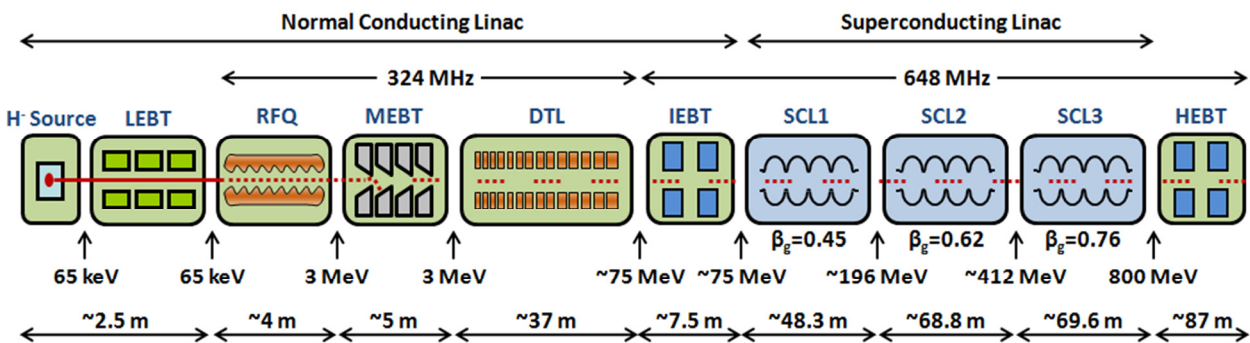


Figure 1: Schematic layout of the new 800 MeV ISIS Linac

Copyright © 2012 by the respective authors — cc Creative Commons Attribution 3.0 (CC BY 3.0)

STATUS OF THE FAIR 70 MeV PROTON LINAC

L. Groening, W. Barth, R. Berezov, G. Clemente, P. Forck, A. Krämer, C. Mühle, R. Hollinger, J. Pfister, W. Vinzenz, G. Schreiber, J. Trüller, C. Will, GSI Helmholtzzentrum für Schwerionenforschung, Darmstadt, Germany
 B. Launé, J. Lesrel, IPNO, IN2P3, CNRS/Orsay, France
 N. Chauvin, O. Delferrière, O. Tuske, C. Simon, IRFU, CEA/Saclay, France
 B. Koubek, H. Podlech, U. Ratzinger, A. Schempp, R. Tiede, Goethe Univ., Frankfurt, Germany

Abstract

To provide the primary proton beam for the FAIR anti-proton research program, a 70 MeV, 70 mA linac is currently under design & construction at GSI. The machine comprises an ECR source, a 3 MeV RFQ, and a DTL based on CH-cavities. Up to 36 MeV pairs of rf-coupled cavities (CCH) are used. A prototype cavity has been built and is prepared for high power rf-testing. An overview of the status as well as on the perspectives of the project is given.

the field flatness is done basically by properly choosing the gap lengths [3]. To this end initially the stems and drift tubes are produced from aluminium. Flatness optimization is done by iterative bead-pull measurements and re-fabrication of the drift tubes. Finally the stems & tubes are drilled from stainless and welded into the cavity. Post fine tuning can just be done by using mobile plungers. The CCH-cavity providing acceleration from 11.6 to 24 MeV (Fig. 2) has been produced and was successfully tuned w.r.t. field flatness. Copper plating is foreseen within this year.

INTRODUCTION

The FAIR proton linac [1] has to provide the primary proton beam for the production of antiprotons. It will deliver a 70 MeV beam with a repetition rate of 4 Hz. Its conceptual layout is shown in Fig. 3 and its main beam parameters are listed in Tab. 1.

Table 1: FAIR Proton Linac Parameters

Final energy	70 MeV
Pulse current	70 mA
Protons per pulse	$7 \cdot 10^{12}$
Repetition rate	4 Hz
Trans. beam emittance	4.2 μm (tot. norm.)
Rf-frequency	325.224 MHz

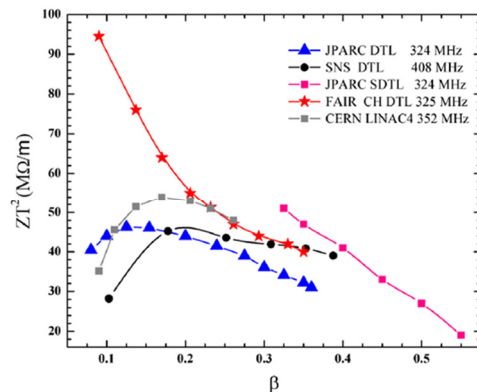


Figure 1: Shunt impedances of several cavity types.

DTL-CAVITIES

Acceleration from 3.0 to 70 MeV is accomplished with six H-mode cavities operated in the TE₂₁₁-mode [2]. Compared to conventional Alvarez cavities these Crossed-bar (CH) cavities feature higher shunt impedance at low energies as shown in Fig. 1. The first three cavities are pairs of two rf-coupled CH-cavities. Rf-coupling is accomplished by merging the first cavity's exit half-drift tube with the second cavity's entrance half-drift tube. This prolonged drift tube of the rf-coupled CHs (CCH) can house a quadrupole triplet. It also provides the rf-coupling cell in the TM₀₁₀-mode. Such CCHs allow for full exploitations of the available rf-power of up to 3 MW per rf-source. After the CCH-section acceleration from 36 to 70 MeV is done with three single CH-cavities. Tuning of

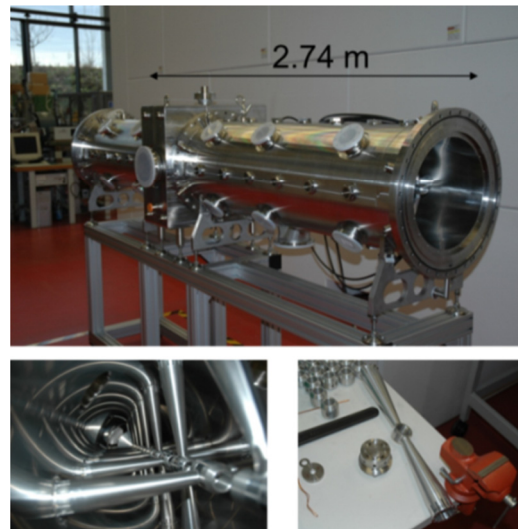


Figure 2: Prototype of CCH-cavity.

EXPERIENCE WITH A 4-ROD CW RADIO FREQUENCY QUADRUPOLE

P. Gerhard*, W. Barth, L. Dahl, W. Hartmann, G. Schreiber, W. Vinzenz, H. Vormann
GSI Helmholtzzentrum f. Schwerionenforschung mbH (GSI), 64291 Darmstadt, Germany

Abstract

The High Charge State Injector (HLI) provides heavy ion beams for the linear accelerator UNILAC at GSI [1]. After 20 years of successful operation its four-rod Radio Frequency Quadrupole (RFQ) was replaced in 2010 [2]. Besides higher beam transmission, the principal intention of this upgrade was to raise the duty factor up to 100%. Commissioning and operational experience from the first years revealed that this goal could not be reached easily. After serious problems with melting of rf contacts were overcome, operation is still restricted. There is strong, modulated rf power reflection, most likely due to mechanical instabilities of the structure. In this paper we present the RFQ design, commissioning results, operational experience and future activities.

INTRODUCTION

The HLI is equipped with an ECR ion source and an RFQ-IH linac which accelerates highly charged ion beams with high duty factor of up to 30% to 1.4 MeV/u for further acceleration in the Alvarez DTL of the UNILAC. Since 1991 main user of these beams is the Super Heavy Element (SHE) research, one of the outstanding projects at GSI [3]. Experiments like TASCA and SHIP strongly benefit from the high average beam intensities. A dedicated cw linac for SHE research at GSI is seriously proposed, with the HLI as its injector. The existing HLI is not designed for cw operation. The replacement of the RFQ in 2010 was the first step towards a cw capable injector.

DESIGN & COMMISSIONING

Due to the high average rf power caused by the cw operation, all parts of the new 4-rod RFQ (electrodes, stems, tuning plates, plungers and coupling loop) had to be directly water cooled. This results in 72 connections and vacuum feedthroughs for cooling water, equipped with pre-vacuum sealing, making the mechanical engineering rather complex. More design properties are given in Tab. 1.

Table 1: Design properties of the new HLI RFQ.

Injection / extraction energy [keV/u]	2.5 / 300
RF frequency [MHz]	108.408
A/q (cw / max.)	6.0 / 8.5
Power (max. avg. / max. pulse) [kW]	60 / 120
Intervane voltage (cw / max.) [kV]	55 / 78
RMS emittance in / out [π mm mrad]	0.1 / 0.1009
Electrode length [m]	2.0

*p.gerhard@gsi.de

The new RFQ was delivered to GSI in autumn 2009. RF and beam commissioning was finished in spring 2010. Achievement of the design beam parameters (transmission, energy, emittance) could be demonstrated (Fig. 1 and [4]). Extensive beam measurements at different locations of the HLI beam line were performed.

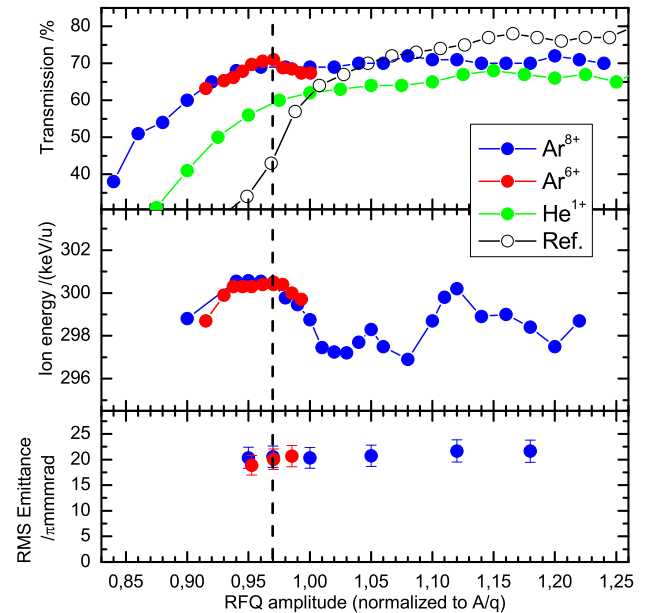


Figure 1: Beam commissioning results (top to bottom): Transmission, ion energy and beam emittance for different ions as a function of the rf amplitude, normalized to the mass-to-charge ratio. Reference data: Old RFQ; dashed line: Derived working point.

THERMAL ASPECTS

During rf commissioning two issues were discovered:

- Insufficient rf contact springs and
- the thermal instability of the 4-rod structure.

Rf contact springs

Several breakdowns of contact springs between the tuning plates and the stems occurred at rf power levels far below the design (s. Fig. 2). The first burning occurred at 16 kW avg. power, possibly due to incorrect mounting of the springs. After two breakdowns, complete renewal with more robust contacts and careful mounting was employed. Nevertheless, damages were found after operation at 24 and 30 kW. Obviously this type of contacts could not handle enough power safely in routine operation. Therefore it was decided to introduce a different contact mechanism using

THE NEW OPTION OF FRONT END OF ION LINAC

A. Kovalenko, JINR, Dubna, Russia

A. Kolomiets, ITEP, Moscow, Russia

Abstract

The standard set of elements consisting of RFQ, two tanks of accelerating IH-structures, external matching and focusing sections is modified to achieve better performances. Special insertions corresponding to buncher and quadrupole triplet are combined within the RFQ tank, whereas superconducting focusing elements are installed between the DTL - structure tanks. Simulation of the system parameters was performed to provide the output beam energy of 5 MeV/u for the ions with charge - to - mass ratio of $0.33 \leq Z/A \leq 1$. Possible application of the considered scheme for the NICA facility at JINR (Dubna, Russia) is discussed.

INTRODUCTION

The work was motivated by our desire to find optimal way of the constructing linear accelerator chain aimed at injection of light ions and protons for the NICA complex at JINR [1] and also for other applications, in particular for the future carbon/proton superconducting (SC) medical synchrotrons [2].

The physics research program at NICA [3] requests the beams of heavy and light ions, protons, polarized deuterons and protons as well. The facility is based on the existing SC synchrotron - Nuclotron that is in operation since 1993 [4] and that was upgraded in 2008-2010[5]. The accelerator complex will include also two separate injection chains, 25 T·m SC booster synchrotron, the collider SC rings, beam transfer channels. The collider will provide heavy ion collisions of average luminosity of $10^{27} \text{cm}^{-2} \text{s}^{-1}$ at the energies of $\sqrt{s_{NN}} \sim (4 - 11) \text{ GeV}$. The collider detector MPD is scheduled for starting data taken in 2017. The fixed target experiment Baryonic Matter at Nuclotron (BM@N) is planned to start data taking in 2015 in the beam of gold ions extracted from the Nuclotron. The NICA will provide polarized proton and deuteron collisions up to $\sqrt{s} = 26 \text{ GeV}$ and 12.5 GeV/u , respectively, with the average luminosity of $10^{31} \text{cm}^{-2} \text{s}^{-1}$.

The two injection chains aimed at heavy ions and protons/light ions (including polarized ones) injection contain respectively the following: high charge state heavy ion source → the new heavy ion linac → SC booster → Nuclotron → collider and the sources of protons, deuterons (including polarized) and light ions → upgraded existing linac LU-20 → Nuclotron → Collider.

The Alvarez type proton linac LU-20 was commissioned in 1974. At the present time LU-20 provides proton beam with energy 20 MeV and light ions ($Z/A \geq 1/3$) up to 5 MeV/u. The LU-20 planned upgrade includes, at the first stage, replacement of old high voltage preinjector by the new one having much lower voltage of the ion source platform ($U = 100 \text{ kV}$) and the

use of RFQ to provide the ion energy required for injection to LU-20.

It is clear, however, that use of LU-20 for acceleration of ions heavier than protons is not very efficient. Moreover it would be very risky to expect reliable operation of the old linac in the coming decades even in the case of complete and very expensive replacement of the drift tubes containing quadrupoles inside.

The main goal of the work is design of compact and efficient linac that can be considered as an option of light ion injector for NICA project.

LIGHT ION INJECTOR

General Layout

Particles that will be accelerated in this device are protons, deuterons (including polarized) and other ions with charge - to - mass ratio of $1/3 \leq Z/A \leq 1/2$, in particular $^{12}\text{C}^{6+}$ and $^{12}\text{C}^{4+}$ as well. The specified values of the beam currents and the expected transverse emittance define the choice of the injector layout and basic parameters of its accelerating structures. After analysis of different possibilities, the scheme shown in Figure 1 is proposed.



Figure 1: Structural scheme of the NICA injector of light and polarized ions. (IS – ion sources)/

Initial part is a combination of RFQ and the DTL that was designed following the idea proposed in [6]. This combination allows to form at output of initial part beam parameters required for injection to DTL 1 and to exclude MEFT with focusing and rf elements for beam matching between RFQ and DTL 1.

DTL 1 and DTL 2 are designed for acceleration of ions with $Z/A = 0.33$ up to final energy 5 MeV/u. DTL 3 is aimed only for proton acceleration and has to be switched off in the other cases.

Superconducting solenoids are used for beam focusing between DTL sections. It allows reducing drift space between cavities and improving longitudinal beam dynamics. Application of superconducting elements in the proposed new injector is logically follows from the NICA basic technology concept and the advanced level of cryogenics in the Laboratory of High Energy Physics.

RFQ

The RFQ is based on a resonant structure with coupling windows developed in ITEP for TWAC facility injector [7]. The main attention at the design stage was devoted to

IRON BEAM ACCELERATION WITH DPIS*

M. Okamura[#], BNL, NY, USA / RIKEN, Saitama, Japan
 T. Yamamoto, Waseda Univ., Tokyo, Japan
 P. Jandovitz, Cornell Univ., NY, USA
 T. Kanetsue, Frankfurt Univ., Frankfurt am Main, Germany
 M. Sekine, TITech, Tokyo, Japan / RIKEN, Saitama, Japan

Abstract

We commissioned an RFQ with a new set of vanes which is for accelerating $q/A > 1/7.2$ ions. RF power was successfully fed and beam commissioning test was done by using high charge state iron beam supplied by a laser ion source. The obtained current reached 4.3 mA at the peak. Silver beam, design particle, test using solenoid confinement with direct plasma injection scheme will be carried on soon.

BACKGROUND

In 2004, we commissioned a 4 vane RFQ in NIRS, Chiba in Japan. The RFQ was constructed by IAP of Frankfurt University and was designed to accommodate high current carbon beam from a laser ion source using direct plasma injection scheme (DPIS). We could demonstrate very high current heavy ion beam acceleration with the DPIS and the measured current after the RFQ reached more than 60 mA of carbon beam[1]. However, due to the radiation safety limitation in NIRS, output beam energy of the RFQ was restricted to be below 100 keV/u. The entire cavity length was 2.0 m and the beam energy reached the energy limitation at 1.42 m point from injection side. So, in the rest of the section, the vanes had no modulation. By passing through under the transversely confinement RF field without acceleration buckets, the beams were completely de-bunched. To verify the feasibility of the DPIS, this RFQ had worked great, however, it was difficult to examine the beam qualities, since the output energy was too low to transport a high current beam and the transverse emittance of de-bunched beam was affected by the RF cycle.

In 2005, we started to design new replacement vanes. Based on experimentally obtained performances of a laser ion source using a 2.3 J Nd-YAG laser, silver $15+$ ion was selected as the design particle[2]. An assembly of the new vanes with supporting stems and a base plate (without outer vessel) was fabricated in 2006 again by IAP.

In 2006, the RFQ and entire experimental equipment was moved from RIKEN in Japan to BNL in USA. In BNL, the study was continued mainly using the old vanes with un-modulated section[3]. Due to a bureaucratic reason, the vane assembly was sent back to Japan after we moved to BNL. However, during the shipment, it was heavily damaged.

A photo taken in Japan is shown in Fig. 1. The assembly was sent to Frankfurt directly from Japan and was straightened and aligned again. The repaired new vanes were installed in 2010 and the commissioning was done in 2011 in BNL.



Figure 1: Deformed vanes.

DESIGN PARAMETERS

The vane parameter design was done assuming 15 mA of Ag^{15+} beam ($q/A = 7.2$) with 0.2π mm mrad (nor. rms) of injection beam transverse emittance. The operating frequency and vane length were retained as 100 MHz and 2.0 m respectively. The beam extraction column voltage applied to laser plasmas was set to 60 keV which corresponds to 8.3 keV/u for Ag^{15+} . The output beam energy was maximized within the limited length. The final modulation factor reached 3.0. Those values are summarized at Table 1 and Fig. 2.

Table 1: Parameters of the RFQ LINAC

RFQ Type	4rod
Frequency	100.1 MHz
Designed Charge to Mass Ratio	1/7.2
Length	2.0 m
Cell Number	143
Input Energy	8.3 keV/u
Output Energy	270keV/u
Designed Vane Voltage	73 kV
Maximum m	3.0
Q value	4500

*Work supported by US. DOE and RIKEN in Japan.

[#]okamura@bnl.gov

ASSEMBLY AND RF TUNING OF THE LINAC4 RFQ AT CERN

C. Rossi, A. Dallochio, J. Hansen, J.B. Lallement, A.M. Lombardi, S. Mathot, D. Pugnati, M. Timmins, G. Vandoni, M. Vretenar, CERN, Geneva, Switzerland
M. Desmons, A. France, Y. Le Noa, J. Novo, O. Piquet, CEA, Gif-sur-Yvette, France

Abstract

The fabrication of Linac4 is progressing at CERN with the goal of making a 160 MeV H- beam available to the LHC injection chain as from 2015. In the Linac4 the first stage of beam acceleration, after its extraction from the ion source, is provided by a Radiofrequency Quadrupole accelerator (RFQ), operating at the RF frequency of 352.2 MHz and which accelerates the ion beam to the energy of 3 MeV. The RFQ, made of three modules, one meter each, is of the four-vane kind, has been designed in the frame of a collaboration between CERN and CEA and has been completely machined and assembled at CERN. The paper describes the assembly of the RFQ structure and reports the results of RF low power measurements, in order to achieve the required accelerating field flatness within 1% of the nominal field profile.

INTRODUCTION

The initial conceptual design of a compact 3 MeV RFQ, published at CERN in 2007 [1], was soon after followed by the detailed study of beam dynamics, performed at CERN, and RF design, jointly done by CERN and CEA, [2]. After the mechanical design, the fabrication of the Linac4 RFQ started in 2009 at CERN and was recently completed with the assembly of the three modules that form the accelerating structure. Aiming for maximum reliability, the design choice was for a traditional four-vane structure with a constant section profile; particular attention was given in the design to avoiding the use of dipole mode suppressors by limiting the RFQ length to 3m (3.5 wavelengths) and by carefully compensating local perturbations. In particular, an original solution was to adopt brazed vacuum ports that could precisely compensate for the local field perturbation introduced by the cavity openings. Remaining errors are compensated by slug tuners.

The very tight tolerances imposed by the compact design, in the absence of resonant coupling cells, have put great pressure on the machining and assembly teams and required intense work at the metrology workshop.

The three 1-m long RFQ modules have been assembled at the end of July at the CERN metrology workshop, then the RFQ has been moved and installed at the 3 MeV Test Stand where the last tuning of the accelerating field is presently being performed, with the finalization of the piston tuners and of the RF power coupler, before the start of the RF commissioning foreseen in November.

Figure 1 shows the RFQ cavity installed at the Test Stand and connected to its cooling system.



Figure 1: The Linac4 RFQ on its support, installed at the 3 MeV Test Stand.

RFQ MODULE FABRICATION

The fabrication of the RFQ is done through two brazing steps: with the first brazing the four RFQ vanes are assembled to form the RFQ cavity, while the second brazing, at lower temperature, is used to assemble the stainless steel flanges of the piston and vacuum ports and the two end flanges [3]. In the following we report the most relevant aspects of the construction of the three modules that form the RFQ. By convention we have called T1 the first module in the beam direction, followed by T2 and T3; in the fabrication process T1 and T3 were fabricated first, being very similar to each other from the mechanical point of view, while T2 was the last module to be built, due to the additional difficulty presented by the large waveguide openings for the RF power coupler.

T1

The fabrication of T1 started in 2009; it has been in fact the prototype on which all procedures have been tested and the fabrication strategy has been tuned. For that reason a considerable amount of metrology checks has been performed during its fabrication in order to assess that the fabrication was progressing well. For the same reason particular attention has been put into the RF bead-pull measurements, which were performed at each step of the assembly phase: mechanical assembly, first brazing and second brazing.

In table 1 the key dates for the construction of the module T1 are presented.

DESIGN OF A FOUR-VANE RFQ FOR CHINA ADS PROJECT*

Zhang Zhouli[#], He Yuan, Shi Aimin, Zhang Bin, Liu Yong, Du Xiaonan, Wang Jing, Li Chao, Jin Xiaofeng, Sun Liepeng, Zhao Hongwei, IMP, Lanzhou 730000, China
 D. Li, S. Virostek, M. Hoff, A. Lambert, J. Staples, LBNL, Berkeley, CA 94720, USA
 C. Zhang, IAP, J.W. Goethe University Frankfurt, Germany

Abstract

A four-vane RFQ accelerator has been designed for the ADS project which has been launched in China since 2011. As one of the two front ends of C-ADS LINAC, the RFQ works at a frequency of 162.5MHz, accelerating the proton beam from 35keV to 2.1MeV. Due to the CW (continuous wave) operation mode, a small Kilpatrick factor of 1.2 was adopted. At the same time, Pi-mode rods are employed to reduce the effect of dipole mode on quadrupole mode, and cavity tuning will be implemented by temperature adjustment of cooling water. Beam dynamics design, RF cavity design and thermal analysis all will be presented in the paper. Some fabrication test of the RFQ cavity will be described, too.

INTRODUCTION

All the countries in the world are confronting energy problems during the process of economic growth and society development nowadays, on one hand more and more energy is required to maintain modernized human life, on the other hand the earth's resources are limited. Although it can help solve the problems, nuclear energy has some drawbacks. First it is not absolutely safe, nuclear radiations caused by accidents happen occasionally; Secondly, management of nuclear waste is difficult [1]. However, the concept of ADS (accelerator driven system) proposed by C. Rubbia and his group has made nuclear energy much more safe and efficient [2]. It makes nuclear reaction controllable and transforms long-lived transuranic elements from conventional

nuclear reactors to short-lived ones while producing electricity at the same time. Due to the advantages of ADS and more and more energy demands, China has launched the ADS project in 2011.

There are two front ends of the linear accelerator for the C-ADS project (as shown in Fig. 1), while IMP (Institute of Modern Physics) is responsible for injector2. The RFQ of injector2 will use the four-vane structure because of the CW operation mode. The frequency of injector2 is 162.5MHz, which will lead to a big size of the RFQ cavity and bring some challenges to the fabrication. Here the design of the RFQ will be presented.

BEAM DYNAMICS DESIGN

The RFQ of C-ADS injector2 is designed to accelerate proton beam from 35keV to 2.1MeV which can lead to small neutron production and material activation [3], and main parameters are listed in table 1. The frequency of 162.5MHz is chosen in order to decrease the power loss density of the cavity. The inter-vane voltage is 65kV, which can well reduce the probability of discharge. The twiss parameters and emittances of output beam are required to be less than 1.5, 0.33 π mm mrad and 1keV ns respectively, table 1 shows all these requirements are met. Because the cavity is 420.8cm long, it will be equally divided into four modules when fabrication.

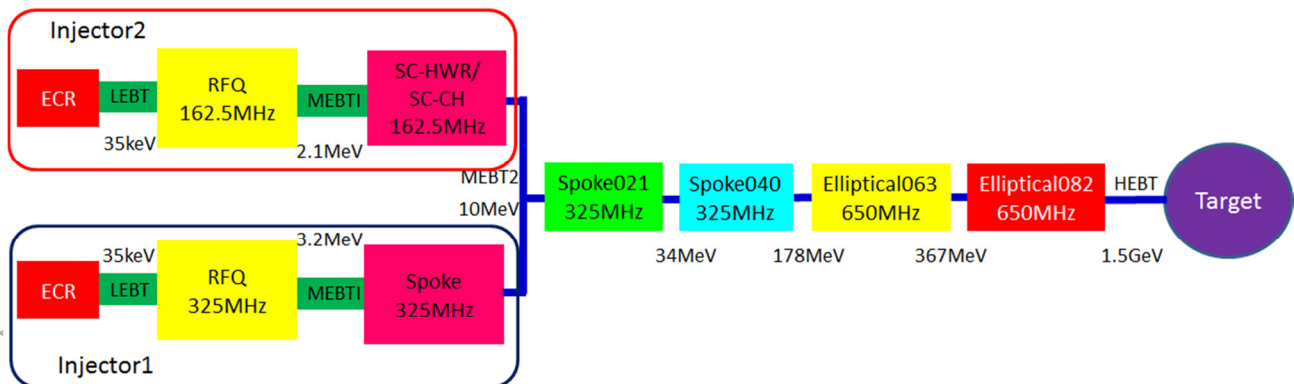


Figure 1: Layout of C-ADS driver accelerator.

* Work supported by NSF under Contract No. 11079001

[#] jolly@impcas.ac.cn

HIGH-POWER RF CONDITIONING OF THE TRASCO RFQ

E. Fagotti, L. Antoniazzi, A. Palmieri, F. Grespan, , INFN-LNL, Legnaro, ITALY
M. Desmons, CEA, Saclay, FRANCE

Abstract

The TRASCO RFQ is designed to accelerate a 40 mA proton beam up to 5 MeV. It is a CW machine which has to show stable operation and provide the requested availability. It is composed of three electromagnetic segment coupled via two coupling cells. Each segment is divided into two 1.2 m long OFE copper modules. The RFQ is fed through eight loop-based power couplers to deliver RF to the cavity from a 352.2 MHz, 1.3 MW klystron. After couplers conditioning, the first electromagnetic segment was successfully tested at full power. RFQ cavity reached the nominal 68 kV inter-vane voltage (1.8 Kilp.) in CW operation. Moreover, during conditioning in pulsed operation, it was possible to reach 83 kV inter-vane voltage (2.2 Kilp.) with a 0.1% duty cycle. The description of the experimental setup and procedure, as well as the main results of the conditioning procedure will be reported in this paper.

EXPERIMENTAL SETUP

The test was performed at CEA Saclay in January, February and March 2012.

The systems involved in the test are:

- RFQ cavity
- RFQ power system
- Vacuum system
- Cooling system
- Control system

The cavity under test is the first electromagnetic segment of the TRASCO RFQ [1], composed by two 1.2 m long OFE copper modules. The first module accommodates 12 gridded vacuum ports, the second one the 2 coupler ports. The RFQ end plates are equipped with dipole stabilizers [2, 3]. RFQ power level and field flatness are monitored by 16 pick-up loops, located inside the tuners along the 4 quadrants. The preservation of field flatness was verified looking at the pick-up signals, after transportation and positioning inside the CEA tunnel (Figure 1).

The core of the RF power system is the CEA 1.3 MW klystron, protected from the reverse power by a 1 MW circulator. The RF power is led into the RFQ tunnel through full-height WR2300 waveguide and then it is tapered to half-height WR2300 for the final distribution to the RFQ. Just upstream the RFQ, the RF power is split by a magic-TEE: two waveguide arms are coupled into the RFQ through 2 coupling loops, the 4th arm goes to a 100 kW water load. Forward and reverse powers are measured by directional couplers in the two waveguide arms before power couplers.

The vacuum system is composed by a dry primary pump, a turbo pump and two cryogenic pumps. The

system was designed to maintain a pressure level $P \leq 1.3 \times 10^{-6}$ mbar under proton gas load. In particular, cryogenic pumps are unnecessary in absence of proton beam and they have not been used for this test. Vacuum gauges are located above couplers and on the vacuum manifold. Gate valves and nitrogen filling channel allow keeping the cavity in inert atmosphere during transports.

Cooling system is designed to remove 300 kW of power and to finely tune the resonant frequency by temperature regulation. For this purpose, it is necessary to have two independent water loops with two regulating temperatures. In the cooling skid, the temperature of each water circuit can be regulated by mixing the cold inlet water with part of the warm water coming from the cavity. Furthermore, the global temperature of the system can be adjusted by regulating the amount of warm water circulating in the heat exchanger. Water flow inside RFQ cooling channel is finely set by flow regulating valves located on each cooling channel. These valves maintain the required flow within $\pm 2\%$ when input pressure varies in the range 1-10 bar. Water flows and input/output temperatures of both water loops are monitored.

Control system [4] is connected to the other subsystems in order to monitor their characteristic parameters (temperature, powers, water flows, pressures), to command their actuators (valves, pumps) and set-up variables (interlock thresholds, water temperatures). In particular, interlocks on temperature, pressure, water flow, forward power are processed by PLC (response time = 10 ms), while arc detectors and reflected power are directly sent to klystron to interrupt power in a few μ s.

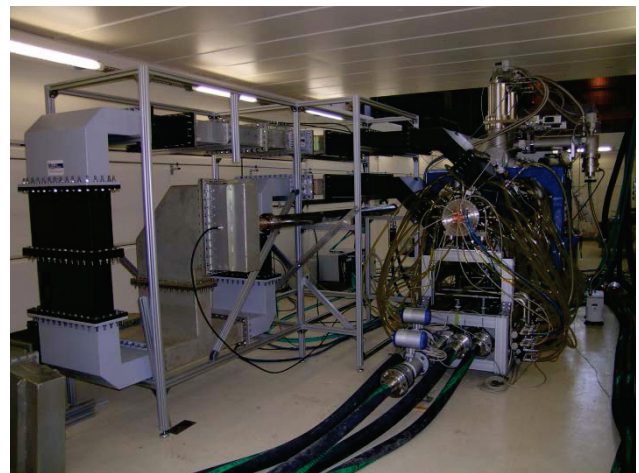


Figure 1: A view of TRASCO RFQ test in the IFMIF tunnel at CEA.

PRODUCTION AND QUALITY CONTROL OF THE FIRST MODULES OF IFMIF-EVEDA RFQ

F. Scantamburlo, A. Pepato, R. Dima, INFN/PD, Padova, Italy,
 C. Roncolato INFN/L.N.L., Legnaro, Italy

Abstract

The IFMIF/EVEDA RFQ, designed to accelerate a 125mA D+ beam from 0.1 MeV to 5 MeV at a frequency of 175 MHz, consists of 18 modules with length of ~550 mm each. The production of the modules has been started and 2 prototype modules plus module 16 have undergone all the production steps, including precision milling and brazing. The progress of the construction and especially the fine tuning of the design and engineering phase are reported.

BRAZING PROCEDURE MODIFICATIONS

Once completed the 2 steps brazing of the 1st module prototype, the acquisition of a continuous active scanning measuring machine (Zeiss Accura) allowed a deep and extensive investigation of the internal geometry of the cavity. A wide series of transversal and longitudinal scanning were then performed. The more detailed and reliable measurements showed a lack of symmetry induced by gravitation effect during the 1st step brazing [1]. The final geometry of the cavity resulted still within the acceptable tolerances range for a single module, but not for the complete line, figures 1 and 2. A vertical brazing assembly, which permitted instead a possibility of a single brazing step, has been developed, figure 3. In this respect, the groove geometry, layout and tooling had to be redesigned. We introduced extensive US scanning (destructive test) and inspection (non-destructive) for the qualification of the brazed surfaces (Cu-Cu and Cu-st. steel).

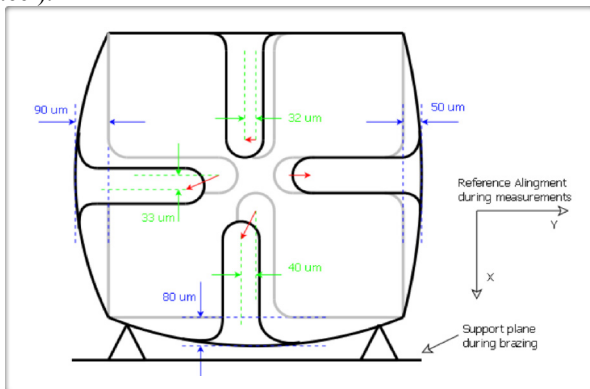
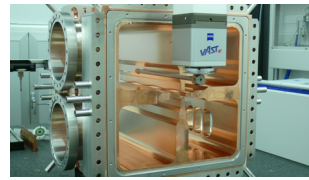


Figure 1: Scheme of the deformation of the cavity of the module 1 prototype after the second brazing



Pole	ΔX [μm]	ΔY [μm]	ΔR_0 [μm]
1	-40	-80	89.44
2	50	0	50.00
3	-32	0	32.00
4	-90	-33	95.86
mean ΔR_0 [μm]			66.83
$\partial f/\partial R_0$ [kHz/ μm]			7.60
Δf [kHz]			507.87

Figure 2: Module 1 prototype during CMM survey (left) and displacements of the tips (right).

R & D FOR SINGLE BRAZING STEP

With a single brazing step, the number of thermal cycles, reducing the mechanical properties of copper (1 annealing step + 1 final brazing step), is minimized.

The overall precision of the final geometry is optimized.

The cost and the timing of the modules production are also optimized.

Some basic tests on specimens having the same groove design, in order to compare vertical to horizontal brazing, have been performed.

Then two almost full scale tests have been performed finalizing an updated tooling set.

A complete inspection by US scan on slices of the brazed surfaces has been done (destructive). The grooves result always completely empty and no significant voids were detected on the brazing planes, figure 4.

Following these results, the production of the final modules started with SuperModule III-HE section. We adopted the vertical brazing approach but still with 2 brazing steps, until all details were well stated.

We completed the production of the module 16 (April '12), the second prototype module (July '12) and the 1st brazing step of module 17 (July '12).

The 1st single brazing step will be adopted on module 15 by October '12.



Figure 3: Full scale single brazing test

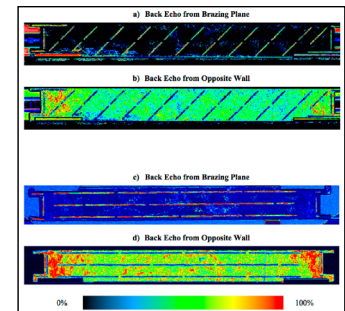


Figure 4: US inspection of two different brazing grooves design

THE RFQ INJECTOR FOR THE RADIOACTIVE ION BEAM OF SPES PROJECT

M. Comunian, A. Palmieri, A. Pisent, F. Grespan, INFN/LNL, Legnaro, Italy

Abstract

A Continuous Wave Radio Frequency Quadrupole Accelerator has been designed for the Radioactive Ion Beam of SPES Project to be used as an Injector of the ALPI Linac. The RFQ frequency is 80 MHz for an input energy of 40 keV, with output energy of 5 MeV and ion ratio $q/A \leq 1/7$. Particular care has been put in the design phase to include an internal bunching section able to reduce the longitudinal output emittance. The details of the RF study of such a cavity are included as well.

BEAM DYNAMICS

Within the project SPES laboratory a new injection line will be built at INFN LNL to transport and match the RIB to the existing ALPI superconducting linac [1].

This line includes a new RFQ (see Tab. 1) that will operate in a CW mode (100% duty factor) at a resonant frequency of 80MHz. This frequency is the same of the lowest energy ALPI superconducting structures. The injection energy of ions was set to 5.7 keV/u. This choice is a compromise between the desire to reduce the ion energy to simplify the LEBT and the RFQ bunching section design and the need to increase the injection energy to increase the beam rigidity in the spectrometer and to reduce space charge effects. The extraction energy was set to 727 keV/u (respect to the 588 keV/u of the present SRFQ), to optimize the beam dynamics of the SRF ALPI linac.

Table 1: Principal RFQ Parameters

Parameter (units)	Value
Operational mode	CW
Frequency (MHz)	80.
Injection Energy (keV/u)	5.7 ($\beta=0.0035$)
Output Energy (keV/u)	727 ($\beta=0.0395$)
Accelerated beam current (μA)	100
Charge states of accelerated ions (Q/A)	7 – 3
Internal bunching section	Yes

The design goals were to minimize the longitudinal and transverse emittances growth and to optimize the RF losses and transmission of the RFQ structure. The RFQ cells were created using the program CORTO, used for the design of CERN linac3 RFQ [2,3], PARMTEQ code package and Toutatis in an iterative cell-by-cell procedure. With this design the RF power consumption is minimized, while a variable voltage profile, like the IFMIF RFQ [4], allows accelerating the beam more effectively at higher velocities and achieving higher output energy. A transition cell was used at both the

entrance and exit of the RFQ. At the exit side, a radial matching section with an appropriate length after the transition cell was also used so that the output beam has the same Twiss parameters in both the horizontal and vertical planes. Table 2 and Figure 1 show the main parameters of the RFQ. The RFQ transmission is more than 95% of accelerated particles, the final longitudinal RMS emittance is 0.15 nskeV/u. The 99% longitudinal emittance is 1.2 nskeV/u, see Figures 2, 3 and 4.

Table 2: RFQ Design Parameters

Parameter (units)	Design 1
Inter-vane voltage V (kV, $A/q=7$)	63.8 – 120
Vane length L (m)	5.97
Average radius R_0 (mm)	5.03 – 9.574
Vane radius ρ to average radius ratio	0.8
Modulation factor m	1.0 – 3.16
Total number of cells	303
Synchronous phase (deg.)	-90 – -20
Focusing strength B	5.28 – 2.8
Peak field (Kilpatrick units)	1.7

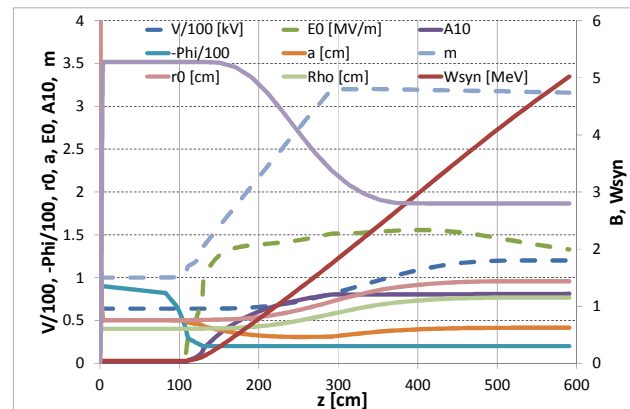


Figure 1: the main RFQ parameters vs. length as for beam dynamics outcomes.

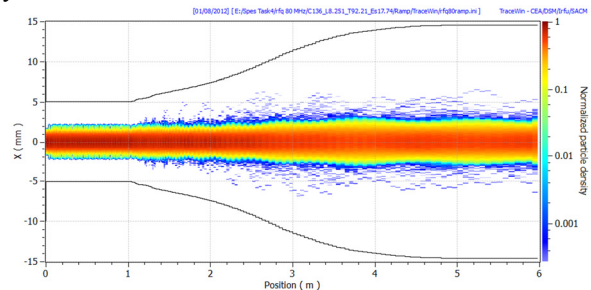


Figure 2: X envelope along the RFQ.

PLANS FOR AN INTEGRATED FRONT-END TEST STAND AT THE SPALLATION NEUTRON SOURCE*

Mark S. Champion[#], Alexander V. Aleksandrov, Mark Crofford, Dale Heidenreich, Yoon W. Kang, John Moss, Tom Roseberry, James Schubert, Oak Ridge National Laboratory, Oak Ridge, TN, USA

Abstract

A spare Radio-Frequency Quadrupole (RFQ) is presently being fabricated by industry with delivery to Oak Ridge National Laboratory planned in late 2012. The establishment of a test stand at the Spallation Neutron Source site is underway so that complete acceptance testing can be performed during the winter of 2012-2013. This activity is the first step in the establishment of an integrated front-end test stand that will include an ion source, low-energy beam transport (LEBT), RFQ, medium-energy beam transport, diagnostics, and a beam dump. The test stand will be capable of delivering an H- ion beam of up to 50 mA with a pulse length of 1 ms and a repetition rate of 60 Hz or a proton beam of up to 50 mA, 100us, 1Hz. The test stand will enable the following activities: complete ion source characterization; development of a magnetic LEBT chopper; development of a two-source layout; development of beam diagnostics; and study of beam dynamics of high intensity beam.

INTRODUCTION

The Spallation Neutron Source (SNS) Radio-Frequency Quadrupole (RFQ) was commissioned with beam in 2003. The RFQ performance has been sufficient to enable high-reliability neutron production, but there have been two sudden detuning events that required retuning of the structure, and there is evidence that the RFQ is being operated near the limits of thermal stability, i.e., reliable operation at higher average power is uncertain. The SNS accelerator presently delivers a 1 MW proton beam to the neutron production target. It is planned to ramp up the beam power to 1.4 MW over the next few years.

The RFQ structure twice experienced a sudden resonant frequency shift of a few hundred kHz. The first event occurred in October of 2003 during beam operation, the second in February 2009 during a maintenance period with no RF power in the cavity. A thorough examination of the RFQ cavity was conducted after the first event but nothing abnormal was found. The cavity was retuned using available tuners and successfully returned to operation in both cases. The root cause of the detuning has not been determined with certainty, but there is a similarity in both cases. The detuning was coincident with cooling system problems: in the first case a failure in the controls system caused the RFQ to cool down to 8°C; in the second case the cooling water pressure inadvertently increased over 100 psi. It is postulated that these events could create an abnormal stress causing a partial

separation of the braze joint between the inner high-purity copper structure and the outer GlidCop exoskeleton.

The RFQ showed resonance control instabilities when operating at a duty factor larger than ~4.2%, and this was one of the limiting factors in reaching 1 MW beam power. The machine downtime due to this RFQ instability was longer than 30 minutes per day, which affected the overall machine availability. The response time (about 5 minutes) of the Resonance Control Cooling System was a major contributing factor. The auto pulse-width adjustment scheme was added to the low level RF control system to provide faster control [1]. With this improvement the SNS RFQ has been confirmed to be stable up to 5.5% RF duty factor at the cost of using up 60 us of available RF pulse width for the temperature control. It is not clear if this solution will work at 7% duty factor required for achieving 1.4 MW beam power.

In order to mitigate the risk of failure of the original RFQ and to prepare for increased beam power, a contract was made for production of a spare RFQ at Research Instruments GmbH near Cologne, Germany. The RFQ is presently in production and delivery to SNS is expected in late 2012. A test stand is being prepared at SNS to support acceptance testing of the RFQ. The test stand will include all infrastructure needed to demonstrate full performance of the RFQ without beam.

It is planned to further develop the test stand thereafter into a fully-integrated front-end test stand that will include an ion source, low-energy beam transport (LEBT), RFQ, medium-energy beam transport (MEBT), diagnostics, and a beam dump. The test stand will be capable of delivering an H- ion beam of up to 50 mA with a pulse length of 1 ms and a repetition rate of 60 Hz or a proton beam of up to 50 mA, 100us, 1Hz. The test stand will enable the following activities: complete ion source characterization; development of a magnetic LEBT chopper; development of a two-source layout; development of beam diagnostics; and study of beam dynamics of high intensity beam.

TEST STAND SITE

The test stand will be installed in the RF Test Facility Annex, building 8320, at the SNS site, as shown in Figure 1. The RF Test Facility, building 8330, is adjacent and presently houses a high-power RF test stand for testing klystrons, RF devices, and cryomodules. Building 8330 also houses infrastructure for superconducting RF development and maintenance activities. This infrastructure includes a clean room, high-purity water system, high-pressure rinsing system, vertical test stand, cryomodule test stand, and cryomodule assembly area.

*ORNL is managed by UT-Battelle, LLC, under contract DE-AC05-00OR22725 for the U.S. Department of Energy.

[#]championms@ornl.gov

RF SETUP OF THE MedAustron RFQ*

B. Koubek, J. Schmidt, A. Schempp, IAP, Goethe University, Frankfurt am Main, Germany
 J. Haeuser, Kress GmbH, Biebergemuend, Germany

Abstract

A Radio Frequency Quadrupole (RFQ) was built for the injector of the cancer treatment facility MedAuston in Austria [1]. For the RF design simulations were performed using CST Microwave Studio® and the structure was manufactured by Firma Kress in Biebergemuend, Germany. The simulations and the RF setup of the delivered RFQ are presented in this paper.

INTRODUCTION

The 216.8 MHz MedAustron RFQ was designed to accelerate protons and carbon ions from 8 keV to 400 keV [2] on an electrode length of 1.25 m. It is a state of the art 4-Rod RFQ with quite slim electrodes and newly developed connections of the stems to the electrodes. Usually clamps were used to fix the electrodes to the stems (see Fig. 2). The accuracy of the machining allows us to remove the clamps. Simulations have shown that these new connections are causing less capacitance and hence less disturbing electric field than the clamps.

Fig. 1 shows the RFQ during its preparation at the Institute of Applied Physics (IAP) in Frankfurt am Main. More details about the RFQ basic design parameter can be found in Table 1.

Table 1: Design Parameters of the MedAustron RFQ

Parameter	Value	
Frequency	216.612	MHz
Input Energy	8	keV
Output Energy	400	keV
Beam Current (max)	4	mA
Aperture (min)	2	mm
Modulation Factor (max)	2	
Electrode Length	1250	mm
Intervane Voltage	70	kV
RF Cells	15	
Beam Height in Tank	19.5	mm
Stem Thickness	20	mm
Stem Distance	68	mm
Tank Length	1233	mm
Wall Thickness	40	mm

SIMULATIONS

Simulations have been performed using CST Microwave Studio® for the RF design. During this process two different shapes of the backside of the electrodes have been in-

* Work supported by BMBF

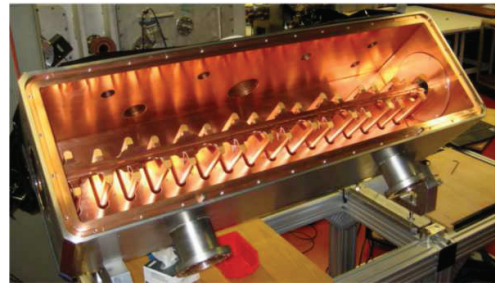


Figure 1: RFQ during preparation at IAP.

vestigated. One is a broad and the other one a more narrow socket of the electrodes backside. A top view of the two different shapes is shown in Fig. 2.

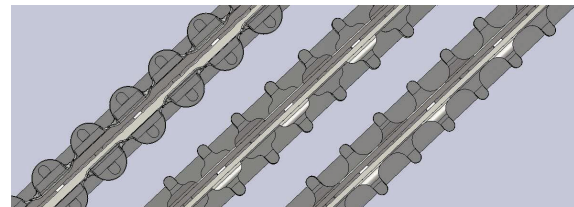


Figure 2: Former clamps (left), new broad (middle) and narrow (right) sockets.

Both shapes are rising the resonance frequency due to less capacitance compared to the old design with clamps. The broad shape increases frequency about one MHz more than the slim one, it shows less inductance and provides a fast and homogenous charge distribution on the electrode tips. Further informations about the RF characteristics of the connections of the electrodes can be found in [3].

MEASUREMENTS AND TUNING

Geometric Measurements

The accuracy of the machining and assembling of the single parts have been checked with a 3-D measurement device. The angle and the distance of the stems, the angle of the electrodes to each other and the position of the beam axis relatively to the reference surfaces have been measured. The measurements have met our expectations. Also no significant longitudinal electrode shift could be measured. Fig. 3 shows the measurement of the angle of the electrodes to each other and the longitudinal shift of the electrodes.

TEST RFQ FOR THE MAX-PROJECT

M. Vossberg, H. Klein, H. Podlech, A. Schempp, C. Zhang IAP, Univ. Frankfurt, Germany
 A. Bechtold, NTG Neue Technologien GmbH und Co KG, Gelnhausen

Abstract

A 17 MeV MHz proton linac is being developed as a front end of the driver accelerator for the MYRRHA facility in Mol. As a part of the MAX (MYRRHA Accelerator Experiment and Development) project a 4-rod Test-RFQ with a resonance frequency of 176 MHz has been designed and built for the MAX-Project. But the RFQ had to be modified to solve the cooling problem at cw-operation, the geometrical precision had to be improved as well as the rf-contacts. The developments led to a new layout and a sophisticated production procedure of the stems and the electrodes. Calculations show an improved Rp-value leading to power losses of <30 kW/m only, which is about 60 % of the power losses which could be achieved safely at cw-operation of the similar Saraf-RFQ. Thermal measurements and simulations with the single components are in progress. The temperature distribution in cw-operation will be measured and the rf-performance checked.

operation of the reactor. Breakdowns of the cw proton beam will cause thermal stress in the reactor core and it will also decrease the lifetime of the reactor. This is the reason why the design of the LINAC and the proton injector part has to be very safe [1]. Figure 1 shows an overview of the MYRRHA linac. A short and effective injector section is recommended by a KONUS (combined zero degree structure) beam dynamics design [2].

MYRRHA INJECTOR

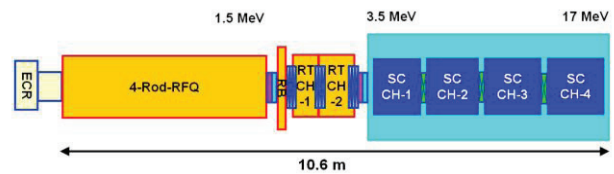


Figure 2: General layout of the MYRRHA injector.

INTRODUCTION

The development of MYRRHA (Multi-purpose hybrid research reactor for high-tech applications) is important to investigate advanced technologies for future power generations. With this test reactor the transmutation of long-lived radioactive waste of nuclear power plants will be studied. Also the reactor will contribute to the present material research and replace the expiring molybdenum reactors, which are essential for the nuclear medicine. An absolutely reliable proton accelerator is required for the

The planned injector (fig. 2) consists of an ECR source, a Radio Frequency Quadrupole (RFQ), two room-temperature CH-cavities and four superconducting CH-cavities. During the EUROTRANS project the RF frequency of the 17 MeV injector part has been set to 352 MHz. The new layout is changed to 176 MHz. The main reason is the possibility to use a flexible and cheap 4-rod-RFQ instead of the 4-vane-RFQ. This 176 MHz RFQ accelerates the particles to 1.5 MeV.

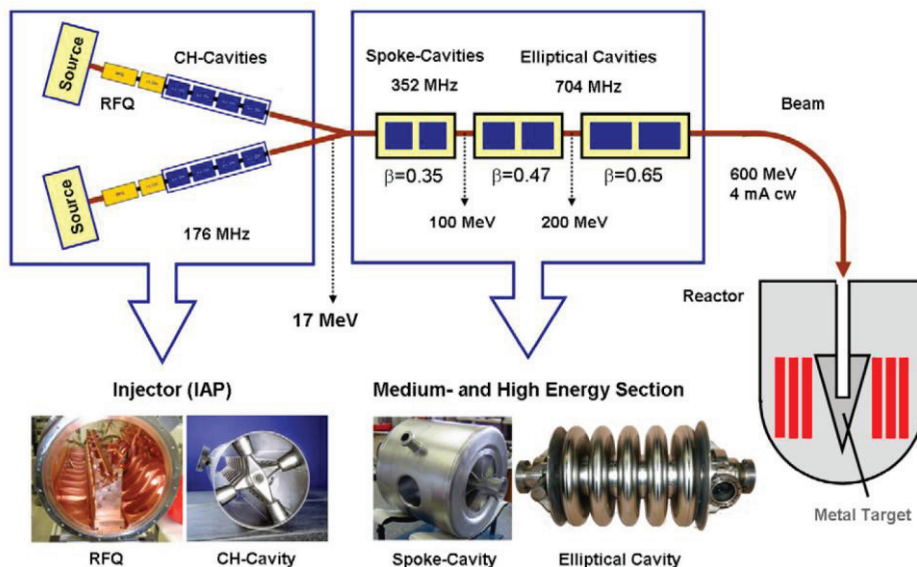


Figure 1: An overview of the MYRRHA driver linac.

Copyright © 2012 by the respective authors — cc Creative Commons Attribution 3.0 (CC BY 3.0)

TUNING STUDIES ON 4-ROD RFQs*

J. Schmidt, B. Koubek, A. Schempp, B. Klump, IAP, Univ. Frankfurt, Germany

Abstract

A NI LabVIEW based Tuning Software has been developed to structure the tuning process of 4-rod Radio Frequency Quadrupoles (RFQs). Its results are compared to measurement data of 4-rod RFQs in different frequency ranges. For the optimization of RFQ design parameters, a certain voltage distribution along the electrodes of an RFQ is assumed. Therefore an accurate tuning of the voltage distribution is very important for the beam dynamic properties of an RFQ. A variation can lead to particle losses and reduced beam quality especially at higher frequencies. Our electrode design usually implies a constant longitudinal voltage distribution. For its adjustment tuning plates are used between the stems of the 4-rod-RFQ. These predictions are based, in contrast to other simulations, on measurements to define the characteristics of the RFQ as it was build - not depending on assumptions of the design. This will lead to a totally new structured process of tuning 4-rod-RFQs in a broad range of frequencies by using the predictions of a software. The results of these studies are presented in this paper.

RESONANT CIRCUITS

A simplified model of the 4-rod RFQ resonator is a chain of LC-oscillators where each RF cell has its own resonance frequency. In these RF cells the stems represent the inductance, while the electrodes form the capacitive part of the circuit. A more detailed model is described in [1].

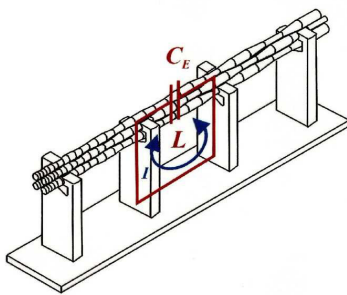


Figure 1: LC Resonator as Equivalent Circuit of a 4-Rod RFQ.

To tune this system, the resonance of each RF cell has to be tuned with tuning plates. They short cut the current path between the stems, to change the inductance of the RF cell. The longitudinal voltage distribution, the so called flatness, is a fundamental parameter in the particle dynamic design of an RFQ. Usually a constant longitudinal voltage along

the electrodes is the basis of our design, but other distributions are possible as well [2].

Following the particle dynamics the longitudinal voltage distribution has to be arranged. It is measured using the capacitive perturbation method. A perturbation capacitor sits on a pair of electrodes of one RF cell to cause a frequency shift due to Thomson's law. The resulting frequency shift of the cell is proportional to its voltage (see Eq. 1).

$$U \propto \Delta f_0 = \frac{1}{\sqrt{LC}} - \frac{1}{\sqrt{L(C + \Delta C)}} \quad (1)$$

THE VOLTAGE TUNING PROCESS

The process of adjusting the flatness is an iterative process of shifting the tuning plates and try to find a set of heights, which results in the desired distribution and total resonance frequency. This process can take some time, especially working on long RFQ structures with a lot of RF cells [3].

Due to several reasons like the changing modulation or differences in the manufacturing, the RFQ has deviations in its characteristics along the electrodes profile [4]. This leads to a different impact of the tuning plates depending on their position in the RFQ.

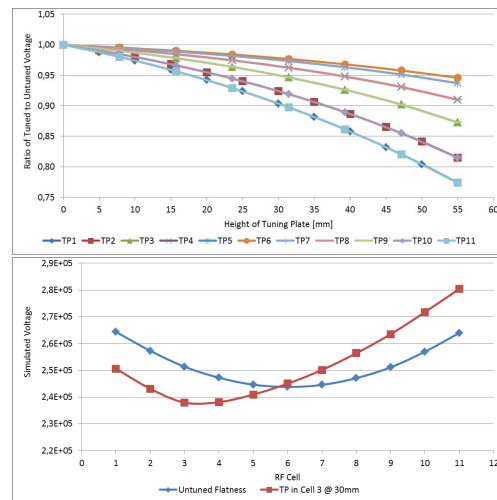


Figure 2: The voltage in $z=k$ from raising tuning plates in all cells (upper graph) and the longitudinal change with a tuning plate in cell $k=3$ (lower graph).

Raising a tuning plate in cell $k \in [1, n]$ decreases the voltage in cell k and its neighboring cells $k \pm i$ with $i < i_0$, while the voltage raises in cells $k \pm i$ with $i \geq i_0$. This behavior is shown in Fig. 2

* Work supported by BMBF

RFQ WITH IMPROVED ENERGY GAIN

A.S. Plastun, NRNU «MEPhI», Moscow, Russia

A.A. Kolomiets, ITEP, Moscow, Russia

Abstract

RFQ structure is practically only one choice for using in front ends of ion linacs for acceleration up to energy about 3 MeV. This limit is due to its relatively low acceleration efficiency. However it isn't intrinsic feature of RFQ principle. It is defined only by vane geometry of conventional RFQ structure with sinusoidal modulation of vanes. The paper presents results of analysis RFQ with modified vane geometries that allow to reach acceleration efficiency compared with IH DTL structures. RFQ with modified vanes was used for design second section of heavy ion injector of TWAC for acceleration of ions with $Z/A=0.33$ up to 5 MeV/u.

INTRODUCTION

An RFQ output energy doesn't usually exceed several MeV. Using conventional RFQ structure for acceleration of particles for higher energies is impractical because RFQ energy gain decreases rapidly with energy at constant modulation.

Many DTL structures were proposed for beam acceleration following RFQ that use magnetic or radio frequency focusing. The structures are well studied, they can provide good accelerating efficiency and are realized in a number of linacs. In the framework of heavy ion injector development for TWAC facility [1] several designs of second section based on these structures have been studied. In addition it was considered option that uses conventional RFQ with relatively minor modification of RFQ electrodes and resonant structure.

81 MHz RFQ – front end of TWAC injector has been recently successfully commissioned [2]. It is designed to accelerate beam from laser ion source with $Z/A = 0.33$ up to energy 1.57 MeV/u.

This paper presents result of study of TWAC injector second section design based on modified RFQ. The main goal of the modification was to provide maximum energy gain at focusing sufficient for acceleration beam with current 30 mA up to 5 MeV/u.

ENERGY GAIN IN RFQ

Vanes with Sinusoidal Modulation

The energy gain of a particle in RFQ is

$$\Delta W = e \frac{Z}{A} UT \cos \varphi_s, \quad (1)$$

e - electron charge, Z - charge number of the particle, A - mass number of the particle, U - voltage between adjacent vanes, T - accelerating efficiency, φ_s - phase of RF field, when synchronous particle is in a maximum of accelerating field.

Voltage U is usually chosen taking into account many different considerations. However it has to be as high as possible to increase energy gain. Its maximum value in this case is fully defined by acceptable surface electric field $E_{s \text{ lim}}$. Most accurately voltage can be found by numerical simulation for real vane geometry and expressed as

$$U = U_{sim} \frac{E_{s \text{ lim}}}{E_{s \text{ sim}}}, \quad (2)$$

Here U_{sim} is voltage between vanes in computer model and $E_{s \text{ sim}}$ is maximum field at vane surface obtained from simulation result.

Figure 1 shows results of field simulation in RFQ cell with code OPERA 3D. Simulated cell length $L_c = \beta\lambda/2$ corresponds particle energy at TWAC RFQ output. Curve 1 presents maximum field at vane surface calculated for sinusoidal modulation in $1 \leq m \leq 5$ range. Aperture for all modulations was constant $a = 8$ mm, that is average distance from axis to vane was changed as $R_0 = a(m+1)/2$. Simulation results show that for surface field limit $E_{s \text{ lim}} = 250$ kV/cm (about 2 Kilpatrick units for frequency $f = 81$ MHz) maximum voltage can reach according formula (2) $U \cong 500$ kV.

Accelerating efficiency T was calculated from simulated distribution of longitudinal field component E_z on axis. T factor for cell with sinusoidal modulation of vanes is limited by value $T \cong 0.7$. It means that the maximum effective accelerating gain per cell with studied parameters doesn't exceed $UT \cong 350$ kV.

Curve 1 shows that there is no sense to increase modulation factor more than $m = 4 \div 5$ because maximum field $E_{s \text{ sim}}$ reduces very slowly for higher m while focusing efficiency rapidly decreases. Figure 2 shows transverse phase advance calculated with the following expression [3]:

$$\sigma^2 = \frac{2}{\pi^2} K^4 + \frac{\pi e UT}{W_{kin}} \sin \varphi,$$

$$K^2 = \frac{Z}{A} \frac{e \bar{G}}{4 W_0} \lambda^2.$$

Here \bar{G} is mean value of simulated transverse field gradient along RFQ cell, W_0 - rest mass of proton, λ - wavelength of RF field. Estimation shows that transverse motion is very close to stability border at $m \cong 4$. It defines limiting capability of conventional RFQ with sinusoidal modulation for higher energy gain acceleration.

It is possible to improve accelerating efficiency using trapezoidal modulation proposed in [4]. Cell with this modulation type is shown in Figure 3. The trapezoidal

IMPROVEMENTS AT THE BNL 200 MeV LINAC*

D. Raparia, J. Alessi, B. Briscoe, J. Fite, O. Gould, V. LoDestro, M. Okamura, J. Ritter, A. Zelenski
 Brookhaven National Laboratory, Upton, NY 11973, USA

Abstract

After reconfiguration of the low energy (35 keV) and the medium energy (750 keV) transport lines in 2009-10, the Brookhaven linac delivered the highest intensity beam since it was built in 1970 (~120 μ A average current of H⁺ to the Brookhaven Linac Isotope Producer). It also delivered lower emittance polarized H⁻ ion beam for the polarized program at RHIC. To increase the intensity further, the match into the RFQ was improved by reducing the distance from the final focusing solenoid to the RFQ and replacing the buncher in the 750 keV line with one with higher Q value, to allow operation at higher power. The transmission efficiencies and beam quality will be discussed in the paper.

INTRODUCTION

The Brookhaven National Laboratory (BNL) 200 MeV drift tube linac (DTL) provides H⁺ beam at 6.67 Hz, 200 MeV for the polarized proton program for Relativistic Heavy Ion Collider (RHIC) and 66-200 MeV for Brookhaven Linac Isotope Production (BLIP). The RHIC program needs 2 pulses every AGS cycle (~4 sec), one for injection into Booster and other for polarization measurement at the 200 MeV polarimeter located in the High Energy Beam Transport line (HEBT). The rest of the pulses are delivered to BLIP. The requirements for

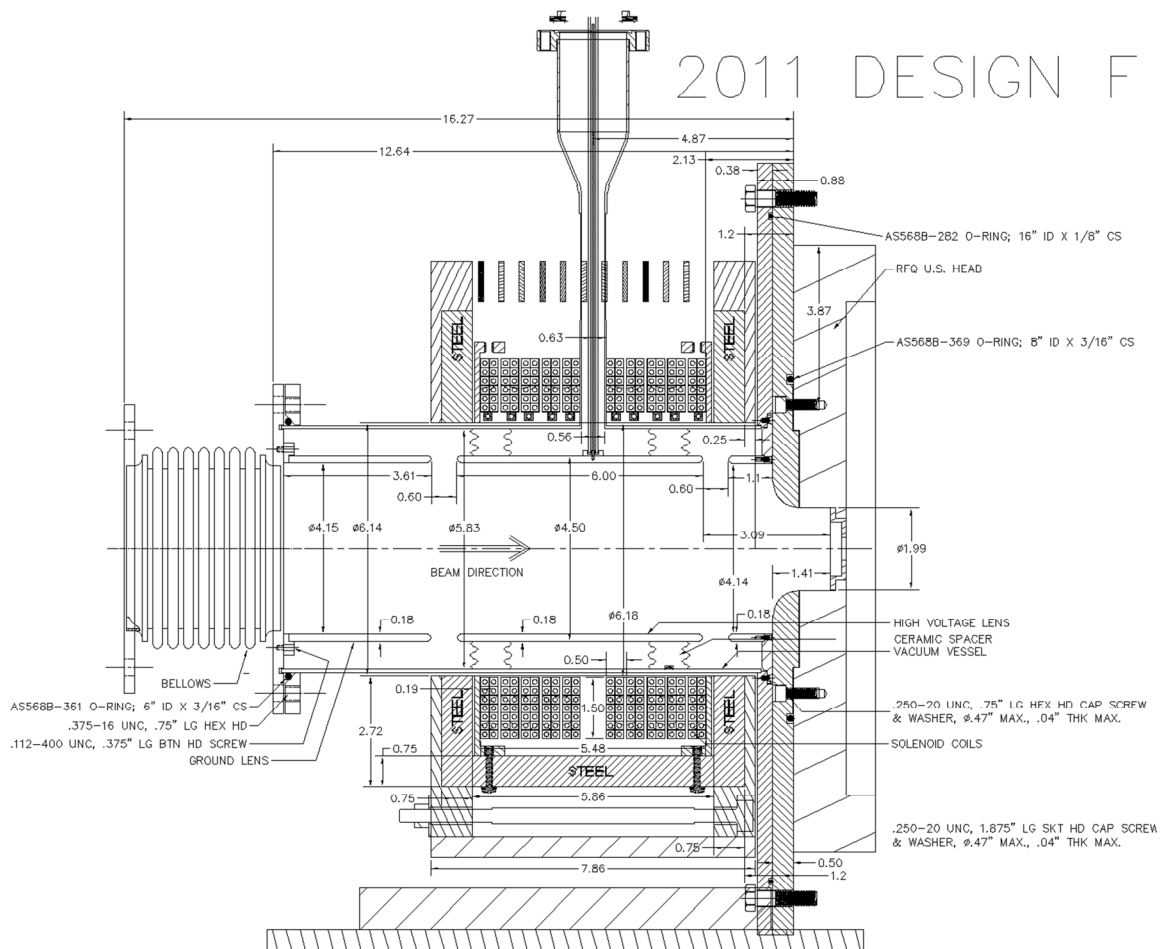


Figure 1: Design of the New Solenoid- and Einzel lens system for the front of the RFQ. The Distance between RFQ and solenoid was decrease by 1.08 inches.

*Work performed under Contract Number DE-AC02-98CH10886 with the auspices of the US Department of Energy
 #raparia@bnl.gov

RECENT PROGRESS WITH THE J-PARC RFQs

Y. Kondo*, T. Morishita, K. Hasegawa, JAEA, Tokai, Naka, Ibaraki, 319-1195, Japan
H. Kawamata, T. Sugimura, F. Naito, KEK, Oho, Tsukuba, 305-0801, Japan

Abstract

In this paper, we will report recent topics about J-PARC RFQs. First, the user operation of the existing RFQ (RFQ I) has been resumed from the long shutdown due to the earthquake. This RFQ has been suffered from a breakdown problem since 2008, therefore we have been developing a back-up RFQ (RFQ II). In April and May 2012, the high power test was successfully performed. Finally, we are fabricating a new RFQ for the beam-current upgrade of the J-PARC linac (RFQ III).

INTRODUCTION

At present, three radio frequency quadrupoles (RFQs) are under operation or development in Japan proton accelerator research complex (J-PARC). The original design energy and peak beam current of the J-PARC linac is 400 MeV and 50 mA, though, at the initial phase, the operation was started with a energy of 181 MeV omitting annular-ring coupled structures[1]. An RFQ built for the Japan hadron facility (JHF) project is used for the initial-phase linac; the design peak beam current of this RFQ is 30 mA[2]. This RFQ is called RFQ I. Because a sparking problem of this RFQ I occurred[3], an RFQ is fabricated as a spare of RFQ I[4]. This is called RFQ II. Moreover, to achieve the original design power of 1 MW (at the neutron target), it is planned to upgrade the linac to the original 400 MeV and 50 mA[5]. To upgrade the beam-current, another RFQ with a design current of 50 mA is newly fabricated and will replace the old one. This 50-mA RFQ is called RFQ III. In Table 1, parameters for each RFQ are listed.

In this paper, the status of each RFQ is described.

RFQ I

Fortunately, there was no damage to the RFQ I due to the Tohoku earthquake. During the period of the linac recovery[6] in 2011, a baking process was applied to desorb the absorbed gases on the surfaces during the operation after the improvement of the vacuum system in 2009[3].

Just after the restart of beam operation, the trip rate was rather high, but it became to be same level (~ 20 times / day) as that of just before the earthquake. Figure 1 shows the history of the trip rate from just after the vacuum improvement to the run end before the long shut down of this summer.

*yasuhiro.kondo@j-parc.jp

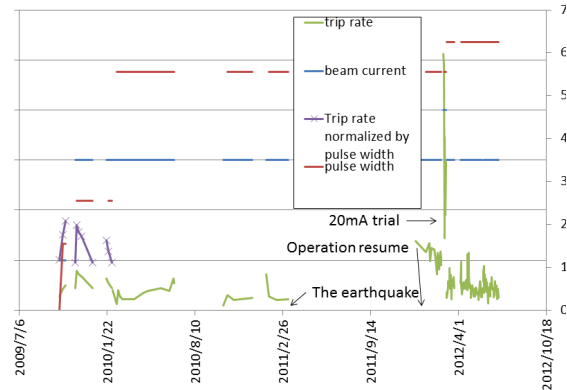


Figure 1: History of the trip rate of RFQ I from just after the vacuum improvement to the last run.

RFQ II

The high-power test of the RFQ II was planned to be completed in March 2011, but it was postponed due to the earthquake till the recovery of the accelerator from the damage of the disaster. After the user operation of the J-PARC was resumed, the high-power test of RFQ II was finally carried out from April to May 2012. Figure 2 is a photograph of RFQ II under high-power test.



Figure 2: High-power testing RFQ II.

After the assembling of high-power tuners, a coupler, and end plates, the measured unloaded Q-value was 9436. This corresponds to the value of 87 % of the SUPERFISH[7] calculation. The coupling factor of the high-power RF-coupler was set to be 1.7. The RFQ II was pumped with one 1700 l/s (for N₂) cryopump and two 400 l/s ion pumps during the high-power test.

In Figure 3, the conditioning history of RFQ II is shown. At first, the pulse height and repetition rate were set to be 30 μ s and 25 Hz. After 15 hours conditioning, the peak

NUMERICAL SIMULATION OF PROJECT-X/PXIE RFQ*

J-F. Ostiguy[†], N. Solyak, A. Saini
 Fermilab, Batavia IL 60510, USA

Abstract

Project-X is a proposed superconducting linac-based high intensity proton source at Fermilab[1]. The machine first stages operate in CW mode from 2.1 to 3 GeV. A high bandwidth chopper is used to produce the required bunch patterns. A 162.5 MHz CW RFQ accelerates the beam from 30 keV to 2.1 MeV. A concern with CW operation is that losses either within the RFQ or in the downstream modules should be well-understood and remain very low to ensure safe and/or reliable operation. In this contribution, we use the code TOUTATIS to perform RFQ simulations.

INTRODUCTION

Project-X is a multi-institutional collaboration. The latter includes LBNL, which in view of its considerable experience, has been assuming the responsibility of designing and delivering the RFQ. The latter is now ready for fabrication; delivery at Fermilab is expected sometime next year. The LBNL design work has been performed using an in-house version of Los Alamos suite of RFQ codes, which includes PARMTEQM. The code is by now well-established and has been used to design numerous successfully operated devices.

The LBNL group has performed extensive numerical studies of its design. In particular, detailed studies of the impact of imperfections on the performance of their RFQ have been reported at a recent Project-X collaboration meeting [3]. In this contribution, we present a first attempt at a similar type of analysis, using TOUTATIS, an alternative RFQ simulation code licensed from CEA/Saclay. This code possesses certain features that are attractive. Among them is the fact that field computations are performed directly from a geometric description of the vanes and are not based on a series expansion. The space charge solver employs a 3D multigrid algorithm and is self-consistent. Integration is performed using time, rather than longitudinal position as an independent variable. Finally, there is, no artificial limitation on the number of particles that can be tracked.

RFQ DESIGN

A set of relevant parameters for the LBNL designed PXIE[2] RFQ is presented in Table 1. It is a conventional device in that it includes the usual radial matcher, gentle buncher and acceleration sections. The downstream termination is of the Crandall type, i.e. it involves one cell where the modulation transitions from $m > 1$ to $m = 1$ followed by another where $m = 1$ whose length is adjusted to

control exit beam parameters and to prevent phase dependent exit kicks. The design provides an output beam which is geometrically round with minimal angular divergence. Sections are clearly distinguishable on Figure 1, which shows the vane profile in the horizontal plane. Overall

Parameter	Value
Vane Length	4.44 m
Energy	30 keV - 2.1 MeV
Input Emittances	0.12,0.12, 0.0 mm-mrad
Output Emittances	0.15 (x),0.15(y), 0.21(z) mm-mrad

Table 1: Some relevant parameters for the Project-X RFQ.

transverse and longitudinal rms beam envelopes are shown in Fig. 2.

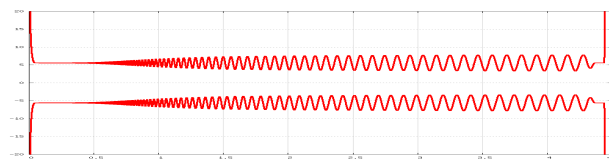


Figure 1: Vane profile in the horizontal plane.

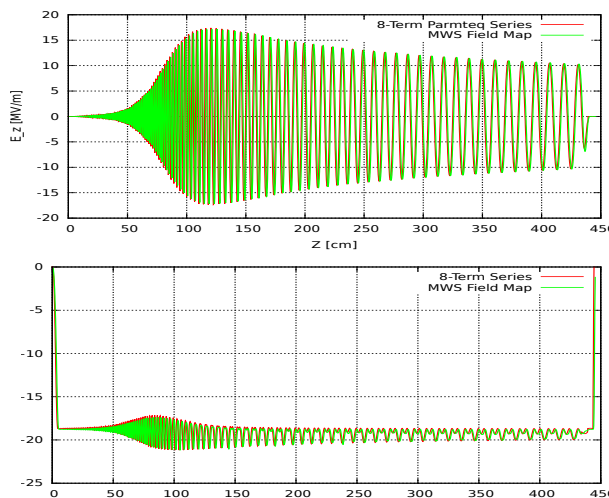


Figure 2: Field profile in the PXIE RFQ.

CODES

The Los Alamos code PARMTEQ is a tracking code where the RFQ field is modelled in the electrostatic approximation between the vanes. The field is obtained from an 8-term axial expansion solution of Laplace's equation. PARMTEQ does not compute the series coefficients; the latter are interpolated from a parametrized table of pre-computed coefficients extracted from a full so-

* Work performed under US DOE contract DE-AC02-76CH03000.

[†] ostiguy@fnal.gov, solyak@fnal.gov

EXPERIMENTAL AND SIMULATION STUDY OF THE LONG-PATH-LENGTH DYNAMICS OF A SPACE-CHARGE-DOMINATED BUNCH*

I. Haber, B. L. Beaudoin, S. Bernal, R. A. Kishek, T. W. Koeth, Y. C. Mo
University of Maryland, College Park, MD 20742, USA

Abstract

The University of Maryland Electron Ring (UMER) is a low-energy (10 KeV) electron facility built to study, on a scaled machine, the long-propagation-length evolution of a space-charge-dominated beam. Though constructed in a ring geometry to achieve a long path length at modest cost, UMER has observed important space-charge physics directly relevant to linear machines. Examples are presented that emphasize studies of the longitudinal dynamics and comparisons to axisymmetric simulations. The detailed agreement obtained between axisymmetric simulation and experiment is presented as evidence that the longitudinal physics observed is not strongly influenced by the ring geometry. Novel phenomena such as soliton formation, unimpeded bunch-end interpenetration, and an instability that occurs after this interpenetration, are discussed.

BACKGROUND

The University of Maryland has had a long-standing program, inspired and nurtured by the late Prof. Martin Reiser, of using electron beams to conduct research, on a scaled basis, into the fundamental physics of intense charged particle beams when the beam evolution is dominated by the influence of space charge. An important and continuing element of this research has been its emphasis on comparison of theory and simulation to experiment. The early successes achieved are a strong motivation for the current research.

During the early years, the primary experimental facility was a 240 mA, 5 KeV electron beam injected into a transport system that consisted of 38 discrete iron core solenoid magnets, placed 13.6 cm apart [1]. Particle-in-cell (PIC) simulations [2] that carefully modelled the iron core solenoids [3] were successful in reproducing, in detail, experimentally observed behavior. The influence of space charge on beam characteristics such as emittance growth in the presence of misalignments and small errors in the initial match [4] were quantitatively reproduced and explained.

A significant milestone in simulation/experiment benchmarking [5] was achieved in an experiment where a mask was placed immediately downstream of the electron gun to produce a five beamlet pattern. This experiment was performed to test the theory that a nonuniform transverse current profile will relax to the lowest-potential-energy uniform profile. The excess energy would be converted to kinetic energy, causing the beam

emittance to grow [6]. Agreement was obtained on the emittance growth between experiment and simulation and theory.

An unexpected downstream re-emergence of the initial five-beamlet pattern was observed on a series of downstream phosphor screen images. Furthermore, the image evolution was reproduced in striking detail in simulation. The simulations assumed uniform emission from the gun with the intrinsic emittance calculated from the cathode temperature and employed no adjustable free parameters. In addition, evolution of the current cross-section was sufficiently sensitive to the initial emittance that only a few percent variation in the initial emittance assumed in the simulation resulted in a noticeable deviation from the experimentally observed patterns. Comparison between simulation and experiment could therefore be used to deduce beam emittance.

To study conversion of the space charge potential energy in a mismatch to kinetic energy, an additional series of experiments was performed where the beam was purposely mismatched. Theoretical predictions of the energy exchange were verified. However, unlike the matched beamlet case where a final distribution with a uniform cross section was observed, the extra kinetic energy was transferred mostly to a beam halo [7].

Additional experiments were also conducted to test longitudinal beam dynamics. Generally good agreement between theory and experiment was also obtained [8]. In investigating both transverse and longitudinal dynamics, many experiments were conducted that validated both theoretical predictions of the physics of the evolution of space-charge dominated beams, as well as, the ability of simulations to predict the observed behavior. However, because of the limited length of the linear transport line, it was not possible to address many significant questions about the physics of space-charge-dominated beams. For example, what are the characteristic of the equilibrium distribution that is reached after long time relaxation of a space-charge-dominated beam? In addition, many questions concerning the longitudinal dynamics, which have a much slower evolution time than the transverse dynamics are inaccessible in a short linear transport system.

UNIVERSITY OF MARYLAND ELECTRON RING (UMER)

Ring Description

In order to address the long pathlength physics of a space charge dominated beam, while remaining within the available space and budgetary limits, the University of Maryland Electron Ring (UMER) was constructed. A

*Work supported by the United States Department of Energy and the Office of Naval Research.

MULTIPOLE FIELD EFFECTS FOR THE SUPERCONDUCTING PARALLEL-BAR/RF-DIPOLE DEFLECTING/CRABBING CAVITIES*

S. U. De Silva^{1,2#}, J. R. Delayen^{1,2},

¹Center for Accelerator Science, Old Dominion University, Norfolk, VA 23529, USA.

²Thomas Jefferson National Accelerator Facility, Newport News, VA 23606, USA.

Abstract

The superconducting parallel-bar deflecting/crabbng cavity is currently being considered as one of the design options in rf separation for the Jefferson Lab 12 GeV upgrade and for the crabbng cavity for the proposed LHC luminosity upgrade. The knowledge of multipole field effects is important for accurate beam dynamics study of rf structures. The multipole components can be accurately determined numerically using the electromagnetic surface field data in the rf structure. This paper discusses the detailed analysis of those components for the fundamental deflecting/crabbng mode and higher order modes in the parallel-bar deflecting/crabbng cavity.

INTRODUCTION

The parallel-bar/RF-dipole deflecting/crabbng cavity has been optimized from a rectangular-shaped design with cylindrical-shaped parallel bars into a design with a cylindrical-shaped outer conductor with trapezoidal-shaped parallel bars [1,2], named the rf-dipole cavity. The improved rf-dipole deflecting/crabbng cavity design operating in TE₁₁-like mode has attractive properties with low and balanced surface fields, high shunt impedance and well separated higher order modes (HOMs). The deflecting/crabbng mode is the lowest mode in the rf-dipole design.

Currently the rf-dipole design is being considered as one of the rf separator options for the Jefferson Lab 12 GeV upgrade and as one of the crabbng cavity options for proposed LHC luminosity upgrade operating at 499 MHz and 400 MHz respectively. A 750 MHz design is also being considered as a crabbng cavity for the proposed medium energy electron-ion collider (MEIC) at Jefferson Lab [3]. The first prototypes of the cylindrical-shaped 499 MHz and 400 MHz rf-dipole cavities (Fig. 1 (A) and (B)) are being fabricated and are in preparation for rf testing [4].

The 400 MHz crabbng cavity design was further modified into a square-shaped outer conductor (Fig. 1(C)) with fixed transverse dimensions of <295 mm, to meet the dimensional constraints of the LHC crabbng system. The design was further improved by curving the bar geometry at the beam aperture (Fig. 1(D)) to reduce the transverse field variation across the beam aperture.

*Authored by Jefferson Science Associates, LLC under U.S. DOE Contract No. DE-AC05-06OR23177. The U.S. Government retains a non-exclusive, paid-up, irrevocable, world-wide license to publish or reproduce this manuscript for U.S. Government purposes. Part of this work was done in collaboration with and supported by Niowave Inc. under the DOE STTR program.
#sdesilva@jlab.org

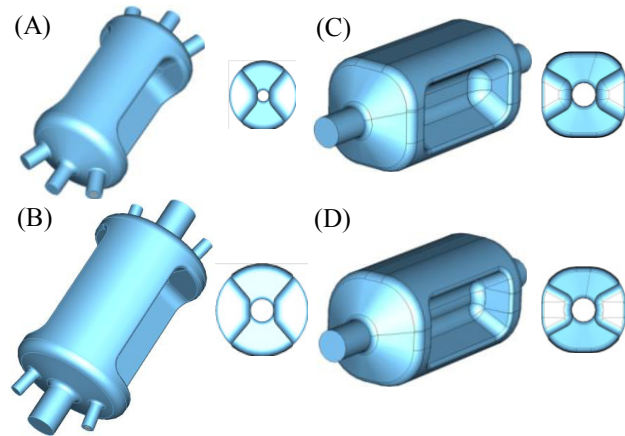


Figure 1: RF-dipole geometries and cross sections of (A) 499 MHz design, (B) cylindrical-shaped 400 MHz design, (C) square-shaped 400 MHz design and (D) square-shaped 400 MHz design with curved inner bar surfaces.

MULTIPOLE FIELD ANALYSIS

In the rf-dipole design, the field varies across the beam aperture off the beam axis generating a non-uniform transverse deflection. The field variation in x and y directions are shown in Fig. 2, for all the rf-dipole designs mentioned in Fig. 1.

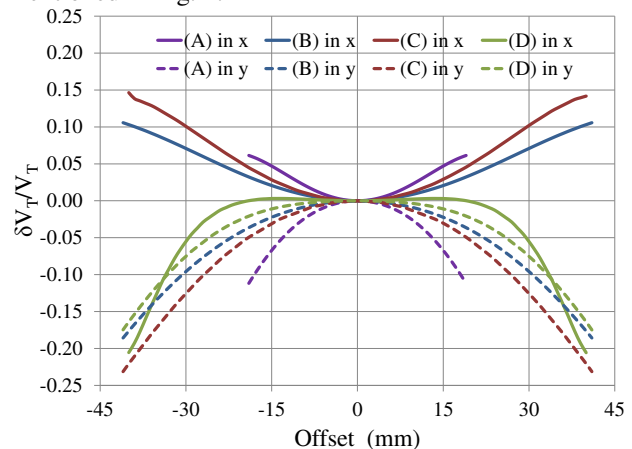


Figure 2: Normalized transverse voltage in x and y directions for designs (A), (B), (C) and (D) in Fig. 1.

The non-uniform transverse fields can generate higher orders of transverse momentum apart from the first order transverse momentum that corresponds to the deflecting or crabbng voltage. These higher order transverse multipole components may lead to perturbations in the beam. This paper presents the higher order multipole components present in the rf-dipole cavity and suppressing of those components by modifying the geometry.

SIMULATED PERFORMANCE OF THE CARIBU EBIS CHARGE BREEDER TRANSPORT LINE*

C. Dickerson[#], S.A. Kondrashev, B. Mustapha, P.N. Ostroumov, ANL, Argonne, IL 60439, U.S.A.

Abstract

An Electron Beam Ion Source (EBIS) has been designed and is being built to charge breed ions from the Californium Rare Isotope Breeder Upgrade (CARIBU) for post acceleration in the Argonne Tandem Linear Accelerator System (ATLAS). The calculated transverse acceptance of the EBIS charge breeder can approach the emittance of the injected ion beam, so beam distortion during transport could lead to incomplete injection and a decrease in the overall system efficiency. The beam quality can be maintained for simulations of the transport line using the ideal ion beam parameters. This paper reports the results of the electrostatic and ion beam transport simulations used to minimize the ion beam distortions by optimizing component designs and configurations.

INTRODUCTION

Acceleration in the Argonne Tandem Linear Accelerator System (ATLAS) requires a $q/A \geq 1/7$, so +1 and +2 fission fragment beams from the Californium Rare Isotope Breeder Upgrade (CARIBU) [1] require charge breeding prior to injection into ATLAS. An Electron Cyclotron Resonance (ECR) ion source is currently used to charge breed the ions, but the contamination of the accelerated beams from plasma-surface interactions within the source obscures the signal of low intensity radioactive ion beams. An Electron Beam Ion Source (EBIS) has been designed [2, 3] and is being built for the CARIBU system, and will improve the purity and intensity of the beams for post acceleration in ATLAS. The CARIBU EBIS is largely based on the Test EBIS developed at Brookhaven National Laboratory [4], and has been designed to operate with a high current, 2 A, and a low current, 0.2 A, electron gun. Ostensibly the high current gun will replicate operating conditions achieved with the Test EBIS, while the low current gun will maximize breeding efficiencies by operating in the closed-shell mode [5]. The low current electron gun was designed to produce 0.2 A to avoid possible virtual cathode formation at the low energies required to match shell closures of the injection ions (~ 2 keV), and the gun will employ a $\varnothing 1.6$ mm cathode to maintain a high current density within the trap, ~ 500 A/cm².

Ion beams from CARIBU, cooled and bunch in a Radio Frequency Quadrupole (RFQ), will have a full emittance of $3 \pi \cdot \text{mm} \cdot \text{mrad}$ at 50 keV for the expected mass range

80-160 amu [6]. Aside from the general desire to maintain the best possible ion beam quality during transport, the normalized emittance corresponding to mass 80 amu, $0.0035 \pi \cdot \text{mm} \cdot \text{mrad}$, is only slightly smaller than the calculated EBIS acceptance under nominal operating conditions with the low current electron gun, $0.0037 \pi \cdot \text{mm} \cdot \text{mrad}$. Another critical function of the transport line is to match the injected ion beam transverse emittance with the EBIS 4D phase space acceptance.

The layout in Fig. 1 indicates the various sections of the system for the offline testing configuration. Transport simulations using generalized components were reported previously [7]. This paper reports the results of the electrostatic and ion beam transport simulations used to optimize the specific component designs and configurations for the transport beamlines by minimizing the transverse emittance growth of the ion beam. The ability of the offline diagnostic line to resolve individual charge states is also discussed.

SIMULATIONS

Ion beam transport simulations were performed with TRACK [8] and CST-EM Studio [9]. TRACK integrates the equations of motion for charged particles in 3D fields, but does not incorporate a numerical solver to calculate external electromagnetic fields explicitly. TRACK can use internal expressions for the fields of a number of idealized components, or can incorporate fields mapped from external solvers. TRACK allows the user to easily scale and rearrange the fields to investigate a wide variety of configurations. EM Studio, part of the CST Studio Suite, incorporates a solid modeler and numeric solver to calculate 3D static fields for arbitrary geometries. EM Studio models can be parameterized and programmatically optimized based on user-defined constraints. EM Studio was used to optimize the optical component geometries within the transport line to minimize beam distortion. Typically, the fields calculated in EM Studio were mapped, extracted, and incorporated into TRACK for particle tracking simulations. The space charge of the ion beam for the ion beam transport simulations was neglected since the maximum expected ion current from the CARIBU source will be ~ 1 nA.

*Work supported by the U.S. Department of Energy, Office of Nuclear Physics, under contract number DE-AC02-06CH11357.

[#]cdickerson@anl.gov

BEAM DYNAMICS TOOLS FOR LINACS DESIGN

A. Setty, THALES Communications, 160 Bld de Valmy 92 700, Colombes, France

Abstract

In the last 25 years, we have been using our in house 3D code PRODYN [1] for electron beam simulations. We have also been using our in house code SECTION for the design of the travelling wave accelerating structures and the beam loading compensation. PRODYN follows in time, the most complicated electron trajectories with relativistic space-charge effects. This code includes backward as well as forwards movements. This paper will describe those two codes and will give some simulations and measurements results.

INTRODUCTION

The electron dynamics are complicated. Their energies varies from zero to more than one MeV in a length comparable to the prebucket dimension. Velocities are different at the same abscissa. On-axis oscillations occur. RF field phase and amplitude laws must be shaped precisely. Radial behaviour can be analyzed by noting optical effects at the input and output regions of the cells. The equivalent lenses have either a convergent, a divergent or a null effect. It depends on the electron beam to RF electrical field dephasing. Their positions can be modified as long as overall longitudinal acceleration occurs.

BEAM DYNAMICS TOOLS

For the design of a linac we use 5 principal codes:

- Our in house code SECTION, for the design of the travelling wave accelerating structures and the beam loading compensation.
- Our in house code PRODYN, for the beam dynamics simulations.
- The well-known EGUN [2] code written by Dr. Hermannfeldt from SLAC, for the gun design.
- The also well-known SUPERFISH code written by Ron. F. Holsinger and Klaus Halbach from LOS ALAMOS for the design of cavities and electric field in accelerating structures.
- The also well-known POISSON code written by the same authors from LOS ALAMOS, for the shielded lenses and solenoids.

SECTION code

SECTION code provides along a travelling wave structure the filling time, the group velocity, the circulating power, the shunt impedance, the electric field and the energy gain.

This code uses the beam loading theory, based upon diffusion equation (Beam loading and transient behavior in travelling wave electron linear accelerators", J.E Leiss

page 151, linear accelerators edited by P. Lapostolle and A. Septier, 1970 North-Holland publishing company-Amsterdam) and the S band measurements mainly the ALS structures ("Les sections accélératrices" page 1194 D. Tronc et Al, L'onde électrique Vol 49, Fasc 11-n°: 513 Dec 1969).

This code was used recently for the design of the ALBA and BESSY accelerating structures, in particular the beam loading effects.

The accelerating structures met the calculated values at ALBA, 53 MeV for 18.8 MW in the first accelerating structure (16 MeV in the buncher) July 2008 Spain.

PRODYN code

PRODYN code tackles particle dynamics, electrons in our case, according to time and in the presence of an electromagnetic field. The code includes backward as well as forward movements and relativistic space-charge effects. The space to be simulated is divided into several elementary cells. Each cell changes the input beam into an output beam that can then be injected into the next cell. If the simulation covers a large number of cells, one can test a change by taking the beam at the output of the cell that precedes the change, and injecting it into the sequence of new cells.

The particle beam is either generated by the code using the entered settings, or read from the particle file supplied by the user.

An elementary particle is represented by its position, its energy, and its phase. To solve differential equations, one uses the Runge-Kutta method with x , y , z , V_x , V_y and V_z as variables, and time as the integration variable.

The provided elements are: RF accelerating cell, drift, magnetic lens, quadripole, dipole and bending magnet. The accelerating cell may include a magnetic lens and a dipole. Subharmonic frequencies can be used.

Space charge module

When calculating dynamics at low beam currents, we can neglect the space charge effects. But with nominal beam currents, as soon as we want to properly define an accelerating section that is self-focused or provided with external focus, we must take the space charge forces into account.

In particular, in the first cavities of a buncher where the beam energy is low, the charge density becomes significant when modulating the beam. This results in significant radial de-focussing.

To elaborate the space charge calculation, we proceed as follows:

Initially, we change the Coulomb law for macro-particles that are close to each other. In order to eliminate

STATUS OF THE BEAM DYNAMICS CODE DYNAC*

E. Tanke, W. Ding, J.A. Rodriguez, W. Wittmer, X. Wu, FRIB, East Lansing, MI 48824, USA
 S. Valero, Consultant, retired from CEA-Saclay, Paris, France

Abstract

The efficacy of using the beam dynamics code DYNAC [1] as an online beam simulation tool for the Facility for Rare Isotope Beams (FRIB) [2] and its concomitant Reaccelerator (ReA) is discussed. DYNAC was originally developed at CERN, where a set of accurate quasi-Liouillian beam dynamics equations was introduced for accelerating elements, applicable to protons, heavy ions and non-relativistic electrons.

A numerical method has been added, capable of simulating a multi-charge state ion beam in accelerating elements (i.e. cavities). Beam line devices such as sextupoles, quadrupole-sextupoles as well as electrostatic devices are now also included. Capability of second order calculations for a multi-charge state beam has been implemented. A Radio Frequency Quadrupole (RFQ) model has been added and a preliminary comparison of beam simulation results with beam measurements on the ReA RFQ is reported. Benchmarking of the code for a multi-charge state beam is discussed. The three space charge routines contained in DYNAC, including a 3D version [3], have remained unchanged.

MAGNETIC DIPOLE WITH GRADIENT

The capability of simulating a multi-charge state beam in a magnetic dipole has been added to DYNAC using a computationally efficient matrix formalism. The FRIB Front End (FE) contains two Electron Cyclotron Resonance (ECR) sources, followed by a source and charge state selection line using magnetic dipoles (see Fig. 1).

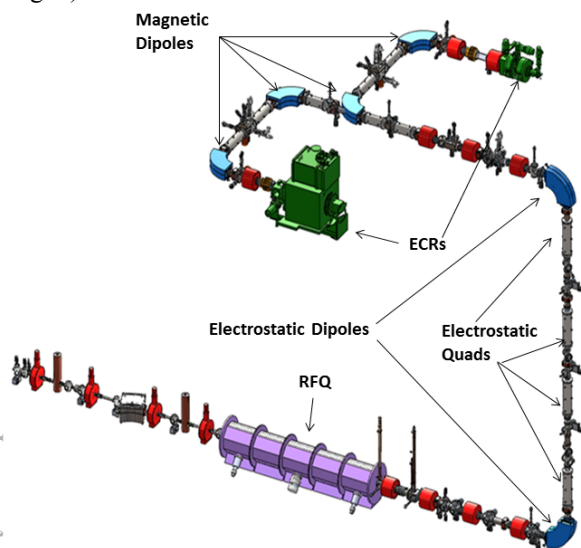


Figure 1: FRIB FE layout.

The DYNAC hard edge model for this dipole, which has an effective field length of 1 m, has been benchmarked against TRACK [4], which used a 3-D representation of the 1.7 m long field. This dipole has a field gradient of about 0.93. The output distributions are shown in Fig. 2 for a 12 keV/u uranium beam with charge states 33+ and 34+. Table 1 shows numerical results based on 4k macro-particles. The differences in the vertical phase plane are smaller than in the horizontal one.

Table 1: DYNAC and TRACK Horizontal Emittance Data for a Multi-Charge State Beam Tracked Through a FE Dipole

Parameter	U ³³⁺	U ³⁴⁺
$\alpha_{x,DYNAC}$	0.431	0.360
$\alpha_{x,TRACK}$	0.465	0.440
$\beta_{x,DYNAC}$	2.586	2.695
$\beta_{x,TRACK}$	2.605	2.551
$\epsilon_{x,DYNAC}$	54.03	53.72
$\epsilon_{x,TRACK}$	54.28	53.94

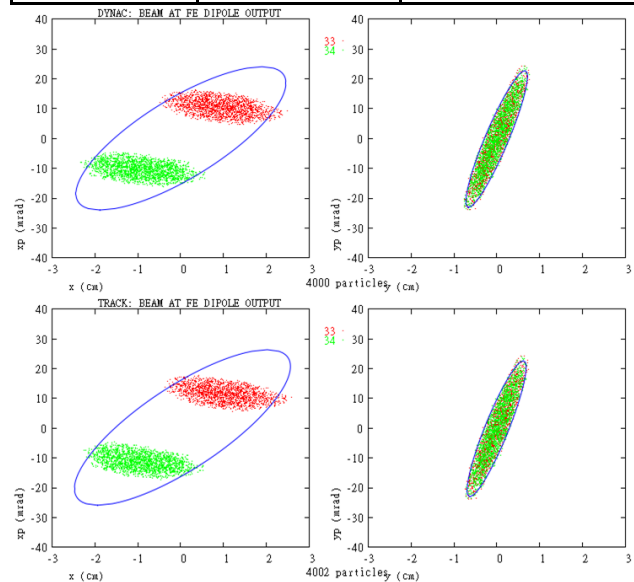


Figure 2: Horizontal emittances (left) and vertical (right) for DYNAC (top) and TRACK (bottom) for a multi-charge state beam tracked through the FE charge selection dipole.

ELECTROSTATIC QUADRUPOLES

To benchmark the electrostatic quadrupole model, a two charge state output beam from the FE charge selection dipole was simulated in a lattice containing six electrostatic quadrupoles. In DYNAC a 20 cm effective length hard edge model was used, whereas TRACK used a 3-D representation of a 30 cm long field. Again, there is good agreement between the two codes (see Table 2).

*This is based upon work supported by the U.S. Department of Energy Office of Science under Cooperative Agreement DE-SC0000661

PHOTOINJECTOR SRF CAVITY DEVELOPMENT FOR BERLinPro *

A. Neumann[†], W. Anders, T. Kamps,
 J. Knobloch - Helmholtz-Zentrum Berlin, Berlin, Germany
 E. Zaplatin - FZJ Jülich, Jülich, Germany

Abstract

In 2010 HZB has received approval to build BERLinPro, an ERL project to demonstrate energy recovery at 100 mA beam current by pertaining a high quality beam. These goals place stringent requirements on the SRF cavity for the photoinjector which has to deliver a small emittance 100 mA beam with at least 1.8 MeV kinetic energy while limited by fundamental power coupler performance to about 230 kW forward power. In order to achieve these goals the injector cavity is being developed in a three stage approach. The current design studies focus on implementing a normal conducting cathode insert into a newly developed superconducting photoinjector cavity. In this paper the fundamental RF design calculations concerning cell shape for optimized beam dynamics as well as SRF performance will be presented. Further studies concentrate on HOM properties, the field-flatness and tuning mechanism for that design.

REQUIREMENTS TO THE CAVITY DESIGN

The BERLinPro ERL will be a prototype facility demonstrating energy recovery with a 100 mA beam at 50 MeV beam energy while preserving a normalized emittance of better than 1 mm mrad at a pulse length of 2 ps or less [1]. This machine will make fully use of superconducting RF technology operated in continuous wave (CW). The injec-

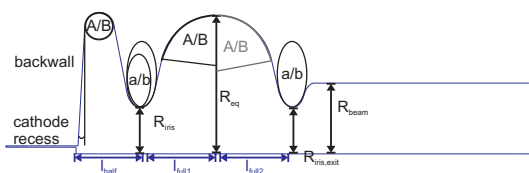


Figure 1: Geometry design parameters used for the cavity optimization scheme.

tor has to deliver a high brightness beam at a high repetition rate, filling every RF bucket, a low emittance allowing for emittance compensation and a compression of the longitudinal phase space in the ps regime. At this high average current also higher order mode excitation and damping have to be considered as well as coupling strongly to the fundamental. The high beam brightness will be achieved by inserting a high quantum efficiency normal conducting semi-conductor cathode within the SC environment of the

cavity. This cathode insert will mainly rely on the design by HZDR used in the ELBE SC 3.5 cell injector cavity [2]. As these are demanding goals, the injector and cavity are developed in a three stage approach. First results of an all superconducting gun cavity with a SC lead cathode were published in [5][6].

RF DESIGN STUDIES

The gun cavity has to fulfill several objectives while limited by some fundamental boundary conditions. The available total power will be limited to about 230 kW by using two KEK-style [3] fundamental power couplers (FPC), whereas the maximum electric peak field E_{peak} was recently demonstrated to reach 45 MV/m [4]. To name a few, regarding SRF and beam based properties the injector cavity has to be designed regarding the following aspects:

- Minimize E_{peak}/E_0 with $E_{cathode} < E_0$: This maximizes the field during beam extraction $E_{launch} = E_{cathode} \cdot \sin \Phi$ compared to the field anywhere on the surface E_{peak} , while it might be helpful to have the maximum on-axis field E_0 away from the cathode to reduce the probability of dark current.
- Minimize H_{peak}/E_{peak} and maximize R/Q to minimize losses. Consider the cutoff of the beam tube and iris diameter for a compromise between R/Q and HOM propagation and cell-to-cell coupling.
- The resonators length determines the launch phase Φ and field level during emission and thus energy gain and emittance. Thereby it also defines the field level for the field emitted dark current at about $\Phi = 90 \pm 20$ degrees.
- Transverse beam properties are influenced by the field during emission (>10 MV/m [7]) as by the transverse focussing due to e.g. retraction of the cathode, back-wall inclination and the transverse field component when the bunch leaves the RF structure.

Figure 1 shows the geometric parameters used in this work to run different optimization steps to converge to a suitable design. The design iteration was done by implementing different optimization schemes, like golden section search and Nead-Melder Simplex algorithms within a MATLABTM wrapper to run the 2-D RF field solver Superfish [8]. The obtained fields were used in the same loop to perform a first field-phase scan of the longitudinal phase space using a simple self written tracking code. Following, a set of candidates were included in ASTRA-based [9] beam dynamics simulations including the solenoid or the whole injector

* Work supported by Bundesministerium für Bildung und Forschung and Land Berlin

[†] Axel.Neumann@helmholtz-berlin.de

FIRST OBSERVATION OF PHOTOEMISSION ENHANCEMENT FROM COPPER CATHODE ILLUMINATED BY Z-POLARIZED LASER PULSE

H. Tomizawa, H. Dewa, A. Mizuno, and T. Taniuchi
 Japan Synchrotron Radiation Research Institute (JASRI/SPRing-8)
 Kouto, Sayo-cho, Sayo-gun, Hyogo 679-5198, Japan

Abstract

Since 2006, we have been developing a novel photocathode gun gated by the laser-induced Schottky-effect. This new type of gun utilizes laser coherency to aim at a compact femtosecond laser oscillator as an IR laser source using Z-polarization on a metal photocathode. This Z-polarization scheme reduces the laser photon energy to excite the cathode with a longer wavelength by reducing its work function due to the Schottky effect. Before this epoch-making scheme emerged, photocathode guns had never utilized a laser's coherency itself. We applied a hollow laser incidence scheme with a hollow convex lens that is focused after passing the beam through a radial polarizer. Based on our calculations (convex lens: $NA=0.15$; 60% hollow ratio), a Z-field of 1 GV/m needs 1.26 MW at peak power for the fundamental wavelength (792 nm) of a Ti:Sapphire laser. To confirm photoemission enhancement effects due to a Z-field of a few GV/m compared with copper's conventional photoemission, we used third harmonic generation (THG: 264 nm) as a pilot experiment and generated a Bessel beam with a hollow axicon lens in a vacuum to relax the phase matching condition of the wavefront on the cathode's focus point. We observed the first Z-field emission enhancement with a copper cathode at THG (264 nm). The enhancement factor was 1.4 times at 1.6 GV/m of the averaged Z-field of the central laser spot (Bessel beam) on the cathode surface.

INTRODUCTION

A conventional photocathode RF gun needs a UV-laser source (~ 260 nm) for robust cathodes like metal copper due to their high work functions that exceed 4 eV. Consequently, the laser system becomes larger and more complex. To make the laser source compact and simple, we need a cathode with a lower work function and high QE. However, such a high QE Negative Electron Affinity (NEA) cathode requires an ultra-high vacuum ($< 10^{-8}$ Pa) and does not have a long lifetime in an RF gun.

One solution to reducing the work function is to apply a high field on the cathode surface. In a field of 1~2 GV/m, the copper cathode's work function is reduced by ~ 2 eV. To achieve such a high field (~ 1 GV/m) on the photocathode, a tungsten needle (radius: ~ 1 μ m) photocathode with photo-assisted field-emission was tested [1]. The obtained QE of the needle tip was found to be proportional to the >10 th power of the electric field

over 500 MV/m and reached 3% of QE at about 800 MV/m. This observed field enhancement of QE is qualitatively explained with a field-emission process that includes the Schottky effect, the tunneling effect, and photoexcitation. However, such a needle cathode tip becomes round and broken in the gun cavity during RF conditioning. The dark current is also very large due to a 100-times longer half-cycle of RF than the pulse duration of the illuminating laser.

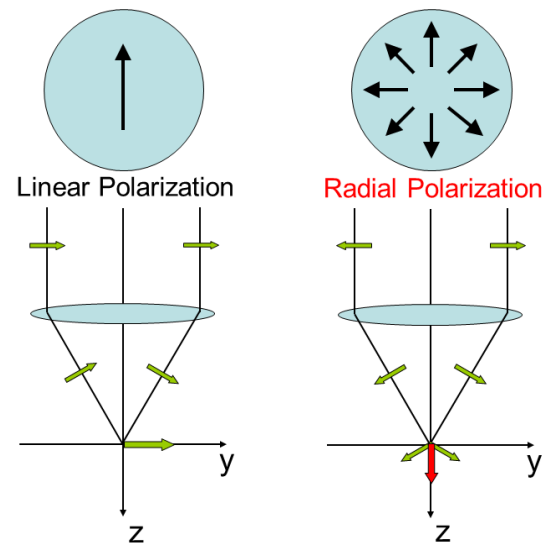


Figure 1: Principle of Z-polarization field on cathode surface generated from radial polarization

Therefore, we started to investigate with a plane-field emitter gated by a laser radiation field by exploiting recent progress in optical technologies to generate radially polarized laser modes. The fundamental mode of radial or azimuthal polarization is the superposition of TEM_{01} and TEM_{10} modes as orthogonal linear polarizations. By focusing a radially polarized laser beam on the photocathode (Fig. 1), the laser's electric field is generated in the laser propagating direction (Z-direction) at the focus point. The generated Z-polarized laser field (Z-field) easily exceeds an electrical field of 1 GV/m with fundamental wavelength from compact femtosecond laser systems. On the other hand, focusing an azimuthally polarized beam on the photocathode results in the zero Z-fields. Comparing the radial and azimuthal polarizations by focusing on metal cathodes, we conducted a feasibility study of Z-field effects on the photocathode [2]. This is also a fundamental study of

BEAM DYNAMICS STUDIES FOR SRF PHOTOINJECTORS*

T. Kamps[†], A. Neumann, J. Voelker
 Helmholtz-Zentrum Berlin, Germany

Abstract

The SRF photoinjector combines the advantages of photo-assisted production of high brightness, short electron pulses and high gradient, low-loss continuous wave (CW) operation of a superconducting radiofrequency (SRF) cavity. The paper discusses beam dynamics considerations for ERL class applications of SRF photoinjectors. One case of particular interest is the design of the SRF photoinjector for BERLinPro, an ERL test facility demanding a high brightness beam with an emittance better than 1 mm mrad at 77 pC and average current of 100 mA.

MOTIVATION

The primary goal of this study is to design an electron injector within the boundary conditions of BERLinPro [1]. For BERLinPro, the electron injector needs to deliver an electron beam with a normalized emittance of $\varepsilon_n = 1$ mm mrad and average current of $I_{avg} = 100$ mA. The rms pulse length must be $\sigma_t \leq 7$ ps in order to reduce emittance growth in the merger, linac and recirculation loop of the ERL. In addition the injector design should be compatible with technical boundary conditions. These translate into rf forward power limits set up by the rf power source and rf input coupler technology of choice. In particular the gun forward power is limited to $P_{fd} = 230$ kW by the rf input couplers. The secondary goal is to develop guidelines and requirements for the microwave design of the SRF cavity.

PRELIMINARIES

The main building blocks for the electron injector of BERLinPro are an SRF gun with drive laser, solenoid and booster section (see Fig. 1). The solenoid and SRF cav-

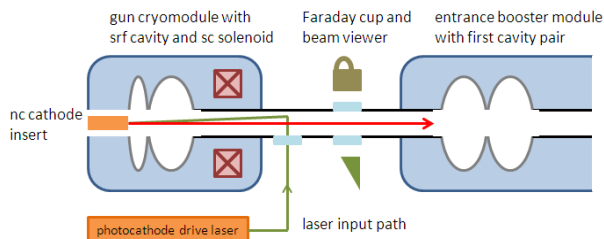


Figure 1: Schematic overview injector system with SRF gun and booster.

*The work is supported by Bundesministerium für Bildung und Forschung and Land Berlin.

[†]kamps@helmholtz-berlin.de

ity are located in a gun cryomodule. The beam exits the cryomodule and is guided through a short warm section with laser input and diagnostics ports before it enters the booster cryomodule. In this study beam parameters are first evaluated after the gun section at the location of the first booster cavity and finally after the booster section, before the beam enters the merger section. All beam dynamics simulations for this study have been carried out with the ASTRA code [2].

EMITTANCE CONTRIBUTIONS

The initial emittance for a beam from a photocathode RF gun is given by the product of initial spot size and the mean transverse energy distribution ($MTE = (h\nu - \phi_{eff})/3$) of the electron distribution after photoemission from the cathode with effective workfunction ϕ_{eff} and single-photon energy $h\nu$ of the drive laser [3]. Low emittance requires a cathode material with a workfunction near the single-photon energy of the drive laser and small initial spot size. The lower limit for the initial spot size is given by the equilibrium between the forces of the image-charge and the accelerating field. This space-charge limited (scl) emission radius is a function of the ratio of bunch charge q_b and launch field E_l the bunch experiences during emission. The resulting thermal (or cathode) emittance and the lower limit for the emission spot size can be expressed by

$$\varepsilon_{th} = \sigma_{in} \sqrt{\frac{MTE}{m_o c^2}} \quad \text{with} \quad \sigma_{in}|_{scl} = \sqrt{\frac{q_b}{4\pi\epsilon_o E_l}} \quad (1)$$

It is clear from Eq. (1) that a high launch field is required to achieve low thermal emittance for a given target bunch charge. The upper limit for the launch field is given by the cathode-to-peak field ratio (given by cavity design) and the achievable peak field in SRF gun cavity structures of $E_{pk} = 45$ MV/m [4]. For BERLinPro we assume a drive laser running at $\lambda = 532$ nm illuminated a photocathode made of CsK₂Sb ($\phi_{eff} = 1.9$ eV) resulting in a divergence term of $\sqrt{MTE/m_o c^2} = 0.51$ mrad. The goal for the BERLinPro injector is to deliver a projected emittance of $\varepsilon_{proj} \leq 1$ mm mrad and slice emittance of $\varepsilon_{slice} \leq 0.6$ mm mrad. To allow for some degradation due to non-linear processes, the target for the thermal emittance is $\varepsilon_{th} = 0.3$ mm mrad. This can be achieved with initial spot size of $\sigma_{in} = 0.6$ mm, resulting in a space-charge limited launch field of $E_l|_{scl} = 5$ MV/m. The gun should be operated at least a factor of two away from this limit to allow for acceleration of the complete bunch including the tail particles. Therefore the launch field the cavity has to

INITIAL RF TESTS OF THE DIAMOND S-BAND PHOTOCATHODE GUN

C. Christou and S. A. Pande
 Diamond Light Source, Oxfordshire, UK

Abstract

An S-band photocathode electron gun designed to operate at repetition rates up to 1 kHz CW has been designed at Diamond and manufactured at FMB. The first test results of this gun are presented. Low-power RF measurements have been carried out to verify the RF design of the gun, and high-power conditioning and RF test has begun. Initial high power tests have been carried out at 5 Hz repetition rate using the S-band RF plant normally used to power the Diamond linac: the benefits and limitations of this approach are considered, together with plans for further testing.

GUN DESIGN

In recent years, the RF photoinjector gun has been increasingly used as a source of high brightness beams for free electron lasers [1, 2], inverse Compton scattering sources [3] and ultrafast relativistic electron diffraction devices [4]. A programme is underway at Diamond Light Source to develop a high repetition rate S-band photocathode gun [5] using a coaxial RF coupler similar to that used at the DESY PITZ gun [6]. Such an approach preserves the axial symmetry of the gun, ensures coupling takes place in a region of low power dissipation and allows the gun main solenoid to be mounted directly around the gun cavity to achieve minimum transverse emittance [7]. The DLS gun is a 1.6-cell design with a removable cathode plug. The RF electric field distribution of the accelerating π mode is shown in Figure 1: the cathode plug is located at the lower left and the coupler is on the right.

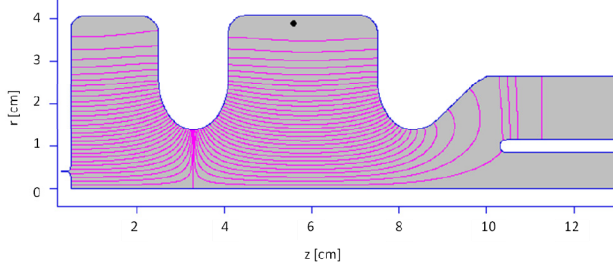


Figure 1: SUPERFISH calculation of π mode

The gun was manufactured at FMB and delivered to Diamond in early 2012: Figure 2 shows the assembled gun and coupler. Gun cavity and coupler are two brazed units connected by a Conflat fitting using one of a range of spacer gaskets of different thickness used to control coupling. The gun includes extensive water cooling channels allowing it to operate at a pulse repetition rate of 1 kHz, and to enable fine tuning of the cavity resonant frequency by control of the water temperature.

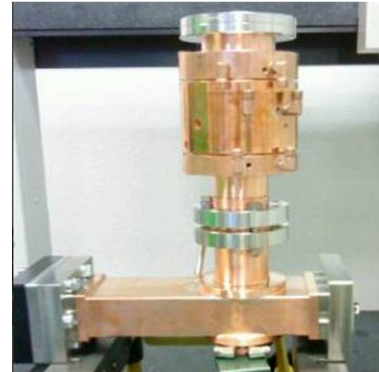


Figure 2: The assembled gun and coupler

LOW POWER TESTS PRIOR TO TUNING

Gun and coupler were probed together at Diamond using a Rohde and Schwarz ZB8 Vector Network Analyzer. Three resonances were measured around 3 GHz: the zero mode (2984 MHz), π mode (3003 MHz) and a small mode at 3021 MHz located at the antenna. The frequency of the π mode at room temperature was designed to be higher than the operating frequency of 2998 MHz in order to compensate for the drop in frequency expected as the cavity warms to its operating temperature when RF power is applied.

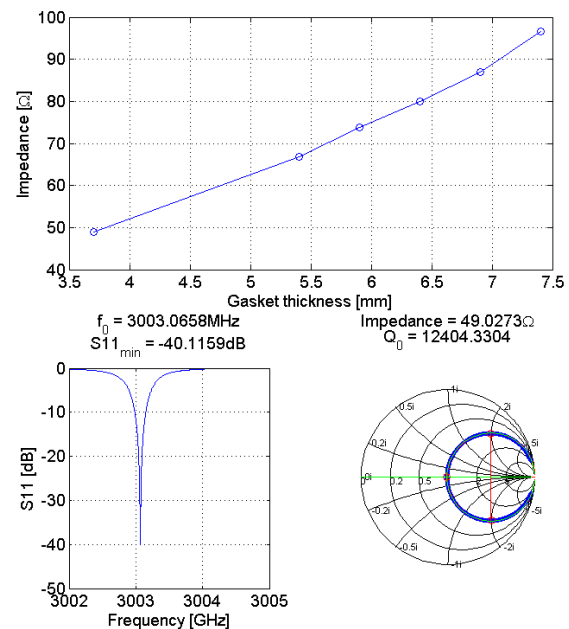


Figure 3: Tuning of gasket thickness for critical coupling (above) and cold test results at critical coupling (below).

A number of coupling gaskets were tested to establish critical coupling. Results are shown in Figure 3, with the

RF PHOTOINJECTOR AND RADIATING STRUCTURE FOR HIGH-POWER THz RADIATION SOURCE

S.M. Polozov, T.V. Bondarenko,

National Research Nuclear University (MEPhI), Moscow, Russia.

Yu.A. Bashmakov, Lebedev Physical Institute of RAS (LPI), Moscow, Russia

Abstract

Sources of high-power electromagnetic radiation in THz band are becoming promising as a new method of a low activation introscopy. Research and development of accelerating RF photoinjector and radiating system for THz radiation source are reported. The photoinjector is based on disk loaded waveguide (DLW). Two different designs of accelerating structure were modelled: widespread 1.6 cell of DLW structure and travelling wave resonator structure (TWR). The resonant models of these structures and the structures with power ports were designed. Electrodynamics characteristics and electric field distribution for all models were acquired. Results of picoseconds photoelectron beam dynamics in simulated structures are reported. Designs of decelerating structures exciting Cherenkov radiation are based on corrugated metal channel or metal channel coated with dielectric. Analysis of radiation intensity and frequency band are presented.

INTRODUCTION

THz radiation is nowadays becoming promising in solving such vital problems as national security, biomedicine and in manufacturing processes control. In national security issue THz radiation can be used in introscopy systems. The definition of the weapons, explosives, drugs and fissionable materials is the main aim of introscopy. The introscopy of cargo transport is much more complicated objective than passenger introscopy issue. The gamma, electron or neutron facilities are used in introscopy system including cargo introscopy at present. The compact electron or ion gun or accelerator is the basic element of such facilities. The main difficulty is the fact that it is necessary to use an electron linear accelerator (LINAC) which can derive the beam with 3-5 times energy variation. LINACs of this type are utterly complex facilities. All of gamma, electron or neutron facilities have a number of disadvantages as needs of environmental shielding and cargo activation.

High-power THz radiation source based on photoinjector and decelerating capillary channel is now one of the most discussable compact facilities providing monochromatic THz radiation of power high enough to be used for cargo introscopy [1].

Facility is based on two main parts: accelerating structure and decelerating radiating channel. Capillary is placed right after the accelerating structures and is made of copper with either dielectric coated inner surface or corrugated surface.

ACCELERATING STRUCTURES

1.6 cell DLW structure

Accelerating structure consists of two accelerators connected sequentially: 1.6 cell DLW and 9 cell TWR structure. First part of facility accelerating system is 1.6 cell standing wave accelerating structure (figure 1). This accelerating structure by itself comes artlessly as a photoinjector part of the accelerating system.

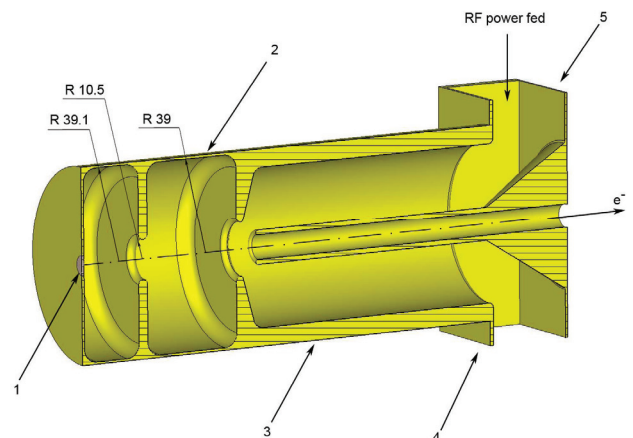


Figure 1. 1.6 accelerating structure: 1 – photocathode, 2 – resonator, 3 – coaxial wave type transformer, 4 – vacuum port, 5 – power input.

This accelerating structure operates on π mode and S-band frequency 2856 MHz ($\lambda=105$ mm). Resonant frequency of the structure was tuned to the desired value by means of cell radius variation. Iris profile was made with rounding to eliminate the possibility of breakdown. First cell length is 0.6 of full-sized cell to obtain maximum field amplitude in the center of the photocathode arranged in the cell's sidewall. Performance of the structures was also increased by rounding of shells edges. The rounding radius value was chosen to provide the highest possible shunt impedance and Q-factor.

Structure RF power input is organized by S-band standard rectangular waveguide with the coaxial coupler. RF power is fed into the structure through only one of the connected waveguides; another is used for structure field symmetry and will be applied for vacuum and other accompanying connections. This scheme provides high level of field symmetry in the system that leads to better quality of the accelerated beam.

This type of wave transformer differs from recently used RF power inputs in photoinjectors like ones in BNL Guns [2]. That type was exploiting the scheme of power

DEVELOPMENT OF A SUPERCONDUCTING FOCUSING SOLENOID FOR CADS*

W. Wu, X.L. Yang, Z.J. Wang, B.M. Wu, S.F. Han, D.S. Ni, W.J. Yang, L. Zhu, S.J. Zheng, L.Z. Ma, Y. He Institute of Modern Physics, Lanzhou, 730000, China

Abstract

A superconducting focusing solenoid has been designed and developed for the China Accelerator Driven System (CADS). In order to meet the requirement of focusing strength and fringe field while minimizing physical size of the solenoid, the novel optimizing design method based on linear programming method was employed. In this report, we will introduce the design of the solenoid including magnetic field optimization, mechanical design and quench protection. The fabrication and the test results of the solenoid will also be introduced in this report.

INTRODUCTION

Accelerator Driven System(ADS) is the effective tool for transmuting the long-lived transuranic radionuclides into shorter-lived radionuclides. A project called CADS is being studied in the Chinese Academy of Sciences. Fig. 1 shows the roadmap of CADS. The linac of CADS will accelerate the proton with beam current 10mA to about 1.5GeV to produce high flux neutrons for transmutation of nuclear waste. The beam dynamics of superconducting linacs operating in the velocity range below 0.4c require a compact accelerating-focusing lattice. Superconducting solenoids together with SC RF resonators within a common cryostat meet this requirement. For its simple design, easily producing and low cost of manufacture, many typical superconducting Linac such as ISAC-II of Canada, Project X of FANL and FRIB of MSU in USA employ solenoid as focusing element[1, 2, 3].

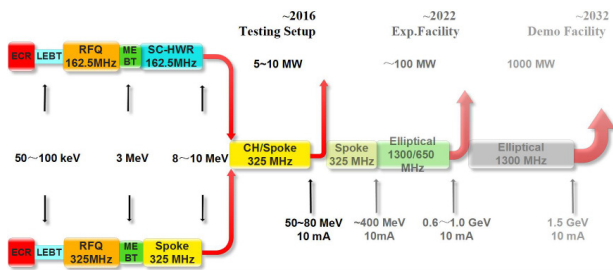


Figure 1: The roadmap of China CADS.

The solenoid will generate stray magnetic field that must be shielded to very low levels at the nearby SRF cavities. Two orthogonal steering dipoles, coaxial to each other and to the solenoid, are required to steer the beam in transverse directions. The specifications of the solenoid are summarized in Table. 1[4].

*Supported by the National Natural Science Foundation of China (Grant No.11079001)

Table 1: Specifications of SC solenoid

Parameters	Value
Center field	7 T
Effective length	150 mm
Stray field 200 Gs line	$\leq 280 \text{ mm}$ from the center
Correction of integral	$> 0.01 T \cdot m$
Bore diameter	44 mm

MAGNETIC DESIGN

The solenoids must have low fringe fields to avoid magnetic-flux capture in the superconducting cavity. Before the SC cavity cooled into superconducting state, the level of the fringe field must be much lower than the earth's magnetic field $50 \mu T$ and according to some estimates should be on the level of $1 \mu T$ [5]. This requires that the solenoid should be constructed only of material with low relative magnetic permeability to minimize remnant fields when the magnet is off. Once the cavity is in the superconducting state, the fringe field of the fully energized magnet is to be less than $20 \sim 40 mT$.

The main goal of the magnetic design is to find a configuration of a solenoid that would meet the major requirements while minimizing the cost. The reverse wound active shielding coils are also used in our design to reduce stray magnetic field as ISAC-II and FRIB did. A two-step method which combines linear programming and a nonlinear optimization algorithm has been employed to design the solenoid[6, 7]. Linear Programming is used to carry out the topology optimization to get the coils' initial location and shape, and then the nonlinear optimizing methods are used as the second step to further simplified the coils' shape.

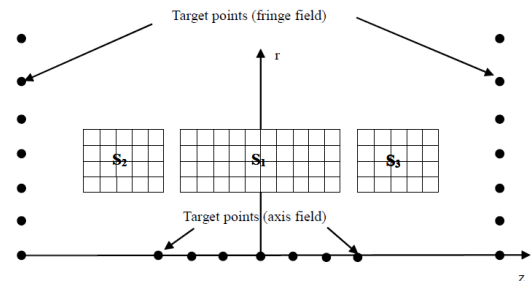


Figure 2: The feasible coil regions with numerical grid.

For a multi-coils magnet the feasible coil space can be divided into several regions and then each section is densely sampled by an array of candidate current loops (Fig. 2). The goal is to determine a set of current loops to create a desired field distribution at the target points while achieving a low fringe field and minimizing the coil volume. This

THE DEVELOPMENT OF TIMING CONTROL SYSTEM FOR RFQ

J. Bai, L. Zeng, S. Xiao, T. Xu

Institute of High Energy Physics, CAS, Beijing, 100049, P.R China

Abstract

In order to meet the need of RFQ accelerator, Timing extension hardware based on VME configuration has been developed. In the future, it will be used in the diagnostics system of CSNS. This paper introduces the function of Timing extension hardware, EPICS driver for Timing extension hardware and MEDM operator interface.

BACKGROUND

The core research of intense-proton beam accelerator is mainly concentrated in the field of beam loss control. Based on the intense-beam RFQ accelerator [1] which accelerates proton beam of 46mA pulse current to 35MeV at more than 7% duty factor, a beam line has been built. In order to do beam loss control experiment, many devices have been developed, one of which is Timing extension hardware. Timing extension hardware, as an important device in the running of RFQ accelerator, provides high accuracy and high stability timing trigger signals for the whole system. In the future, it will be used in the CSNS (Chinese Spallation Neutron Source). CSNS adopts EPICS [2] (Experimental Physics and Industrial Control System) as its software environment. So it is necessary to develop EPICS driver [3] for timing extension hardware.

INTRODUCTION OF TIMING EXTENSION HARDWARE

Timing extension hardware uses VME bus of A24 nonprivileged data access address modifier [6]. It is listed below as fig. 1. Since A24 space is of predicable size 16MB, default window encompassing the full space is always provided. The A24 window is for VME bus address from 0x000000 to 0xfffff, which is usually mapped by VxWorks subroutine sysBusToLocalAdrs to local memory from 0xfa000000 to 0xfaffffff [6].

```
#define VME_AM_STD_USR_DATA 0x39 /* A24, nonprivileged data access*/
```

Figure 1: Address Modifiers of A24 nonprivileged data access

Timing extension hardware based on VME configuration is not only consistent with RFQ requirement, it but also avoids the disadvantage of original timing control system, achieving parameters remedy on line. When operators need to remedy parameters of original timing control system, they have to stop the accelerator and calculate the parameters according to the request of experiments, and then use dip switch to change the parameters. The whole process will

last almost two hours and affect the efficiency, stability and continuity. Besides, Timing extension hardware based on VME architecture achieves utility of the same hardware to perform different functions by using reconfiguration of the FPGA, which enhances the flexibility of timing extension hardware.

Timing extension hardware has two types of functions [4]. One is providing primary timing signals for RFQ and secondary timing signals which divide frequency of primary timing signals for beam commissioning and RF system. The other is providing delaying or broadening timing signals according to the needs of various devices. In fact, the principle of these two functions is calculating clock signals. For example, primary timing outputs a timing pulse when it calculates the clock signal to the certain amount. Broadening hardware is triggered by timing signal and starts counting program. It will output a TTL pulse with the width of 3us when counting program reaches to the setting value.

Fig. 2 shows timing signals of RFQ, and the timing extension hardware is shown in Fig. 3.

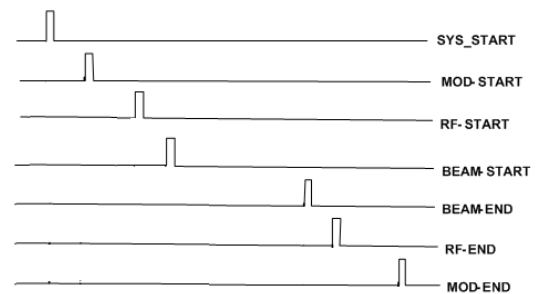


Figure 2: Timing signals of RFQ



Figure 3: The timing extension hardware

STATUS OF E-XFEL STRING AND CRYOMODULE ASSEMBLY AT CEA-SACLAY

C. Madec, S. Berry, P. Charon, J.-P. Charrier, C. Cloué, A. Daël, M. Fontaine, O. Napoly, N. Sacépé, C. Simon, B. Visentin, A. Brasseur, Y. Gasser, S. Langlois, R. Legros, G. Monnereau, J.-L. Perrin, D. Roudier, Y. Sauce, T. Vacher, CEA/Irfu, Gif-sur-Yvette, France

Abstract

As In-Kind contributor to the E-XFEL project, CEA is committed to the integration on the Saclay site of the 100 cryomodules (CM) of the superconducting linac as well as to the procurement of the magnetic shieldings, superinsulation blankets and 31 cold beam position monitors (BPM) of the re-entrant type. The assembly infrastructure has been renovated from the previous Saturne Synchrotron Laboratory facility: it includes a 200 m² clean room complex with 112 m² under ISO4, 1325 m² of assembly platforms and 400 m² of storage area. In parallel, CEA has conducted industrial studies and three cryomodule assembly prototyping both aiming at preparing the industrial file, the quality management system and the commissioning of the assembly plant, tooling and control equipment. In 2012, the contract of the integration has been awarded to ALSYOM. The paper will summarize the outputs of the preparation and prototyping phases and the status of the up-coming industrial phase.

INTRODUCTION

The 17.5 GeV superconducting RF linac of the E-XFEL project [1] will comprise 100 cryomodules (cf fig.1), after the injector module. These twelve-meter long cryomodules, deriving from the FLASH technology, include a string of eight 1.3 GHz RF cavities with an average gradient of 24 MV/m, followed by a BPM and a superconducting quadrupole.

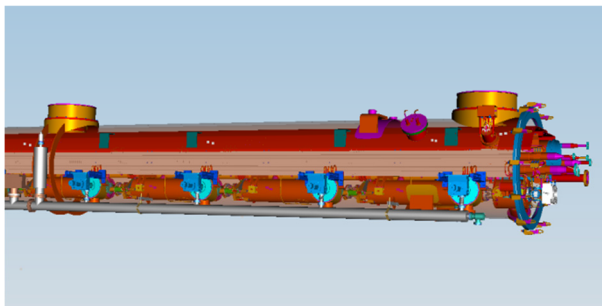


Figure 1: XFEL Cryomodule 3D-model

This string is closed by two gate valves at both ends. Within the Accelerator Consortium (AC), CEA is committed to the assembly of the 103 cryomodules over 2013 to mid-2015 with the goal to deliver one cryomodule per week to DESY for RF acceptance. Strategic decisions, shared by the AC, were taken in 2008 first to host the assembly plant on CEA premises at Saclay, using the former Saturne Synchrotron Laboratory

accelerator and experimental halls, second to subcontract the 103 modules, assembly work, including 3 pre-series modules, to an industrial company for. The layout of the assembly plant (see Fig. 2), was optimized by breaking down the assembly work in seven successive blocks of one-week procedures, leading to one clean room complex for coupler and string assembly, and five cryostating workstations for the remaining cryostating work, including alignment and control operations. To allow for a fluid circulation of the cryomodules along the assembly chain even when a repair is needed at one workstation, each workstation, but the vacuum vessel cantilever (see Fig. 3), has been doubled to offer module parking possibilities.

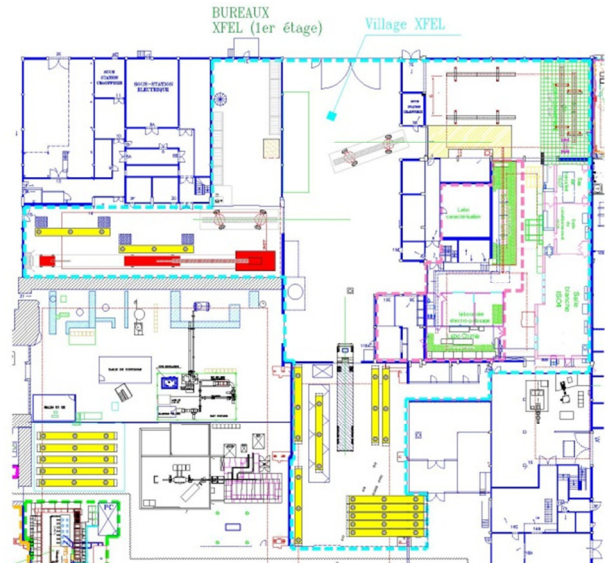


Figure 2: Layout of the XFEL infrastructure



Figure 3: Vacuum vessel and cold mass on the cantilever

OUTPUTS FROM THE PREPARATION PHASE

To ensure the integration of 103 CM at the rate of one cryomodule per week, CEA has set up a program to form

A LOW-LEVEL RF CONTROL SYSTEM FOR A QUARTER-WAVE RESONATOR*

J. W. Kim, D. G. Kim Institute for Basic Science, Daejeon, Korea
C. K. Hwang, Korea Atomic Energy Research Institute, Daejeon, Korea

Abstract

A low-level rf control system was designed and built for an rf deflector, which is a quarter wave resonator with a resonance frequency near 88 MHz. Its required phase stability is approximately $\pm 1^\circ$ and amplitude stability less than $\pm 1\%$. The control system consists of analog input and output components, and a digital system based on an FPGA for signal processing. It is a cost effective system, while meeting the stability requirements. Some basic properties of the control system were measured. Then the capability of the rf control has been tested using a mechanical vibrator made of a dielectric rod attached to an audio speaker system, which induced regulated perturbation in the electric fields of the resonator. The control system is flexible such that its parameters can be easily configured to compensate for disturbance induced in the resonator.

INTRODUCTION

The low-level rf (LLRF) system is a control device to stabilize electromagnetic fields of the rf resonators used for electron and ion beam applications. A quarter-wave resonator was built to deflect a secondary electron beam to measure the longitudinal beam emittance of a low-energy ion beam [1, 2]. Stability required for the resonator in measuring the charge distribution of a beam bunch is around $\pm 1^\circ$ in rf phase and $\pm 1\%$ in amplitude, respectively.

The LLRF system is composed of analogue components in the front ends and a digital signal processing board using a field programmable gate array (FPGA), which is controlled by software based on Windows OS. The feedback loop in the FPGA needs a large phase margin to avoid loop instabilities. This kind of approach utilizing both analog and digital devices have successfully been applied to different accelerator systems [3], which often asks for more strict rf stabilities. A major merit of this system is that the rf components are readily available as commercial products employing a simple architecture, and thus curtails its cost. The properties of the LLRF system were first measured with signals generated using an attenuator to replace the pick-up signal of the cavity.

The test of the LLRF was performed using the vibrator and a model rf deflector which has a fundamental resonance frequency at 87.9 MHz in the deflection mode.

The frequency of disturbance induced for testing is less than a hundred Hz because this low frequency range corresponds to resonance bandwidth for the mechanical structure similar to that of the rf deflector [4].

Numerical simulations have been performed using MATLAB tools [5] to test control methods such as one using ESO (extended state observer) and simple PID. We plan to adapt this LLRF system to use for superconducting cavities operating around at 80 MHz with further works on simulation and testing.

CHARACTERISTICS OF LLRF SYSTEM

Figure 1 shows a schematic circuit diagram of the LLRF system designed and constructed, and a photo of the components connected. The method that we chose utilizes both digital and analogue components. An analogue IQ demodulator (Analog Device model 8348) is used to convert the pick-up signal into I (in phase) and Q (quadrature phase) signals.

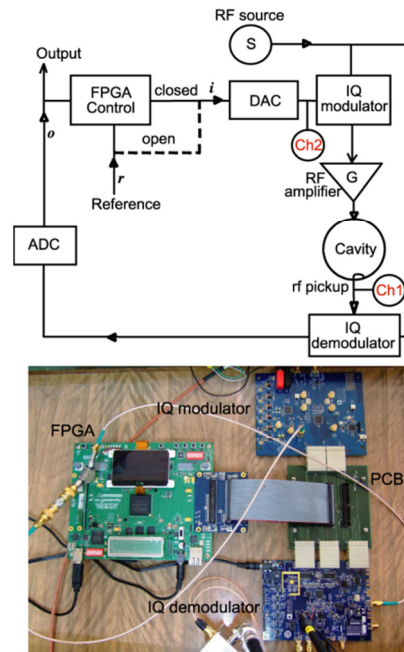


Figure 1: Upper: Schematic diagram of the LLRF system, Lower: Photo of the LLRF system showing major components. A printed circuit board (PCB) used for cable connections is also shown on the photo.

A detailed connection scheme describing the actual components used in the circuit is shown in Fig. 2. The

LLRF AUTOMATION FOR THE 9mA ILC TESTS AT FLASH

J. Branlard^{1*}, V. Ayvazyan¹, G. Cancelo², J. Carwardine³, W. Cichalewski⁴, B.C. Chase², O. Hensler¹, W. Jałmużna⁴, S. Michizono⁵, C. Schmidt¹, N.J. Walker¹, M. Walla¹, H. Schlarb¹,
¹DESY, Germany, ²FNAL, USA, ³ANL, USA, ⁴DMCS-TUL, Poland, ⁵KEK, Japan

Abstract

Since 2009 and under the scope of the International Linear Collider (ILC) research and development, a series of studies takes place twice a year at the free electron laser accelerator in Hamburg (FLASH) DESY, in order to investigate technical challenges related to the high-gradient, high-beam-current design of the ILC. Such issues as operating cavities near their quench limit with high beam loading or in klystron saturation regime are investigated. To support these studies, a series of automation algorithms have been developed and implemented at DESY. These include automatic detection of cavity quenches, automatic adjustment of the superconducting cavity quality factor, and automatic compensation of detuning including Lorentz force detuning. This paper explains the functionality of these automation tools and shows the experience acquired during the last 9mA ILC test which took place at DESY in February 2012. The benefits of these algorithms and operation experience with them are discussed.

INTRODUCTION

In pulsed accelerators, like FLASH or the ILC, the electric field inside a cavity is ramped up at the beginning of each pulse and then held constant both in amplitude and phase for the entire duration of the beam train. To meet luminosity goals, the vector sum flat top gradient should be regulated and controlled to better than 0.1% in amplitude and 0.1 degree in phase, according to ILC specifications. At FLASH like in the ILC design, one klystron provides power to several cryomodules. Due to performance disparities among cavities, the klystron RF power is distributed according to the individual cavity gradient limits. At FLASH, this is achieved by fixing the waveguide distribution system so that the spread in power distribution matches the spread among cavity gradients within a cryomodule. As a consequence, the beam loading also differs from cavity to cavity, resulting in positive or negative gradient tilts during the flat top while the vector sum of all cavity gradients remains perfectly flat. While this tilting effect is negligible for low beam currents (below 1 mA), it can induce 10 to 20% tilts on single cavities for high beam currents such as the 9 mA ILC upgrade design, as illustrated in Fig. 1. It was demonstrated that a physical misalignment of cavities combined with a gradient tilt during beam acceleration results in a transverse dispersion of the beam [1], and would force lowering the operational gradient in the machine.

One of the goals of the ILC 9mA runs at FLASH was to demonstrate the flattening of individual beam-induced

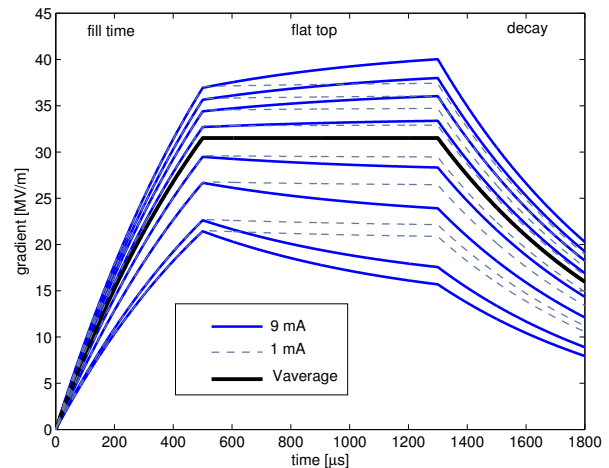


Figure 1: Cavity gradients for one cryomodule (8 cavities) with 1 mA (dotted) and 9 mA (solid) beam currents. The normalized vector-sum gradient is shown in black.

cavity tilts using loaded quality factor (Q_L) adjustments. The test was carried out on the last two cryomodules of the accelerator (ACC6 and ACC7), which contain the cavities with the highest gradient performance and are equipped with motorized controllers of the cavity Q_L .

AUTOMATION

Automation for Machine Operation

Automatic Q_L control. Gradient flattening studies require frequent changes of the cavity Q_L , so the automation of these settings was necessary. A middle-layer DOOCS [2] server was implemented for this purpose. When a new Q_L setting is requested, the server compares it to the current Q_L value, which is computed for all cavities and at each RF pulse. The server then moves the coupler motor to modify the position of the coupler antenna, effectively changing the cavity Q_L and bandwidth, until the measured Q_L value matches its setting. A discrete-time feedback control scheme is applied, where the input error is the difference between measured Q_L and setting, and the controller output directly drives the coupler motor. To avoid over exercising the coupler motor, a move is only requested if the Q_L error exceeds a certain threshold. The server robustness was improved by taking into account exceptions such as out-of-range Q_L settings, invalid Q_L measurements or motor reaching the end of its excursion, etc. A complete description of the automatic Q_L server is found in [3].

* julien.branlard@desy.de

PRECISION REGULATION OF RF FIELDS WITH MIMO CONTROLLERS AND CAVITY-BASED NOTCH FILTERS

C. Schmidt*, S. Pfeiffer, J. Branlard, H. Schlarb (DESY, Hamburg),
W. Jalmuzna (TUL-DMCS, Poland)

Abstract

The European XFEL requires a high precision control of the electron beam, generating a specific pulsed laser light demanded by user experiments. The low level radio frequency (LLRF) control system is certainly one of the key players for the regulation of accelerating RF fields. A uTCA standard LLRF system was developed and is currently under test at DESY. Its first experimental results showed the system performance capabilities. Investigation of regulation limiting factors evidenced the need for control over fundamental cavity modes, which is done using complex controller structures and filter techniques. The improvement in measurement accuracy and detection bandwidth increased the regulation performance and contributed to integration of further control subsystems.

INTRODUCTION

The European Free Electron Laser XFEL is a free electron laser generating X-Ray laser light of tunable wavelength by the SASE process, using an electron beam accelerated to about 17.5 GeV, in a pulsed operation mode. Providing its users stable and reproducible photons, requires a very precise control of acceleration fields. Developing and studying LLRF hardware and control strategies for the XFEL benefits from implementing and testing concepts at the Free electron LASer Hamburg FLASH. The latest renovation of the LLRF system is a change of the controller hardware to an uTCA based technology standard. One major impact for the LLRF regulation is the change of field detection, sampling frequency and precision of signal processing. Especially the higher sampling frequency allow for direct measure of further dynamics in the feedback loop.

It is well known that next to the acceleration mode, there exist further fundamental modes in a resonator effecting the closed loop system [1]. Especially the so called $8\pi/9$ -mode generating a significant limitation on the maximum loop gain. In this paper a control concept is presented which has been implemented and tested at FLASH. Filtering approaches and measurements for the next fundamental mode are outlined. This allows to keep the relative amplitude and absolute phase error below the XFEL requirements of 0.01 % (rms) and 0.01 degrees (rms).

* christian.schmidt@desy.de

REGULATION LIMITING FUNDAMENTAL CAVITY MODES

The Tesla type cavities used for the XFEL linear accelerator are operated in the so called π -mode. Next to the acceleration mode there exist further fundamental modes hosted by this resonator. Resonance frequencies have been measured and further theoretical background can be found in [1]. A sketch of the on axis electrical field distribution in beam direction for these modes can be found in Fig. 1.

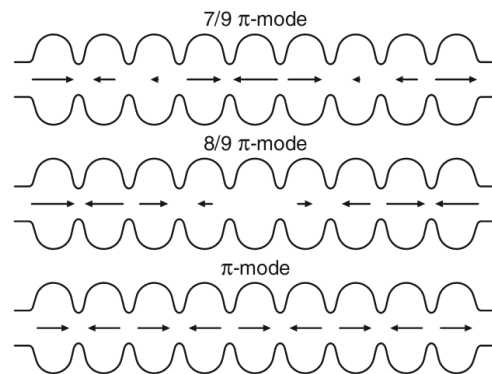


Figure 1: Sketch of electrical field \vec{E}_z distribution along the axis for the acceleration and the two next fundamental modes of Tesla type cavities [1]

Exciting this resonance modes lead to a degradation of the regulation performance up to an unstable loop. Furthermore it is limiting the parameter area which can be used for the controller design. So far only aliased contributions have been measurable due to the lower sampling frequency of $f_s = 1$ MHz, and actively suppressed using a complex feedback controller. Identifying the location has been done by bandwidth sweeping techniques in iterative processes [2]. With the upgrade of the LLRF system the sampling frequency of the LLRF digital processing has been increased to 9 MHz to meet the given intra train bunch repetition frequency of XFEL. This allows to measure directly the next two fundamental modes, $8\pi/9$ and $7\pi/9$, which are located about 800 kHz and 3 MHz below the π -mode carrier frequency of 1.3 GHz. Excitation measurements have been tested at FLASH to identify there exact location.

MEASUREMENT RESULTS

Defining the necessary system control parameters requires knowledge of the particular system dynamics. Be-

MAGNETIC CHARACTERIZATION OF THE PHASE SHIFTER PROTOTYPES BUILT BY CIEMAT FOR E-XFEL*

I. Moya[#], J. Calero, J.M. Cela-Ruiz, J. de la Gama, L. García-Tabarés, A. Guirao, J.L. Gutiérrez, L.M. Martínez, T. Martínez de Alvaro, E. Molina Marinas, L. Sanchez, S.Sanz**, F. Toral, C. Vázquez, CIEMAT, Madrid, Spain
 J. Campmany, J. Marcos, V. Massana, CELLS, Barcelona, Spain

Abstract

The European X-ray Free Electron Laser (E-XFEL) will be based on a 10 to 17.5 GeV electron linac that will accelerate the beam used in the undulator system to obtain ultra-brilliant X-ray flashes for experimentation. The so-called intersections are the transitions between undulators, where a quadrupole on top of a precision mover, a beam position monitor, two air coils and a phase shifter are allocated. CIEMAT participates in the development of the phase shifters (PS), as part of the Spanish in-kind contribution to the E-XFEL project. The updated design of the phase shifter is presented here to improve its behaviour as a result of the measurements on the first prototype, which did not fulfil the first field integral specification. This paper describes the magnetic measurements carried out on the last two prototypes in the test bench at CELLS, together with the tuning process to decrease the field integral dependence with gap.

from TESLA project [3]. Up to now, CIEMAT has developed three prototypes in collaboration with industry, as part of the Spanish in-kind contribution to the facility. The first CIEMAT prototype design [4] was based on the previous DESY prototype. Some design modifications were already introduced, agreed with the E-XFEL counterparts, in order to ease fabrication and assembly. That prototype fulfilled all the specifications, except the most challenging one, the variation of the first field integral with the gap (DESY prototype had failed as well).

In agreement with the E-XFEL, CIEMAT had developed a magnetic measurement bench based on a moving long coil connected to an analog integrator [5]. However, there are still some problems to get the required accuracy, incompatible with the project timeline.

Table 1: Technical Specifications

Magnetic specifications	
Min. phase integral at gap 10.5 mm (21°C)	23,400 T ² mm ³
Max. variation of 1 st field integral with gap	± 0.004 T·mm
Max. variation of 2 nd field integral with gap	± 67 T·mm ²
Mechanical specifications	
Gap	10.5 to 100 mm
Gap repeatability in bidirectional movement	± 50 µm
Gap repeatability in unidirectional movement	± 10 µm
Gap speed	0.01 to 10 mm/s

INTRODUCTION

The E-XFEL phase shifter will be located at the intersections in-between the undulators (Figure 1). The role of the phase shifter is to adjust the phase of the electron beam and the radiation when entering into an undulator according to different required beam energies and wavelengths. The main specifications [1, 2] that the device must currently satisfy can be found in Table 1.

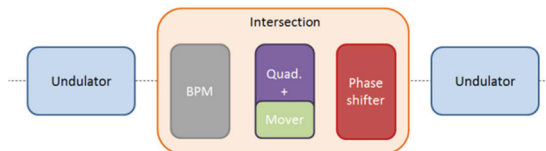


Figure 1: Undulator system intersection layout.

Four magnetic modules in a hybrid Halbach array produce a double sinus magnetic field in the mid-plane. The magnetic modules are surrounded by a pure iron yoke to enhance the phase integral value and weaken the fringe fields at nearby elements (Figure 2). The variation of the magnetic field strength is obtained by approaching or moving further the magnetic modules. Upper and lower modules move simultaneously with a unique spindle.

DEVELOPMENT OVERVIEW

The conceptual design and a first prototype were developed by DESY [1], based on the experience gained

*Work supported by Spanish Ministry of Science and Innovation under SEI Resolution on 17-Sept.-2009 and project ref. AIC-2010-A-000524

**S.Sanz is now with Tecnalia Energy, Spain.

#ivan.moya@ciemat.es



Figure 2: Third CIEMAT prototype

MACHINE PROTECTION ISSUES AND SOLUTIONS FOR LINEAR ACCELERATOR COMPLEXES

M. Jonker, H. Schmickler, R. Schmidt, D. Schulte, CERN, 1211 Genève 23, Switzerland
M. Ross, SLAC, Menlo Park, CA 94025-7015, USA

Abstract

The workshop “Machine Protection focusing on Linear Accelerator Complexes” was held from 6-8 June 2012 at CERN. This workshop brought together experts working on machine protection systems for accelerator facilities with high brilliance or large stored beam energies, with the main focus on linear accelerators and their injectors. An overview of the machine protection systems for several accelerators was given. Beam loss mechanisms and their detection were discussed. Mitigation of failures and protection systems were presented. This paper summarises the workshop and reviews the current state of the art in machine protection systems.

WORKSHOP OBJECTIVES

Machine protection has become a major concern in the design stages of the high power linear accelerators now under construction or being planned (e.g. high intensity protons linacs, XFEL, electron positron colliders). Due to the increased beam power the need for a dependable machine protection system becomes imperative. For this reason we organized this workshop on machine protection with a main focus on Linear Accelerator Complexes.

The objective of this workshop was to bring together for the first time experts on machine protection from various origins and disciplines, and to exchange experience and ideas for machine protection systems. The workshop was organized at CERN and could profit from the recent experience of the LHC collider, an accelerator where the need for a machine protection system was taken into account already during the design phase.

WORKSHOP ORGANISATION

The workshop was attended by 60 participants with a significant number from outside CERN.

Over 30 presentations were made in 6 half day sessions leaving ample time for discussion. The workshop sessions focused on the following topics:

Introduction: The session assessed the objectives for machine protection and reviewed existing solutions and challenges faced by future installations.

Beam loss mechanisms: The experience with beam loss mechanisms in existing installations and the outlook for future accelerator complexes were reviewed.

Failure detection: The session addressed the detection of failures that may lead to uncontrolled beams.

Failure mitigation: The session discussed various failure specific mitigations strategies.

Operational aspects: The session was dedicated to the operational aspects of machine protection (e.g.

commissioning, intensity ramp, availability) and to risk management (risk assessment and management tools).

Summing up and closing: These five sessions were followed by a workshop summary session.

It is not in the scope of this paper to make a thorough report of these presentations. Here we highlight key issues and identify new trends and recommendations.

MACHINE PROTECTION

The purpose of machine protection is to protect the accelerator equipment from beam induced damage.

We did not consider equipment protection from other threats, (e.g. overheating of a power supply, protection of super conducting magnets). However, beam induced quenches and the effect of a magnet quench on the beam should be evaluated in the scope of machine protection.

Machine protection must not be confounded with personnel protection. Personnel protection is more stringent and need to fulfil legal requirements while the applied approach and solutions are often more basic.

Machine protection is not limited to the interlock system and its control and surveillance software. There are many more elements within the scope of machine protection ranging from failure studies to spares policies. The following list is non-exhaustive:

1. The passive protection devices (collimators and masks) to limit the damage caused by unmanageable failures.
2. The active beam-abort systems to dispose of any present beam upon detection of instabilities, including beam observation instrumentation, abort kicker-magnets, beam dumps and other beam inhibit systems.
3. A beam interlock system to inhibit the beam in case of equipment failures.
4. A strategy to limit the rate with which magnetic fields and device positions can change.
5. A post cycle beam and equipment quality assessment system to inhibit the next cycle when performance parameters are outside predefined limits.
6. A beam-stop restart system: i.e. an intensity ramp sequence that provides an appropriate protection depending on the machine mode and state.
7. A version control and parameter change authorization system.
8. A fault recording, analysis and playback system.
9. The written procedures to introduce changes in the parameters that control the machine protection system.
10. A set of test procedures to thoroughly test the components of the machine protection system after each change in the system.

RECENT IMPROVEMENTS IN SPRING-8 LINAC FOR EARLY RECOVERY FROM BEAM INTERRUPTION

S. Suzuki, T. Asaka, H. Dewa, T. Kobayashi, T. Magome, A. Mizuno,
T. Taniuchi, H. Tomizawa, K. Yanagida and H. Hanaki
Japan Synchrotron Radiation Research Institute (JASRI/SPRING-8)
Kouto, Sayo-cho, Sayo-gun, Hyogo, 679-5198 Japan

Abstract

The 1GeV SPRING-8 linac is an injector for the SPRING-8 synchrotron radiation storage ring with 8GeV booster synchrotron. In recent years, backup systems were installed to eliminate long-time interruption of the beam injections. The main gun system is usually operated, and the backup gun is always pre-heated and can inject electron beams into the buncher section at intervals of several minutes if the main gun fails. The first klystron, which feeds the RF powers to the buncher system and the downstream klystrons, can be relieved by the next klystron in about 20 minutes by switching the waveguide circuit. When one of the eleven working klystrons fails, one of the standby klystrons, which are kept on line as hot spares, is automatically activated to accelerate beams instead of the failed one to avoid beam interruption. The total downtime in FY 2011 was 0.11% in the top-up operation user time. The averaged fault frequency was 0.2 times per day.

INTRODUCTION

The SPRING-8 accelerator complex is composed of a 1-GeV electron linac, an 8-GeV booster synchrotron, and an 8-GeV storage ring. The linac injects electron beams into the booster synchrotron and the 1.5-GeV storage NewSUBARU ring of the University of Hyogo.

In the early stage of SPRING-8 operation, the linac injected beams one or two times a day into each ring. In 2004, the top-up operation of the SR and the NewSUBARU ring (at 1 GeV) started to stabilize the stored currents and realized constant SR lights. At present, SR is being injected every 20 seconds to five minutes depending on the filling pattern, and the stored current stability is 0.03% at 99.5 mA. The NewSUBARU ring runs the injection every six or seven seconds with current stability of 0.01% at 250 mA.

To maintain such frequent injections to both rings without interruptions, injector linacs are strongly required to minimize device failures and the recovery time from such failures. We thus improved various components of linac and enhanced its stability and reliability. Important improvements achieved in recent years include the introduction of a twin gun system, a backup system for the first klystron, and the automatic exchange of a standby klystron. These improvements gradually reduced linac's downtime to 0.11% in FY 2011.

IMPROVEMENT OF ELECTRON GUN SYSTEM

The SPRING-8 linac was equipped with only one electron gun system, i.e., a high-voltage inverter type pulse power supply, a pulse transformer, a high-voltage deck, and an electron gun. When any of these parts fail, the linac cannot inject beams into the booster synchrotron until the failure is fixed. In particular, the replacement of a cathode assembly requires at least three days to complete the mounting processes for a new cathode assembly and cathode evacuation and activation. Therefore, the construction of a backup system is an important issue for enhancing the reliability of the electron gun system and to reduce the downtime of the beam injection during gun failures. Thus we made the following improvements:

- 1) Composition of a twin electron gun system.
- 2) Development of a reliable high-voltage pulse power supply.

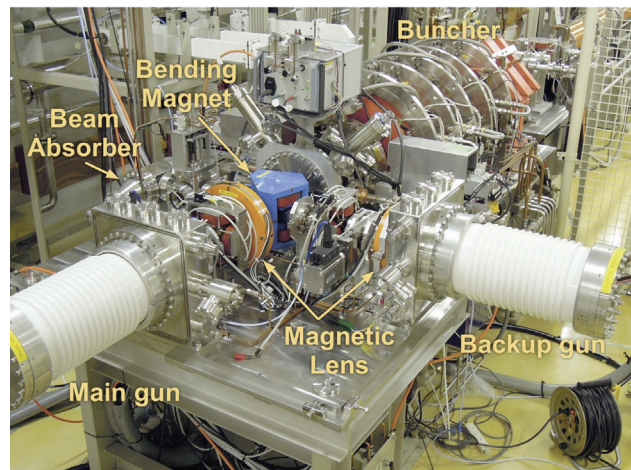


Figure 1 : Twin electron gun.

Twin Electron Gun System

We considered two ideas to realize a twin gun system: duplicating the present electron gun or doubling the present injector part, including the gun and the buncher system, for example. We built a backup gun and its power supply and considered the following issues in our backup gun design.

- 1) The original performance of the main gun must be maintained after the backup gun's installation, but the backup gun's performance for the backup operation, the

PERFORMANCE OF BEAM CHOPPER AT SARAF VIA RF DEFLECTOR BEFORE THE RFQ

A. Shor, D. Berkovits, I. Fishman, A. Grin, B. Kaiser, L. Weissman
Soreq Nuclear Research Center, Yavne 81800, Israel

Abstract

We describe performance of a beam chopper at the SARAF accelerator consisting of a HV deflector preceding the RFQ. The deflector and electronics, developed at LNS Catania, was designed to provide slow beam chopping for beam testing and diagnostics where low beam power is necessary. The HV deflector sweeps away the low energy beam onto a water-cooled beam catcher, while a fast HV switch momentarily switches off the HV whenever a transmitted beam to the RFQ is desired. We report on measurements with this chopping system, where minimum transmitted beam pulse of 180 ns duration is attained and where individual nano-bunches of the RFQ are visible. Comparisons are made with beam dynamics calculations that simulate the LEBT and the RFQ. The simulations suggest that single RFQ bunch selection can be attained with appropriate alternating positive-negative deflecting HV waveform, where single bunch transmission occurs during the positive-negative crossover.

THE SARAF ACCELERATOR: PHASE I

The SARAF accelerator complex [1] is designed to provide CW proton or deuteron beams of up to 5 mA and 40 MeV. Currently, phase I of SARAF has been installed and has undergone commissioning, and is currently operational for experimental work. SARAF phase I consists of an ECR ion source (EIS), a 176 MHz radio-frequency quadrupole (RFQ), and a prototype superconducting module (PSM). The PSM contains 6 superconducting half-wave resonators (HWR) and 3 superconducting solenoids, and provides acceleration up to about 5 MeV. Figure 1 shows the layout for SARAF phase I, including the EIS ion source and LEBT, the RFQ, MEBT, the PSM and D-plate, and the magnetic beam line transporting the beam either to the beam dump or to target station for experimentation.

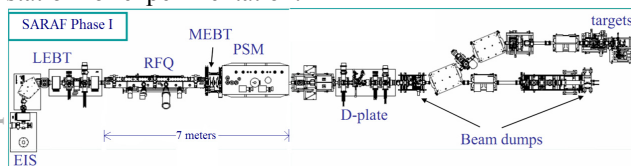


Figure 1: Layout of SARAF phase I showing EIS source, LEBT, RFQ, MEBT, PSM, D- plate, and beam lines.

SLOW CHOPPER AT SARAF

The slow chopper at SARAF consists of deflection plates and electronics developed at LNS Catania within the SPIRAL II program [2] and mounted in SARAF for tests and evaluation. The slow chopper consists of a set of parallel plates on which HV is applied for deflecting a low energy beam at an angle of 20° . For a transmitted beam, a fast switch shuts off the HV for the required beam on-time. The slow chopper was provided to SARAF along with electronics that enable applying a potential of up to 10 kV, and controls for varying the duration, frequency and phase for the off-time. The electronics provided allows for minimum off-time of about 180 ns and maximum switching repetition rate of up to 800 Hz. The slow chopper was installed in the SARAF LEBT between the second and third solenoids. The slow chopper provides a simple mechanism for lowering beam current and/or duty factor without having to pulse the ion source. Pulsing of the beam is especially required in order to tune the high intensity beam when using the downstream beam-destructive diagnostics. Figure 2 shows a schematic diagram of the LEBT and placement of the slow chopper, including the water cooled beam catcher at 20° , and also the RFQ and MEBT.

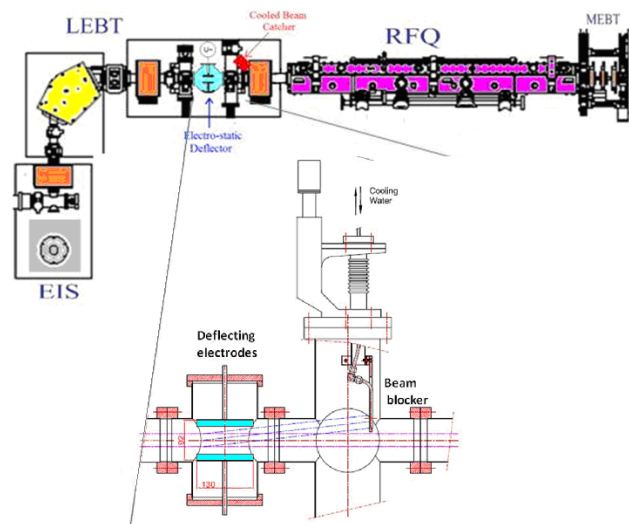


Figure 2: Schematic diagram of the EIS source, LEBT, RFQ and MEBT, with placement of slow chopper and beam catcher in the LEBT. A detailed drawing of the LEBT section containing the chopper and beam blocker is shown in the inset.

DESIGNING OF A PHASE-MASK-TYPE LASER DRIVEN DIELECTRIC ACCELERATOR FOR RADIOBIOLOGY*

K. Koyama[†], A. Aimidula, Y. Matsumura, M. Uesaka, The University of Tokyo, Tokai, Japan
M. Yoshida, T. Natsui, KEK, Tsukuba, Japan

Abstract

In order to develop a useful tool for the basic investigation of the radiobiology, the laser driven dielectric accelerator is studied. From the viewpoint of the fabrication, our effort is focused on the phase-modulation-mask-type laser-driven dielectric accelerator (PLDA). The required beam energy and bunch charge, which depend on the thickness of the specimen, are in the range of 100 keV to 1 MeV and 0.1 fC to 1 fC, respectively. The simulation results by using the FDTD simulation code, Meep, showed that the minimum grating period, was $L_G/\lambda = 0.5$ for the original type of PLDA provided that the accelerator structure was made of silica. The initial electron speed was $v = 0.5c$ (79 keV) to match the minimum grating period of PLDA. The optimistic value of the required total laser energy is 4 mJ for obtaining 1 MeV electron bunch. The acceleration field was also produced by the inside-out accelerator structure. However, L_G/λ was limited to longer than 0.6 in the preliminary simulation result.

INTRODUCTION

Radiobiologists desire to understand basic radiobiological processes around DNAs in living cells in order to estimate the health risk associated with a low radiation dose. Compact devices which deliver the spatially and temporally defined particle bunches or X-ray pulses serve to accomplish the purpose. The suitable beam size is as small as the resolving power of an optical microscope with a spatial resolution of a few hundred nanometers. The required beam energy and bunch charge, which depend on the thickness of the specimen, are in the range of 100 keV to 1 MeV and 0.1 fC to 1 fC, respectively. Moreover, it is required that one can aim at the target specimen using the optical microscope. Photonic crystal accelerators (PCAs) are capable of delivering nanometer beams of subfemtosecond pulses because the characteristic length and frequency of accelerators are on the order of those of laser light.

A phase-modulation-mask-type laser-driven dielectric accelerator (PLDA) has a simpler structure [1] than other types of PCAs[2,3]. Since the required output energy of the accelerator for the radiobiology is in the non-relativistic or weakly relativistic region the parameters of the PLDA is different from previously published one [1]. The structure and dimensions of the PLDA as well as the required laser power are discussed in this paper.

*This work was supported by KAKENHI, Grant-in-Aid for Scientific Research (C) 24510120.

[†]koyama@nuclear.jp

DIMENSIONS OF THE ACCELERATOR

The structure of the original type of PLDA is expressed in terms of the grating period L_G , the width of the grating pillar L_p , the height of the pillar H_p , and the distance between opposite pillars D as shown in Fig. 1. The thickness of the base plate can be adopted arbitrary value. The maximum length of the pillar, i.e., the width of the accelerator channel W , is restricted by the suppliable laser power. The accelerator is energized by the face-to-face irradiation of laser pulses in a orthogonal direction to the electron beam. Laser pulses, which are linearly polarized parallel to the axis of the electron beam, pass through the pillar and vacuum depending on their longitudinal position of the accelerator. An electric field along the beam axis behaves similar to a standing wave when the optical path difference between two paths through the pillar and vacuum is tuned to the half-period of the laser light. In order

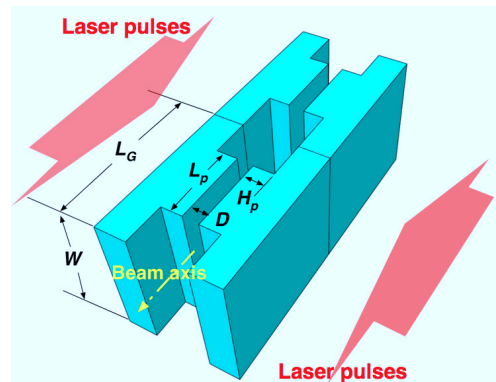


Figure 1: Schematic drawing of two periods of an accelerator unit.

to accelerate the electron, the speed of the injected electron, v_0 must be tuned to satisfy $v_0/c = L_G/\lambda$, where the electric field distribution is approximated by a sine wave and c and λ are the speed of light and the wavelength of the laser, respectively. The normalized pillar height is approximated to be $H_p/\lambda \approx 1/(2(n-1))$ by considering a path difference of π , where n is the refractive index of the pillar material [4]. The distance between opposite pillars is assumed to be $D/\lambda < 1/4$ by considering the diffraction blurring from the pillar edge. According to the reference [1], the acceleration field strength decreases by 20 percent by increasing D/λ from 0.25 to 0.5 in case of silica (SiO_2 , $\epsilon = n^2 = 2.07$ for $\lambda = 1\mu\text{m}$). Accurate values of these parameters are determined with help of the numerical simulation code.

HIGH-POWER SOURCES OF RF RADIATION DRIVEN BY PERIODIC LASER PULSES*

S.V. Kuzikov[#], IAP RAS, Nizhny Novgorod, Russia and Omega-P Inc., New Haven, USA
 A.V. Savilov, IAP RAS, Nizhny Novgorod, Russia.

Abstract

A short, periodic laser pulses can be applied for phase and frequency locking of RF sources operated in a single-mode regime. In particular, these pulses, irradiating GaAs sample, are able to produce fast modulation of Q-factor (due to inserted time dependent losses) with frequency to be close to natural single-mode oscillation frequency. In a steady state regime a phase of oscillations automatically slaves to provide minimum of the losses in GaAs. Another possible principle is to provide electron beam modulation in a cavity excited by periodically modulated current, the resulted beam with modulated density in this case generates RF power in next output cavity. The necessary exciting current can be provided by means of a DC generator those current due to a photoconductivity is externally modulated with definite frequency by laser which irradiates GaAs isolator inserted in-between electrodes. This klystron principle also solves a problem of phase locking.

pulses, it is natural to use RF sources those frequency and phase are controllable by the same laser pulses. A possible scheme, showing how to use these new sources, is shown in Fig. 1.

Many well-known RF oscillators acquire new properties, if one modulates a quality factor of its electrodynamic systems [1]. A switch of Q-factor (Q-switch) might be based on GaAs semiconductor which has several unique properties. Laser radiation with photon energy near 1.43 eV, corresponding to GaAs band gap, causes an induced photoconductivity in a penetration depth $\sim 1 \mu\text{m}$ so that GaAs becomes an absorber for less than 0.1 ns and recovers itself for $\sim 0.6 \text{ ns}$ [2]. At 1 GHz for low electron concentration in the conducting zone ($N_e < 10^{13} \text{ cm}^{-3}$) GaAs is a dielectric, for high $N_e (> 10^{17} \text{ cm}^{-3})$ GaAs is similar to metal, good absorber (to be used for Q-switch) takes place for $N_e \sim 10^{15} \text{ cm}^{-3}$. Typical necessary laser power is 1-100 nJ/mm² using popular Ti:Sa lasers with wavelength $\lambda=870 \text{ nm}$.

INTRODUCTION

Because high-gradient accelerators typically have a photoinjector, where electron bunches are born by laser

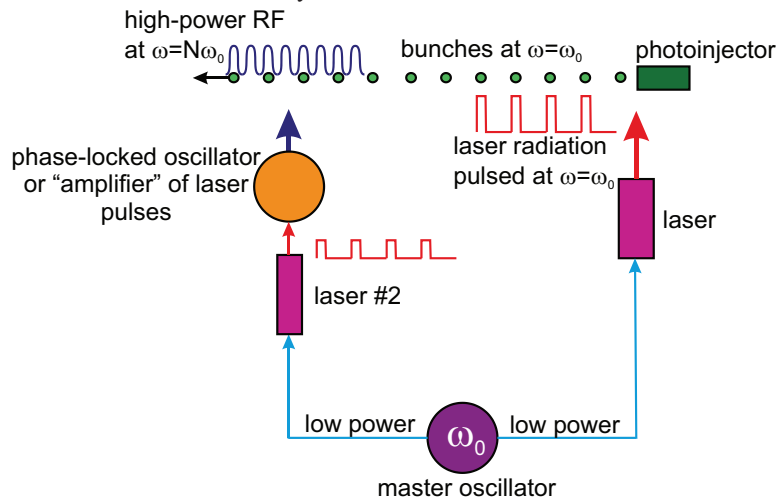


Figure 1: Scheme of accelerator with RF source driven by periodic laser light.

RF OSCILLATORS CONTROLLED BY PERIODIC LASER PULSES

If one irradiates GaAs by pulses cycling with frequency $\leq 1 \text{ GHz}$ and put it in RF cavity, where electrons generate RF power, such a new device might lock frequency and

phase (Fig. 2). Indeed, among all possible RF oscillations, which electron beam can excite, only oscillations with a proper frequency and a phase, corresponded to minimum of absorption in GaAs, are able to survive.

This principle was tested in a well known Van Der Pol oscillator, which allows to simulate a non-linear electron device having a threshold of the self-excitation [3]. In Fig. 3 one can see oscillations in dependence on normalized time ($x=\omega_0 t$) in the mentioned generator those

Copyright © 2012 by the respective authors — cc Creative Commons Attribution 3.0 (CC BY 3.0)

* Supported in part by DoE USA.

[#]kuzikov@appl.sci-nnov.ru

FRIB FRONT END DESIGN STATUS*

E. Pozdeyev[#], N. Bultman, G. Machicoane, G. Morgan, X. Rao, Q. Zhao, FRIB, East Lansing, MI 48824, USA

L.M. Young, LANL, Los Alamos, NM 87545 USA

J. Stovall, CERN, Geneva, Switzerland

V. Smirnov, S. Vorozhtsov, JINR, Dubna, Russia

L. Sun, IMP, Lanzhou, China

Abstract

The Facility for Rare Isotope Beams (FRIB) will provide a wide range of primary ion beams for nuclear physics research with rare isotope beams. The FRIB SRF linac will be capable of accelerating medium and heavy ion beams to energies beyond 200 MeV/u with a power of 400 kW on the fragmentation target. This paper presents the status of the FRIB Front End designed to produce uranium and other medium and heavy mass ion beams at world-record intensities. The paper describes the FRIB high performance superconducting ECR ion source, the beam transport designed to transport two-charge state ion beams and prepare them for the injection in to the SRF linac, and the design of a 4-vane 80.5 MHz RFQ. The paper also describes the integration of the front end with other accelerator and experimental systems.

FRONT END LAYOUT AND PARAMETERS

The FRIB Front End is designed to provide stable ion beams up to uranium with intensity sufficient to achieve 400 kW beam power on the FRIB target [1]. The FRIB Front End includes two ECR ion sources, two charge selection systems, LEBT, RFQ, and MEBT. To enhance availability and maintainability, the ECR sources and their charge selection systems are placed at the ground level in the support building about 10 m above the linac tunnel floor. Table 1 shows principle parameters of the Front End. The Front End layout is shown in Figure 1.

FRONT END SYSTEMS

Ion Sources

FRIB Front End includes two ion sources: a superconducting high-power source based on the VENUS ECRIS developed at LBNL [2] and, primarily for commissioning, a room-temperature ECR ARTEMIS. The sources are placed on high voltage platforms to match the RFQ injection energy for all beams.

The ARTEMIS ECR source, built at MSU and based on the AECR-U ECR developed at LBNL, operates at 14.5 GHz with room temperature coils. Minimal re-configuration of the source is required to make the source compatible with operation on a high voltage platform.

*Work supported by the U.S. Department of Energy Office of Science under Cooperative Agreement DE-SC0000661 and grant #DE-FGO2-08ER41553

#pozdeyev@frib.msu.edu

Table 1: FRIB Front End principle parameters

LEBT (before RFQ)	
Energy (keV/u)	12
Nominal beam current (eμA, typ.)	400
Emittance (πμm, 99.5%, norm.)	0.9
MEBT (after RFQ)	
Energy (keV/u)	500
Nominal current (eμA, typ.)	330
Emittance (πμm, 99.5%, norm.)	1.1
Long. Emittance (πkeV/u·ns, 99.5%)	1.5
Bunch repetition rate (MHz)	40.25, 80.5
Beam pulse length (μs)	0.6 – CW

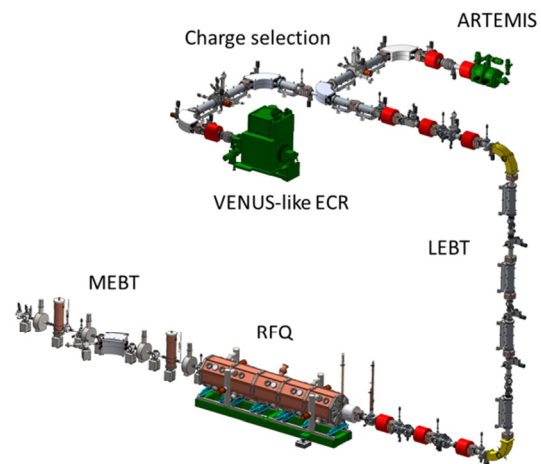


Figure 1: FRIB Front End Layout. Two ECR sources are located at the ground level. The RFQ and MEBT are located in the linac tunnel 10 m below grade.

The superconducting high-performance source will be based on the design of VENUS ECR ion source operating at a maximum frequency of 28 GHz. In 2007, VENUS demonstrated intensity required for FRIB for a 238U beam with the two charges states, 33+ and 34+, combined. Based on this result, FRIB was designed to accelerate two charge states from an ion source to double intensity. Recent beam tests demonstrated that better

HEAVY ION STRIPPERS *

F. Marti, FRIB/MSU, East Lansing, MI 48824, USA

Abstract

Stripping of high current heavy ion beams is a key technology for future accelerators as FAIR (Germany) [1] and FRIB (USA) [2] and current ones as RIBF (RIKEN, Japan) [3]. A small change in the peak charge state produced at the stripper could require a significant expense in additional accelerating stages to obtain the required final energy.

The main challenges are the thermal effects due to the high power deposition ($\sim 50 \text{ kW/mm}^2$) and the radiation damage due to the high energy deposition. The effects of heavy ion beams are quite different from proton beams because of the much shorter range in matter.

We present an overview considering charge stripping devices like carbon foils and gas cells used worldwide as well as the current research efforts on plasma stripping, liquid metal strippers, etc. The advantages and disadvantages of the different options will be presented.

INTRODUCTION

The use of strippers in heavy ion accelerators provides a way of increasing the final energy without increasing the total accelerating voltage. But there are drawbacks. Usually the stripper efficiency is low, especially when only one charge state can be accelerated like it occurs in cyclotrons, and only a fraction of the incoming particles are in the correct charge state. In the new high beam power regimes proposed for linear accelerators under construction an additional problem occurs because of the high power deposition in the stripping media.

STRIPPER CHALLENGES

Power Deposition and Radiation Damage

The major issue associated with beam strippers for high intensity heavy ion accelerators compared with H-accelerators is the much larger energy deposition per unit length of the heavy ions compared with the protons. Using the code SRIM [4] we can calculate the energy loss. As an example, a U ion at 16.5 MeV/u (FRIB stripper case) deposits 25.7 MeV/ μm and has a range of 0.14 mm in a C foil (2.25 g/cm^3), while a 1 GeV proton (i.e. SNS stripper) deposits about 0.44 keV/ μm and has a range of 1.62 m; a ratio of close to 60000 in linear energy deposition.

This much higher linear energy deposition produces significantly larger radiation damage effects in solids.

* This material is based upon work supported by the U.S. Department of Energy Office of Science under Cooperative Agreement DE-SC0000661

Thermal Effects

Although the beam powers are quite different (40 kW at the FRIB stripper and 1.4 MW at the SNS stripper) the much higher linear energy deposition more than compensates it and the thermal effects are also more severe. These become important when gas or liquid strippers are proposed to avoid the radiation damage to the solid lattice. They could produce density variations that result in large energy spreads of the stripped beam.

EXAMPLES OF STRIPPERS IN USE

Brookhaven National Laboratory

The Relativistic Heavy Ion Collider (RHIC) is the major heavy ion accelerator at Brookhaven National Laboratory (BNL) (see Figure 1). The Au beam was until recently accelerated in a tandem (now an EBIT is being used) with the first stripper in the tandem terminal (S1), a second stripper after the tandem (S2), a third between the Booster and the AGS (S3) and a fourth one between the AGS and the Collider (S4) [5].

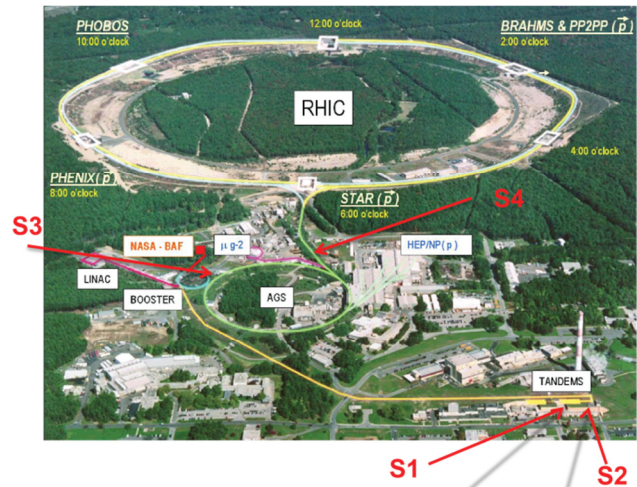


Figure 1: Layout of the RHIC accelerator at BNL showing the location of the four strippers, S1 at the tandem terminal, S2 after the tandem, S3 between the Booster and the AGS and S4 after the AGS.

The two more challenging strippers are S1 and S3. The first stripper (S1) is very thin, just 2 micro grams/ cm^2 . The Au ions are stripped from Au^{-1} to Au^{+12} . The lifetime of this stripper when using evaporated carbon foils was short. The introduction of foil produced by laser ablation of carbon extended the average lifetime by a factor of three. A ladder with several hundred foils is located at the terminal and oscillates to spread the beam damage over a larger surface.

LIGHT ION ECR SOURCES STATE OF THE ART FOR LINACS

R. Gobin*, N. Chauvin, O. Delferrière, O. Tuske, D. Uriot, Commissariat à l’Energie Atomique et aux Energies Alternatives, CEA/Saclay, DSM/IRFU, 91191 - Gif/Yvette, France

Abstract

Since the middle of the 90’s development of high intensity light ion injectors are undertaken at CEA-Saclay. The first 100 mA proton beam has been produced by the SILHI ECR source in the framework of the IPHI project. Ever since, more than 100 mA of protons or deuteron beams, with high purities, have been regularly produced in pulsed or continuous mode, and with very good beam characteristics analyzed in dedicated beam diagnostics. CEA-Saclay is currently involved in several high intensity LINAC projects such as Spiral2, IFMIF-EVEDA and FAIR, and is in charge of their source and LEBT design and construction.

This article reports the latest developments and experimental results carried out at CEA-Saclay for the 3 projects. In addition, a review of the developments and beam results performed in other laboratories worldwide are also presented.

INTRODUCTION

For several decades numerous projects are based on high intensity beam interaction with different targets, either for industrial applications or research facilities. High intensity light ion beam projects are often ranked in the HPPA (High Power Proton Accelerator) family. Table 1 gives a list of worldwide research facility projects based on positive ions. One could note, numerous projects based on negative ion production (mainly H-) also exist and are not listed here.

Table 1: List of several HPPA around the world

	Particles	Intensity	Pulse length	Repetition	Duty Factor	Emittance
	p/d/H-	mA	ms	Hz	%	π mm.mrad
LEDA	H ⁺	100	CW	-	100	0.25
IPHI*	H ⁺	100	CW	-	100	0.25
TRASCO	H ⁺	30	CW	-	100	0.2
SARAF	H ⁺ , D ⁺	2	CW	-	100	0.2
IFMIF*	D ⁺	140	CW	-	100	0.25
Spiral2*	H ⁺ , D ⁺	5	CW	-	100	0.25
PEFP	H ⁺	20	2	-	8-20	-
MYRRHA	H ⁺	10/25	CW	-	100	0.25
Chinese ADS	H ⁺	10	CW	-	100	-
FAIR*	H ⁺	100	1	4	0.4	0.3
ImPUF	H ⁺ , D ⁺	5	CW	-	100	-
ESS	H ⁺	60/90	2.9	14	4	0.3

Like for all ion accelerators, the general lay out (fig. 1) shows the first element of such HPPA is the ion source.

email: rjgobin@cea.fr

The ion source has to provide the requested beam with characteristics giving the best conditions to inject the beam into the 1st accelerating cavity. Thus the source has to be designed to minimize the beam emittance. The 1st accelerating cavity is generally an RFQ (Radiofrequency Quadrupole) which bunches and accelerates the beam up to few MeV. A LEBT (Low energy Beam Transport), follows the source and allows matching the beam at the entrance of the RFQ. As shown in table 1, the requested rms normalized emittance value turns out to be 0.25π .mm.mrad at the RFQ entrance. As a consequence, for an HPPA, while designing an injector, one has to consider not only the source but the ion source, the extraction system and the LEBT as a whole[1].

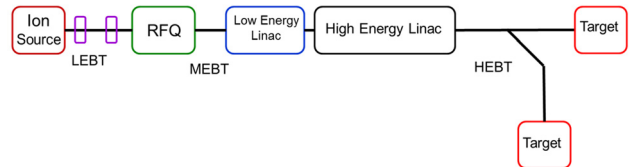


Figure 1: Schematic lay out of a high intensity Linac

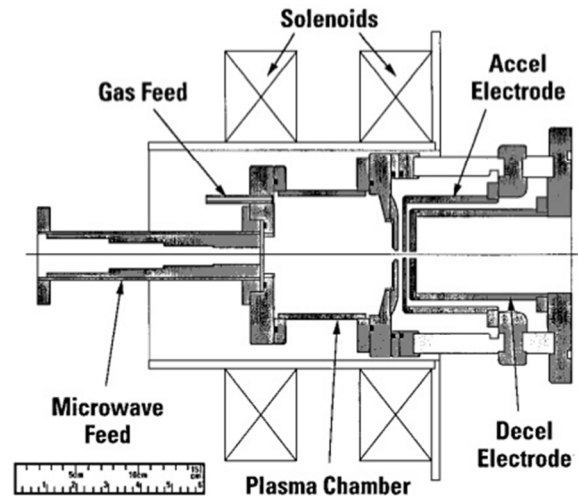


Figure 2: 1st ECR ion source dedicated to HPPA, developed in Chalk River

Then, after the RFQ, the main part of the accelerator consists of a long string of cavities (generally superconducting cavities) separated by matching sections and equipped with well-adapted diagnostics.

IN FLIGHT ION SEPARATION USING A LINAC CHAIN*

M. Marchetto[†], F. Ames, P. Bender, B. Davids, N. Galinski, A. Garnsworthy, G. Hackman, O. Kirsebom, R.E. Laxdal, D. Miller, A.C. Morton, A. Rojas, C. Unsworth, TRIUMF, Vancouver, Canada
L. Evitts, C. Nobs, University of Surrey and TRIUMF

Abstract

The ISAC accelerator complex now can accelerate radioactive heavy ion beams to above the Coulomb Barrier. Recently an ECR type charge state booster has been added to allow the acceleration of radioactive beams with masses $A > 30$. A characteristic of the ECR source is the efficient ionization of background species that can overwhelm the low intensity RIB beam. The long linac chain at ISAC can be used to provide some in flight separation both in the time domain and in the spatial domain analogous to fragment separators at in-flight fragmentation facilities. The paper summarizes the work done at TRIUMF to develop tools for the filtration and diagnosis of beam purity in the post acceleration of charge bred beams.

INTRODUCTION

Radioactive ion beams (RIB) are produced and post accelerated at the TRIUMF ISAC facility, represented in Fig. 1, via the isotope separation on line (ISOL) method.

The ISAC RIB production uses protons from the TRIUMF cyclotron. The radioactive species released by the thick target are singly charged and extracted at source potential. The radioactive ions are magnetically separated and can be post accelerated to a variable final energy. The post-accelerator chain is composed of a radio frequency quadrupole (RFQ), a drift tube linac (DTL) and a superconducting (SC) linac.

In order to reach high energies and limit the cost of the post-accelerators the singly charged beam is stripped to a higher charge state. Light masses ($A \leq 30$) are stripped downstream of the RFQ by means of a thin carbon foil. Heavy masses ($A > 30$) are stripped before injection into the RFQ by means of an ECR type charge state booster (CSB).

The charge state booster ionizes both the RIB but also any other element present in its vacuum chamber and immediate surroundings. Such elements belong either to the background residual gas or to the materials that constitute the vacuum chamber itself. The ionization of these contaminants generates a background current of orders of magnitude higher than the radioactive species. This background makes identifying and selecting the RIB extremely challenging. In most of the cases the contaminants to RIB ra-

tio can be improved in favor of radioactive species but the contaminants can not be completely suppressed. Also the necessary cleaning of the beam from contaminants has the side effect of losing part of the produced RIB.

In order to suppress the contaminants a toolkit of separation and filtration techniques as well as software and diagnostic aids to plan and streamline the beam tuning and delivery is in place.

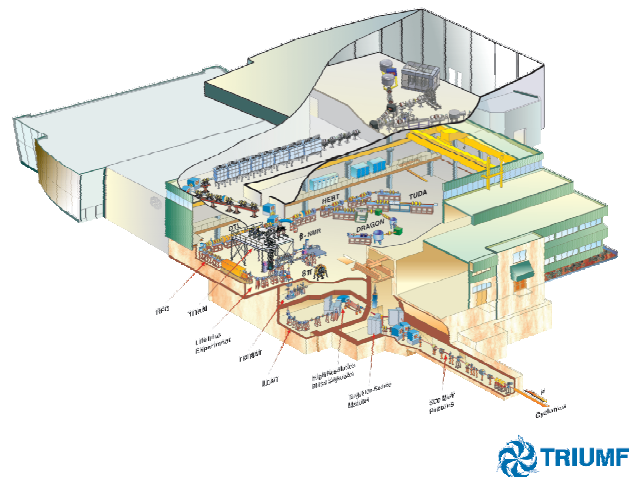


Figure 1: Artistic overview of the ISAC facility at TRIUMF.

THE ISAC FACILITY

The ISAC facility plan view is represented in Fig. 2. The detailed description of the facility can be found in previous proceedings [1].

The RIB production takes place in one of the two underground target stations (ITE and ITW see shaded area in Fig. 2) at a time using 500MeV up to $100\mu\text{A}$ of current (namely up to 50kW of beam power). Different target materials can be used to produce the neutral beams. Two types of production target containers are available, rated as low and high power relatively to the proton beam current. The production target material and type are chosen based on the experimental needs.

The produced neutral atoms diffuse into the ion source. Different sources are available (surface, LASER, FEBIAD) and others are under development (ECR). Each target is combined with the proper sources to optimized the overall

*TRIUMF receives federal funding via a contribution agreement through the National Research Council of Canada

[†]marco@triumf.ca

SARAF PHASE II P/D 40 MeV LINAC DESIGN STUDIES*

P.N. Ostroumov, Z.A. Conway, M.P. Kelly, A.A. Kolomiets, S.V. Kutsaev and B. Mustapha
Argonne National Laboratory, Argonne, IL 60441, USA
J. Rodnizki[#], Soreq NRC, Yavne, Israel

Abstract

The Soreq NRC initiated the establishment of SARAF – Soreq Applied Research Accelerator Facility [1]. SARAF will be a multi-user facility for basic research, e.g., nuclear astrophysics, radioactive beams, medical and biological research; neutron based non-destructive testing (using a thermal neutron camera and a neutron diffractometer) and radio-pharmaceuticals research, development and production. The SARAF continuous wave (CW) accelerator is planned to produce variable energy (5-40 MeV) proton and deuteron beam currents (0.04-5 mA). Phase I of SARAF (ion source, radio-frequency quadrupole (RFQ), and one cryomodule housing 6 half-wave resonators (HWR)) was installed and is operating at Soreq NRC delivering CW 1mA 3.5 MeV proton beams and low-duty cycle (10^{-4}) 0.3 mA 4.7 MeV deuteron beams [2]. SARAF is designed to enable hands-on maintenance, which implies very low beam losses for the entire accelerator. This paper presents the physics design of two options to subsequently develop a conceptual design for extending the SARAF Phase I linac to its planned Phase-II beam parameters (40 MeV, 5 mA protons and deuterons).

INTRODUCTION

We present the physics design of two options for a CW linac capable of delivering 200-kW beams of 40-MeV, 5-mA protons and deuterons [3, 4]. The two options analyzed are (1) a linac based on superconducting (SC) halfwave resonators (HWRs) operating at a fundamental frequency of 176 MHz; and (2) a linac based on SC quarter-wave resonators (QWRs) operating at a fundamental frequency of 109 MHz. Both options include a CW radio frequency quadrupole (RFQ) designed for acceleration of protons or deuterons from 20 keV/u to 1.3 MeV/u.

The main SC cavity parameters are based on recent Argonne National Laboratory (ANL) experience with a performance margin. These parameters are used to develop baseline designs of the SC linacs. The ANL approach for CW RFQs for both options is described. Significant effort was devoted to the electromagnetic (EM) optimization of both QWRs and HWRs. The concepts for the engineering and beam physics design of the linac and its cryomodules are discussed. The results of detailed beam dynamics simulations with realistic fields and machine errors are presented.

[#]jacob@soreq.gov.il

* This work was supported by the ANL WFO No. 85Y47

CHOICE OF SC CAVITY PARAMETERS

The choice of SC cavity parameters for SARAF Phase II is based on the demonstrated performance of TEM-class cavities at ANL. The horizontal bands in Fig. 1 show the proposed operating regions for each of the two pairs of 109-MHz QWRs and 176-MHz HWRs. The critical point is that in all cases there is a performance margin with respect to demonstrated Argonne cavity performance in the ATLAS energy upgrade cryomodule [5]. Overall, the choice of operating parameters is weighted toward maintaining E_{PEAK} at or below 36 MV/m because the performance margin with respect to B_{PEAK} is relatively larger. Based on the most recent ANL experience with the development of new 72 MHz QWRs for the ATLAS efficiency and intensity upgrade [6], it is most likely that the margin in both electric and magnetic fields will be increased up to 100% [7].

Generally, the proposed quarter-wave option has a modestly larger margin due to the lower value of B_{PEAK} for a given value of E_{PEAK} in QWR geometries versus HWR geometries.

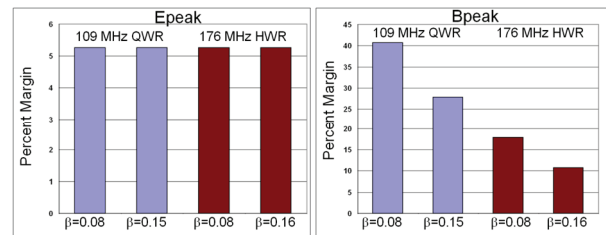


Figure 1: Operating margin with respect to already demonstrated performance in ATLAS.

RFQ BEAM AND EM DESIGN

To maintain a high level of operational reliability, we recommend the development and fabrication of a new 1.3-MeV/u RFQ with reduced RF power losses relative to the existing SARAF Phase-I 4-rod RFQ. The new RFQ would be based on a 4-vane structure. The main requirements for the RFQ for the high-intensity SARAF linac are as follows:

- Absolutely reliable CW operation for both protons and deuterons.
- Formation of a beam with extremely low halo in the longitudinal phase space.
- Moderate peak fields to avoid any possible breakdowns and avoid long conditioning of the resonator. In particular, the peak electric fields should be below 1.8EK where EK is the Kilpatrick limiting field.

RECOVERY OF THE J-PARC LINAC FROM THE EARTHQUAKE

K. Hasegawa[#]

Accelerator Division of J-PARC, KEK/JAEA, Tokai, Ibaraki, 319-1195, Japan

Abstract

J-PARC was severely damaged by the March 11 Great East Japan Earthquake in 2011. When the earthquake struck, we had a beam study operation of the linac, and the machine automatically stopped immediately. The damages to the facilities and infrastructure were very serious over the entire site. Thanks to the significant effort of restoration, we resumed beam operation in December 2011 and user operation in January 2012. We learnt many lessons from the earthquake.

INTRODUCTION

J-PARC, which stands for Japan Proton Accelerator Research Complex, consists of the linac, the 3 GeV rapid cycling synchrotron (RCS), the 30 GeV Main Ring synchrotron (MR) and three experimental facilities[1]. The linac consists of a negative hydrogen ion source, a 3 MeV RFQ (Radio Frequency Quadrupole linac), a 50 MeV DTL (Drift Tube Linac) and a 191 MeV SDTL (Separated-type DTL) as shown in Fig. 1. But currently, the last 2 SDTL cavities are used as debunchers with no acceleration, and then the injection energy to the RCS is 181 MeV. Construction of superconducting linac (SCL) from 400 to 600 MeV and experimental facilities for the Accelerator Driven Transmutation System (ADS) are planned in the next construction phase of J-PARC. A proton beam from the RCS is injected to Materials and Life Science Experimental Facility (MLF) for neutron and muon experiments. The MR has two beam extraction systems. One is a fast extraction for the neutrino beam line for the Tokai-to-Kamioka (T2K) experiment, and the other is a slow extraction for Hadron Experimental Facility.

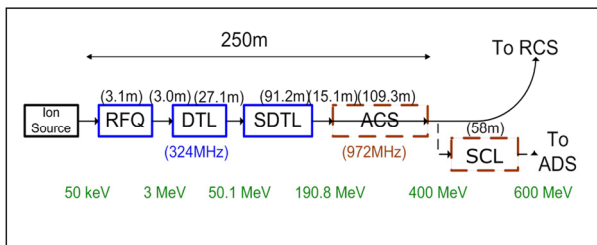


Figure 1: The structure of the J-PARC linac.

Coincidentally no user services were scheduled in the daytime of March 11, 2011. Beam study at the linac, and radiation survey work at the RCS and MR tunnels were carried out. The earthquake occurred when we suspended a beam for changing a beam destination from the linac to the RCS. The earthquake intensity was 6 lower at Tokai, which is the third highest intensity of the ten-ranked Japanese seismic scale. Whereas we prepared up to 8 m

tsunami, the actual level was much lower at 3 m. It was extremely fortunate that no one was injured or missing.

STATUS BEFORE THE EARTHQUAKE

Commissioning of the linac started in 2006 and entire accelerators started operation in 2009. We had a discharge trouble at the RFQ, but this was settled during the summer shutdown of 2009 by improving the vacuum system. Since then, we had kept stable operation for users, concretely 90 to 95% availability. We ramped up the beam power from the RCS to the MLF to 120 kW in the 2009 fall and then to 200 kW in November 2010. Corresponding linac beam power is simply calculated by the ratio of energy, $0.060=(181/3,000)$, e.g. 200 kW RCS power corresponds 12.0 kW linac power. At the MLF, many neutron beam lines were in operation and numerous data had been accumulated before the earthquake. We also performed 400 kW (equivalent current beam) acceleration for higher power demonstration in January 2011.

The MR had been increased beam power steadily and had delivered beam at 145 kW to the neutrino beam line. Muon neutrinos may convert to electron neutrinos while travelling J-PARC to the Super-Kamiokande detector in 295 km distance. Detailed study results before the earthquake revealed that there were 6 possible events of the appearance of electron neutrinos.

The MR slow extracted beam to the Hadron Facility was 3 kW. Many experiment just started and the first data of the penta quark search were obtained.

THE EARTHQUAKE DISASTER

The big earthquake with magnitude of 9.0 hit the northeastern Japan on March 11, 2011. The J-PARC is located at about 200 km from the epicenter and had significant damage. Because the status of the J-PARC facility in general is described in some references[2,3], this paper mainly focus on that of the linac.

Linac

The linac building had the most seriously damages among all other buildings. A wide area at the entrance of the linac building subsided about 1.5 m, and almost all water supply and drainage pipes were broken as shown in Fig. 2. We could not get into the building until March 17 due to many strong aftershocks. It was found that there were fortunately no severe damages on the accelerator components themselves, but found that water was accumulated by 1 cm in depth on the linac tunnel floor. When we entered the tunnel again a week later on the 24th, the water level increased to approximately 10 cm. The leakage speed in this week was much faster than that of the first week from the earthquake. Therefore, we

[#]hasegawa.kazuo@jaea.go.jp